Evaluation of the Stimulatory Effects of EBC-46 on Dermal Fibroblast and Keratinocyte Wound Healing Responses *in Vitro* and Correlation to Preferential Healing *in Vivo*

Rachael Louise Moses BSc, MSc

Thesis presented for the degree of

Doctor of Philosophy

Stem Cells, Wound Repair & Regeneration,
Oral and Biomedical Sciences,
Cardiff Institute of Tissue Engineering & Repair (CITER),
School of Dentistry,
College of Biomedical and Life Sciences,
Cardiff University,
Cardiff, UK

August, 2016

Dedication

I would like to dedicate this thesis to my Mum, you have been an inspiration to me and given me every opportunity. I am truly thankful for your unconditional love and support, making this PhD possible. Thank you for always being there; I love you.

Acknowledgements

Firstly, I would like to give utmost thanks and appreciation to my two supervisors, Dr Ryan Moseley and Dr Robert Steadman. You have provided invaluable expertise, support, encouragement and enthusiasm throughout my project; I have thoroughly enjoyed this project. I have greatly appreciated your guidance and encouragement of my future career in research.

In addition, I am hugely grateful to all who have assisted me and provided support from the School of Dentistry, Institute of Nephrology and Tenovus Building. Particular thanks go to Dr Adam Midgeley, who has provided vital support and advice on experimental procedures and subsequent analysis. I would like to thank Professor Rachel Errington, Dr Rachel Howard-Jones and Marie Wiltshire, their assistance and knowledge on flow cytometry procedures and the specialised analysis software was greatly appreciated. I would also like to thank the technical team at the School of Dentistry; who have all contributed to the successful running of the department, along with providing equipment expertise and knowledge.

Additionally, I would like to express huge thanks to Dr Glen Boyle and Professor Peter Parsons, for allowing me the opportunity to perform Microarray analysis at Queensland Institute of Medical Research (QIMR), along with crucial training on undertaking these studies, and access and training on the specialised analysis software. I would like to thank the rest of the department at QIMR for graciously welcoming me and providing support and friendship, in particular Carly, Pei, Tash, Jacinta, Jenny and Vaish.

I have been lucky to work with a number of great colleagues and friends in the School of Dentistry, who have provided scientific support, brilliant friendships, great humour; and personal support and encouragement, especially on those night shifts with cell cycle analysis! I would like to thank my friends, Nic, Rhi, Châni, Jen, Liv, Karina and Shannon, who have been there for me throughout this project, providing fantastic friendships and unlimited support.

This project was funded by QBiotics Ltd., and I would like to take this moment to thank Dr Paul Reddell and Dr Victoria Gordon for giving me this wonderful opportunity to undertake a research project that I have thoroughly loved. I am also grateful for the funding received by CITER, enabling my research travel to QIMR, giving me an amazing experience and obtaining essential data.

Finally, I would like to express heartfelt thanks to my wonderful family, in particular my Mum, Steve and grandparents; you have provided unlimited and unwavering support, encouragement and love throughout my project, keeping me somewhat sane! You have been there for me at every stage; I love you all very much and greatly appreciate all that you have done for me.

Abstract

The novel epoxy-tiglianes, EBC-46 and 'lesser activity' EBC-211, are sourced from seeds of the Fountain's Blushwood Tree (*Fontainea picrosperma*), indigenous to Queensland Tropical Rainforest. Australian biotechnology company, QBiotics Ltd., has demonstrated that EBC-46 stimulates exceptional dermal wound healing responses *in vivo*, following cancer treatment and tumour destruction in domesticated animals. Consequently, QBiotics is developing EBC-46 as a veterinary anti-cancer pharmaceutical and performing human clinical trials. However, little is known on how EBC-46 induces its exceptional healing effects, manifested as accelerated wound re-epithelialisation, closure and reduced scarring.

This study aimed to elucidate how EBC-46 and EBC-211 mediates these exceptional wound healing effects *in vitro*, through analysis of HaCaT keratinocyte and dermal fibroblast/myofibroblast genotypic and phenotypic responses, following epoxy-tigliane treatment (0.001-100µg/ml). A number of key wound healing responses were assessed, including proliferation, cell cycle progression, scratch wound repopulation; and transforming growth factor-β_1 (TGF-β_1)-driven, fibroblast-myofibroblast differentiation.

Studies demonstrated that both EBC-46 and EBC-211 induced fibroblast and HaCaT cytotoxicity at 100µg/ml. EBC-46 and EBC-211 (0.001-10µg/ml) significantly retarded fibroblast proliferation and delayed S/G2 cell cycle transition, but exerted no significant effects on fibroblast migratory responses. Although EBC-46 had no effects on α-smooth muscle actin (α-SMA) expression, stress fibre organization and myofibroblast formation (0.001-0.01µg/ml and 1-10µg/ml), EBC-46 significantly inhibited α-SMA expression and stress fibre formation at 0.1µg/ml, with cells retaining normal fibroblast morphologies. EBC-211 induced similar effects at 10µg/ml.

Both EBC-46 and EBC-211 (0.001-10µg/ml) stimulated significant HaCaT proliferation, G1/S and S/G2 cell cycle transitions; and accelerated scratch wound repopulation, even with mitomycin C. Microarray analysis and protein level validation, identified numerous differentially expressed genes in epoxy-tigliane-treated, HaCaTs. Up-regulated genes included certain keratins and others associated with promoting cell cycle progression, proliferation and migration. Down-regulated genes included other keratins and genes associated with inhibiting cell cycle progression and proliferation, including certain cytokines and chemokines.

This study has provided evidence to explain the enhanced re-epithelialisation and reduced scarring responses observed in epoxy-tigliane-treated skin. Furthermore, it highlights the potential of epoxy-tiglianes as novel therapeutics for impaired dermal wound healing and excessive scarring situations.

Patents, Prizes and Presentations

Research-Related Patents Filed To Date

Methods and Compositions for Wound Healing. Inventor on the following Patents in collaboration with QBiotics Ltd. and collaborators at the QIMR Berghofer Medical Research Institute (Queensland, Australia), relating to the application of epoxy-tigliane compounds, such as EBC-46 and EBC-211, in the promotion of dermal wound healing and reduced scarring:-

AU20140253608, CA2909653, CN105308052, EA201591996, EP2986615, KR20160023651, PH12015502405, SG11201508588X, US2016068499; and WO201416935.

Conferences Prizes

Young Investigators' Poster Prize. *28th Annual Postgraduate Research Day*, Cardiff University, UK (November, 2013).

Poster Prize. *European Tissue Repair Society Annual Conference*, Edinburgh, UK (September, 2014).

Guest Speaker

Identification of gene expression profiles underlying preferentially stimulated keratinocyte wound healing responses and re-epithelialisation by novel epoxy-tigliane pharmaceuticals. *Wound Healing: Collaboration and Innovation for Health and Wealth*. Cardiff Institute of Tissue Engineering & Repair (CITER), Cardiff University, UK (February, 2016).

Other Presentations Directly Related to the Contents of This Thesis

1. Contrasting stimulatory effects of EBC-46 on dermal fibroblast and keratinocyte wound healing responses *in vitro*. **Moses RL**, Boyle GM, Reddell P, Steadman R, Moseley R. *Proceedings of the 28th Annual Postgraduate Research Day*, 55. Wales College of Medicine, Cardiff University, Cardiff, UK (November, 2013).

2. Preferential stimulation of keratinocyte proliferation and migratory responses by novel tigliane pharmaceuticals contribute to enhanced wound re-epithelialisation. **Moses RL**, Reddell P, Steadman R, Moseley, R. *European Tissue Repair Society Annual Conference*, Edinburgh, UK (September, 2014). *Wound Repair and Regeneration* (2014), **22:** A92.

3. Preferential stimulation of keratinocyte proliferation and migratory responses by novel tigliane pharmaceuticals contribute to enhanced wound re-epithelialisation. **Moses RL,** Reddell P, Steadman R, Moseley, R. *Proceedings of the 12th Cardiff Institute of Tissue Engineering and Repair (CITER) Scientific Meeting*, P21. Stradey Park Hotel, Llanelli, UK (September, 2014).

4. Pharmaceutical evaluation of novel tigliane compounds as modulators of dermal fibroblast-myofibroblast differentiation, scar tissue resolution and fibrosis; and elucidation of their underlying mechanisms of action. Dally J, **Moses RL**, Midgley AC, Reddell PW, Steadman R, Moseley R. *Proceedings of the 1st Sêr Cymru (Life Sciences Research Network Wales) Annual Scientific Meeting*, P4. St David's Hotel, Cardiff, UK (December, 2014).

5. Epoxy-tiglianes modulate dermal fibroblast-myofibroblast wound healing responses and reduce scarring. Dally J, **Moses RL**, Midgley AC, Howard-Jones RA, Errington RJ, Reddell PW, Steadman R, Moseley R. British Society for Oral and Dental Research Annual Meeting, Cardiff, UK (September, 2015). *Journal of Dental Research* (2015), **94B:** 137.

6. Epoxy-tiglianes stimulate keratinocyte proliferative and migratory responses, enhancing wound re-epithelialisation. **Moses RL**, Boyle GM, Reddell P, Steadman R, Moseley R. British Society for Oral and Dental Research Annual Meeting, Cardiff, UK (September, 2015). *Journal of Dental Research* (2015), **94B:** 141.

7. Identification of gene expression profiles underlying preferentially stimulated keratinocyte wound healing responses and re-epithelialisation by novel epoxy-

tigliane pharmaceuticals. **Moses RL**, Boyle GM, Reddell P, Steadman R, Moseley R. *Proceedings of the 13th Cardiff Institute of Tissue Engineering and Repair (CITER) Scientific Meeting*, 18. Cadbury House Hotel, Bristol, UK (September, 2015).

8. Modulatory effects of novel epoxy-tigliane pharmaceuticals on dermal fibroblast-myofibroblast wound healing responses mediate their enhanced anti-scarring properties. Dally J, **Moses RL**, Midgley AC, Howard-Jones RA, Errington RJ, Reddell PW, Steadman R, Moseley R. *Proceedings of the 13th Cardiff Institute of Tissue Engineering and Repair (CITER) Scientific Meeting*, 50. Cadbury House Hotel, Bristol, UK (September, 2015).

9. Modulatory effects of novel epoxy-tigliane pharmaceuticals on dermal fibroblast-myofibroblast wound healing responses mediate their enhanced anti-scarring properties. Dally J, **Moses RL**, Midgley AC, Howard-Jones RA, Errington RJ, Reddell PW, Steadman R, Moseley R. *European Tissue Repair Society Annual Conference*, Copenhagen, Denmark (October, 2015). *Wound Repair and Regeneration* (2015), **23:** A6.

10. Identification of gene expression profiles underlying preferentially stimulated keratinocyte wound healing responses and re-epithelialisation by novel epoxy-tigliane pharmaceuticals. **Moses RL**, Boyle GM, Reddell P, Steadman R, Moseley R. *European Tissue Repair Society Annual Conference*, Copenhagen, Denmark (October, 2015). *Wound Repair and Regeneration* (2015), **23:** A21.

Chapter 1 – Introduction

Table of Contents

Chapter 2 - Materials and Methods

Table of Contents

Chapter 3 - Effects of EBC-46 and EBC-211 on Dermal Fibroblast Wound Healing Responses

Table of Contents

Chapter 4 - Effects of EBC-46 and EBC-211 on Keratinocyte Wound Healing Responses

Table of Contents

Chapter 5 - Effects of EBC-46 and EBC-211 on Global Gene Expression in HaCaTs

Table of Contents

Chapter 6 – Validation of Differential HaCaT Gene Expression Responses Induced by EBC-46 and EBC-211

Table of Contents

Chapter 7 – Discussion

Table of Contents

List of Abbreviations

5-FU	5-Fluorouracil
α-SMA	α-Smooth muscle actin
ACT	α-1-Antichymotrypsin
AhR	Aryl hydrocarbon
AKT3	V-AKT murine thymoma viral oncogene homolog 3
ALKs	Activin-receptor-like kinases
AP	Activator protein
APCs	Antigen presenting cells
bFGF	Basic fibroblast growth factor
β-ME	β-Mercaptoethanol
BAMBI	Bone morphogenetic protein and activin membrane-bound inhibitor
BSA	Bovine serum albumin
cDNA	Copy DNA
cRNA	Antisense RNA
CCL	Chemokine (C-C motif) ligand
CCNA2	Cyclin A2
CCNB1	Cyclin B1
CCNB2	Cyclin B2
CDCA7	Cell division cycle associated 7
CDKs	Cyclin-dependent protein kinases
CDKN1A	Cyclin-dependent kinase inhibitor 1A
CDKN3	Cyclin-dependent kinase inhibitor 3
CEP55	Centrosomal protein 55kDa
COX-2	Cyclooxygenase-2 enzyme
CTGF	Connective tissue growth factor
CXCL	Chemokine (C-X-C motif) ligand
DAG	Diacylglycerol
DMEM	Dulbecco's modified eagle's medium
DMSO	Dimethyl sulfoxide
E2F2	E2F transcription factor 2

EBC-211	(12-tigloyl-13-(2-methylbutanoyl)-5,6-epoxy-4,5,9,12,13,20-hexahydroxy-1-tigliane-3-one)
EBC-46	(12-tigloyl-13-(2-methylbutanoyl)-6,7-epoxy-4,5,9,12,13,20-hexahydroxy-1-tigliane-3-one)
ECM	Extracellular matrix
EGF	Epidermal growth factor
EGFR	Epidermal growth factor receptor
ELISAs	Enzyme-linked immunosorbent assays
ERK	Extracellular signal-regulated kinase
FCS	Foetal calf serum
FDA	Food and drug administration
FGF	Fibroblast growth factor
FOXO1	Forkhead box O1
F-SCM	Fibroblast-serum containing media
FST	Follistatin
GINS2	GINS complex subunit 2
GM-CSF	Granulocyte macrophage colony-stimulating factor
HaCaTs	Human adult, spontaneously immortalized, epidermal keratinocytes
HAS	Hyaluronan synthase
HB-EGF	Heparin-binding epidermal growth factor
HGF/SF	Hepatocyte growth factor/scatter factor
HMMR	Hyaluronan mediated motility receptor
IFN	Interferon
IL	Interleukin
IPA®	Ingenuity pathway analysis
ITE	2-(1′H-indole-3′-carbonyl)-thiazole-4-carboxylic acid methyl ester
JAK	Janus kinase
JNK	c-Jun N-terminal kinase
JUN	Jun proto-oncogene/c-Jun
KGF	Keratinocyte growth factor
Krt	Keratin
K-SCM	Keratinocyte-serum containing media
MAPK	Mitogen-activated protein kinases

MCP-1	Monocyte chemoattractant protein-1
MEK	MAPK/ERK Kinase
MMP	Matrix metalloproteinase
MPF	Mitosis-promoting factor
MTT	[3-(4,5-dimethyl-2-thiazolyl)-2,5-diphenyltetrazolium bromide]
NF	Normal dermal fibroblast
NGF	Nerve growth factor
ṄO	Nitric oxide
NPWT	Negative pressure wound therapy
PAI	Plasminogen activator inhibitor
PBS	Phosphate buffered saline
PDGF	Platelet-derived growth factor
PI3	Peptidase inhibitor 3
PI3K	Phosphatidylinositide 3-kinase
PI-8	Protease inhibitor 8
PKC	Protein kinase C
PLC	Phosphoinositide phospholipase C
POLE2	Polymerase (DNA directed), epsilon 2, accessory subunit
PTHLH	Parathyroid hormone-like hormone
qPCR	Quantitative polymerase chain reaction
ROCK	Rho-associated kinase
ROS	Reactive oxygen species
R-SMADs	Receptor-associated SMADs
SARA	SMAD anchor for receptor activation
SCCA	Squamous cell carcinoma antigen
SDF-1	Stromal cell-derived factor-1
SDS	Sodium dodecyl sulphate
SERPINs	Serpin peptidase inhibitors
STAT	Signal transducers and activators of transcription
TβRs	TGF-β receptors
TAE	Tris-acetate-EDTA
TBS	Tris-buffered saline
TF	Tissue factor

TGF-α	Transforming growth factor-α
TGF-β_1	Transforming growth factor-β_1
TGF-β_2	Transforming growth factor-β_2
TGF-β_3	Transforming growth factor-β_3
TIMPs	Tissue inhibitors of metalloproteinases
TLR	Toll-like receptor
TNF-α	Tumour necrosis factor-α
tPA	Tissue-type plasminogen activator
UBE2C	Ubiquitin-conjugating enzyme E2C
uPA	Urokinase-type plasminogen activator
UV	Ultraviolet
VEGF	Vascular endothelial growth factor

Chapter 1 – Introduction

Chapter 1 – Introduction

1.1 Overview

EBC-46 was found in the seeds of the Fountain's Blushwood Tree (*Fontainea picrosperma*), indigenous to the Queensland Tropical Rainforest. EBC-46 was sourced due to its' potential to have potent bioactivity and was developed by QBiotics Ltd. (Queensland, Australia). EBC-46 was discovered to have an anti-cancer effect through the palliative treatment of solid tumours on cats, dogs and horses. This treatment was shown to have remarkable success in the ablation of the tumours and sarcoids, without evidence of any long term side effects (QBiotics Ltd.). An exceptional wound healing response at treatment sites was observed, following tumour ablation; producing good cosmetic outcomes in affected areas. In light of these obvious beneficial anti-tumour and pro-healing effects, QBiotics Ltd. are developing EBC-46 as a veterinary pharmaceutical for the treatment of solid tumours in these animals (QBiotics Ltd.). Furthermore, as QBiotics Ltd. has compelling proof-of-concept data of the drug's efficacy and safety both in cancer models in mice and in other domesticated animals, QBiotics Ltd. is rapidly advancing the drug towards the necessary regulatory approvals for conducting human clinical phase I/II trials (QBiotics Ltd.).

As a result of this observed exceptional wound healing effect and with little information regarding how EBC-46 induces this effect, this PhD study has focused on elucidating how it affects two cell types strongly involved in the acute skin wound healing response, i.e. dermal fibroblasts and epidermal keratinocytes (Singer & Clark 1999; Guo & DiPietro 2010). Dermal fibroblasts were used throughout this project from normal skin; and a keratinocytes cell line, human adult, spontaneously immortalized, epidermal keratinocytes (HaCaTs), were also used (Boukamp et al. 1988). A number of *in vitro* studies were performed to determine the effect of EBC-46 on various aspects of the wound healing process. These included assays to assess cell proliferation, viability, cell cycle progression, migration, differentiation, global gene expression; and finally protein expression and activity. This is the first time the effects of these novel epoxy-tiglianes on wound healing cells have been analysed.

These cells were chosen as they will hopefully replicate the *in vivo* effects seen in the animal palliative studies (Reddell et al. 2014). Comparisons were also made between EBC-46 and a 'lesser activity' analogue, EBC-211, across a range of concentrations (0-100µg/ml). This aimed to determine the optimal dose range *in vitro*, while observing the effects of these novel epoxy-tiglianes on the normal genotypic and phenotypic responses of both fibroblasts and keratinocytes. It had been previously shown through preliminary studies that EBC-46 may act as a protein kinase C (PKC) regulator. The global gene expression analysis may confirm this through differentially expressed genes downstream of this pathway (Boyle et al. 2014; Reddell et al. 2014).

1.2 Skin Structure and Function

The skin is the largest organ of the body performing various vital functions, such as providing a protective barrier from the external environment. The level of protection provided by the skin is multi-factorial, encompassing protection against pathogens and preventing ultraviolet (UV) damage, along with protection against chemical, physical and immune damage (Menon 2002; Walters & Roberts 2002; Denning 2004; Candi et al. 2005; Ovaere et al. 2009; Darlenski et al. 2011; D'Orazio et al. 2013). It also acts as a protection against free radical molecules, reducing the chance of oxidative damage occurring (Menon 2002; Baumann 2007). The skin is predominantly responsible for maintaining homeostasis of a number of key functions, such as thermoregulation and preventing the loss of water (Kalinin et al. 2002; Menon 2002; Walters & Roberts 2002; Candi et al. 2005; Darlenski et al. 2011). It is also one of the major sensory organs providing great detail about the surroundings (Menon 2002; Walters & Roberts 2002; Boulais & Misery 2008; Darlenski et al. 2011).

There are a large number of cells associated with these functions, which are constantly regenerated to maintain their actions; keeping the balance between proliferation, differentiation and apoptosis of the cells to maintain the functionality of the skin (Haake et al. 2001; Walters & Roberts 2002; Moll et al. 2005; Gurtner et al. 2008; Merad et al. 2008; Pastar et al. 2014; Ghatak et al. 2015). There are three layers separating the muscle layer from the environment: the epidermis, dermis and hypodermis, depicted in Figure 1.1 (Song et al. 1997; Braiman-Wiksman et al. 2007;

Stephens & Genever 2007; Bottcher-Haberzeth et al. 2010). The hypodermis is present directly above the muscle layer and is also termed the subcutaneous layer. It contains adipocytes providing protection and insulation (Song et al. 1997; Stephens & Genever 2007). The epidermis and dermis comprise the skin, each comprising of a number of cells, although the level of organisation of the cells varies considerably. The epidermis is more cellular and the dermis consists mainly of ECM proteins (Song et al. 1997; Haake et al. 2001; Moll et al. 2005; Boulais & Misery 2008; Merad et al. 2008; Eckes et al. 2010; Tracy et al. 2016). The epidermis has a structured appearance with layers of each cell type as they differentiate along the pathway (Song et al. 1997; Menon 2002; Stephens & Genever 2007; Bragulla & Homberger 2009). In contrast, the dermis is less regimentally organised, it is divided into two main sections: the papillary region and the reticular region (Song et al. 1997; Sorrell & Caplan 2004; Stephens & Genever 2007).

Preserving or re-establishing the integrity of the skin is vital, as loss of the protective barrier can allow contamination of the injury site and affect the normal functionality of the skin (Singer & Clark 1999; Fuchs 2007; Ovaere et al. 2009; Darlenski et al. 2011). Millions of people are affected worldwide each year as a result of a loss of the protective barrier, this is primarily a result of burns and chronic wounds, but can significantly affect the lives of those affected (Singer & Clark 1999; Menke et al. 2007; Pastar et al. 2014; Dreifke et al. 2015). Due to the major importance of the skin and all the functions it performs, it is vital for the continual regeneration and rapid repair of any injuries to prevent loss of integrity and prevent any subsequent disability resulting from this loss of integrity (Walters & Roberts 2002; Kondo & Ishida 2010; Pastar et al. 2014). There is a degree of elasticity present in the skin allowing for more flexibility with movement and to prevent tearing of the skin with the slightest alteration. This is essential, as the skin has to extend and retract as muscles contract and relax, without causing damage to the skin (Kielty et al. 2002; Sherratt 2009; McGrath & Uitto 2010). This flexibility is enabled through the presence of elastic fibres within the connective tissue of the dermis. However, this elasticity decreases with age, reducing the tensile strength of the skin (Kielty et al. 2002; Baumann 2007; Sherratt 2009; Cheng et al. 2011; Tobin 2016). This elasticity increases the durability of the skin allowing it to withstand a large amount of forces that are exerted against it, including shear force and

Figure 1.1: Section through the skin showing epidermis, dermis and hypodermis. The epidermal layers are depicted with desmosomes and hemidesmosomes, providing an adhesion role within the epidermis (McGrath & Uitto 2010).

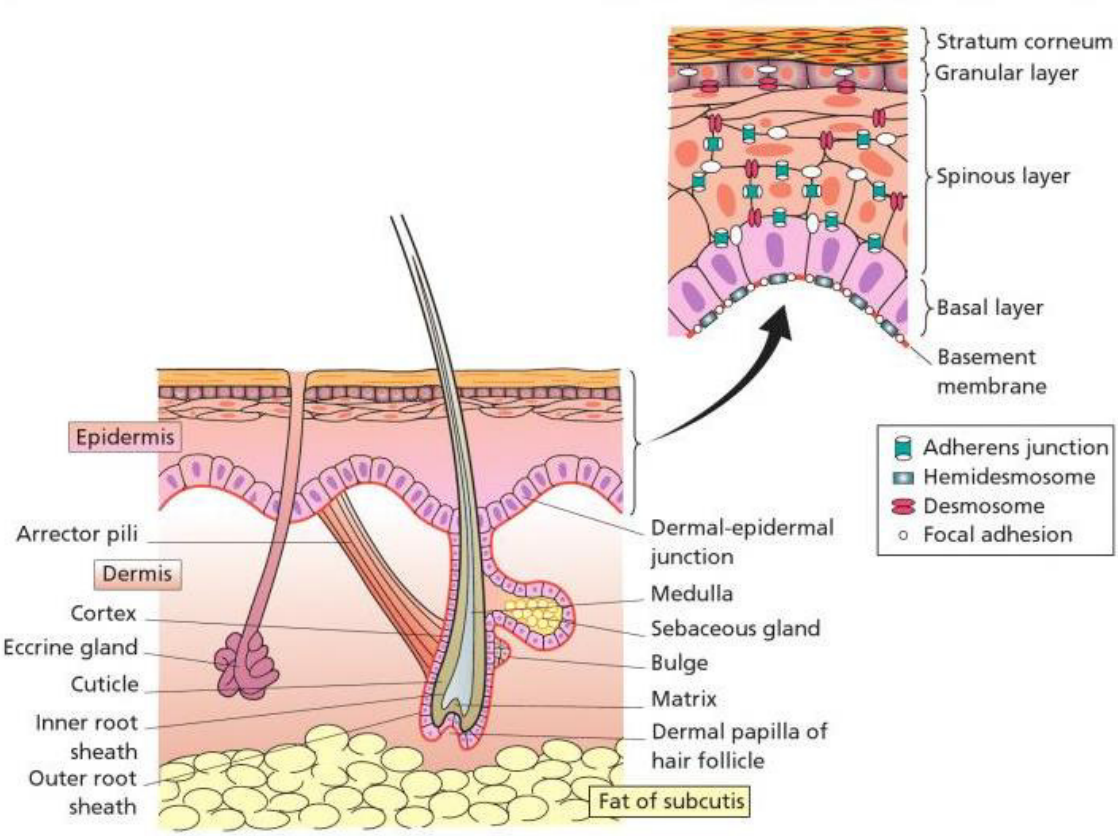

friction (McGrath & Uitto 2010).

1.2.1 Epidermis

The cells in the epidermis are organised in a way that as they differentiate; they move progressively further away from the basement membrane, until the uppermost layer of dead cells is removed (Kalinin et al. 2002; Walters & Roberts 2002; Candi et al. 2005; Bragulla & Homberger 2009; Eckhart et al. 2013). The epidermis consists of stratified squamous epithelial cells, with keratinocytes forming the majority of cells present, approximately 95%; with the other 5% consisting of melanocytes, Merkel cells and Langerhan's cells (Menon 2002; Romani et al. 2003; Moll et al. 2005; Boulais & Misery 2008; Bragulla & Homberger 2009; Sprenger et al. 2013). Keratinocytes are present at different points of differentiation, starting from the layer above the basement membrane going to the uppermost layer of the skin, forming a 100-150µm thickness: the *stratum basale*, the *stratum spinosum*, *stratum granulosum* and the *stratum corneum*, as depicted in Figure 1.1 (Menon 2002; Walters & Roberts 2002; Fuchs 2007; D'Orazio et al. 2013; Pastar et al. 2014). The columnar cells in the *stratum basale* are the only dividing cells within the four sections, with terminal differentiation occurring across the others, committing the cells to differentiate through the four layers until reaching the skin surface forming the dead, but functional, cell layer (Fuchs 1995; Haake et al. 2001; Menon 2002; Blanpain et al. 2004; D'Orazio et al. 2013; Eckhart et al. 2013; Pastar et al. 2014). As the cells differentiate, they migrate towards the skin surface and adapt to perform the functions specific to that layer. The cells also change morphology as they progress along the differentiation pathway, increasing in size and flattening (Eckert & Rorke 1989; Fuchs 1995; Haake et al. 2001; Lian & Yang 2004; Lippens et al. 2005; Eckhart et al. 2013).

Cells in the *stratum basale* are involved in the process for the protection of cells from UV damage. This involves melanocytes present both in the basal layer and the suprabasal layer (Yamashita et al. 2005; Katagiri et al. 2006; D'Orazio et al. 2013; Natarajan et al. 2014). These cells are pigment producing cells that synthesise melanin from tyrosine; the melanin is then used to 'cap' the basal cells (Tsatmali et al. 2002; Yamashita et al. 2005; Katagiri et al. 2006; Cichorek et al. 2013). This protects the cells at the earliest point in the differentiation process, preventing the mutation of cells

at the *stratum basale* and the subsequent differentiation of these mutated cells to the skin surface (Walters & Roberts 2002; Yel et al. 2014). Melanocytes form attachments with keratinocytes through the use of the transmembrane protein, epithelial cadherin (E-cadherin), forming an adherent junction between the two cells allowing the transfer of melanin to the keratinocytes (Haake et al. 2001; Tsatmali et al. 2002; Boissy 2003; Natarajan et al. 2014; Tarafder et al. 2014). Also present in the *stratum basale* are slow cycling stem cells, which also need to be protected from sun exposure (Menon 2002; Fuchs 2007; D'Orazio et al. 2013; Panich et al. 2016). As one daughter stem cell remains a stem cell and the other differentiates along the pathway, it is important to prevent the mutation of these cells (Watt 1998; Haake et al. 2001; Panich et al. 2016).

Other epidermal cells are Merkel cells, mechanoreceptors which are involved in sensation of touch (Ogawa 1996; Moll et al. 2005; Boulais & Misery 2007; Boulais & Misery 2008; Woo et al. 2015). Merkel cells are closely associated with the nerves. Epidermal Merkel cells produce nerve growth factor (NGF) and the dermal Merkel cells produce the receptor for this growth factor providing the connection to the nerves (Haake et al. 2001; Boulais & Misery 2007; Woo et al. 2015). Langerhan's cells are also present in the epidermis and are part of immune system in the skin through the role of antigen presenting cells (APCs; Boulais & Misery 2008; Merad et al. 2008; Igyarto & Kaplan 2013). Langerhan's cells are the skin specific form of dendritic cells and like other dendritic cells; these interact with T cells to perform the function of presenting foreign antigens (Haake et al. 2001; Romani et al. 2003; Merad et al. 2008; Igyarto & Kaplan 2013). The cells within layers and between layers are connected through desmosomes, while cells in the *stratum basale* are connected to the basement membrane by hemidesmosomes; as shown in Figure 1.1 (Garrod 1993; Burdett 1998; Nievers et al. 1999; Menon 2002; Walters & Roberts 2002; Calkins & Setzer 2007; Fuchs 2007; Suter et al. 2009).

1.2.1.1 Keratinocytes

Keratinocytes are a form of squamous epithelial cells and account for approximately 95% of the epidermis (Kalinin et al. 2002; Menon 2002; Denning 2004; Sprenger et al. 2013). These cells are, therefore, a vital cell to focus on in regards to epidermal

wounding and the subsequent re-epithelialisation (Varani 1998; Menon 2002; Patel et al. 2006; Koivisto et al. 2012; Pastar et al. 2014). Keratinocytes are present across the four layers of the epidermis, with slightly altered cell morphology in each layer; with the different morphologies corresponding to their functions at each epidermal depth (Eckert & Rorke 1989; Fuchs 1995; Menon 2002; McGrath & Uitto 2010).

During wound healing, an increased presence of keratinocytes is required to allow for successful re-epithelialisation. Keratinocytes are already present at the wound site, although terminal differentiation is halted in those required in the healing process (Braiman-Wiksman et al. 2007; Bader & Kao 2009; Koivisto et al. 2012; Pastar et al. 2014). This prevents the basal keratinocytes from differentiating through the epidermal layers before becoming part of the cornified layer and eventually 'shed' from the skin (Eckert & Rorke 1989; Kalinin et al. 2002; Candi et al. 2005; Eckhart et al. 2013). Keratinocytes can sense their environment, due to the presence of sensory proteins and a close connection to sensory neurons. This allows them to convey information about their surroundings and can cause the keratinocytes to change their shape or action. It may also play a part in the detection of injury to the epidermal layers (O'Toole 2001; Haase et al. 2003; Gilcrease 2007; Boulais & Misery 2008). Keratinocytes are also able to sense the surrounding ECM and use this ability when they are migrating across a wound edge. Migration occurs via the extension of the cell edge forming lamellipodia-like structures and form focal adhesions with the extracellular matrix (ECM) through the use of integrin receptors (O'Toole 2001; Fuchs 2007; Li et al. 2007; Suter et al. 2009; Pastar et al. 2014). Through this signalling mechanism, keratinocytes are able to sense the presence of fibronectin in the epithelial layers through the integrins, $\alpha5\beta1$ and $\alpha3\beta1$ (Grinnell 1992; Kim et al. 1992; O'Toole 2001; Grose et al. 2002; Gilcrease 2007; Li et al. 2007; Pastar et al. 2014).

Keratinocytes possess integrin attachments, which need to be disassembled to allow the leading edge of the cell to protrude and release the traction tension at the trailing edge of the cell. This is achieved by a cyclical process of protrusion, adhesion and retraction (Cooper 2000; Van Haastert & Devreotes 2004; Gilcrease 2007; Vicente-Manzanares & Horwitz 2011; Petrie & Yamada 2012). Focal adhesions between the cell and the ECM provide a degree of stability to the cell. However, a balance is

required, as the strength of adhesion and speed of migration operate in opposite ways, with strong focal adhesions slowing the migratory speed of cells (Palecek et al. 1997; Maheshwari et al. 2000; Chan et al. 2011; Velnar et al. 2009; Vicente-Manzanares & Horwitz 2011; Kim & Wirtz 2013). In order to stabilise the attachment of the epidermis to the dermis, there are anchoring filaments that can connect the basement membrane to the dermis. This is performed by type VII collagen, part of the anchoring fibrils group of collagens (Borradori & Sonnenberg 1996; Aumailley & Rousselle 1999; O'Toole 2001; Li et al. 2007; Suter et al. 2009; Gordon & Hahn 2011; Mouw et al. 2014). However, this appears to be slow to develop at wound sites, affecting the integrity of the epidermal to dermal connection and resulting in a less stable structure, compared to unwounded areas (Gras et al. 2001; O'Toole 2001; Nyström et al. 2013).

The majority of integrin receptors recognise a specific amino acid sequence, RGD (arginine, glycine and aspartic acid; Kim et al. 1992; Ruoslahti 1996; O'Toole 2001; Li et al. 2007). This sequence is present in the cell attachment region of the integrin and binds to ECM proteins, such as fibronectin and vitronectin (Ruoslahti 1996; O'Toole 2001; Humphries et al. 2006; Li et al. 2007). The integrins that recognise and attach to RGD sequences are the αv integrins, α5β1, α8β1 and αIIbβ. Other integrin binding sequences are used for the attachment to other ECM proteins, such as to collagen and laminin (O'Toole 2001; Humphries et al. 2006; Li et al. 2007; Reynolds et al. 2008; Parsons et al. 2010). Some of these integrins are vital for the migration of keratinocytes to occur, such as α2β1 integrin that binds to a specific binding sequence on type 1 collagen and enables the cell to traverse across the collagen matrix (Kim et al. 1992; O'Toole 2001; Grose et al. 2002; Fuchs 2007). This assistance in cell motility is by the integrins present on the keratinocytes binding to the specific ligand present on the ECM proteins and forming cell adhesions. This connects the actin cytoskeleton of the cell to the ECM and can be used to pull the cell along the surface of the matrix (Revenu et al. 2004; Fuchs 2007; Gilcrease 2007; Parsons et al. 2010). After injury, there is an up-regulation of integrins present in the epidermis, including those that act as a receptor for fibronectin, vitronectin and laminin; some of which have a low presence in the unwounded epidermis but play a part in the migration of cells to the injury site (Gilcrease 2007; Koivisto et al. 2012; Longmate & DiPersio 2014).

Keratinocytes produce matrix metalloproteinases (MMPs) at the wound site, in particular MMP-1, -2 and -9 (Martin 1997; Pilcher et al. 1997; Varani 1998; Li et al. 2007; Philips et al. 2011). These allow the breakdown of the fibrin clot and sever the anchoring structures connecting the basal keratinocytes to the basement membrane; and allows their migration to the surface for re-epithelialisation (Martin 1997; O'Toole 2001; Philips et al. 2011; Graves et al. 2014). This expression is normally present, but there is a noticeable increase in the expression of these MMPs during cell migration. This allows for the movement of keratinocytes from both the wound edge and those anchored at the basement membrane (Martin 1997; O'Toole 2001; Joo & Seomun 2008; Stevens & Page-McCaw 2012; Pastar et al. 2014; Caley et al. 2015). The migrating keratinocytes are responsible for the production of the MMPs involved in degrading collagen type I and III, which aids their migration through the breakdown of the ECM (O'Toole 2001; Bigg et al. 2007; Hattori et al. 2009; Caley et al. 2015; Rohani & Parks 2015; Van Doren 2015).

Keratinocytes are recruited and activated through the actions of specific growth factors. This is apparent during the different phases of acute skin wound healing, where certain factors are responsible for the stimulation of keratinocyte migration to wound site and other factors stimulating their subsequent proliferation at the site (Broughton et al. 2006a; Koivisto et al. 2012; Peplow & Chatterjee 2013; Longmate & DiPersio 2014; Seeger & Paller 2015). During the initial haemostasis stage of wound healing, it is the release of interleukin (IL)-1 and tumour necrosis factor-α (TNF-α) from macrophages present at the wound site, that attracts keratinocytes to the area and their presence is required for successful and rapid re-epithelialisation (Chen et al. 1995; Banno et al. 2004; Broughton et al. 2006b; Brancato & Albina 2011; Koh & DiPietro 2011). As the wound healing process develops, other components are responsible for producing the growth factors and cytokines necessary for stimulating the migration and proliferation of keratinocytes to the injured site (Bennett & Schultz 1993; Gillitzer & Goebeler 2001; Barrientos et al. 2008; Peplow & Chatterjee 2013; Seeger & Paller 2015).

The epidermal growth factor (EGF) family have been shown to play a role in this activation, along with keratinocyte growth factor (KGF), which has been shown to also

possess a potent proliferative stimulation of keratinocytes (Guo et al. 1993; Martin 1997; Maas-Szabowski et al. 2000; auf demKeller et al. 2004; Barrientos et al. 2008; Reinke & Sorg 2012). Within the EGF family of growth factors, there are a number that are associated with this regulatory function acting on keratinocytes, stimulating their proliferation and migration. These include EGF, heparin binding epidermal growth factor (HB-EGF) and transforming growth factor-α (TGF-α), all of which use the EGF receptor for the keratinocyte activation and proliferation at the wound edge (Gailit & Clark 1994; Martin 1997; Haase et al. 2003; Hernández-Quintero et al. 2006; Barrientos et al. 2008; Gurtner et al. 2008; Peplow & Chatterjee 2013). The EGF receptor is located throughout the epidermal layers, but is more concentrated at the basal layer and is partly responsible for successful re-epithelialisation, as its presence allows the growth factors to stimulate keratinocyte proliferation and migration to the wound site (Nanney et al. 1984; Martin 1997; Barrientos et al. 2008; Pastore et al. 2008).

Some of these growth factors have a dual function, such as IL-1 and TNF-α, which have been shown to have a chemotactic and stimulative effect on keratinocytes, directly and indirectly, respectively (Tang & Gilchrest 1996; Maas-Szabowski et al. 1999; Werner & Grose 2003; Banno et al. 2004; Barrientos et al. 2008). These factors also increase the expression of KGF, through a paracrine mechanism depicted in Figure 1.2. KGF is released by fibroblasts and induces a proliferative action on keratinocytes (Guo et al. 1993; Tang & Gilchrest 1996; Maas-Szabowski et al. 1999; auf demKeller et al. 2004; Witte & Kao 2005; Broughton et al. 2006a; Barrientos et al. 2008; Menon et al. 2012). Another dual function example is with EGF, which has been shown to have a stimulatory effect on keratinocyte migration (Uchi et al. 2000; Peplow & Chatterjee 2013; Seeger & Paller 2015). It has a mitogenic effect on keratinocytes through the activation of GTPase Rac proteins, involved in the cell crawling process through the facilitation of focal adhesion formation and the movement of the lamellipodia across the substrate (Martin 1997; Li et al. 2007; Barrientos et al. 2008; Seeger & Paller 2015).

Keratinocytes themselves also express a number of growth factors, both for their own benefit acting in an autocrine manner, but also in a paracrine way, producing growth

Figure 1.2: The autocrine and paracrine relationship between fibroblasts and keratinocytes, depicting the growth factors and cytokines released from each cell type. The factors in bold are involved in stimulating KGF release by fibroblasts, through direct stimulation of KGF release (IL-1α and IL-1β), along with regulating KGF expression (IL-6, PTHrP and PDGF-BB) acting through paracrine mechanisms; and stimulation of keratinocyte proliferation (TGF-α) through autocrine mechanisms (Bader & Kao 2009).

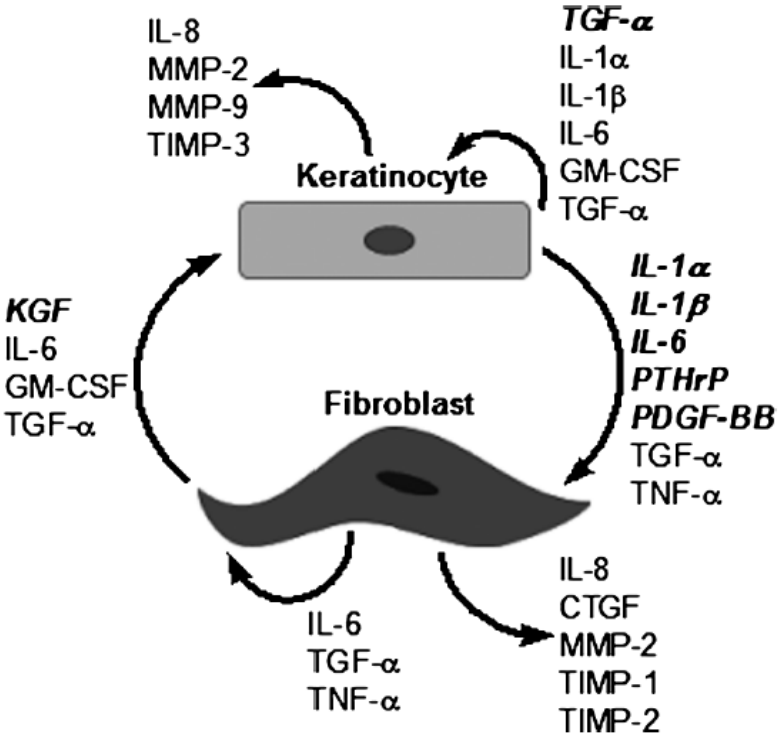

factors that will activate other cells (Maas-Szabowski et al. 1999; Witte & Kao 2005; Barrientos et al. 2008; Bader & Kao 2009). The main example of this autocrine and paracrine relationship occurring is with the mutualistic relationship between fibroblasts and keratinocytes during wound healing (Martin 1997; Maas-Szabowski et al. 1999; Witte & Kao 2005; Werner et al. 2007; Barrientos et al. 2008; Bader & Kao 2009; Menon et al. 2012). IL-6 is one of the growth factors that both fibroblasts and keratinocytes express in an autocrine and paracrine manner, as shown in Figure 1.2 (Uchi et al. 2000; Werner et al. 2007; Bader & Kao 2009). Fibroblasts secrete KGF-1 and KGF-2, which along with IL-6 have a proliferative and migratory effect on keratinocytes, directing them towards the wound site (Broughton et al. 2006a; Hernández-Quintero et al. 2006; Barrientos et al. 2008; Turabelidze & DiPietro 2012).

Keratinocytes also have a role in angiogenesis at the wound site through the production of vascular endothelial growth factor (VEGF) and basic fibroblast growth factor (bFGF; Broughton et al. 2006a; Werner et al. 2007; Barrientos et al. 2008; Velnar et al. 2009; Johnson & Wilgus 2014). VEGF is produced by other cells present in both the dermis and epidermis, although it appears that keratinocytes are the main contributor to the release of this growth factor (Werner & Grose 2003; Broughton et al. 2006a; Werner et al. 2007; Barrientos et al. 2008; Seeger & Paller 2015). This stimulates the growth of new capillaries and the production of endothelial cells (Tonnesen et al. 2000; Broughton et al. 2006a; Barrientos et al. 2008; Johnson & Wilgus 2014). Expression of VEGF by keratinocytes is stimulated by a number of other growth factors and at different stages in the wound healing process (Werner & Grose 2003; Barrientos et al. 2008; Velnar et al. 2009; Johnson & Wilgus 2014). Initially VEGF expression is stimulated by the release of IL-1 and TNF-α from macrophages, followed by the release of KGF-2 and transforming growth factor-β_1 (TGF-β_1), the latter of which is involved in the differentiation of fibroblasts to contractile myofibroblasts (Frank et al. 1995; Koyama et al. 2002; Broughton et al. 2006a; Barrientos et al. 2008; Bao et al. 2009; Pakyari et al. 2013). Keratinocytes also express nitric oxide (ṄO), and the combined presence of ṄO and VEGF increases the expression of VEGF at the wound site (Broughton et al. 2006a; Bao et al. 2009). ṄO has been demonstrated to stimulate keratinocyte migration, acting through a

cGMP/PKG-Rho-GTPase pathway. This is believed to impact on the cytoskeleton, inducing this migratory response (Zhan et al. 2015).

KGF, also referred to as fibroblast growth factor-7 (FGF-7), has a highly proliferative effect on keratinocytes and is released by fibroblasts (Ruehl et al. 2002; auf demKeller et al. 2004; Barrientos et al. 2008; Bader & Kao 2009). The expression of KGF by fibroblasts is stimulated by the release of factors from keratinocytes, such as IL-1α and IL-1β, again showing the close association between the two cells types and the autocrine and paracrine relationship, depicted in Figure 1.2 (Tang & Gilchrest 1996; Maas-Szabowski et al. 1999; Werner et al. 2007; Bader & Kao 2009; Menon et al. 2012; Seeger & Paller 2015). KGF has another angiogenic affect, besides increasing VEGF expression; it induces a mitogenic effect on vascular endothelial cells required for the production of new capillaries (Frank et al. 1995; Barrientos et al. 2008; Bao et al. 2009). In an effort to maintain high levels of keratinocytes at the wound site, KGF expression decreases the apoptosis of keratinocytes by decreasing the action of reactive oxygen species (ROS), responsible for causing cellular damage and the subsequent cell apoptosis. KGF increases the detoxification of ROS through the transcription of enzymes involved in the detoxifying ROS (Werner 1998; Beer et al. 2000; Kovacs et al. 2009).

The proliferation of keratinocytes is also increased by the presence of fibrin, an integral component of the fibrin clot necessary to provide a temporary protective barrier before re-epithelialisation occurs. This proliferation of keratinocytes drives the re-epithelialisation process (Yamamoto et al. 2005; Broughton et al. 2006a; Menon et al. 2012). This stimulation of keratinocytes occurs through fibrin increasing the release of TGF-α from keratinocytes (Yamamoto et al. 2005). TGF-α has been shown to increase the proliferation activity of both keratinocytes and fibroblasts, acting in an autocrine and paracrine manner, respectively. It also indirectly increases the proliferation and migration of keratinocytes by increasing the binding capacity of the EGF receptor (Miller et al. 2005; Yamamoto et al. 2005; Bader & Kao 2009; Seeger & Paller 2015).

There have been conflicting opinions on the effect of TGF-β_1 on keratinocyte proliferative ability, some indicate inhibition and others that increased expression stimulates proliferation. Furthermore, it is has been shown that increased TGF-β_1 expression stimulated keratinocyte migration, through upregulation of the integrins involved in keratinocyte migration (Koivisto et al. 2012; Peplow & Chatterjee 2013; Hameedaldeen et al. 2014; Longmate & DiPersio 2014). Less information is known regarding the effects of TGF-β_2 and TGF-β_3 on keratinocyte migration, although TGF-β_3 has been described as contributing to keratinocyte migration, through TGF-β receptor II (Bandyopadhyay et al. 2006; Barrientos et al. 2008; Le et al. 2012; Rad et al. 2015).

1.2.1.2 Keratins

Keratinocytes contain keratin intermediate filaments forming bundles within the cells (Fuchs 1995; Magin et al. 2007; Moll et al. 2008; Bragulla & Homberger 2009; Ramms et al. 2013). There are specific pairs associated with each of the four levels of the epidermis, with an overlap across the layers as differentiation of each cell type occurs (Fuchs 1995; Haake et al. 2001; Menon 2002; Gu & Coulombe 2007; Moll et al. 2008; Bragulla & Homberger 2009). In the *stratum basale*, the keratin (Krt) pair is 5 and 14. The *stratum spinosum* contain the pair 1 and 10. This pair converts from 1 to 2 and from 10 to 11 in the *stratum granulosum* layer, with Krt pair 1 and 10 being present again in the *stratum corneum*, along with disulphide bonds to increase the structural support (Fuchs 1995; Freedberg 2001; Haake et al. 2001; Menon 2002; Vaidya & Kanojia 2007; Moll et al. 2008; Bragulla & Homberger 2009). The presence of these pairs alters during wound healing with a decreased expression of Krt1 and Krt10 and an increased presence of Krt6 and Krt16, due to their roles in differentiation and proliferation, respectively (Fuchs 1995; Haake et al. 2001; Magin et al. 2007; Vaidya & Kanojia 2007; Bragulla & Homberger 2009).

Each keratin present has a specific function in maintaining a functional epidermal layer to provide the strong protective barrier of the skin (Menon 2002; Gu & Coulombe 2007; Magin et al. 2007; Bragulla & Homberger 2009). Due to the functionality of these proteins being reliant on interactions with other keratin filaments, in most cases both keratin types are required to be present for normal function to occur (Magin et al.

2007; Moll et al. 2008; Arin 2009; Bragulla & Homberger 2009; Ramms et al. 2013). However in other cases, another keratin type can be used as a replacement if the original form is absent or mutated. An example of this is evident in epidermis bullosa simplex, which affects the spinous layer of the epidermis (Bragulla & Homberger 2009). This is a result of a mutation occurring in the gene for Krt5 or Krt14. In the case of Krt14, the substitute Krt15 may be used; however, it still produces some symptoms, but in a less severe form (Fuchs 1995; Lloyd et al. 1995; Moll et al. 2008; Arin 2009; McLean & Moore 2011; Ramms et al. 2013). In contrast, if the gene for Krt5 is affected, there is no substitute suitable so a more severe form of epidermis bullosa simplex is evident (Steinert 2001; Bragulla & Homberger 2009). There are other types of keratin present in the other components of the skin, with specific functions, such as the hair follicles. A number of keratins are present in the hair follicle which are specific to this site and used to be named reflecting this; Krt6hf (hair follicle expression), Krt6irs1-4 (inner root sheath) and Krt25irs1-4, now termed Krt75, Krt71-74 and Krt25-28, respectively (Fuchs 1995; Vaidya & Kanojia 2007; Moll et al. 2008; Bragulla & Homberger 2009; McLean & Moore 2011). The outer root sheath and companion layer also contain Krt5 and Krt14; and Krt6 and Krt16, respectively (Waseem et al. 1999; Fuchs 2007; Vaidya & Kanojia 2007; Bragulla & Homberger 2009). The hair follicle bulge has also been shown to contain a reservoir of epithelial stem cells, with Krt15 considered a biomarker for these stem cells (Whitbread & Powell 1998; Liu et al. 2003; Ohyama 2007; Bose et al. 2013).

Krt6 and Krt16, along with Krt17, have been shown to be upregulated in response to injury and are thought to play a part in the re-epithelialisation process, although the mechanism behind their actions is not yet fully understood (Fuchs 1995; Santos et al. 2002; Mazzalupo et al. 2003; Sivamani et al. 2007; Bragulla & Homberger 2009). The upregulation of Krt6 and Krt16 during wound healing has been shown to be induced by both EGF and TGF-α (Jiang et al. 1993; Fuchs 1995; Freedberg et al. 2001; Komine et al. 2000; Barrientos et al. 2008; Bragulla & Homberger 2009). These two keratin types, along with Krt17, are considered to be a keratinocyte marker for when the cells are in an activated state, such as in the wound healing response or the hyperproliferation observed in cancer. During this state, the keratinocytes proliferate, migrate and change their cell structure as a result of cell crawling (Paladini &

Coulombe 1998; Freedberg et al. 2001; Bragulla & Homberger 2009). IL-1 is strongly involved in this activation process and has been shown to increase the expression of Krt6 (Freedberg et al. 2001). Receptors to IL-1 are present on the keratinocyte surface, allowing the activation of keratinocytes to be initiated (Freedberg et al. 2001; Komine et al. 2001). TNF-α and TGF-α, both associated with keratinocyte functions, have been shown to behave in a regulatory manner towards Krt6, resulting in a specific response to the stimulus depending on whether an inflammatory or proliferative response is required, respectively (Jiang et al. 1993; Fuchs 1995; Freedberg et al. 2001; Komine et al. 2001). However, this increased proliferative response of the keratinocytes can be detrimental, as increased expression of Krt17 has been shown to correlate to an increased severity of the skin disorder, psoriasis (Bonnekoh et al. 1995; Leigh et al. 1995; Gudmundsdottir et al. 1999; Zhang et al. 2012; Jin & Wang 2014).

1.2.2 Dermis

There are a number of different components in the dermis, including the connective tissue layer of the skin involved in producing elastic force and tensile strength to the tissue (Haake et al. 2001; Kielty et al. 2002; McGrath et al. 2004; Sherratt 2009). The dermis performs many functions, some of which are required to maintain the strength and flexibility of the skin. The main functions are: protection from injury, thermoregulation and sensory receptors to detect pressure (Haake et al. 2001; Menon 2002; McGrath et al. 2004; Darlenski et al. 2011; Hubmacher & Apte 2013).

There are numerous proteins present in the ECM, which are involved in maintaining dermal functions; including collagens, proteoglycans and glycoproteins. The ECM is synthesised by fibroblasts, which are a major cell type present in the dermis (Agren & Werthén 2007; Schultz & Wysocki 2009; Frantz et al. 2010; Guo & DiPietro 2010; Reinke & Sorg 2012; Hubmacher & Apte 2013). Fibroblasts are especially important in injury and healing due to their ability to produce ECM components in order to repair the defect site and reinstating the damaged protective barrier functions (Agren & Werthén 2007; Schultz & Wysocki 2009; Frantz et al. 2010; Reinke & Sorg 2012; Bainbridge 2013; Tracy et al. 2016). There are other components present which are also essential for the synthesis of the ECM, such as cytokines and growth factors (Barrientos et al. 2008; Schultz & Wysocki 2009; Kim et al. 2011; Behm et al. 2012).

There are 28 types of collagen that are known, several of which are involved in various roles in skin. The majority present are two of the fibrillar collagens, type I (approximately 80%) and type III collagen (10%; O'Toole 2001; Gelse et al. 2003; Ricard-Blum & Ruggiero 2005; Heino 2007; Schultz & Wysocki 2009; Gordon & Hahn 2011; Xue & Jackson 2015; Tracy et al. 2016). In type I collagen, three collagen α-chains are joined together in a proline rich triple helical structure, consisting of a (glycine-X-Y) formation. This comprises a procollagen molecule, before it is transported out of the cell and undergoes a number of post-translational modifications; the most common modification is with prolyl hydroxylase, which induces the hydroxylation of prolines and forming 4-hydroxyproline, required for collagen triple helix formation (O'Toole 2001; Gelse et al. 2003; Myllyharju 2003; Ricard-Blum & Ruggiero 2005; Gorres & Raines 2010; Gordon & Hahn 2011; Krieg & Aumailley 2011; Mouw et al. 2014). Procollagen peptidases are involved in removing the C- and N-terminals of procollagen, producing tropocollagen. Numerous tropocollagen proteins form collagen fibrils (Stadelmann et al. 1998; Ricard-Blum & Ruggiero 2005; Mouw et al. 2014). These fibrils then undergo covalent cross-links with other collagen fibrils, forming collagen fibres which increase the tensile strength and stability of the structure through the use of the enzyme, lysyl oxidase (Gelse et al. 2003; Diegelmann & Evans 2004; Krieg & Aumailley 2011; Hubmacher & Apte 2013; Mouw et al. 2014; Xue & Jackson 2015; Tracy et al. 2016). Collagens are able to interact with cells through the presence of collagen specific receptors on cell surfaces. The largest family of receptors involved are the integrins. In the dermis, fibroblasts connect to collagens through multiple integrins, specifically α1β1, α2β1 and α3β1 (O'Toole 2001; Moulin & Plamondon 2002; Ricard-Blum & Ruggiero 2005; Agren & Werthén 2007; Heino 2007; Schultz & Wysocki 2009; Xue & Jackson 2015; Tracy et al. 2016).

1.2.2.1 Fibroblasts

Fibroblasts possess a spindle-shape morphology and are one of the major cell types involved in acute skin wound healing (Moulin & Plamondon 2002; Wozniak et al. 2004; Birch et al. 2005; Agren & Werthén 2007; Schultz & Wysocki 2009; Li & Wang 2011; Bainbridge 2013; Tracy et al. 2016). Fibroblasts have a number of functions in the dermis, including the production of ECM components, contraction of the wound

through differentiation to myofibroblasts, supporting re-epithelialisation through the autocrine and paracrine interaction with keratinocytes at the wound site; and the production of granulation tissue and new capillaries (Maas-Szabowski et al. 1999; Agren & Werthén 2007; Werner et al. 2007; Barrientos et al. 2008; Schultz & Wysocki 2009; Guo & DiPietro 2010; Bainbridge 2013; Tracy et al. 2016). Fibroblasts also provide the contractile force required to pull the wound edges together, as a result of the differentiation of dermal fibroblasts to contractile myofibroblasts (Gabbiani 2003; Desmouliere et al. 2005; Broughton et al. 2006a; Li & Wang 2011; Micallef et al. 2012; Darby et al. 2014). There are two sub-populations of fibroblasts in the dermis, present in the upper papillary dermis and the lower reticular dermis. There are differences in fibroblast functions between these sub-population, with papillary fibroblasts releasing less KGF and greater granulocyte macrophage colony-stimulating factor (GM-CSF) than reticular fibroblasts. These differences impact on keratinocyte proliferation and differentiation responses (Schafer et al. 1985; Sorrell & Caplan 2004; Sorrell et al. 2004; Sorrell et al. 2008). Due to the variation between the fibroblasts present in these two sub-populations, there are differences between the ECM present in each layer, including the type of collagen fibres present (Sorrell & Caplan 2004; Sorrell et al. 2004). In the papillary dermis, the collagen fibres synthesised are thin structures. In contrast, the collagen fibres produced in the reticular dermis are more densely comprised (Sorrell & Caplan 2004; Sorrell et al. 2004; Watt & Fujiwara 2011). Some of the fibroblasts present at the wound site migrate to the area in response to chemotactic signals, such as TNF-α, platelet-derived growth factor (PDGF), EGF and insulin-like growth factor-1 (IGF-1; Seppa et al. 1982; Bennett & Schultz 1993; Barrientos et al. 2008; Bainbridge 2013; Olczyk et al. 2014). However, some fibroblasts at the wound site are derived from multipotent cells present in the undamaged dermis and have the ability to differentiate into dermal fibroblasts (Toma et al. 2001; Fernandes et al. 2004; Shaw & Martin 2009; Reilkoff et al. 2011). These cells are circulating fibrocytes, which are a distinct population from fibroblasts, but also possess a number of fibroblastic features. These include the synthesis of ECM components, release of cytokines and growth factors required for wound healing, inducing contraction required for wound closure; and stimulating angiogenesis (Metz 2003; Quan et al. 2004; Kao et al. 2011; Bianchetti et al. 2012; Blakaj & Bucala 2012; Suga et al. 2014). Due to this variety of functions, they are capable of contributing to

the wound healing process directly and through their ability to differentiate into dermal fibroblasts and contractile myofibroblasts (Metz 2003; Bellini & Mattoli 2007; Strieter et al. 2009; Blakaj & Bucala 2012; Van Linthout et al. 2014).

In addition to new ECM synthesis, fibroblasts are responsible for the organisation and remodelling of the newly-deposited ECM (Agren & Werthén 2007; Schultz & Wysocki 2009; Eckes et al. 2010; Olczyk et al. 2014; Tracy et al. 2016). Therefore, a dysfunction in dermal fibroblasts or conversion to senescent fibroblasts will have a resulting impact on ECM architecture, potentially leading to impaired healing (Cook et al. 2000; Sorrell & Caplan 2004; Wall et al. 2008; Schultz & Wysocki 2009; Wells et al. 2015). Fibroblasts regulate the turnover of the ECM by controlling the expression of the MMPs responsible for the breakdown of the ECM, along with the inhibitors of these proteases, tissue inhibitors of metalloproteinases (TIMPs; Nagase et al. 2006; Gill & Parks 2008; Schultz & Wysocki 2009; Li & Wang 2011; Watt & Fujiwara 2011; Behm et al. 2012; Caley et al. 2015; Rohani & Parks 2015). The presence of TGF-β_1 decreases the turnover of the ECM by decreasing the expression of MMPs and increasing the expression of TIMPs (Overall et al. 1989; Zeng et al. 1996; Barrientos et al. 2008; Schultz & Wysocki 2009; Watt & Fujiwara 2011). If ECM synthesis is higher than degradation, this can lead to an unorganised ECM structure and the formation of fibrotic tissue. This is as a result of the new ECM being continually deposited without a regulated degradation occurring (Li et al. 2007; Kisseleva & Brenner 2008; Schultz & Wysocki 2009; Watt & Fujiwara 2011). If a high presence of activated fibroblasts remain at the wound site, this results in ECM synthesis continuing without adequate degradation, leading to excessive ECM deposition and scar tissue formation (Li et al. 2007; Eckes et al. 2010; Watt & Fujiwara 2011; Jumper et al. 2015; Xue & Jackson 2015). Dysfunctional ECM turnover is also present in chronic wounds; although in this situation, there is increased degradation of the ECM, believed to be a result of increased expression of proteases at the wound site (Trengrove et al. 1999; Cook et al. 2000; Agren & Werthén 2007; McCarty & Percival 2013).

The migration of fibroblasts into the wound site is modulated by chemotactic signals. The source of the growth factors responsible for chemotaxis varies throughout the

wound healing process (Seppa et al. 1982; Pierce et al. 1989; Werner & Grose 2003; Li et al. 2004; Broughton et al. 2006a; Andrae et al. 2008; Schultz & Wysocki 2009; Schneider et al. 2010; Bainbridge 2013; Olczyk et al. 2014; Balaji et al. 2015). Initially, platelets and macrophages produce PDGF, which activates the fibroblasts and stimulates them to produce ECM components, including collagens, glycosaminoglycans and fibronectin; re-establishing the dermal matrix (Broughton et al. 2006a; Agren & Werthén 2007; Barrientos et al. 2008; Pakyari et al. 2013; Olczyk et al. 2014). Increased expression of PDGF stimulates fibroblast proliferation and subsequent ECM synthesis. This increase is also beneficial for the production of new capillaries in the granulation tissue (Sato et al. 1993; Battegay et al. 1994; Barrientos et al. 2008; Raica & Cimpean 2010; Watt & Fujiwara 2011; Reinke & Sorg 2012). PDGF has also been shown to upregulate MMPs during the remodelling stage of wound healing, allowing for the removal of damaged ECM. This is necessary for the successful remodelling of the ECM and allowing for an organised deposition of the new ECM to be assembled (Jinnin et al. 2005; Risinger et al. 2006; Barrientos et al. 2008; Gill & Parks 2008; Schultz & Wysocki 2009; Risinger et al. 2010; Reinke & Sorg 2012). FGF, also produced by fibroblasts has also been shown to increase ECM synthesis. Additionally, it increases the migration of more fibroblasts to the wound site, allowing for further production of ECM components (Wilkie et al. 1995; Barrientos et al. 2008; Xie et al. 2008; Schultz & Wysocki 2009).

A positive feedback system exists between fibroblasts and keratinocytes, with the dermal fibroblasts producing a number of growth factors and cytokines, which stimulate the proliferation of keratinocytes and induce release of factors shown to subsequently increase fibroblast proliferation (Maas-Szabowski et al. 1999; Maas-Szabowski et al. 2000; Werner & Smola 2001; Werner & Grose 2003; Bader & Kao 2009). Both cells exert autocrine and paracrine actions, through the release of such factors which stimulate their own proliferation and the release of soluble factors to increase the proliferation of the other cell type (Witte & Kao 2005; Werner et al. 2007; Bader & Kao 2009). This autocrine and paracrine interaction between the fibroblasts and keratinocytes is shown in Figure 1.2 (Bader & Kao 2009). TGF-β_1 also increases the expression of connective tissue growth factor (CTGF) from fibroblasts and acts in an autocrine manner by increasing the proliferation of fibroblasts; and it has been

shown to produce some of the components required for ECM synthesis (Igarashi et al. 1993; Frazier et al. 1996; Sorrell & Caplan 2004; Daniels et al. 2003; Barrientos et al. 2008). During wound healing, TGF-β_1 and TGF-β_2 from the TGF-β superfamily exhibit the highest presence; TGF–β_3 is also present, although at a lower level (Frank et al. 1996; Yang et al. 1999; Barrientos et al. 2008; Reinke & Sorg 2012). TGF-β_2 has been shown to have a potent attractant for fibroblasts to the wound site, whilst TGF-β_3 has been shown to have a positive effect on the migration of fibroblasts. TGF-β_3 has also been shown to possess potent anti-scarring properties (Shah et al. 1995; Frank et al. 1996; Barrientos et al. 2008; Kishi et al. 2012; Lichtman et al. 2016).

Before the conversion of fibroblasts to contractile myofibroblasts, there is a weak contractile force produced by the fibroblasts, forming stress fibres consisting of bundles of actin fibres; these 'active' fibroblasts have been referred to as proto-fibroblasts (Hinz et al. 2001; Tomasek et al. 2002; Hinz 2007; Shaw & Martin 2009). The main contractile force is generated once myofibroblasts are activated by the presence of TGF-β_1 (Desmoulière et al. 1993; Grinnell 1994; Serini & Gabbiani 1999; Gabbiani 2003; Desmouliere et al. 2005; Shaw & Martin 2009). Fibroblasts produce a tensile force as a result of the interaction between actin and myosin. These are involved in the cell crawling process as the cytoskeleton changes conformation and form adhesions to the ECM, as the cell migrates across the ECM (Kolega et al. 1991; Conrad et al. 1993; Lauffenburger & Horwitz 1996; Ananthakrishnan & Ehrlicher 2007; Li & Wang 2011; Reinke & Sorg 2012). In addition to involvement in wound contraction, TGF-β_1 has been shown to increase the expression of a number of integrins for collagen, fibronectin and vitronectin (Gailit et al. 1994; Thannickal et al. 2003; Schultz & Wysocki 2009; Watt & Fujiwara 2011; Hameedaldeen et al. 2014).

Other soluble factors in this process, such as IL-1α and IL-1β, are involved with stimulating the release of other factors, such as IL-6 and IL-8 from keratinocytes and fibroblasts, respectively (Uchi et al. 2000; Werner et al. 2007; Bader & Kao 2009). The benefit of the close association between fibroblasts and keratinocytes is seen in successful wound healing, as both cells are vital to this mechanism (Werner et al. 2007; Bader & Kao 2009; Guo & DiPietro 2010; Schreml et al. 2010; Menon et al. 2012; Bainbridge 2013; Pastar et al. 2014). This mutually beneficial interaction between

fibroblasts and keratinocytes is important for the regulation of the ECM, ensuring that re-epithelialisation occurs successfully and the synthesis and degradation of the ECM is tightly regulated (Sawicki et al. 2005; Witte & Kao 2005; Werner et al. 2007; Menon et al. 2012). It is thought that the connection between the fibroblasts and keratinocytes is mediated through the AP-1 family of transcription factors present in fibroblasts and therefore, fibroblasts are believed to oversee the regulation of ECM synthesis and re-epithelialisation (Angel et al. 2001; Florin et al. 2004; Sorrell & Caplan 2004; Schultz & Wysocki 2009).

1.2.2.2 Myofibroblasts

When tissue injury occurs, some fibroblasts present at the injury site are activated to differentiate into myofibroblasts. This is due to a combination of mechanical stress on the tissue, along with activation by TGF-β_1 (Desmouliere et al. 2005; Hinz 2007; Meran et al. 2008; Li & Wang 2011; Leung et al. 2012). In addition, the splice variant of the glycoprotein, fibronectin (ED-A), is also involved in activating this differentiation to a myofibroblast phenotype (Gabbiani 2003; Desmouliere et al. 2005; Hinz 2007; Li & Wang 2011). The activation of fibroblasts to myofibroblasts occurs in a two-step process, with the production of a proto-myofibroblast as an intermediate step, as shown in Figure 1.3 (Tomasek et al. 2002; Daniels et al. 2003; Gabbiani 2003; Desmouliere et al. 2005; Li & Wang 2011; Darby et al. 2014). The function of myofibroblasts is essential for the closure of the wound, as they impart a contraction on the wound edges to bring them together (Tomasek et al. 2002; Gabbiani 2003; Hinz 2007; Li & Wang 2011; Sarrazy et al. 2011).

This contractile force is generated from α-smooth muscle actin (α-SMA), which are expressed by the myofibroblasts and deemed as a characteristic marker of true myofibroblasts (Serini & Gabbiani 1999; Tomasek et al. 2002; Gabbiani 2003; Hinz 2007; Hinz et al. 2007; Eckes et al. 2010; Darby et al. 2014). There are different forms of smooth muscle actin present at the intermediate step where proto-myofibroblasts are present; α-actin is not present at this stage, but β- and γ-actin isoforms are present instead (Tomasek et al. 2002; Gabbiani 2003; Desmouliere et al. 2005). This

Figure 1.3: Process of differentiation from fibroblast to proto-myofibroblast to myofibroblasts; and the factors involved in the conversion, TGF-β_1 and ED-A splice variant fibronectin (Tomasek et al. 2002).

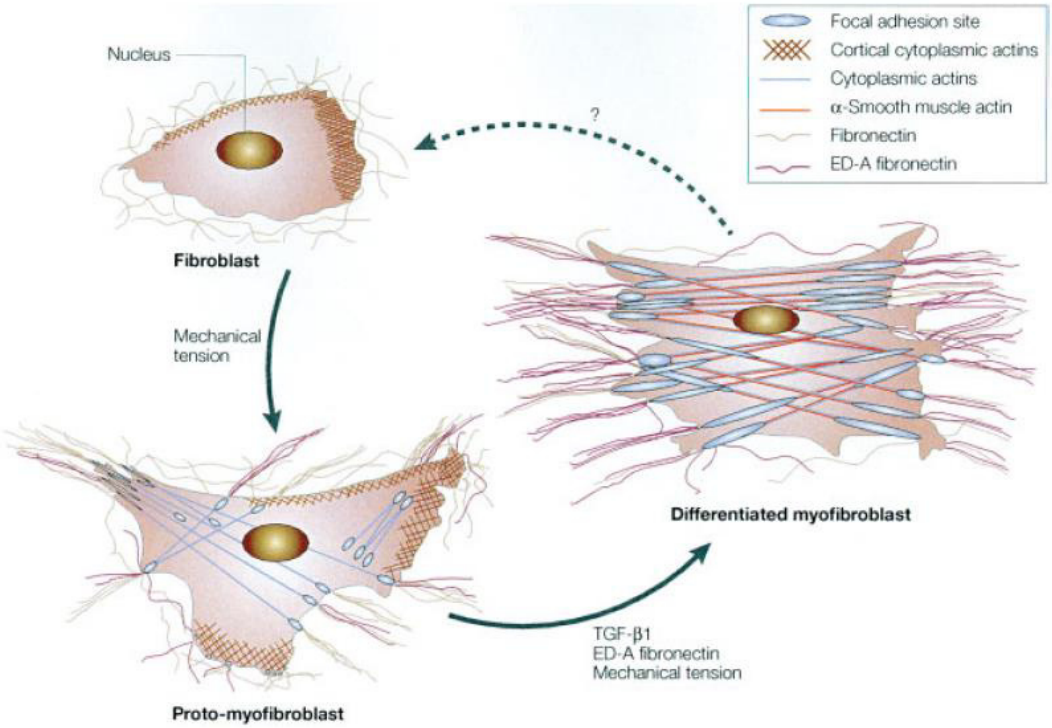

conversion of actin types present between the intermediate and fully activated myofibroblast confirms that α-SMA is a reliable marker for the active form of myofibroblasts (Gabbiani 2003; Desmouliere et al. 2005; Li & Wang 2011). Other filament types that are used as a positive marker for myofibroblasts are the intermediate filament, vimentin and in some tissues desmin. These cells can be distinguished from fibroblasts by the absence of desmin and α-SMA, although fibroblasts also test positive for the presence of vimentin (Eyden 2008; Gabbiani 1992; Li & Wang 2011; Darby et al. 2014). Myofibroblasts contain a network of microfilaments that are arranged in bundles, these microfilaments need a connection to the surrounding ECM, so that the contractile force generated can be exerted onto the matrix (Tomasek et al. 2002; Gabbiani 2003; Hinz 2007; Micallef et al. 2012; Darby et al. 2014). These connections are termed focal adhesion sites, which connect the intracellular actin with the ECM for both the proto-myofibroblast and the activated myofibroblast (Tomasek et al. 2002; Gabbiani 2003; Hinz 2007; Eckes et al. 2010; Li & Wang 2011; Darby et al. 2014).

The benefit of closing the wound space at the dermal level is the provision of a protective barrier for the underlying connective tissue (Li & Wang 2011; Eming et al. 2014). Contraction takes place during the proliferative stage of the wound healing process, when high numbers of fibroblasts are present at the wound site, with the potential to differentiate into myofibroblasts (Desmouliere et al. 2005; Hinz 2007; Li & Wang 2011; Darby et al. 2014). This contraction and subsequent closure of the wound needs to be tightly regulated, as too much or too little contraction can have implications on the healing mechanism (Tomasek et al. 2002; Gabbiani 2003; Eckes et al. 2010; Li & Wang 2011; Hinz et al. 2012; Van De Water et al. 2013; Darby et al. 2014; Darby et al. 2016). Too little contraction may prevent successful closure of the wound, whilst excess contraction can affect the appearance of the scar, but more importantly may cause a loss of function in that area (Gabbiani 2003; Moulin et al. 2004; Eckes et al. 2010; Li & Wang 2011; Micallef et al. 2012; Eming et al. 2014; Rabello et al. 2014). Furthermore, as the dermal layers close, this allows successful re-epithelialisation to occur due to the closer proximity of the two edges (Martin 1997; Häkkinen et al. 2011; K J Rolfe & Grobbelaar 2012; Rittié 2016). Another function of myofibroblasts is their ability to produce large quantities of ECM proteins at the injury

site, in particular type I-VI collagens, type XVIII collagen, glycoproteins, glycosaminoglycans and proteoglycans. All of these ECM components are vital for the effective synthesis of new dermal tissue (Tomasek et al. 2002; Hinz 2007; Li & Wang 2011; Darby et al. 2014). In addition, myofibroblasts produce components that are necessary for the remodelling of the ECM, such as MMPs and TIMPs (Powell et al. 1999; Li & Wang 2011).

TGF-β_1 induces its response on fibroblasts through binding to TGF-β receptors (TβRs) and activating downstream intracellular signalling molecules. These transcription regulators are part of the SMAD family, as depicted in Figure 1.4 (Kretzschmar & Massague 1998; Schiller et al. 2004; ten Dijke & Hill 2004; Verrecchia et al. 2006; Ross & Hill 2008; Xu et al. 2012). The ligand binds to TβRII, which subsequently binds to TβRI, forming a complex; this complex phosphorylates and activates SMAD regulators (Heldin et al. 1997; Kretzschmar & Massague 1998; Schiller et al. 2004; ten Dijke & Hill 2004; Verrecchia et al. 2006; Ross & Hill 2008; Xu et al. 2012). There are multiple type I and II receptors, these are referred to as Activin-receptor-like kinases (ALKs); ALK4, ALK5 and ALK7 are involved in SMAD2 and SMAD3 phosphorylation (Miyazono 2000; ten Dijke & Hill 2004; Moustakas & Heldin 2008). Receptor-associated SMADs (R-SMADs), SMAD2 and SMAD3, are phosphorylated by the TβRs; the recruitment of R-SMADs to the TβR complex is aided by a SMAD anchor for receptor activation (SARA). Once the R-SMAD has been phosphorylated, co-SMAD4 forms a complex with this phosphorylated R-SMAD. This complex is subsequently internalised into the nucleus and gene transcription initiated (Heldin et al. 1997; Inman et al. 2002; Javelaud & Mauviel 2004; Schiller et al. 2004; ten Dijke & Hill 2004; Verrecchia et al. 2006; Ross & Hill 2008; Xu et al. 2012). R-SMAD2, R-SMAD3 and co-SMAD4 are the SMADs present in vertebrates and involved in TGF-β signalling (Attisano & Wrana 1998; Kretzschmar & Massague 1998).

TGF-β exerts its response through this SMAD signalling pathway and induces the differentiation of fibroblasts to myofibroblasts. SMAD3 has been demonstrated to play a key role in producing a fibrotic response and SMAD2 overexpression induced increased α-SMA expression (Evans et al. 2003; Javelaud & Mauviel 2004; Schiller et al. 2004; Verrecchia et al. 2006; Darby et al. 2014). However, there are inhibitory

Figure 1.4: TGF-β/SMAD signalling pathway, showing binding of TGF-β to TβRs, initiating activation of downstream signalling through SMADs and initiating gene transcription (Schiller et al. 2004).

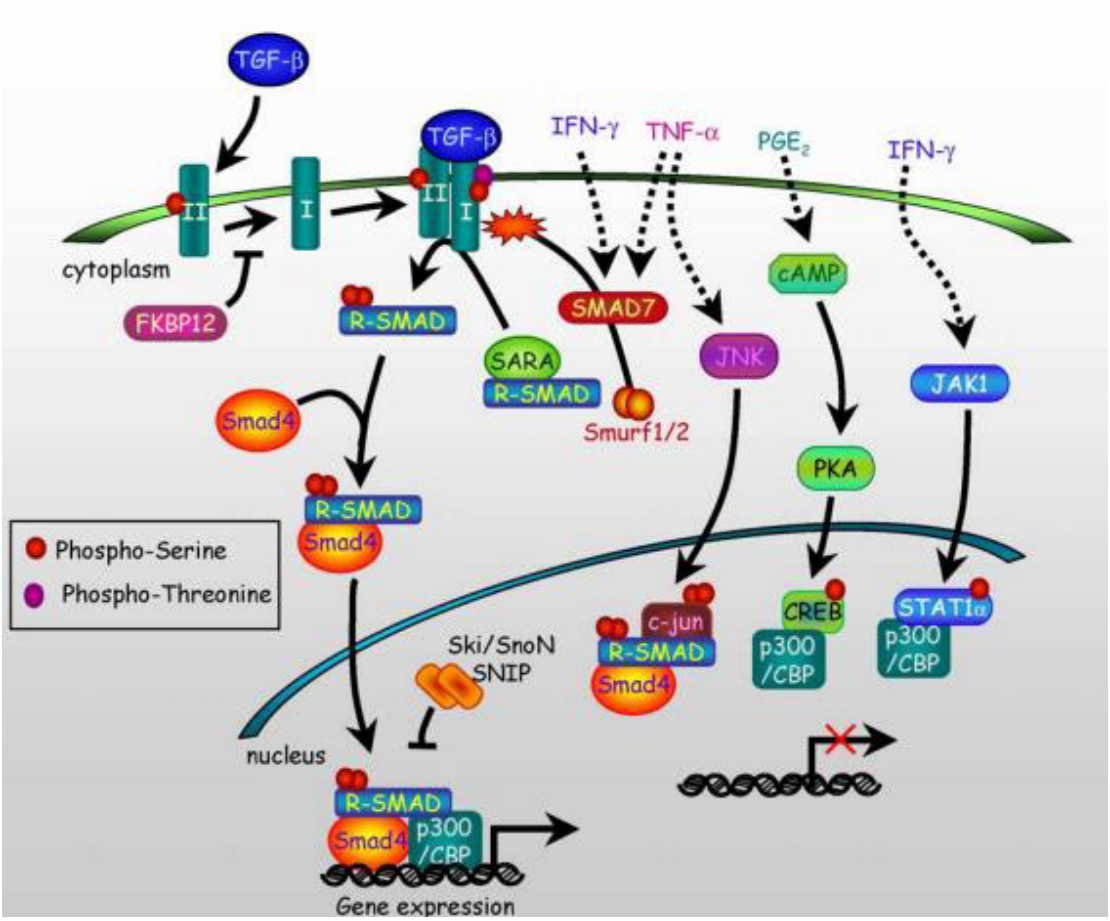

SMADS, SMAD6 and SMAD7, which are involved in opposing this fibrotic response. SMAD7 has been shown to inhibit TGF-β signalling, through inhibiting SMAD3 phosphorylation and preventing the formation of R-SMAD and co-SMAD complexes; and the subsequent downstream signalling (Kretzschmar & Massague 1998; Miyazono 2000; Javelaud & Mauviel 2004; Schiller et al. 2004; Moustakas & Heldin 2008).

Hyaluronan, a glycosaminoglycan found in the ECM, has been demonstrated to be involved in TGF-β_1-mediated, fibroblast to myofibroblast differentiation (Jenkins et al. 2004; Meran et al. 2007; Webber et al. 2009a). It has been shown to be a vital part of inducing differentiation, although inhibition of hyaluronan synthesis does not affect phosphorylation of SMAD3. However, SMAD3 is involved in TGF-β_1-mediated, fibroblast proliferation (Webber et al. 2009a). Formation of a hyaluronan pericellular coat is involved in fibroblast to myofibroblast differentiation; as production of the pericellular coat was absent with inhibited hyaluronan synthesis, which resulted in inhibition of differentiation to myofibroblasts (Webber et al. 2009a, 2009b). This involvement of hyaluronan in TGF-β_1-mediated, differentiation is evident in dermal fibroblasts, but not oral fibroblasts (Meran et al. 2007). Oral mucosal fibroblasts resist TGF-β_1-mediated differentiation, this is thought to be partly due to a decreased expression of hyaluronan compared to dermal fibroblasts. This is potentially due to the decreased expression of hyaluronan synthase 2 enzyme (HAS2) by oral mucosal fibroblasts (Meran et al. 2007, 2008). Additionally, high expression of HAS3 was evident in oral fibroblasts, compared to a much lower expression in dermal fibroblasts; whereas HAS1 was not expressed by oral fibroblasts, but was by dermal fibroblasts. However, alteration of HAS1 expression levels in oral mucosal or dermal fibroblasts did not impact on TGF-β_1-mediated, differentiation (Meran et al. 2007; Glim et al. 2014). TGF-β_1 is also involved in synthesis of tumour necrosis factor-stimulating gene-6 (TSG-6), which is a hyaluronan binding protein and involved in pericellular coat formation. CD44 and EGF receptor (EGFR) are cell surface receptors, which are involved in the downstream actions of hyaluronan. Hyaluronan associates with CD44, inducing its co-localisation to EGFR, initiating the downstream pathways and resulting in myofibroblast formation (Midgley et al. 2013; Midgley et al. 2015).

When myofibroblasts are no longer required within the wound once closure is achieved, it is believed that myofibroblasts undergo apoptosis preventing further contractile forces acting on the wound site (Desmoulière et al. 1995; Desmoulière et al. 1997; Martin 1997; Hinz 2007; Häkkinen et al. 2011; Li & Wang 2011; Darby et al. 2014). Another mechanism for the cessation of contraction at the wound site are thought to be 'stop signals' released as the mechanical tension at the wound site is eased, due to closure of the injured tissue. Decreased α-SMA is also evident when tension decreases (Martin 1997; Hinz et al. 2001; Tomasek et al. 2002; Gabbiani 2003; Hinz 2007). Although programmed cell death is the most accepted fate for redundant myofibroblasts, there is also a theory that they may revert their phenotype back into a fibroblast (Gabbiani 2003; Desmouliere et al. 2005; Li & Wang 2011). However, it is not yet known how this dedifferentiation would occur and which factors may support this conversion (Gabbiani 2003; Li & Wang 2011).

1.2.3 Extracellular Matrix

The ECM is a vital component of skin, amongst other tissues; and represents the non-cellular aspect of tissues. One of its main functions is providing strength and structure to the tissue, through a variety of ECM components (Frantz et al. 2010; Lu et al. 2011; Hubmacher & Apte 2013; Mouw et al. 2014; Naba et al. 2016). It is often referred to as being the 'gel-like' component surrounding the cells, being comprised of water, proteins and polysaccharides (Schultz & Wysocki 2009; Eckes et al. 2010; Frantz et al. 2010). The different components of the ECM have specific functions. For instance, collagens are the predominate protein component of the ECM and involved in the scaffold structure, providing integrity to the tissue (Gelse et al. 2003; Eckes et al. 2010; Frantz et al. 2010; Gordon & Hahn 2011; Mouw et al. 2014). There are a number of collagen types present in the skin, but type I and III collagen are the main forms secreted by fibroblasts in the newly formed granulation tissue (Bazin et al. 1976; Haukipuro et al. 1991; Gelse et al. 2003; Schultz & Wysocki 2009; Olczyk et al. 2014). Collagen type I is the predominate form, but there is a higher presence of type III collagen in foetal wounds compared to adult, dermal wounds (Gelse et al. 2003; Cuttle et al. 2005; Schultz & Wysocki 2009; Cheng et al. 2011; Leung et al. 2012; Olczyk et al. 2014). The intrinsic differences between the two fibrillar collagens may account for the difference in scar formation following wounding. Type III collagen is associated

with more elastic tissues. Therefore, the higher presence of this type may result in a less rigid wound site and produce a scarless healing response (Gelse et al. 2003; Cuttle et al. 2005; Leung et al. 2012; Muiznieks & Keeley 2013; Olczyk et al. 2014).

Other proteins present in the ECM include elastin, laminin and fibronectin (Schultz & Wysocki 2009; Eckes et al. 2010; Mouw et al. 2014; Olczyk et al. 2014). Elastin is comprised of cross-linked tropoelastin subunits and is also associated with providing elasticity to the tissue (Debelle & Tamburro 1999; Midwood & Schwarzbauer 2002; Tamburro et al. 2005; Frantz et al. 2010; Singh et al. 2010; Kim et al. 2011; Tracy et al. 2016). Additionally, along with collagen, elastin provides structural support to the tissues allowing tissues to withstand tensile stress (Frantz et al. 2010; Muiznieks & Keeley 2013; Mouw et al. 2014). Elastin is closely linked to collagen fibres to provide the degree of flexibility, with the collagen fibres reducing the degree that the fibres can extend. The combination of these two predominant ECM proteins results in a strong tissue that is able to withstand stresses (Frantz et al. 2010; Van Doren 2015). An important observation is the lack of elastin in the newly-deposited granulation tissue following injury. This could contribute to the more rigid matrix observed in scar tissue (Schultz & Wysocki 2009; Eckes et al. 2010). Another glycoprotein contributing to the tensile strength of the skin is laminin. It is referred to as an adhesive protein and is a major component of the basement membrane (Nishiyama et al. 2000; Bosman & Stamenkovic 2003; Eckes et al. 2010; Kim et al. 2011; Mouw et al. 2014). Laminins have a variety of functions, in addition to providing the structural integrity of the basement membrane. They are strongly involved in cell-matrix interaction, through the basement membrane (Korang et al. 1995; Bosman & Stamenkovic 2003; Schneider et al. 2007; Mouw et al. 2014). Other functions include an involvement in cell proliferation, migration and differentiation. Laminin-332, after cleavage by MMPs present, is thought to be involved in keratinocyte migration at the wound edge through the provision of pro-migratory tracks for the keratinocytes to migrate across (Schneider et al. 2007; Schultz & Wysocki 2009; Eckes et al. 2010; Schlage et al. 2015). Fibronectin, is another adhesive protein present in the ECM, in particular in the basement membrane zone (Ruoslahti 1984, 1988a; Schultz & Wysocki 2009; Eckes et al. 2010; Singh et al. 2010; Mouw et al. 2014; Tracy et al. 2016). This glycoprotein also possesses many functions, including structural support, cell adhesion and

regulating cell-matrix interactions (Corbett et al. 1997; Schultz & Wysocki 2009; Eckes et al. 2010; Singh et al. 2010; Tracy et al. 2016). It has a vital role in the acute wound healing response, through the formation of a provisional matrix with fibrin. This matrix allows the infiltration of fibroblasts and other cells required to synthesise a new ECM, along with providing a structure for keratinocytes to migrate across during re-epithelialisation (Clark et al. 1982; Greiling & Clark 1997; Agren & Werthén 2007; Schultz & Wysocki 2009; Eckes et al. 2010; Olczyk et al. 2014; Reinke & Sorg 2012).

In addition to the structural proteins and adhesive glycoproteins, the ECM is also comprised of various proteoglycans and glycosoaminoglycans. These surround the ECM proteins and help organise the arrangement of collagen fibrils to increase tissue strength (Ruoslahti 1988b; Agren & Werthén 2007; Schultz & Wysocki 2009; Eckes et al. 2010; Mouw et al. 2014; Tracy et al. 2016). Proteoglycans are negatively charged molecules comprised of a protein backbone, with polysaccharide (glycosoaminoglycan) chains attached. These are present in the ECM and in the basement membrane (Ruoslahti 1988b; Kjeuin & Lindahl 1991; Schultz & Wysocki 2009; Eckes et al. 2010; Ghatak et al. 2015; Smith & Melrose 2015; Tracy et al. 2016). They are hydrophilic molecules and capable of holding large volumes of water, approximately 1000-times their volume. This provides hydration to the tissue and contributes to the gel-like composition of the ECM (Ruoslahti 1988b; Schultz & Wysocki 2009; Culav et al. 1999; Eckes et al. 2010; Schaefer & Schaefer 2010; Smith & Melrose 2015; Tracy et al. 2016). There are two main categories of proteoglycans, heparan sulphate proteoglycans and chondroitin sulphate proteoglycans (Ruoslahti 1988b; Kjeuin & Lindahl 1991; Kim et al. 2011; Mouw et al. 2014; Ghatak et al. 2015; Smith & Melrose 2015). Heparan sulphate proteoglycans include perlecan and syndecan, present in the early stages of wound healing (Gallagher et al. 1986; Oksala et al. 1995; Bishop et al. 2007; Kim et al. 2011; Sarrazin et al. 2011; Olczyk et al. 2014). Perlecan has a role in regulating VEGF, PDGF and FGF2; and their subsequent wound healing functions, such as angiogenesis, cell proliferation, migration and adhesion (Iozzo 1998; Guimond & Turnbull 1999; Bosman & Stamenkovic 2003; Bishop et al. 2007; Eckes et al. 2010; Kim et al. 2011). Chondroitin sulphate proteoglycans include versican and the small leucine-rich proteoglycans, decorin and biglycan. These occur later in the wound healing process, approximately 2 weeks after

injury (Kjeuin & Lindahl 1991; Iozzo 1998; Iozzo & Proteoglycans 1999; Agren & Werthén 2007; Schaefer & Iozzo 2008; Kim et al. 2011; Olczyk et al. 2014). Versican has been shown to have a role in the stimulation of fibroblast and keratinocyte proliferation. However, for fibroblast proliferation, this appears to be true for versican V1 isoform, with V2 isoform showing an inhibitory response on proliferation (Zimmermann et al. 1994; Zhang et al. 1998; Bosman & Stamenkovic 2003; Sheng et al. 2005; Wight et al. 2014). Other functions of the chondroitin sulphate proteoglycans include the provision of strength to the tissue, through resisting compressive force (Iozzo 1998; Bosman & Stamenkovic 2003; Eckes et al. 2010). Decorin plays a role in collagen fibril formation, which contributes to skin integrity. This response has been demonstrated through knockout animal studies, displaying abnormal collagen fibril organisation and a large variety in the diameter of these fibrils, leading to a decreased level of tensile strength (Iozzo 1998; Reed & Iozzo 2002; Muiznieks & Keeley 2013; Smith & Melrose 2015).

The most prevalent glycosaminoglycan in the skin is hyaluronan, which is involved in fibroblast proliferation, migration, differentiation to myofibroblasts; and in collagen production (Agren & Werthén 2007; Meran et al. 2007; Huang et al. 2008; Meran et al. 2008; Tracy et al. 2016). However, there appears to be a difference in wound healing responses depending on the size of hyaluronan present, impacting on inflammation, proliferation, ECM synthesis and myofibroblast differentiation (Tolg et al. 2014a; Ghatak et al. 2015; Tracy et al. 2016). Native, larger molecule-weight hyaluronan (>500 kDa) decreased inflammation, increased synthesis of type III collagen, and increased expression of TGF-β_3 from dermal fibroblasts; all these actions contribute to preferential healing responses (David-Raoudi et al. 2008; Tolg et al. 2014b; Tracy et al. 2016). Whereas, smaller molecular-weight hyaluronan (<400 kDa) has a contrasting response, with increased inflammation, increased synthesis of type I collagen, enhanced proliferation of fibroblasts; and increased expression of TGF-β_1 from dermal fibroblasts and resultant differentiation to myofibroblasts (David-Raoudi et al. 2008; Tolg et al. 2012; Tolg et al. 2014b; Tracy et al. 2016). As previously mentioned, hyaluronan has been shown to influence the TGF-β_1 signalling pathway, mediating the differentiation to myofibroblasts (Jenkins et al. 2004; Meran et al. 2007; Webber et al. 2009a). Increased presence of these smaller molecular-weight

hyaluronan fragments leads to fibrosis. These fragments are produced through degradation of native hyaluronan by hyaluronidases and reactive oxygen species present in adult skin (David-Raoudi et al. 2008; Tolg et al. 2014b; Ghatak et al. 2015; Tracy et al. 2016). However, in contrast, a high level of intact, native hyaluronan is seen in foetal wounds. This decreased fibrotic response is characteristic of the scarless healing observed in early-gestational, foetal healing (David-Raoudi et al. 2008; Schultz & Wysocki 2009b; Tolg et al. 2014b; Tracy et al. 2016).

The ECM is essential for cells to exert a number of functions. This is also true for the re-epithelialisation process, through the provision of the scaffold matrix and basement membrane, allowing the migration of keratinocytes across the wound site (Clark et al. 1982; O'Toole 2001; Schultz & Wysocki 2009; Hubmacher & Apte 2013). The supportive ECM and basement membrane also provide a structure for the differentiation of keratinocytes, from the basal layer to the formation of corneocytes (Watt 1989; Menon 2002; Hubmacher & Apte 2013). In addition, the interaction between the cells and the ECM, along with direct ECM-growth factor interactions, are vital for the normal function of the skin. Such events mediate cell responses and the remodelling of the ECM itself (Agren & Werthén 2007; Schultz & Wysocki 2009; Eckes et al. 2010; Tracy et al. 2016). There is a continual turnover of the ECM, through synthesis and degradation, involving MMPs and TIMPs. This turnover process is especially important during wound healing and the ECM remodelling phase, this is discussed further in Section 1.3.4 (Parks 1999; Schultz & Wysocki 2009; Kim et al. 2011; Olczyk et al. 2014; Arpino et al. 2015; Caley et al. 2015; Xue & Jackson 2015). Variations in these interactions can result in detrimental effects; such examples of dysfunctional ECM turnover are demonstrated in fibrosis and chronic wounds. In chronic wounds the ECM does not remodel successfully, due to excessive degradation and insufficient ECM synthesis. In contrast, excessive ECM synthesis and reduced degradation contributes to fibrotic tissue formation (Trengrove et al. 1999; Agren & Werthén 2007; Wynn 2008; Schultz & Wysocki 2009; Eckes et al. 2010; Watt & Fujiwara 2011; McCarty & Percival 2013; Xue & Jackson 2015; Tracy et al. 2016).

1.3 Acute Skin Wound Healing

The skin is capable of self-repair through a set of overlapping phases of acute skin wound healing. These are performed in a particular order to ensure successful repair. The main stages involved are haemostasis, inflammation, migration and proliferation of cells to form the new epithelium and dermal ECM; and finally, the remodelling of the affected tissue, as depicted in Figure 1.5 (Beanes et al. 2003; Braiman-Wiksman et al. 2007; Li et al. 2007; Velnar et al. 2009; Guo & DiPietro 2010; Kondo & Ishida 2010; Reinke & Sorg 2012; Portou et al. 2015). Rapid contraction and closure of the wound occurs to re-instate the protective barrier (Gabbiani 2003; Desmouliere et al. 2005; Li et al. 2007; Velnar et al. 2009; Eckes et al. 2010; Bainbridge 2013). There is also a rapid synthesis of the newly formed ECM. However, the new ECM is deposited in a disorganised manner below the newly-formed epidermis (Shah et al. 1995; Traversa & Sussman 2001; Beanes et al. 2003; Velnar et al. 2009; Xue & Jackson 2015). The combination of these two processes results in the production of fibrotic scar tissue (Velnar et al. 2009; Li & Wang 2011; Watt & Fujiwara 2011; Reinke & Sorg 2012; Xue & Jackson 2015). In normal acute skin wound healing, this is a very tightly regulated mechanism, with all aspects of the process carefully balanced to produce the successful healing of the injury. This requires an optimal amount of ECM components deposited to allow healing without the formation of excess scar tissue. Conversely, ECM degradation needs to be regulated, as excess degradation is shown to occur in chronic wounds (Bullen et al. 1995; Stadelmann et al. 1998; Menke et al. 2007; Muller et al. 2008; Xie et al. 2008; Velnar et al. 2009; Cox & Erler 2011; Reinke & Sorg 2012).

As mentioned previously, it is the interaction between different cells and between cells and the ECM that results in successful wound healing (Werner et al. 2007; Barrientos et al. 2008; Eckes et al. 2010; Watt & Fujiwara 2011; Reinke & Sorg 2012). These interactions control a number of functions during the overlapping wound healing phases, including cell proliferation, migration, differentiation; and synthesis of new ECM components. There is an overlap of functions for these mediators, with many belonging to several categories or families, depending on the effects they exert

Figure 1.5: Overlapping phases of the wound healing process, depicting the four main stages, haemostasis, inflammation, proliferation and remodelling (Beanes et al. 2003).

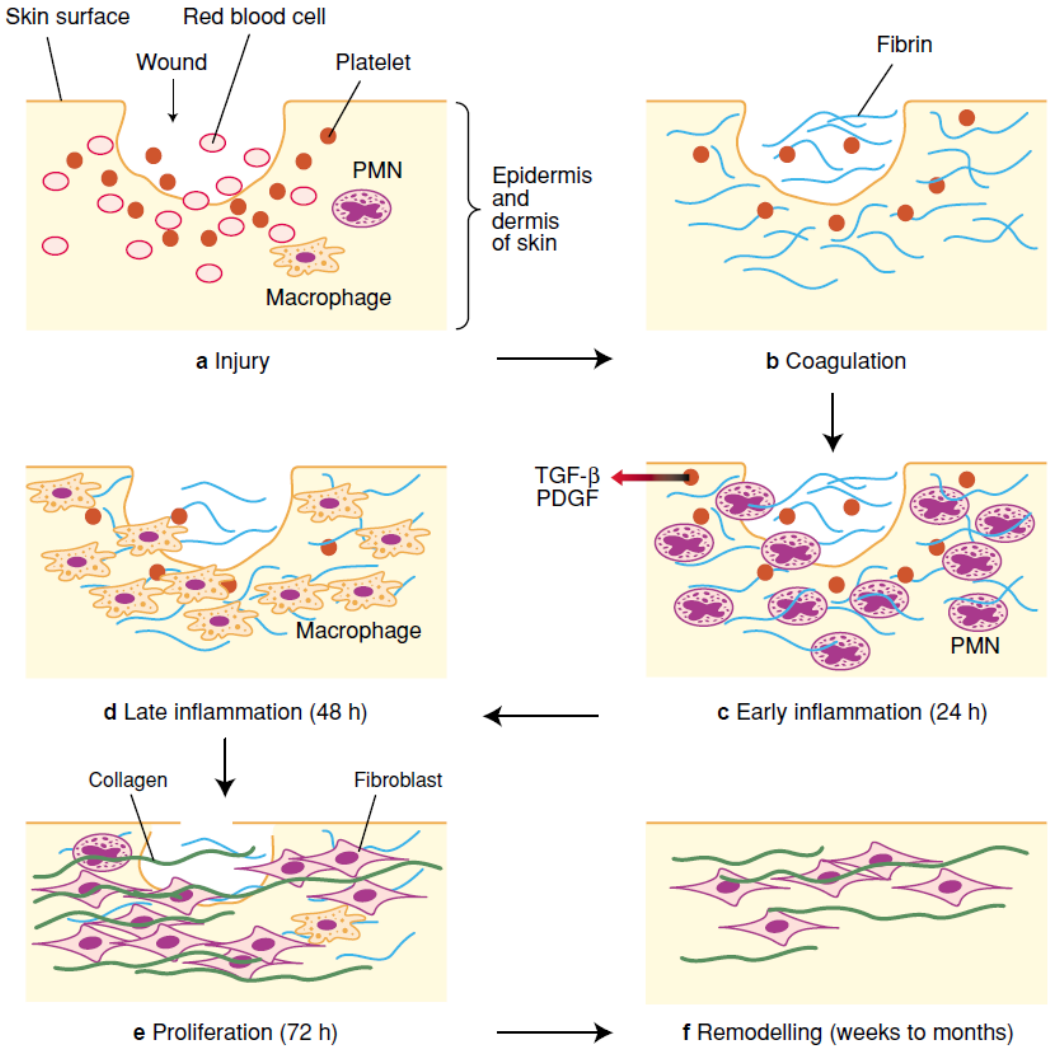

(Gillitzer & Goebeler 2001; Diegelmann & Evans 2004; Birch et al. 2005; Li et al. 2007; Barrientos et al. 2008; Guo & DiPietro 2010; Behm et al. 2012; Reinke & Sorg 2012). A number of pro-inflammatory cytokines are released following wounding, including TNF-α, IL-1 and IL-6. An overview of their functions is described in Table 1.1 (Hübner et al. 1996; Gillitzer & Goebeler 2001; Lin et al. 2003; Broughton et al. 2006a; Barrientos et al. 2008; Behm et al. 2012; Reinke & Sorg 2012). There are several growth factors involved in acute skin wound healing; some of the main factors are described in Table 1.2 (Hashimoto 2000; Broughton et al. 2006a; Barrientos et al. 2008; Schultz & Wysocki 2009; Toriseva & Kähäri 2009; Behm et al. 2012; Turabelidze & DiPietro 2012; Pastar et al. 2014).

1.3.1 Haemostasis

Haemostasis is a very rapid process, occurring instantaneously after injury with the aim to minimise blood loss from the injury site (Gurtner et al. 2008; Li et al. 2007; Velnar et al. 2009; Guo & DiPietro 2010; Reinke & Sorg 2012; Bielefeld et al. 2013). Vasoconstriction of nearby capillaries occurs as a reflex reaction to injury in an effort to halt or reduce bleeding (Rendell et al. 2002; Monaco & Lawrence 2003; Velnar et al. 2009; Beldon 2010; Reinke & Sorg 2012). However, it has been shown that a difference in blood flow through a wound is determined at a microvascular level and may be the cause behind abnormal scarring in some instances (Clark & Leung 1996; Rendell et al. 1997; Amadeu et al. 2003). The formation of a fibrin clot forms an alternative protective barrier from the environment to minimise infection of the wound (Martin 1997; Clark 2001; Monaco & Lawrence 2003; Li et al. 2007; Schäfer & Werner 2008; Velnar et al. 2009). The fibrin clot also provides a provisional matrix necessary in the later stages of acute skin wound healing (Corbett et al. 1997; Greiling & Clark 1997; Clark 2001; Broughton et al. 2006a; Li et al. 2007; Velnar et al. 2009; Reinke & Sorg 2012; Olczyk et al. 2014). Incoming cells that are required for the remodelling of the ECM, along with immune cells required for the clearance of debris from the wound site, bind to this temporary scaffold to enable them to carry out their vital function in this process (Traversa & Sussman 2001; Li et al. 2007; Gurtner et al. 2008; Velnar et al. 2009; Reinke & Sorg 2012; Portou et al. 2015; Xue & Jackson 2015).

Table 1.1: Predominant cytokines and chemokines involved in acute skin wound healing (Gillitzer & Goebeler 2001; Werner & Grose 2003; Broughton et al. 2006a; Broughton et al. 2006b; Behm et al. 2012; Turabelidze & DiPietro 2012; Balaji et al. 2015).

Mediator	Source	Function
TNF-α	Neutrophils Macrophages	Inflammation Re-epithelialisation
IFN-γ	T-helper lymphocytes Cytotoxic T cells Natural killer cells	Antigen presentation Antiviral activity Cytokine production
IL-1	Neutrophils Monocytes Macrophages Keratinocytes	Inflammation Re-epithelialisation
IL-6	Neutrophils Macrophages Keratinocytes	Inflammation Re-epithelialisation
IL-8	Macrophages Keratinocytes	Re-epithelialisation ECM turnover Inflammation
IL-10	T-helper lymphocytes Keratinocytes	Inhibition of angiogenesis Inhibition of fibroblast motility
CCL2 (MCP-1)	Keratinocytes	Inflammation Monocyte chemotaxis Mast cell chemotaxis
CCL5 (RANTES)	Keratinocytes	Inflammation Monocyte chemotaxis Lymphocyte chemotaxis
CXCL10 (IP-10)	Keratinocytes	Inflammation Lymphocyte chemotaxis Monocyte chemotaxis Delays re-epithelialisation

Table 1.2: Predominant growth factors involved in acute skin wound healing (Werner & Grose 2003; Broughton et al. 2006a; Broughton et al. 2006b; Barrientos et al. 2008; Toriseva & Kähäri 2009; Behm et al. 2012; Turabelidze & DiPietro 2012).

Mediator	Source	Function
PDGF	Platelets Macrophages Fibroblasts Keratinocytes Endothelial cells	Inflammation Granulation tissue formation ECM synthesis/degradation Re-epithelialisation
CTGF	Fibroblasts Platelets	Re-epithelialisation Granulation tissue formation ECM synthesis/degradation
IGF	Platelets Keratinocytes Fibroblasts	Re-epithelialisation ECM synthesis
FGF-7 (KGF)	Fibroblasts	Re-epithelialisation Neovascularisation
FGF-2 (bFGF)	Keratinocytes Fibroblasts Macrophages	Angiogenesis Granulation tissue formation ECM synthesis/degradation Re-epithelialisation
TGF-β_1	Platelets Keratinocytes Fibroblasts Macrophages	Contraction Inflammation Re-epithelialisation Angiogenesis ECM synthesis
VEGF	Platelets Macrophages Keratinocytes Endothelial cells Fibroblasts Neutrophils	Angiogenesis Vascular permeability Granulation tissue formation
EGF	Platelets Macrophages Fibroblasts	Re-epithelialisation ECM synthesis/degradation
TGF-α	Platelets Neutrophils Macrophages Keratinocytes	Re-epithelialisation

Immediately after injury occurs, the coagulation cascade is initiated; the extrinsic pathway is activated following disruption to the blood vessels (Hoffman et al. 1995; Monaco & Lawrence 2003; Mackman 2004; Li et al. 2007; Reinke & Sorg 2012; Palta et al. 2014). This disruption exposes the subendothelial cell-surface glycoprotein, tissue thromboplastin (Factor III), also known as tissue factor (TF), to calcium-activated, factor VIIa, which circulates in the blood stream. The activated complex formed is TF:FVIIa, which further activates factors in the extrinsic pathway and initiates a coagulation response (Hoffman et al. 1995; Walsh 2003; Mackman 2004; Palta et al. 2014). Aggregated platelets at the wound also stimulate the chemotaxis of necessary cells to the injured site and the subsequent activation of downstream processes. This allows successful dermal wound repair to occur (Monaco & Lawrence 2003; Broughton et al. 2006a; Reinke & Sorg 2012; Portou et al. 2015). The insoluble fibrin clot is a combination of fibrin fibres with platelets interspersed within the fibrin scaffold. It also contains a number of growth factors and cytokines, including PDGF, TGF-β_1, EGF and IGFs; contained within the α-granules of platelets (Martin 1997; Monaco & Lawrence 2003; Li et al. 2007; Velnar et al. 2009; Portou et al. 2015). The high concentrations of growth factors and cytokines act as a chemotactic stimulus to inflammatory cells, together with the cells required to re-establish the epidermal and dermal layers (Deuel et al. 1982; Martin 1997; Heldin & Westermark 1999; Monaco & Lawrence 2003; Li et al. 2007; Velnar et al. 2009).

Fibrin fibres are produced through the cleavage of fibrinogen by thrombin (Martin 1997; Monaco & Lawrence 2003; Mackman 2004; Li et al. 2007; Olczyk et al. 2014; Palta et al. 2014). Other glycoproteins present in this matrix include, plasma fibronectin, vitronectin and thrombospondin, which are released from platelet α-granules. These glycoproteins also have a role in haemostasis through platelet aggregation and formation of the blood clot (Ruoslahti 1988a; Greiling & Clark 1997; Monaco & Lawrence 2003; Li et al. 2007; Velnar et al. 2009; Reinke & Sorg 2012; Olczyk et al. 2014; Palta et al. 2014). Additionally, these glycoproteins are involved in cell-matrix interactions, matrix-matrix interactions, cell migration and cell proliferation (Ruoslahti 1984; Ruoslahti 1988a; Mutsaers et al. 1997; Monaco & Lawrence 2003; Schultz & Wysocki 2009; Eckes et al. 2010). Fibronectin, vitronectin and thrombospondin are part of a group of ECM ligands for integrins, which are

strongly involved in cell adhesion (Ruoslahti 1996; Mutsaers et al. 1997; Preissner & Seiffert 1998; Santoro & Gaudino 2005; Li et al. 2007; Kim et al. 2011; Longmate & DiPersio 2014; Olczyk et al. 2014). One member of the integrin family, glycoprotein IIb/IIIa, is present on the cell membranes of platelets and play a role in the aggregation to each other forming a clot (Ruoslahti 1996; Mutsaers et al. 1997; Yang et al. 1999; Beanes et al. 2003; Gilcrease 2007; Palta et al. 2014). It is through the contact between platelets or other blood components with the exposed collagen as a result of tissue injury, that the release of factors from platelets is triggered. These released factors include growth factors, clotting factors and ECM proteins (Diegelmann & Evans 2004; Li et al. 2007; Velnar et al. 2009; Olczyk et al. 2014; Palta et al. 2014). Pro-inflammatory factors, such as serotonin, prostaglandins and thromboxane A2, are also released from the platelets present in the fibrin clot. It is the high concentrations of these factors that act as a cue to initiate the inflammatory phase, due to the chemoattractant signals towards immune cells (Martin 1997; Stadelmann et al. 1998; Traversa & Sussman 2001; Li et al. 2007; Velnar et al. 2009; Palta et al. 2014).

1.3.2 Inflammatory Phase

Overlapping with the late stage of haemostasis, the inflammatory phase commences responding to chemoattractant cues signalling to inflammatory cells, such as neutrophils and monocytes. However, the inflammatory stage can be divided into an early and late stage, where the neutrophils are most active at the earlier stages, with macrophages taking over in the late stages (Diegelmann & Evans 2004; Martin & Leibovich 2005; Li et al. 2007; Velnar et al. 2009; Koh & DiPietro 2011; Reinke & Sorg 2012; Olczyk et al. 2014). During the early stage, the complement cascade is activated, a process known to play a part in the immune response at the wound site (Stadelmann et al. 1998; Beanes et al. 2003; Velnar et al. 2009; Koh & DiPietro 2011). One aspect of this process is the production of complement components, C3a and C5a, which along with TGF-β_1, have been shown to behave as chemoattractants towards neutrophils. Bacterial and platelet peptides produced by fibrinolysis at the wound site also exert a chemoattractant signal towards neutrophils (Beanes et al. 2003; Monaco & Lawrence 2003; Chin et al. 2004; Velnar et al. 2009; Reinke & Sorg 2012; Olczyk et al. 2014). This process is very rapid, allowing neutrophils to migrate to the wound site within minutes of injury occurring. These remain at the injured site for a few days,

or until they have succeeded in clearing the cell debris and bacteria (Martin 1997; Dovi et al. 2004; Li et al. 2007; Velnar et al. 2009; Reinke & Sorg 2012; Wilgus et al. 2013).

Neutrophils are initially present in high numbers as their main function is to remove any contaminants, such as bacteria present in the wound and damaged tissue. This is achieved through phagocytosis and the production of ROS (Monaco & Lawrence 2003; Dovi et al. 2004; Schäfer & Werner 2008; Velnar et al. 2009; Guo & DiPietro 2010; Reinke & Sorg 2012; Wilgus et al. 2013; Olczyk et al. 2014). Neutrophils digest the bacteria present at the wound site through the use of proteases, with different enzymes being required depending on the digestion target (Yager & Nwomeh 1999; Broughton et al. 2006a; Toriseva & Kähäri 2009; Velnar et al. 2009; Lu et al. 2011; Reinke & Sorg 2012; Wilgus et al. 2013). The unwounded area adjacent to the injury site is protected from these highly active enzymes by the high presence of protease inhibitors. This is sufficient as a protection mechanism unless there is an excessive inflammatory response overwhelming the inhibitory proteases (Yager & Nwomeh 1999; Broughton et al. 2006a; Koh & DiPietro 2011; McCarty & Percival 2013; Wilgus et al. 2013). Although the phagocytosis of bacteria and cell debris is thought to be the main function of neutrophils at a wound site, they have also been shown to be a reservoir of pro-inflammatory cytokines and chemokines (Martin 1997; Scapini et al. 2000; Reinke & Sorg 2012; Wilgus et al. 2013; Olczyk et al. 2014; Tecchio et al. 2014; Tecchio & Cassatella 2016).

Neutrophils migrate to the wound site through a series of cell adhesion processes. Firstly, there are changes to the cell surface adhesion molecules on the neutrophils causing them to become ‘sticky’ and along with a selectin-dependent cell adhesions, a weak attachment to the endothelial cell layer occurs (Springer 1994; Martin 1997; Monaco & Lawrence 2003; Broughton et al. 2006a; Petri & Bixel 2006; Velnar et al. 2009). This weak bond causes the neutrophils to roll along the endothelium at a slower pace allowing a stronger β_2 integrin-mediated adhesion to occur. The subsequent strong bond results in diapedesis occurring, where neutrophils and other leukocytes migrate through the blood vessel walls to the wound site (Butcher et al. 1991; Ager 1994; Springer 1994; Martin 1997; Monaco & Lawrence 2003; Petri & Bixel 2006; Velnar et al. 2009). The gaps within the endothelial cell layer occur as a result of the

synthesis of leukotrienes and prostaglandins, both of which cause an inflammatory reaction. This leads to the vasodilation of blood vessels (Hedqvist et al. 2000; Broughton et al. 2006a; Pober & Sessa 2007; DiStasi & Ley 2009). The initial synthesis of these two inflammatory molecules is through the activation of the cyclooxygenase-2 enzyme (COX-2), which causes the downstream synthesis of prostaglandins and leukotrienes, resulting in vasodilation and inflammation, respectively (Broughton et al. 2006a; Li et al. 2007; Pober & Sessa 2007; DiStasi & Ley 2009). This inflammatory effect causes gaps to form within the endothelial cell layer, also known as a leaky capillary wall; and allows the migration of neutrophils out of the blood vessel. Proteins have also been shown to migrate through these gaps and cause a local swelling reaction (Hedqvist et al. 2000; Broughton et al. 2006a; Pober & Sessa 2007; DiStasi & Ley 2009; Velnar et al. 2009). A beneficial effect of the action of COX-2 is that the vasodilation and leaky blood vessels allows for the translocation of leukocytes from the circulating blood to the wound site (Broughton et al. 2006a; Pober & Sessa 2007; DiStasi & Ley 2009).

Monocytes are initially attracted to the wound site before undergoing differentiation to macrophages. Monocytes circulate in the blood allowing a ready supply to be converted to macrophages and activated at sites of injury (Martin 1997; Monaco & Lawrence 2003; Li et al. 2007; Velnar et al. 2009; Guo & DiPietro 2010; Brancato & Albina 2011; Olczyk et al. 2014). Macrophages also produce signalling factors initially released from the both neutrophils and degranulating platelets (Monaco & Lawrence 2003; Diegelmann & Evans 2004; Velnar et al. 2009). Once the neutrophils have cleared the bacteria and contaminants, macrophages activated at the wound site clear the apoptotic neutrophils that have fulfilled their job of clearing the wound debris. They have also been shown to induce apoptosis of neutrophils and other immune cells (Monaco & Lawrence 2003; Martin & Leibovich 2005; Li et al. 2007; Velnar et al. 2009; Guo & DiPietro 2010; Brancato & Albina 2011; Koh & DiPietro 2011; Wilgus et al. 2013). Neutrophils need to be cleared from the wound site without causing a new inflammatory reaction, performed by two main mechanisms. Neutrophils can undergo apoptosis and then rely on macrophages to remove them from the site. Alternatively, neutrophils can migrate to the wound surface and be shed from the skin surface (Monaco & Lawrence 2003; Li et al. 2007; Velnar et al. 2009; Guo & DiPietro 2010;

Koh & DiPietro 2011; Wilgus et al. 2013). As macrophages have a longer lifespan, these remain for a longer time-period at the wound site than the neutrophils and continue the work of the neutrophils. Macrophages are further capable of working in lower pH conditions (Martin 1997; Mosser & Edwards 2008; Velnar et al. 2009; Guo & DiPietro 2010; Parihar et al. 2010; Reinke & Sorg 2012; Olczyk et al. 2014).

Macrophages need to undergo activation so they can carry out a number of functions. The main function is inducing the transition from the inflammatory phase to the proliferative phase. This is achieved through stimulation of fibroblasts and keratinocytes to the wound site; these cells are required in the proliferative phase. Another function is stimulating angiogenesis to ensure sufficient blood supply to the repaired area (Martin & Leibovich 2005; Li et al. 2007; Velnar et al. 2009; Guo & DiPietro 2010; Koh & DiPietro 2011; Reinke & Sorg 2012; Lech & Anders 2013; Lucas et al. 2010; Portou et al. 2015; Snyder et al. 2016). Macrophages stimulate these cells through the production of growth factors and other mediators, such as TGF-β_1, TGF-α, FGF, HB-EGF and collagenase (Monaco & Lawrence 2003; Diegelmann & Evans 2004; Li et al. 2007; Velnar et al. 2009; Brancato & Albina 2011; Koh & DiPietro 2011; Reinke & Sorg 2012). There are two categories of macrophages, M1 and M2, referred to as the classically activated and the alternatively activated, respectively. These two subtypes of macrophages induce different responses during wound healing (Mosser & Edwards 2008; Lucas et al. 2010; Koh & DiPietro 2011; Snyder et al. 2016). M1 macrophages are developed from resting macrophages, the transition is induced by pro-inflammatory cytokines or microbial components. These activated macrophages are then capable of expressing pro-inflammatory cytokines, along with chemokines to attract further immune cells to the wound site (Mosser & Edwards 2008; Koh & DiPietro 2011; Ashcroft et al. 2012; Lech & Anders 2013; Snyder et al. 2016). M2 macrophages are also referred to as the resolution macrophages, due to their contrasting role to M1 macrophages. They induce anti-proliferative cytokines and reduce the expression of pro-inflammatory cytokines (Lucas et al. 2010; Parihar et al. 2010; Snyder et al. 2016). In addition, their functions include angiogenesis, ECM remodelling and MMP production, all of which contribute to a reparative response (Lucas et al. 2010; Lech & Anders 2013; Snyder et al. 2016).

Neutrophils and macrophages release cytokines, which act as a chemoattractant to T-lymphocytes. These cells migrate to the wound site after the inflammation stage has concluded and are necessary for the next process to take place. The chemoattractant agents towards T-lymphocytes are IL-1, complement components and the degradation products of IgG. Lymphocytes also require activation at the wound site to perform their actions (Scapini et al. 2000; Velnar et al. 2009; Guo & DiPietro 2010; Olczyk et al. 2014). Approximately 2-3 days after injury, macrophages continue to clear the wound of any contaminants, then along with lymphocytes, these produce enzymes in response to IL-1 and TNF-α to degrade wound components before the ECM remodelling process occurs (Monaco & Lawrence 2003; Velnar et al. 2009; Reinke & Sorg 2012; Olczyk et al. 2014). MMPs are mainly involved in this degradation of the damaged ECM. They are expressed by a number of cells involved in wound healing, allowing this process to occur across the various phases (Monaco & Lawrence 2003; Broughton et al. 2006a; Velnar et al. 2009; McCarty & Percival 2013; Rohani & Parks 2015). Initially, monocytes and macrophages are responsible for the MMP production, with this role later undertaken by fibroblasts and keratinocytes (Broughton et al. 2006a; Velnar et al. 2009; McCarty & Percival 2013; Olczyk et al. 2014; Caley et al. 2015).

1.3.3 Proliferative Phase

The proliferative phase lasts for approximately 2 weeks and commences within a few days of injury. It is necessary to produce the large numbers of fibroblasts and keratinocytes required for the production of the ECM and epidermis, respectively (Stadelmann et al. 1998; Beanes et al. 2003; Li et al. 2007; Gurtner et al. 2008; Velnar et al. 2009; Reinke & Sorg 2012; Bainbridge 2013; Olczyk et al. 2014; Xue & Jackson 2015). The proliferative phase is focused mainly on the reparative process; the initial phases could be considered as damage control with the cessation of blood flow and formation of a temporary barrier. The inflammation phase ensures that the wound site is free from contaminants before restoration of the epidermis and underlying dermis (Stadelmann et al. 1998; Li et al. 2007; Velnar et al. 2009; Kondo & Ishida 2010; Reinke & Sorg 2012; Olczyk et al. 2014). The two main aspects of the proliferative phase are re-epithelisation, to establish a more permanent barrier replacing the temporary fibrin clot; and the synthesis of new ECM by the fibroblasts that have

migrated to the wound site (Stadelmann et al. 1998; Velnar et al. 2009; Kondo & Ishida 2010; Reinke & Sorg 2012; Bainbridge 2013; Olczyk et al. 2014; Pastar et al. 2014).

1.3.3.1 Re-epithelialisation

For the re-epithelialisation aspect of this phase, undamaged keratinocytes migrate from the wound edge. Additionally, epidermal stem cells migrate from the stem cell bulge in the hair follicles, along with from sebaceous glands and sweat glands (Watt 1998; Li et al. 2007; Guo & DiPietro 2010; Koivisto et al. 2012; Reinke & Sorg 2012; Olczyk et al. 2014; Pastar et al. 2014; Ojeh et al. 2015). The migration of keratinocytes from both the basement membrane and the undamaged areas adjacent to the wound site allows re-epithelialisation, creating a more permanent barrier than the temporary fibrin clot (Broughton et al. 2006b; Li et al. 2007; Koivisto et al. 2012; Pastar et al. 2014; Seeger & Paller 2015). Initially, the focus of migrating keratinocytes is to re-establish the uppermost layers of the epidermis to seal the wound, before re-constructing the basement membrane and allowing terminal differentiation of keratinocytes to continue and re-build each epidermal layer in an ascending manner (Broughton et al. 2006b; Patel et al. 2006; Li et al. 2007; Velnar et al. 2009; Koivisto et al. 2012; Kroeze et al. 2012; Reinke & Sorg 2012; Olczyk et al. 2014; Pastar et al. 2014). As the epidermal layers are re-established, there are various changes in keratin expression at the wound site, as previously described (Section 1.2.1.2, Fuchs 1995; Haake et al. 2001; Santos et al. 2002; Magin et al. 2007; Bragulla & Homberger 2009). Keratins appear to be less segmented between the layers of the epidermis, with keratin pairs expressed in additional layers to their normal expression site in unwounded skin (Martin 1997; Haake et al. 2001; Magin et al. 2007; Bragulla & Homberger 2009). Additional keratins are also expressed at the wound sites that are not present in unwounded skin. These include Krt6, Krt16 and Krt17, which are upregulated following epidermal injury (Fuchs 1995; Martin 1997; Santos et al. 2002; Mazzucchelli 2002; Sivamani et al. 2007; Bragulla & Homberger 2009; Moll et al. 2008).

In order for the keratinocytes to migrate across the fibrin clot from the unwounded epidermis, the fibrin clot needs to be removed. In addition, hemidesmosomes, the connections between the keratinocytes and the ECM, need to be disrupted to allow the migration of keratinocytes through the epidermal levels to replace those lost during

injury (Martin 1997; Li et al. 2007; Reinke & Sorg 2012; Longmate & DiPersio 2014; Pastar et al. 2014; Rohani & Parks 2015; Seeger & Paller 2015). Hemidesmosomes hold keratinocytes in place to the ECM, along the basal lamina. The keratinocytes themselves produce the enzymes required to dissociate from their tethered positions and migrate to the wound site (Martin 1997; Li et al. 2007; Koivisto et al. 2012; Longmate & DiPersio 2014; Pastar et al. 2014; Rohani & Parks 2015). Plasmin is responsible for dissolving the fibrin clot and breaking the hemidesmosomes connection to keratinocytes. Plasminogen is the precursor to plasmin and is present as part of the fibrin clot (Jensen & Lavker 1996; Martin 1997; Cesarman-maus & Hajjar 2005; Koivisto et al. 2012). Cleavage and activation of plasminogen to form the reactive plasmin is achieved through the action of tissue-type plasminogen activator (tPA) or urokinase-type plasminogen activator (uPA). Plasmin can act in a positive feedback mechanism, by cleaving both tPA and uPA, which in turn can cleave and activate plasminogen (Blasi 1988; Novokhatny et al. 1995; Bugge et al. 1996; Martin 1997; Cesarman-maus & Hajjar 2005; Koivisto et al. 2012). The actions of tPA and uPA are fibrin specific, with these activators specifically targeting plasminogen bound to fibrin. The activity of tPA is greatly increased in the presence of fibrin, allowing for the cleavage and activation of plasminogen (Blasi 1988; Collen & Lijnen 2005, 2009). The presence of tPA and uPA are increased by keratinocytes that have migrated to the wound site. These keratinocytes also provide a complementary receptor for uPA. The combination of these components present allows plasmin to be activated and achieve the desired result of dissolving the temporary fibrin clot (Grøndahl-Hansen et al. 1988; Rømer et al. 1991, 1994; Martin 1997; Koivisto et al. 2012). The gene expression for both uPA and its respective receptor are upregulated by the enzymes associated with keratinocyte proliferation and migration, such as EGF and KGF (Tsuboi et al. 1993; Clark 1996; Ploug 2003).

MMPs within the wound site are also responsible for dissolving the fibrin clot and the surrounding ECM, including MMP-1, -9 and -10. Each MMP has a different target for enzymatic breakdown. As with the action of plasmin, keratinocytes present at the wound site are responsible for the production of these proteinases (Martin 1997; Li et al. 2007; Behm et al. 2012; Koivisto et al. 2012; Hameedaldeen et al. 2014; Olczyk et al. 2014; Pastar et al. 2014; Rohani & Parks 2015). However, not all of the MMPs

present are produced by keratinocytes of the same origin. MMP-1 is produced by migrating keratinocytes from the basal and suprabasal layers and MMP-10 is produced by the undamaged keratinocytes that are present along the wound edge (Martin 1997; Pilcher et al. 1997; Krampert et al. 2004; Koivisto et al. 2012; Pastar et al. 2014; Rohani & Parks 2015). All three of these MMPs are classified into different groups within the MMP family of enzymes, according to their function. MMP-1 is part of the collagenase family, MMP-9 from the gelatinase family; and MMP-10 from the stromelysins (Martin 1997; Koivisto et al. 2012; Olczyk et al. 2014; Rohani & Parks 2015).

MMP-1 is responsible for the cleavage of interstitial collagens, typically types I and III collagen, allowing for the migration of keratinocytes into the wound space. Type I collagen is known to form a large part of the ECM prior to its repair (Martin 1997; Pilcher et al. 1997; Li et al. 2007; Gill & Parks 2008; Olczyk et al. 2014; Pastar et al. 2014; Rohani & Parks 2015). Type IV and type VII collagen are cleaved by the action of MMP-9, due to their roles in the basal lamina and as an anchoring fibril collagen, respectively (Hudson et al. 1993; Martin 1997; Bigg et al. 2007; Abreu-Velez & Howard 2012; Olczyk et al. 2014). This is believed to allow the migration of keratinocytes from the basal layer to the wound site and basement membrane remodelling (Martin 1997; Falanga 2005; Li et al. 2007; Koivisto et al. 2012). MMP-10 is upregulated in wound healing and expressed by migrating keratinocytes. It also has the least specificity out of the three MMPs involved (Martin 1997; Krampert et al. 2004; Gill & Parks 2008; Koivisto et al. 2012; Rohani & Parks 2015). An excessive presence of proteinases will affect the normal healing process and may be one of the causes for impaired healing and wound closure in chronic wounds (Martin 1997; Schultz & Wysocki 2009; Toriseva & Kähäri 2009; Guo & DiPietro 2010; Koivisto et al. 2012; Pastar et al. 2014; Rohani & Parks 2015).

During normal healing, ECM degradation is regulated to prevent excessive ECM breakdown; this is essential for normal tissue function (Li et al. 2007; Schultz & Wysocki 2009; Velnar et al. 2009; Cox & Erler 2011). Keratinocytes eventually downregulate MMP expression and return to their normal function of terminal differentiation throughout the epidermal layers, along with the formation of new

hemidesmosomes (Martin 1997; Li et al. 2007; Koivisto et al. 2012; Longmate & DiPersio 2014). It is through this tightly regulated production of cytokines and growth factors and their interaction with the ECM components that increases and decreases the production of MMPs. This affects the synthesis of newly formed ECM (Schultz & Wysocki 2009; Toriseva & Kähäri 2009; Velnar et al. 2009; Behm et al. 2012). One such example is TGF-β_1, which has been shown to stimulate the production of various ECM components. It also regulates MMP and TIMP expression, involved in ECM degradation (Li et al. 2007; Schultz & Wysocki 2009; Toriseva & Kähäri 2009; Velnar et al. 2009; Watt & Fujiwara 2011). TGF-β_1 has also been shown to upregulate the expression of MMP by keratinocytes, contributing to keratinocyte migration (Gill & Parks 2008; Philips et al. 2011; Pastar et al. 2014).

During keratinocyte migration to the wound site, a process called cell crawling occurs. This involves the action of integrins and the keratinocyte actin cytoskeleton. This process involves a series of steps that are repeated until the cell has reached the required location (Cooper 2000; Haase et al. 2003; Li et al. 2007; Velnar et al. 2009; Reinke & Sorg 2012). The steps involved are the initial protrusion of the leading edge of the cell; cell focal adhesions are then formed between the leading edge and the substratum to increase stability. Finally, dissociation of focal adhesions at the rear of the cell occurs, allowing the retraction of the trailing edge of the cell to the cell body (Van Haastert & Devreotes 2004; Gilcrease 2007; Clainche & Carlier 2008; Velnar et al. 2009; Vicente-Manzanares & Horwitz 2011; Krause & Gautreau 2014; Seeger & Paller 2015). Actin filaments possess a natural polarity and when they undergo polymerisation in cell crawling. New actin monomers are added at the positive end and removed from the negative end in a process referred to as ‘actin treadmilling’. It is the repeated addition to the positive end that pushes the cell structure out at the leading edge and facilitates the movement of the cell (Clainche & Carlier 2008; Velnar et al. 2009; Parsons et al. 2010; Krause & Gautreau 2014).

The focal adhesion complexes formed and activated between the cell and the substratum occur from the binding of integrins to specific proteins present in the ECM and the actin filaments present at the leading edge (Cooper 2000; Wozniak et al. 2004; Velnar et al. 2009; Vicente-Manzanares & Horwitz 2011; Kim & Wirtz 2013;

Longmate & DiPersio 2014). The proteins involved in connecting actin to integrin are α-actinin, vinculin and talin (Cooper 2000; Wozniak et al. 2004; Vicente-Manzanares & Horwitz 2011; Koivisto et al. 2012). The direction of movement of the cell is determined by a polarity effect and a chemoattractive substance, attracting the cells to the wound site (Van Haastert & Devreotes 2004; Clainche & Carlier 2008; Velnar et al. 2009; Vicente-Manzanares & Horwitz 2011; Kim & Wirtz 2013). The chemoattractant force directs the cell to a specific location, the injury site, in a positive chemotactic direction through the production of a chemical gradient. The new position is stabilised with the formation of focal adhesion complexes (Li et al. 2007; Velnar et al. 2009; Parsons et al. 2010; Reinke & Sorg 2012; Krause & Gautreau 2014). However, this provides a tension on the focal adhesion complexes still present at the trailing edge, requiring these to be dissociated to allow the retraction of the back of the cell (Clainche & Carlier 2008; Velnar et al. 2009; Parsons et al. 2010; Krause & Gautreau 2014). The contractile force that takes place within the cell uses the actomyosin filaments to allow the retraction of the trailing edge of the cell. Myosin motor proteins and their connection to the actin filaments are involved in producing this force and breaking the connections between the actin cytoskeleton and the integrins at the trailing edge (Gilcrease 2007; Clainche & Carlier 2008; Velnar et al. 2009; Parsons et al. 2010; Kim & Wirtz 2013).

Dependent on the cells desired at the site, there are specific chemotactic agents required to produce the signal. This is dependent on the stage of the wound healing process, as the attraction of inflammatory cells is stimulated by the products of the haemostasis process, degranulating platelets and growth factors specific to that stage (Scapini et al. 2000; Traversa & Sussman 2001; Monaco & Lawrence 2003; Velnar et al. 2009; Reinke & Sorg 2012; Olczyk et al. 2014). In the proliferation stage, products of the inflammation stage are used as chemoattractants, such as TGF-β_1 and PDGF. These growth factors attract fibroblasts to the site, in order to produce the ECM components required for the synthesis of new ECM, replacing the temporary matrix present during the earlier stages (Seppa et al. 1982; McDougall et al. 2006; Li et al. 2007; Velnar et al. 2009; Reinke & Sorg 2012; Olczyk et al. 2014). The migration of keratinocytes commences earlier in the healing process, approximately a few hours after wounding due to the importance of re-establishing the protective barrier.

Therefore, chemoattractant agents, such as TGF-α and EGF, provide the chemotactic signals for these cells along with enhancing the proliferative action of keratinocytes (Li et al. 2007; Velnar et al. 2009; Koivisto et al. 2012; Olczyk et al. 2014; Pastar et al. 2014; Seeger & Paller 2015).

The production of new integrins at the leading edge and the dissolution of those at the trailing edge takes time, resulting in the delay seen before migration occurs. The type of integrin expressed depends on the ECM protein it will bind to (Grinnell 1992; Larjava et al. 1993; Martin 1997; Humphries et al. 2006; Velnar et al. 2009; Longmate & DiPersio 2014). These specificities are determined by receptors expressed on the surface of integrins. Some examples are α5β1 and αvβ6 expressing the receptors for fibronectin and tenascin respectively; and αvβ5 expressing the vitronectin receptor. Some integrins can express receptors for multiple targets, such as α2β1 integrin expressing the receptor for both collagen and laminin (Larjava et al. 1993; Martin 1997; Humphries et al. 2006; Gilcrease 2007; Koivisto et al. 2012; Longmate & DiPersio 2014). In addition to expressing the appropriate receptors for each protein, integrins are also able to convey information between the cell and ECM, acting in a two-directional manner allowing for cell migration regulation (Humphries et al. 2006; Gilcrease 2007; Velnar et al. 2009; Koivisto et al. 2012; Longmate & DiPersio 2014). These integrins form a connection to the cytoskeleton. The keratinocyte cytoskeleton is comprised of a network of keratin intermediate fibres, providing structure to the cell whilst also allowing for a degree of flexibility in the cell, necessary for cell migration (Gu & Coulombe 2007; Windoffer et al. 2011; Hobbs et al. 2012). Different cells can migrate at different speeds. It is mainly dependent on the strength of adhesion to the ECM, as reduced adhesion strength can allow more rapid migration of the cells requiring a balance between migration and adhesion to be established (Maheshwari et al. 2000; Velnar et al. 2009; Nardini et al. 2016). Speed of cell motility is also dependent on the phase of wound healing and the resultant chemoattractive force. Initially, there is a high chemoattractive signal for migrating cells causing a rapid migration of cells to the wound site, but as the healing process occurs, there is less demand for more cells to migrate to the area. This results in a decreased chemoattractant signal and reduced cell migration speed (Van Haastert & Devreotes 2004; Li et al. 2007; Velnar et al. 2009; Reinke & Sorg 2012).

There are a number of growth factors involved in the cell crawling process, along with general re-epithelisation, some of which are part of the positive feedback loop between the fibroblasts and keratinocytes, such as KGF; which has a vital role in keratinocyte proliferation (Finch et al. 1989; Werner 1998; Maas-Szabowski et al. 1999; auf demKeller et al. 2004; Barrientos et al. 2008; Bader & Kao 2009; Shirakata 2010; Koivisto et al. 2012; Seeger & Paller 2015). Rapid re-epithelisation is a beneficial property for restoring the protective barrier with the aim of preventing infection of the wound site. This is especially important in patients with burns or chronic wounds, where large areas of the epidermis may be affected (Martin 1997; Usui et al. 2008; Koivisto et al. 2012; Pastar et al. 2014; Rowan et al. 2015; Seeger & Paller 2015; Rose & Chan 2016). There are two systems in place for re-establishing the vasculature to the dermis and epidermis, through the repair of damaged vessels or through neovascularisation. The growth factors involved in promoting angiogenesis are FGF, VEGF, TGF-β_1, TGF-α and angiogenin. A number of cells are responsible for the production of these angiogenic factors, including macrophages, fibroblasts and keratinocytes (Tonnesen et al. 2000; Uchi et al. 2000; Barrientos et al. 2008; Velnar et al. 2009; Reinke & Sorg 2012; Johnson & Wilgus 2014). Although multiple cell types are involved in the neovascularisation process, it is the keratinocytes that are mainly responsible for the production of new capillaries. Macrophages and fibroblasts release growth factors that act on the keratinocytes and stimulate them to release VEGF and produce the resultant capillary growth (Frank et al. 1995; Tonnesen et al. 2000; Broughton et al. 2006a; Li et al. 2007; Velnar et al. 2009; Johnson & Wilgus 2014). There is an angiogenic inhibitor also present at the wound site, angiostatin. This is to ensure that the new capillary growth does not go unregulated (Cesarman-maus & Hajjar 2005; Velnar et al. 2009; Johnson & Wilgus 2014; Olczyk et al. 2014).

1.3.3.2 Dermal Extracellular Matrix Synthesis

ECM synthesis is required to produce granulation tissue as a replacement for the temporary fibrin scaffold formed earlier in the wound healing process. However, a balance between ECM synthesis and degradation is necessary for sufficient organisation of the ECM to occur (McDougall et al. 2006; Velnar et al. 2009; Kim et al. 2011; Reinke & Sorg 2012; Olczyk et al. 2014; Xue & Jackson 2015). Granulation

tissue consists of a number of components, including macrophages, fibroblasts, fibronectin, fibrinogen, hyaluronan, collagen and the newly re-established vasculature (Schultz & Wysocki 2009; Velnar et al. 2009; Eckes et al. 2010; Mouw et al. 2014; Olczyk et al. 2014; Xue & Jackson 2015; Tracy et al. 2016).

The synthesis of the ECM is dictated by the production of ECM components and proteases by fibroblasts. The ECM components produced include procollagen types I and III, fibronectin, hyaluronan and proteoglycans (Gelse et al. 2003; Agren & Werthén 2007; Schultz & Wysocki 2009; Velnar et al. 2009; Guo & DiPietro 2010; Olczyk et al. 2014; Tracy et al. 2016). The production of these ECM components by fibroblasts provides a degree of structure and stability to the matrix. The organisation of the matrix has high importance to allow the normal functions of the dermal matrix to occur and provide the scaffold for migrating cells (Schultz & Wysocki 2009; Velnar et al. 2009; Frantz et al. 2010; Hubmacher & Apte 2013; Tracy et al. 2016). The migration of fibroblasts to the wound site occurs a few days after injury and they initiate the formation of granulation tissue. There is an initial delay in fibroblast migration, due to there being in an inactive or quiescent state (Martin 1997; Monaco & Lawrence 2003; Li et al. 2004; Velnar et al. 2009; Bainbridge 2013; Olczyk et al. 2014). The proliferation of fibroblasts at the wound site is mediated indirectly through an autocrine mechanism by the activation of TGF-β_1. This growth factor has been shown to be involved in stimulating fibroblast proliferation (Cordeiro et al. 2000; Broughton et al. 2006a; Li et al. 2007; Meran et al. 2008; Olczyk et al. 2014; Tracy et al. 2016).

Fibroblasts are attracted quite specifically to the wound site by the presence of growth factors sending out chemoattractant signals. The growth factors involved in this chemotaxis are TGF-β_1 and PDGF (Pierce et al. 1989; Heldin & Westermark 1999; McDougall et al. 2006; Li et al. 2007; Velnar et al. 2009; Behm et al. 2012; Bainbridge 2013; Olczyk et al. 2014). These growth factors are present at the wound site, due to their release from degranulating platelets and inflammatory cells. The expression of PDGF is further increased by fibroblasts at the wound site by autocrine stimulation from the fibroblasts, increasing the chemoattractant signal to other migrating fibroblasts (Pierce et al. 1989; Broughton et al. 2006a; Schultz & Wysocki 2009;

Velnar et al. 2009; Olczyk et al. 2014). Fibroblasts synthesise and deposit collagen, initially a high proportion of type III collagen is synthesised. Approximately 40% of the collagen present in granulation tissue is type III collagen, compared to only 25% type III collagen present in unwounded tissue (Li et al. 2007; Velnar et al. 2009; Cheng et al. 2011; Reinke & Sorg 2012; Bainbridge 2013; Olczyk et al. 2014; Xue & Jackson 2015; Tracy et al. 2016). The benefit of type III collagen being laid down initially is the rapid speed with which it can be synthesised, providing a temporary structure for other matrix molecules to develop around (Mutsaers et al. 1997; Monaco & Lawrence 2003; Li et al. 2007; Velnar et al. 2009; Bainbridge 2013). Some fibroblasts at the wound site undergo differentiation into myofibroblasts, which are strongly associated with the contraction of the wound site, enabling closure between the wound edges. This contraction at the wound site is required for wound closure, but also contributes to scar formation; therefore this process needs to be tightly regulated as previously mentioned (Gabbiani 2003; Desmouliere et al. 2005; Broughton et al. 2006a; Li et al. 2007; Eckes et al. 2010; Reinke & Sorg 2012; Bainbridge 2013; Olczyk et al. 2014).

An important aspect of re-establishing an ECM is the production of a blood supply to the newly synthesised matrix. There are multiple angiogenic factors that are released to promote both the formation of new capillaries and the repair of damaged vessels (Tonnesen et al. 2000; Li et al. 2007; Velnar et al. 2009; Reinke & Sorg 2012; DiPietro 2013; Olczyk et al. 2014). In addition, migration of the cells responsible for these angiogenic functions to the wound site is necessary. There are a number of chemoattractants involved, including TGF-α, VEGF, angiopoietin, fibrin and lipid growth factors (Tonnesen et al. 2000; Szpaderska et al. 2005; Li et al. 2007; Velnar et al. 2009; Reinke & Sorg 2012; DiPietro 2013; Johnson & Wilgus 2014; Olczyk et al. 2014). Presence of a blood supply to the matrix is necessary for providing oxygen to the cells required in cell metabolism. Degradation of existing structures, including the basal lamina, are required to allow formation of new vasculature to both the epithelial layers and the dermal matrix (Tonnesen et al. 2000; Li et al. 2007; Velnar et al. 2009; Reinke & Sorg 2012; DiPietro 2013; Johnson & Wilgus 2014).

MMPs are involved in the degradation of the damaged ECM, allowing a new matrix to be synthesised without any damaged components being incorporated. There are

specific proteases depending on the target of degradation, for example damaged collagen fibres are degraded by the actions of collagenases (Martin 1997; Broughton et al. 2006a; Li et al. 2007; Kim et al. 2011; Bainbridge 2013; Rohani & Parks 2015; Xue & Jackson 2015). Another target of the MMPs is the remaining debris from the earlier wound healing stages, such as any remaining immune and inflammatory cells that have completed their job of clearing the bacteria and providing the chemotactic signals to the fibroblasts and other cells required later in the process (Monaco & Lawrence 2003; Broughton et al. 2006a; Olczyk et al. 2014). TGF-β_1 has opposing responses on different MMPs, with MMP-1 inhibited and MMP-2 stimulated, along with increased TIMP activity in fibroblasts (Schultz & Wysocki 2009; Philips et al. 2011; Watt & Fujiwara 2011; Xue & Jackson 2015). Additionally, the expression of MMP-1 is up-regulated through the actions of IL-1β and IL-6; whereas the expression of TIMPs is upregulated by the actions of TNF-α and TGF-β_1 (Circolo et al. 1991; Dasu et al. 2003; Behm et al. 2012).

1.3.4 Remodelling Phase

Variations in the levels of MMPs and TIMPs occur during the remodelling phase, with the aim is to increase the tensile strength of the tissue by modulating the composition of the matrix (Monaco & Lawrence 2003; Li et al. 2007; Velnar et al. 2009; Philips et al. 2011; Bainbridge 2013; Xue & Jackson 2015). A careful balance between MMPs and their inhibitors, TIMPs, is required for optimal healing. If excessive production of MMPs is present, this may lead to failure to heal the wound site as degradation of the matrix will occur at a faster rate that ECM deposition (Trengrove et al. 1999; Mwaura et al. 2006; Li et al. 2007; Menke et al. 2007; Rayment et al. 2008; Schultz & Wysocki 2009). Conversely, decreased expression of some MMPs, including MMP-1 and MMP-9, may lead to the decreased degradation of ECM causing an excess granulation tissue deposition (Lafuma et al. 1994; Broughton et al. 2006a; Li et al. 2007; Lee et al. 2015; Rohani & Parks 2015). A balance between the actions of MMPs and TIMPs is normally reached approximately 3 weeks after the injury occurred. This remodelling period, where the ECM undergoes a turnover process, can last anywhere between a number of months up to a couple of years, depending on the size of the area undergoing remodelling (Li et al. 2007; Velnar et al. 2009; Reinke & Sorg 2012; Xue & Jackson 2015).

One of the major changes seen between the ECM composition during the proliferative and remodelling stages is the percentages of type I and III collagen present (Monaco & Lawrence 2003; Li et al. 2007; Reinke & Sorg 2012; Bainbridge 2013; Olczyk et al. 2014; Xue & Jackson 2015). Type III collagen is initially laid down in the proliferative stage, resulting in a higher proportion of type III collagen present in granulation tissue, compared to unwounded tissue. It is during the remodelling stage that type III collagen is gradually replaced by type I collagen (Haukipuro et al. 1991; Broughton et al. 2006a; Li et al. 2007; Cheng et al. 2011; Olczyk et al. 2014). The proportion of type I and III collagen present in the remodelled ECM, after the maturation of the granulation tissue, alters to approximately the same proportion as in unwounded tissue; scar formation typically occurs at this point (Broughton et al. 2006a; Li et al. 2007; Olczyk et al. 2014; Xue & Jackson 2015). The intrinsic differences between the two fibrillar collagens may account for the difference in scar formation following wounding. Type I collagen is associated with a higher tissue tensile strength, but also has a degree of stiffness (Gelse et al. 2003; Bainbridge 2013). In contrast, type III collagen is associated with more elastic tissues. Therefore, the higher presence of this type in early-gestational, foetal wound healing may result in a less rigid wound site and produce a scarless healing response (Gelse et al. 2003; Cuttle et al. 2005; Li et al. 2007; Leung et al. 2012; Olczyk et al. 2014). There is a proportionate relationship between the amount of type I collagen present and the strength of the granulation tissue. However, the remodelled tissue only reaches approximately 80% of the tensile strength found in unwounded tissue (Monaco & Lawrence 2003; Broughton et al. 2006a; Li et al. 2007; Velnar et al. 2009; Olczyk et al. 2014; Xue & Jackson 2015; Rose & Chan 2016). The increase in tensile strength is associated with the organised formation of the fibres and the cross-linking that occurs between fibres. The cross-linking is controlled by the enzymes lysyl and prolyl oxidases, increasing the tissue strength. These enzymes are released by the fibroblasts still present in the newly-synthesised matrix (Gelse et al. 2003; Gordon & Hahn 2011; Mouw et al. 2014; Olczyk et al. 2014; Xue & Jackson 2015; Tracy et al. 2016).

Throughout the remodelling stage, there is a decreased turnover of the ECM, resulting in a decreased production of proteoglycans and other matrix components, due to

decreased chemoattraction to migrating cells (Monaco & Lawrence 2003; Velnar et al. 2009; Reinke & Sorg 2012). This leads to an overall decrease in the metabolic demand of the wound site, due to a decreased action by the cells. In addition, there is a reduction in the number of cells present at the wound site, as cells no longer required undergo apoptosis (Desmoulière et al. 1995; Desmoulière et al. 1997; Greenhalgh 1998; Velnar et al. 2009; Reinke & Sorg 2012). Initially, during the proliferative stage, small vessels were formed in response to angiogenic factors, a microvasculature to provide the oxygenation of the tissues. During the remodelling stage, these capillaries combine together to form larger vessels. This is in response to the changing environment of the ECM as the granulated tissue matures and remodels, the resultant decreased cell metabolism lowers the overall oxygen demand (Baum & Arpey 2005; Li et al. 2007; Velnar et al. 2009; Reinke & Sorg 2012; Olczyk et al. 2014; Portou et al. 2015).

A number of growth factors are also implicated in this remodelling phase, in particular PDGF, TGF-β_1 and FGF. Their role at this point is the continual closure of the wound site, an action initially stimulated by the fibroblasts and their conversion to the contractile myofibroblast phenotype (Mutsaers et al. 1997; Traversa & Sussman 2001; Baum & Arpey 2005; Velnar et al. 2009; Bainbridge 2013). The role of TGF-β_1 in the remodelling stage is to push the turnover balance more towards the deposition of the newly synthesised matrix. This is achieved through increasing the presence of TIMPs at the wound site, which subsequently decreases the action of MMPs (O'Kane & Ferguson 1997; Broughton et al. 2006a; Watt & Fujiwara 2011; Micallef et al. 2012; Xue & Jackson 2015).

1.4 Preferential Healing Situations

1.4.1 Foetal Wound Healing

There is evidence of scarless healing occurring in early foetal wounds producing normal skin architecture at the wound site. This only appears to occur in foetal injuries before the end of the second trimester. In contrast, all foetal injuries that occur after this time-point heal in the same manner as adult wounds, with the production of fibrous tissue leading to scar formation (Lorenz et al. 1992; Mast et al. 1992; Lorenz & Adzick 1993; Ferguson & Kane 2004; Lo et al. 2012; Rolfe & Grobbelaar 2012; Turabelidze

& DiPietro 2012; Malik et al. 2015). It was initially thought that the sterile environment of the uterus was involved in this scarless healing process. However, it was shown that it may be a result of intrinsic differences between foetal tissue and adult tissue (Adzick & Lorenz 1994; Dillon et al. 1994; Broker et al. 1999; Longaker et al. 2001; Bullard et al. 2003; Wagner & Wehrmann 2007; Rolfe & Grobbelaar 2012; Yagi et al. 2016). Foetal wound healing occurs more rapidly than the adult wound healing, despite the same stages of wound healing occurring. There are differences seen between the cell types present and the respective ratios of these cells, which may account for the variation in wound healing and skin architecture observed between the tissue types (Lorenz & Adzick 1993; Adzick & Lorenz 1994; Lee & Eun 1999; Bullard et al. 2003; Broughton et al. 2006b; Lo et al. 2012; Rolfe & Grobbelaar 2012; Yagi et al. 2016). Additionally, there are variations between the lengths of time that each stage lasts for, such as a reduced inflammation stage. This reduced response may account for the rapid healing observed in foetal tissue, compared to a longer healing period observed in adult dermal healing (Mast et al. 1992; Adzick & Lorenz 1994; Cass et al. 1997; Broker et al. 1999; Ferguson & Kane 2004; Chen et al. 2007; Rajan & Murray 2008; Nauta et al. 2011; Kishi et al. 2012; Malik et al. 2015; Yagi et al. 2016). It has been proposed that the difference in healing patterns between the two tissue types may be a result of foetal tissue undergoing regeneration, as opposed to the repair mechanism that occurs in adult dermal healing (Mast et al. 1992; Adzick & Lorenz 1994; Longaker et al. 2001; Bullard et al. 2003; Kishi et al. 2012; Yagi et al. 2016).

Correlating with the differences seen between adult and foetal wound healing, in regards to cell types present in the healing processes, there are also subtle variations seen between the stages of the wound healing process (Mast et al. 1992; Wagner & Wehrmann 2007; Rolfe & Grobbelaar 2012; Yagi et al. 2016). Initially, there is a reduced aggregation of platelets in foetal wounds; contact between the aggregated platelets and collagen is still required for the production of a number of growth factors, TGF-β_1, TGF-β_2 and PDGF. The level of growth factors produced by this contact is much reduced, compared to adult dermal healing (Adzick & Lorenz 1994; Cass et al. 1997; Broker et al. 1999; Bullard et al. 2003; Larson et al. 2010; Kishi et al. 2012; Yagi et al. 2016). These three growth factors are associated with a profibrotic function, so their much reduced presence may contribute to the scarless healing observed in

foetal wounds. Although TGF-β_1 and TGF-β_2 are still present in foetal wounds, it has been shown that they are rapidly cleared from the wound site (Mast et al. 1992; Adzick & Lorenz 1994; Belford 1997; Cass et al. 1997; Broker et al. 1999; Bullard et al. 2003; Ferguson & Kane 2004; Larson et al. 2010; Rolfe & Grobbelaar 2012; Yagi et al. 2016). A higher expression of TGF-β_3 has been shown in foetal wounds TGF-β_3 has been proposed as an anti-scarring therapy, due to its association with improved scar formation (Soo et al. 2003; Wagner & Wehrmann 2007; Rajan & Murray 2008; Larson et al. 2010; Kishi et al. 2012; Lo et al. 2012; Rolfe & Grobbelaar 2012; Malik et al. 2015; Yagi et al. 2016).

Foetal tissue appears to produce a greatly reduced inflammatory response, potentially resulting from the decreased inflammatory signals normally produced by platelets, through the release of TGF-β_1 and PDGF. These growth factors are involved in the recruitment of inflammatory and immune cells to the wound site in adult dermal healing (Cass et al. 1997; Bullard et al. 2003; Larson et al. 2010; Kishi et al. 2012; Rolfe & Grobbelaar 2012). The reduced inflammation stage correlates with a much reduced presence of the immune and inflammatory cells, in particular neutrophils, macrophages and mast cells (Adzick & Lorenz 1994; Bullard et al. 2003; Larson et al. 2010; Kishi et al. 2012; Lo et al. 2012; Rolfe & Grobbelaar 2012). These cells have been shown to be present at higher levels during adult wound healing, with mast cells associated with the production of fibrotic tissue resulting in scar formation (Mak et al. 2009; Gauglitz et al. 2011; Leung et al. 2012). In addition to the reduced numbers of inflammatory cells present at the wound site, the length of time that they remain at the site for is also reduced, along with a lower activity. Expression levels of pro-inflammatory cytokines, such as IL-6 and IL-8, are also lowered in foetal wounds. It is thought that the reduced presence of immune cells in foetal wound healing is due to the development of the immune system not being fully functional (Mast et al. 1992; Adzick & Lorenz 1994; Cowin et al. 1998; Liechty et al. 1998; Liechty et al. 2000; Rolfe & Grobbelaar 2012). At the end of the second trimester, it is thought that the immune system is more developed and as a result will produce a higher inflammatory response to injury and subsequent scarring. This leads to the theory that the level of inflammation has a marked effect on the production of fibrotic tissue (Cowin et al. 1998; Rajan & Murray 2008; Larson et al. 2010; Kishi et al. 2012; Yagi et al. 2016).

In addition to a reduced production of fibrotic tissue at the dermal layer, there is an increased re-epithelialisation process of foetal wounds, compared to adult dermal wounds (Wagner & Wehrmann 2007; Coolen et al. 2010; Kishi et al. 2012; Lee et al. 2012; Lo et al. 2012; Rolfe & Grobbelaar 2012). The cell crawling process of the keratinocytes does not occur in foetal wounds. Instead, a process referred to as 'purse string closure' occurs through the use of an actin cable. This is a much more rapid process, compared to the adult wound re-epithelialisation as the dissociation and forming of new integrins is not required, allowing wound closure to begin promptly after injury (Belford 1997; Martin 1997; Redd et al. 2004; Wagner & Wehrmann 2007; Lee et al. 2012; Rolfe & Grobbelaar 2012). There are different keratins present in early-gestational, foetal epithelia, compared to adult skin epithelia. Krt15 has been shown to have a continuous presence in early-gestational, foetal epithelia; whereas, in adult skin epithelia, this expression is discontinuous. Krt15 has also been associated as a characteristic keratin present in epidermal stem cells (Waseem et al. 1999; Bragulla & Homberger 2009; Bose et al. 2013).

There is a difference in the predominant cell type present in adult and foetal wound healing. In adult wound healing, macrophages are the predominant cell type present; whereas in foetal wound healing, fibroblasts are the predominant cell type (Adzick & Lorenz 1994; Cowin et al. 1998; Broker et al. 1999; Larson et al. 2010; Rolfe & Grobbelaar 2012). This could account for the rapid healing that is seen in foetal healing, due to rapid migration of foetal fibroblasts to the wounded site. This high abundance of fibroblasts can increase the synthesis of new ECM components and remodel the ECM in a shorter time period, compared to adult dermal healing (Mast et al. 1992; Bullard et al. 2003; Lo et al. 2012; Yagi et al. 2016). Despite the high presence of fibroblasts in foetal wounds and their early presence, due to their rapid migration to the wound site, there is an absence of myofibroblasts in foetal wounds at day 14, reducing the contraction of the wound. This often leads to scarring, which may be related to the low levels of TGF-β_1 present in foetal wounds (Adzick & Lorenz 1994; Lee & Eun 1999; Leung et al. 2012; Lo et al. 2012; Yagi et al. 2016). In addition, bFGF has been shown to be expressed at a higher level in scarless foetal wounds, compared to adult scarring wounds. This growth factor exerts a number of important

functions, including fibroblast proliferation, ECM synthesis, angiogenesis and keratinocyte mobility (Sogabe et al. 2006; Barrientos et al. 2008; Xie et al. 2008; Akita et al. 2012; Rolfe & Grobbelaar 2012). Another growth factor difference observed is the increased presence of VEGF in foetal wounds, contributing to angiogenesis, through increased permeability of the vasculature. Despite this increase in VEGF expression, studies indicated that development of new vessels is not significantly increased, compared to a control capable of scarring (Bullard et al. 2003; Colwell et al. 2005; Yagi et al. 2016). However, there are conflicting reports on VEGF expression in foetal wounds, with other studies suggesting that VEGF levels were reduced in scarless healing wounds and addition of VEGF induces a fibrotic response (Wilgus et al. 2008; Satish & Kathju 2010; Johnson & Wilgus 2014).

In addition to the rapid speed in which the new ECM is laid down in the wounded site of foetal injuries, there is also a difference in the composition of the healed foetal wounds, compared to adult dermal wounds. There is a much higher proportion of type III collagen to type I collagen present in the newly synthesised foetal ECM, compared to the ratio in adult dermal wounds (Adzick & Lorenz 1994; Bullard et al. 2003; Larson et al. 2010; Leung et al. 2012; Lo et al. 2012; Rolfe & Grobbelaar 2012; Yagi et al. 2016). The organisation of the collagen fibres is notably different between the two wound healing types. In adult wounds, fibres are present in thick bundles of type III collagen fibres, with cross-linking evident between fibres, leaving the appearance of a disorganised pattern of laid down collagen (Mast et al. 1992; Adzick & Lorenz 1994; Larson et al. 2010; Leung et al. 2012; Lo et al. 2012). In contrast, in foetal wounds, it is often difficult to distinguish between the unwounded site and the newly repaired site; this is thought to be a result of thinner type I collagen fibres being deposited in a reticular pattern (Mast et al. 1992; Broker et al. 1999; Bullard et al. 2003; Larson et al. 2010; Leung et al. 2012; Lo et al. 2012; Yagi et al. 2016). There is also a reduced presence of lysyl oxidase in foetal wounds, resulting in less collagen cross-linking occurring. In contrast, a much increased activity of prolyl hydroxylase is seen in foetal wounds. This enzyme functions as a rate-limiting step in collagen synthesis (Lorenz & Adzick 1993; Bullard et al. 2003; Rolfe & Grobbelaar 2012). The presence of type III collagen and reduced collagen cross-linking may be responsible for an increased

elasticity of the wound and therefore, preventing the rigid structure often reported with fibrotic tissue in scarring (Bullard et al. 2003; Larson et al. 2010; Leung et al. 2012).

Another important compositional difference between adult and foetal wounds is the high levels of hyaluronan and hyaluronan receptor present in foetal wounds (Longaker et al. 1991; Laurent et al. 1995; Fraser et al. 1997; Chen & Abatangelo 1999; Bullard et al. 2003; Larson et al. 2010; Leung et al. 2012; Rolfe & Grobbelaar 2012). Hyaluronan has been shown to increase the migration of foetal fibroblasts to the wound site, enhancing their presence. Once at the site, hyaluronan is deposited rapidly. Hyaluronan has been shown to remain at the wound site for a prolonged period in early-gestational foetal healing, indicating that hyaluronan is required for synthesising a new ECM with an organised structure. This is in comparison to adult wounds where lower amounts of hyaluronan are present earlier and more briefly (Longaker et al. 1991; Mast et al. 1992; Alaish et al. 1994; Huang et al. 2008; Larson et al. 2010; Leung et al. 2012; Lo et al. 2012; Rolfe & Grobbelaar 2012; Yagi et al. 2016). Increased presence of hyaluronan has also been thought to result in reduced deposition of collagen in the granulation tissue, reducing the subsequent scar formation. This was demonstrated through fibrosis occurring in the absence of hyaluronan (Chen & Abatangelo 1999; Yagi et al. 2016). Due to the ability of hyaluronan to increase type III collagen and TGF-β_3 levels, both of which have been associated with a scarless healing outcome; increased presence of native hyaluronan may contribute to the scarless healing phenotype associated with early-gestational foetal wound healing (David-Raoudi et al. 2008; Kishi et al. 2012; Lee et al. 2012; Leung et al. 2012; Lo et al. 2012).

The synthesis and remodelling of new ECM is a tightly regulated process, with a careful balance between MMPs and their inhibitors, TIMPs. The combination of both play a vital part in the remodelling process of the ECM. In foetal wounds, a higher MMP presence and a decreased TIMP presence is observed, resulting in an increase in ECM turnover, allowing scarless healing to occur (Bullard et al. 2003; Dang et al. 2003; Satish & Kathju 2010; Rolfe & Grobbelaar 2012; Yagi et al. 2016). In scarring wounds, there is an increased expression of both TIMP-1 and -2, along with a decreased MMP-2 expression. This decreases the rate of ECM turnover leading to the

formation of fibrotic tissue (Lafuma et al. 1994; Lee et al. 2015; Rohani & Parks 2015). In foetal scarless healing, there is a quicker and upregulated expression of MMP-1, -2, -9 and -14. MMP-1 is associated with a preference for the breakdown of type III collagen, which has an increased presence in foetal wounds, compared to adult dermal wounds (Welgus et al. 1981; Nwomeh et al. 1998; Dang et al. 2003; Dasu et al. 2003; Lu et al. 2011; Rolfe & Grobbelaar 2012). Additionally, the presence of either TGF-β_1 or -β_3 in foetal scarless wounds is associated with an increased expression of MMP-13 increasing the ECM turnover; whereas MMP-13 expression is undetectable in adult dermal wounds (Ravanti et al. 1999, 2001; Toriseva & Kähäri 2009).

All of these variations in MMP and TIMP expression between adult and foetal wound healing results in an increased ECM turnover occurring in foetal wounds, potentially leading to a more organised composition of the new ECM. This is due to an increased ECM turnover preventing an excessive deposition of newly-synthesised ECM and the resultant formation of fibrotic tissue in the dermis (Bullard et al. 2003; Larson et al. 2010; Lo et al. 2012; Rolfe & Grobbelaar 2012; Yagi et al. 2016). The discovery that the newly synthesised ECM in foetal wounds is present in an organised manner was a surprising find. It was originally thought that the rapid laying down of collagen fibres would result in a disorganised structure (Mast et al. 1992; Larson et al. 2010; Lo et al. 2012; Malik et al. 2015; Yagi et al. 2016). It is the composition and structure of the underlying dermis that determines the presence and appearance of a scar, with an unorganised ECM being a major contributor to scarring. Therefore, there is the potential that synthesising a new ECM in an organised fashion can aid in the prevention of scar development (Mast et al. 1992; Shah et al. 1995; Larson et al. 2010).

1.4.2 Oral Mucosal Wound Healing

During oral mucosal wound healing, there is a dramatically reduced scar formation, but it is not thought to be completely scarless, as seen with early-gestational foetal wound healing (Whitby & Ferguson 1991; Szpaderska et al. 2003; Enoch et al. 2008; Nauta et al. 2011; Turabelidze & DiPietro 2012; Glim et al. 2013). Oral mucosal wounds undergo the same wound healing stages as adult dermal wounds. However, the length of time that each stage lasts for varies and there are intrinsic differences between the dermal and oral fibroblasts (Szpaderska et al. 2003; Mak et al. 2009; Nauta

et al. 2011). In addition, despite similarities between the compositions of the skin and the oral mucosal epithelium, there are intrinsic differences between these two types of epithelium, as shown in Figure 1.6 (Stephens & Genever 2007). The oral mucosal epithelium has been show to produce a reduced angiogenic response, compared to the response in skin wounds. This could contribute to the differences in scarring seen between the two tissue types (Szpaderska et al. 2005; Novak et al. 2008; Mak et al. 2009; Chen et al. 2010). As seen with early-gestational foetal wound healing, there are differences in the keratins present in the oral mucosal epithelia, compared to adult skin epithelia. Krt13 has been shown to be present at a much higher level in oral mucosal epithelia, compared to adult skin epithelia (Waseem et al. 1999; Presland & Dale 2000; Bragulla & Homberger 2009; Turabelidze et al. 2014).

As with foetal wound healing, there is evidence of a reduced inflammatory response during oral mucosal wound healing, along with rapid re-epithelialisation; both of which contribute to the minimal scar formation of oral mucosal wounds (Szpaderska et al. 2003; Enoch et al. 2008; Mak et al. 2009; Nauta et al. 2011; Turabelidze et al. 2014). The reduced inflammatory stage is consistent with the decreased levels of neutrophils, macrophages and T cells present in oral mucosal wounds. In addition, similar to the response seen in early-gestational foetal healing, there is a reduced presence of pro-inflammatory cytokines, such as IL-6 and IL-8, along with reduced presence of growth factors, such as TGF-β_1 (Szpaderska et al. 2003; Mak et al. 2009; Chen et al. 2010; Nauta et al. 2011; Glim et al. 2015). Another contributing factor for reduced scarring is the decreased presence of pro-inflammatory cytokines, such as IL-1 and TNF-α. This coincides with the absence of the JAK-STAT signalling pathway, which has been associated with the activation of immune and inflammatory responses (Chen et al. 2010; Turabelidze & DiPietro 2012).

As previously mentioned, intrinsic differences between dermal fibroblasts and oral mucosal fibroblasts have been shown, resulting in this population being genotypically and phenotypically distinct from dermal fibroblasts (Enoch et al. 2008; Glim et al. 2013). The oral mucosal fibroblasts have been shown to possess a ‘younger’ phenotype, compared to patient-matched dermal fibroblasts. This ‘young’ phenotype is similar to the foetal fibroblast phenotype; and may be responsible for rapid and

Figure 1.6: A schematic diagram showing the composition of the oral mucosa with the cells present in each section, compared to the composition of skin (Stephens & Genever 2007).

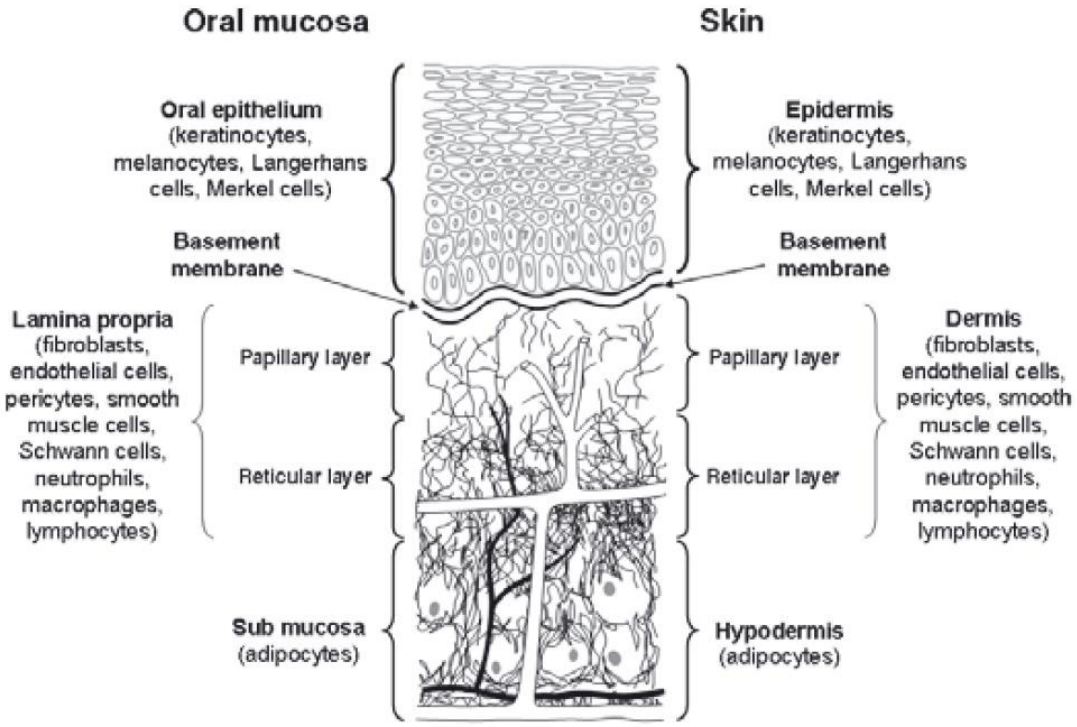

minimally scarred healing observed in oral mucosal wounds (Enoch et al. 2009, 2010). Oral mucosal fibroblasts have also been shown to senesce at much later time points than dermal fibroblasts, after undergoing a longer proliferative lifespan and a greater number of population doublings. Proliferation has also been reported to occur at a faster rate, compared to dermal fibroblasts. The delayed senescence that occurs in oral mucosal fibroblasts is due to their ability to retain their telomere length for a longer period of time, compared to population doubling level-matched, dermal fibroblasts (Lee & Eun 1999; Shannon et al. 2006; Enoch et al. 2009, 2010; Glim et al. 2013, 2014; Peake et al. 2014). Analysis was performed on the level of telomerase activity, the enzyme involved in reducing the breakdown of telomeres. However, neither oral mucosal or dermal fibroblasts expressed any active telomerase. Therefore, the oral mucosal fibroblasts are telomerase-independent, yet still able to maintain a longer proliferative lifespan. This may be an intrinsic function of this population that allows the preservation of the telomere length (Enoch et al. 2009; Marynka-Kalmani et al. 2010).

Oral mucosal fibroblasts are capable of migrating to the wound site much quicker than their dermal counterparts, resulting in a quicker re-population of the damaged area and synthesis of the new ECM (al-Khateeb et al. 1997; Shannon et al. 2006; Meran et al. 2007; Enoch et al. 2008, 2010). There are also differences in the composition of the ECM synthesised by oral fibroblasts, compared to dermal ECM. Increased presence of fibronectin and chondroitin sulphate has been observed in oral wounds. However, another study has demonstrated a less prolonged expression of fibronectin splice variant ED-A in oral wounds, compared to dermal wounds. Decreased presence of elastin has been observed in oral wounds despite a more elastic phenotype. This is potentially due to increased presence of other elastic fibres, including oxytalan and elaunin (Wong et al. 2009; Glim et al. 2013, 2014). Oral fibroblasts also impact on the organisation of the ECM, with increased organisation evident compared to dermal fibroblasts (Stephens et al. 2001a; Shannon et al. 2006; Enoch et al. 2010). Fibroblasts are associated with the synthesis of MMPs, which are vital for the remodelling of the ECM. It has been shown that there is an increased expression and production of MMP-2 by oral mucosal fibroblasts. This increased expression of MMP-2 may be a result of

a decreased expression of both TIMP-1 and TIMP-2, reducing the inhibitory action on the metalloproteinases (Stephens et al. 2001a; Chen et al. 2010; Enoch et al. 2010; Glim et al. 2013, 2014). However, a number of other MMPs were shown to have reduced presence, compared to in skin wounds; these include MMP-1, MMP-8, MMP-9, MMP-10 and MMP-13 (Chen et al. 2010). Another growth factor potentially involved in the remodelling of the ECM is hepatocyte growth factor/scatter factor (HGF/SF), which has mitogenic, motogenic and morphogenic actions. HGF increases the migratory action towards fibronectin. Oral mucosal fibroblasts have been shown to have a significantly increased expression and activity compared to dermal fibroblasts (Stephens et al. 2001b; Poomsawat et al. 2003; Shannon et al. 2006; Enoch et al. 2008).

Despite playing a vital role in blood vessel growth and subsequent delivery of oxygen and nutrients required at the wound site, it has been proposed that a high angiogenic response may contribute to the scarring phenotype. Therefore, the reduced angiogenesis observed in oral mucosal wounds may reduce scarring (Mak et al. 2009; Chen et al. 2010; Tonnesen et al. 2000; Nauta et al. 2011; Johnson & Wilgus 2014). There was also a decreased expression of certain pro-angiogenic factors in oral mucosal wounds, compared to adult dermal wounds; these include VEGF and TGF-β_1 (Szpaderska et al. 2005; Mak et al. 2009; Turabelidze et al. 2014). Resulting from the decreased TGF-β_1 expression, there is a lower ratio of TGF-β_1 to TGF-β_3 in oral mucosal wounds. This is similar to the effect seen in foetal wounds, where there is a higher TGF-β_3 to TGF-β_1 ratio, leading to the proposal that decreased TGF-β_1 or increased TGF-β_3 contributes to scarless or minimally scarred healing (Bullard et al. 2003; Shannon et al. 2006; Nauta et al. 2011; Yagi et al. 2016). Oral mucosal fibroblasts were shown to be resistant to the differentiation to myofibroblasts via TGF-β_1 stimulation. This was shown through the lack of α-SMA expression and stress fibre formation (Shannon et al. 2006; Meran et al. 2007; Enoch et al. 2008). This is compared to dermal fibroblasts, which upon activation by TGF-β_1, differentiate into the contractile phenotype myofibroblasts. This resistance to differentiating into myofibroblasts by the oral mucosal fibroblasts may contribute to the minimal scarring observed in oral mucosal wounds (Meran et al. 2007; Enoch et al. 2008). In addition, resistance to differentiation in oral fibroblasts was associated with failure of induction

of HAS1 and HAS2 transcription and failure of pericellular coat assembly. Furthermore, inhibition of HA synthesis in dermal fibroblasts significantly attenuated TGF1-mediated differentiation (Yamada et al. 2004; Meran et al. 2007; Glim et al. 2013).

Although oral mucosal wounds healed in a similar manner to dermal wounds, they exhibit a scarless healing phenotype similar to early-gestational foetal wound healing. There are a number of similarities between these two scarless healing mechanisms, including reduced inflammatory responses, reduced fibroblast differentiation to myofibroblasts, rapid fibroblast migration to the wound site; and rapid re-epithelialisation (Meran et al. 2007; Mak et al. 2009; Wong et al. 2009; Enoch et al. 2010; Glim et al. 2013; Turabelidze et al. 2014).

1.5 Dysfunctional Wound Healing Situations

As previously mentioned, the wound healing process is tightly regulated. This is required in order for successful wound closure and repair to occur (Li et al. 2007; Velnar et al. 2009; Reinke & Sorg 2012). Variations in this response can lead to detrimental wound healing responses. There are two main categories of dysfunctional wound healing, pathological scarring and chronic wounds (Menke et al. 2007; Bran et al. 2009; Shih et al. 2010; Frykberg & Banks 2015). Due to the importance of fibroblast and keratinocyte functions during wound repair, it is changes in the normal functions of these cells that have a vital impact on normal acute, dermal wound healing (Li et al. 2007; Menke et al. 2007; Bran et al. 2009).

1.5.1 Pathological Scarring

Scar formation is a normal hallmark of acute skin wound healing and is a result of wound contraction and altered collagen composition of the wound (Velnar et al. 2009; Olczyk et al. 2014). However, in some instances, pathological scarring can occur. The two main examples of this are keloids and hypertrophic scarring (English & Shenefelt 1999; Szulgit et al. 2002; Bran et al. 2009; Gauglitz et al. 2011; Huang et al. 2013). Keloids are scars that have grown past the margin of the wound site, into the surrounding healthy tissue. They also typically do not resolve over time and can cause

pain to the patient (Bran et al. 2009; Gauglitz et al. 2011; Viera et al. 2012). In addition, as some keloids can extend quite far beyond the margin, it can impact the patient's life, through both the resultant impaired functionality and the psychological impact it can have (Bran et al. 2009; Shih et al. 2010; Viera et al. 2012). This form of pathological scarring is quite rare, although there is a higher incidence in dark-pigmented populations, with approximately 6-16% incidence in African populations. There also seems to be a strong familial inheritance, with over half of keloid patients having a family history of keloid scarring (Bran et al. 2009; Russell et al. 2010; Gauglitz et al. 2011; Viera et al. 2012; Jumper et al. 2015).

There are a number of histological differences between a normal scar that occurs following wound healing and a keloid scar. Some of the main differences include no myofibroblasts, higher type I to type III collagen ratio and thick, disorganised collagen fibres, along with an increased production of ECM components (Uitto et al. 1985; Lim et al. 2002; Bran et al. 2009; Gauglitz et al. 2011; Jumper et al. 2015). The inflammatory phase appears to last longer, with a higher presence of mast cells, macrophages and lymphocytes, further promoting inflammation (Boyce et al. 2001; Shih et al. 2010; Gauglitz et al. 2011; Jumper et al. 2015). There is also an increased presence of pro-inflammatory cytokines and growth factors during inflammation, compared to normal wound healing. An up-regulation of TNF-α, IL-6, interferon (IFN)-β, TGF-β_1 and TGF-β_2 was observed in keloids, along with an increased response to PDGF and TGF-β_1 by higher levels of receptors present on fibroblasts (Mccauley et al. 1992; Tuan & Nichter 1998; Xue et al. 2000; Chen et al. 2003; Bran et al. 2009; Shih et al. 2010; Gauglitz et al. 2011). The prolonged inflammatory phase and subsequent increased release of cytokines and growth factors recruits a greater number of cells to the wound site during the proliferative phase, resulting in excessive proliferation. The increased fibroblast proliferation contributes to the fibrotic response seen in keloids (Shih et al. 2010; Gauglitz et al. 2011).

Keloid fibroblast behaviour is intrinsically different to normal dermal fibroblasts. They undergo more rapid migration and proliferation than normal dermal fibroblasts, increasing their presence at the wound site (Bettinger et al. 1996; Calderon et al. 1996; Funayama et al. 2003; Shih et al. 2010). Due to the strong paracrine feedback system

between keratinocytes and fibroblasts, it is thought that the increased activities of fibroblasts are a result of increased release of cytokines, such as IL-1 from keratinocytes (Maas-Szabowski et al. 1999; Maas-Szabowski et al. 2000; Bader & Kao 2009; Gauglitz et al. 2011; Dong et al. 2013). There are also alteration in the expression of keratins, with an increased expression of keratin 16. This keratin is typically upregulated after wounding, but is also an associated hyperproliferation marker (Mazzalupo et al. 2003; Ong et al. 2010; Jumper et al. 2015). Keloids appear to have a thickened epidermis, which may be a result of excessive keratinocyte proliferation. The increased keratinocyte presence will also feedback into the paracrine system with the fibroblasts, enhancing their activity (Lim et al. 2001; Chua et al. 2011; Gauglitz et al. 2011; Jumper et al. 2015).

Keloid fibroblasts are also capable of producing more collagen than dermal fibroblasts, approximately 2-3 times more (Uitto et al. 1985; English & Shenefelt 1999; Satish et al. 2004; Huang et al. 2013). Additionally, in some keloids, there is a decreased breakdown of the ECM, as a result of down-regulated MMP-9, although MMP-2 has been shown to be up-regulated (Satish et al. 2004; Imaizumi et al. 2009; Ulrich et al. 2010; Gauglitz et al. 2011). There is also an altered expression of hyaluronan. It is typically present in the papillary dermis in normal dermal wounds, but is present between the epidermal layers in keloids. Despite the increased presence of hyaluronan, especially smaller molecular weight fragments (<400 kDa) associated with fibrosis, keloids possess a decreased presence of hyaluronan compared to normal scar tissue and unscarred tissue, leading to the potential treatment option of high molecular weight hyaluronan addition to keloid tissue (David-Raoudi et al. 2008; Meyer et al. 2000; Tan et al. 2011; Hoffmann et al. 2012; Jumper et al. 2015; Tracy et al. 2016). Hyaluronan is an important ECM component and has shown to be increased in scarless healing responses. It has important functions in regulating inflammation and is involved in fibroblast proliferation and migration (Longaker et al. 1991; Mast et al. 1992; Meyer et al. 2000; Ghatak et al. 2015; Jumper et al. 2015; Tracy et al. 2016). This increased collagen production may also be due to reduced IFN-α and IFN-γ in keloids, which normally reduce the synthesis of collagen type I mRNA, by increasing the expression of p53, a pro-apoptotic gene (Satish et al. 2004; Bran et al. 2009; De Felice et al. 2009; Berman 2010; Viera et al. 2012). It appears that keloid fibroblasts undergo reduced

apoptosis, potentially due to a mutation in tumour suppressor gene, p53. This increases the presence of fibroblasts, which results in greater ECM production. The reduced apoptosis of keloid fibroblasts retains the wound healing process in a proliferative state, as opposed to continuing into the maturation phase, where proliferation and ECM synthesis decrease steadily (Ladin et al. 1998; Saed et al. 1998; Funayama et al. 2003; Broughton et al. 2006b; Bran et al. 2009; De Felice et al. 2009; Shih et al. 2010; Jumper et al. 2015).

Although keloid and hypertrophic scars are both examples of pathological scarring, they are characteristically different from each other. The most notable example is that although hypertrophic scars are also raised due to excessive scarring, the scarring does not extend past the wound margins (English & Shenefelt 1999; Broughton et al. 2006b; Bran et al. 2009; Gauglitz et al. 2011; Ding & Tredget 2015; Trace et al. 2016). There is a high incidence of hypertrophic scarring following surgery (40-70%) and even higher following burn injuries (<90%). However, unlike keloids, hypertrophic scars can regress within a few years. This scarring is more prevalent than keloids and doesn't have a higher incidence in any population. It appears within several weeks of injury, grows over a period of months, before regressing (Stadelmann et al. 1998; Bran et al. 2009; Gauglitz et al. 2011; Penn et al. 2012; Xue & Jackson 2015).

The histology of hypertrophic scars is quite different to keloids, with a higher proportion of type III collagen in hypertrophic scars, which is organised in fine, parallel bundles to the epidermal surface (Bran et al. 2009; Oliveira et al. 2009; Verhaegen et al. 2009; Gauglitz et al. 2011; Rabello et al. 2014). There are also myofibroblast containing nodules within the scar tissue, which stains positively for α-SMA. Apoptosis of these cells occurred much later than in normal acute wound healing, after a few years instead of a few weeks. This excess myofibroblast activity results in excessive contraction of the wound site (Moulin et al. 2004; Broughton et al. 2006b; Slemp & Kirschner 2006; Bran et al. 2009; Gauglitz et al. 2011; Sarrazy et al. 2011; Rabello et al. 2014). Some other characteristic features of hypertrophic scars include increased cell presence, increased vasculature, increased chondroitin sulphate and increased collagen synthesis. The increased collagen deposition is not due to abnormal responses to growth factors, as seen with keloids; the synthesis of ECM

occurs over an extended period of time, resulting in excess deposition (Kischer et al. 1975; Scott et al. 1995; Bran et al. 2009; Rabello et al. 2014; Zhu et al. 2016). Fibroblast presence is increased in hypertrophic scars, compared to normal wounds, but proliferative ability is not affected. The increased number of fibroblasts, together with an overexpression of TGF-β_1 increases the presence of contractile myofibroblasts (Nedelec et al. 2001; Wang et al. 2008; Gauglitz et al. 2011; Sarrazy et al. 2011; Rabello et al. 2014).

1.5.1.1 Existing Therapies for Pathological Scarring

Both of these pathological scarring phenotypes have an impact on patients quality of life, with some causing considerable disability and psychological implications. It has a huge clinical burden, as approximately 100 million patients per year in the developed world, develop a scar following surgery (English & Shenefelt 1999; Al-Attar et al. 2006; Gurtner et al. 2008; Gauglitz et al. 2011; Ding & Tredget 2015; Andrews et al. 2016). There are a number of treatment options available for keloids and hypertrophic scars, often one of the first options is surgery to remove the excess scar tissue. Hypertrophic scars do not recur following surgical removal of the scar tissue and may resolve themselves if left for a longer period (English & Shenefelt 1999; Niessen et al. 1999; Broughton et al. 2006b; Bran et al. 2009; Gauglitz et al. 2011; Rabello et al. 2014). In nearly 100% of the cases, keloid scar tissue will reoccur and despite this probability, it is often still the first treatment strategy. However, as surgical excision creates another wound site, many cases have shown the formation of a larger keloid at the original site (Berman & Bieley 1996; English & Shenefelt 1999; Al-Attar et al. 2006; Broughton et al. 2006b; Slemp & Kirschner 2006; Bran et al. 2009; Gauglitz et al. 2011; Rabello et al. 2014) .

In patients known to form keloids or hypertrophic scar, there are a variety of preventative treatment options; these include pressure therapy, silicone gel sheeting, silicone gel and flavonoids (English & Shenefelt 1999; Al-Attar et al. 2006; Slemp & Kirschner 2006; Gauglitz et al. 2011; Gold et al. 2014; Andrews et al. 2016; Trace et al. 2016). These treatment options are prophylactic, so are not suitable on formed keloids or hypertrophic scars, they can only be used in a preventative manner. These treatments often need to be performed for several months, in order to prevent scar

formation (Kischer et al. 1975; English & Shenefelt 1999; Gauglitz et al. 2011; Gold et al. 2014). Pressure therapy has been shown to be successful, but requires pressure to be exerted onto the site for 18-24 hours, for several months. It is thought that this pressure impacts on ECM synthesis and degradation, increasing degradation and resulting in decreased presence of chrondroitin sulphate. Additionally, compression therapy has been shown to increase prostaglandin E_2 (PGE_2) levels, reducing collagen synthesis. This process resolves the scar, however, due to the discomfort with this therapy, there is a reduced patient compliance (Kischer et al. 1975; Reno et al. 2001; Al-Attar et al. 2006; Broughton et al. 2006b; Gauglitz et al. 2011; Trace et al. 2016). Silicone gel sheeting, or silicone gel in areas of continuous movement, is another recognised therapy. It is thought that the beneficial response is a result of maintained hydration of the wound site (Lyle 2001; Broughton et al. 2006b; Zurada et al. 2006; Atiyeh 2007; Ogawa 2010; Gauglitz et al. 2011; Gold et al. 2014; Rabello et al. 2014). This hydration may have a positive effect on the keratinocytes and result in beneficial fibroblast function and response to growth factors and the subsequent reduced deposition of collagen (Niessen et al. 1998; Lyle 2001; Broughton et al. 2006b; Zurada et al. 2006; Atiyeh 2007; Mustoe 2008; Rabello et al. 2014). Flavonoids are a topical cream, which are thought to possess anti-fibrotic properties, through the inhibition of fibroblast proliferation, synthesis of collagen and wound contracture (Atiyeh 2007; Cho et al. 2010; Gauglitz et al. 2011; Kandasamy et al. 2011).

The current therapies available for treating developed scars, include corticosteroids, cryotherapy, scar revision, radiotherapy and laser therapy (Al-Attar et al. 2006; Broughton et al. 2006b; Slemp & Kirschner 2006; Atiyeh 2007; Ogawa 2010; Gauglitz et al. 2011; Gold et al. 2014; Rabello et al. 2014; Trace et al. 2016). Corticosteroids are often one of the main initial treatment options, especially for keloids. This dampens the inflammatory response, which reduces the downstream responses, resulting in reduced fibroblast proliferation and collagen deposition. Several applications are typically required and successful scar resolution can occur in 50-100% cases. However, recurrence can occur in up to 50% of cases (Maguire Jr. 1965; Chowdri et al. 1999; Niessen et al. 1999; Roques & Téot 2008; Gauglitz et al. 2011; Gold et al. 2014; Rabello et al. 2014). Cryotherapy is of use in small scars and induces damage to the vasculature through spray application of liquid nitrogen. Application has been

delivered through intralesional-needle cryoprobe, which reduces scar volume by approximately 50% (Zouboulis et al. 1993; Zouboulis et al. 2002; Har-Shai et al. 2003; Broughton et al. 2006b; Gauglitz et al. 2011; Trace et al. 2016). Radiotherapy has been a therapeutic option towards keloids for many years and successful treatment probabilities have increased over the years, with approximately 64-98% successful scar resolution. It is thought to inhibit the proliferation of fibroblasts in the keloid, increase the rate of keloid fibroblast apoptosis, decreasing collagen deposition. However, the treatment dose is restricted due to potential side effects, including atrophy and erythema (Levy et al. 1976; Niessen et al. 1999; Ogawa et al. 2003; Al-Attar et al. 2006; Broughton et al. 2006b; Gauglitz et al. 2011; Lee & Park 2015). Laser therapy has been used on keloids, using a pulsed-dye laser. This is also beneficial to early hypertrophic scars. It is also thought to impact on fibroblast proliferation and the downstream functions of the cell, whilst causing minimal contraction of the scar (Alster & Williams 1995; Alster & Nanni 1998; Broughton et al. 2006b; Bouzari et al. 2007; Parrett & Donelan 2010; Gauglitz et al. 2011; Jin et al. 2013). Despite the wide range of treatment options, often requiring multiple applications, there are few studies showing their effectiveness. Additionally, there is a wide range in the chance of a successful outcome, with a high incidence of recurrence for keloid scars; a number of side effects have also been associated with these treatments (Al-Attar et al. 2006; Broughton et al. 2006b; Slemp & Kirschner 2006; Gauglitz et al. 2011; Gold et al. 2014; Rabello et al. 2014; Trace et al. 2016).

More recently introduced therapies include interferon (IFN-α-2b) and 5-fluorouracil (5-FU); both of which are injected into the scar tissue site (Al-Attar et al. 2006; Broughton et al. 2006b; Atiyeh 2007; Ogawa 2010; Gauglitz et al. 2011; Gold et al. 2014; Rabello et al. 2014; Trace et al. 2016). IFN-α was shown to be decreased in keloids and injection of IFN-α-2b may impair fibroblast function, in particular the deposition of collagen. This is also due to increased collagenase activity. It has also been shown to reduce the proliferative action of fibroblasts, reducing their overall presence at the scar site; although some studies have reported this treatment to be ineffective (Wong et al. 1994; Berman & Flores 1997; Al-Attar et al. 2006; Broughton et al. 2006b; Davison et al. 2006; Slemp & Kirschner 2006; Gauglitz et al. 2011; Gold et al. 2014; Rabello et al. 2014). However, there are side effects with application of

IFN-α-2b. These are typically flu-like symptoms, including fever, along with pain on injection, in addition it is an expensive therapy (Al-Attar et al. 2006; Broughton et al. 2006b; Slemp & Kirschner 2006; Gauglitz et al. 2011; Rabello et al. 2014). 5-FU increases fibroblast apoptosis in keloids and inflamed hypertrophic scars. This along with an inhibited fibroblast proliferation reduces their presence and the subsequent amount of collagen synthesised (Uppal et al. 2001; Kontochristopoulos et al. 2005; Broughton et al. 2006b; Gauglitz et al. 2011; Wilson 2013; Gold et al. 2014; Rabello et al. 2014; Jones et al. 2015; Shah et al. 2016). It has been shown to more effective when given alongside corticosteroid treatment, with a reduction in scar size by approximately 50% appears to occur in most patients (Asilian et al. 2006; Broughton et al. 2006b; Davison et al. 2009; Gauglitz et al. 2011; Gold et al. 2014; Rabello et al. 2014). Despite the beneficial responses seen, there are a few side effects observed in this treatment, including pain on injection, burning sensation and formation of ulcers (Apikian & Goodman 2004; Kontochristopoulos et al. 2005; Al-Attar et al. 2006; Gauglitz et al. 2011; Trace et al. 2016). More successful treatment options are essential for the resolution of these debilitating pathological scars. Consequently, further understanding of the aetiology and pathogenesis of keloids and hypertrophic scars may elucidate target mechanisms for successful outcomes (Al-Attar et al. 2006; Slemp & Kirschner 2006; Atiyeh 2007; Gauglitz et al. 2011; Rabello et al. 2014; Trace et al. 2016).

1.5.2 Chronic Wounds

Chronic wounds are one of the predominate examples of impaired healing, where the integrity of the skin is not restored following injury. This increases the risk of contamination and a potential loss of function at the site. There are a range of wounds that fall under this category, including venous leg ulcers, diabetic ulcers and pressure ulcers. Incidence of these chronic wounds increases with age and prevalence of diabetes (Gosain & DiPietro 2004; Menke et al. 2007; Posnett & Franks 2008; Gorecki et al. 2009; Dreifke et al. 2015; Demidova-Rice et al. 2012a; Frykberg & Banks 2015). These non-healing wounds can last for a considerable length of time, typically a minimum of 3 months, but a large proportion last over a year. This has a significant impact on the patient, through pain, lack of mobility, psychological impact and increased morbidity (Posnett & Franks 2008; Sen et al. 2010; Agale 2013; Trøstrup et

al. 2013; Dreifke et al. 2015; Frykberg & Banks 2015). In addition to the impact on patients, there is also an extensive clinical burden on the NHS caused by treating these chronic wounds. It is estimated to cost approximately £5 billion per year, equating to about 3% of the UK healthcare expenditure. This cost has almost doubled in less than a decade. This is broken down to approximately £2 billion per year, spent on long-lasting wounds, which healed within a year; and £3 billion per year, on wounds which did not heal during the study duration (Posnett & Franks 2008; Trøstrup et al. 2013; Guest et al. 2015; Guest et al. 2016).

A common feature of chronic wounds and burn injuries is the lack of re-epithelialisation. Without re-establishing the protective barrier, the wound site is vulnerable to infection and further morbidity. There are a number of intrinsic differences in chronic wounds, compared to acute wounds, which contribute to this non-healing phenotype and lack of re-epithelialisation (Stojadinovic et al. 2005; Menke et al. 2007; Agren & Werthén 2007; Usui et al. 2008; Wikramanayake et al. 2014; Dreifke et al. 2015; Frykberg & Banks 2015). Keratinocyte function is often directly impaired in diabetic patients, in particular migratory ability. This is partly due to dysfunctional ECM and a reduced response to EGF and other growth factors involved in promoting keratinocyte migration (Stojadinovic et al. 2005; Agren & Werthén 2007; Brem et al. 2007; Usui et al. 2008; Schultz & Wysocki 2009; Dreifke et al. 2015). It is thought that an impaired response to EGF is a result of over-activation of β-catenin, preventing keratinocytes from responding to the growth factor signals promoting migration. One theory regarding this reduced response to EGF signalling is that the EGF receptor typically present on the keratinocyte membrane is found in the cytoplasm of keratinocytes in chronic wounds, preventing the induction of migratory signals (Nanney et al. 1984; Stojadinovic et al. 2005; Brem et al. 2007; Barrientos et al. 2008). EGF is also thought to be proteolytically degraded due to the high presence of metalloproteinases in the chronic wound exudate (Robson 1997; Yager et al. 1997; Trengrove et al. 1999; Barrientos et al. 2008). Additionally, β-catenin over-activation also has a downstream response, over-activating oncogene c-myc. This results in excessive cycling of epidermal stem cells, reducing their ability to respond effectively to wounding (Arnold & Watt 2001; Stojadinovic et al. 2005; Agren & Werthén 2007). Some studies have also indicated a senescent phenotype of the keratinocytes present

at chronic wounds, which could account for the reduced re-epithelialisation response (Telgenhoff & Shroot 2005; Frykberg & Banks 2015). High levels of IL-8 has been detected in chronic wounds, expression of this inflammatory cytokine has been shown to further stimulate the chemotaxis of immune cells, including neutrophils contributing to the excessive inflammation. However, it has also been shown to induce a proliferative and migratory effect on keratinocytes (Rennekampff et al. 2000; Scapini et al. 2000; Barrientos et al. 2008; Wiegand et al. 2010; Jiang et al. 2012; Singh et al. 2016).

Levels of bFGF have been shown to be reduced in chronic wounds. This growth factor is involved in re-epithelialisation, through increasing keratinocyte motility by Rac activation. Fibroblast migration is also reduced with lowered expression of bFGF, along with a reduced synthesis of ECM components and MMPs (Sogabe et al. 2006; Barrientos et al. 2008; Xie et al. 2008; Akita et al. 2012). TGF-β_1 and its receptor are also reduced in chronic wounds, again potentially degraded by the proteolytic environment. Potentially contributing to the reduced TGF-β_1 expression, levels of PDGF are also lowered in chronic wounds. This growth factor indirectly stimulates the release of TGF-β_1, in addition to stimulating angiogenesis, re-epithelialisation, fibroblast proliferation and subsequent ECM synthesis (Cooper et al. 1994; Robson 1997; Yager et al. 1997; Barrientos et al. 2008; Demidova-Rice et al. 2012b). Chronic wound fibroblasts have often been described as being senescent, or exhibiting decreased proliferation, potentially due to the high levels of oxidative stress in the wound environment (Mendez et al. 1998; Cook et al. 2000; Telgenhoff & Shroot 2005; Menke et al. 2007; Wall et al. 2008; Frykberg & Banks 2015). It is thought that the chronic wound fibroblasts still synthesise similar quantities of ECM, although it may be defective. This may be partly a result of variations in MMP and TIMP expression levels. Decreased MMP-1 and MMP-2 expression occurs with increased TIMP-1 and TIMP-2 expression (Cook et al. 2000). Other studies have shown that the wound fluid contains higher level of MMPs, due to the excessive inflammation. These MMPs are thought to degrade a number of vital growth factors required to successful ECM deposition (Yager et al. 1996; Yager et al. 1997; Trengrove et al. 1999; Yager & Nwomeh 1999; Telgenhoff & Shroot 2005; Menke et al. 2007; Frykberg & Banks 2015). The inflammatory response in chronic wounds has been reported to last longer

than in acute wounds. This is reported to be a result of a detrimental feedback system, where neutrophils are continually recruited to the wound site and release factors, which stimulates further chemotactic signals to neutrophils (Fivenson et al. 1997; Moseley et al. 2004; Eming et al. 2007; Menke et al. 2007; Wiegand et al. 2010; Wilgus et al. 2013). The wound environment appears to be causing this feedback system, by hypoxia or bacterial presence (Stephens et al. 2003; Jones et al. 2004; Menke et al. 2007; Schultz & Wysocki 2009). Diabetic wounds are thought to possess high levels of MMPs, due to the hyperglycaemic increased expression of TNF-α and IL-1β. This contributes to the impaired ECM synthesis (Lobmann et al. 2002; Muller et al. 2008; Lev-Tov et al. 2013; Xu & Graves 2013; Dreifke et al. 2015). The dysfunctional ECM is thought to impede keratinocyte migration, as a result of a lack of basement membrane components required for lamellipodial cell movement across the matrix (Agren & Werthén 2007; Usui et al. 2008; Krishnaswamy & Korrapati 2014; Thamm et al. 2015). All of these factors contribute to the phenotype observed in chronic non-healing wounds, impacting across the wound healing phases, including excessive inflammation, impaired re-epithelialisation, dysfunctional ECM synthesis (Menke et al. 2007; Demidova-Rice et al. 2012a; Trøstrup et al. 2013; Dreifke et al. 2015).

1.5.2.1 Existing Therapies for Chronic Wounds

Despite the huge clinical burden and a need for therapies, there are no wound healing strategies that are adequate enough to resolve these wounds. Consequently, this burden is only going to increase with an increased prevalence of diabetes and an ageing population (Posnett & Franks 2008; Werdin et al. 2009; Sen et al. 2010; Trøstrup et al. 2013; Dreifke et al. 2015). There are a number of treatment options available, but these typically involve debriding the wound of any contaminants and applying topical dressings (Bradley 1999; O'Donnell & Lau 2006; Agren & Werthén 2007; Menke et al. 2007; Dreifke et al. 2015).

There a number of topical ECM therapies, which categorised into 4 main families, collagen-based, non-collagen, biosynthetic composite scaffolds and processed native skin; these are all acellular therapies (O'Donnell & Lau 2006; Agren & Werthén 2007; Demidova-Rice et al. 2012b; Dreifke et al. 2015; Frykberg & Banks 2015). There are a variety of collagen-based ECM topical products, including: Oasis®, Promogran® and

Matrix Collagen™. These are decellularised human or animal tissue, that can provide a stable scaffold for the influx of cells required to establish a more permanent ECM and aid wound repair. Some improvements in wound healing rates have been observed with these dressings, although with some collagen-based topical dressings, this is not a significant improvement compared to good wound care (Veves et al. 2002; Niezgoda et al. 2005; O'Donnell & Lau 2006; Agren & Werthén 2007; Holmes et al. 2013; Lev-Tov et al. 2013; Dreifke et al. 2015; Frykberg & Banks 2015). One of the main non-collagen based ECM therapies is hyaluronan, due to its important role in promoting wound healing process. The most notable example of this dressing is Hyalofill®, an esterified hyaluronic acid. This treatment appeared to be more beneficial to wound closure and repair than standard wound care practice (Edmonds et al. 2000; Lobmann et al. 2003; Vazquez et al. 2003; Agren & Werthén 2007; Voigt & Driver 2012; Longinotti 2014; Boateng & Catanzano 2015; Dreifke et al. 2015). The two main biosynthetic composite scaffolds are Biobrane and Integra, made from porcine and bovine collagen with a silicone layer, respectively. Both were typically used in the treatment of burns, but Integra has also more recently been used to treat chronic wounds (Ruszczak 2003; Agren & Werthén 2007; Mcheik et al. 2014; Dreifke et al. 2015; Frykberg & Banks 2015; Rowan et al. 2015). Biobrane has been shown to result in increased infection rates, through an increase in bacterial presence at the site. This is not optimal for chronic wounds where increased risk of infection already occurs (Agren & Werthén 2007; Schultz & Wysocki 2009; Dreifke et al. 2015; Tan et al. 2015; Schulz et al. 2016). Processed native skin dressings can be human or animal-derived, this includes human cadaver graft, Alloderm® and porcine graft, E-Z Derm™. Alloderm® is considered for use on full-thickness diabetic ulcers, whereas E-Z Derm™ is considered for use on pressure ulcers; both are acellular biologic dressings (Wainwright 1995; Callcut et al. 2006; Agren & Werthén 2007; Broussard & Powers 2013; Rowan et al. 2015). Despite the wide range of dressing options, there are few studies on their effectiveness, whilst some have considered that repeated dressing changes may be detrimental to the wound healing response, due to the disruption of the wound surface (O'Donnell & Lau 2006; Agren & Werthén 2007; Boateng & Catanzano 2015; Dumville et al. 2015; Harding 2015).

Another popular wound healing therapy is negative pressure wound therapy (NPWT), which uses a suction method on the chronic wound site to remove any contaminants and wound exudate (Kasuya & Tokura 2014; Boateng & Catanzano 2015; Dumville et al. 2015; Frykberg & Banks 2015; Harding 2015). The suction pressure on the wound is also thought to aid wound contraction, drawing the wound edges together. Antimicrobials can also be delivered to the site, aiding the clearance of infection from the wound (Saxena et al. 2004; Armstrong et al. 2005; Kirby 2007; Vikatmaa et al. 2008; Frykberg & Banks 2015). This treatment modality can be used in combination with another option, such as topical dressings, to further increase the chance of wound resolution (Scherer et al. 2008; Isaac et al. 2014; Frykberg & Banks 2015). It is a more expensive treatment option, compared to the relatively low cost topical dressings. However, studies have indicated positive effects on wound healing following its application (Kirby 2007; de Leon et al. 2009; Frykberg & Banks 2015; Harding 2015). Conversely, other studies have suggested a bias in these positive outcomes and questioned the efficacy of the treatment. However, as it can benefit the wound site, through the clearance of infection, it is widely used on chronic wounds (Armstrong et al. 2005; Kirby 2007; Vikatmaa et al. 2008; Frykberg & Banks 2015; Harding 2015).

Split-thickness autografts are considered one of the best treatment options for chronic wounds, through application of donor or cultured skin grafts over the chronic wound site (Sheridan & Tompkins 1999; Loss et al. 2000; Atiyeh & Costagliola 2007; Dreifke et al. 2015; Frykberg & Banks 2015). There are a number of limitations with this treatment option, including a high risk of scar tissue formation at the wound site and limited sites available for harvesting of donor skin (Weber et al. 1995; Hallock 1999; Atiyeh & Costagliola 2007; Dreifke et al. 2015). In addition, the use of donor epidermal keratinocytes carries the risk of donor-site complications and donor keratinocytes from younger adults have an increased response to growth factors, in particular KGF (Harris 1998; Koller et al. 2002; Dreifke et al. 2015). However, cultured epithelial autografts requires an additional wound site on the patient for extraction of the cell required. This delays treatment while the cultured cells expand to form a graft, but also carries no risk of graft rejection. Additionally, there is a high cost associated with this treatment option (Loss et al. 2000; Atiyeh & Costagliola 2007; Dreifke et al. 2015).

As often, vital growth factors are degraded by the high level of proteases in chronic wounds, direct topical application of growth factors has been evaluated as a therapy, including recombinant EGF and PDGF (Robson 1997; Niezgoda et al. 2005; Barrientos et al. 2008; Hardwicke et al. 2010; Ching et al. 2011). A masking technique was used with dextrin, to shield the growth factor from degradation, until at the wound site, where enzymatic degradation of the biodegradable dextrin polymer. The conjugate of dextrin-recombinant human EGF was analysed and determined a potential beneficial wound healing response on keratinocytes proliferation and migration (Hardwicke et al. 2008, 2010). This indicates a potential use in chronic wounds, although replacement of one growth factor only targets one aspect of the impaired wound healing observed in chronic wounds (Robson 1997; Menke et al. 2007; Hardwicke et al. 2010; Ching et al. 2011; Frykberg & Banks 2015).

Another growth factor therapy available is becaplermin gel, marketed as Regranex®, which is a recombinant form of isoform PDGF-BB. This is applied as a topical gel to the wound site and is the only pharmaceutical currently approved by the Food and Drug Administration (FDA) for chronic wounds (Edmonds et al. 2000; Goldman 2004; Barrientos et al. 2008; Fang & Galiano 2008; Dreifke et al. 2015; Frykberg & Banks 2015). As mentioned previously, PDGF has a number of beneficial functions during wound healing, including chemoattraction of immune cells, fibroblast proliferation and involvement in stimulation of ECM synthesis. It has also been shown to have reduced presence in chronic wounds, potentially due to its degradation by the high expression of wound proteases (Pierce et al. 1989a; Greenhalgh et al. 1990; Robson 1997; Uchi et al. 2000; Barrientos et al. 2008; Fang & Galiano 2008). Application of this topical gel has shown an increased wound closure ability, although there have been conflicting results, resulting in a wide percentage of successful wound closure. This is partially dependent on the type of chronic wound (Rees et al. 1999; Smiell et al. 1999; Goldman 2004; Niezgoda et al. 2005; Fang & Galiano 2008). However, in approximately a third of cases, there was evidence of recurrence of diabetic ulcers. In addition, concerns have been raised about the risk of tumour formation after use of 3 or more tubes of Regranex®. This warning, issued by the FDA, was aimed at patients with a previous history of malignancies, but questions whether the benefit is sufficient

to outweigh these risks (Lacci & Dardik 2010; Papanas & Maltezos 2010; Ziyadeh et al. 2011; Dreifke et al. 2015).

Despite all the treatment options described, chronic wounds are still highly prevalent, causing reduced quality of life for a number of patients and a major clinical burden on healthcare systems. The therapies available are not adequate enough to tackle rising burden, requiring alternative, cost-effective treatment options to be developed, with the aim of resolving chronic wounds in a shorter time frame, successful re-epithelialisation of the wound and remodelling of the underlying dermal matrix (Posnett & Franks 2008; Werdin et al. 2009; Sen et al. 2010; Trøstrup et al. 2013; Boateng & Catanzano 2015; Dreifke et al. 2015; Frykberg & Banks 2015).

1.6 EBC-46 and EBC-211

An Australian drug discovery company, EcoBiotics Ltd. (Queensland, Australia) have developed the technology, EcoLogic. Through an understanding of how the rainforest ecosystem is maintained, specific knowledge was collected on a number of plant species allowing those with the potential to produce chemicals with highly desirable properties to be selected for further development, with the aim of novel drug development (EcoBiotics Ltd). A subsidiary company of EcoBiotics Ltd; QBiotics Ltd. was demerged from EcoBiotics Ltd. due to the different expertise required in each company. Through EcoLogic, the naturally derived epoxy-tigliane, EBC-46 (12-tigloyl-13-(2-methylbutanoyl)-6,7-epoxy-4,5,9,12,13,20-hexahydroxy-1-tigliane-3-one), was discovered in the Queensland tropical rainforest and found to possess potent bioactivity.

EBC-46 was found in the seeds of the Fountain's Blushwood Tree (*Fontainea picrosperma*), indigenous to the Queensland Tropical Rainforest, and developed by QBiotics Ltd. (Queensland, Australia). EBC-46 was shown to act as a chemical deterrent to predation, in particular to the native marsupials in the surrounding area due to the high presence of an inflammatory chemical (QBiotics Ltd.). EBC-211 (12-tigloyl-13-(2-methylbutanoyl)-5,6-epoxy-4,5,9,12,13,20-hexahydroxy-1-tigliane-3-one) is a 'lesser activity' analogue of EBC-46, with approximately a 100-fold reduced

activity (QBiotics Ltd.). The chemical structure of EBC-46 (Figure 1.7A), was determined through a series of experiments to allow for large scale production to occur and it has been shown to be relatively easy to harvest. The chemical structure of EBC-211 is also shown (Figure 1.7B).

EBC-46 had been shown to possess a potent anti-cancer response, through rapid ablation of solid tumours and sarcoids, both cutaneous and non-cutaneous. The compound was administered through intra-lesional injection. This anti-tumour response has been successfully shown on melanomas, sarcomas, carcinomas, mast cell tumours and sarcoids during veterinary studies on tumours that were previously deemed inoperable. These veterinary trials have been performed on domesticated animals as a palliative treatment. Examples of these responses are shown in Figures 1.8 and 1.9 (QBiotics Ltd.). The veterinary case studies showed a significant reduction in volume of the solid tumours and sarcoids. In light of these obvious beneficial anti-tumour effects, QBiotics Ltd. has developed and registered EBC-46 as a veterinary pharmaceutical for the treatment of solid tumours in these animals. In addition, as QBiotics Ltd. has compelling proof-of-concept data of the drug's efficacy and safety both in cancer models in mice and in other domesticated animals, EBC-46 is currently undergoing development during human Phase I/II clinical trials.

These novel epoxy-tiglianes have been shown to act through the activation of classical PKC isoforms (PKC-βI, -βII, -α, and -γ), although predominantly through PKC-β (Boyle et al. 2014). Through a number of studies, it has been hypothesised that EBC-46 remains at the tumour site, due to low detection in the plasma. It is also thought to play a role in the disruption of blood supply to the tumour, through increased permeability of the cells at the tumour site causing damage to the vasculature at the specific tumour site (Boyle et al. 2014). This disruption results in sloughing of the entire tumour, with minimal impact on healthy surrounding tissue (Boyle et al. 2014; QBiotics Ltd.). Tumour ablation appears to be long-acting, due to the lack of tumour recurrence within 12 month post-treatment in the majority of cases (Boyle et al. 2014). It is thought that neutrophils also play a small part in the tumour reduction. However, the full mechanism of action has not yet been determined and further is work is being undertaken to elucidate this pathway (Boyle et al. 2014). An unexpected exceptional

Figure 1.7: Chemical structure of (A) EBC-46 and (B) EBC-211, found in seeds of Blushwood Tree (*Fontainea picrosperma*) and several species of the Fontainea, sourced in Queensland, Australia.

A

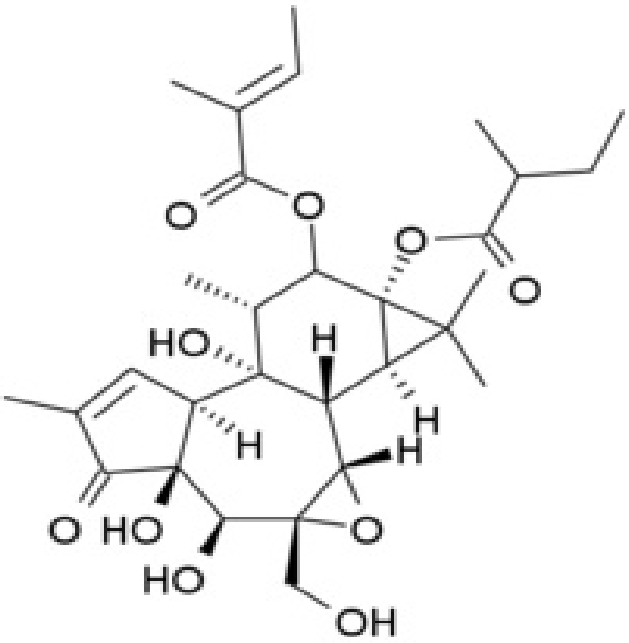

B

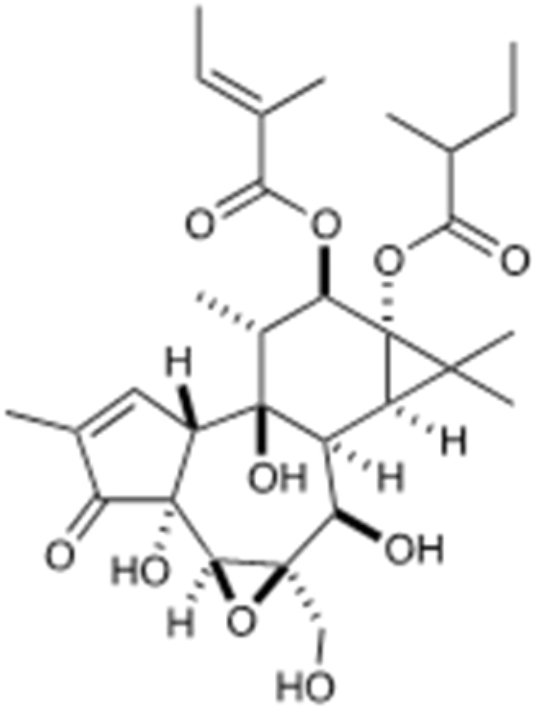

Figure 1.8: Intra-lesional injection of a large equine sarcoid with EBC-46. Left-hand image: prior to treatment. Right-hand image: 22h post-treatment, with ablation of tumour mass evident (Reddell et al. 2014; QBiotics Ltd.).

Figure 1.9: Intra-lesional injection of equine sarcoid with EBC-46. Left-hand image: Day 6 following injection of 0.75mg EBC-46. Right-hand image: Day 10 following final injection of 1.5mg EBC-46, with almost complete sarcoid loss and wound resolution (Reddell et al. 2014; QBiotics Ltd.).

wound healing response was observed following tumour ablation in these cancer studies, manifested as rapid re-epithelialisation, wound closure, reduced scarring and the reformation of skin appendages (Reddell *et al*. 2014).

Following the beneficial responses observed during the *in vivo* anti-tumour studies and *in vitro* studies, wound healing veterinary trials were initiated. Many of the cases included in these trials were on wounds that were previously unresponsive to months of treatment under current wound care strategies. These veterinary trials has demonstrated similarly significant enhancements in wound healing outcomes (Reddell et al. 2014). The case study presented in Figure 1.10 shows a deep necrosing facial wound that was previously unresponsive to 3 months treatment using current routine wound care strategies. Following application of EBC-46, rapid re-epithelialisation occurred, resolving the wound and producing an exceptional cosmetic effect. Throughout these preliminary veterinary trials and safety studies, there has been no evidence of any significant adverse effects following treatment with EBC-46 (QBiotics Ltd.).

TGF-β_1-mediated dermal fibroblast-myofibroblast differentiation is essential to wound closure, contraction and scarring, with persistence of myofibroblasts observed in fibrosis. Therefore, fibroblasts and myofibroblasts are a viable pharmaceutical target to explain the minimal scarring observed with epoxy-tigliane treatment. Additionally, due to the huge clinical burden associated with chronic wounds and burn injuries, where wounds fail to re-epithelialise, keratinocytes would be a pharmaceutical target of great interest as a result of their role in re-epithelialisation.

Figure 1.10: Effect of topical EBC-46 gel applications on a non-healing deep necrosing facial wound at 28 days. A single dose was injected into multiple sites around wound area (0.5mg/ml EBC-46). (A) Prior to treatment; (B) 3 days after commencement of treatment; (C) 28 days after topical treatment protocol, prior to injection into wound site; (D) 104 days following commencement of treatment, and 76 days following injectable treatment (QBiotics Ltd.).

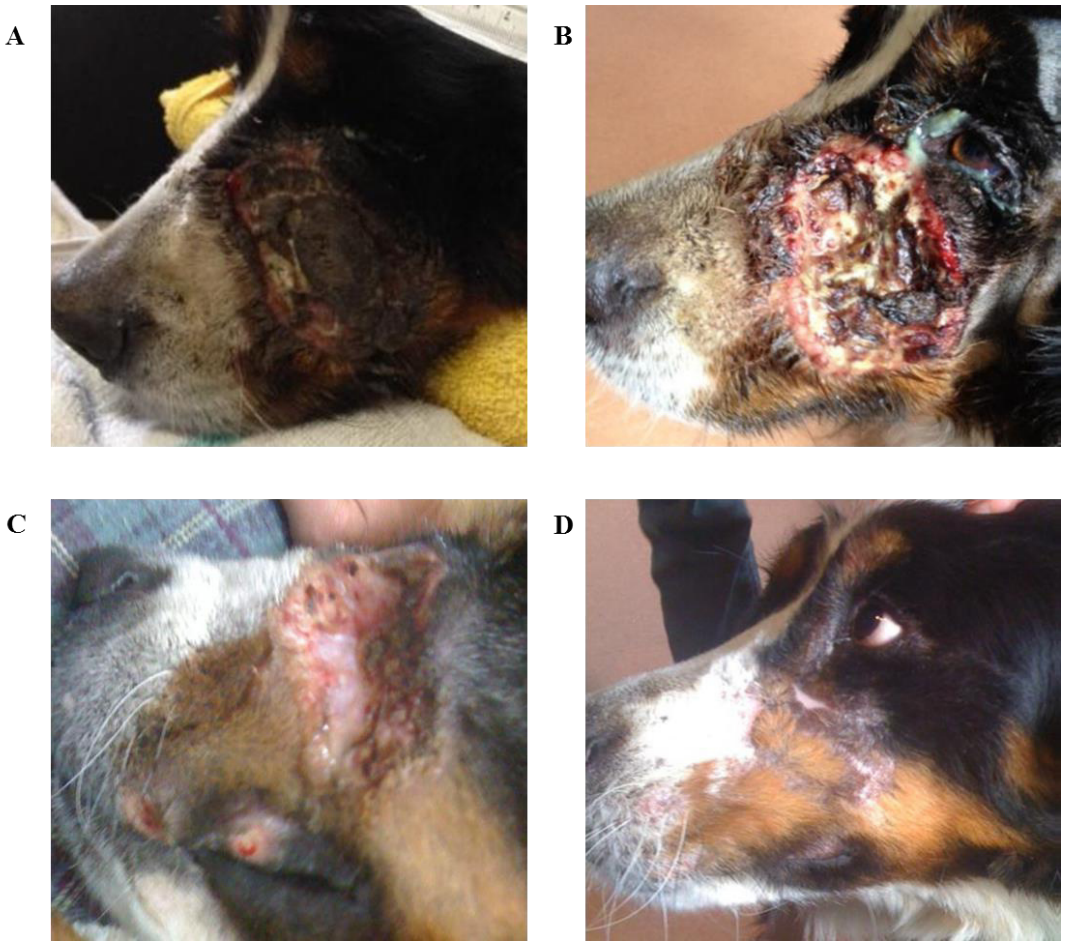

1.7 Aims of the Study

Despite the significant beneficial effects on wound healing previously observed, little is known about how the novel epoxy-tiglianes exert these responses (Reddell et al. 2014; QBiotics Ltd.). The aim of this PhD was to determine how this exceptional wound healing response is produced, through analysing the effects of EBC-46 and the 'lesser active' EBC-211 on dermal fibroblasts, myofibroblasts and keratinocytes *in vitro*; the major cell types involved in the acute skin wound healing process. In addition, the study aims to identify and elucidate the mechanisms of action responsible for these exceptional *in vivo* wound healing responses.

The specific aims of this PhD are:

- Determine whether EBC-46 and the 'lesser active' EBC-211 modulate fibroblast and keratinocyte viability, proliferation, cell cycle progression, migration and cellular morphology.
- Determine whether EBC-46 and the 'lesser active' EBC-211 modulate TGF-β_1-driven, fibroblast-myofibroblast differentiation.
- Determine the effect of EBC-46 and the 'lesser active' EBC-211 on gene expression in keratinocytes.
- Validate any key differentially expressed genes detected during global gene analysis, following treatment with EBC-46 and the 'lesser active' EBC-211.

The hypothesis of this project is that these novel epoxy-tiglianes, EBC-46 and EBC-211, may induce a more regenerative healing response, as opposed to the typical reparative healing process, which results in scar formation. By undertaking these studies, it is envisaged that a more comprehensive understanding of epoxy-tigliane responses and mechanisms of action will be gained. This could provide justification for the development of these pharmaceuticals as wound treatments for impaired and/or excessive scarring situations in skin.

Chapter 2 – Materials and Methods

Chapter 2 - Materials and Methods

2.1 Preparation of EBC-46 and EBC-211

EBC-46 and the 'lesser activity' form, EBC-211, were both supplied by QBiotics Ltd. (Queensland, Australia) and solubilised in dimethyl sulfoxide (DMSO, >99.9%, Sigma-Aldrich Company Ltd., Dorset, U.K). EBC-46 and EBC-211 were solubilised in DMSO at concentrations of 100mg/ml, and 10mg/ml respectively. Aliquots of 20µl and 25µl EBC-46 and EBC-211 were prepared respectively, so that only the required volumes were thawed when required. The solubilised compounds were stored at -20°C, where stable for several months.

Prior to use, EBC-46 and EBC-211 were warmed to room temperature. As numerous concentrations were required for analysis, stock solutions of both were diluted as appropriate to produce the required concentrations (0.001µg/ml, 0.01µg/ml, 0.1µg/ml, 1µg/ml, 10µg/ml and 100µg/ml). Each concentration was diluted in Fibroblast-Serum Containing Media (F-SCM; Section 2.2.1) or Keratinocyte-Serum Containing Media (K-SCM; Section 2.2.2). Fresh EBC-46 and EBC-211 culture medium solutions were prepared on a weekly basis, as these were stable at 4°C for a period of 1 week. Untreated controls were also prepared containing 1% DMSO, to account for the DMSO in compound containing media, due to EBC-46 and EBC-211 solubilisation in DMSO.

2.2 General Cell Culture Methods

To ensure sterility of the working environment, safety cabinets and equipment were sprayed with 70% ethanol prior to carrying out any cell culture. In addition, the incubators, safety cabinets and water baths were cleaned on a weekly basis. All consumables, glassware, some plastics, phosphate buffered saline (PBS) and double-distilled water, were sterilised through autoclaving (123°C, 15lb/m^2, 15 minutes); and any equipment required remained in the tissue culture laboratory.

2.2.1 Dermal Fibroblast Culture

Normal dermal fibroblast (NF) cultures were obtained from previously collected biopsies carried out on healthy, adult patients (*n=4*), undergoing routine oral surgery at the School of Dentistry, Cardiff University, Cardiff, UK Biopsies (6mm) were previously obtained from uninjured skin with informed consent from patients and Local Research Ethical Committee approval (09/WSE03/18) was obtained prior to the sample collection by Professor Phil Stephens, as previously described (Enoch et al. 2009, 2010). NF cultures were used in all experiments from these biopsies between passages 7-17.

NF were seeded at a cell density of $1.5x10^5/75cm^2$ tissue culture flask (Sarstedt, Leicester, UK), cultured in F-SCM (10ml), containing Dulbecco's Modified Eagle's Medium (DMEM), supplemented with 1% antibiotics (100U/ml penicillin G sodium, 100µg/ml streptomycin sulphate and 0.25µg/ml amphotericin B), 1% L-glutamine (2mM) and 10% foetal calf serum (all purchased from Thermo Fisher Scientific, Leicestershire, UK). NF were maintained in 37°C, in 5% CO_2/95% air, with F-SCM changed every 48-72h. When NF reached 80-90% confluence, cells were sub-cultured, re-suspended in F-SCM and counted to determine cell density.

2.2.2 Epidermal Keratinocyte Culture

Human adult, spontaneously immortalized, epidermal keratinocytes (HaCaT cells) were provided by Dr X.Q. Wei (School of Dentistry, Cardiff University, Cardiff, UK); and seeded at a cell density of $1.5x10^5/75cm^2$ tissue culture flask, cultured in K-SCM (10ml), containing Dulbecco's Modified Eagle's Medium (DMEM), supplemented with 1% antibiotics (100U/ml penicillin G sodium, 100µg/ml streptomycin sulphate and 0.25µg/ml amphotericin B), 1% L-glutamine (2mM) and 10% foetal calf serum (all purchased from Thermo Fisher Scientific). HaCaTs were maintained in 37°C, in 5% CO_2/95% air, with K-SCM changed every 24-48h. When HaCaTs reached 70-80% confluence, cells were sub-cultured and re-suspended in K-SCM and counted to determine cell density.

2.2.3 Cell Subculture and Counting

When NF and HaCaTs reach desired confluence, cells were passaged to maintain appropriate cell density levels. NF and HaCaTs were washed in PBS, incubated with trypsin (3ml/75cm^2 tissue culture flask, Thermo Fisher Scientific) for approximately 5min at 37°C, in 5% CO_2/95% air. Trypsin was neutralised by the addition of F-SCM or K-SCM (7ml/75cm^2 tissue culture flask) for both NF and HaCaTs. The cell suspensions containing trypsin and culture media were centrifuged at 1500xg for 5min and the resulting supernatants removed. The remaining pellets consisting of NF or HaCaTs were re-suspended in fresh F-SCM or K-SCM (10ml), respectively. Cell densities were then determined through counting viable cells. Cell suspensions (10µl) were taken and mixed well with Trypan Blue (10µl, Sigma-Aldrich Company Ltd.); 10µl of this mixture was transferred to the Neubauer Improved Haemocytometer (Thermo Fisher Scientific). As viable cells with an intact cell membrane do not allow the trypan blue stain to pass through, viable cell counts were determined through counting the non-stained cells. This was performed using a light microscope at x100 magnification (CK2 Inverted Microscope, Olympus UK Ltd., Middlesex, UK). Following cell counting, NF and HaCaTs were sub-cultured in their respective media (10ml/75cm^2), as described above.

2.2.4 Cryopreservation and Cell Retrieval

To maintain stores of cells with low passages, excess cells produced through sub-culturing were cryopreserved. The cell pellets produced through sub-culturing (Section 2.2.3), were re-suspended in a freezing solution, consisting of 10% DMSO and 90% foetal calf serum. The cell/freezing solution mixtures were placed in cryovials (Greiner Bio-One Ltd., Gloucestershire, UK) and frozen gradually over a 24h period to -80°C, through the use of an isopropanol freezing container (Sigma-Aldrich Company Ltd.); which cools cells at 1°C/minute. After the slow freezing process in the -80°C freezer, cryovials were transferred to liquid nitrogen for long term storage at -196°C.

For cell retrieval, NF and HaCaTs were removed from their storage in liquid nitrogen and the cryovials rapidly thawed at 37°C. The cells were washed in either F-SCM or K-SCM respectively, through the addition of 9ml of culture medium to 1ml of

cells/cryovial and centrifugation at 1500xg for 5min. The cell pellets obtained were re-suspended in fresh culture medium (10ml, F-SCM or K-SCM) through agitation of the pellet, before seeding the cells in fresh 75cm^2 tissue flasks.

2.2.5 Screening for Mycoplasma Contamination

Routine checks were performed on cells to determine whether mycoplasma contamination was present. This process was performed by Dr Rachael Jordan and Dr Maria Stack (School of Dentistry, Cardiff University, UK). Samples of culture media were obtained when cells reached 90-100% confluence. Samples were stored at -20°C until required for assessment, then thawed on ice before incubated at 95°C for 5min. Cellular debris was removed by centrifugation and polymerase chain reaction (PCR) Master Mix was established containing; nuclease-free water, GoTaq Green buffer, magnesium chloride, primer/nucleotide mix, internal control, GoTaq polymerase (all from Promega Ltd., Hampshire, UK). A negative control of nuclease-free water only and a positive control DNA, were used to determine whether mycoplasma contamination was present. To achieve this, a PCR reaction was prepared as follows: 2min at 94°C, followed by 39 cycles of: 30s at 94°C, 30s at 55°C, 30s at 72°C. The samples were maintained at 4°C and run on 2% agarose gels at 100V for 20min using a Mini-Horizontal Electrophoresis Unit (Jencons-PLS, Bedfordshire, UK). A positive mycoplasma contamination was shown by the presence of a strong band present at 267bp. An internal control always produces a band at 191bp to show the reaction had worked. However, if there was a strong mycoplasma contamination, this internal control band at 191bp was not visible. Any mycoplasma positive cells were either discarded or treated, as detailed below.

If samples were found to be mycoplasma positive, they were subsequently treated with BM Cyclin (Roche, Sussex, UK) for 3 weeks, consisting of 3 cycles of treatment. Contaminated culture medium was removed, with fresh medium containing BM Cyclin 1 (4µl of stock solution/ml, final concentration 10µg/ml) added. Cells were cultured as previously described for three days; and passaged when necessary. Culture medium containing BM Cyclin 1 was subsequently removed and replaced with fresh medium containing BM Cyclin 2 (4µl of stock solution/ml, final concentration 5µg/ml). Cells were cultured as previously described

for 4 days; and passaged when necessary. This 7 day treatment cycle was performed 3 times, before a fresh sample of culture medium was reassessed to confirm eradication of mycoplasma contamination.

2.3 General *in Vitro* Wound Healing Methods

2.3.1 Cell Viability and Proliferation

Cellular viability and proliferation was determined through use of an MTT [3-(4,5-dimethyl-2-thiazolyl)-2,5-diphenyltetrazolium bromide] Dye-Reduction assay, assessing cells at 24h, 72h, 120h and 168h. Confluent NF and HaCaTs were trypsinized, counted and seeded in F-SCM and K-SCM respectively, into 96-well microtitre plates (Sarstedt Ltd., Leicestershire, UK), at cell densities of $2.5x10^3$ cells/well and $5x10^3$ cells/well, respectively for 24h. Culture media was then removed and replaced with serum-free F-SCM or K-SCM (DMEM, 1% antibiotics and 1% L-glutamine), respectively for a further 24h; in order to growth arrest the cells. Serum-free media was subsequently removed and replaced with the respective 1% serum containing culture medium (F-SCM or K-SCM; DMEM, 1% antibiotics, 1% L-glutamine and 1% foetal calf serum), as described in Section 2.1, with different concentrations of EBC-46 and EBC-211 (0.001µg/ml, 0.01µg/ml, 0.1µg/ml, 1µg/ml, 10µg/ml or 100µg/ml). Untreated controls were also established, 0µg/ml, containing 1% DMSO as described in Section 2.1. A blank control containing no cells, but the respective culture medium only, was included to show no absorbance in cell-free wells. These concentrations were used for both EBC-46 and EBC-211, with 6 wells/concentration (Figure 2.1), for each time point. Cultures were maintained at 37°C, in a 5% CO_2/95% air environment, with culture medium changed every 48h.

At 24h, 72h, 120h and 168h, sterile MTT (25µl of a 5mg/ml MTT solution in PBS, Sigma-Aldrich Company Ltd.) was added to culture medium in each well and incubated at 37°C, in a 5% CO_2/95% air environment, for 4h. The culture medium/MTT mixture was removed after 4h and 100µl MTT Extraction Buffer was added to each well. MTT extraction buffer consists of sodium dodecyl sulphate (20g; SDS, Sigma-Aldrich Company Ltd.), N,N-dimethylformamide (50ml, Sigma-Aldrich Company Ltd.) and double-distilled water (50ml). Following solubilisation, the pH

Figure 2.1: Representation of the culture plate set up for the MTT assay.

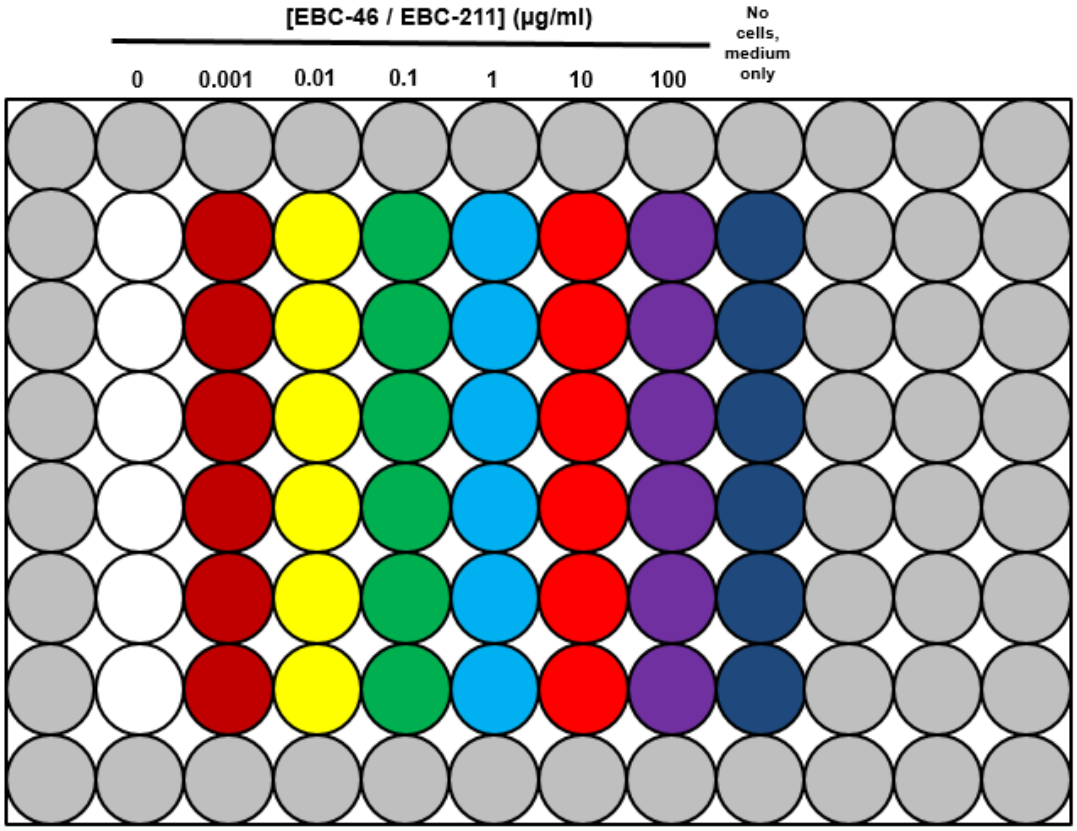

was adjusted to 4.7 by the addition of 3ml 'acid mix', which consists of glacial acid (80ml; Thermo Fisher Scientific), 1M hydrochloric acid (HCl, 2.5ml, Thermo Fisher Scientific) and double-distilled water (17.5ml).

Following the addition of Extraction Buffer, the 96-well plates at each time-point were wrapped in cling film and maintained at 37°C, in a 5% CO_2/95% air environment, for a further 4h. At 4h, the absorbance values were read at 540nm using Bio-Tek Instruments Microplate Autoreader EL311 (Thermo Fisher Scientific). These experiments were performed on 3 separate occasions, the data was expressed as percentage data compared to the untreated control, with averages and standard error values for each concentration assessed. Statistical analysis was performed using one-way ANOVA with post-test Tukey analysis; and statistical significance considered at $p<0.05$.

2.3.2 Cell Cycle Analysis

Flow cytometry was performed to analyse the effects of EBC-46 and EBC-211 (0.001-10µg/ml) on dermal fibroblast and HaCaT cell cycle progression, compared to untreated controls (0µg/ml). The percentages of cells present in each phase of the cell cycle following EBC-46 or EBC-211 treatment were analysed at a number of time-points; and compared to the respective untreated controls.

2.3.2.1 Dermal Fibroblast Culture

Following trypsinisation, dermal fibroblasts were seeded into 6-well, microtitre plates (Sarstedt Ltd.) at a cell density of $7.5x10^4$cells/well in F-SCM (Section 2.2.1). Fibroblasts were maintained at 37°C in a 5% CO_2/95% air atmosphere for 24h and subsequently cell cycle synchronized through culturing in serum-free F-SCM for 24h. Serum-free DMEM was removed and replaced with F-SCM containing 10% foetal calf serum, in addition to EBC-46 or EBC-211 (0µg/ml, 0.001µg/ml, 0.01µg/ml, 0.1µg/ml 1µg/ml or 10µg/ml; 2ml/well). An untreated control (0µg/ml) was also included, containing 1% DMSO. Fibroblasts were maintained at 37°C in 5% CO_2/95% air, for 22h, 29h and 36h; with T0 (0h) analysed at time of treatment.

2.3.2.2 Epidermal Keratinocyte Culture

Following trypsinisation, HaCaTs were seeded into 6-well, microtitre plates (Sarstedt Ltd.) at a cell density of $7.5x10^4$cells/well in K-SCM (Section 2.2.2). HaCaTs were maintained at 37°C in a 5% CO_2/95% air atmosphere for 24h and subsequently synchronized through culturing in serum-free K-SCM for 24h. Serum-free DMEM was removed and replaced with K-SCM containing 1% foetal calf serum, in addition to EBC-46 or EBC-211 (0µg/ml, 0.001µg/ml, 0.01µg/ml, 0.1µg/ml 1µg/ml or 10µg/ml; 2ml/well). An untreated control (0µg/ml) was also included, containing 1% DMSO. HaCaTs were maintained at 37°C in 5% CO_2/95% air, for 9h, 17h, 26h, 32h, 40h and 48h; with T0 (0h) analysed at time of treatment.

2.3.2.3 Cell Fixation

At each time-point, treated media was removed, wells washed with PBS (x1) before the addition of trypsin (500µl/well). After cell detachment, trypsin was neutralised with F-SCM or K-SCM (1ml). Cells were centrifuged at 1500xg for 5min, the supernatants were carefully removed and the pellets re-suspended in PBS (1ml). Samples were centrifuged at 1500xg for 5min and the supernatant discarded. Pellets were re-suspended in 4% paraformaldehyde solution in PBS (1ml; Santa Cruz Biotechnology Inc., Middlesex, UK); and incubated on ice for 30min before centrifugation at 1500xg for 5min and the supernatants discarded. Pellets were re-suspended in PBS (volume calculated to give $\leq 4x10^5$ cells/ml). Aliquots (250µl) of each cell/PBS mix were transferred to Falcon Round bottom, 5ml polystyrene tubes (Scientific Laboratory Supplies Ltd., Nottinghamshire, UK), with Draq5 (1µl; BioStatus Ltd., Leicestershire, UK) added and mixed. Cells were incubated in Draq5 at 37°C for 5min, before being run through the Flow Cytometer System.

2.3.2.4 Flow Cytometry

Cells were run through the Flow Cytometer System (FACScalibur, Becton Dickinson, Oxfordshire, UK), at an approximate speed of 150 events/second. These datasets were analysed using a number of software packages. Cell cycle analysis was performed using FlowJo Software LLC, Version 7.6 (Ashland, Oregon, U.S.A.), with a fixed mean for G1 and G2 peaks to determine the percentage of cells in each phase of the cell cycle. This experiment was performed on 3 separate occasions, with the

data obtained expressed as percentage data, detailing the percentage of cells in each phase of the cell cycle (G1, S and G2), compared to the untreated control. Averages and standard error values for each concentration were assessed at each time-point studied. Statistical analysis was performed using one-way ANOVA with Dunnett Multiple Comparisons Test analysis, using the untreated control as the control for comparison. Statistical significance considered at $p<0.05$.

2.3.3 Cell Morphology

Confluent NF and HaCaTs were trypsinized, counted, and seeded into 24-well BD Falcon microtitre plates (BD Biosciences, Oxfordshire, UK) at a cell density of $1.56x10^4$ cells/well and $3.12x10^4$ cells/well, respectively. NF and HaCaTs were seeded in F-SCM and K-SCM respectively (Sections 2.2.1 and 2.2.2) for 24h. Culture media was then removed and replaced with serum-free culture media, as Section 2.3.1, for 24h. Serum-free medium was subsequently removed and replaced with each respective 1% serum culture medium, containing EBC-46 or EBC-211 (0.001µg/ml, 0.01µg/ml, 0.1µg/ml, 1µg/ml, 10µg/ml or 100µg/ml) as detailed in Section 2.1, with 3 wells/concentration. An untreated control (0µg/ml) was also included, which further contained 1% DMSO. Cultures were maintained at 37°C, in a 5% CO_2/95% air environment, with culture medium changed every 48h. This experiment was performed on 3 separate occasions. Cellular morphology images were taken at x100 magnification for each concentration of EBC-46 and EBC-211, along with the untreated control, at 24h, 72h, 120h and 168h to correlate with the MTT data. Images were obtained using Nikon Eclipse TS100 Inverted Microscope (Nikon UK Ltd., Surrey, UK).

2.3.4 Scratch Wound Assay

Confluent NF and HaCaTs were trypsinized, counted and seeded into 24-well BD Falcon microtitre plates (BD Biosciences), at cell densities of $2.5x10^4$ cells/well and $7.5x10^4$ cells/well, respectively. NF and HaCaTs were seeded in F-SCM and K-SCM respectively (Sections 2.2.1 and 2.2.2) for 48h. Culture media was removed and replaced with serum-free F-SCM or K-SCM for 24h. At 24h, a scratch was made across each cell layer using a sterile pipette and washed (x2) with PBS to remove cell debris. Following this, each respective 1% serum culture medium containing

different concentrations of EBC-46 and EBC-211 (0-100µg/ml; as in Section 2.1) was added to the respective wells, with 3wells/concentration. An untreated control (0µg/ml) was also included, containing 1% DMSO. Cultures were maintained at 37°C, in a 5% CO_2/95% air environment, with the migration of cells into the denuded area monitored through use of Time Lapse Microscopy, using the Leica TCS SP5 Confocal Microscope (Leica Microsystems (UK) Ltd., Buckinghamshire, UK). Digital images were taken every 20min over the 48h period; and converted to a video using LAS AF Lite (Leica Software, Version 4.0.11706, Leica Microsystems (UK) Ltd). Each experiment was performed on 3 separate occasions.

Wound repopulation was analysed using ImageJ Software (NIH Software, Version 1.49). Fibroblast cell movement was tracked using Image J tracking plugin, with distance travelled, cell displacement, speed and velocity calculated for 6 cells/video over 3 separate experiments, resulting in 18 data points/culture condition. Averages and standard error values for each condition were calculated. HaCaT migration was also analysed through ImageJ, by calculating the percentage closure of the wound site at 24h and 48h time-points, with averages and standard error values calculated for each culture condition analysed. Statistical analysis of both fibroblast and HaCaT wound repopulation was performed using one-way ANOVA with post-test Tukey analysis; and statistical significance considered at $p<0.05$.

2.3.4.1 Optimisation of Mitomycin C Treatment

Based on the findings of the effects of EBC-46 and EBC-211 on HaCaT proliferation and migration (Chapter 4), the scratch wound repopulation was performed in the presence of anti-proliferative agent, Mitomycin C (Santhiago et al. 2012; Wang et al. 2012; Lü et al. 2013). Migration was analysed to determine the effect of EBC-46 and EBC-211 on wound repopulation, independent of proliferation. The optimal concentration of Mitomycin C for HaCaT culture conditions was determined through use of an MTT [3-(4,5-dimethyl-2-thiazolyl)-2,5-diphenyltetrazolium bromide] Dye-Reduction assay. The aim of this MTT assay was determine the concentration required to inhibit the proliferative response, without having a cytotoxic effect on the HaCaTs.

Confluent HaCaTs were trypsinized, counted and seeded into 96-well microtitre plates, at a cell density of $5x10^3$ cells/well. HaCaTs were seeded in K-SCM (Section 2.2.2) for 24h; then replaced with serum free K-SCM for 24h. Serum free medium was removed from cell cultures and replaced with respective 1% serum culture medium (K-SCM) containing different concentrations of Mitomycin C: 0.5µg/ml, 1µg/ml, 2.5µg/ml, 5µg/ml or 10µg/ml, and a negative control containing no Mitomycin C. There were 6 wells/concentration (similar to Figure 2.1) at 24h, 72h and 120h. Cell cultures were maintained at 37°C, in a 5% CO_2/95% air environment, with culture medium changed every 48h. At 24h, 72h and 120h, the MTT process was carried out as described in Section 2.3.1. Absorbance was read at 540nm using Bio-Tek Instruments Microplate Autoreader EL311. This experiment was carried out on 3 separate occasions, with averages and standard error values calculated for each concentration.

2.3.4.2 Scratch Wound Repopulation in Presence of Mitomycin C

Confluent HaCaTs were trypsinized, counted and seeded into 24-well BD Falcon microtitre plates (BD Biosciences) at a cell density of $5x10^4$ cells/well respectively. HaCaTs were seeded in K-SCM (Section 2.2.2) for 48h, then replaced with serum free K-SCM for 24h. As described in Section 2.3.4, a scratch was made across the cell layer using a sterile pipette, then washed twice with PBS. Following this, each respective 1% serum culture medium containing different concentrations of EBC-46 and EBC-211 (0-100µg/ml; as in Section 2.3.1) was added to the respective wells. The calculated optimal concentration of Mitomycin C (1µg/ml) was also added to each epoxy-tigliane containing media. Two epoxy-tigliane untreated controls were also included, one in the presence and one in the absence of Mitomycin C (1µg/ml). Cell cultures were maintained at 37°C, in a 5% CO_2/95% air environment. Migration of cells into denuded area was monitored through use of Time Lapse Microscopy using the Leica TCS SP5 Confocal Microscope, as described previously (Section 2.3.3). Digital images were taken every 20min for 48h, with each experiment performed on 3 separate occasions. Migration was analysed by calculating percentage wound closure at 24h and 48h using ImageJ. Averages and standard error values for each condition were calculated. Statistical analysis of HaCaT wound

repopulation was performed using one-way ANOVA with post-test Tukey analysis; and statistical significance considered at $p<0.05$.

2.3.5 Dermal Fibroblast-Myofibroblast Differentiation

2.3.5.1 Immunocytochemistry

Confluent NFs were trypsinized, counted and seeded into 8-well, Permanox chamber slides (VWR International Ltd., Leicestershire, UK). NFs were seeded in F-SCM (250µl) at a cell density of $2.5x10^4$ cells/ml; and maintained at 37°C, in a 5% CO_2/95% air environment for duration of the experiment. When cells reached approximately 50-60% confluence levels, cells were growth arrested through culturing in serum-free, F-SCM (250µl) for 48h. Serum-free media was replaced with serum-free F-SCM containing EBC-46 or EBC-211 (0µg/ml, 0.001µg/ml, 0.01µg/ml, 0.1µg/ml, 1µg/ml or 10µg/ml; 3 wells/concentration) in the presence or absence of Transforming Growth Factor β_1, (TGF-β_1, 10ng/ml; PeproTech Ltd., London, UK). Cells were maintained in treated serum-free F-SCM (250µl) for 72h.

At 72h, media was removed from cells, the wells washed with PBS (x1) and the cells fixed in 4% paraformaldehyde solution in PBS (100µl) for 10min, before being re-washed in PBS (x1). Cells were permeabilised in 0.1% Triton X-100 (200µl; Sigma-Aldrich Company Ltd.) for 5min and washed in PBS (x1). Cells were then blocked in 1% bovine serum albumin (BSA)-PBS for 30min at room temperature and washed in 0.1% BSA-PBS (x3). Cells were incubated in primary antibody, monoclonal mouse anti-actin, α-smooth muscle antibody (1:100 in 0.1% BSA-PBS; Sigma-Aldrich Company Ltd.), overnight at 4°C. Cells were washed in 0.1% BSA-PBS (x3), then re-washed in 0.1% BSA-PBS for 5min (x3). Cells were subsequently incubated in secondary antibody, Alexa Fluor 488 goat anti-mouse IgG antibody (1:1000 in 0.1% BSA-PBS; Thermo Fisher Scientific), for 1h at room temperature, under darkness. Cells were washed in 0.1% BSA-PBS (x3) and re-washed in 0.1% BSA-PBS for 5min (x3). Cells were then incubated in Hoechst Solution (1:2000 in 0.1% BSA-PBS; Sigma-Aldrich Company Ltd.) for 30min at room temperature, under darkness. Cells were washed in 0.1% BSA-PBS (x3) and re-washed in 0.1% BSA-PBS for 5min (x3). The chambers were removed and wells sealed with Fluor Save Reagent

(Merck Millipore, Darmstadt, Germany) and Gerhard Menzel Coverslips (Thermo Fisher Scientific). Slides were viewed using a Leica Dialux 20 Fluorescent Microscope (Leica Microsystems UK Ltd., Buckinghamshire, UK). Images were taken at a magnification of x400, with each experiment performed on 3 separate occasions.

2.3.5.2 Quantitative Polymerase Chain Reaction (qPCR)

2.3.5.2.1 Cell Culture

Confirmation of differentiation from dermal fibroblasts to myofibroblasts was performed through analysis of α-Smooth Muscle Actin (α-SMA) expression by quantitative Polymerase Chain Reaction (qPCR), at 72h. This was analysed for both EBC-46 and EBC-211 (0.001µg/ml, 0.01µg/ml, 0.1µg/ml, 1µg/ml and 10µg/ml; 3wells/concentration) in the presence or absence of TGF-β_1 (10ng/ml). Two untreated controls were also included, one in the presence and one in the absence of TGF-β_1 for each experiment to establish control expression levels for both TGF-β_1 positive (0µg/ml + TGF-β_1) and TGF-β_1 negative (0µg/ml - TGF-β_1) conditions, to allow comparison to epoxy-tigliane treated cells. Cells were maintained in treated serum-free F-SCM (2ml) for 72h.

Confluent NFs were trypsinized, counted and seeded into 6-well, microtitre plates. NFs were seeded in F-SCM at a cell density of $5x10^4$ cells/ml and maintained at 37°C, in a 5% CO_2/95% air environment for the duration of the experiment. As previously described in Section 2.3.5.1, cells were growth arrested through culturing in serum-free F-SCM for a further 48h. Serum-free media was replaced with serum-free F-SCM containing EBC-46 or EBC-211 (0µg/ml, 0.001µg/ml, 0.01µg/ml, 0.1µg/ml, 1µg/ml or 10µg/ml; 3 wells/concentration) in the presence or absence of Transforming Growth Factor β_1, (TGF-β_1, 10ng/ml; PeproTech Ltd., London, UK). Cells were maintained in treated serum-free F-SCM (2ml) for 72h.

2.3.5.2.2 Extraction of High Quality RNA

At 72h, samples were harvested and RNA was extracted using Qiagen RNeasy Mini Kit (Qiagen Ltd., Lancashire, UK), according to manufacturer's instructions. This

Kit is designed to extract up to 100µg of purified, high-quality RNA from cells; and is suitable for sensitive applications. An additional on-column DNase digestion was performed to remove any DNA contamination from the samples, using a RNase-Free DNase Set Qiagen (Qiagen Ltd.). Digestion of any residual DNA is necessary due to the sensitive nature of TaqMan RT-PCR analysis, as the presence of even small amounts of DNA may affect the results obtained.

Cells were harvested from wells by the addition of Buffer RLT (350µl) to each well. Cell/Buffer RLT samples were transferred to an RNase free tube and vortexed for 1min to disrupt and homogenise cells, in order to release all RNA from the cells and allow efficient binding of RNA to the spin columns.

One volume of 70% ethanol (350µl) was added to each sample and mixed well by pipetting, before immediate transfer to RNeasy Spin Column placed in collection tubes (in Kit). Spin Columns were centrifuged at ≥8000xg for 15s; and flow-through eluate discarded. Buffer RW1 (350µl) was used to wash the columns. Columns were centrifuged at 10,000xg for 15s and subsequent flow-through eluate discarded, as above. From additional on-column DNase digestion, 10µl DNase I Stock solution was added to 70µl Buffer RDD (in Kit). This was mixed gently and centrifuged at 10,000xg for 5s. DNase I incubation mix (80µl) was added directly to the Spin Columns and incubated at room temperature for 15min. Buffer RW1 (350µl) was added to the Spin Columns containing DNase I incubation mix, centrifuged at 10,000xg for 15s and flow-through eluate discarded.

Buffer RPE (500µl) containing 4 volumes of 96-100% ethanol was added to the Spin Columns as a further wash step, centrifuged at 10,000xg for 15s and flow-through eluate discarded. A second volume of Buffer RPE (500µl) was added to the Spin Columns and centrifuged at 10,000xg for 2min. Spin Columns were transferred to new 2ml collection tubes and centrifuged at 10,000xg for 1min, to ensure complete elimination of Buffer RPE from the spin columns. RNeasy Spin Columns were transferred to new 1.5ml collection tubes (in Kit). RNase-free water (30µl) was added to each Spin Column, incubated for 1min at room temperature and centrifuged at 10,000xg for 1min, to elute RNA from the columns.

RNA concentrations were determined using a NanoDrop® ND-8000 Spectrophotometer (Thermo Fisher Scientific). RNA purity was determined using the ratio between absorbance values at 260 and 280nm (260/280 ratio), with purities over 1.7 considered sufficient for downstream applications.

2.3.5.2.3 Reverse Transcription and Synthesis of Copy DNA (cDNA)

RNA was converted to cDNA through the use of High Capacity cDNA Reverse Transcription Kits (Thermo Fisher Scientific), according to manufacturer's instructions. 2X Reverse Transcription Master Mix was prepared on ice (10X RT Buffer, 2µl; 25X dNTP Mix (100mM), 0.8µl; 10X RT Primers, 2µl; Multiscribe Reverse Transcriptase, 1µl; RNase Inhibitor, 0.5µl; Nuclease-free H_2O, 3.7µl; in Kit); and mixed gently. 10µl 2X RT Master Mix was pipetted into each tube, along with RNA sample (volume calculated according to RNA concentration) and nuclease-free water to a final volume of 10µl and mixed gently. Tubes were briefly centrifuged and loaded into the PTC-225 Peltier Thermal Cycler (Bio-Rad Laboratories Ltd., Hertfordshire, UK) and programmed accordingly (25°C for 10min, 37°C for 120min, 85°C for 5min and held at 4°C).

2.3.5.2.4 Quantitative Polymerase Chain Reaction (qPCR) Amplification and Detection

Target cDNA was amplified and probes hybridised to target sequence through the use of TaqMan® Fast Universal PCR Master Mix (2X), No AmpErase® UNG (Thermo Fisher Scientific), according to manufacturer's instructions. Reaction mix was prepared (Master Mix, 10µl; H_2O, 4µl; α-SMA Gene Expression Assay Mix (containing forward PCR Primer, reverse PCR primer and TaqMan probe), 1µl; Eukaryotic 18S rRNA Endogenous Control, 1µl); and mixed gently. Reaction mixtures (16µl) were added to each well of 96-well plates, with cDNA sample (4µl) added to respective wells. Plates were sealed and centrifuged at 10,000xg for 2min, then transferred to 7900HT Fast Real Time PCR System (Thermo Fisher Scientific). The Thermal Cycler was set for an initial cycle at 95°C for 1s, followed by 40 cycles of 95°C for 1s, then 60°C for 20s. Comparative CT (ΔΔCT) method was used for relative quantification of α-SMA gene expression. Each experiment was performed

on 3 separate occasions, with averages and standard error values calculated for each experimental condition. Statistical analysis was performed using one-way ANOVA with post-test Tukey analysis; and statistical significance considered at $p<0.05$.

2.4 Microarray Analysis of Global Gene Expression

Microarray analysis was undertaken to obtain data on gene expression changes that occurred following HaCaT treatment with a range of EBC-46 and EBC-211 concentrations (0.001µg/ml, 0.1µg/ml or 10µg/ml), at 24h and 48h. Differential gene expression was then compared versus untreated control HaCaTs.

2.4.1 Epidermal Keratinocyte Culture

Following trypsinisation, HaCaTs were seeded into separate T-75 tissue culture flasks (VWR International, UK); at a cell density of $2x10^6$ cells/flask in K-SCM. HaCaTs were maintained at 37°C in a 5% CO_2/95% air atmosphere for 24h and subsequently growth arrested for 24h in serum-free K-SCM. Serum-free DMEM was removed and replaced with 1% serum containing K-SCM; in addition to 0µg/ml, 0.001µg/ml, 0.1µg/ml or 10µg/ml EBC-46 or EBC-211 (10ml/flask). Untreated controls (0µg/ml) also included 1% DMSO (as described in Section 2.1); HaCaTs were maintained at 37°C in 5% CO_2/95% air atmosphere, for 24h and 48h. Therefore, 12 x T-75 tissue culture flasks/experiment were established for a total of 4 separate experiments (Table 2.1), with 0.1µg/ml EBC-46 and EBC-211 being analysed at 48h only. At 24h and 48h, all culture medium (10ml) was removed, then immediately replaced along with RNAprotect Cell Reagent : media (4.5ml/flask, Qiagen Ltd.), to maintain the 5:1 ratio and transferred to 15ml Falcon tubes (VWR International, UK). HaCaTs were maintained at 4°C, until subsequent shipping to the Berghofer Queensland Institute of Medical Research (QIMR), Queensland, Australia; where further experimental work and analysis of these samples was performed.

2.4.2 Extraction and Purification of High Quality RNA

RNA was extracted from each HaCaT sample, using Qiagen RNeasy Plus Mini Kits (Qiagen Pty Ltd., Victoria, Australia), according to manufacturer's instructions. This

Table 2.1: Summary of the 12 HaCaT conditions analysed through Microarray analysis of global gene expression following EBC-46 and EBC-211 treatment; 4 separate samples were obtained for each condition, resulting in 48 samples analysed through Microarray analysis.

Treatment Number	[EBC-46] or [EBC-211] (µg/ml)	Time-point (h)
1	0 (1% DMSO)	24
2	0 (1% DMSO)	48
3	0.001 (EBC-46)	24
4	0.001 (EBC-46)	48
5	0.001 (EBC-211)	24
6	0.001 (EBC-211)	48
7	0.1 (EBC-46)	48
8	0.1 (EBC-211)	48
9	10 (EBC-46)	24
10	10 (EBC-46)	48
11	10 (EBC-211)	24
12	10 (EBC-211)	48

Kit is designed to extract up to 100µg of purified, high-quality RNA from cells, suitable for sensitive applications. Cell/RNAprotect samples (500µl) were transferred to an RNase-free tube and centrifuged at 10,000xg for 1min. Supernatants were carefully removed and pellets resuspended in Buffer RLT Plus (350µl; in Kit), (10µl β-mercaptoethanol (β-ME)/10ml Buffer RLT Plus). The lysates were homogenised through vortexing and pipetting, before transfer to gDNA Eliminator Spin Columns, placed in collection tubes (in Kit). Spin Columns were centrifuged at 10,000xg for 1min, discarding Spin Columns with captured genomic DNA, whilst resultant flow-through was retained. One volume of 70% ethanol (350µl) was added to each collected flow-through, mixed by pipetting and transferred to RNeasy Spin Columns placed in collection tubes (in Kit). Spin columns were centrifuged at 10,000xg for 15s, and flow-through eluates were discarded. Buffer RW1 (700µl, in Kit) was added to retained RNeasy Spin Columns to wash the columns; being centrifuged at 10,000xg for 15s, with subsequent flow-through eluates discarded. Buffer RPE (500µl, in Kit) containing 4 volumes of 96-100% ethanol was added to Spin Columns as an additional Spin Column wash step, and centrifuged at 10,000xg for 15s. Subsequent flow-through was discarded and Spin Columns centrifuged at ≥8000xg for 1min, to ensure all Buffer RPE had been eliminated from the Spin Columns. The RNeasy Spin Columns were transferred to fresh 1.5ml collection tubes (in Kit). RNase-free water (50µl) was added to each Spin Column and centrifuged at 10,000xg for 1min, to elute collected RNA from the Spin Column.

2.4.3 Quantifying RNA and Confirmation of Purity and Integrity

RNA concentrations were determined using a NanoDrop® Lite (Thermo Fisher Scientific, Australia Pty Ltd., Victoria, Australia), which also provided the purity of each RNA sample through ratio between the absorbance values at 260 and 280nm (260/280 ratio). Purities over 1.7 were considered sufficient for downstream applications. RNA integrity was confirmed by 1% agarose gel electrophoresis with ethidium bromide staining. A 2:1 ratio of 28S rRNA to 18S rRNA confirmed the integrity of the RNA samples. Agarose (1%) gels were produced by agarose (Seakem® LE Agarose, Lonza Pty Ltd., New South Wales, Australia) and 1x Tris-acetate-EDTA (TAE) buffer (Tris, Thermo Fisher Scientific, Australia; acetic acid, Merck Millipore, Victoria, Australia; and EDTA, Univar Australia Pty Ltd., New

South Wales, Australia). Agarose was dissolved through heating and mixed well to ensure equal concentrations throughout. Once cooled, 10mg/ml ethidium bromide (8µl; Sigma-Aldrich Pty. Ltd., New South Wales, Australia) was added to the agarose/TAE and mixed well. Agarose/TAE was poured into prepared RNase-free moulds and allowed to set at room temperature, for approximately 30min. RNA samples were loaded into wells (10µl), together with a 1kb DNA marker (10µl; Thermo Fisher Scientific, Australia). Electrophoresis was applied to the loaded gels, at 90V for 30min, in 1xTAE running buffer. Gel images were captured under UV light (312nm); and viewed using a UV Imager (Vilber Lourmat, Fisher Biotec, Western Australia, Australia), using the DNA marker as a guide for molecular size.

2.4.4 Generation of Biotinylated, Amplified Antisense RNA (cRNA) and Quantification

RNA was amplified and labelled through the use of Illumina® TotalPrep RNA Amplification Kits (Thermo Fisher Scientific, Australia), to provide antisense RNA ready for hybridisation with Illumina Sentrix® Arrays. Approximately 500ng of total RNA was transferred to RNase-free microcentrifuge tubes and adjusted to a final volume of 11µl with nuclease-free water. To synthesise first strand cDNA, Reverse Transcription Master Mix was prepared, according to manufacturer's instructions (T7 Oligo(dT) Primer, 1µl; 10X First Strand Buffer, 2µl; dNTP Mix, 4µl; RNase Inhibitor, 1µl; ArrayScript, 1µl), mixed by vortexing and centrifuged at 10,000xg for 15s. Reverse Transcription Master Mix (9µl) was transferred to each sample, mixed thoroughly and centrifuged at 10,000xg for 15s, before incubation at 42°C for 2h in GeneAmp PCR System 2400 (Perkin Elmer, Victoria, Australia).

Second Strand Master Mix was prepared on ice, according to manufacturer's instructions (nuclease-free water, 63µl; 10X Second Strand Buffer, 10µl; dNTP Mix, 4µl; DNA Polymerase, 2µl; RNase H, 1µl), mixed by vortexing and centrifuged at 10,000xg for 15s. Second Strand Master Mix (80µl) was added to each sample, mixed thoroughly and centrifuged at 10,000xg for 15s, before incubation at 16°C for 2h in a a GeneAmp PCR System 2400 (Perkin Elmer), to synthesise second strand cDNA.

cDNA Binding Buffer (250µl, in Kit) was added to each sample of second strand cDNA, mixed thoroughly and centrifuged at 10,000xg for 15s. cDNA samples were transferred to cDNA Filter Cartridges placed in collection tubes and centrifuged at 10,000xg for 1min discarding each flow-through. Wash Buffer containing 100% ethanol (500µl, in Kit), was added to the cDNA Filter Cartridges and centrifuged at 10,000xg for 1min; subsequent flow through eluate was discarded. Filter Cartridges were re-spun to ensure all Wash Buffer had been removed, before being transferred to cDNA Elution Tubes. Nuclease-free water (20µl), preheated to 55°C, was added to cDNA Filter Cartridge, left at room temperature for 2min; and then centrifuged at 10,000xg for 1.5min to elute purified cDNA.

IVT Master Mix was prepared according to manufacturer's instructions (T7 10X Reaction Buffer, 2.5µl; T7 Enzyme Mix, 2.5µl; Biotin-NTP Mix, 2.5µl), mixed well through vortexing and centrifuged at 10,000xg for 15s. IVT Master Mix (7.5µl) was added to each cDNA sample, mixed thoroughly and centrifuged at 10,000xg for 15s. Samples were incubated at 37°C for 16h in a Thermal Cycler, to synthesise cRNA. After 16h, reactions were stopped through the addition of nuclease-free water (75µl) to each cRNA sample; and mixed by gentle vortexing.

cRNA Binding Buffer (350µl, in Kit) was added to each sample, followed by addition of ACS reagent grade 100% ethanol (250µl). Samples were mixed through pipetting and transferred immediately to cRNA Filter Cartridges (in Kit). Wash Buffer (650µl, in Kit) was added to each cRNA Filter Cartridge, centrifuged at 10,000xg for 1min discarding resultant flow-through, and centrifuged again at 10,000xg for 1min to ensure all Wash Buffer had been removed. cRNA Filter Cartridges were transferred to new cRNA collection tubes. Nuclease-free water (100µl), preheated to 50-60°C, was added to the cRNA Filter Cartridges and the cartridge left at room temperature for 2min, prior to centrifugation at 10,000xg for 2min to obtain purified cRNA.

As previously described (Section 2.4.3), RNA concentrations were determined using a NanoDrop® Lite. RNA purity was also obtained through 260/280 ratio; purities over 1.7 were considered sufficient for downstream applications.

2.4.5 Illumina Hybridisation of Antisense RNA (cRNA)

Hybridization of cRNA samples to complementary gene-specific sequence BeadChips was performed using the Illumina® Whole-Genome Gene Expression Direct Hybridization Assay System (Illumina®, Victoria, Australia), according to manufacturer's instructions. HYB and HCB tubes (in Kit) were incubated at 58°C and mixed thoroughly for 10min, prior to use. BeadChips were warmed to room temperature, prior to use. Each cRNA sample (750ng) was aliquoted into separate hybridization tubes and volumes made up to 5µl with RNase-free water. Samples were heated at 65°C for 5min, briefly centrifuged at 250xg and cooled to room temperature; before HYB Mix (10µl; in Kit) was added to each sample.

Hyb Chambers were assembled with all four Hyb Chamber inserts. HCB (200µl) was added to the eight humidifying buffer reservoirs, for hybridisation of four BeadChips. Prepared cRNA mix (15µl) was loaded onto Illumina® Expression BeadChips. All BeadChips were loaded into the Hyb Chambers, securely sealed and incubated on a rocker at 58°C for 16h.

After incubation, a series of hybridisation and wash steps were performed, according to the Whole-Genome Gene Expression Direct Hybridization Assay Guide (Illumina®), as detailed below. BeadChips were removed from Hyb Chamber and submerged face up in Wash E1BC solution (6ml E1BC buffer in 2L RNase-free water) and the cover-seals removed. BeadChips were transferred to slide racks submerged in Wash E1BC solution (250ml), the slide racks were transferred to a Hybex Waterbath containing High Temperature Wash buffer (250ml; Illumina®); and incubated for 10min. Slide racks were transferred to fresh Wash E1BC buffer (250ml), plunged in and out of solution (x10); and transferred to an orbital shaker, set on medium-low for 5min at room temperature. Slide racks were transferred to fresh 100% ethanol (250ml), plunged in and out of solution (x10), before being transferred to an orbital shaker, set on medium-low for 10min at room temperature. Slides were then transferred back to Wash E1BC buffer (250ml), plunged in and out of solution (x10), before transferred to orbital shaker, set on medium-low for 2min at room temperature.

BeadChips were placed face up in wash trays on a rocker. Block E1 buffer (4ml; Illumina®) was added to each wash tray and rocked at a medium speed for 10min at room temperature. BeadChips were transferred to wash trays, containing Cy3-Streptavidin (1:1000 dilution of Cy3-Streptavidin in Block E1 buffer; 2ml), with the wash tray lids used to protect the Cy3-Streptavidin from light. Wash trays were subsequently placed on a rocker set at medium speed for 10min at room temperature. BeadChips were transferred to slide racks in Wash E1BC buffer (250ml), plunged in and out of solution (x5), before being transferred to a orbital shaker, set on medium-low for 5min at room temperature. Slide racks containing BeadChips were placed in a centrifuge and spun at 1,000xg for 4min at room temperature.

2.4.6 Microarray Data Acquisition and Data Analysis

BeadChips were scanned using the iScan System on an Agilent GS2565 Microarray Scanner (Agilent Technologies Australia, Victoria, Australia). This system uses a laser to excite the fluor of the single-base extension product on the beads, with subsequent light emissions recorded and analysed. BeadChips were scanned according to the Whole-Genome Gene Expression Direct Hybridization Assay Guide (Illumina®), with decoded data input into the iScan System to correspond to specific BeadChips.

The Human HT-12 v4 Expression BeadChips cover more than 47,000 transcripts and known splice variants across the human transcriptome, providing genome-wide transcriptional coverage of >25,000 characterised genes, gene candidates and splice variants. Raw data files were filtered and normalised using BeadScan Software and data extracted using BeadStudio Gene Expression Module (Illumina®). Data was subsequently imported into GeneSpring GX v12.5 Expression Analysis Software (Agilent Technologies), for normalisation, filtering based on detection score, statistical analysis and heatmap visualization/clustering. The expression values were normalized using quantile normalization with default settings. The entities were filtered based on detection score calculated by Genome Studio, where $p \leq 0.05$ was considered significant. Data from each treatment group (*n=4* separate experiments) was grouped for combined analysis using Ingenuity Pathway Analysis (IPA®)

Software. Further analysis of Microarray data using IPA® Software, used Ingenuity Knowledge Base to visualise gene pathways, to aid interpretation of the Microarray dataset.

Various databases were further used to identify characteristics and functions of genes of interest, in addition to the information gained from GeneSpring GX v12.5 Expression Analysis Software and Ingenuity Pathway Analysis (IPA®) Software. Databases used included PubMed (*http://www.ncbi.nlm.nih.gov/gene/*), GeneCards (*http://www.genecards.org/*) and OMIM (*http://www.omim.org*).

2.5 Microarray Validation

2.5.1 Quantitative Polymerase Chain Reaction (qPCR)

Following on from Microarray studies, qPCR experiments were performed on a number of key genes (Krt13, Krt15, Krt16, Krt17, MMP-1 and Cyclin B2), identified to be differentially expressed by EBC-46 and EBC-211, in order to validate the Microarray data obtained and to further quantify the expression of these genes. All experiments were performed in triplicate.

To prepare samples for qPCR, the samples initially underwent reverse transcription of the total RNA. Firstly, a Master Mix containing RNasin (1µl; Promega, New South Wales, Australia), Oligo d(T15) at 0.5µg/µl (1µl; Thermo Fisher Scientific, Australia), 10mM dNTP Mix (1µl; Promega, Australia) and Ultra-Pure Distilled Water (1µl; Thermo Fisher Scientific, Australia), was prepared, mixed and centrifuged at ≥8000xg for 15s, before the addition of 4µg/ml total RNA (24µl) to each PCR tube. Reverse transcription Master Mix and RNA were mixed well and centrifuged at ≥8000xg for 15s, before heating at 70°C for 10min in a Thermal Cycler (GeneAmp PCR System 9700, Thermo Fisher Scientific, Australia). The Thermal Cycler program was paused and samples transferred to ice for 2min to break the secondary structure of RNA, before being re-centrifuged at ≥8000xg for 15s and heated in the Thermal Cycler, at 50°C for 10min.

Another Master Mix was prepared on ice containing 5x First Strand Buffer (8µl), 100mM DTT (2µl) and SuperScript III (200units/µl; 2µl; all from Thermo Fisher Scientific, Australia). Aliquots (12µl) were added to each RNA sample, gently mixed and centrifuged at ≥8000xg for 15s, before incubation in a Thermal Cycler at 50°C for 1h. This was followed by heating to 70°C for 15min for inactivation of the enzyme to occur. Samples were diluted 1:10 using Elution Buffer (Qiagen, Australia); and stored at -20°C for future use.

Master Mix for qPCR was prepared, comprising of 2x SYBR® Green PCR Master Mix (10µl; Thermo Fisher Scientific, Australia), Ultra-Pure Distilled Water (3µl; Thermo Fisher Scientific, Australia), 10mM Forward Primer (1µl) and 10mM Reverse Primer (1µl). Primers were designed using qPrimerDepot and provided by Sigma-Aldrich Pty Ltd. Primers were diluted to 1:10 ratio using Elution Buffer, to obtain the correct concentration for qPCR. Master Mix (15µl) was vortexed, centrifuged and added to each 100µl tube. cDNA samples (5µl) were added to each respective tube. Tubes were transferred to Corbett Rotor Gene 6000 machine (Corbett Research Pty Ltd., New South Wales, Australia) and heated at 95°C for 15min, run through 40 cycles of 95°C for 30s, 60°C for 30s and 72°C for 30s, before a final melt step which heated samples from 72°C - 95°C at 1°C increments.

2.5.2 Western Blot Analysis

Following trypsinisation, HaCaTs were seeded into separate T-75 tissue culture flasks, at a density of $2x10^6$ cells/flask in K-SCM (10ml; Section 2.2.2). HaCaTs were maintained at 37°C in a 5% CO_2/95% air atmosphere for 24h, then growth arrested for 24h in serum-free K-SCM. Serum-free K-SCM was removed and replaced with 1% serum-containing K-SCM, containing a range of EBC-46 and EBC-211 concentrations (0.001-10µg/ml, 10ml/flask). Untreated controls (0µg/ml), were also used for comparison at each time-point, which included 1% DMSO. HaCaTs were maintained at 37°C in 5% CO_2/95% air, for 24 and 48h. Each experiment was performed on 3 separate occasions.

At 24 and 48h, treated K-SCM was collected and centrifuged at 1,200xg to pellet cell debris. HaCaTs were washed in ice-cold PBS (x2) and cell/extracellular matrix

(ECM) extracts obtained by scraping the flask contents into ice-cold RIPA buffer (1000µl, Thermo Fisher Scientific), containing protease inhibitors (Complete Protease Inhibitor Cocktail Tablets, Roche, West Sussex, UK) and sonicated (Digital SLPe Cell Disruptor, Branson Ultrasonics Corp., Connecticut, USA). Cell/ECM suspensions were centrifuged (15,000xg/4°C, 5min) and each supernatant protein concentration quantified using Pierce® BCA Protein Assay Kit (Thermo Fisher Scientific), according to manufacturer's instructions. Western Blot analysis was carried out for Krt13, Krt15, Krt16, Krt17, Krt6B, Cyclin B1, Cyclin B2, Cyclin A2, UBE2C, CDKN3 and CDKN1A.

Protein samples (15µg) were separated under reducing conditions by mixing with 4x Laemmli buffer (Bio-Rad Laboratories), heated to 95°C for 5min, centrifuged and stored on ice. Samples underwent SDS-PAGE separation (100V, 75min), using pre-formed 4–15% gradient TGX™ gels (Bio-Rad Laboratories) and Mini-Protean® Tetra Cell System (Bio-Rad Laboratories). A Kaleidoscope Protein Ladder was also loaded onto each gel (Bio-Rad Laboratories). Proteins were transferred onto polyvinylidene difluoride membranes (Hybond™-P; Thermo Fisher Scientific), using Mini Trans-Blot® Electrophoretic Transfer Cell (100V, 1h; Bio-Rad Laboratories).

Membranes were blocked with 5% semi-skimmed milk/1% Tween 20 (Thermo Fisher Scientific) in Tris-buffered saline (TBS), for 1h at room temperature. Membranes were incubated with primary antibody for 1h at room temperature or 4°C overnight in 5% semi-skimmed milk/1% Tween 20. Primary antibodies used and incubation conditions are shown in Table 2.2 (all supplied by Abcam, Cambridgeshire, UK). Protein loading levels were confirmed for each blot using a β-actin Loading Control (1:4000; Abcam). After primary antibody incubation, membranes were washed in 1% Tween 20/TBS (x3); and incubated for 1h at room temperature in secondary antibody (HRP-conjugated polyclonal swine anti-rabbit Ig's; 1:3000, Dako UK Ltd., Cambridgeshire, UK), in 5% semi-skimmed milk/1% Tween 20/TBS. Membranes were washed (x3), followed by an additional wash in TBS for 5min. Membranes were incubated in Amersham ECL™ Prime Detection Reagent (1:1 ratio; (VWR International, UK), for 5min in the dark at room temperature and autoradiographic films (Hyperfilm™-ECL, Thermo Fisher

Table 2.2: Summary of primary antibodies and conditions used for Western blot analysis.

Antibody	Concentration (mg/ml)	Expected Molecular Weight	Incubation Conditions
Krt13	**0.022**	**50kDa**	**4°C o/n**
Krt15	**0.029**	**45kDa**	**1h at RT**
Krt16	**0.163**	**51kDa**	**4°C o/n**
Krt17	**0.060**	**48kDa**	**4°C o/n**
Krt6B	**1.000**	**60kDa**	**1h at RT**
Cyclin B1	**0.316**	**58kDa**	**1h at RT**
Cyclin B2	**1.369**	**45kDa**	**1h at RT**
Cyclin A2	**1.000**	**49kDa**	**4°C o/n**
UBE2C	**0.218**	**20kDa**	**4°C o/n**
CDKN3	**1.260**	**24kDa**	**1h at RT**
CDKN1A	**0.681**	**21kDa**	**1h at RT**
Beta-actin	**0.400**	**42kDa**	**1h at RT**

Scientific) developed, according to manufacturer's instructions. Immunoblot images were quantified by densitometry (Gel Doc™ EZ System and Image Lab™ Software, Bio-Rad Laboratories). Each experiment was performed on 3 separate occasions. Statistical analysis was performed using one-way ANOVA, with Dunnett Multiple Comparisons Test analysis, using the untreated control as the control for comparison. Statistical significance considered at $p<0.05$.

2.5.3 Matrix Metalloproteinase (MMP) Activity Assays

Supernatants collected in Section 2.5.2 were centrifuged for 10min at 1000xg/4°C and stored at -70°C, until required for further experiments. Matrix metalloproteinase (MMP) analysis was undertaken to observe changes in activity following HaCaT treatment with a range of EBC-46 and EBC-211 concentrations (0.001µg/ml, 0.01µg/ml, 0.1µg/ml, 1µg/ml or 10µg/ml), at 24h and 48h. Activity levels were compared versus an untreated HaCaT control at each time-point. MMP-1/-7/-10 activities in the samples were quantified using SensoLyte® 520 MMP-1/-7/-10 Activity Assay Kits, respectively (Fluorimetric; AnaSpec Inc., Cambridge, UK), and performed according to manufacturer's instructions.

Pro-MMPs were activated through the incubation of culture media samples with APMA (1mM; in Kits) immediately before each experiment. Samples were maintained on ice once activated. MMP-1 containing samples were activated at 37°C for 3h, MMP-7 containing samples activated at 37°C for 1h; and MMP-10 containing samples activated at 37°C for 24h. Once activated, samples were incubated with respective MMP-1/-7/-10 substrates. MMP substrates were diluted 1:100 in Assay Buffer (in Kits). MMP-1/-7-/10 containing samples (50µl/well) were added to black, flat-bottomed, 96 well microplates (Thermo Fisher Scientific). Assay buffer (50µl) was added to three wells as a substrate control. MMP-1/-7/-10 Substrate Mix (50µl/well, in Kits) was added to the sample and control wells; and mixed well by gentle shaking the plate for 30s. Fluorescence signals were measured at end-point by incubating the plate at 37°C for 1h, avoiding direct light. Fluorescence intensity was measured every 10min at an excitation of 490nm and emission of 520nm. The average values obtained for the substrate control wells were used to blank correct the fluorescent readings for each sample. This experiment was performed on 3 separate

sample sets for each MMP analysed. The corrected values obtained were used to calculate average values and standard errors determined. Statistical analysis was performed using one-way ANOVA with post-test Tukey analysis; and statistical significance considered at $p<0.05$.

2.5.4 Enzyme-Linked Immunosorbent Assays (ELISAs)

Supernatants collected in Section 2.5.2 were centrifuged for 10min at 1000xg/4°C and stored at -70°C, until required for further experiments. Enzyme-linked immunosorbent assays (ELISAs) were undertaken to observe changes on expression levels following HaCaT treatment with a range of EBC-46 and EBC-211 concentrations (0.001µg/ml, 0.01µg/ml, 0.1µg/ml, 1µg/ml or 10µg/ml), at 24h and 48h. Expression levels were compared versus an untreated HaCaT control at each time-point. Interleukin (IL)-6, IL-8, CCL5 and CXCL10 expression levels were quantified using Human IL-6 Immunoassay, Human CXCL8/IL-8 Immunoassay, Human CCL5/RANTES Immunoassay and Human CXCL10/IP-10 Immunoassay, respectively (Quantikine® ELISA; R&D Systems Ltd., Oxfordshire, UK), and performed according to manufacturer's instructions.

Assay Diluent RD1W (100µl) was added to microplate wells (in Kit), followed by either the standards, samples or controls (100µl); and incubated for 2h at room temperature. Each well was aspirated and washed (x4) using Wash Buffer (400µl; in Kit), with complete removal of liquid after each wash step, especially after final wash step. Human IL-6 Conjugate (200µl; in Kit) was added to each well and incubated for 2h at room temperature. Wash steps were repeated as before (x4), with complete removal of liquid after each wash. Substrate Solution (200µl; in Kit) was added to each well and incubated for 20min at room temperature, under darkness. Stop Solution (50µl; in Kit) was added to each well to stop the reaction and tapped gently to ensure thorough mixing. The optical density of each well was determined through taking readings of each well at 450nm. Readings were also taken at 540nm and subtracted from the 450nm readings, as an additional internal control. This ELISA was performed on 3 separate sample sets. The corrected values were used to calculate average values and standard errors. Statistical analysis was performed using

one-way ANOVA with post-test Tukey analysis; and statistical significance considered at $p<0.05$.

ELISA protocol was repeated for IL-8. Assay Diluent RD1-85 (100µl) was added to microplate wells (in Kit), followed by either the standards, samples or controls (50µl); and incubated for 2h at room temperature. Each well was aspirated and washed (x4) using Wash Buffer (400µl; in Kit), with complete removal of liquid after each wash step, especially after final wash step. Human IL-8 Conjugate (100µl; in Kit) was added to each well and incubated for 1h at room temperature. Wash steps were repeated as before (x4), with complete removal of liquid after each wash. Substrate Solution (200µl; in Kit) was added to each well, and incubated for 30min at room temperature, under darkness. Stop Solution (50µl; in Kit) was added to each well to stop the reaction and tapped gently to ensure thorough mixing. The optical density of each well was determined through taking readings of each well, as described for IL-6 above; and IL-8 expression levels calculated. Statistical analysis was performed using one-way ANOVA with post-test Tukey analysis; and statistical significance considered at $p<0.05$.

ELISA protocol was repeated for CCL5 (also known as RANTES). Assay Diluent RD1W (100µl) was added to microplate wells (in Kit), followed by either the standards, samples or controls (100µl); and incubated for 2h at room temperature. Each well was aspirated and washed (x3) using Wash Buffer (400µl; in Kit); with complete removal of liquid after each wash step, especially after final wash step. Human RANTES Conjugate (200µl; in Kit) was added to each well and incubated for 1h at room temperature. Wash steps were repeated as before (x3), with complete removal of liquid after each wash. Substrate Solution (200µl; in Kit) was added to each well and incubated for 20min at room temperature, under darkness. Stop Solution (50µl; in Kit) was added to each well to stop the reaction and tapped gently to ensure thorough mixing. The optical density of each well was determined through taking readings of each well, as described for IL-6 above; and CCL5 expression levels calculated. Statistical analysis was performed using one-way ANOVA with post-test Tukey analysis; and statistical significance considered at $p<0.05$.

ELISA protocol was repeated for CXCL10 (also known as IP-10). Assay Diluent RD1-56 (150µl) was added to microplate wells (in Kit), followed by either the standards, samples or controls (100µl); and incubated for 2h at room temperature. Each well was aspirated and washed (x4) using Wash Buffer (400µl; in Kit); with complete removal of liquid after each wash step, especially after final wash step. Human IP-10 Conjugate (200µl; in Kit) was added to each well and incubated for 2h at room temperature. Wash steps were repeated as before (x4), with complete removal of liquid after each wash. Substrate Solution (200µl; in Kit) was added to each well and incubated for 30min at room temperature, under darkness. Stop Solution (50µl; in Kit) was added to each well to stop the reaction and tapped gently to ensure thorough mixing. The optical density of each well was determined through taking readings of each well, as described for IL-6 above; and CXCL10 expression levels calculated. Statistical analysis was performed using one-way ANOVA with post-test Tukey analysis; and statistical significance considered at $p<0.05$.

Chapter 3 - Effects of EBC-46 and EBC-211 on Dermal Fibroblast Wound Healing Responses

Chapter 3 - Effects of EBC-46 and EBC-211 on Dermal Fibroblast Wound Healing Responses

3.1 Introduction

EBC-46 is a naturally-derived, epoxy-tigliane compound, sourced and developed from within seeds of the Fountain's Blushwood Tree in Queensland's Tropical Rainforest by Australian biotechnology company, QBiotics Ltd. (described in Section 1.7; Reddell & Gordon 2007). EBC-46 has been demonstrated to possess potent anti-cancer effects on solid tumours and sarcoids; this led to the hypothesis that an anti-fibrotic response may be involved in tumour ablation, in particular as sarcoids are primarily composed of fibroblasts (Reddell & Gordon 2007; Boyle et al. 2014). An unexpected beneficial response following tumour sloughing was the rapid wound closure, with reduced scarring evident and the reformation of skin appendages (Reddell & Gordon 2007).

Fibroblasts are a key cell involved in the acute skin wound healing response and perform a number of essential wound healing functions, such as extracellular matrix (ECM) production (Martin 1997; Reinke & Sorg 2012; Bainbridge 2013). The differentiation of fibroblasts to myofibroblasts is a vital function due to the contractile force exerted by the myofibroblasts to aid closure of the wound site (Li & Wang 2011). Fibroblasts express a number of vital growth factors required during wound healing, with some acting in an autocrine response on fibroblasts and others in a paracrine effect on keratinocytes. There is a positive feedback system between these key wound healing cells, contributing to wound repair (Barrientos et al. 2008; Schultz & Wysocki 2009). Acute skin wound healing responses are tightly regulated processes and alterations in these can produce detrimental healing responses, as seen with chronic non-healing wounds where re-epithelialisation is impaired (Chapter 4), or during dermal fibrosis, such as with keloid and hypertrophic scars (Section 1.5; Bran et al. 2009; Shih et al. 2010).

Keloid and hypertrophic scars are a result of excessive scarring at the wound site, with hypertrophic scars possessing an increased presence of myofibroblasts, resulting in excessive wound contraction (Gauglitz et al. 2011; Jumper et al. 2015; Kelsh et al. 2015). This increased production of matrix components may be a result of an increased presence of fibroblasts at the wound site, following enhanced chemoattraction by immune cells, in addition to the increased fibroblast proliferation observed in keloid fibroblasts (Shih et al. 2010; Gauglitz et al. 2011; Ding & Tredget 2015; Jumper et al. 2015; Kelsh et al. 2015). Burn injuries have a high incidence of hypertrophic scar formation, higher than the incidence following surgery (Gauglitz et al. 2011). This is thought to be a result of increased activation of the fibroblasts following increased immune and inflammatory responses after thermal injury, leading to increased matrix deposition and differentiation to contractile myofibroblasts (Gauglitz et al. 2011; Ding & Tredget 2015). Burn injuries result in damaged and necrotic tissue, impacting the normal acute wound healing response, by impacting the infiltration of numerous growth factors to the wound site as a result of impaired angiogenesis (Rose & Chan 2016).

Chronic wounds have common features impacting their healing mechanisms, despite the variety of wounds and ulcers; including excessive inflammatory response, impaired ECM remodelling, increased metalloproteinase activity, bacterial colonisation and biofilm formation (Stephens et al. 2003; Wall et al. 2008; Guo & DiPietro 2010; Demidova-Rice et al. 2012; Percival et al. 2012; Eming et al. 2014; McInnes et al. 2014). Alterations in the phenotype of fibroblasts present in chronic wounds have been observed, with reduced proliferation, migration, response to growth factors and ECM turnover (Agren & Werthén 2007; Menke et al. 2007; Wall et al. 2008). One theory was that dermal fibroblasts were becoming senescent, which would reduce fibroblast proliferative ability and matrix synthesis (Telgenhoff & Shroot 2005; Wall et al. 2008; Eming et al. 2014). Other theories on impaired fibroblast functions in chronic wounds include a reduced ability to respond to signals from growth factors due to faulty signalling pathways, or faulty adhesion receptor activation, resulting in dysfunctional formation of the matrix (Agren & Werthén 2007; Menke et al. 2007; Frykberg & Banks 2015). Fibroblast migration is also impaired in chronic wounds, with reduced mitogenic function to stimuli, including a number of growth factors. This

has been partly attributed to the wound exudate present in chronic wounds and a reduced presence of the receptors required to propagate these migratory responses (Raffetto et al. 2001; Menke et al. 2007). Additionally, the high presence of bacteria and biofilm formation contributes to this dysfunctional healing response. It has been proposed that the excessive inflammation present in chronic wounds induces an aged phenotype of the tissue, resulting in reduced functionality and vasculature formation (Wall et al. 2008; Guo & DiPietro 2010; Eming et al. 2014).

There are subtle differences between adult dermal wound healing and the preferential responses of oral mucosal and early-gestational foetal healing, including attenuated inflammatory response, altered cytokine/growth factor profiles; and contrasting collagen synthesis (Nauta et al. 2011; Leung et al. 2012; Rolfe & Grobbelaar 2012). Fibroblast responses are enhanced in early-gestational foetal healing, with increased proliferative and migratory abilities; more organised ECM synthesis occurs by foetal fibroblasts (Yates et al. 2012; Helmo et al. 2013). Presence of myofibroblasts in foetal wounds has been disputed, with some claiming that they are not present and others that they are present earlier in the wound healing process than in adult wound responses. Other claims are that they are completely absent from early non-scarring foetal wounds but are present during later-gestational foetal wounds, which result in scar formation (Larson et al. 2010; Rolfe & Grobbelaar 2012; Yates et al. 2012). Myofibroblasts undergo apoptosis once the tissue has been remodelled and is of sufficient tensile strength; scarless healing wounds have shown increased caspase 7 levels, the active form, which potentially increases apoptosis of a number of cells, including myofibroblasts (Satish & Kathju 2010; Rolfe & Grobbelaar 2012; Mcilwain et al. 2013; Darby et al. 2014; Balaji et al. 2015).

Oral fibroblasts appear to respond earlier to TGF-β isoforms, resulting in earlier but less sustained contraction compared to dermal fibroblasts, with also a resistance of oral fibroblasts differentiation to contractile myofibroblasts (Lee & Eun 1999; Meran et al. 2008; Enoch et al. 2010; Nauta et al. 2011). A study has shown that the level of hyaluronan may play an important role in fibroblast response to TGF-β signalling, with increased hyaluronan resulting in stimulated fibroblast proliferation; reduced levels of hyaluronan are evident in oral mucosal wounds, leading to a reduced proliferative

response (Meran et al. 2008). Production of certain MMPs, in particular MMP-2 and MMP-3, is up-regulated in oral fibroblasts compared to dermal fibroblasts. This increased presence may impact on the ECM remodelling ability through a quicker remodelling ability and wound contraction, as rapid, scarless healing is a known response of oral mucosal healing (Stephens et al. 2001; McKeown et al. 2007; Enoch et al. 2010).

Similar beneficial wound healing responses, characterised by rapid re-epithelialisation and minimal scarring, were observed in veterinary case studies with EBC-46 treatment on wounds that were previously unresponsive to current wound care strategies (Reddell et al. 2014). However, despite the significant beneficial effects on wound healing previously observed, little was known about how the novel epoxy-tiglianes exert these responses (Reddell et al. 2014). The healed wound site is more representative of a preferential healing process, such as early-gestational foetal and oral mucosal wounds (Mak et al. 2009; Nauta et al. 2011; Rolfe & Grobbelaar 2012). Nonetheless, given the prominent role that fibroblasts play in acute skin wound healing, a greater understanding of the effects on the fibroblast wound healing responses was required; this is vital in order to progress with these novel epoxy-tiglianes as a novel wound healing agent.

3.2 Aims

Due to the importance of the fibroblasts in acute skin wound healing, any alterations in the genotypic or phenotypic responses could alter the healing mechanisms. This alteration could produce a favourable scarless response, as discussed previously. Therefore, the aims of this Chapter were to assess the effects of EBC-46 or EBC-211 on key fibroblastic wound healing responses, such as viability, proliferation, cell cycle progression, morphology; and cellular migration. In addition, the effects of EBC-46 and EBC-211 on the differentiation of fibroblasts to myofibroblasts were evaluated, due to their importance to wound contraction, closure and scarring outcome *in vivo*.

3.3 Materials and Methods

3.3.1 Preparation of EBC-46 and EBC-211

EBC-46 and the lesser active analogue, EBC-211, were both supplied by QBiotics Ltd., Queensland, Australia. EBC-46 and EBC-211 were solubilised in DMSO (Section 2.1). For both compounds, concentrations of 0.001μg/ml, 0.01μg/ml, 0.1μg/ml, 1μg/ml, 10μg/ml and 100μg/ml were prepared in 1% F-SCM for the assessment of dermal fibroblast wound healing responses (Section 2.2.1).

3.3.2 Dermal Fibroblast Culture

Dermal fibroblasts were sourced, cultured, sub-cultured, counted, cryopreserved and mycoplasma screened, as previously described (Sections 2.2.1, 2.2.3, 2.2.4 and 2.2.5 respectively).

3.3.3 Assessment of Dermal Fibroblast Viability and Proliferation

The viability and proliferation of dermal fibroblasts was assessed through the use of an MTT [3-(4,5-dimethyl-2-thiazolyl)-2,5-diphenyltetrazolium bromide] Dye-Reduction assay at 24h, 72h, 120h and 168h, as previously described (Section 2.3.1).

3.3.4 Assessment of Dermal Fibroblast Cell Cycling

Dermal fibroblasts were seeded and cultured for cell cycle analysis, with samples obtained at T0, T22, T29 and T36 after treatment with EBC-46 or EBC-211 (0μg/ml, 0.001μg/ml, 0.01μg/ml, 0.1μg/ml, 1μg/ml and 10μg/ml). Samples were prepared, Draq5 DNA dye added and analysed by Flow Cytometry (FACScalibur, Becton Dickinson, Oxfordshire, U.K.), as previously discussed (Sections 2.3.2.1, 2.3.2.3 and 2.3.2.4).

3.3.5 Assessment of Dermal Fibroblast Morphology

Morphology of dermal fibroblasts was assessed by light microscopy, as previously described (Section 2.3.3).

3.3.6 Assessment of Dermal Fibroblast Repopulation

Dermal fibroblast repopulation was assessed through the use of an *in vitro* 'scratch wound' assay, with images captured every 20min over 48h using Time-Lapse Microscopy, as previously described (Section 2.3.4).

3.3.7 Assessment of Dermal Fibroblast-Myofibroblast Differentiation

The assessment and confirmation of dermal fibroblast to myofibroblast differentiation in the presence and absence of TGF-β_1 was performed through immunocytochemistry and quantitative polymerase chain reaction (qPCR) analysis, as previously described (Sections 2.3.5.1 and 2.3.5.2, respectively).

3.4 Results

3.4.1 Effects of EBC-46 and EBC-211 on Dermal Fibroblast Viability and Proliferation

The viability and proliferation study was performed on fibroblasts cultured in EBC-46 or EBC-211 (0.001µg/ml, 0.01µg/ml, 0.1µg/ml, 1µg/ml, 10µg/ml and 100µg/ml), with untreated controls included for comparison purposes (0µg/ml) for both compounds. Average absorbance values were obtained at each EBC-46 and EBC-211 concentration at 24h, 72h, 120h and 168h. Values were used to calculate the variation from the untreated control for each concentration and time-point; and percentage calculations produced versus each untreated control (Figures 3.1A and 3.2A).

Both EBC-46 and EBC-211 were shown to be cytotoxic at 100µg/ml. This was evident by the significantly decreased percentage data obtained; this was observed for both EBC-46 and EBC-211, from 24h onwards ($p<0.001$; Figures 3.1A and 3.2A, respectively), compared to the untreated controls (0µg/ml). However, there was a delayed cytotoxic effect of EBC-211, compared to EBC-46, which confirmed the reduced activity of EBC-211. This was evident by the longer time period required for a complete cytotoxic effect to occur.

EBC-46 also appeared to have an anti-proliferative effect on the fibroblasts across the majority of concentrations. At 24h and 120h, this was only significant at a few

Figure 3.1: (A) Dermal fibroblast viability and proliferation percentage differences, following culture in the presence of EBC-46 (0µg/ml, 0.001µg/ml, 0.01µg/ml, 0.1µg/ml, 1µg/ml, 10µg/ml and 100µg/ml), at 24h, 72h, 120h and 168h; (*N=3, average±SE*). (B) Cross-statistical analysis of significant changes in dermal fibroblast proliferation, following treatment with EBC-46 (0.001-100µg/ml) over 168h, versus untreated controls (p<0.05, **p<0.01, ***p<0.001*).**

A

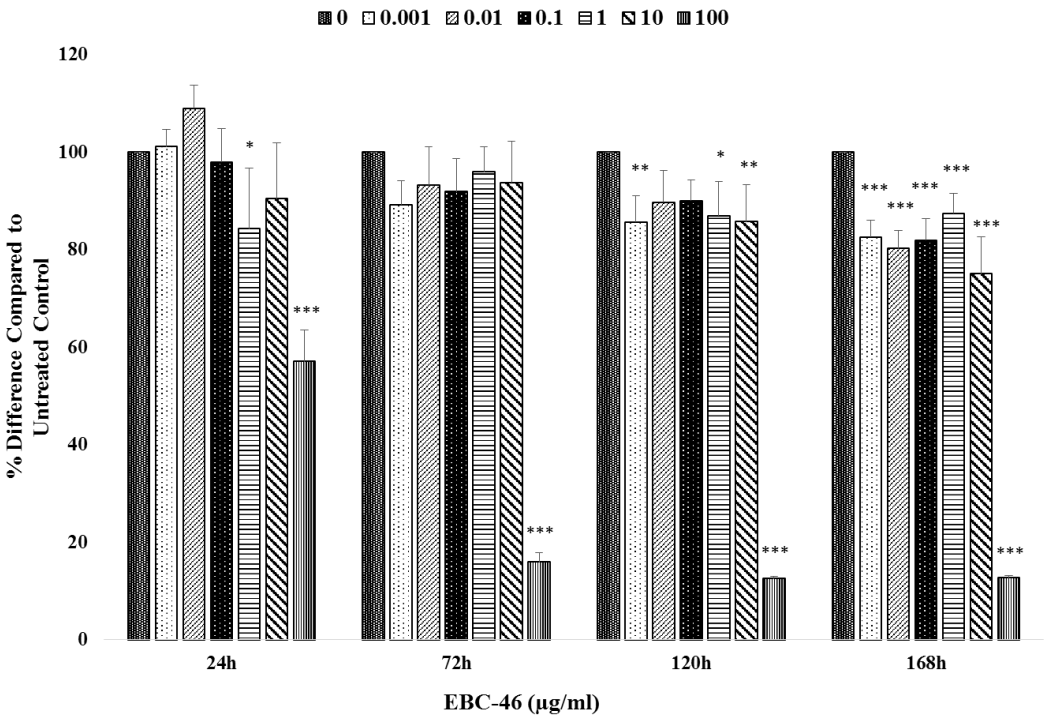

B

24h

	0	0.001	0.01	0.1	1	10	100
0					*		***
0.001					**		***
0.01					***	*	***
0.1							***
1							***
10							***
100							

72h

	0	0.001	0.01	0.1	1	10	100
0							***
0.001							***
0.01							***
0.1							***
1							***
10							***
100							

120h

	0	0.001	0.01	0.1	1	10	100
0		**			*	**	***
0.001							***
0.01							***
0.1							***
1							***
10							***
100							

168h

	0	0.001	0.01	0.1	1	10	100
0		***	***	***	***	***	***
0.001							***
0.01							***
0.1							***
1						**	***
10							***
100							

Figure 3.2: (A) Dermal fibroblast viability and proliferation percentage differences, following culture in the presence of EBC-211 (0µg/ml, 0.001µg/ml, 0.01µg/ml, 0.1µg/ml, 1µg/ml, 10µg/ml and 100µg/ml), at 24h, 72h, 120h and 168h; (*N=3, average±SE*). (B) Cross-statistical analysis of significant changes in dermal fibroblast proliferation, following treatment with EBC-211 (0.001-100µg/ml) over 168h, versus untreated controls (p<0.05, **p<0.01, ***p<0.001*).**

A

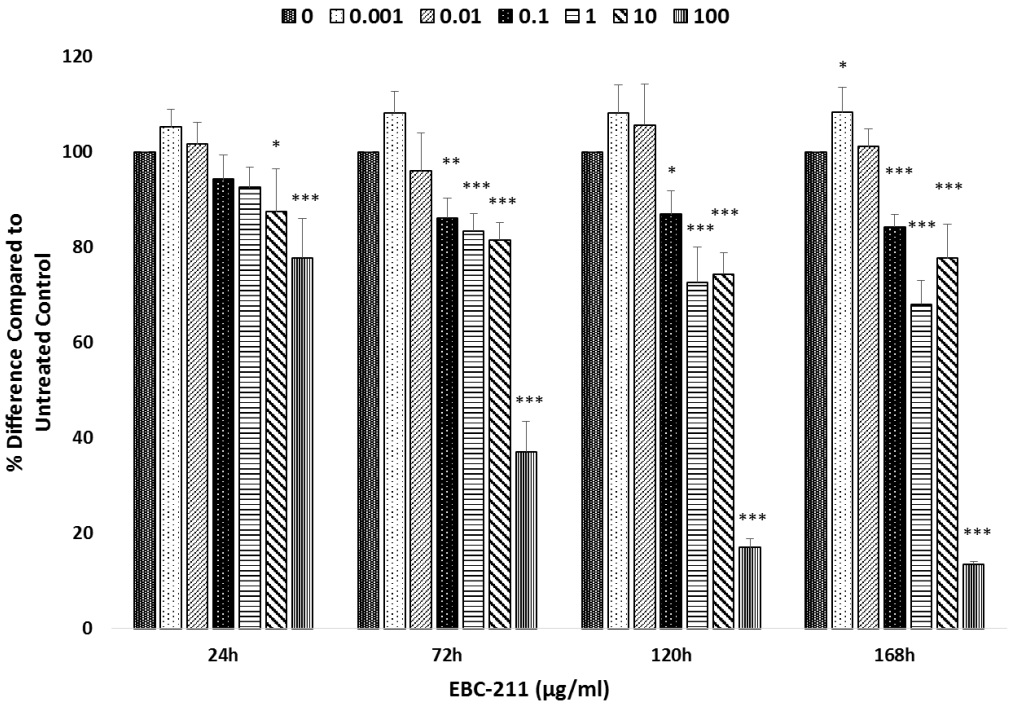

B

24h

	0	0.001	0.01	0.1	1	10	100
0						*	***
0.001				*	*	***	***
0.01						**	***
0.1							***
1							***
10							
100							

72h

	0	0.001	0.01	0.1	1	10	100
0				**	***	***	***
0.001			**	***	***	***	***
0.01					**	**	***
0.1							***
1							***
10							***
100							

120h

	0	0.001	0.01	0.1	1	10	100
0				*	***	***	***
0.001				***	***	***	***
0.01				***	***	***	***
0.1					**		***
1							***
10							***
100							

168h

	0	0.001	0.01	0.1	1	10	100
0		*		***	***	***	***
0.001				***	***	***	***
0.01				***	***	***	***
0.1					***		***
1						**	***
10							***
100							

concentrations (0.001µg/ml, 1µg/ml and 10µg/ml), compared to untreated controls ($p<0.01$-0.05); there was no significant anti-proliferative effect evident at 72h ($p>0.05$). In contrast, at 168h, there was a highly significant anti-proliferative effect across all the concentrations, in comparison to untreated controls ($p<0.001$; Figure 3.1A). As seen with EBC-46, an anti-proliferative effect was also observed with EBC-211 (Figure 3.2A). This reduction in proliferation was significant for 0.1-10µg/ml at 72h, 120h and 168h, in addition to 10µg/ml at 24h, when compared to untreated control responses ($p<0.001$-0.05; Figure 3.2A). A positive proliferative effect on dermal fibroblasts was evident upon culture with 0.001µg/ml EBC-211, significant in comparison to untreated controls at 168h ($p<0.05$; Figure 3.2A). Cross-statistical analysis was performed for both EBC-46 and EBC-211 (0.001-100µg/ml), comparing epoxy-tigliane treated cells between concentrations for both EBC-46 and EBC-211. This comparison only showed a few significant differences between concentrations of EBC-46. At 24h, there were significant differences between 0.001µg/ml and 0.01µg/ml compared to 1µg/ml; and 0.1µg/ml compared to 10µg/ml ($p<0.001$-0.05; Figure 3.1B). In addition, at 168h, there was a significant difference between 1µg/ml and 10µg/ml EBC-46 ($p<0.01$; Figure 3.1B). The cross-statistical analysis between concentrations for EBC-211 showed response differences between high and low concentrations. Significant differences were observed between all comparisons, the only exception being between 0.1µg/ml and 10µg/ml EBC-211 ($p<0.001$-0.05; Figure 3.2B).

3.4.2 Effects of EBC-46 and EBC-211 on Dermal Fibroblast Cell Cycling

In light of the potential anti-proliferative effects identified in Section 3.4.1, Flow Cytometry was further performed to determine whether treatment with EBC-46 or EBC-211 (0.001µg/ml, 0.01µg/ml, 0.1µg/ml, 1µg/ml and 10µg/ml) had an effect on the cell cycle progression of dermal fibroblasts, compared to untreated controls (0µg/ml); and whether this contributed to the anti-proliferative effects observed. A growth curve was initially performed to calculate the cycling time for an untreated control fibroblasts (Supplement 3.1). This determined the time-points required to observe the different phases of the cell cycle for the untreated fibroblast controls. The time-points identified were T0 (at the point of treatment), T22 (22h after treatment), T29 (29h after treatment) and T36 (36h after treatment). The T0 time-point was

analysed at point of treatment to ensure all cells were at the same synchronised state after serum starvation, with any differences that subsequently followed at later time-points being a consequence of epoxy-tigliane treatment. Data obtained at T0 for both EBC-46 and EBC-211 showed no significant differences, compared to untreated control. This confirmed that the cells were all synchronised to the same cell cycle phase before analysis of the later time-points to determine significant changes in cell cycle progression ($p>0.05$; Figures 3.3A and 3.7A).

Treatment with EBC-46 (0.001-10µg/ml) showed the significantly delayed progression of dermal fibroblasts through the cell cycle phases at T22 and T29. This was evident at 0.01-10µg/ml EBC-46 at T22 and 0.001-10µg/ml EBC-46 at T29 ($p<0.01$-0.05; Figures 3.4A and 3.5A, respectively). This was shown to have a greater impact at T29 across the full range of EBC-46 concentrations. The untreated cells had progressed back into G1 phase, whereas the EBC-46 treated cells remained in S and G2 phases, demonstrating the delayed progression ($p<0.01$-0.05; Figure 3.5A). There was no significant difference evident at T36, between the EBC-46 treated cells and the untreated controls ($p>0.05$; Figure 3.6A). It is thought that this may be a result of different lengths of the dermal fibroblast cell cycle phases, with G1 being the longest and G2/M the shortest. This gives the appearance that the cells have caught up to the same cell cycle phase by T36. The accompanying cell cycle histogram shows a proportion of cells treated with EBC-46 remaining in G2 phase (Figure 3.6B). The cell cycle histograms show all conditions synchronised at T0, with the normal progression through the cell cycle phases for the untreated controls (Figures 3.3B, 3.4B, 3.5B and 3.6B). However, the EBC-46 treated cells progressed through at a slower rate; this delayed progression through the cell cycle could contribute to the anti-proliferative responses previously observed.

Treatment with EBC-211 showed a similar effect (Figures 3.7-3.10A), with a significantly delayed progression through the cell cycle at 1-10µg/ml EBC-211 at T22 and 0.001-10µg/ml EBC-211 at T29 ($p<0.01$-0.05; Figures 3.8A and 3.9A, respectively). Due to the lesser activity of EBC-211, the lower concentrations (0.001-0.01µg/ml) appeared to progress at a similar rate to the untreated control at T22 ($p>0.05$; Figure 3.8A). This was evident in the corresponding histograms (Figures

Figure 3.3: (A) Dermal fibroblast cell cycle analysis at T0, following culture in the presence of EBC-46 (0.001µg/ml, 0.01µg/ml, 0.1µg/ml, 1µg/ml and 10µg/ml), compared to untreated controls (0µg/ml; *N=3, average % in each phase±SE*). Statistical analysis (*all p>0.05*). (B) Corresponding cell cycle histogram at T0, following culture in the presence of EBC-46 (0-10µg/ml).

A

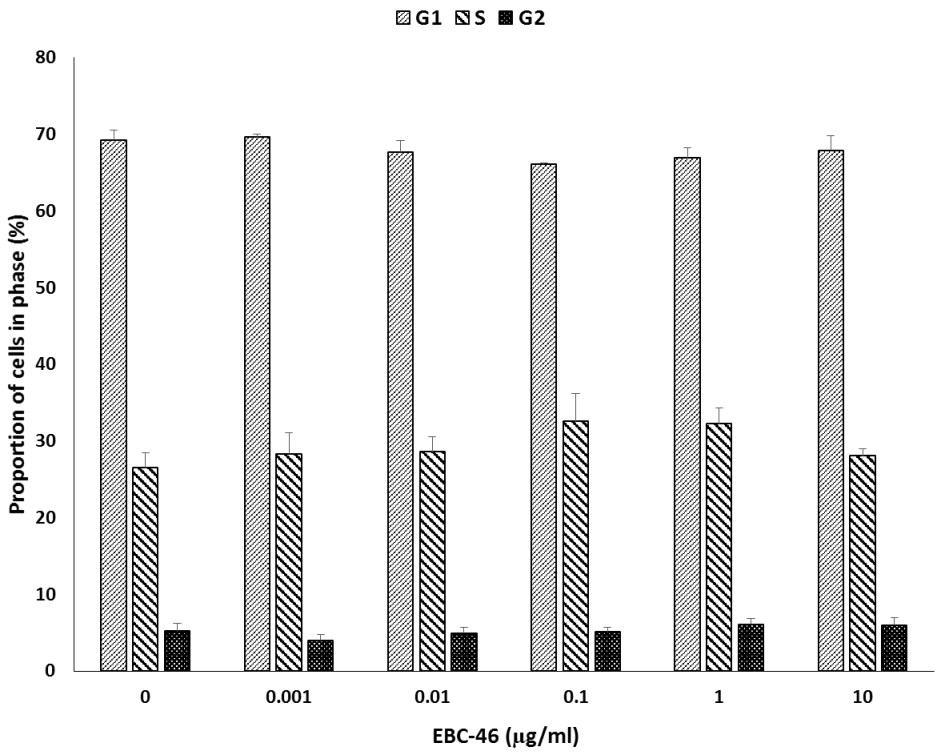

B

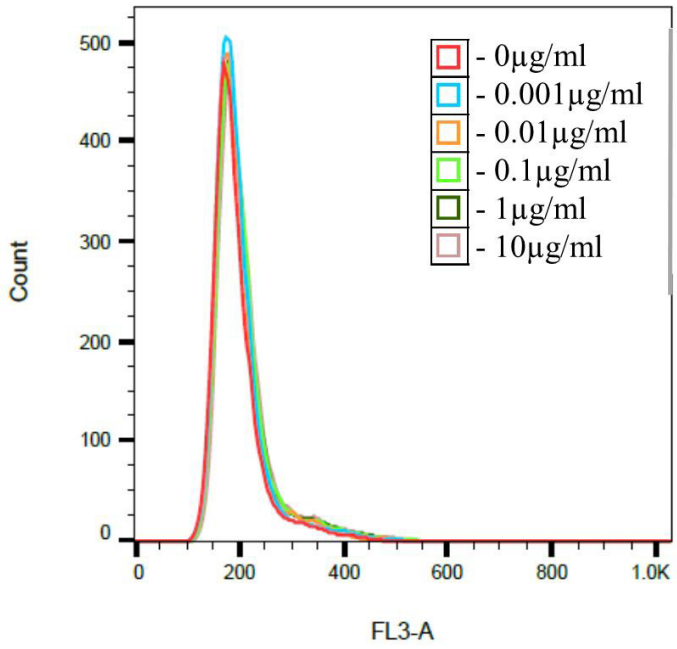

Figure 3.4: (A) Dermal fibroblast cell cycle analysis at T22, following culture in the presence of EBC-46 (0.001µg/ml, 0.01µg/ml, 0.1µg/ml, 1µg/ml and 10µg/ml), compared to untreated controls (0µg/ml; *N=3, average % in each phase±SE*). Statistical analysis (p<0.05, **p<0.01*). (B) Corresponding cell cycle histogram at T22, following culture in the presence of EBC-46 (0-10µg/ml).**

A

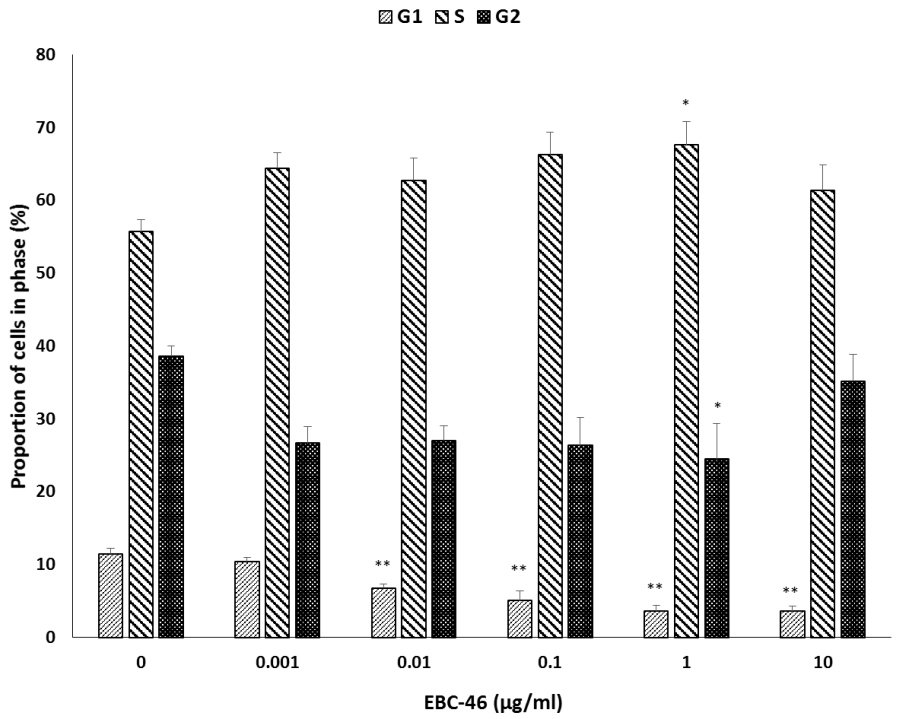

B

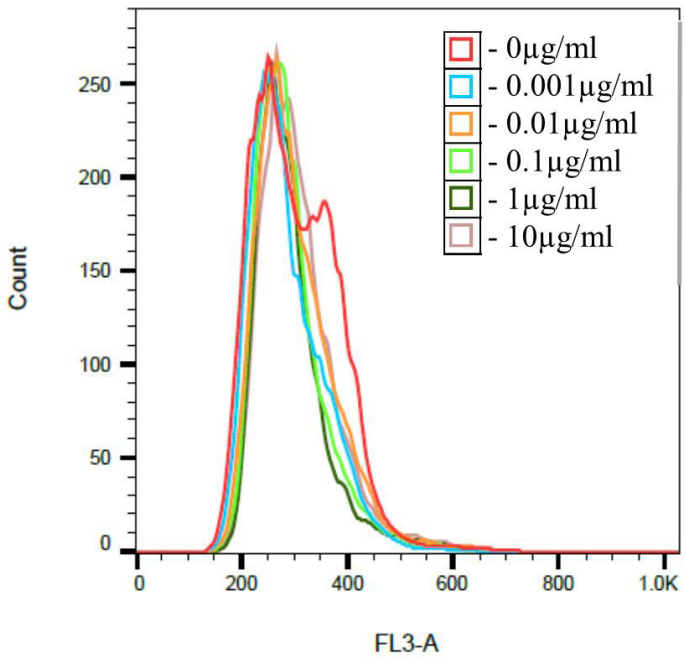

Figure 3.5: (A) Dermal fibroblast cell cycle analysis at T29, following culture in the presence of EBC-46 (0.001µg/ml, 0.01µg/ml, 0.1µg/ml, 1µg/ml and 10µg/ml), compared to untreated controls (0µg/ml; *N=3, average % in each phase±SE*). Statistical analysis (p<0.05, **p<0.01*). (B) Corresponding cell cycle histogram at T29, following culture in the presence of EBC-46 (0-10µg/ml).**

A

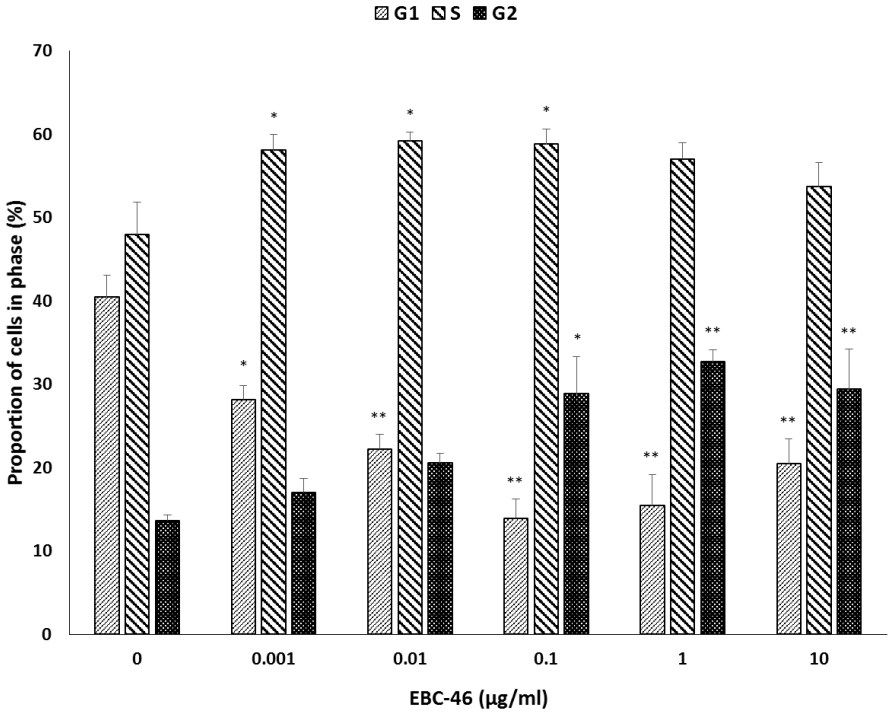

B

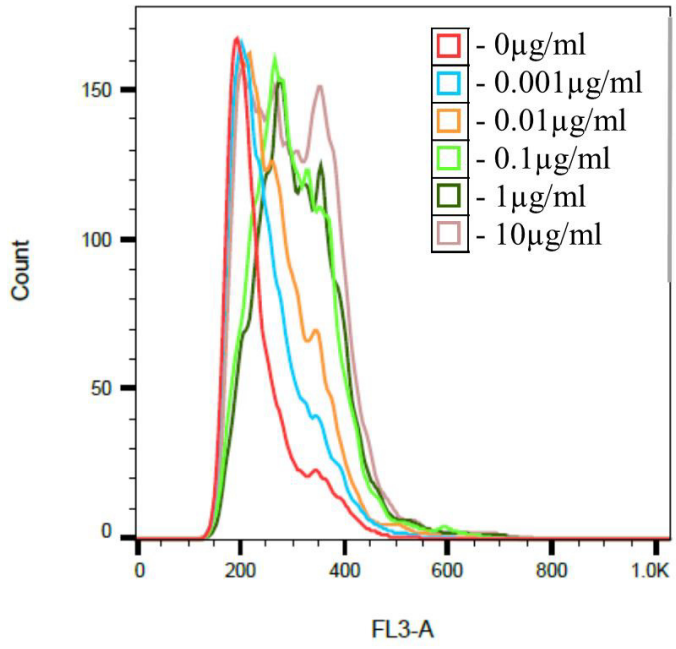

Figure 3.6: (A) Dermal fibroblast cell cycle analysis at T36, following culture in the presence of EBC-46 (0.001µg/ml, 0.01µg/ml, 0.1µg/ml, 1µg/ml and 10µg/ml), compared to untreated controls (0µg/ml; *N=3, average % in each phase±SE*). Statistical analysis (*all p>0.05*). (B) Corresponding cell cycle histogram at T36, following culture in the presence of EBC-46 (0-10µg/ml).

A

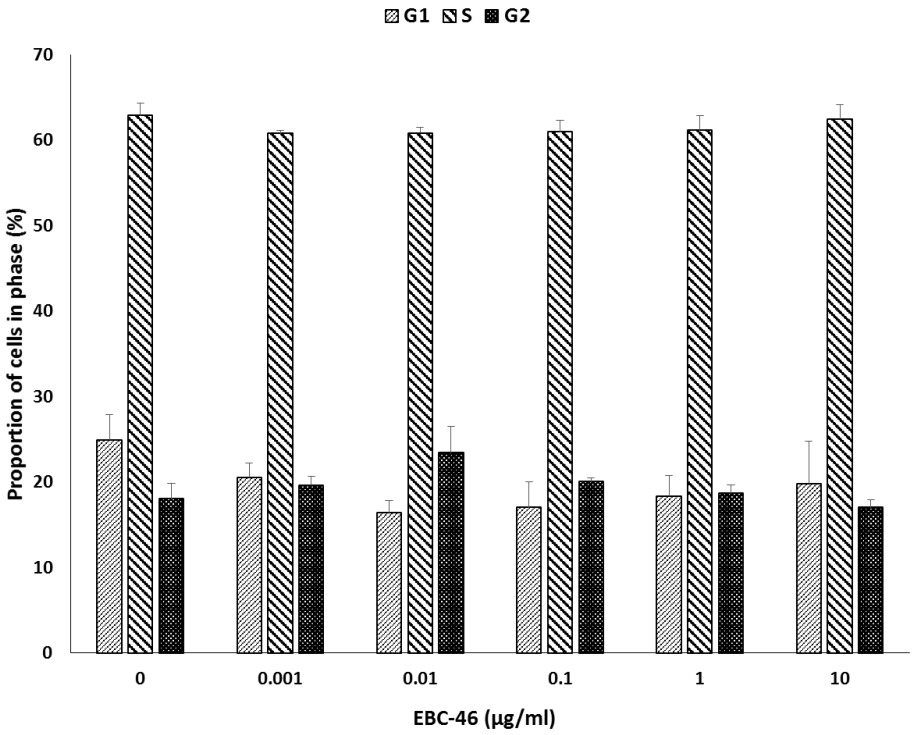

B

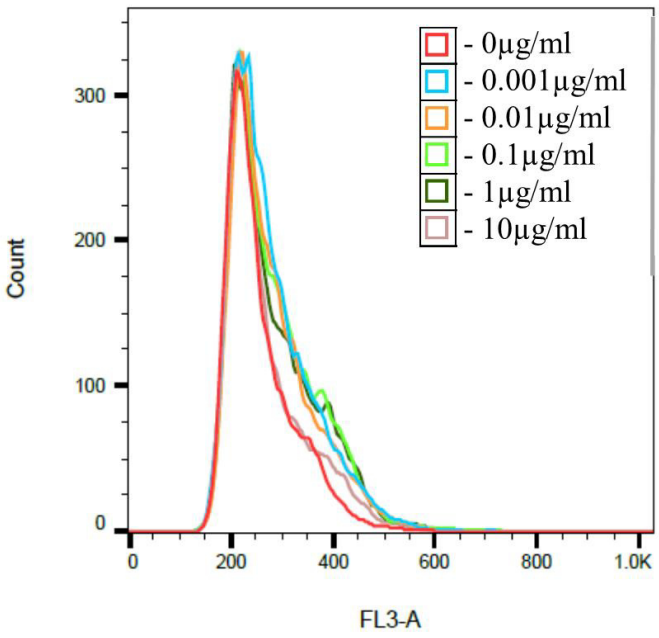

Figure 3.7: (A) Dermal fibroblast cell cycle analysis at T0, following culture in the presence of EBC-211 (0.001µg/ml, 0.01µg/ml, 0.1µg/ml, 1µg/ml and 10µg/ml), compared to untreated controls (0µg/ml; *N=3, average % in each phase±SE*). Statistical analysis (*all p>0.05*). (B) Corresponding cell cycle histogram at T0, following culture in the presence of EBC-211 (0-10µg/ml).

A

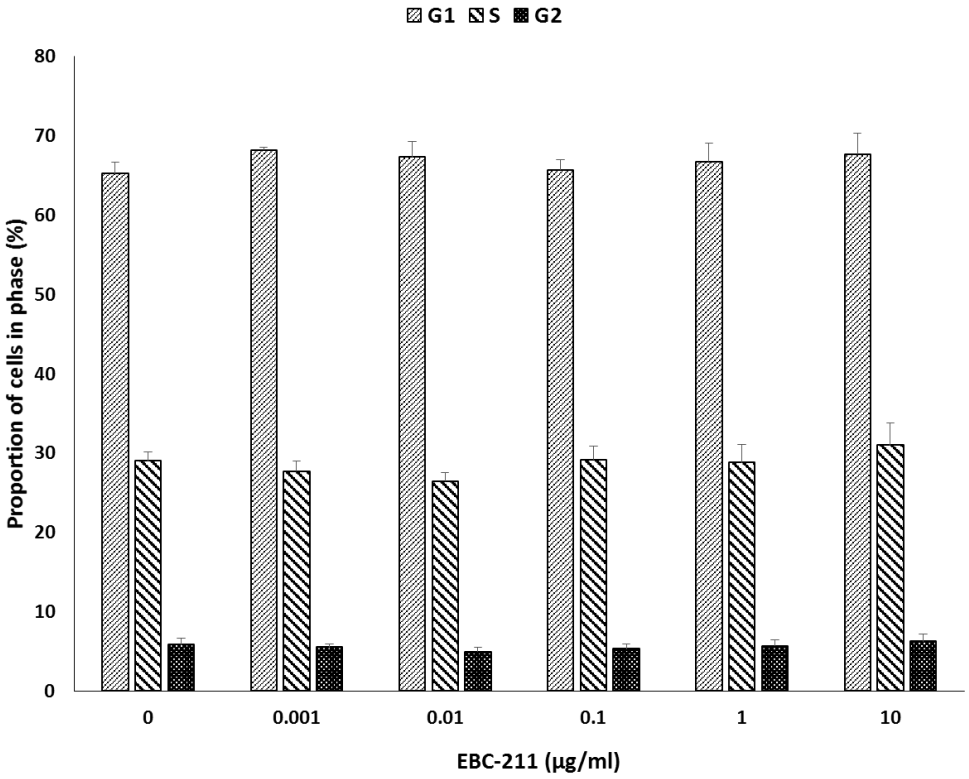

B

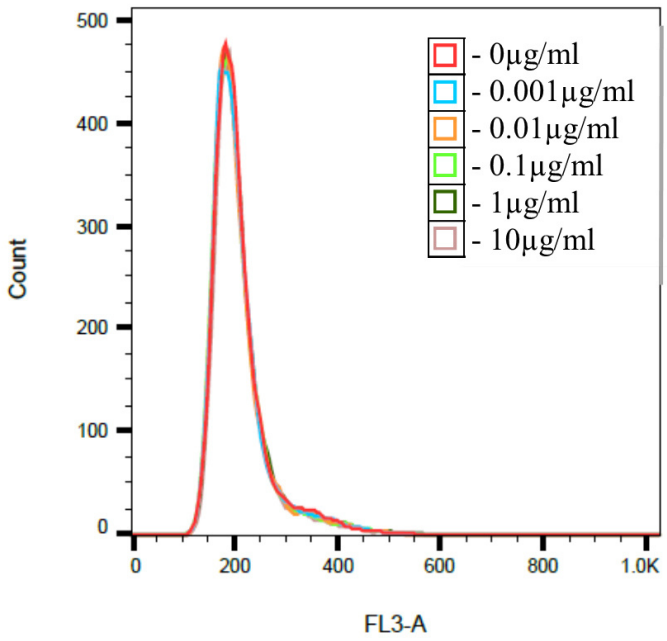

Figure 3.8: (A) Dermal fibroblast cell cycle analysis at T22, following culture in the presence of EBC-211 (0.001µg/ml, 0.01µg/ml, 0.1µg/ml, 1µg/ml and 10µg/ml), compared to untreated controls (0µg/ml; *N=3, average % in each phase±SE*). Statistical analysis (p<0.05, **p<0.01*). (B) Corresponding cell cycle histogram at T22, following culture in the presence of EBC-211 (0-10µg/ml).**

A

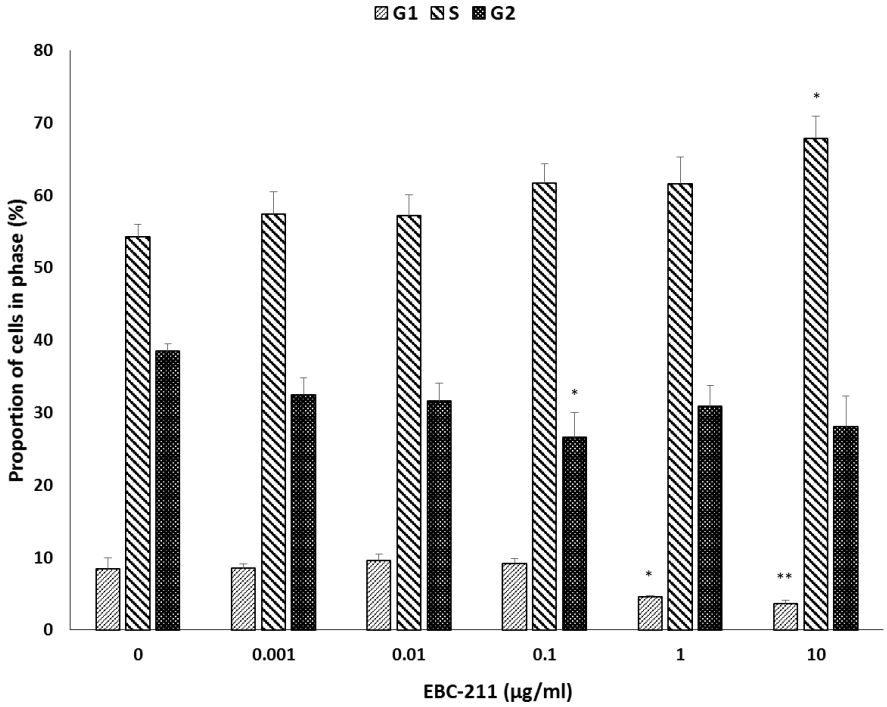

B

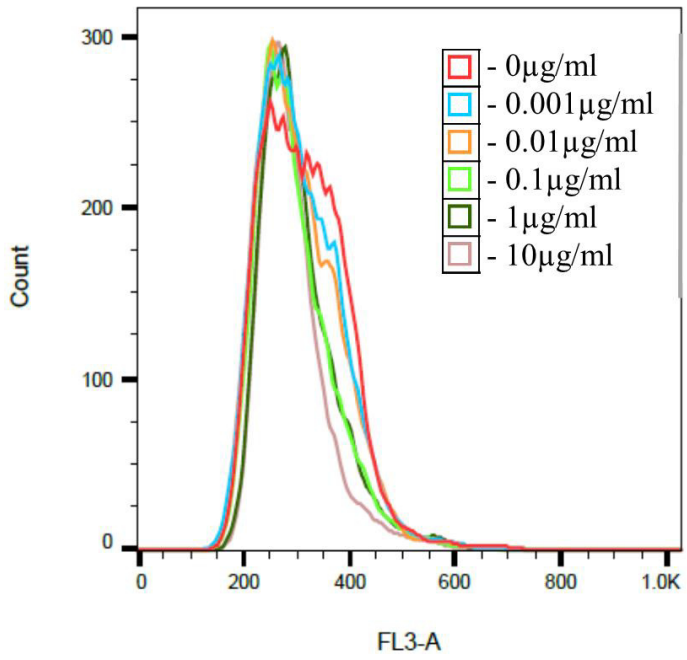

Figure 3.9: (A) Dermal fibroblast cell cycle analysis at T29, following culture in the presence of EBC-211 (0.001µg/ml, 0.01µg/ml, 0.1µg/ml, 1µg/ml and 10µg/ml), compared to untreated controls (0µg/ml; *N=3, average % in each phase±SE*). Statistical analysis (p<0.05, **p<0.01*). (B) Corresponding cell cycle histogram at T29, following culture in the presence of EBC-211 (0-10µg/ml).**

A

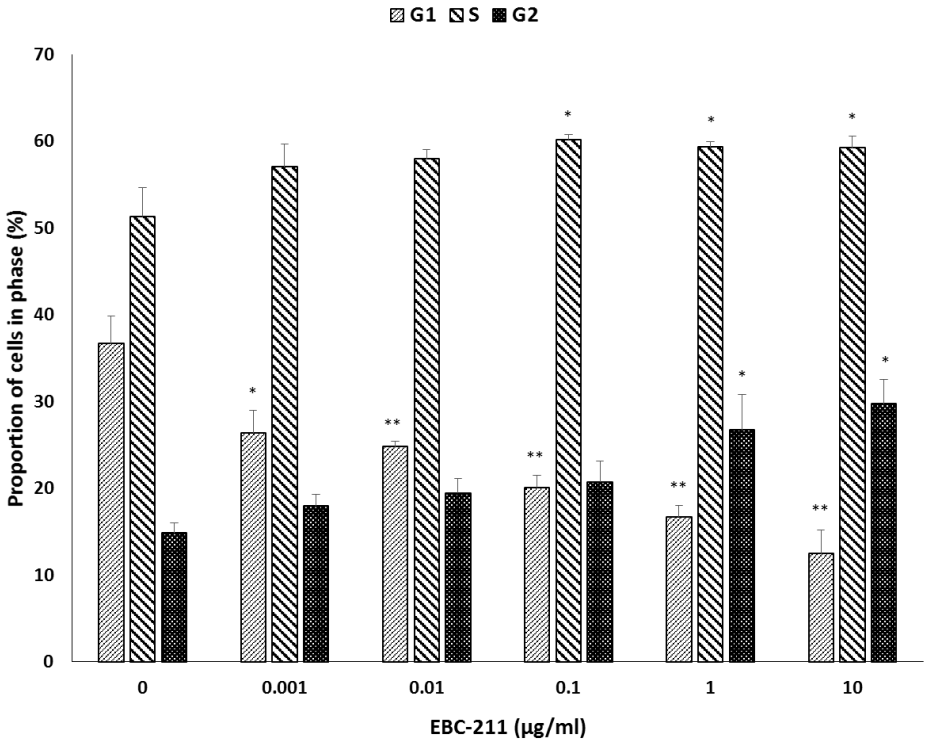

B

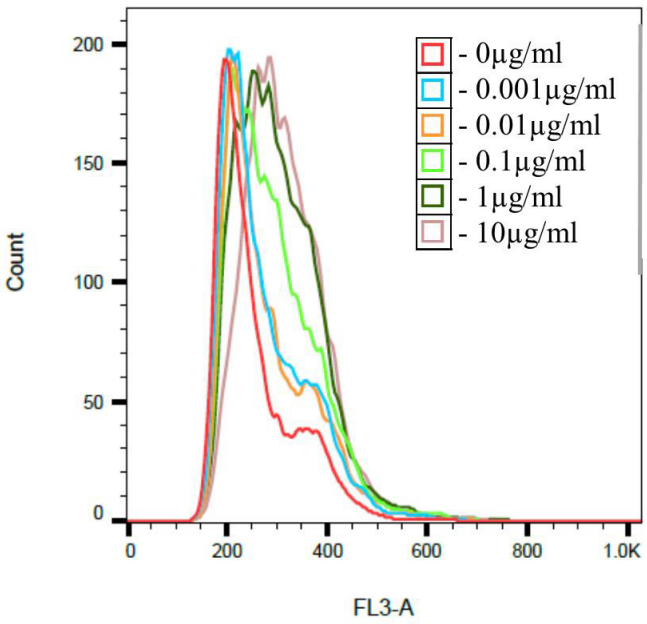

Figure 3.10: (A) Dermal fibroblast cell cycle analysis at T36, following culture in the presence of EBC-211 (0.001µg/ml, 0.01µg/ml, 0.1µg/ml, 1µg/ml and 10µg/ml), compared to untreated controls (0µg/ml; *N=3, average % in each phase±SE*). Statistical analysis (*all p>0.05*). (B) Corresponding cell cycle histogram at T36, following culture in the presence of EBC-211 (0-10µg/ml).

A

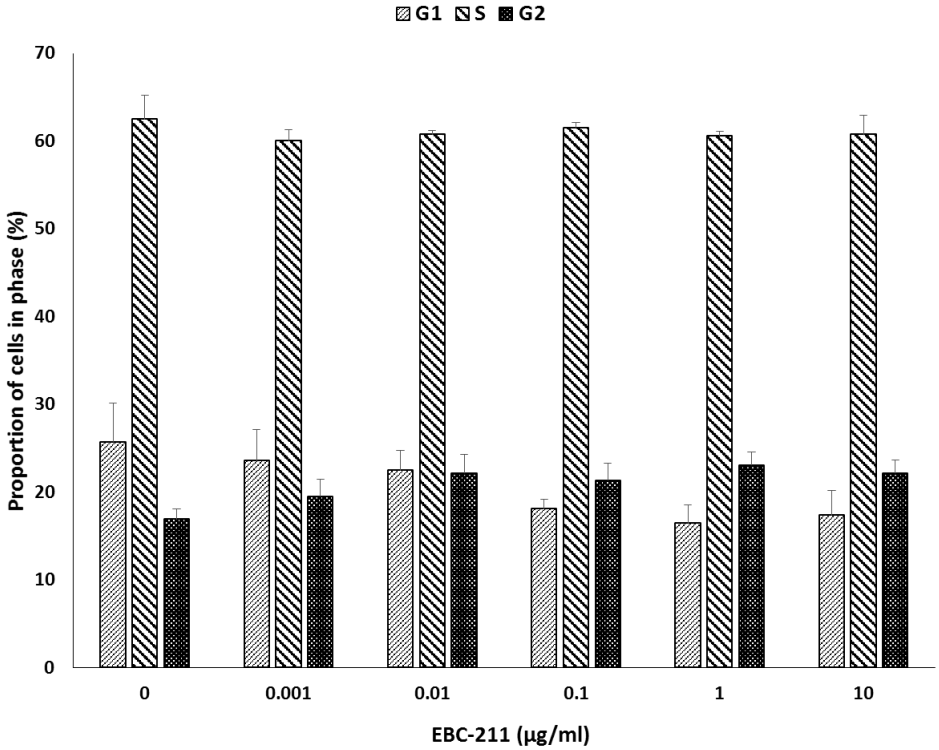

B

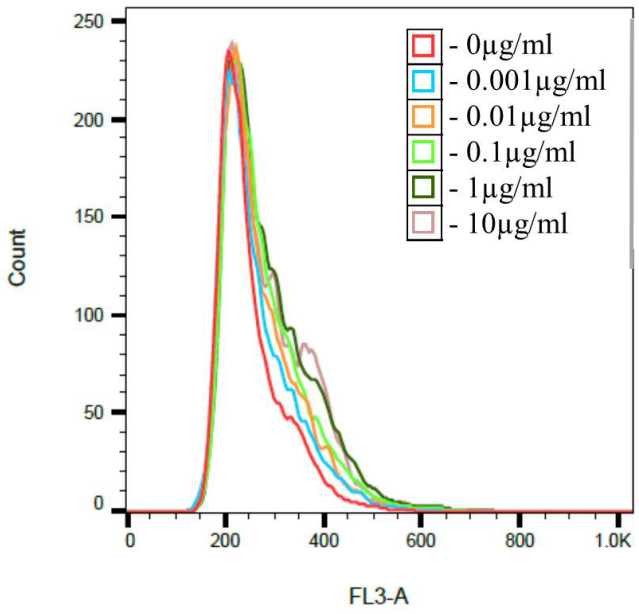

3.7B, 3.8B, 3.9B and 3.10B). However, by T29, the delayed cell cycle progression was also significant at these concentrations ($p<0.01$-0.05; Figure 3.9A). For both compounds, the delayed cell cycle progression appeared to be a result of progression of the cells into S phase, due to delayed progression of the cells treated with epoxy-tiglianes from G1 to S phase, compared to untreated controls. The untreated controls appear to have progressed into S phase by T22, whereas the epoxy-tigliane treated cells progression into S phase only occurs by T29. This appeared to be a dose-dependent reaction, with the lower concentrations behaving in a similar manner to the untreated controls, progressing through the cell cycle phases at a similar rate. This was particularly evident with EBC-211, due to the lesser activity of this epoxy-tigliane (Figure 3.8B).

3.4.3 Effects of EBC-46 and EBC-211 on Dermal Fibroblast Morphology

EBC-46 and EBC-211 were shown to be highly cytotoxic to dermal fibroblasts at 100µg/ml, corroborating previous proliferation data. Cellular morphology studies confirmed this, with the rounding and subsequent potential apoptosis or necrosis of fibroblasts. There was also a noticeable reduction in the number of fibroblasts present with the progressing time-points, along with an increased production of cell debris. Following 24h treatment with 100µg/ml EBC-46, some viable cells remained; whereas at 72h, 120h and 168h after treatment, only a few cells were present along with the resultant cell debris (Figures 3.11G, 3.12G, 3.13G and 3.14G). In comparison, viable cells were present in decreasing quantities at 24h, 72h and 120h, after treatment with 100µg/ml EBC-211; whilst 168h was the only time-point where no viable cells remained (Figures 3.15G, 3.16G, 3.17G and 3.18G).

Culturing fibroblasts in EBC-46 (0.01-10µg/ml) showed a dramatically altered morphology at 24h, producing much larger, more stellate-shaped fibroblasts, as opposed to the spindle-shaped cells that are characteristic of dermal fibroblasts. There also appeared to be an increased presence of stress fibres, showing a significant alteration on the cytoskeleton of the fibroblasts. In contrast, 0.001µg/ml EBC-46 appeared to not affect the fibroblasts in the same way as the higher concentrations, with these cells retaining the normal morphological appearance of dermal fibroblasts (Figure 3.11B). Additionally, by 72h, it also appeared that the altered morphological

Figure 3.11: Dermal fibroblast morphology, cultured in the presence of (A) 0µg/ml, (B) 0.001µg/ml, (C) 0.01µg/ml, (D) 0.1µg/ml, (E) 1µg/ml, (F) 10µg/ml; and (G) 100µg/ml EBC-46 for 24h (*N=3*). Scale bar = 100µm.

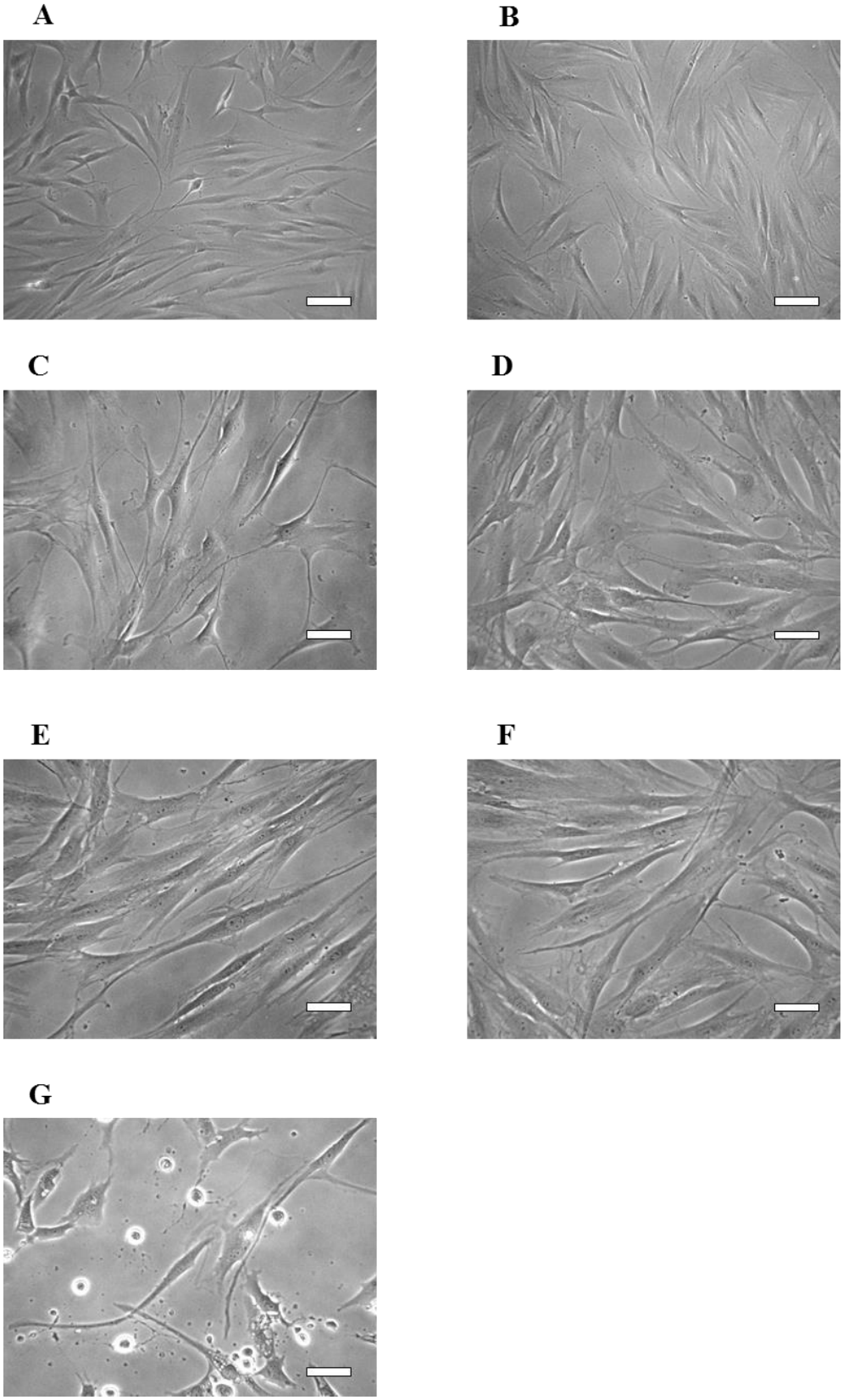

Figure 3.12: Dermal fibroblast morphology, cultured in the presence of (A) 0µg/ml, (B) 0.001µg/ml, (C) 0.01µg/ml, (D) 0.1µg/ml, (E) 1µg/ml, (F) 10µg/ml; and (G) 100µg/ml EBC-46 for 72h (*N=3*). Scale bar = 100µm.

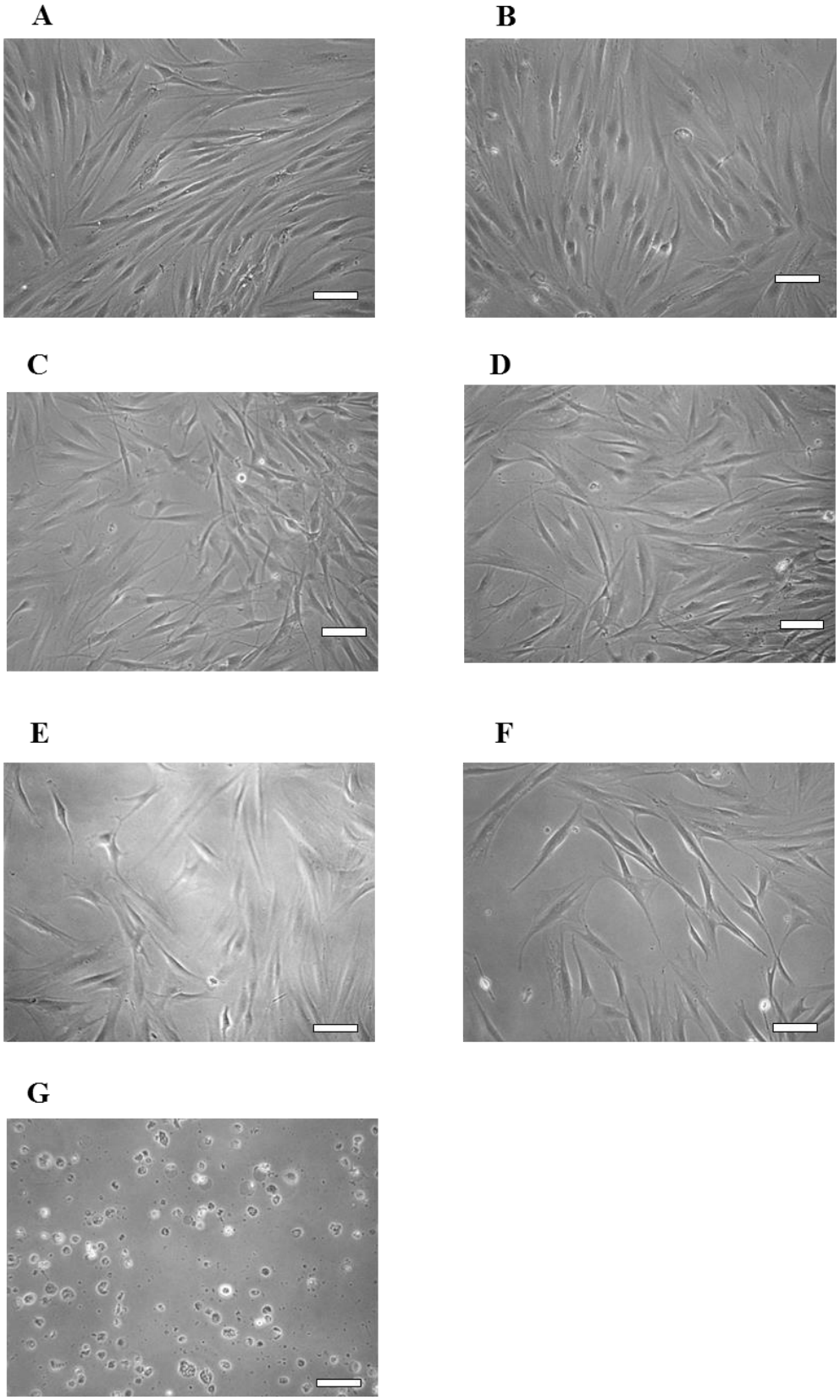

Figure 3.13: Dermal fibroblast morphology, cultured in the presence of (A) 0µg/ml, (B) 0.001µg/ml, (C) 0.01µg/ml, (D) 0.1µg/ml, (E) 1µg/ml, (F) 10µg/ml; and (G) 100µg/ml EBC-46 for 120h (*N=3*). Scale bar = 100µm.

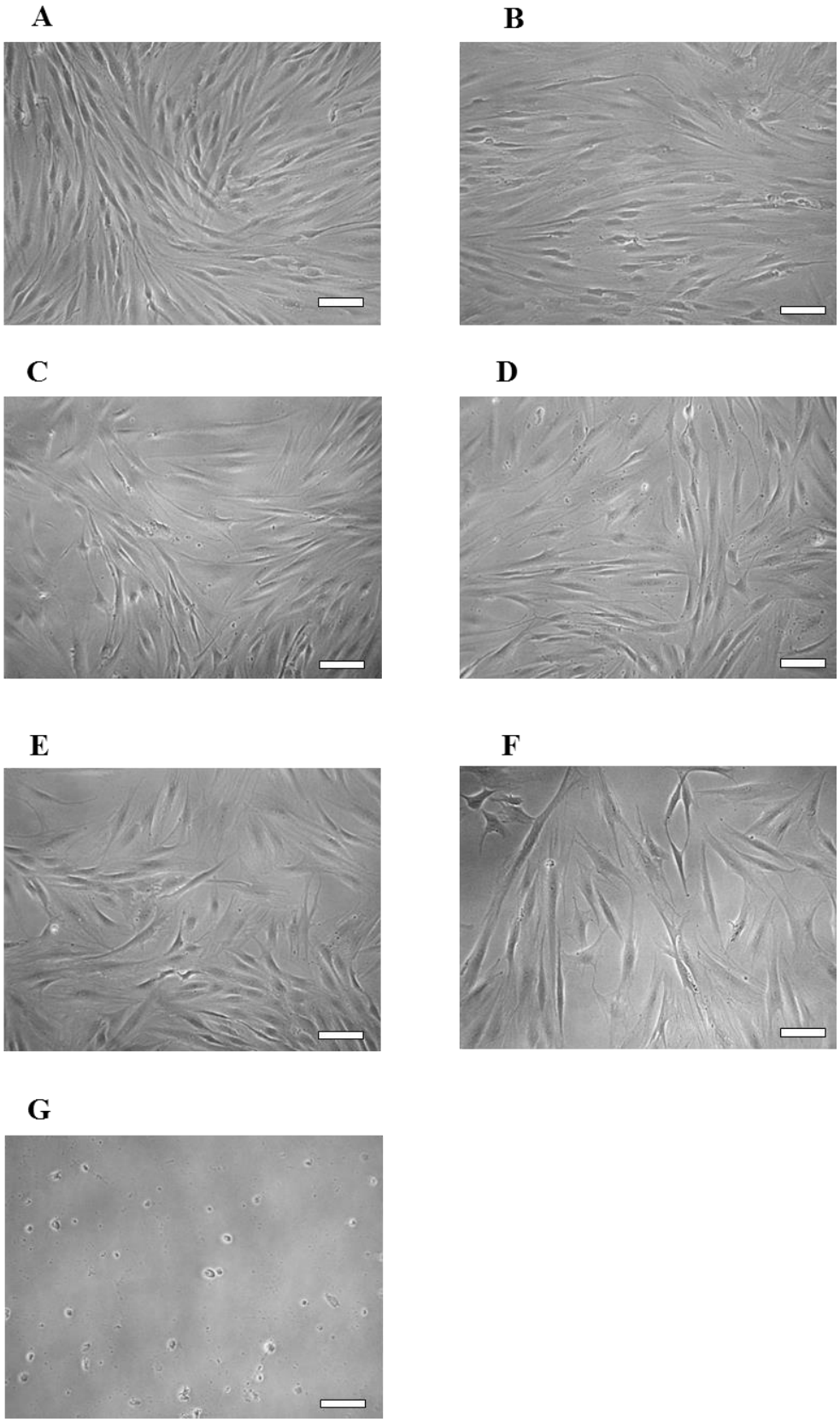

Figure 3.14: Dermal fibroblast morphology, cultured in the presence of (A) 0µg/ml, (B) 0.001µg/ml, (C) 0.01µg/ml, (D) 0.1µg/ml, (E) 1µg/ml, (F) 10µg/ml; and (G) 100µg/ml EBC-46 for 168h (*N=3*). Scale bar = 100µm.

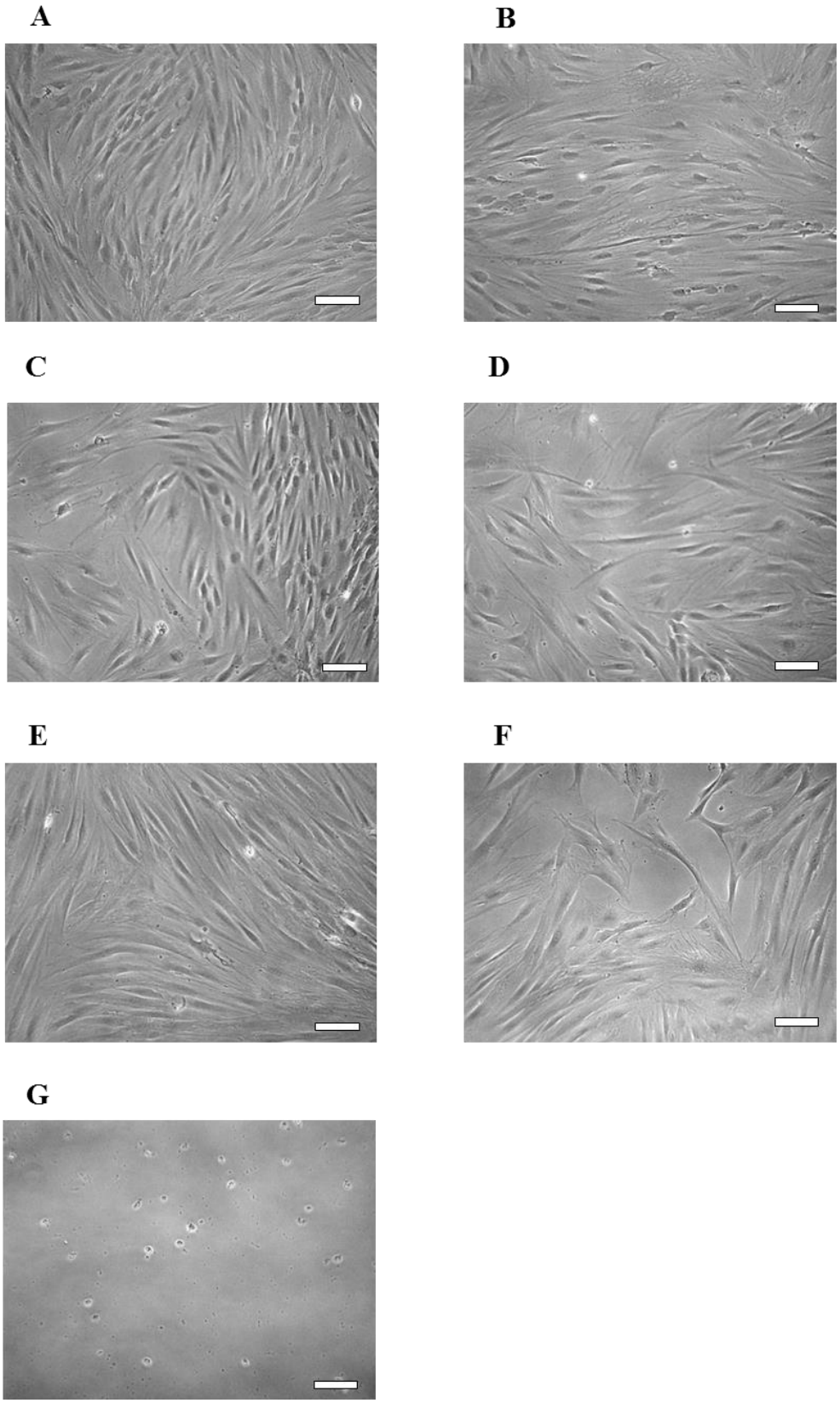

Figure 3.15: Dermal fibroblast morphology, cultured in the presence of (A) 0µg/ml, (B) 0.001µg/ml, (C) 0.01µg/ml, (D) 0.1µg/ml, (E) 1µg/ml, (F) 10µg/ml; and (G) 100µg/ml EBC-211 for 24h (*N=3*). Scale bar = 100µm.

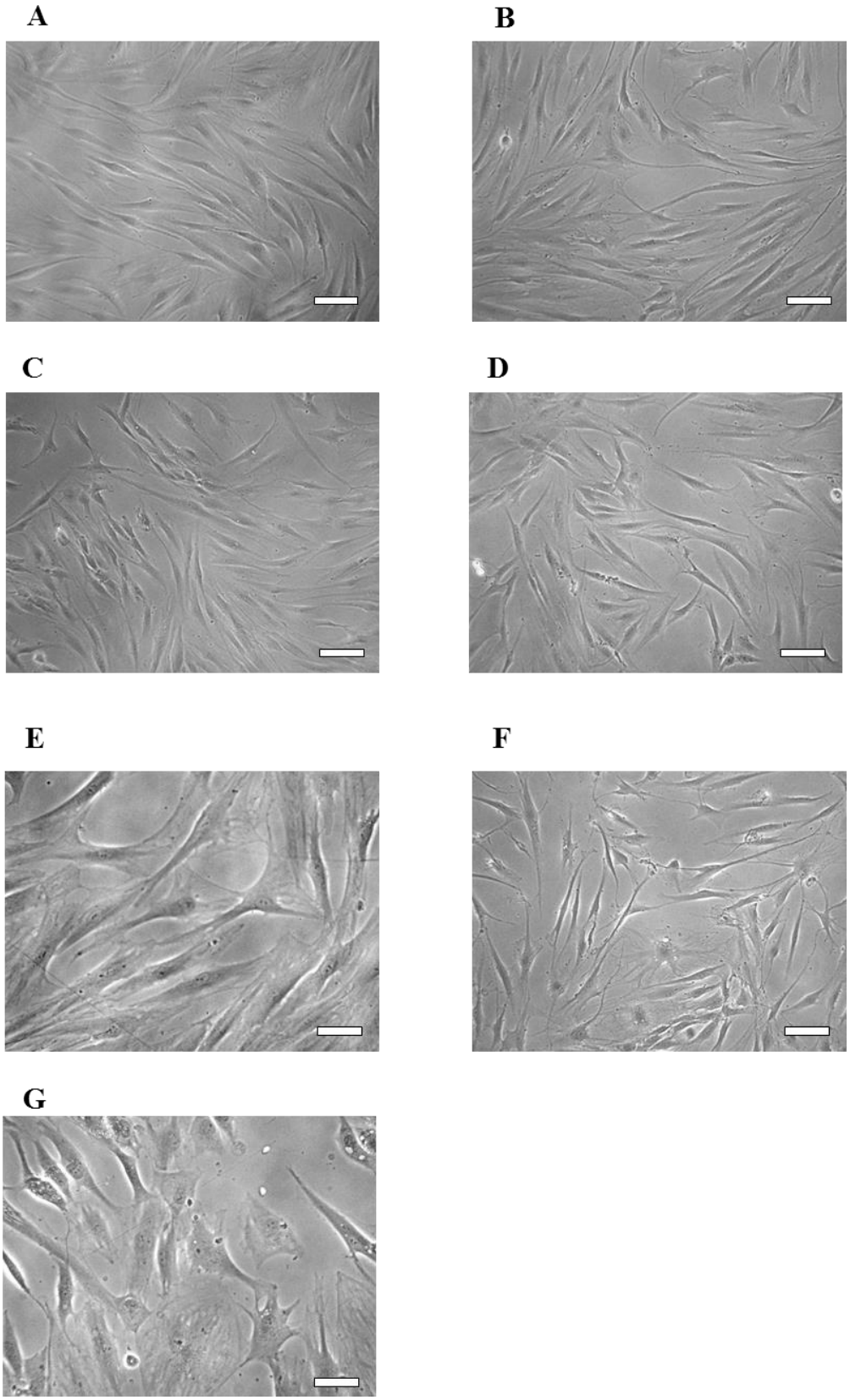

Figure 3.16: Dermal fibroblast morphology, cultured in the presence of (A) 0µg/ml, (B) 0.001µg/ml, (C) 0.01µg/ml, (D) 0.1µg/ml, (E) 1µg/ml, (F) 10µg/ml; and (G) 100µg/ml EBC-211 for 72h (*N=3*). Scale bar = 100µm.

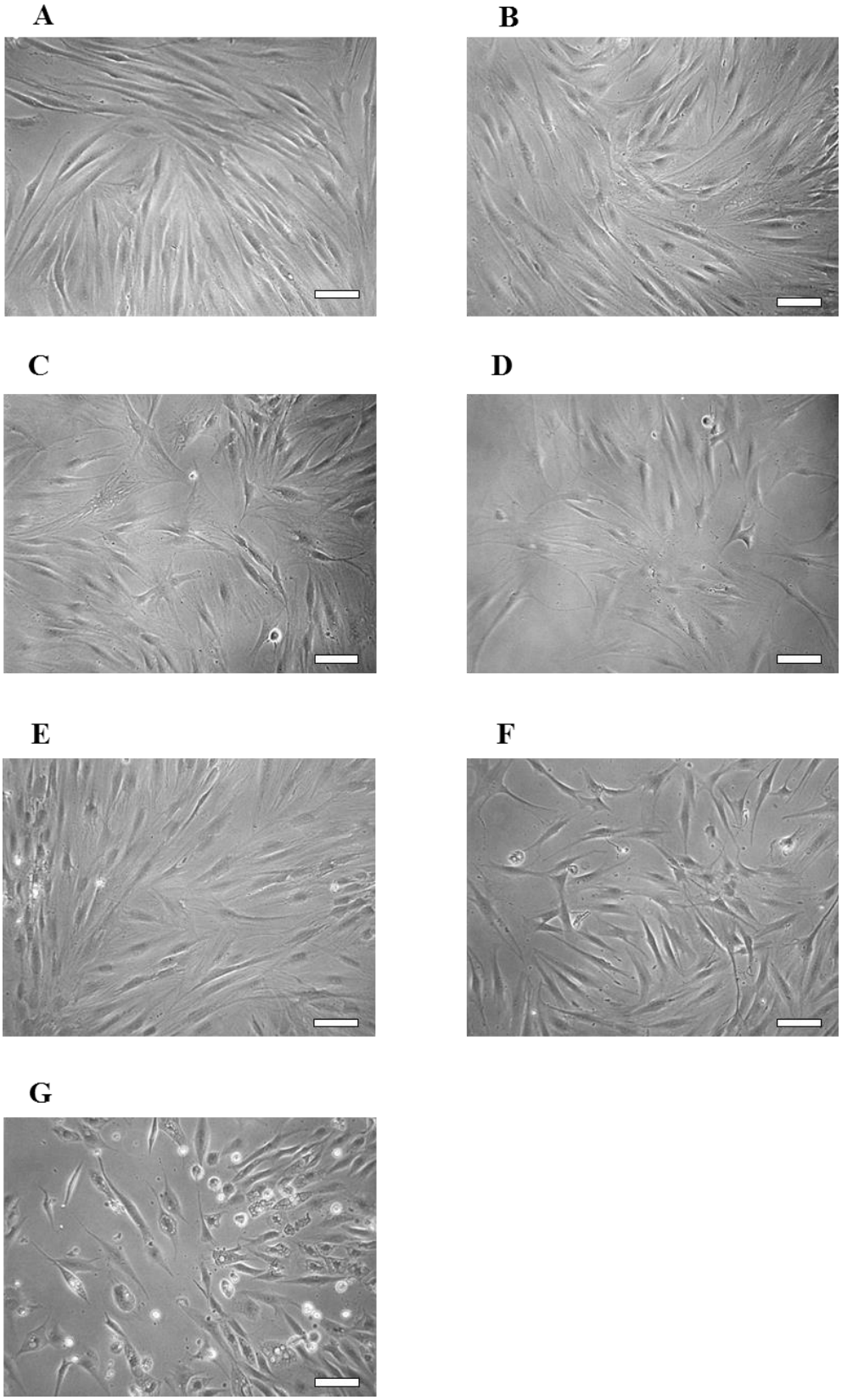

Figure 3.17: Dermal fibroblast morphology, cultured in the presence of (A) 0µg/ml, (B) 0.001µg/ml, (C) 0.01µg/ml, (D) 0.1µg/ml, (E) 1µg/ml, (F) 10µg/ml; and (G) 100µg/ml EBC-211 for 120h (*N=3*). Scale bar = 100µm.

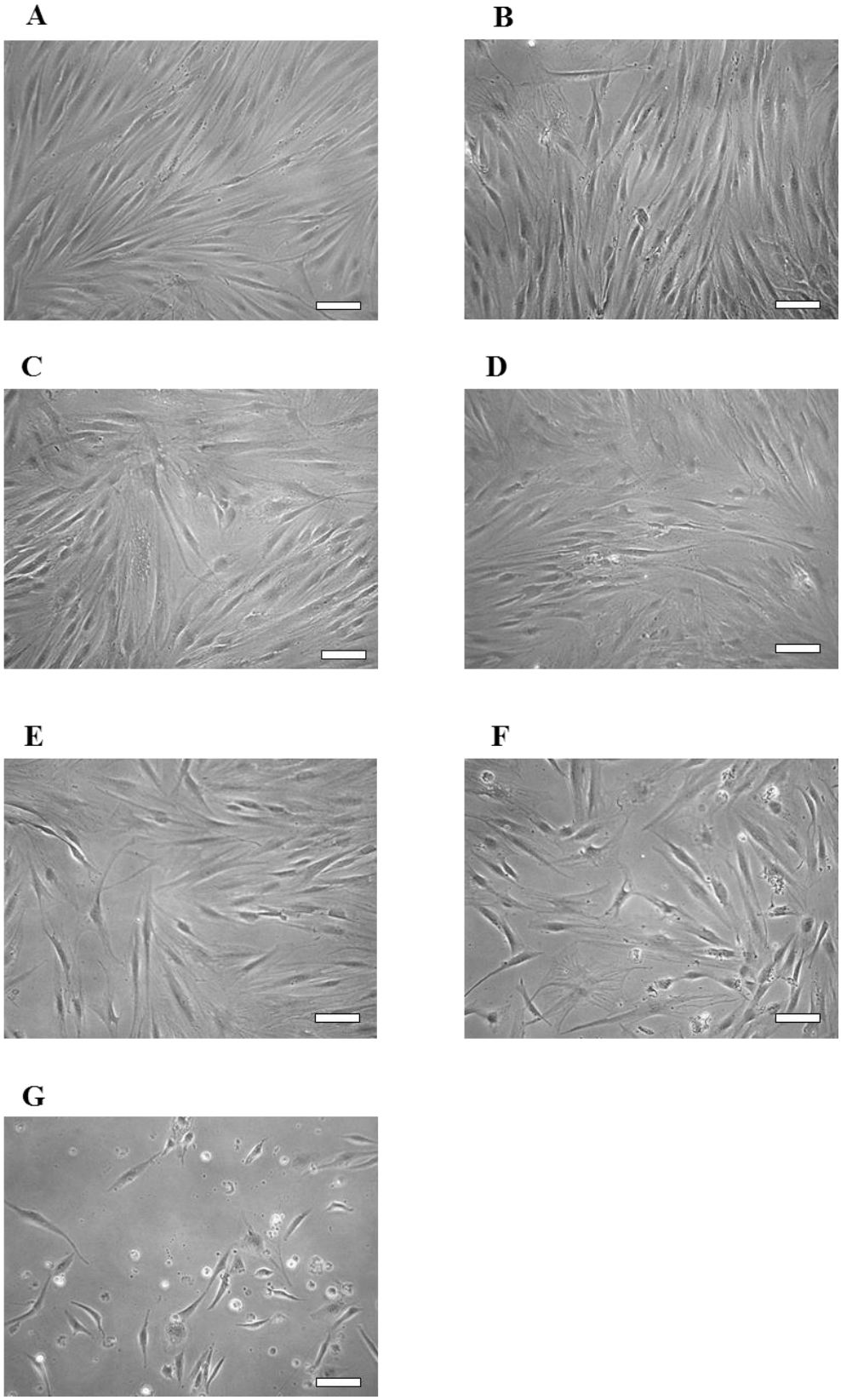

Figure 3.18: Dermal fibroblast morphology, cultured in the presence of (A) 0µg/ml, (B) 0.001µg/ml, (C) 0.01µg/ml, (D) 0.1µg/ml, (E) 1µg/ml, (F) 10µg/ml; and (G) 100µg/ml EBC-211 for 168h (*N=3*). Scale bar = 100µm.

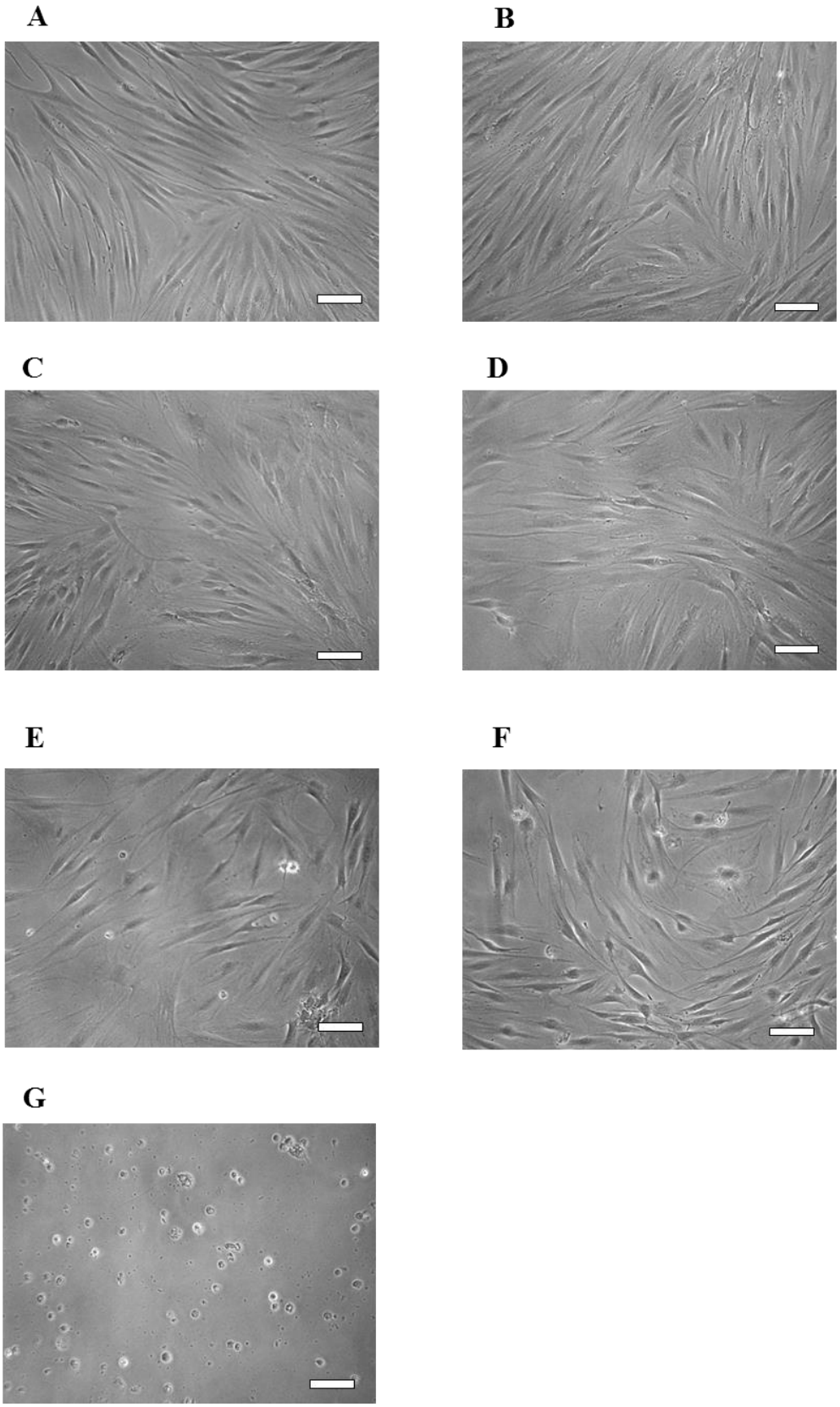

changes induced by 24h, revert back to a more normal spindle-shaped morphology, which remained this way through 120h and 168h. There also appeared to be reduced cell numbers across the EBC-46 concentrations, compared to untreated controls (0µg/ml); in line with the data obtained from the viability and proliferation studies.

Fibroblasts at the higher concentrations of EBC-211 (1-10µg/ml) also showed the same altered morphology as EBC-46, with a more stellate-structure and presence of stress fibres (Figures 3.15E-F). As with EBC-46, there was a reversion back to a more typical fibroblast morphology by 72h, which remained at 120h and 168h. In contrast, at the lower concentrations of EBC-211 (0.001-0.1µg/ml), there was little effect on fibroblast morphology at any time-point, with morphologies retaining the normal spindle-shape similar to untreated controls. Confirming the anti-proliferative effect of EBC-211, there again appeared to be reductions in cell number at the higher concentrations, compared to untreated controls (0µg/ml) at the later time-points, in line with the previous viability and proliferation data.

3.4.4 Effects of EBC-46 and EBC-211 on Dermal Fibroblast Repopulation

Digital images obtained over 48h showed the repopulation of the denuded sites by dermal fibroblasts. Cells were cultured in EBC-46 or EBC-211 (0.001µg/ml, 0.01µg/ml, 0.1µg/ml, 1µg/ml, 10µg/ml and 100µg/ml), with untreated controls (0µg/ml) included for comparison purposes (Figures 3.19 and 3.20, respectively). The digital images were converted into time-lapse movies (Supplement 3.2), using LAS AF lite (Leica Software, Version 4.0.11706, Leica Microsystems (UK) Ltd), to show the repopulation of dermal fibroblasts over the 48h time-period.

As expected, untreated controls showed complete re-population of the denuded site within 48h, with normal migration and proliferation of dermal fibroblasts occurring. Confirming previous proliferation data, the cytotoxic nature of both EBC-46 and EBC-211 was observed at 100µg/ml for both epoxy-tiglianes. At 100µg/ml, EBC-46 and EBC-211, the fibroblasts did not migrate into the denuded space and were seen to round up and undergo cell death, releasing cell debris as a result, over the 48h period (Figures 3.19G and 3.20G, respectively).

Figure 3.19: Dermal fibroblast scratch wound repopulation, in the presence of (A) 0µg/ml, (B) 0.001µg/ml, (C) 0.01µg/ml, (D) 0.1µg/ml, (E) 1µg/ml, (F) 10µg/ml; and (G) 100µg/ml EBC-46, over 48h (*N=3*). Red dashed lines show original scratch wound distance at 0h. Scale bar = 100µm.

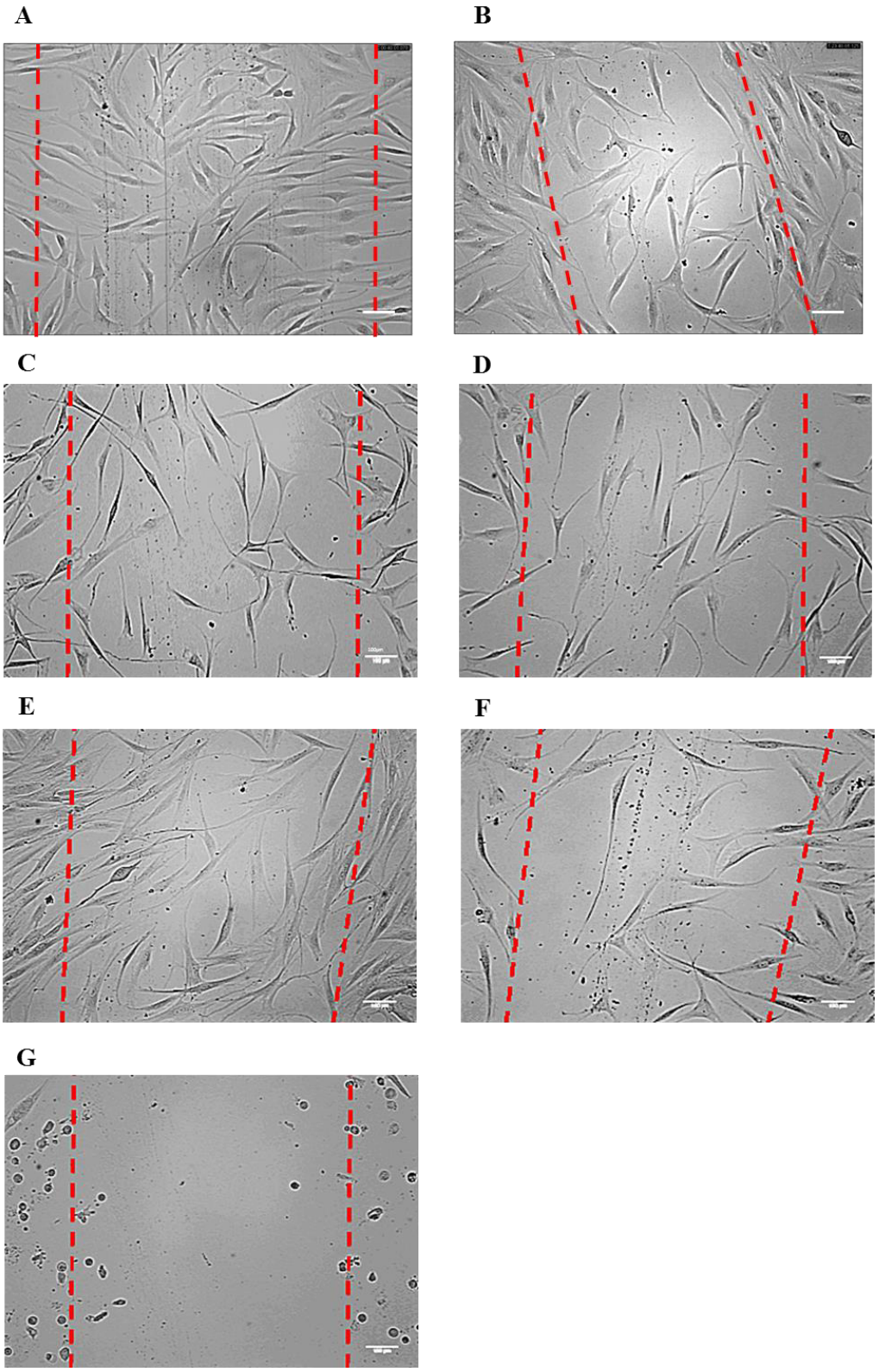

Figure 3.20: Dermal fibroblast scratch wound repopulation, in the presence of (A) 0µg/ml, (B) 0.001µg/ml, (C) 0.01µg/ml, (D) 0.1µg/ml, (E) 1µg/ml, (F) 10µg/ml; and (G) 100µg/ml EBC-211, over 48h (*N=3*). Red dashed lines show original scratch wound distance at 0h. Scale bar = 100µm.

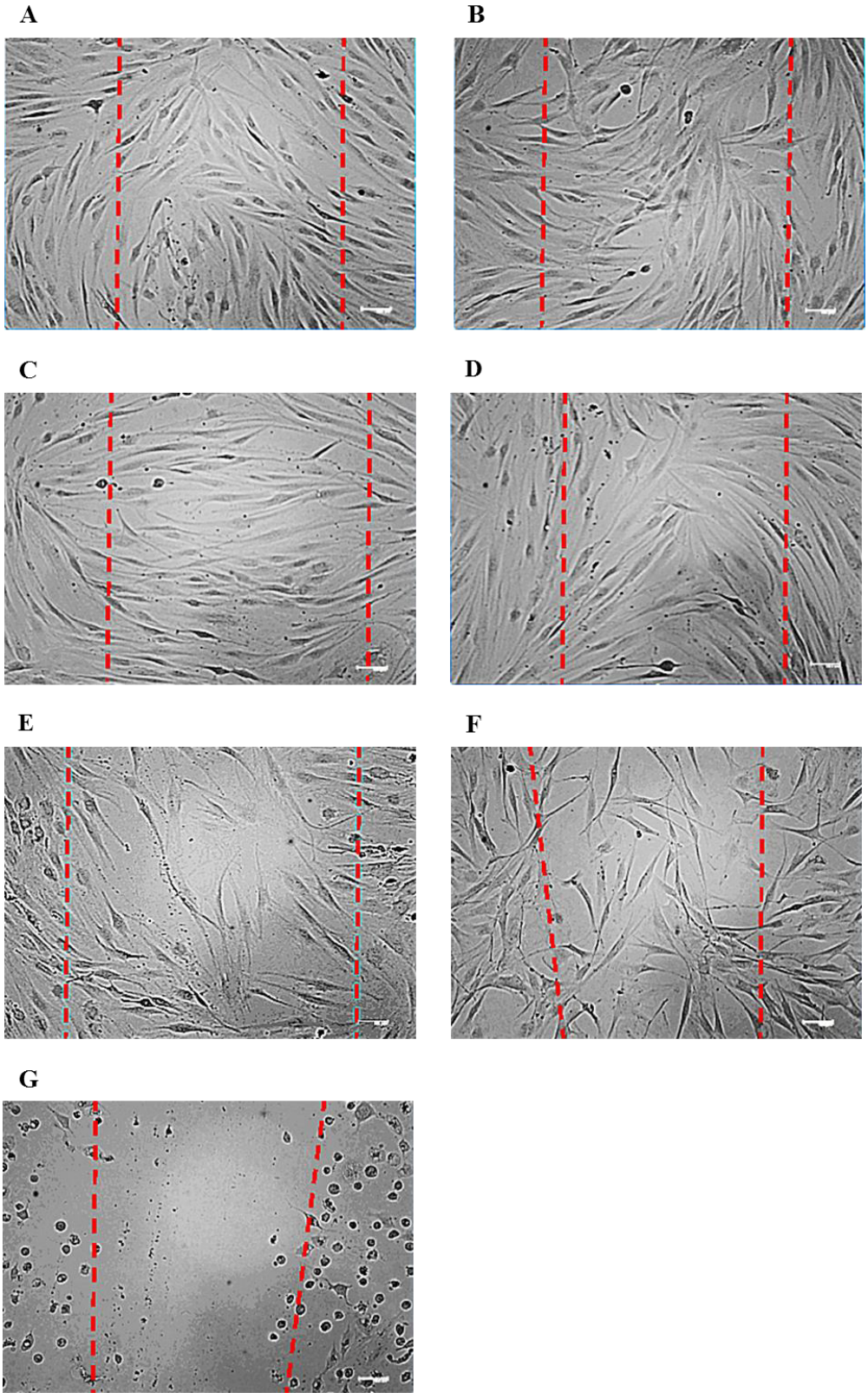

Repopulation data for the other concentrations of EBC-46 (0.001-10µg/ml) assessed, confirmed previous viability and proliferation findings, showing a reduced cell number present compared to untreated controls; although the fibroblasts were seen to increase in size and produce long processes from their cytoskeleton (Figure 3.19A-F). At 0.01-10µg/ml EBC-46, there was a perceived reduced number of fibroblasts observed in the denuded sites, compared to untreated controls; and therefore, reduced closure of the wound space. However, the large stellate morphology of the fibroblasts may give the appearance of successful wound closure (Figure 3.19).

The lower concentrations of EBC-211 (0.001-0.01µg/ml) appeared to achieve wound closure within 48h, in a comparable manner to untreated controls (0µg/ml; Figure 3.20B-C). In contrast, 0.1-10µg/ml EBC-211 showed an apparently reduced repopulation, through a reduced number of fibroblasts evident in the denuded sites. At these concentrations, the fibroblasts appeared to be larger, more stellate-shaped and produce long processes (Figure 3.20D-F).

The fibroblast repopulation data was further analysed using ImageJ to identify any significant differences in various parameters associated with the fibroblast migratory responses, in the presence of EBC-46 and EBC-211 (0.001-100µg/ml), compared to untreated controls. These included distance travelled (Figures 3.21A and 3.22A, respectively), cell displacement (Figures 3.21B and 3.22B, respectively), speed (Figures 3.21C and 3.22C, respectively); and overall cell velocity (Figures 3.21D and 3.22D, respectively).

Due to the high variability in the movements of fibroblasts treated with EBC-46 (0.01-10µg/ml), no significant differences were observed, when compared to untreated controls for the distance travelled, cell displacement, speed or overall velocity ($p>0.05$). For these EBC-46 concentrations, there was a large variability in the motility responses of the fibroblasts, ranging from rapid migration across the well to inhibited or greatly reduced migration. Further evidence of this can be viewed in the time-lapse movies (Supplement 3.2). This large variability in cell behaviour accounts for the high error bars, which prevented any significant differences being observed across the concentrations.

Figure 3.21: Dermal fibroblast migration analysis, in the presence of EBC-46 (0µg/ml, 0.001µg/ml, 0.01µg/ml, 0.1µg/ml, 1µg/ml and 10µg/ml), (A) distance travelled (Tt), (B) cell displacement (Td), (C) speed (Tt/min) and (D) overall velocity (Td/min) at 48h (*N=3, average±SE, p>0.05*).

A

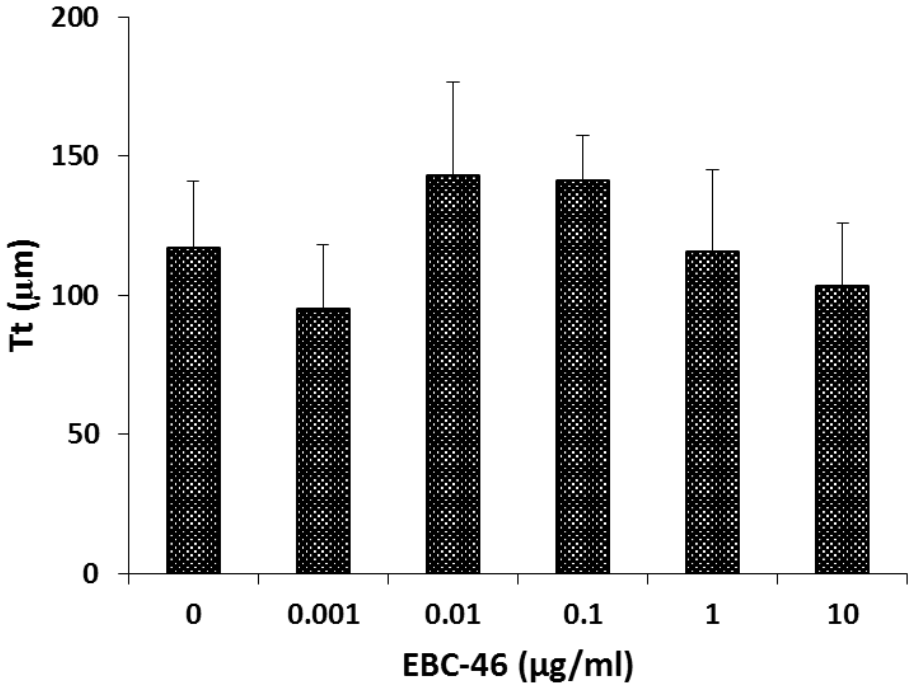

B

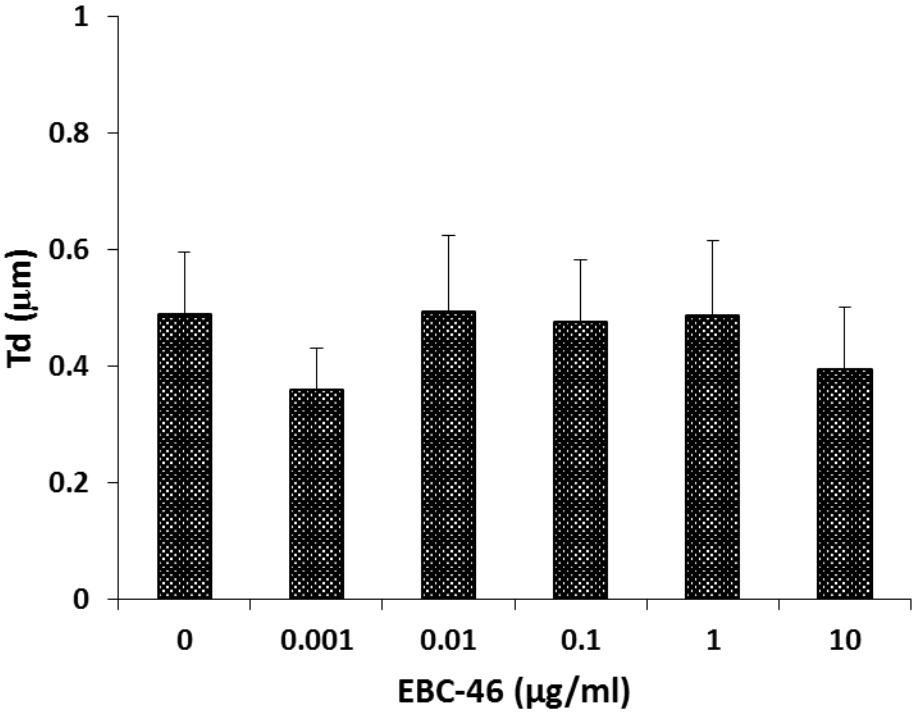

C

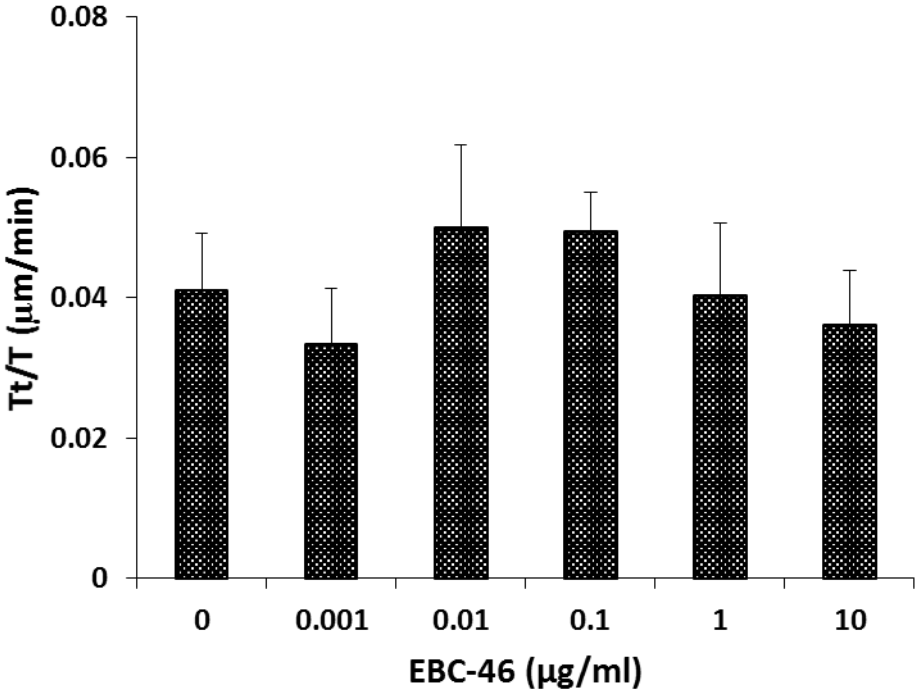
0.08
0.06
0.04
0.02
0
Tt/T (µm/min)
0
0.001
0.01
0.1
1
10
EBC-46 (µg/ml)

D

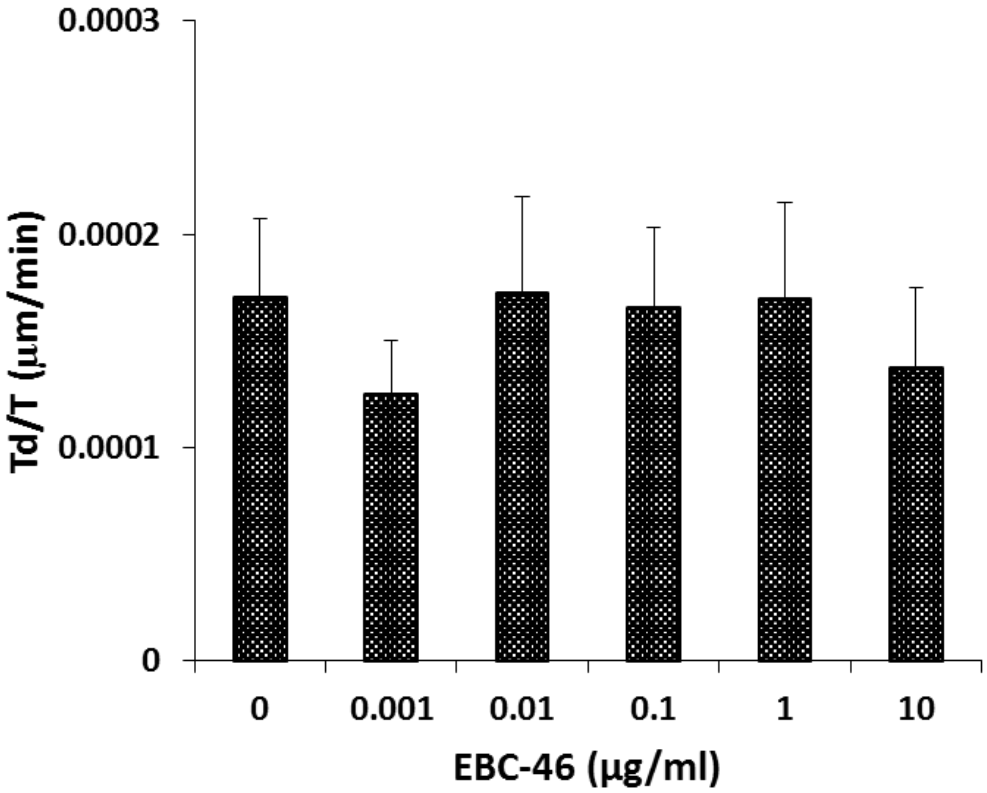
0.0003
0.0002
0.0001
0
Td/T (µm/min)
0
0.001
0.01
0.1
1
10
EBC-46 (µg/ml)

Figure 3.22: Dermal fibroblast migration analysis, in the presence of EBC-211 (0µg/ml, 0.001µg/ml, 0.01µg/ml, 0.1µg/ml, 1µg/ml and 10µg/ml), (A) distance travelled (Tt), (B) cell displacement (Td), (C) speed (Tt/min) and (D) overall velocity (Td/min) at 48h (*N=3, average±SE, p<0.01*).

A

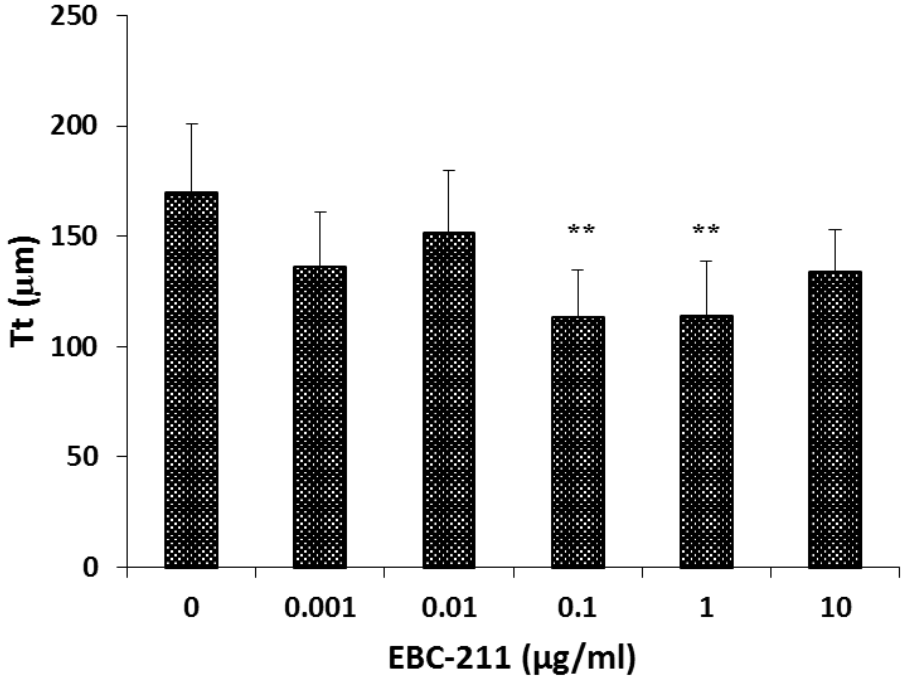

B

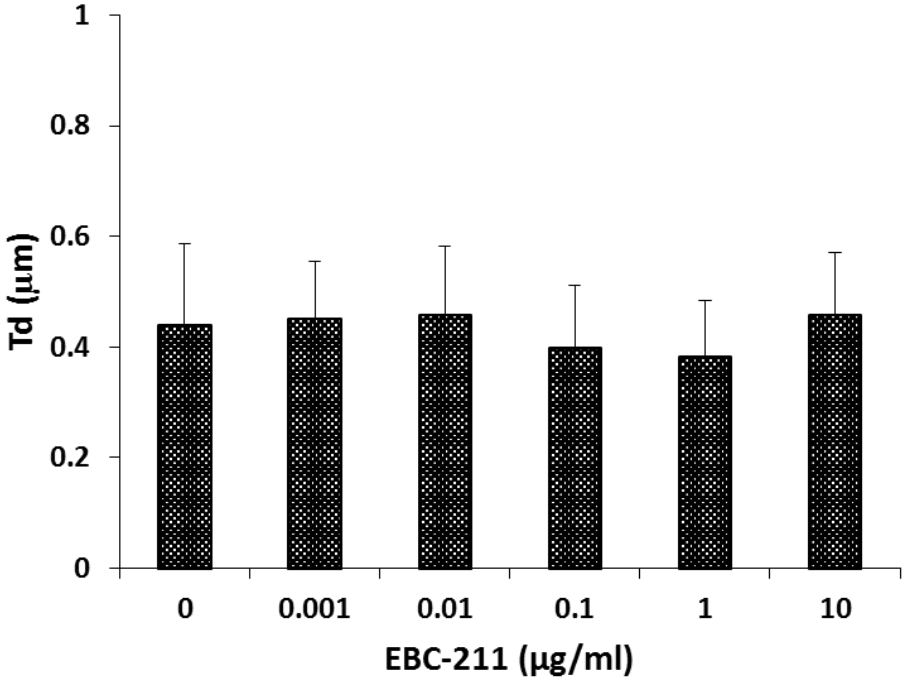

C

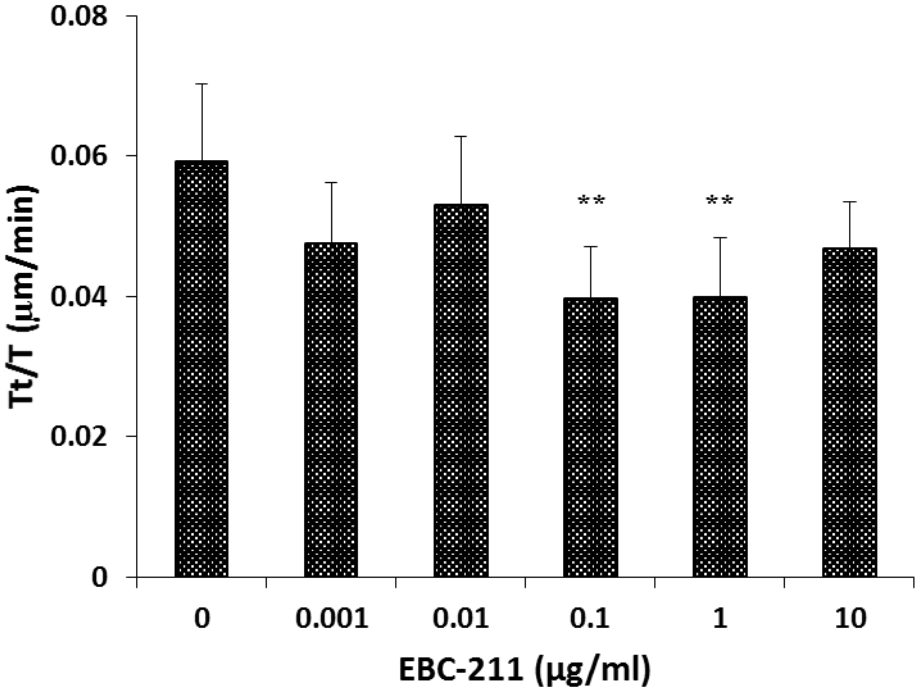
0.08
0.06
0.04
0.02
0
Tt/T (μm/min)
**
**
0
0.001
0.01
0.1
1
10
EBC-211 (μg/ml)

D

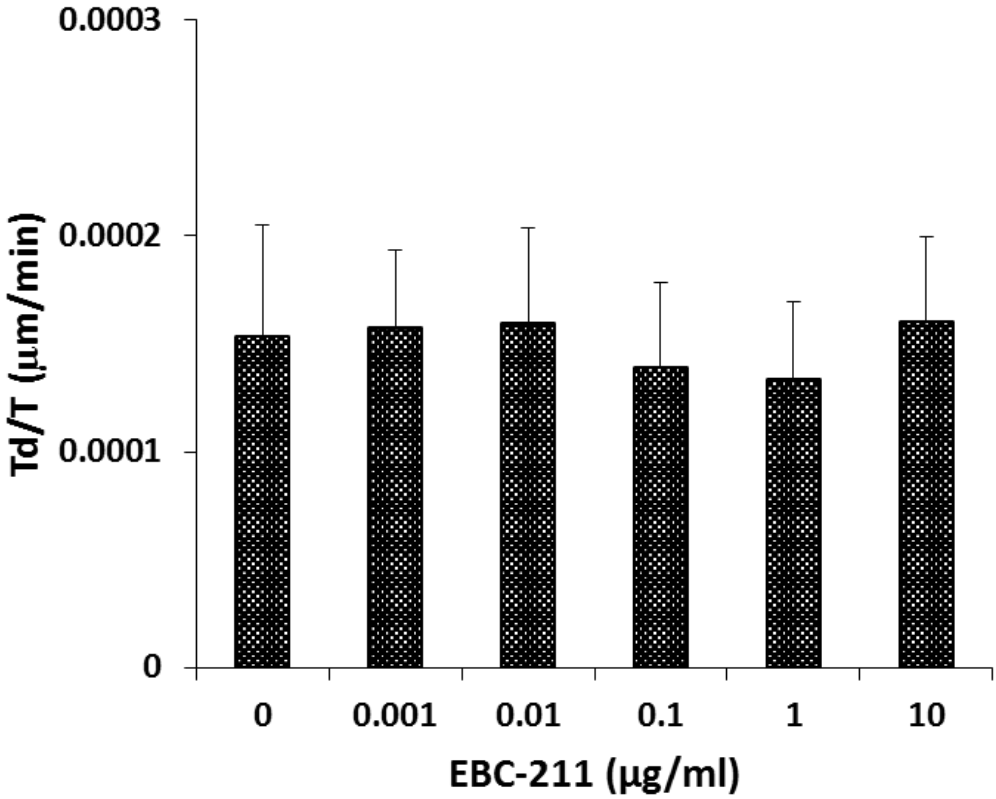
0.0003
0.0002
0.0001
0
Td/T (μm/min)
0
0.001
0.01
0.1
1
10
EBC-211 (μg/ml)

Similar observations were apparent with EBC-211 (0.001-0.01µg/ml and 10µg/ml), with no significant differences observed in distance travelled, cell displacement, speed or overall velocity, when compared to untreated controls ($p>0.05$). However, significant differences in fibroblast distance travelled and speed were observed at 0.1-1µg/ml EBC-211 (Figures 3.22A and 3.22C, respectively; $p<0.01$), with a reduction in both parameters compared to untreated controls; which could account for the reduced repopulation observed in the time-lapse movies (Supplement 3.2).

3.4.5 Effects of EBC-46 and EBC-211 on Dermal Fibroblast-Myofibroblast Differentiation by Immunocytochemistry

Immunocytochemical analysis was performed on dermal fibroblasts cultured in either EBC-46 or EBC-211 (0.001µg/ml, 0.01µg/ml, 0.1µg/ml, 1µg/ml and 10µg/ml), with an untreated control included for comparison purposes (0µg/ml) for both compounds. These experiments were performed in the presence and absence of TGF-β_1 (10ng/ml). Confirmation of dermal fibroblast differentiation to a contractile myofibroblast was through positive staining of α-smooth muscle actin (α-SMA) and the presence of stress fibres at 72h, especially evident in cultures supplemented with TGF-β_1 (Gabbiani 2003; Li & Wang 2011). An additional control was included without the incubation of the primary α-SMA antibody, this confirmed that non-specific binding of the secondary antibody was not occurring as no α-SMA staining was evident (Figures 3.23H, 3.24H, 3.25H and 3.26H; Burry 2011).

Fibroblasts cultured with EBC-46 (0.001-10µg/ml) and in the presence of TGF-β_1 (10ng/ml), showed varying results when compared to untreated controls (Figure 3.23A-F). The lower concentrations of EBC-46 (0.001-0.01µg/ml) displayed no obvious differences compared to the controls, with a comparable presence of α-SMA and stress fibres. However, there were noticeable morphological differences observed at 0.1µg/ml EBC-46, as despite α-SMA staining, this was localised to the perinuclear region of the cells only. Consequently, there was a distinct lack of stress fibres present in 0.1µg/ml EBC-46-treated cells. The α-SMA staining and lack of stress fibres appeared more representative of the untreated control in the absence of TGF-β_1 (Figure 3.23G); although the α-SMA staining for 0.1µg/ml EBC-46 appeared to extend along

Figure 3.23: Immunocytochemical analysis of dermal fibroblast differentiation to myofibroblasts in the presence of TGF-β_1 and (A) 0µg/ml, (B) 0.001µg/ml, (C) 0.01µg/ml, (D) 0.1µg/ml, (E) 1µg/ml, (F) 10µg/ml EBC-46, (G) 0µg/ml in the absence of TGF-β_1 and (H) primary antibody-free control, for 72h (*N=3*). Scale bar = 100µm.

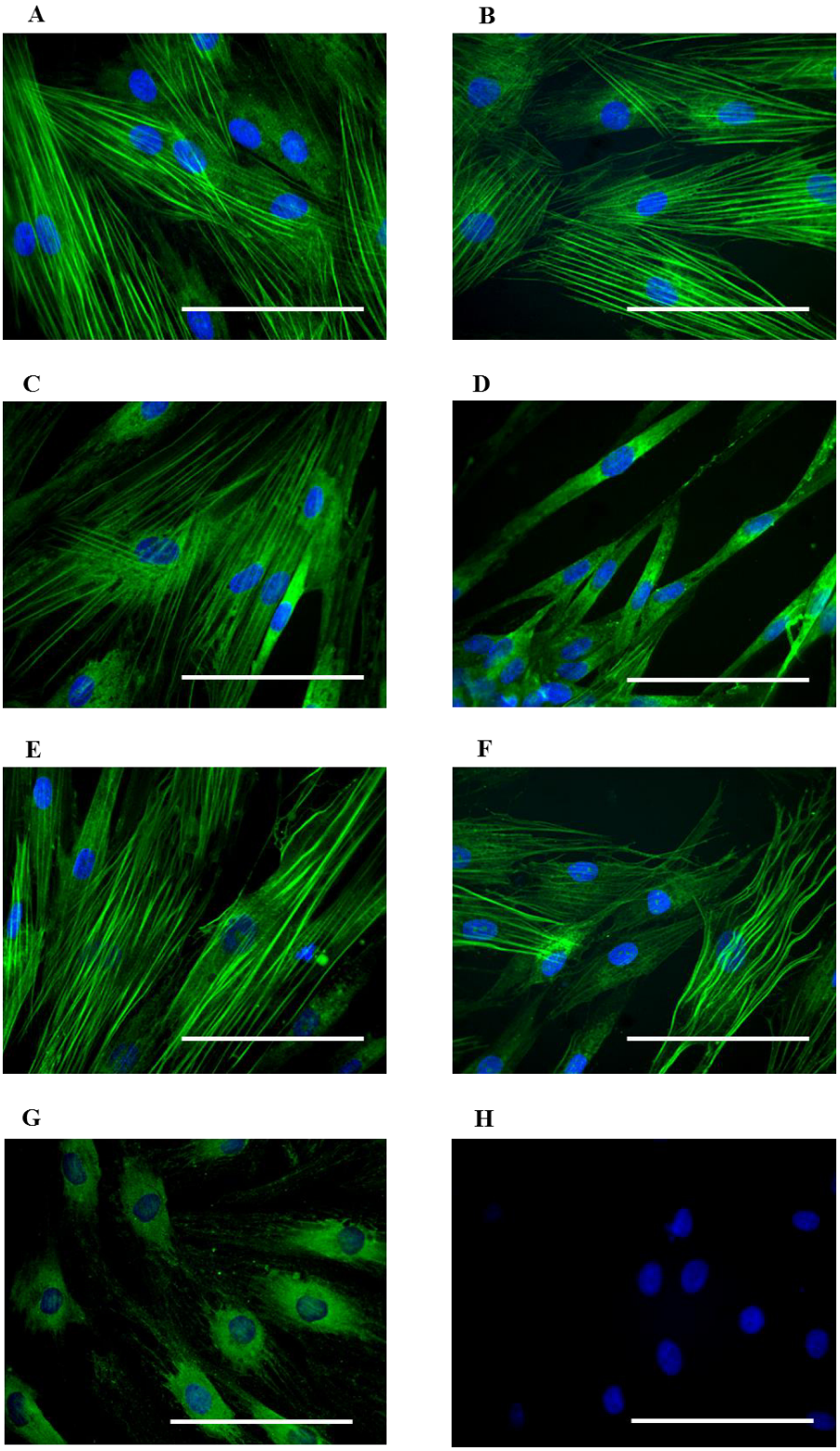

Figure 3.24: Immunocytochemical analysis of dermal fibroblast differentiation to myofibroblasts in the presence of TGF-β_1 and (A) 0µg/ml, (B) 0.001µg/ml, (C) 0.01µg/ml, (D) 0.1µg/ml, (E) 1µg/ml, (F) 10µg/ml EBC-211, (G) 0µg/ml in the absence of TGF-β_1 and (H) primary antibody-free control, for 72h (*N=3*). Scale bar = 100µm.

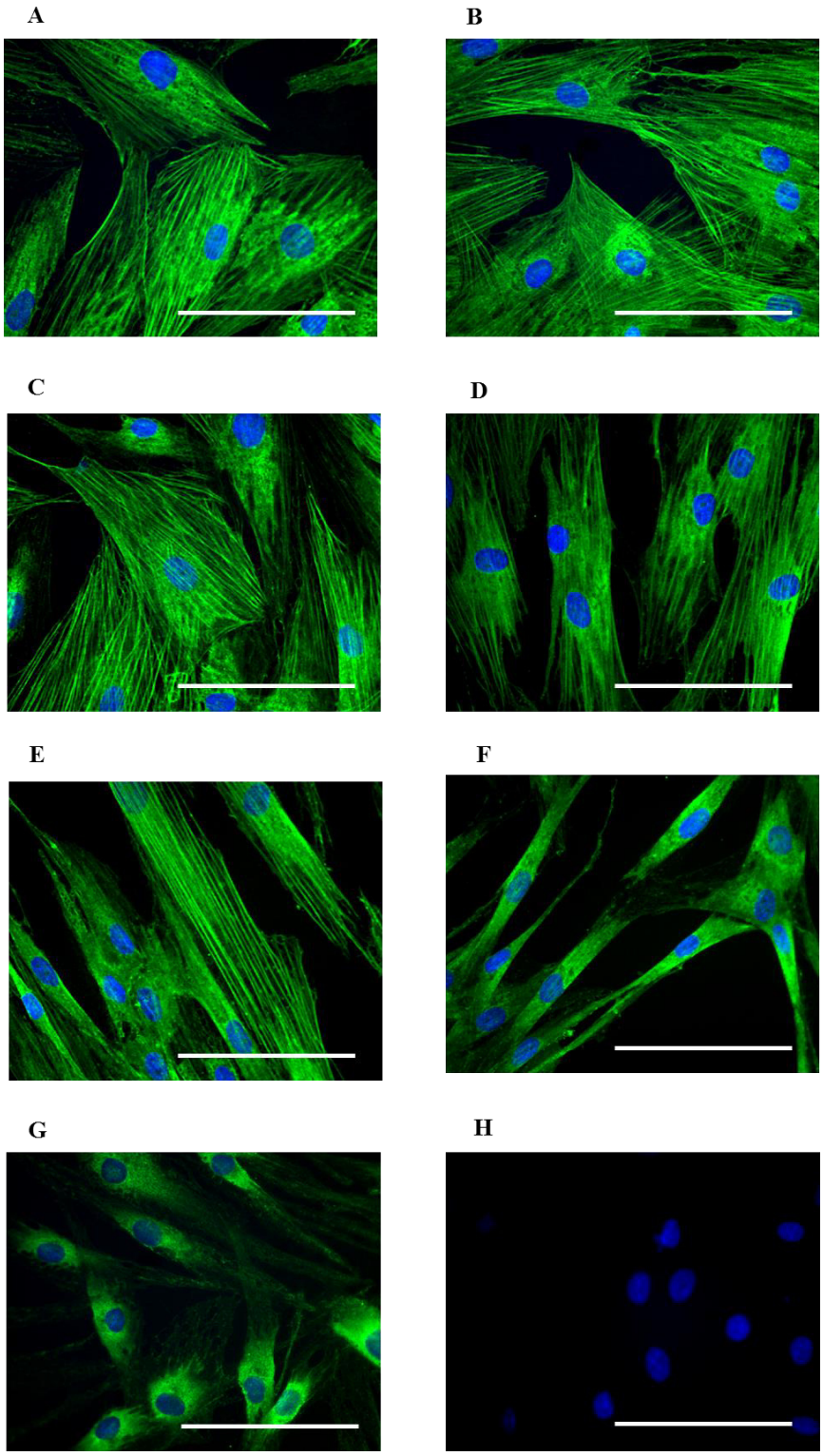

Figure 3.25: Immunocytochemical analysis of dermal fibroblast differentiation to myofibroblasts in the absence of TGF-β_1 and (A) 0µg/ml, (B) 0.001µg/ml, (C) 0.01µg/ml, (D) 0.1µg/ml, (E) 1µg/ml, (F) 10µg/ml EBC-46; (G) 0µg/ml in the presence of TGF-β_1 and (H) primary antibody free-control, for 72h (*N=3*). Scale bar = 100µm.

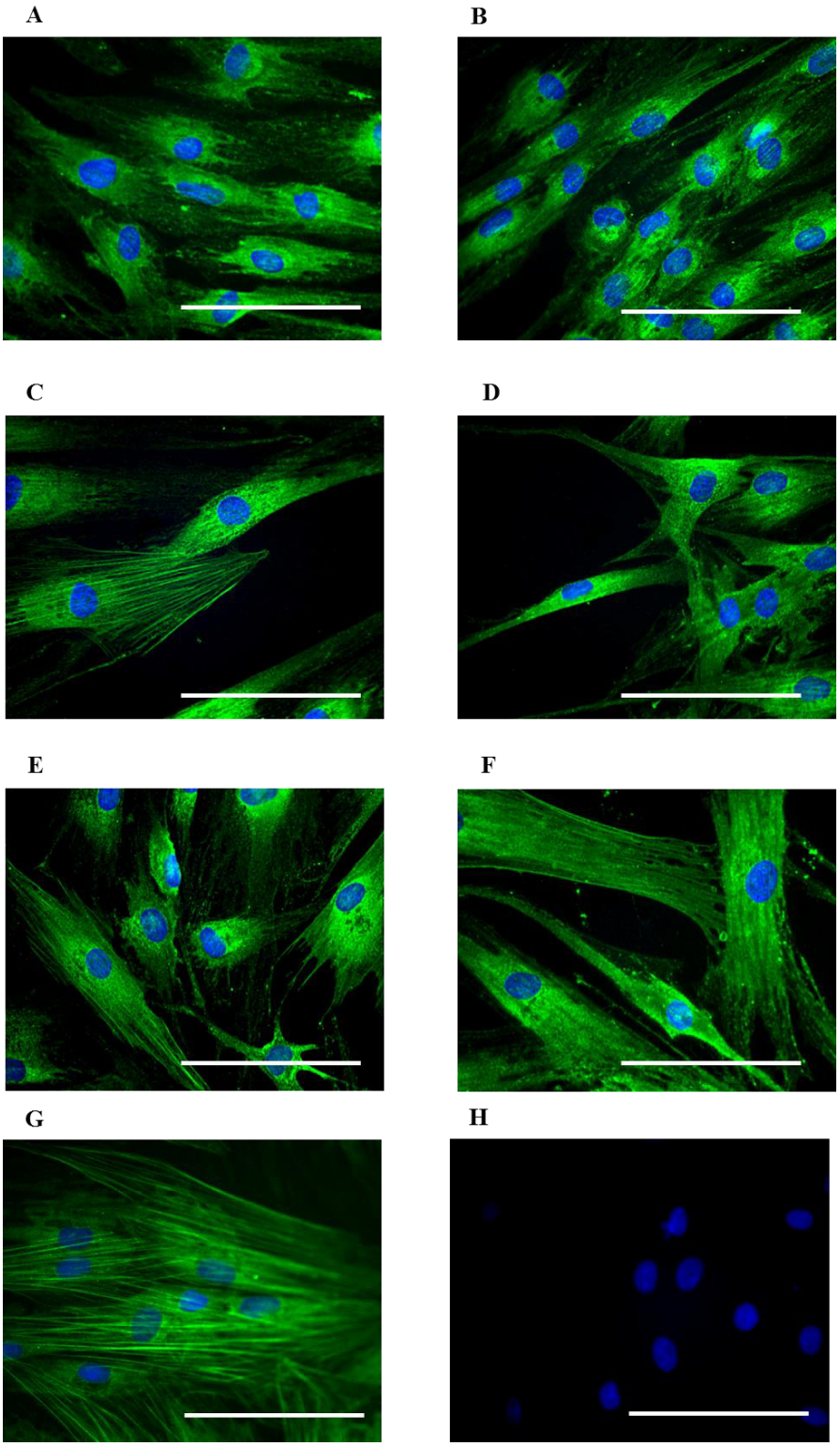

Figure 3.26: Immunocytochemical analysis of dermal fibroblast differentiation to myofibroblasts in the absence of TGF-β_1 and (A) 0µg/ml, (B) 0.001µg/ml, (C) 0.01µg/ml, (D) 0.1µg/ml, (E) 1µg/ml, (F) 10µg/ml EBC-211, (G) 0µg/ml in the presence of TGF-β_1 and (H) primary antibody-free control, for 72h (*N=3*). Scale bar = 100µm.

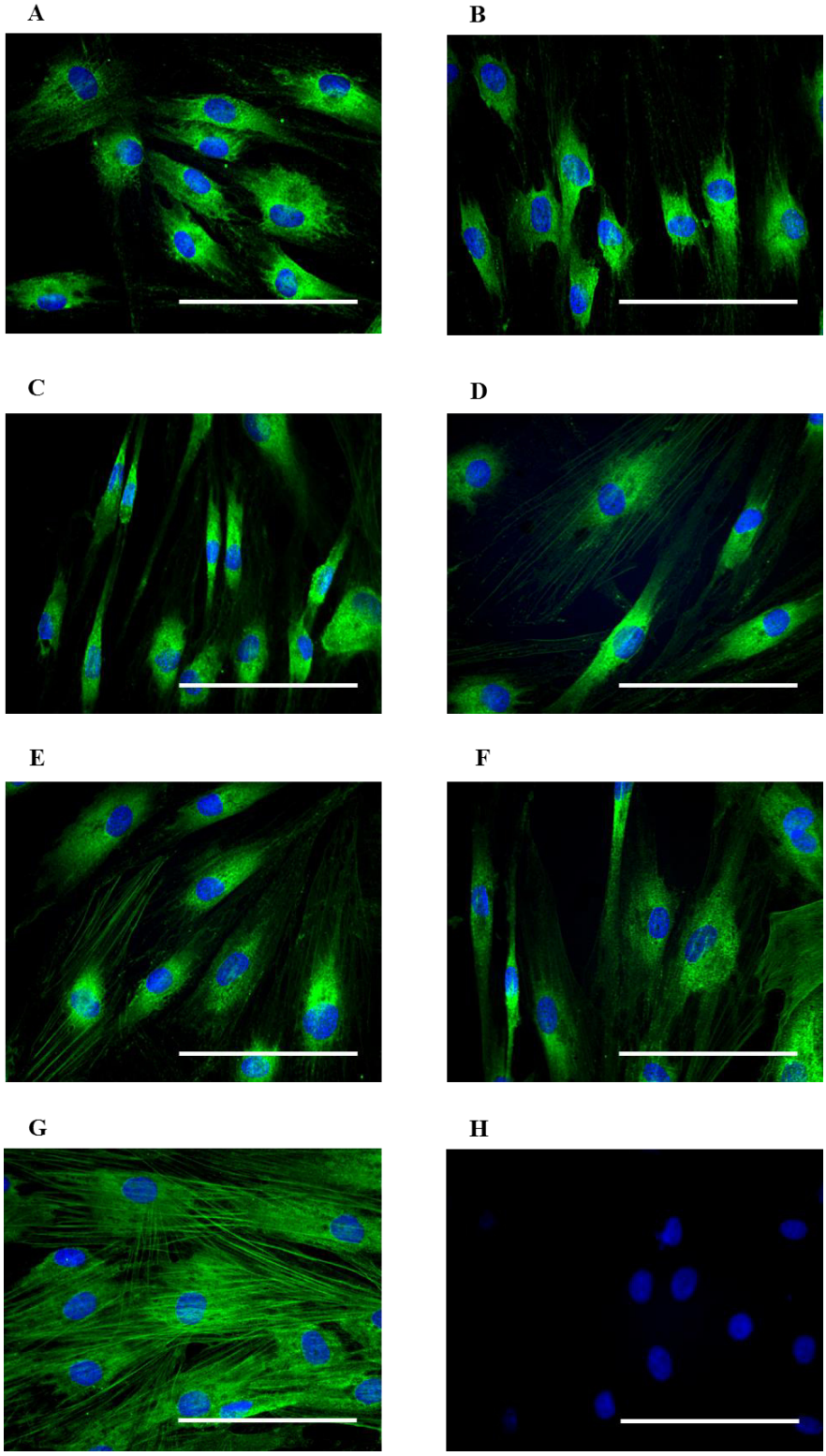

the length of the cell, as opposed to being localised around the nuclear region in the untreated control. At higher concentrations of EBC-46 (1-10µg/ml), α-SMA staining were again present along with the stress fibres, although there were some alterations from the typical myofibroblast morphology, as the stress fibres appeared less uniform and were not organised as tightly around the nuclear region.

Similar results were seen when fibroblasts were cultured with EBC-211 (0.001-10µg/ml) in the presence of TGF-β_1 (Figure 3.24A-F). The lower concentrations of EBC-211 (0.001-0.01µg/ml) showed no major differences in α-SMA staining or in the organisation of the stress fibres, when compared to untreated controls (Figure 3.24B-C). However, at 10µg/ml EBC-211, there was again a distinct lack of stress fibres, despite the presence of α-SMA staining localised around the perinuclear region, showing similarities to the morphology and α-SMA staining seen in the untreated control in the absence of TGF-β_1 (Figure 3.24G); as seen previously with 0.1µg/ml EBC-46. At 0.1-1µg/ml EBC-211, cells exhibited a slightly altered morphology compared to untreated controls, as the stress fibres were present and uniform in their organisation (Figures 3.24D-E). However, they appeared to demonstrate a narrower cell shape, with the stress fibres remaining quite close to the nuclear region.

These studies were repeated for EBC-46 (0.001-10µg/ml), but in the absence of TGF-β_1 (Figure 3.25A-F). There were no major differences observed in either the α-SMA content or in cell morphology at 0.001µg/ml EBC-46, compared to controls. However, at higher EBC-46 concentrations (0.01-10µg/ml), cells had altered morphologies with the production of α-SMA stress fibres, despite cultures containing no TGF-β_1. This was similar to the altered morphologies evident in the light microscopy studies (Section 3.4.3). In addition, cells at 0.1-10µg/ml EBC-46 also showed altered morphologies, with more stellate-shaped cells and the production of actin protrusions, as seen previously with the fibroblast repopulation studies (Section 3.4.4), with the increased fibroblast size and production of long processes from their cytoskeleton. These morphologies, with the presence of TGF-β_1 and stress fibres, appear more representative of the untreated control in the presence of TGF-β_1 (Figure 3.25G).

When repeated with EBC-211 (0.001-10µg/ml) in the absence of TGF-β_1 (Figure 3.26A-F), there were no major differences observed in the morphology of the cells or the α-SMA content between the lower concentrations of EBC-211 (0.001-0.01µg/ml) and the untreated controls (Figures 3.26B-C). At the higher concentrations of EBC-211 (0.1-10µg/ml), there was evidence of stress fibre formation and altered morphologies, similar to those seen previously with the morphology and repopulation studies (Figures 3.26D-F). Similar to the response seen with EBC-46, these morphologies, with the presence of TGF-β_1 and stress fibres, appear more representative of the untreated control in the presence of TGF-β_1 (Figure 3.26G).

3.4.6 Confirmation of EBC-46 and EBC-211 Effects on Dermal Fibroblast-Myofibroblast Differentiation by Quantitative Polymerase Chain Reaction (qPCR)

Following on from the immunocytochemistry studies, qPCR analysis was performed to determine the gene expression levels of α-SMA upon culture in EBC-46 or EBC-211 (0.001µg/ml, 0.01µg/ml, 0.1µg/ml, 1µg/ml and 10µg/ml), with an untreated control also included for comparison purposes (0µg/ml) for both compounds. These experiments were performed in the presence and absence of TGF-β_1 (10ng/ml), for 72h.

Fibroblasts cultured with EBC-46 (0.001-10µg/ml) and in the presence of TGF-β_1 (10ng/ml) were compared to two untreated controls (Figure 3.27A), one in the presence of TGF-β_1 (positive control) and the other in the absence of TGF-β_1 (negative control). Some EBC-46 concentrations (0.01µg/ml and 1-10µg/ml) showed no significant difference in α-SMA expression, compared to the TGF-β_1 positive control ($p>0.05$; Figure 3.27A). This confirmed the immunocytochemistry data (Figure 3.23C, E and F), where no major differences were observed. However, there was a significant increase in α-SMA expression at 0.001µg/ml EBC-46, compared to the positive controls ($p<0.05$; Figure 3.27A), suggesting the presence of more α-SMA stained stress fibres (Figure 3.23B). However, at 0.1µg/ml EBC-46, there was a significant reduction in the expression of α-SMA, compared to positive controls, with approximately 2.5-fold lower expression ($p<0.001$; Figure 3.27A). This corroborated the lack of stress fibres observed by immunocytochemistry and the unique and specific

Figure 3.27: α-SMA expression during dermal fibroblast-myofibroblast differentiation in the presence of TGF-β$_1$ and (A) EBC-46 and (B) EBC-211, at (0µg/ml, 0.001µg/ml, 0.01µg/ml, 0.1µg/ml, 1µg/ml and 10µg/ml) for 72h; (*N=3, average±SE; *p<0.05, **p<0.01, ***p<0.001, compared to untreated controls*).

A

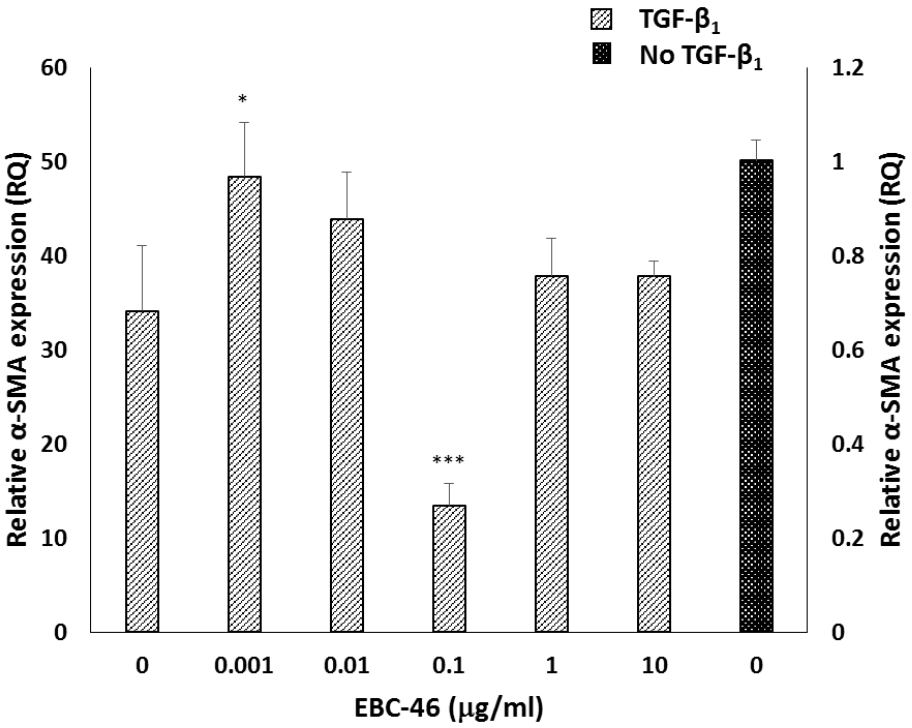

B

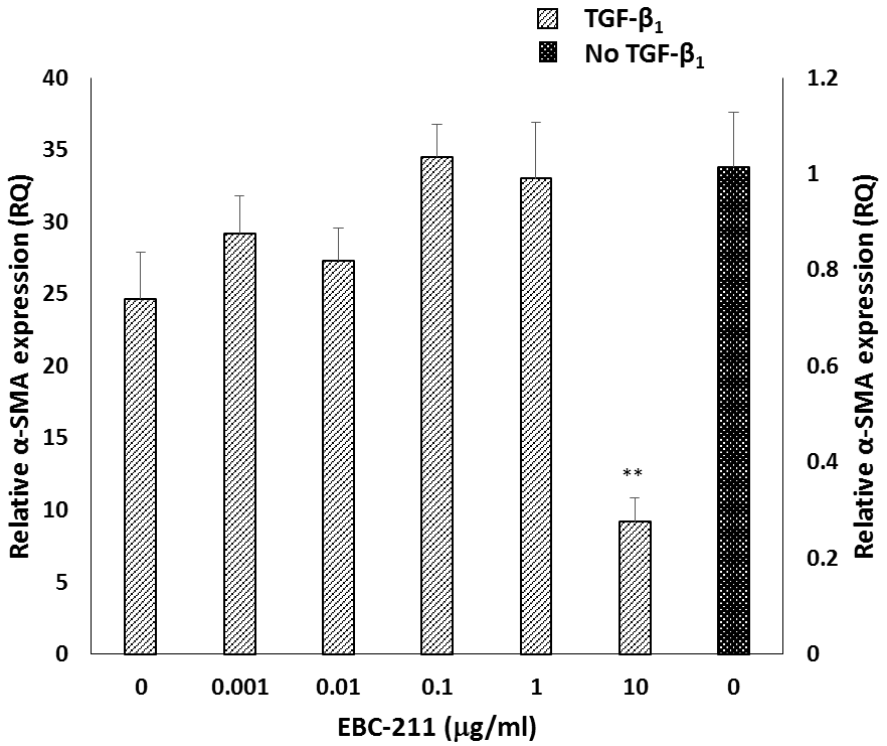

Figure 3.28: α-SMA expression during dermal fibroblast-myofibroblast differentiation in the absence of TGF-β_1 and in the presence of (A) EBC-46 and (B) EBC-211, at (0µg/ml, 0.001µg/ml, 0.01µg/ml, 0.1µg/ml, 1µg/ml and 10µg/ml) for 72h; (*N=3, average±SE; *p<0.05, ***p<0.001, compared to untreated controls*).

A

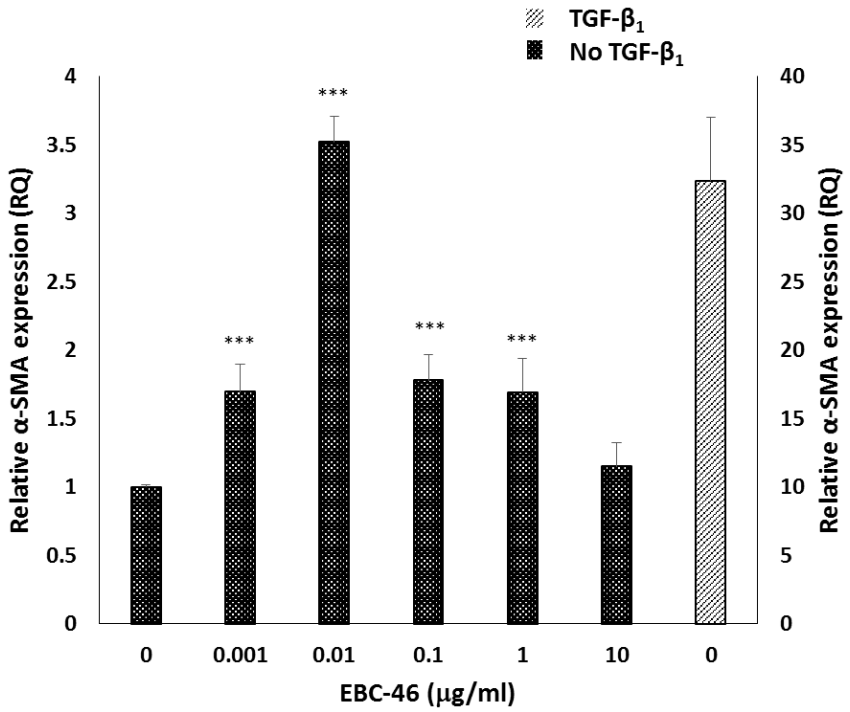

B

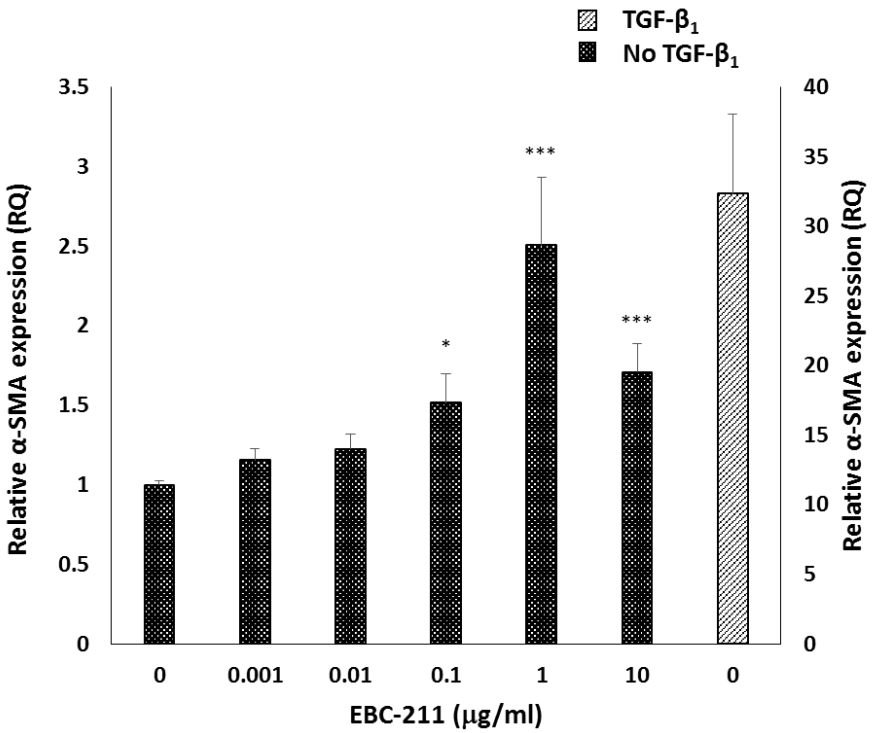

response at this concentration (Figure 3.23D). Interestingly, the α-SMA expression at this concentration was approximately 13-fold higher than the negative controls (Figure 3.27A). This showed that expression of α-SMA is still induced in fibroblasts at 0.1µg/ml EBC-46, but not to the same extent as in stimulated fibroblasts.

α-SMA expression after treatment with EBC-211 (0.001-1µg/ml) was not significantly different to the positive controls ($p>0.05$; Figure 3.27B), corroborating the previous immunocytochemistry data (Figure 3.24B-E). However, at 10µg/ml EBC-211, there was a significant reduction in α-SMA expression, also approximately 2.5-fold lower, compared to stimulated fibroblasts ($p<0.01$; Figure 3.27B). As evident with 0.1µg/ml EBC-46; this result also showed a higher expression of α-SMA than the negative control, approximately 9-fold higher.

The fibroblasts that were treated with 0.001-1µg/ml EBC-46 and in the absence of TGF-β_1 showed a significant increase in α-SMA expression, compared to untreated negative controls ($p<0.001$; Figure 3.28A), whereas there was no significant increase in expression with the highest concentration of EBC-46 (10µg/ml; $p>0.05$; Figure 3.28A). Despite there being a significant increase in α-SMA expression (approximately 1.5-3.5-fold), compared to the negative controls, the levels of α-SMA expression were still much lower than the positive controls (approximately 10-fold lower), than in the presence of TGF-β_1 (Figure 3.28A). The increased α-SMA expression corroborated the immunocytochemistry studies, where an increased presence of stress fibres was observed following 0.001-1µg/ml EBC-46 treatment, in the absence of TGF-β_1 (Figure 3.25B-E).

Treatment with EBC-211 in the absence of TGF-β_1 (Figure 3.28B) showed a similar response to previously seen with EBC-46. However, due to the approximately 100-fold reduced activity of EBC-211, compared to EBC-46 (Boyle et al. 2014; Reddell et al. 2014), this increase was significant at 0.1-10µg/ml EBC-211, compared to the negative control ($p<0.001$-0.05; Figure 3.28B). As before, the increased α-SMA expression (approximately 1.5-2.5-fold) compared to the negative control, corroborated the immunocytochemistry studies, where there was an increased presence of stress fibres after EBC-211 treatment at these concentrations (Figure

3.26D-F). However, the α-SMA expression levels were still much lower (approximately 13-fold lower), than the stimulated fibroblasts following treatment with TGF-β_1 (Figure 3.28B).

3.5 Discussion

This Chapter focused on assessing the effect of the novel epoxy-tiglianes, EBC-46 and EBC-211, on key fibroblast wound healing responses, due to their necessary roles in acute skin wound healing processes. The palliative animal studies performed by QBiotics Ltd. have previously demonstrated the profound effects of these compounds *in vivo* (Reddell & Gordon 2007; Reddell et al. 2014). However, in order to progress towards human clinical trials, it was necessary to fully understand these events at a cellular level. It is already known that there is a fine balance between the successful and impaired healing of wounds, as slight changes in gene expression or the function of fibroblasts may have a detrimental effect on wound healing outcomes. This is shown through multiple forms of impaired healing, such as chronic wounds or the excessive scar tissue formation observed with keloid and hypertrophic scars (Bran et al. 2009; Shih et al. 2010). However, it may be possible to induce a regenerative response and allow adult wounds to heal preferentially, as opposed to the remodelling process that normally occurs. This regenerative healing process would potentially result in the rapid, scarless healing typically only seen in early-gestational foetal wounds and in the oral mucosa (Nauta et al. 2011; Rolfe & Grobbelaar 2012). The palliative animal studies undertaken by QBiotics Ltd. appeared to show this beneficial response by the exceptional healing response and a distinct lack of visible scarring, following EBC-46 treatment, implying that EBC-46 and other epoxy-tiglianes may exert these effects, at least in part, via the mediators of preferential healing.

The initial proliferation and viability studies observed through use of an MTT assay determined the cytotoxic level of both epoxy-tiglianes as 100µg/ml. This is evident within 24h of treatment and resulted in no viable cells remaining by 168h for both EBC-46 and EBC-211. This was found to be highly significant ($p<0.001$), evident by a dramatic reduction in the cell viability readings, in comparison to the respective untreated controls. However, EBC-46 showed a more profound cytotoxic effect than

EBC-211, due to the 100-fold lesser activity of EBC-211 (Boyle et al. 2014; Reddell et al. 2014). This was evident by a cytotoxic response at 24h for EBC-46 treatment and at 72h for EBC-211 treatment. The cytotoxic effect was also visualised during the morphology and repopulation studies, where cells initially rounded up and eventually burst, with blebbing occurring. A resultant loss of integrity to the cell membrane resulted in the cells releasing their contents. This observation suggested that necrosis was responsible for the cytotoxic effect observed, rather than apoptosis (Ogbourne et al. 2004; Elmore 2007). Despite it appearing to be a necrotic process, it is still possible that apoptosis was occurring, as the cells were cultured *in vitro* and therefore any apoptotic bodies would not be phagocytosed. This lack of clearance of apoptotic bodies leads to secondary necrosis, also termed apoptotic necrosis, which may be what was being observed in this study (Saraste & Pulkki 2000; Ziegler & Groscurth 2004; Fink & Cookson 2005; Elmore 2007; Elliott & Ravichandran 2010). Apoptosis and necrosis used to be described as opposite responses. However, it has been shown that there may be intermediate forms, especially in terms of *in vitro* studies. There are numerous other cell death mechanisms known, such as oncosis, autophagy and pyroptosis, so further studies would be required to determine which cell death mechanism is occurring (Ziegler & Groscurth 2004; Fink & Cookson 2005; Elmore 2007).

At the other concentrations of EBC-46 (0.001-10µg/ml), there appeared to be an overall anti-proliferative response in fibroblasts after EBC-46 or EBC-211 treatment, particularly at the later time-point (168h) for 0.001-10µg/ml EBC-46 and at 72h, 120h and 168h for 0.1-10µg/ml EBC-46. This decrease in fibroblast proliferation is believed to be a result of a direct anti-proliferative action, as opposed to the cytotoxic effect observed at 100µg/ml. This conclusion is based on the visualisation of viable cells for the full 168h duration of the study. Despite this anti-proliferative response being statistically significant, the decrease in proliferative ability compared to untreated controls appears to be marginal, especially following treatment with EBC-46; therefore, there is a possibility that this anti-proliferative response will not be biologically significant. It is possible that the anti-proliferative responses observed are a result of a phenotypic change in the fibroblasts to resemble those present at a wound site, which have a decreased proliferative ability, but are involved in collagen

production to fill the denuded site (Beldon 2010). Indeed, as described previously, there were dramatic morphological changes in the fibroblasts at 24h, to form a more stellate-shaped structure. This morphology is similar to that of senescent cells or those undergoing differentiation, with the formation of stress fibres (Gabbiani 2003; Campisi & d'Adda di Fagagna 2007).

However, this dramatic morphological alteration of the fibroblasts was found to be reversible, with normal stellate-shaped fibroblasts returning by 72h and remaining for the duration of the experiment. Although, it is currently unknown what is occurring to induce this response, the potential benefits could be significant, if treatment with the novel epoxy-tiglianes are capable of stimulating a reversible fibrosis response. This would have profound implications on the wide array of fibrotic diseases, including the excessive scarring observed in keloid and hypertrophic scars (Darby et al. 2014). A number of studies have been performed to reduce the incidence of excessive scarring, through reduction of myofibroblast activity. This included inducing myofibroblast apoptosis, reducing myofibroblast function, activation of inhibitory myofibroblast differentiation factors; and the reduction of stimulatory myofibroblast differentiation factors (Chitturi et al. 2015). Further studies would be required to determine whether any of these mechanisms are induced following epoxy-tigliane treatment, in particular the stimulation or inhibition of crucial factors, resulting in inhibition of myofibroblast differentiation; differentially expressed factors could be elucidated through global gene analysis on myofibroblast treated with epoxy-tiglianes.

An initial theory was that the cells were becoming senescent, due to the anti-proliferative response and increased morphology of the cell, features seen in senescent fibroblasts (Hayflick 1965; Campisi & d'Adda di Fagagna 2007). Senescent cells prevent cell growth by halting progression through the cell cycle; this could explain why the fibroblasts did not proliferate at a normal rate, despite the medium being replenished every 48 hours, but also remain viable as senescent cells resist apoptosis (Campisi & d'Adda di Fagagna 2007). As senescent cells have an altered gene expression from those that continue normally through the cell cycle, gene analysis could be performed to determine whether these cells are indeed senescent. By assessing for specific markers that are associated with senescence, such as senescence-

associated β-galactosidase, p53, $p21^{WAFI}$, $p16^{INK4A}$, senescence-associated DNA-damage foci and senescence-associated heterochromatin foci (Campisi & d'Adda di Fagagna 2007; Rodier & Campisi 2011). However, despite the anti-proliferative response following treatment with EBC-46 or EBC-211, the fibroblasts were observed to continue proliferating across the 168h time period of the viability/proliferation study. Therefore, it is thought that treatment with EBC-46 or EBC-211 results in a delayed cell cycle progression, not an induction of senescence.

This response was confirmed with the flow cytometry studies, assessing the progression and proportion of cells in the cell cycle phases at 0h, 22h, 29h and 36h; an overall anti-proliferative response was observed. This delayed progression of the cell cycle after EBC-46 or EBC-211 treatment appeared to be a result of a delayed progression of the cells into S phase, which could be a result of S phase checkpoints promoting the delayed progression of the cell cycle. This would reduce the replicative activity of the cell and contribute to the anti-proliferative effect (Bartek et al. 2004). Such responses may have an impact on the ablation of solid tumours and sarcoids, through decreasing the volume of fibroblasts present at the tumour site and fibroblast-rich sarcoids; and the reduced activation to contractile myofibroblasts (Knottenbelt 2005; Darby et al. 2014). Chronic wound fibroblasts are typically associated with a decreased proliferative capabilities and premature senescence. In contrast, an increased presence and activation of fibroblast proliferation occurs in keloid and hypertrophic scars, reiterating the delicate balance between successful and impaired healing (Wall et al. 2008; Bran et al. 2009; Peake et al. 2014; Jumper et al. 2015; Roper et al. 2015).

In addition to the anti-proliferative responses evident following EBC-46 or EBC-211 treatment, a potentially reduced migratory and wound closure ability in these fibroblasts was also observed through the incomplete closure of *in vitro* scratch wounds. This was shown through a decreased number of cells appearing to repopulate denuded sites, compared to untreated controls. This response along with the anti-proliferative action potentially results in a reduction of fibroblasts at the wound site, decreasing the potential for subsequent myofibroblast formation. Additionally, the time-lapse movies showed atypical motility of the fibroblasts following epoxy-tigliane

treatment (Supplement 3.2). The higher concentrations of EBC-46 (0.01-10µg/ml) and EBC-211 (0.1-10µg/ml), in particular, showed abnormal fibroblast motility. The dramatically altered behaviour of fibroblasts was demonstrated in the time-lapse movies, with rapid mobility observed in some fibroblasts and a perceived impaired mobility in others following EBC-46 or EBC-211 treatment. However, potentially due to this wide variability in cellular behaviour, there were no significant differences in migration observed following EBC-46 treatment, despite the noticeable effect on wound repopulation. Following EBC-211 treatment, there was no significant effect on cell displacement or overall velocity. However, there was a significant decrease in distance travelled and speed of the fibroblasts at 0.1-1µg/ml EBC-211, resulting in a decreased migratory action at these conditions. Impaired fibroblast migratory responses are observed in chronic wounds, due to reduced growth factor presence, resulting from increased proteolytic degradation (Menke et al. 2007; Barrientos et al. 2008). Migration of fibroblasts into the wound site is crucial for successful synthesis of ECM components; in addition to wound contraction, aiding wound closure (Reinke & Sorg 2012; Bainbridge 2013).

Profound changes in the cell structure were also evident during this time-lapse procedure, with some cells exhibiting a much larger morphology, which could give the appearance of wound repopulation and closure, due to individual cells covering a larger area. In addition to the larger, stellate-shaped fibroblasts, cells with very long processes were also observed in epoxy-tigliane treated fibroblasts, prior to migration. It is possible that these processes are part of the actin cytoskeleton in fibroblasts, responsible for forming projections during cell crawling, in order to migrate (Ananthakrishnan & Ehrlicher 2007). However, it appears that the actin cytoskeleton is significantly affected by treatment with EBC-46 or EBC-211, due to the production of numerous projections instead of one uniform projection towards a chemotactic signal, along with failure to retract the projection after movement (Van Haastert & Devreotes 2004; Ananthakrishnan & Ehrlicher 2007). It is not yet known what is causing such changes to the atypical fibroblast morphology and cytoskeletal structure. It is possible that the cytoskeletal changes are a result of alterations in Rho family GTPases, within the Ras superfamily. These proteins, Rho, Rac and CDC42, are involved in actin cytoskeleton regulation, cell migration, stress fibre and focal

adhesion formation (Kaibuchi et al. 1999; Wozniak et al. 2004; Parri & Chiarugi 2010; Parsons et al. 2010; Petrie & Yamada 2012). Downstream from Rho, the Rho-associated kinase (ROCK) is involved in stress fibre formation, contraction and focal adhesion formation. This effector is capable of maintaining tension, through ROCK-mediated contraction, with ROCK1 appearing to be the form involved in stress fibre formation (Schwartz 2004; Wozniak et al. 2004; Amano et al. 2010; Parsons et al. 2010). Rac is primarily involved in the motility of fibroblasts, through activation at the leading edge and needed for lamellipodia extension; in addition to a vital role in focal adhesion formation, activating when cells adhere to the ECM (Schwartz 2004; Parri & Chiarugi 2010; Parsons et al. 2010; Petrie & Yamada 2012). Changes in the gene expression for these could be elucidated through global gene analysis, following epoxy-tigliane treatment, indicating whether changes in stress fibre and focal adhesion formation are present. The fibroblasts were cultured in 1% foetal calf serum (FCS), so a low expression of growth factors were present which stimulate growth and viability of cells. Therefore, there is a possibility that treatment with the novel epoxy-tiglianes, along with 1% FCS may result in a fibroblast-myofibroblast differentiation response, producing the altered morphology observed (Gabbiani 2003; Zheng et al. 2006).

As mentioned, myofibroblasts have a different morphology to fibroblasts, with myofibroblasts expressing higher α-SMA levels and possessing stress fibres. A combination of these two factors positively confirm the presence of true myofibroblasts. α-Actin is the form present in myofibroblasts, while β- and γ-actin are present in fibroblasts. Therefore, α-SMA is the isoform used as a marker to detect that myofibroblast differentiation has occurred (Gabbiani 2003). Proto-myofibroblasts are an intermediate point between fibroblasts and smooth muscle cells, possessing some stress fibres, but these do not express high levels of the α-actin isoform that characterise myofibroblasts. The differentiation of fibroblasts to myofibroblasts is activated by the presence of TGF-β_1 (Evans et al. 2003; Gabbiani 2003). Actin fibres also produce cell to cell connections, which are necessary for the contractile function of myofibroblasts. This contraction is essential in wound healing for closing the wound edges together; however, increased contraction does lead to increased scar tissue formation (Evans et al. 2003; Li & Wang 2011).

At 0.1µg/ml EBC-46 and 10µg/ml EBC-211 in the presence of TGF-β_1, despite α-SMA being expressed, it was not present along stress fibres as typically observed following TGF-β_1 stimulation, but remained localised to the perinuclear regions of the cells. Due to the definition that a true myofibroblast must possess both α-SMA staining and have the contractile stress fibres present, these cells are not true myofibroblasts (Gabbiani 2003). This was confirmed with qPCR studies, where there was a significant reduction in α-SMA expression, although this was still markedly higher than the TGF-β_1-free control. Nonetheless, such findings imply that at these specific EBC-46 and EBC-211 concentrations, there is an inhibition of myofibroblast formation. As mentioned previously, mechanisms of myofibroblast inhibition have been studied and a number of compounds have been shown to reduce or inhibit this fibrotic response. One agent capable of inhibiting TGF-β_1-induced, myofibroblast differentiation is endogenous aryl hydrocarbon (AhR) ligand, 2-(1′H-indole-3′-carbonyl)-thiazole-4-carboxylic acid methyl ester (ITE), which has potential as an anti-fibrotic therapy (Lehmann et al. 2011). Another agent able to inhibit fibrosis is the synthetic PPAR-γ agonist, triterpenoid, through blocking TGF-β/Smad and Akt signalling pathway; the synthetic triterpenoid is oleanane 2-cyano-3,12-dioxoolean-1,9-dien-28-oic (CDDO), which has been shown to a possess good safety profile, resulting in a promising potential as an anti-scarring therapy (Wei et al. 2014). There are a number of other biologically-derived and synthetic pharmaceuticals that possess TGF-β-mediated anti-fibrotic responses on a variety of tissues, including ginsan, trichostatin A, relaxin, resveratrol and curcumin (Heeg et al. 2005; Olson et al. 2005; Masamune et al. 2006; Glenisson et al. 2007; Guo et al. 2009; Ahn et al. 2011). As mentioned in Chapter 1, TGF-β-mediated responses act through SMAD signalling pathway to induce the fibroblast-myofibroblast differentiation. Therefore, EBC-46 and EBC-211 may exert their responses through inhibition of SMADs; previous studies have shown SMAD3 inhibition reduces myofibroblast formation, resulting in an anti-fibrotic therapy (Evans et al. 2003; Javelaud & Mauviel 2004; Schiller et al. 2004; Darby et al. 2016). Additionally, hyaluronan is also involved in TGF-β-mediated fibroblast to myofibroblast differentiation, with inhibition of hyaluronan synthesis inhibiting this response; therefore, the epoxy-tigliane-mediated responses may occur due to hyaluronan synthesis inhibition (Jenkins et al. 2004; Meran et al. 2007; Webber et al. 2009). Further studies would be required to determine which mechanism is impacted

by epoxy-tigliane treatment to inhibit fibroblast-myofibroblast differentiation at 0.1µg/ml EBC-46 and 10µg/ml EBC-211; comparisons to the other epoxy-tigliane concentrations would also be of interest to determine why this response only occurs at these specific concentrations.

As activation of protein kinase C (PKC) isoforms and subsequent downstream signalling pathways have previously been associated with these novel epoxy-tiglianes, in particular EBC-46; this could be the mechanism by which EBC-46 and EBC-211 mediate these responses during myofibroblast formation (Boyle et al. 2014). Further work will be necessary to look at the impact of epoxy-tigliane treatment on TGF-β_1-mediated, fibroblast-myofibroblast differentiation, using pan- and specific-PKC inhibitors, to determine what roles PKCs have in stress fibre formation. Alternatively, due to the lack of stress fibre formation, but the expression of α-SMA, albeit reduced, it is possible that the cells present are not either a differentiated myofibroblast or an undifferentiated fibroblast. Therefore, further studies are required to understand this situation fully. An initial theory was that the cells were forming an intermediate proto-myofibroblast form. However, as mentioned previously, proto-myofibroblasts also possess stress fibres, which are noticeably absent at 0.1µg/ml EBC-46 and 10µg/ml EBC-211 (Gabbiani 2003; Micallef et al. 2012). In addition α-actin is present, albeit at a lower expression than seen in true myofibroblasts, whereas β- and γ-actin are the forms known to be present in proto-myofibroblasts, with no expression of α-SMA (Gabbiani 2003; Micallef et al. 2012; Darby et al. 2014). Consequently, the presence of the α-actin isoform seems to indicate that this theory is unlikely. Another probability is that they could be transforming into fibrocytes, a circulating cell type involved in wound repair and fibrotic tissue development; capable of expressing α-SMA albeit at lower levels (Reilkoff et al. 2011; Calderhead & Goo 2014). In a similar scenario, the studies performed in the absence of TGF-β_1 show an increase of α-SMA expression, albeit reduced compared to positive controls, with some stress fibre formation. This could be another example of the differentiation to a myofibroblast phenotype not being complete.

This dramatic effect on the myofibroblast differentiation process at these specific concentrations of EBC-46 and EBC-211 may indicate the potential action these novel

epoxy-tiglianes have on myofibroblast differentiation by inhibiting or reducing the contractile myofibroblast formation. If this is the case, EBC-46 or EBC-211 may have a use as an anti-scarring treatment and be of particular use in excessive scarring situations, such as keloid and hypertrophic scarring (Gauglitz et al. 2011). Foetal wound healing is an example of successful wound healing with a reduced presence of α-SMA expressing myofibroblasts, with actin 'purse-string' closure observed in early-gestational foetal wounds. Of interest, myofibroblast presence increases with gestational age, with late-gestational wounds displaying myofibroblast presence and scarring (Redd et al. 2004; Satish & Kathju 2010; Otranto et al. 2012; Yates et al. 2012). Oral mucosal wounds have also been associated with a minimal scarring response following injury, this is despite an enhanced collagen contraction, potentially due to the increased motility of oral fibroblasts resulting in an increased migration into the wound site to re-establish the ECM (Shannon et al. 2006; Meran et al. 2008). The reduced scarring response may be a result of a significantly lowered presence of TGF-β_1 expression in oral wounds, when compared to dermal wounds; as TGF-β_1 is strongly involved in the induction of fibroblast to myofibroblast differentiation, this decreased expression also results in a reduced α-SMA expression in oral mucosa and the potentially subsequent reduction in myofibroblast presence (Szpaderska et al. 2003; Shannon et al. 2006). Low levels of TGF-β_1 have been observed in both early-gestational foetal and oral mucosal wounds, leading to the theory that it is a reduced presence of myofibroblasts that allows scarless or minimal scarred healing to occur; and not an overall reduction in contraction of the wound (Bullard et al. 2003; Szpaderska et al. 2003; Shannon et al. 2006; Meran et al. 2008; Yates et al. 2012). Therefore, the implication of the reduced α-SMA expression following treatment of certain concentrations of EBC-46 (0.1µg/ml) and EBC-211 (10µg/ml); and subsequent reduced myofibroblast formation, may lead to a minimal scarring response following injury. This theory fits in with the previous *in vivo* animal studies performed by QBiotics Ltd., demonstrating a reduced scarring healing response following treatment with novel epoxy-tiglianes (Reddell et al. 2014). However, it is not yet understood why these inhibitory myofibroblast responses only occur at 0.1µg/ml EBC-46 and 10µg/ml EBC-211, but not at the other concentrations of both epoxy-tiglianes. In addition, it is not yet known the comparable concentration used during *in vivo* studies and whether

these optimal concentrations were used, resulting in the observed reduced scarring response.

EBC-46 has been shown to act primarily through the activation of classical PKC-β isoforms, along with other classical and novel isoforms, albeit to a much lower level (Boyle et al. 2014). This is a calcium-activated, phospholipid and diacylglycerol (DAG) dependent serine/threonine protein kinase, which requires DAG and calcium for activation (Breitkreutz et al. 2007; Roffey et al. 2009; Sumagin et al. 2013). PKC-β is involved in regulating mitochondrial function and subsequent apoptosis, cell survival and mitosis. This apoptosis regulation may confirm the cell death mechanism occurring during the cytotoxicity studies (Breitkreutz et al. 2007; Ali et al. 2009; Saba & Levy 2012; Mehta 2014). This PKC isoform also plays a role in vascular endothelial growth factor (VEGF) induced cell proliferation, impacting on the permeability of the blood vessel (Boyle et al. 2014). Treatment with EBC-46 subsequently resulted in leaky vasculature (Graff et al. 2005; Ali et al. 2009). PKC-β is also thought to be activated in a high glucose environment, therefore is shown to be upregulated in experimental diabetes and contributes to renal fibrosis. Inhibition of this isoform is thought to reduce the progression of diabetic nephropathy (Kelly et al. 2003; Meier et al. 2007; Geraldes & King 2010). PKC-β is also involved in actin polymerisation, allowing the migration of smooth muscle cells (Larsson 2006; Mochly-Rosen et al. 2012). Other functions of PKC signalling include cell transformation, cell growth and apoptosis, acting down the mitogen-activated protein kinases (MAPK) pathway affecting cell growth through an effect on cyclins. Due to these important roles, dysfunctional MAPK pathway signalling has been implicated in cancer development (Larsson 2006; Ali et al. 2009; Hampson et al. 2010; Mason et al. 2010; Mochly-Rosen et al. 2012). MAPK signalling is activated by epidermal growth factor (EGF) family binding to EGF receptor. This pathway has been shown to regulate cell proliferation and differentiation, in particular the downstream signalling pathways, c-Jun N-terminal kinase (JNK), extracellular signal-regulated kinase (ERK)1/2 and p38, with an apparent opposing roles from the different downstream pathways (Zhang & Liu 2002; Mccubrey et al. 2007; Hampson et al. 2010). These MAPK downstream signalling pathways have also been shown to play an important role in cell migration, in particular JNKs, with inhibitors shown to impair fibroblast migratory responses

(Huang et al. 2004; Kajanne et al. 2007). Upregulated activity of JNKs has been shown to affect stress fibres in fibroblasts, resulting in morphological changes in the cells. Gene analysis following epoxy-tigliane treatment may determine whether any of these downstream signalling pathways are altered, resulting in the *in vitro* and *in vivo* responses previously observed (Rennefahrt et al. 2002; Huang et al. 2004).

The role of PKC-βII has been well-studied and has shown to impact angiogenesis, B cell survival and the AKT pathway, involved in cell survival mechanisms and shown to exert an anti-apoptotic effect. However, less is known about PKC-βI function (Martiny-Baron & Fabbro 2007; Reyland 2007; Serova et al. 2008; Saba & Levy 2012). PKC-βI appears to function in opposing manners, in some cases it also promotes cell survival and stimulates proliferation mediated through VEGF (Ali et al. 2009). In contrast, it also seems to have a pro-apoptotic role, again potentially confirming the cell death mechanism discussed previously, along with an inhibitory effect on cell cycle progression (Poole et al. 2004; Ali et al. 2009; Saba & Levy 2012). An important PKC-β-dependent process is plasminogen activator inhibitor (PAI) synthesis, which impacts a number of key features of wound healing, such as migration, cell attachment to extracellular matrix and angiogenesis. Therefore, stimulation of PKC-β will enhance these functions (Berg et al. 2005).

Novel PKC isoform, epsilon (ε), has also been shown to have an involvement in wound closure and myofibroblast formation, along with a decreased α-SMA expression and subsequent stress fibre formation; targeting this isoform may be of use for excessive scarring situations, such as hypertrophic scarring, by reducing the presence of the contractile myofibroblasts (Leask et al. 2008). This decreased α-SMA expression and myofibroblast formation is similar to the response seen at EBC-46 (0.1µg/ml) and EBC-211 (10µg/ml), indicating a potential reduction in activity of this novel isoform (Leask et al. 2008). In addition to the inhibitory effect on myofibroblast formation when PKC-ε is knocked out, there is also a reduction in migration response. Although no significant difference was observed following epoxy-tigliane treatment, there was a perceived reduction in wound closure ability observed by a lack of repopulation of the denuded site (Leask et al. 2008). PKC-δ has also been associated with the migratory response of dermal fibroblasts, through the activation of Stat3, a factor

involved in wound healing. This isoform has also been shown following activation by EGF to increase fibronectin expression, an essential component of the wound healing process, involved in re-epithelialisation, ECM formation and clot production (Mimura et al. 2004; Fan et al. 2006). PKC-δ has also been shown to have an important role in the impaired wound healing response observed in diabetic wounds, focusing on fibroblast responses, with enhanced diabetic wound repair following inhibition of PKC-δ. This response was also demonstrated by inducing impaired wound healing in healthy situations through an excessive expression of PKC-δ (Khamaisi et al. 2016). Determining the specific PKC isoforms involved in inducing the potential anti-fibrotic response observed during the veterinary trials will help elucidate the mechanism of action of the novel epoxy-tiglianes and understand what changes to the normal acute skin wound healing response are occurring.

Overall, there is a profound effect following treatment with EBC-46 or EBC-211 on dermal fibroblasts, including delayed cell cycle progression and an overall anti-proliferative effect; and a modulatory effect on the actin cytoskeleton resulting in the inhibition of myofibroblast formation. However, there was no overall effect on the migratory responses of dermal fibroblasts following epoxy-tigliane treatment, potentially due to the large variability in fibroblast motility; the only exceptions being the reduced fibroblast distance travelled and speed at 0.1-1µg/ml EBC-211. Many of these responses can be attributed to PKC-β stimulation. The veterinary trials previously performed with EBC-46 have already demonstrated wound healing responses similar to those in preferential healing tissues, with the lack of visible scarring. However, no studies have yet been performed to observe the histology of the dermis to determine the composition of the wound site and if there is a presence of granulation tissue, myofibroblasts or the ratio of type I collagen to type III collagen. These are all factors of the wound healing response that differ in early-gestational foetal and oral mucosal wound healing, compared to normal acute skin wound healing responses (Rolfe & Grobbelaar 2012; Yates et al. 2012). Further studies are, therefore, required to understand how these modulatory effects on the dermal fibroblasts are achieved and whether myofibroblast inhibition is occurring, resulting in a potentially scarless healing outcome.

Chapter 4 - Effects of EBC-46 and EBC-211 on Keratinocyte Wound Healing Responses

Chapter 4 - Effects of EBC-46 and EBC-211 on Keratinocyte Wound Healing Responses

4.1 Introduction

As described in Chapter 3, the epoxy-tiglianes, EBC-46 and EBC-211, were demonstrated to possess significant anti-proliferative effects in dermal fibroblasts, in addition to the ability to inhibit transforming growth factor-β_1 (TGF-β_1)-driven, dermal fibroblast-myofibroblast differentiation at certain concentrations. Previous veterinary studies undertaken by QBiotics Ltd. have demonstrated that EBC-46 induces enhanced wound healing responses, such as rapid wound closure and reduced scarring (Section 1.7). Such *in vitro* findings may shed light on the mechanisms responsible for these preferential wound healing outcomes *in vivo*. In addition to the fibroblast-mediated wound healing responses, rapid wound re-epithelialisation is also a common feature of enhanced healing in EBC-46 treated skin (Reddell et al. 2014). These responses were evident during wound healing studies undertaken by QBiotics Ltd., comprising veterinary cases that were previously unresponsive to months of treatment under current wound healing strategies (Reddell et al. 2014).

Re-epithelialisation is a vital process during acute skin wound healing, as it restores the protective barrier of the skin; there are numerous cells involved in this function, although as approximately 95% of the epidermis consists of keratinocytes, these contribute the largest role to re-epithelialisation (Martin 1997; Menon 2002). Terminal differentiation of keratinocytes is halted in wound healing, as the keratinocytes undergo proliferation and migration to re-establish the protective barrier, with differentiation only resumed once the epidermal barrier has been restored (Candi et al. 2005; Bader & Kao 2009; Portou et al. 2015). The basement membrane is also re-established before normal keratinocyte differentiation can resume, through the re-formation of anchors between keratinocytes and the basal layer; the hemidesmosome complex provides stability to the differentiating keratinocytes (Martin 1997; Menon 2002; Li et al. 2007). It has been reported that when epidermal keratinocytes are

stimulated by certain signals, such as basic fibroblast growth factor (bFGF) or epidermal growth factor (EGF), they are capable of undergoing dedifferentiation to a less differentiated state (Fu et al. 2001; Li et al. 2007; Sun et al. 2011). It has been hypothesised that the extracellular signal-regulated kinase (ERK), mitogen-activated protein kinases (MAPK)-dependent signalling pathway is strongly involved in this dedifferentiation process and re-establishing a profound proliferative potential of the keratinocytes (Sa et al. 2009). This dedifferentiated state enables keratinocytes to possess a higher proliferative capacity and obtain characteristics of stem cells or become a precursor cell to the differentiated epidermal keratinocyte. This is confirmed through the presence of specific markers, such as cytokeratin 19 and β1 integrin, which have been associated as positive epidermal stem cell markers (Sa et al. 2009; Zhang et al. 2010; Sun et al. 2011). This dedifferentiation may result in a regenerative healing process, as opposed to remodelling, which typically occurs after injury (Zhang et al. 2010; Sun et al. 2011).

Some components necessary for the remodelling of the extracellular matrix (ECM) are synthesised by keratinocytes in the epithelia, such as metalloproteinases, laminin proteins and tenascin C glycoprotein. These components play a role in aiding keratinocyte migration at the wound edge (Schultz & Wysocki 2009). Keratinocytes at the wound healing edge can sense the ECM, allowing for migration across the dermal layer (Martin 1997; Li et al. 2007). As mentioned in Section 1.2.1.1, there is a 'double paracrine' process between keratinocytes and fibroblasts, stimulating wound healing responses in the other cell type (Werner et al. 2007; Bader & Kao 2009).

As with fibroblasts, keratinocyte function is tightly regulated as variation in normal phenotype can have detrimental effects on overall wound healing outcomes, such as with chronic wounds and burn injuries, where there is a loss of skin integrity, increasing the risk of contamination or infection of the wound site; and a resultant loss in functionality (Singer & Clark 1999; Menke et al. 2007; Dreifke et al. 2015). An example of this loss in function is the potential lack of response to migratory signals (Tomic-Canic et al. 2004; Agren & Werthén 2007; Li et al. 2007). Additional causes of impaired re-epithelialisation are the inability of keratinocytes to migrate over

chronic wound sites, either due to presence of infection or a dysfunctional ECM (Agren & Werthén 2007; Li et al. 2007).

Unfortunately, current wound healing strategies are not sufficient to tackle this major clinical burden, a burden that is only going to increase with the ageing population and prevalence of diabetes. Chronic wounds associated with diabetes include foot ulcers, can lead to amputation if not diagnosed early and treatment is not successful (Menke et al. 2007; Posnett & Franks 2008; Dreifke et al. 2015). As mentioned previously, there is another pharmaceutical agent currently available, Regranex® with isoform PDGF-BB as the main active component; decreased levels of PDGF are present in chronic wounds, indicating their essential role in the wound healing response (Beer et al. 1997; Barrientos et al. 2008; Fang & Galiano 2008). This treatment was approved by the Food and Drug Administration (FDA) for treatment of chronic wounds, in particular diabetic ulcers (Goldman 2004; Barrientos et al. 2008; Howard et al. 2014). However, the findings on the effectiveness of this agent are not encouraging, with recurrence of ulcers observed in approximately 30% of patients (Niezgoda et al. 2005; Fang & Galiano 2008). A theory for this lack of effectiveness is that there are numerous changes to the wound environment in chronic wounds and the addition of one growth factor is not sufficient to resolve this. One of the main issues is the high levels of inflammatory cytokines and proteases at the chronic wound site, degrading PDGF, along with other vital growth factors, such as FGF and transforming growth factor-β (TGF-β) (Fang & Galiano 2008). In addition, there has since been a warning issued from the FDA of an increased mortality after use of 3 or more tubes of Regranex® gel. This warning was aimed at patients with a history of malignancy and questions whether the potential beneficial response outweighs the risk (Lacci & Dardik 2010; FDA). Despite the wide array of treatment options for chronic wounds described in Section 1.5.2.1, these are not adequate enough to ease the rising burden of chronic wounds (Fang & Galiano 2008; Dumville et al. 2015; Harding 2015). Therefore, alternative options are required to ease this clinical burden and resolve wounds quicker with successful re-epithelialisation and dermal remodelling (Niezgoda et al. 2005; Dumville et al. 2015; Harding 2015).

Due to the previous palliative veterinary studies performed by QBiotics Ltd., we are aware that the treatment of previously unresponsive veterinary chronic wounds with EBC-46 results in rapid wound closure with exceptional cosmesis (Reddell et al. 2014). Rapid re-epithelialisation responses are a recognised feature of preferential healing in tissues, such as early-gestational foetal healing and oral mucosal healing (Coolen et al. 2010; Turabelidze et al. 2014). The rapid re-epithelialisation seen in oral mucosal wounds appears to be partly a result of increased keratinocyte proliferation (Chen et al. 2010; Turabelidze et al. 2014). Studies have shown that there are a number of differentially regulated genes between dermal keratinocytes and oral keratinocytes. In addition, there is a different presence of keratins, with keratins 8 and 19 present in the foetal epidermal layer, but absent in adult epidermal layers (Coolen et al. 2010; Turabelidze et al. 2014). Some of these gene changes may result in this exceptional healing response, with genes upregulated leading to enhanced keratinocyte proliferation and migration in oral mucosal wounds (Colwell et al. 2008; Turabelidze et al. 2014). This shows that despite similarities in the wound healing processes of these tissues, the preferential benefits are a result of core changes in gene expression on crucial functions of the cells, such as keratinocyte migration (Turabelidze et al. 2014).

4.2 Aims

Keratinocytes are another key cell type involved in acute skin wound healing, where they perform the essential role of re-forming the epidermal barrier to close the wound site, thereby protecting against infection. As with dermal fibroblasts (Chapter 3), any alterations in the genotypic or phenotypic responses of the keratinocytes could alter their mechanisms of action and healing outcomes. Therefore, the aims of this chapter were to assess the effects of EBC-46 or EBC-211 on key keratinocyte wound healing responses, such as viability, proliferation, cell cycle progression, morphology and migration. HaCaTs were used instead of primary keratinocytes, as this immortalised cell line has been widely used to assess epidermal responses, due to their close similarity of functional response to normal adult epidermal keratinocytes (Boukamp et al. 1988; Pessina et al. 2001; Wilson 2014).

4.3 Materials and Methods

4.3.1 Preparation of EBC-46 and EBC-211

EBC-46 and the lesser active analogue, EBC-211, were both supplied by QBiotics Ltd., Queensland, Australia. EBC-46 and EBC-211 were solubilised in DMSO (Section 2.1). For both compounds, concentrations of 0.001µg/ml, 0.01µg/ml, 0.1µg/ml, 1µg/ml, 10µg/ml and 100µg/ml were prepared in 1% K-SCM for the assessment of epidermal keratinocyte wound healing responses (Section 2.2.2).

4.3.2 HaCaT Culture

Epidermal keratinocyte cell line (HaCaTs) were sourced, cultured, sub-cultured, counted, cryopreserved and screened for mycoplasma, as previously described (Sections 2.2.2, 2.2.3, 2.2.4 and 2.2.5, respectively).

4.3.3 Assessment of HaCaT Viability and Proliferation

The viability and proliferation of keratinocyte cell line (HaCaTs) was assessed through the use of an MTT [3-(4,5-dimethyl-2-thiazolyl)-2,5-diphenyltetrazolium bromide] Dye-Reduction assay at 24h, 72h, 120h and 168h, as previously described (Section 2.3.1).

4.3.4 Assessment of HaCaT Cell Cycling

Keratinocyte cell line (HaCaTs) were seeded and cultured for cell cycle analysis, with samples obtained at T0, T9, T17, T26, T32, T40 and T48 after treatment with EBC-46 or EBC-211 (0µg/ml, 0.001µg/ml, 0.01µg/ml, 0.1µg/ml, 1µg/ml and 10µg/ml). Samples were prepared, Draq5 DNA dye added and analysed by Flow Cytometry (FACScalibur, Becton Dickinson, Oxfordshire, U.K.), as previously discussed (Sections 2.3.2.2, 2.3.2.3 and 2.3.2.4).

4.3.5 Assessment of HaCaT Morphology

Morphology of keratinocyte cell line (HaCaTs) was assessed by light microscopy, as previously described (Section 2.3.3).

4.3.6 Assessment of HaCaT Repopulation

Keratinocyte cell line (HaCaTs) migration was assessed through the use of an *in vitro* 'scratch wound' assay, with images captured every 20min over 48h using Time-Lapse Microscopy, as previously described (Section 2.3.4).

4.3.7 Assessment of HaCaT Migration in Presence of Mitomycin C

HaCaTs were cultured in the presence of mitomycin C (1µg/ml) and migration assessed by *in vitro* 'scratch wound' assay, with images captured every 20min over 48h using Time-Lapse Microscopy, as previously described (Sections 2.3.4.1 and 2.3.4.2).

4.4 Results

4.4.1 Effects of EBC-46 and EBC-211 on HaCaT Viability and Proliferation

The viability and proliferation study was performed on HaCaTs cultured in EBC-46 or EBC-211 (0.001µg/ml, 0.01µg/ml, 0.1µg/ml, 1µg/ml, 10µg/ml and 100µg/ml), with untreated controls included for comparison purposes (0µg/ml) for both compounds. Average absorbance values were obtained at each EBC-46 and EBC-211 concentration at 24h, 72h, 120h and 168h. Values were used to calculate the variation from the untreated control for each concentration and time-point; and percentage calculations produced versus each untreated control (Figures 4.1A and 4.2A).

As with the fibroblast studies (Chapter 3), it was shown that EBC-46 and the lesser active analogue, EBC-211, were both cytotoxic at 100µg/ml from 24h onwards (Figures 4.1 and 4.2, respectively). This was evident by the significantly decreased percentage data obtained ($p<0.001$; Figures 4.1A and 4.2A, respectively), compared to the untreated controls (0µg/ml). However, the delayed cytotoxic effect of EBC-211, compared to EBC-46, confirmed the reduced activity of EBC-211. This was evident by the longer time period required for a complete cytotoxic effect to occur.

There was a stimulated proliferative response evident across the remaining concentrations of both EBC-46 and EBC-211 (0.001-10µg/ml). However, at 24h, any increases were deemed to be non-significant, compared to untreated controls ($p>0.05$).

Figure 4.1: (A) HaCaT viability and proliferation percentage differences following culture in the presence of EBC-46 (0µg/ml, 0.001µg/ml, 0.01µg/ml, 0.1µg/ml, 1µg/ml, 10µg/ml and 100µg/ml), at 24h, 72h, 120h and 168h (*N=3, average±SE*). (B) Cross-statistical analysis of significant changes in HaCaT proliferation following treatment with EBC-46 (0.001-100µg/ml) over 168h, versus untreated controls (p<0.05, **p<0.01, ***p<0.001*).**

A

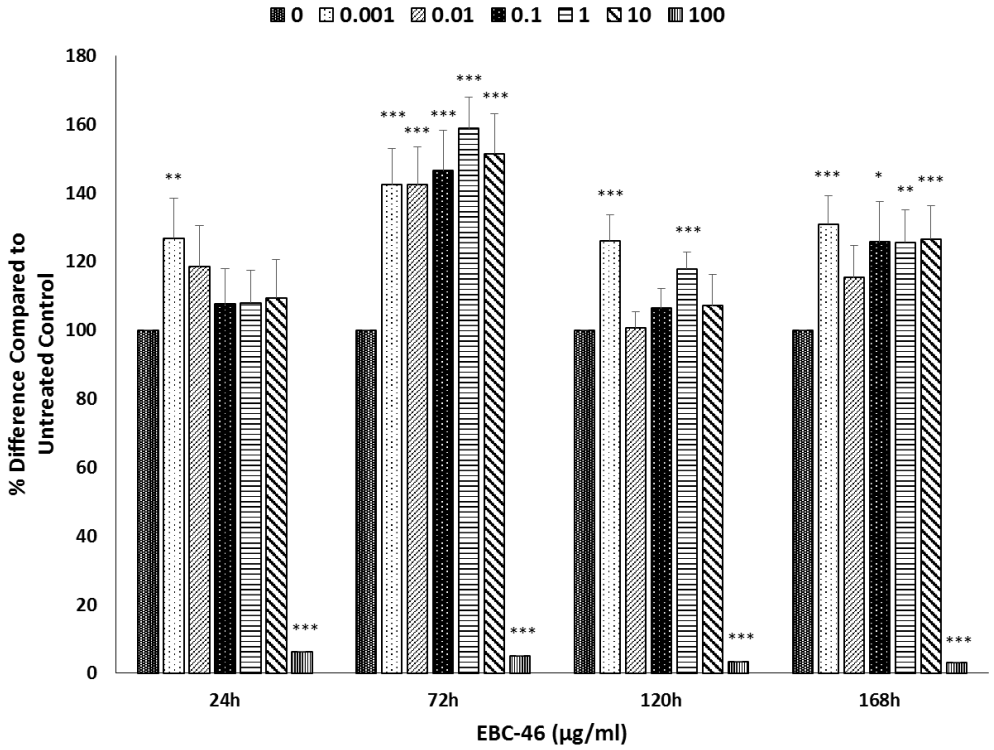

B

24h

	0	0.001	0.01	0.1	1	10	100
0		**					***
0.001						*	***
0.01							***
0.1							***
1							***
10							***
100							

72h

	0	0.001	0.01	0.1	1	10	100
0		***	***	***	***	***	***
0.001							***
0.01							***
0.1							***
1							***
10							***
100							

120h

	0	0.001	0.01	0.1	1	10	100
0		***			***		***
0.001			***	**		**	***
0.01					***		***
0.1							***
1							***
10							***
100							

168h

	0	0.001	0.01	0.1	1	10	100
0		***		*	**	***	***
0.001							***
0.01							***
0.1							***
1							***
10							***
100							

Figure 4.2: (A) HaCaT viability and proliferation percentage differences, following culture in the presence of EBC-211 (0µg/ml, 0.001µg/ml, 0.01µg/ml, 0.1µg/ml, 1µg/ml, 10µg/ml and 100µg/ml), at 24h, 72h, 120h and 168h (*N=3, average±SE*). (B) Cross-statistical analysis of significant changes in HaCaT proliferation following treatment with EBC-211 (0.001-100µg/ml) over 168h, versus untreated controls (p<0.05, **p<0.01, ***p<0.001*).**

A

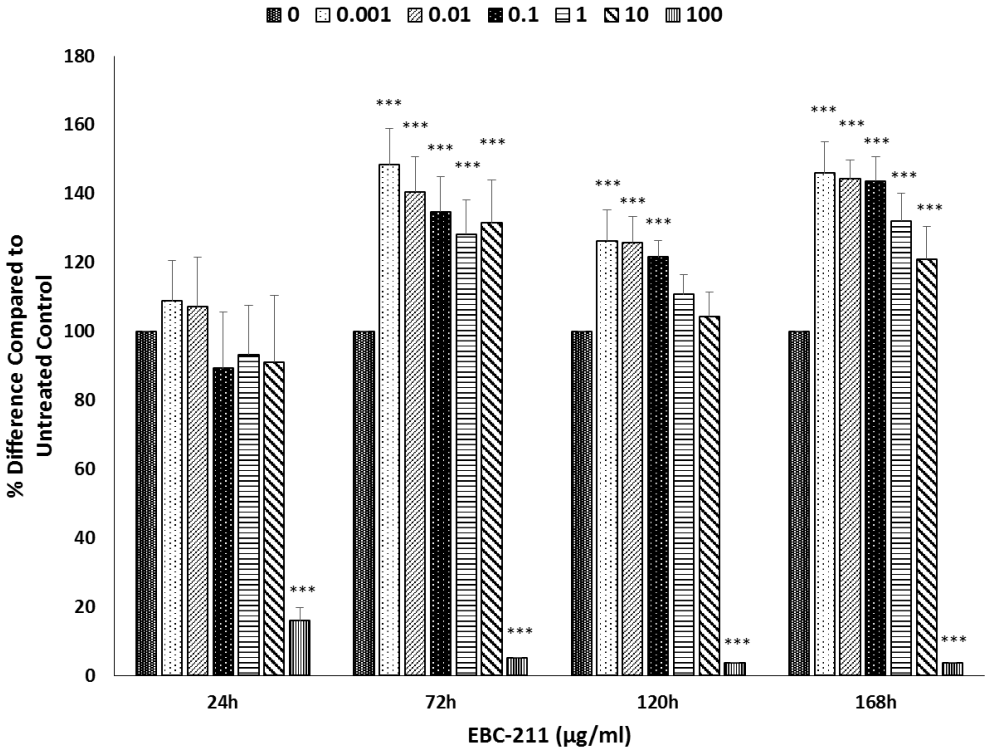

B

24h

	0	0.001	0.01	0.1	1	10	100
0							***
0.001							***
0.01							***
0.1							***
1							***
10							***
100							

72h

	0	0.001	0.01	0.1	1	10	100
0		***	***	***	***	***	***
0.001					*		***
0.01							***
0.1							***
1							***
10							***
100							

120h

	0	0.001	0.01	0.1	1	10	100
0		***	***	***			***
0.001					**	***	***
0.01					*	***	***
0.1						**	***
1							***
10							***
100							

168h

	0	0.001	0.01	0.1	1	10	100
0		***	***	***	***	***	***
0.001						***	***
0.01						***	***
0.1						***	***
1							***
10							***
100							

The only exception was 0.001µg/ml EBC-46, where a significant increase in proliferation was observed ($p<0.01$; Figure 4.1A). At 72h, the most profound proliferative responses were observed across all EBC-46 and EBC-211 concentrations (0.001-10µg/ml; $p<0.001$; Figures 4.1A and 4.2A, respectively). Increased proliferation was also observed at 120h and 168h for EBC-46, although this was not considered to be as significant as the responses seen at 72h ($p<0.001$-0.05; Figure 4.1A). EBC-211 also showed an increase in proliferation across the concentrations (0.001-10µg/ml) at 120h and 168h. This was deemed significant for 0.001-0.1µg/ml EBC-211 at 120h and 0.001-10µg/ml at 168h (Figure 4.2A; $p<0.001$). The continual increase in the absorbance values for EBC-211 at each subsequent time-point, showed a consistent increase in proliferation.

As the greatest increase in cell proliferation for EBC-46 treated cells occurred at 72h, there was a possibility that the cells were fully confluent by this time-point and therefore, unable to proliferate to the same extent beyond this time-point. The proliferation study was repeated with a lower cell density to account for this observation; however, the greatest increase in cell proliferation occurred again at 72h (Supplement 4.1). This leads to the theory that there may be a profound proliferative burst occurring between 24h and 72h, to produce the significant increase in HaCaT proliferative response at 72h. Cross statistical analysis was performed for both EBC-46 and EBC-211 (0.001-100µg/ml), comparing epoxy-tigliane treated cells to untreated controls. In addition, comparisons were made between concentrations for both EBC-46 and EBC-211. Cross-statistical analysis between EBC-46 concentrations only showed a few conditions that were considered significant, including between 0.001µg/ml and 10µg/ml at 24h and 120h; also between 0.01-0.1µg/ml and 10µg/ml, along with 0.01µg/ml and 1µg/ml at 120h ($p<0.001$-0.05; Figure 4.1B). EBC-211 cross-statistical analysis showed significant between 0.001-0.1µg/ml and 10µg/ml at 120h and 168h; in addition, to between 0.001-0.01µg/ml and 1µg/ml at 120h, and 0.001µg/ml and 1µg/ml at 168h ($p<0.001$-0.05; Figure 4.2B).

4.4.2 Effects of EBC-46 and EBC-211 on HaCaT Cell Cycling

In light of the potential pro-proliferative effects identified in Section 4.4.1, flow cytometry was further performed to determine whether treatment with EBC-46 or

EBC-211 (0.001-10µg/ml) had an effect on HaCaT cell cycle progression and whether this contributed to the profound stimulatory effects observed. A growth curve was initially performed to calculate the cycling time for an untreated control (Supplement 4.2). This determined the time-points required to observe the different phases of the cell cycle for the untreated HaCaT controls. The time-points identified were T0 (at point of treatment), T9 (9h after treatment), T17 (17h after treatment), T26 (26h after treatment), T32 (32h after treatment), T40 (40h after treatment) and T48 (48h after treatment). The T0 time-point was analysed at point of treatment to ensure cells across all conditions were at the same synchronised state after serum starvation; and any differences that follow at the later time-points are a result of the epoxy-tigliane treatment. Data obtained at T0 for both EBC-46 and EBC-211 showed no significant differences, compared to untreated control. This confirmed that the cells were all synchronised to the same cell cycle phase before analysis of the later time-points to determine significant changes in cell cycle progression ($p>0.05$; Figures 4.3A and 4.10A).

There was no significant difference between EBC-46-treated cells and the untreated controls at T0 and T9 ($p>0.05$; Figures 4.3A and 4.4A, respectively), although there were indications that the cells were progressing through the cycle at a quicker rate. This was observed by following the progression of the cell populations through the cell cycle phases at each time-point. The rapid transition from G1 at T17 to G2 phase at T26, through S phase, was evident ($p<0.01$-0.05; Figures 4.5A and 4.6A). This led to the possibility that either the G1 to S or S to G2 transitions, or both, were stimulated by epoxy-tigliane treatments. At T17, T26, T32 and T40, an increase in cell cycle progression, compared to untreated controls, was evident across all EBC-46 concentrations (0.001-10µg/ml). These were deemed significant at each of these time-points ($p<0.01$-0.05; Figures 4.5A, 4.6A, 4.7A and 4.8A). The most profound differences were observed at T40, where the acceleration through the cell cycle caused significant differences across all phases ($p<0.01$-0.05; Figure 4.8A). At this time-point, untreated controls predominantly remained in G1 phase, compared to EBC-46-treated cells, which had progressed through S phase and into the G2 phase. This corroborated the previous proliferation data (Section 4.4.1), where the burst of proliferation appeared to occur between 24h and 72h, to produce the dramatic increase in cell

Figure 4.3: (A) HaCaT cell cycle analysis at T0, following culture in the presence of EBC-46 (0.001µg/ml, 0.01µg/ml, 0.1µg/ml, 1µg/ml and 10µg/ml), compared to untreated controls (0µg/ml) (*N=3, average % in each phase±SE*). Statistical analysis (*all p>0.05*). (B) Corresponding cell cycle histogram at T0, following culture in the presence of EBC-46 (0-10µg/ml).

A

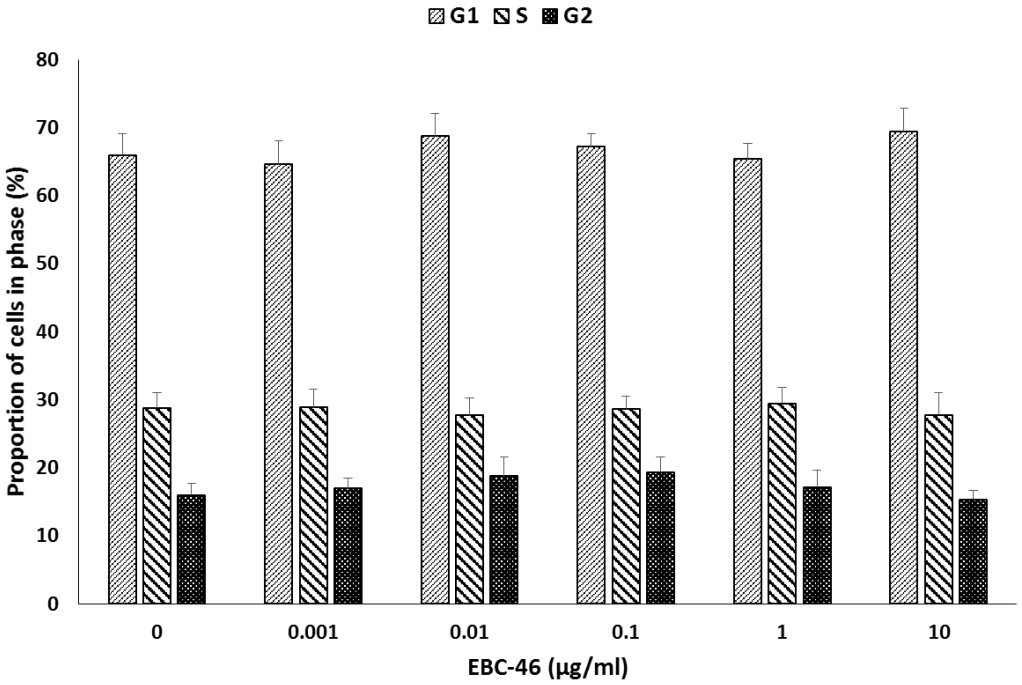

B

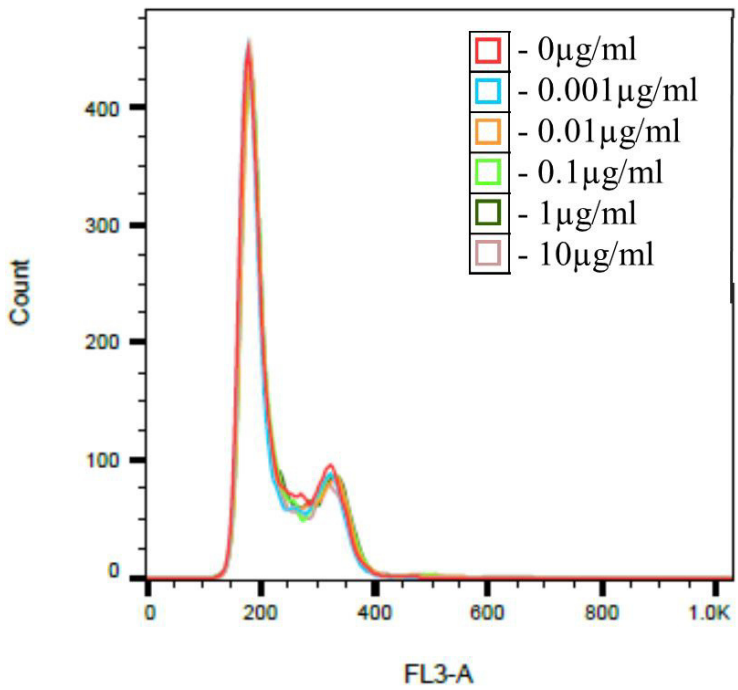

Figure 4.4: (A) HaCaT cell cycle analysis at T9, following culture in the presence of EBC-46 (0.001µg/ml, 0.01µg/ml, 0.1µg/ml, 1µg/ml and 10µg/ml), compared to untreated controls (0µg/ml) (*N=3, average % in each phase±SE*). Statistical analysis (*all p>0.05*). (B) Corresponding cell cycle histogram at T9, following culture in the presence of EBC-46 (0-10µg/ml).

A

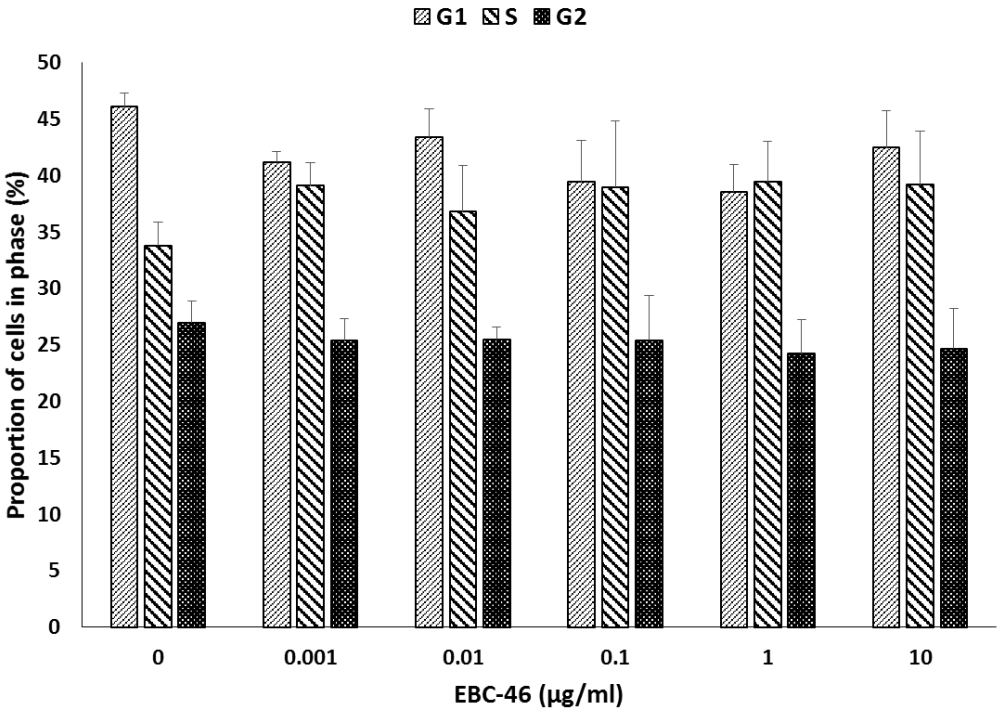

B

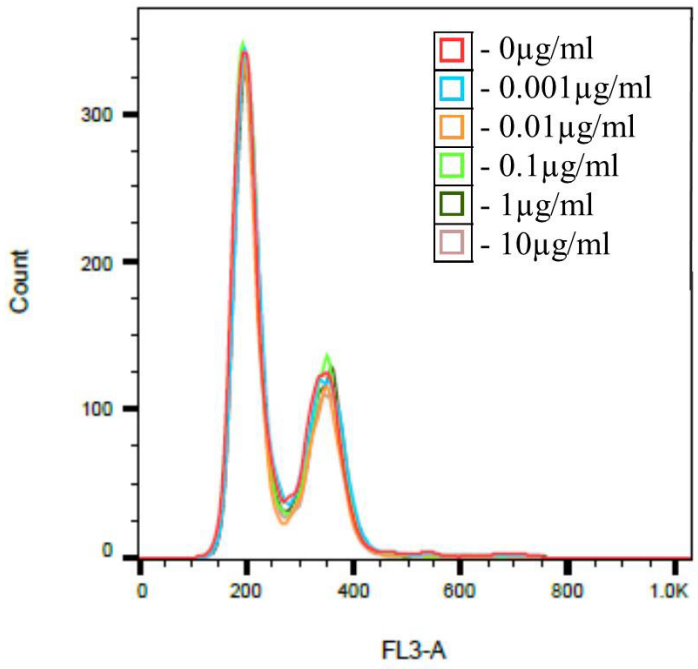

Figure 4.5: (A) HaCaT cell cycle analysis at T17, following culture in the presence of EBC-46 (0.001µg/ml, 0.01µg/ml, 0.1µg/ml, 1µg/ml and 10µg/ml), compared to untreated controls (0µg/ml) (*N=3, average % in each phase±SE*). Statistical analysis (p<0.05, **p<0.01*). (B) Corresponding cell cycle histogram at T17, following culture in the presence of EBC-46 (0-10µg/ml).**

A

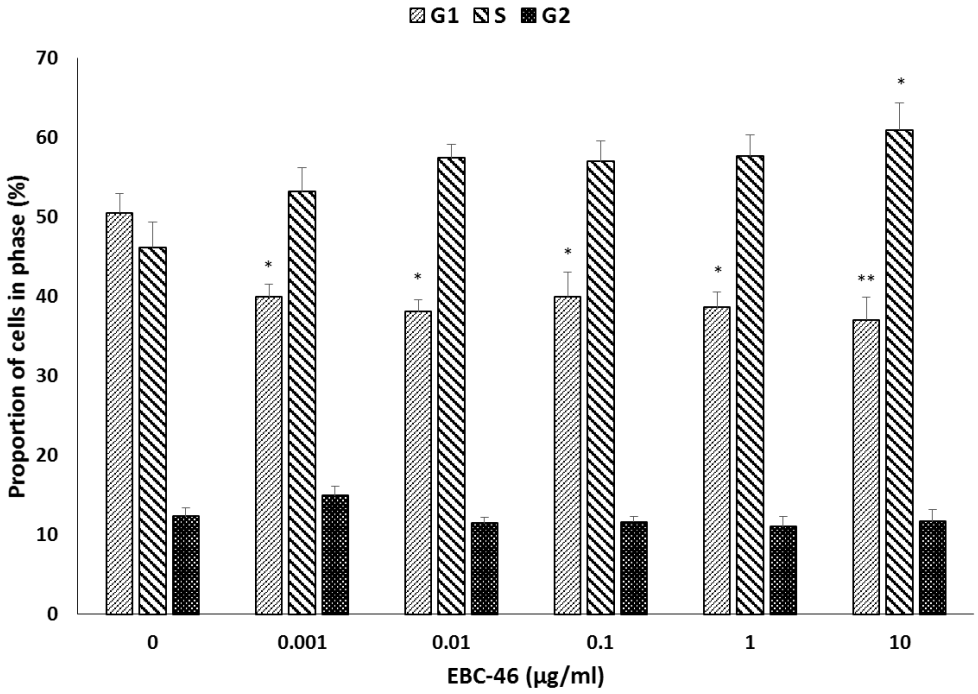

B

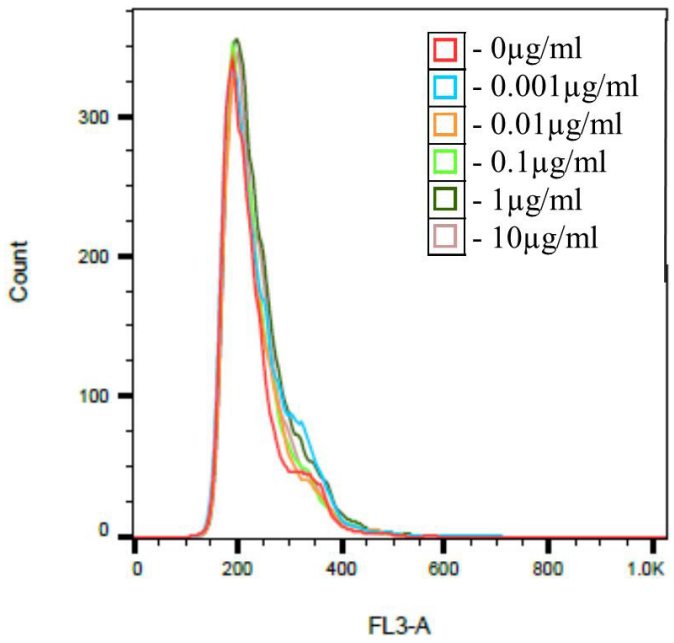

Figure 4.6: (A) HaCaT cell cycle analysis at T26, following culture in the presence of EBC-46 (0.001µg/ml, 0.01µg/ml, 0.1µg/ml, 1µg/ml and 10µg/ml), compared to untreated controls (0µg/ml) (*N=3, average % in each phase±SE*). Statistical analysis (p<0.05, **p<0.01*). (B) Corresponding cell cycle histogram at T26, following culture in the presence of EBC-46 (0-10µg/ml).**

A

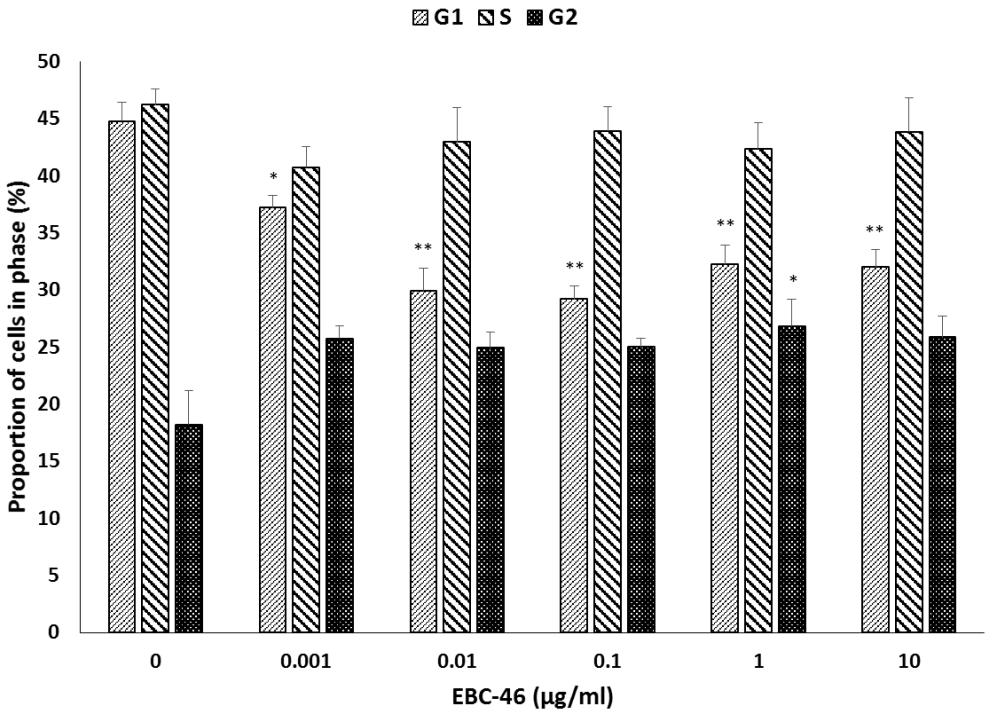

B

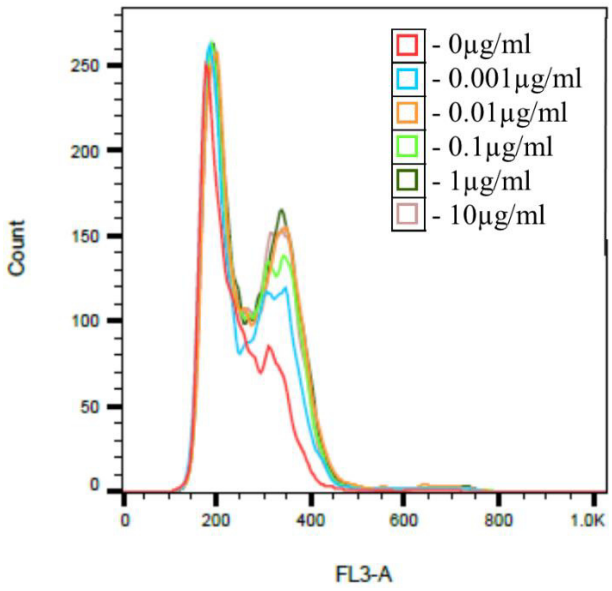

Figure 4.7: (A) HaCaT cell cycle analysis at T32, following culture in the presence of EBC-46 (0.001µg/ml, 0.01µg/ml, 0.1µg/ml, 1µg/ml and 10µg/ml), compared to untreated controls (0µg/ml) (*N=3, average % in each phase±SE*). Statistical analysis (p<0.05, **p<0.01*). (B) Corresponding cell cycle histogram at T32, following culture in the presence of EBC-46 (0-10µg/ml).**

A

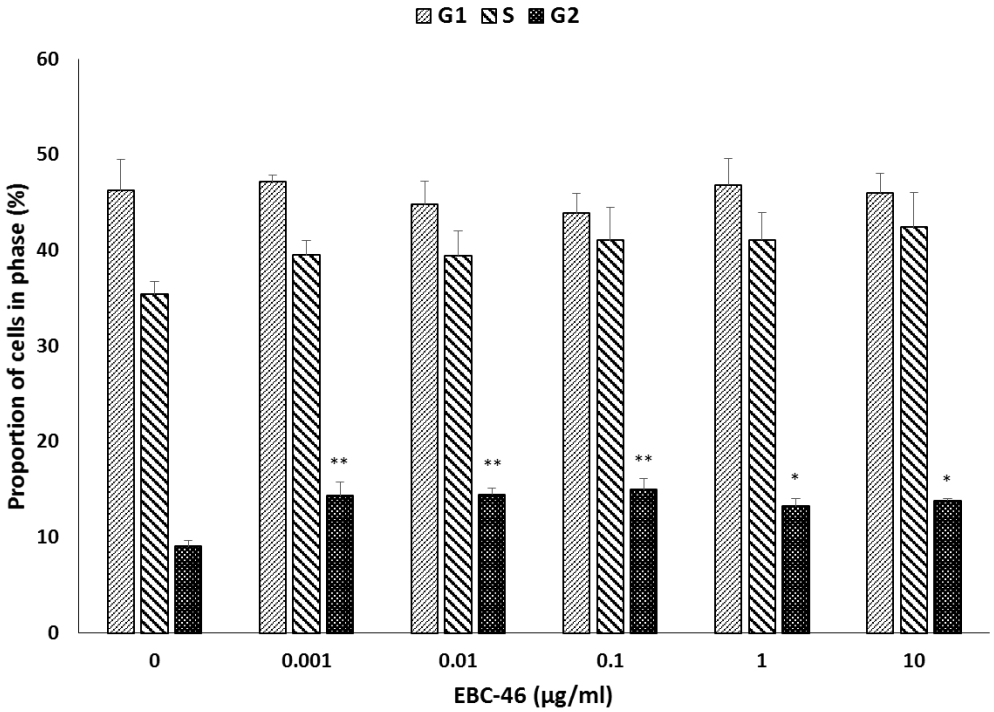

B

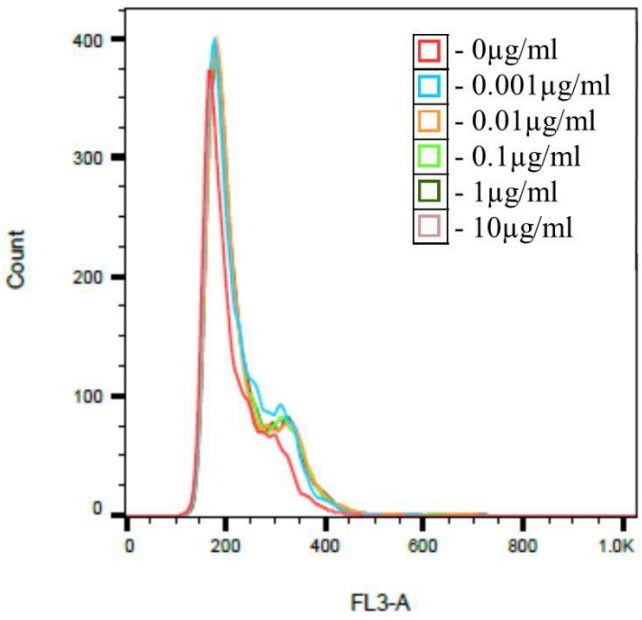

Figure 4.8: (A) HaCaT cell cycle analysis at T40, following culture in the presence of EBC-46 (0.001µg/ml, 0.01µg/ml, 0.1µg/ml, 1µg/ml and 10µg/ml), compared to untreated controls (0µg/ml) (*N=3, average % in each phase±SE*). Statistical analysis (p<0.05, **p<0.01*). (B) Corresponding cell cycle histogram at T40, following culture in the presence of EBC-46 (0-10µg/ml).**

A

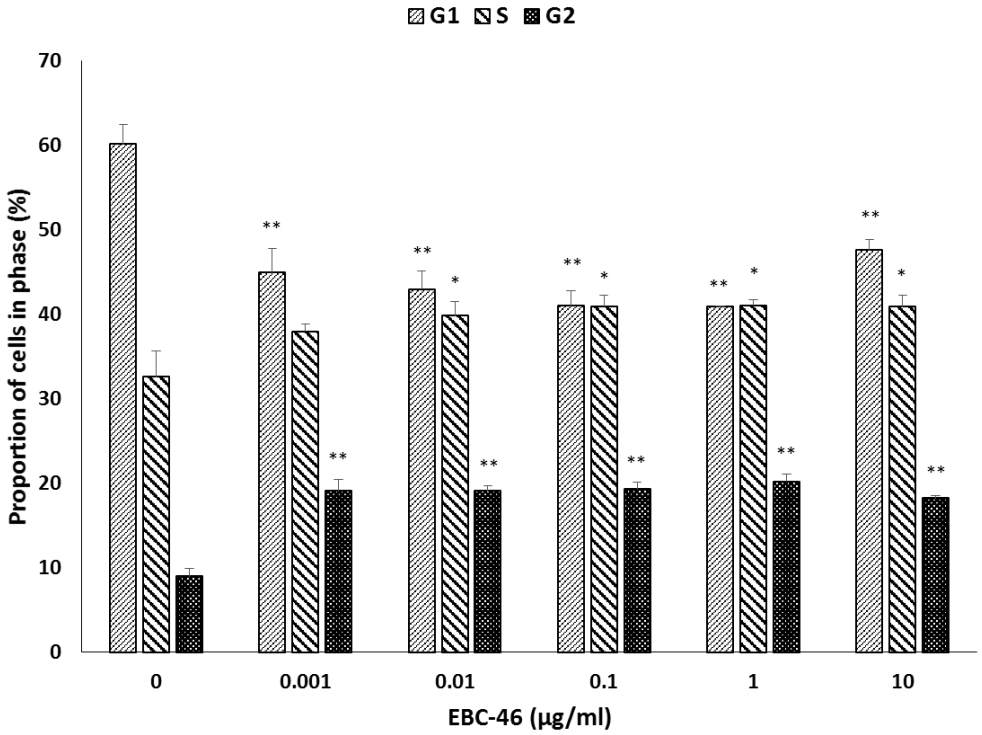

B

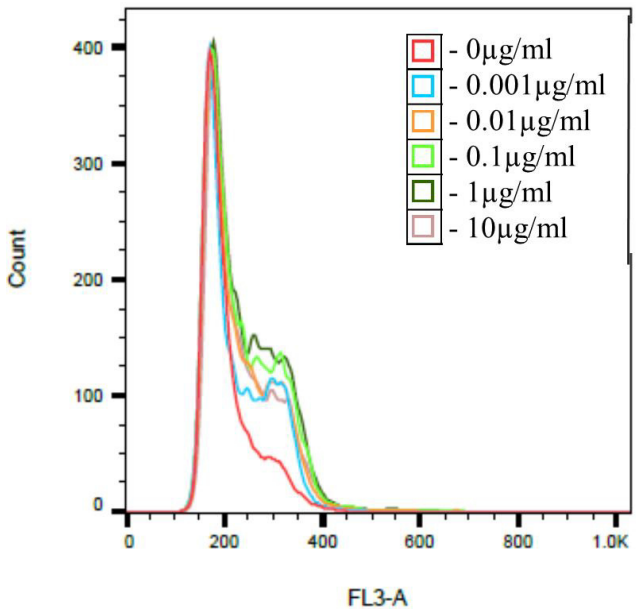

Figure 4.9: (A) HaCaT cell cycle analysis at T48, following culture in the presence of EBC-46 (0.001µg/ml, 0.01µg/ml, 0.1µg/ml, 1µg/ml and 10µg/ml), compared to untreated controls (0µg/ml) (*N=3, average % in each phase±SE*). Statistical analysis (p<0.05*). (B) Corresponding cell cycle histogram at T48, following culture in the presence of EBC-46 (0-10µg/ml).**

A

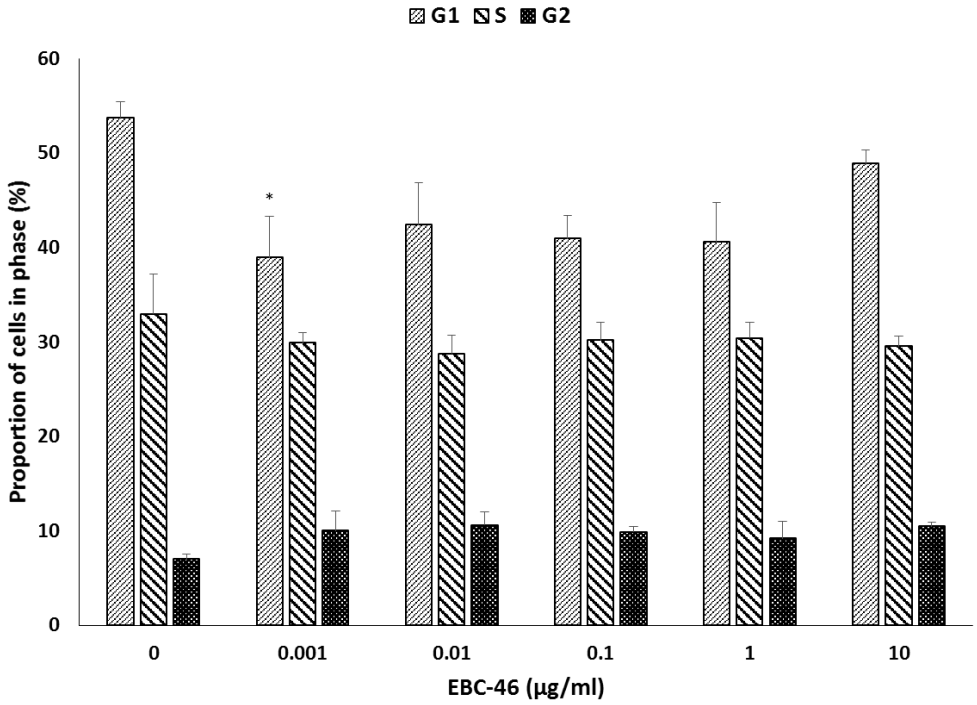

B

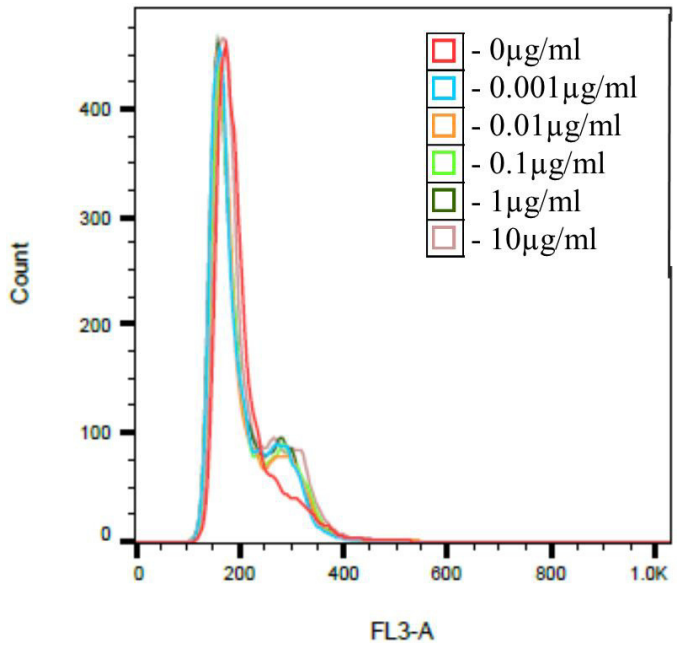

number at 72h (Figure 4.1A). The accompanying cell cycle histograms (Figures 4.3B, 4.4B, 4.5B, 4.6B, 4.7B, 4.8B and 4.9B) further show these dramatic and significant differences in cell distribution throughout the phases of the cell cycle, particularly at T26 and T40 (Figures 4.6B and 4.8B, respectively). There was also only a marginal increase in cell cycle progression at T48, although this was deemed to be significant, with 0.001µg/ml EBC-46 in G1 phase ($p<0.05$; Figure 4.9A). It is thought that due to the different lengths of cell cycle phases, with G1 being the longest and G2/M the shortest, the cells appear to catch up to the same cell cycle phase, G1, by T48; although the accompanying cell cycle histogram shows a proportion of cells treated with EBC-46 remaining in G2 phase, with the untreated controls present in G1 phase (Figure 4.9B).

EBC-211-treated cells showed similar effects to EBC-46, with increased cell cycle progression, compared to untreated controls (Figures 4.10A, 4.11A, 4.12A, 4.13A, 4.14A, 4.15A and 4.16A). There were no significant differences observed at T0, T9 or T17, although as before, there was evidence that the cells were moving from G1 to S phase at a more rapid rate. However, this was not statistically significant ($p>0.05$; Figures 4.10A, 4.11A and 4.12A, respectively). By T26, this acceleration through the cell cycle was significant across all concentrations of EBC-211 (0.001-10µg/ml; $p<0.01$-0.05; Figure 4.13A). This acceleration continued at T32, T40 and T48 ($p<0.01$-0.05; Figures 4.14A, 4.15A and 4.16A, respectively), potentially due to the lesser activity of EBC-211. There was a greater degree of significant differences obtained to the untreated controls with EBC-211, than EBC-46 at T48, as a result of a slightly less dramatic acceleration through the cell cycle. The corresponding cell cycle histograms (Figures 4.10B, 4.11B, 4.12B, 4.13B, 4.14B, 4.15B and 4.16B) again confirmed the rapid and significant cell cycle progression, compared to untreated controls; which particularly showed the clear differences in cell distribution within the cell cycle phases at T26 and T40 (Figures 4.13B and 4.15B).

Figure 4.10: (A) HaCaT cell cycle analysis at T0, following culture in the presence of EBC-211 (0.001µg/ml, 0.01µg/ml, 0.1µg/ml, 1µg/ml and 10µg/ml), compared to untreated controls (0µg/ml) (*N=3, average % in each phase±SE*). Statistical analysis (*all p>0.05*). (B) Corresponding cell cycle histogram at T0, following culture in the presence of EBC-211 (0-10µg/ml).

A

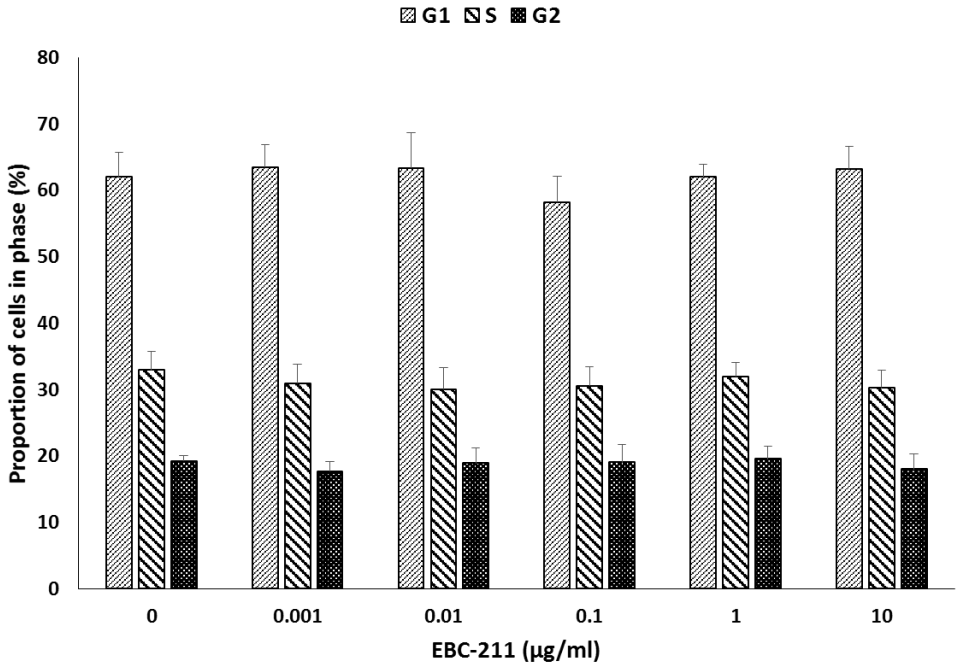

B

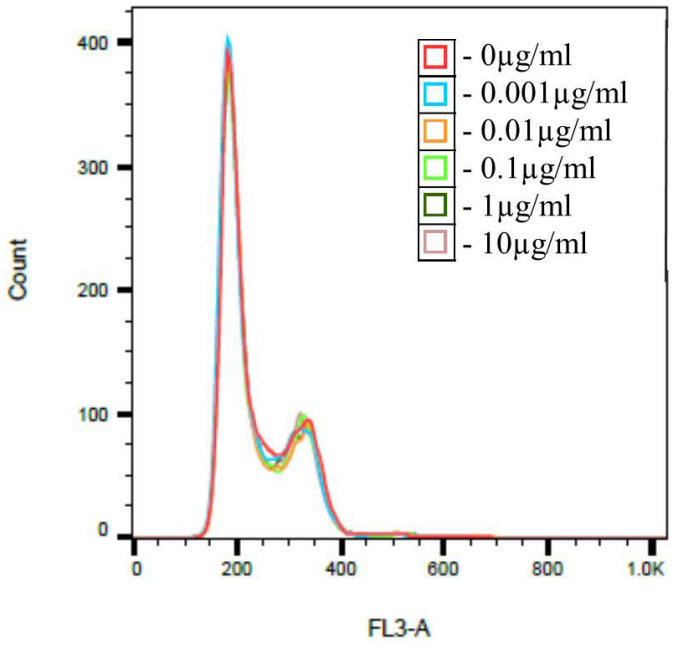

Figure 4.11: (A) HaCaT cell cycle analysis at T9, following culture in the presence of EBC-211 (0.001µg/ml, 0.01µg/ml, 0.1µg/ml, 1µg/ml and 10µg/ml), compared to untreated controls (0µg/ml) (*N=3, average % in each phase±SE*). Statistical analysis (*all p>0.05*). (B) Corresponding cell cycle histogram at T9, following culture in the presence of EBC-211 (0-10µg/ml).

A

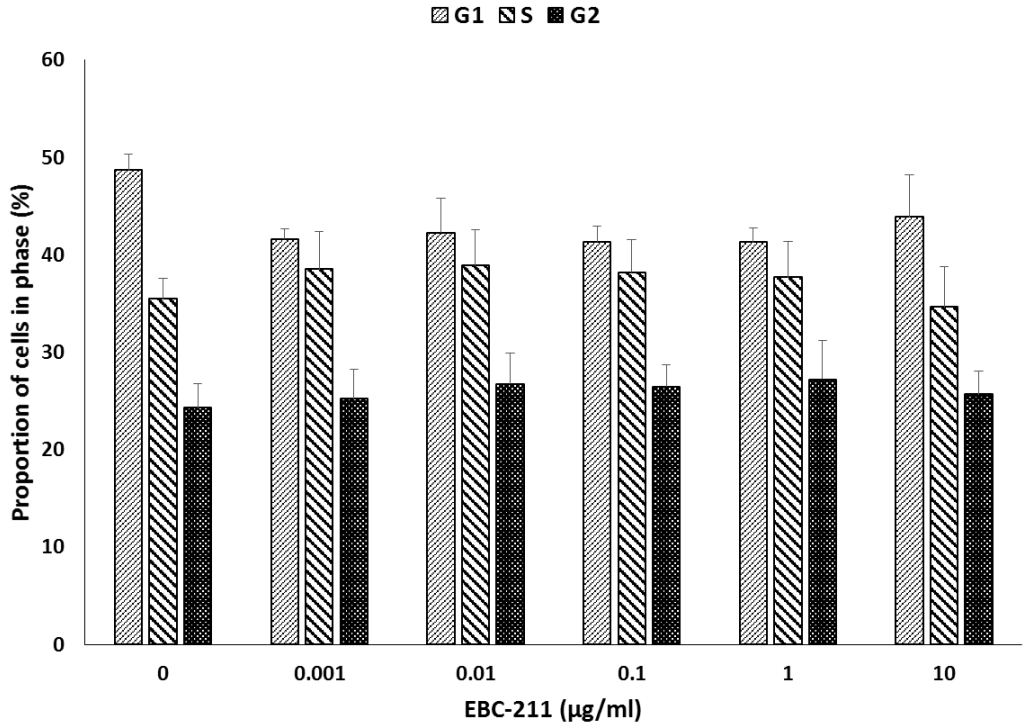

B

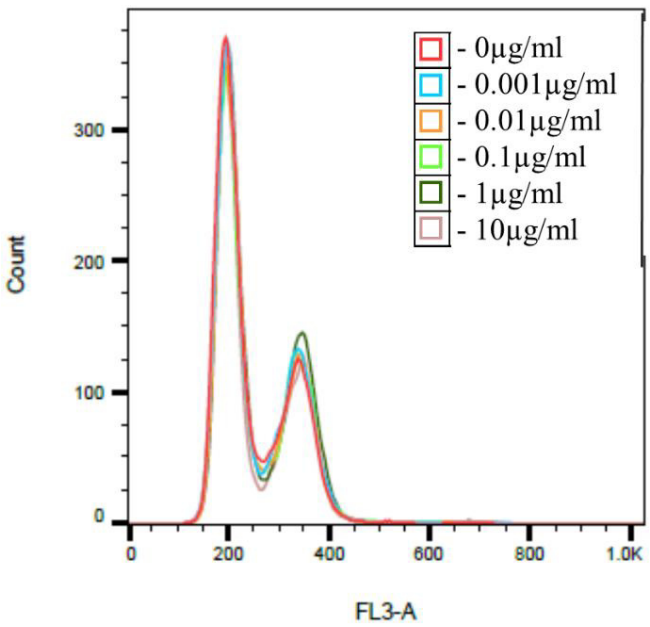

Figure 4.12: (A) HaCaT cell cycle analysis at T17, following culture in the presence of EBC-211 (0.001µg/ml, 0.01µg/ml, 0.1µg/ml, 1µg/ml and 10µg/ml), compared to untreated controls (0µg/ml) (*N=3, average % in each phase±SE*). Statistical analysis (*all p>0.05*). (B) Corresponding cell cycle histogram at T17, following culture in the presence of EBC-211 (0-10µg/ml).

A

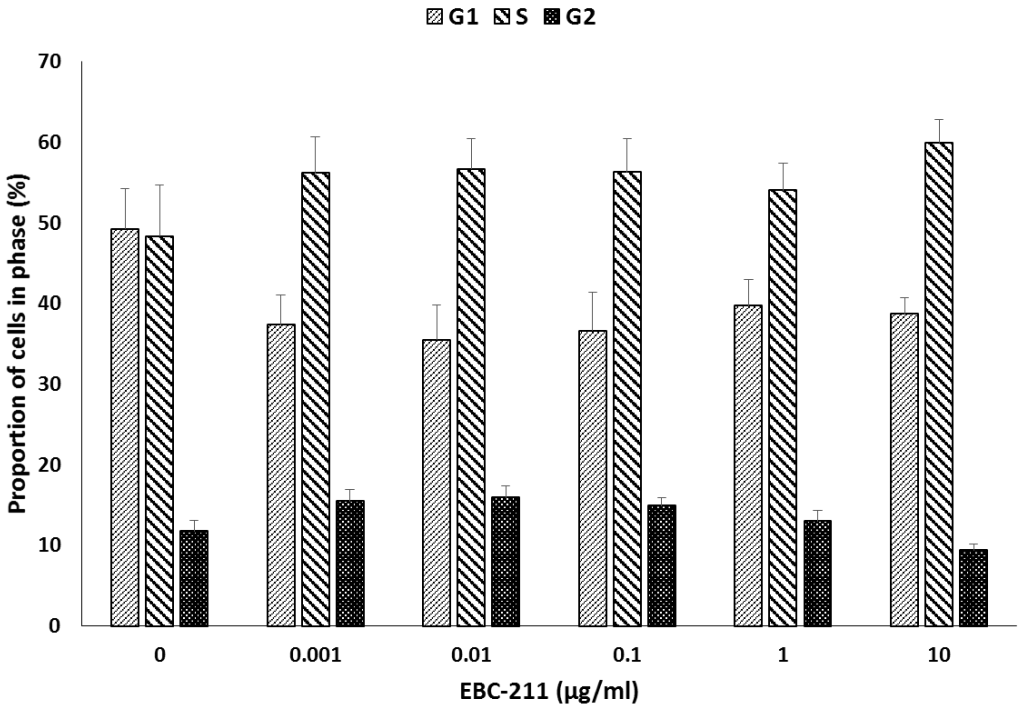

B

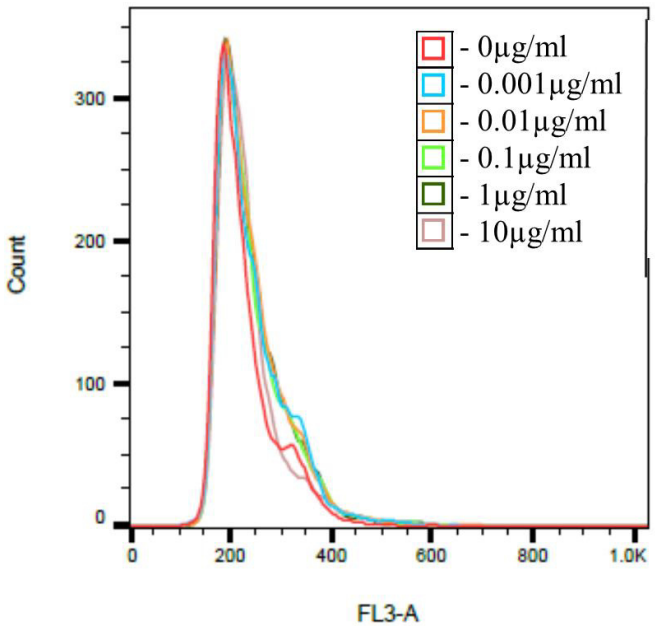

Figure 4.13: (A) HaCaT cell cycle analysis at T26, following culture in the presence of EBC-211 (0.001µg/ml, 0.01µg/ml, 0.1µg/ml, 1µg/ml and 10µg/ml), compared to untreated controls (0µg/ml) (*N=3, average % in each phase±SE*). Statistical analysis (p<0.05, **p<0.01*). (B) Corresponding cell cycle histogram at T26, following culture in the presence of EBC-211 (0-10µg/ml).**

A

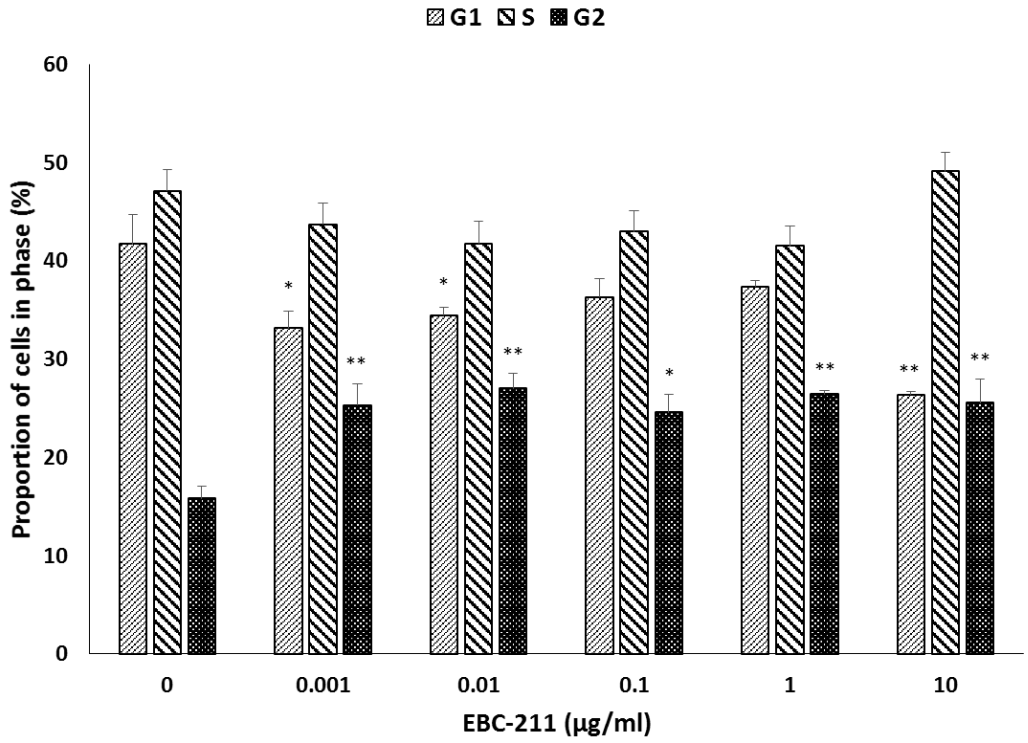

B

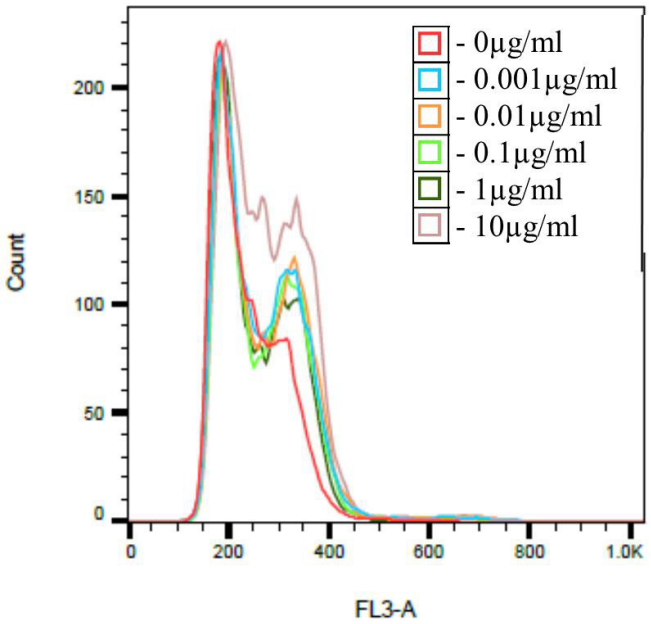

Figure 4.14: (A) HaCaT cell cycle analysis at T32, following culture in the presence of EBC-211 (0.001µg/ml, 0.01µg/ml, 0.1µg/ml, 1µg/ml and 10µg/ml), compared to untreated controls (0µg/ml) (*N=3, average % in each phase±SE*). Statistical analysis (p<0.05, **p<0.01*). (B) Corresponding cell cycle histogram at T32, following culture in the presence of EBC-211 (0-10µg/ml).**

A

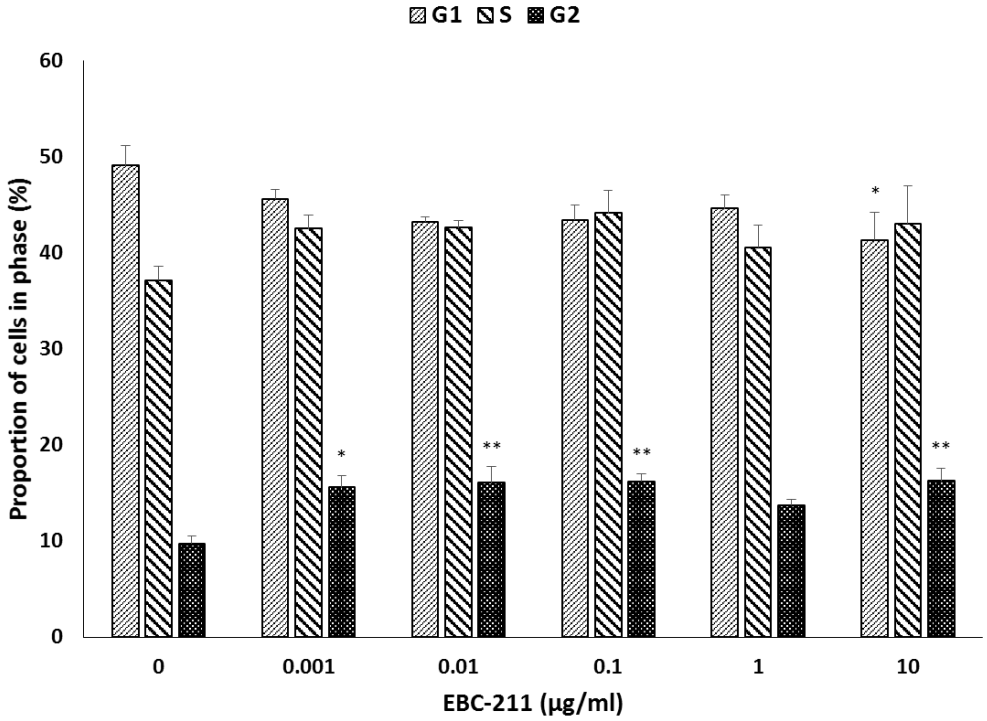

B

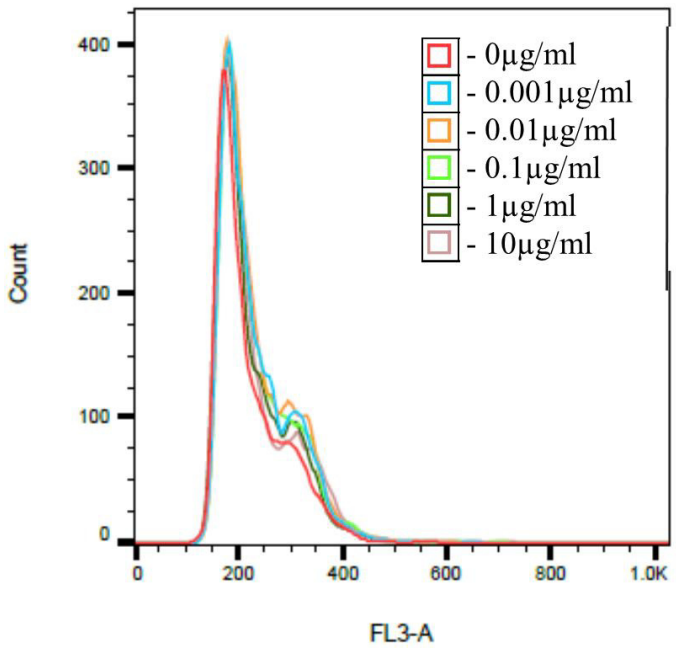

Figure 4.15: (A) HaCaT cell cycle analysis at T40, following culture in the presence of EBC-211 (0.001µg/ml, 0.01µg/ml, 0.1µg/ml, 1µg/ml and 10µg/ml), compared to untreated controls (0µg/ml) (*N=3, average % in each phase±SE*). Statistical analysis (p<0.05, **p<0.01*). (B) Corresponding cell cycle histogram at T40, following culture in the presence of EBC-211 (0-10µg/ml).**

A

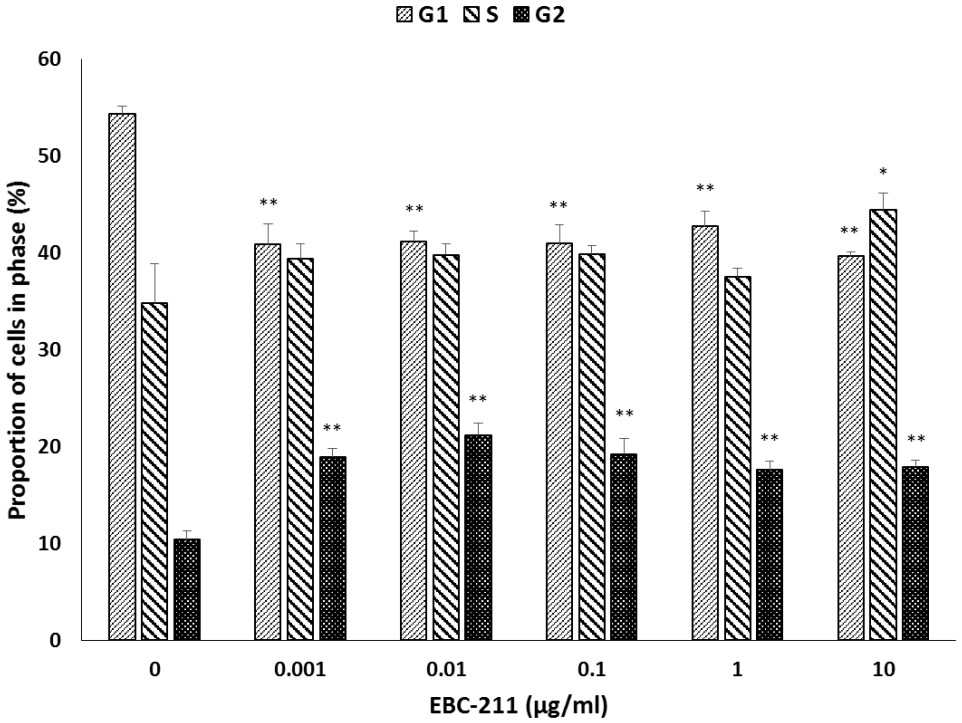

B

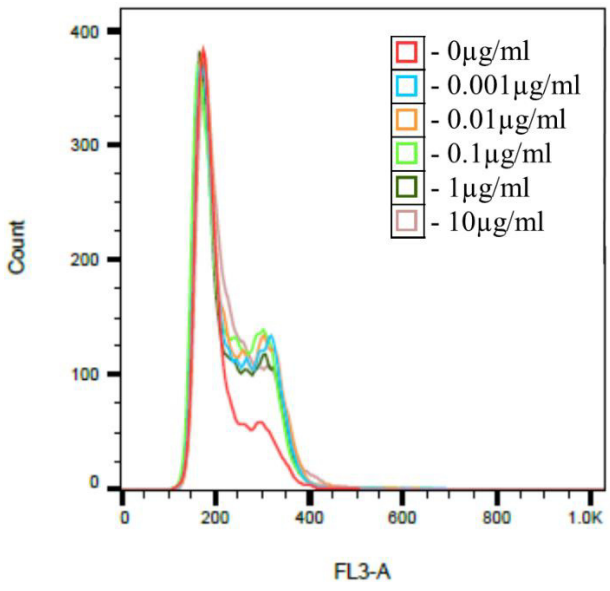

Figure 4.16: (A) HaCaT cell cycle analysis at T48, following culture in the presence of EBC-211 (0.001µg/ml, 0.01µg/ml, 0.1µg/ml, 1µg/ml and 10µg/ml), compared to untreated controls (0µg/ml) (*N=3, average % in each phase±SE*). Statistical analysis (*p<0.01*). (B) Corresponding cell cycle histogram at T48, following culture in the presence of EBC-211 (0-10µg/ml).**

A

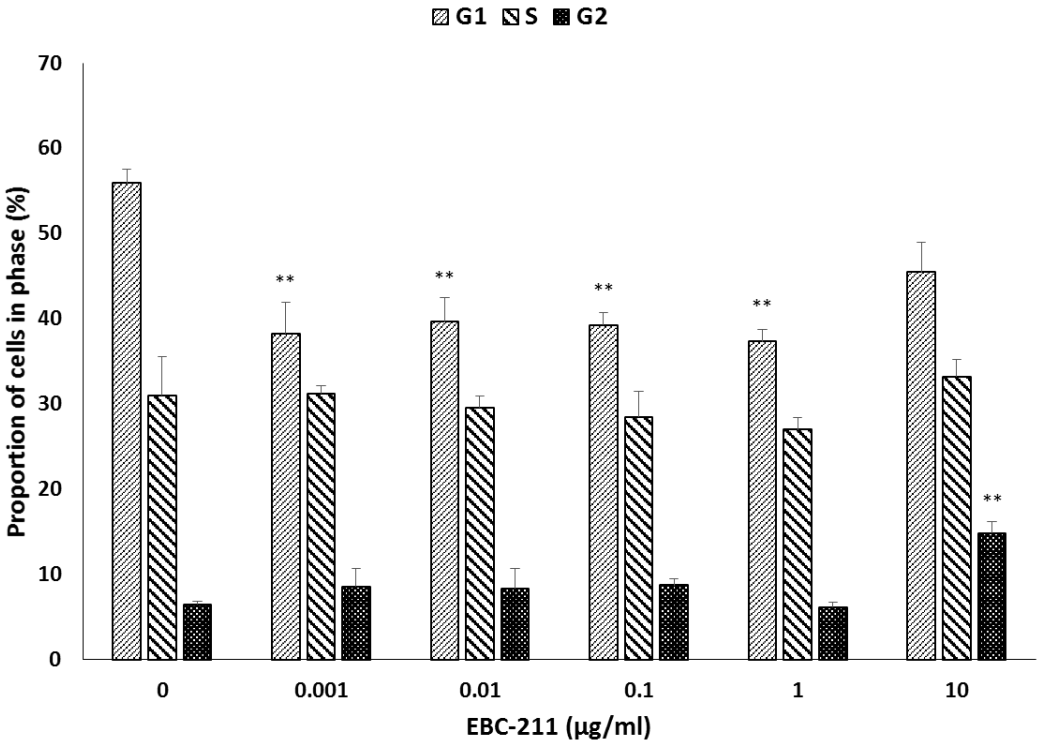

B

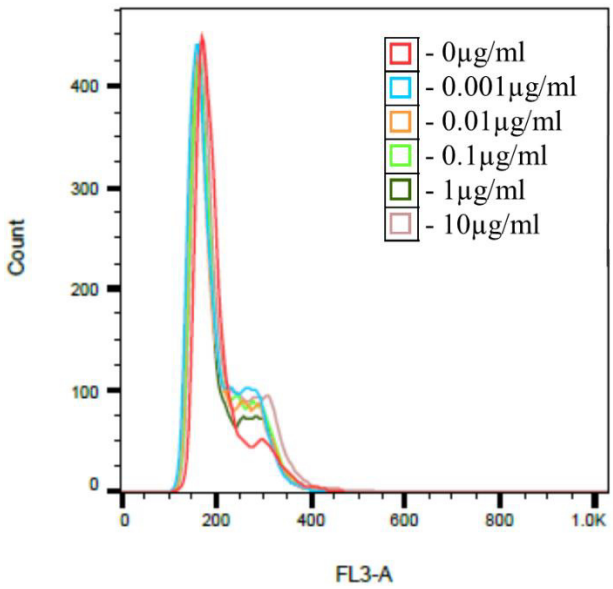

4.4.3 Effects of EBC-46 and EBC-211 on HaCaT Morphology

EBC-46 was shown to be highly cytotoxic to the HaCaTs at 100µg/ml, as shown initially with the proliferation data. This was confirmed through the cellular morphology studies with the potential apoptosis of the HaCaTs. There was a large reduction in the number of HaCaTs present, along with a high content of cell debris at the earlier time-points (Figures 4.17G, 4.18G, 4.19G and 4.20G). The cytotoxicity of EBC-211 at 100µg/ml was also confirmed through the HaCaT morphology studies. However, it also showed a slightly reduced cytotoxic effect than seen with EBC-46, again confirming the lesser activity of EBC-211. At 24h, there was evidence of a few viable cells remaining; whereas at 72h, 120h and 168h, there were no viable cells remaining (Figures 4.21G, 4.22G, 4.23G and 4.24G).

At the other EBC-46 concentrations (0.001-10µg/ml), there were no major differences in morphology or cell number visible at 24h, compared to untreated controls (0µg/ml; Figure 4.17A-F). In contrast, at 72h, 120h and 168h, the profound proliferative effect initially observed from the viability and proliferation studies was confirmed through the cellular morphology studies, by increased presence of cells evident (Figures 4.18, 4.19 and 4.20A-F). However, there did not appear to be any noticeable differences between the EBC-46 concentrations. Unlike the fibroblast studies, no obvious morphological changes in the HaCaTs were evident, with the cells retaining the typical cobble-stone morphology at all concentrations and throughout the entire culture period.

The other concentrations of EBC-211 (0.001-10µg/ml) also showed no obvious differences in morphology or cell number, when compared to untreated controls (0µg/ml) at 24h (Figures 4.21A-F). At 72h, 120h and 168h, the profound proliferation that occurs across the range of EBC-211 concentrations (0.001-10µg/ml) was evident, in comparison to untreated controls (Figures 4.22, 4.23 and 4.24A-F). However, as with EBC-46, there was no noticeable difference in cell numbers between EBC-211 concentrations. Again, there were no obvious morphological changes in the HaCaTs when cultured with EBC-211, as the cells retained their typical cobble-stone structure at all concentrations throughout the culture period.

Figure 4.17: HaCaT morphology, cultured in the presence of (A) 0µg/ml, (B) 0.001µg/ml, (C) 0.01µg/ml, (D) 0.1µg/ml, (E) 1µg/ml, (F) 10µg/ml; and (G) 100µg/ml EBC-46 for 24h (*N=3*). Scale bar = 100µm.

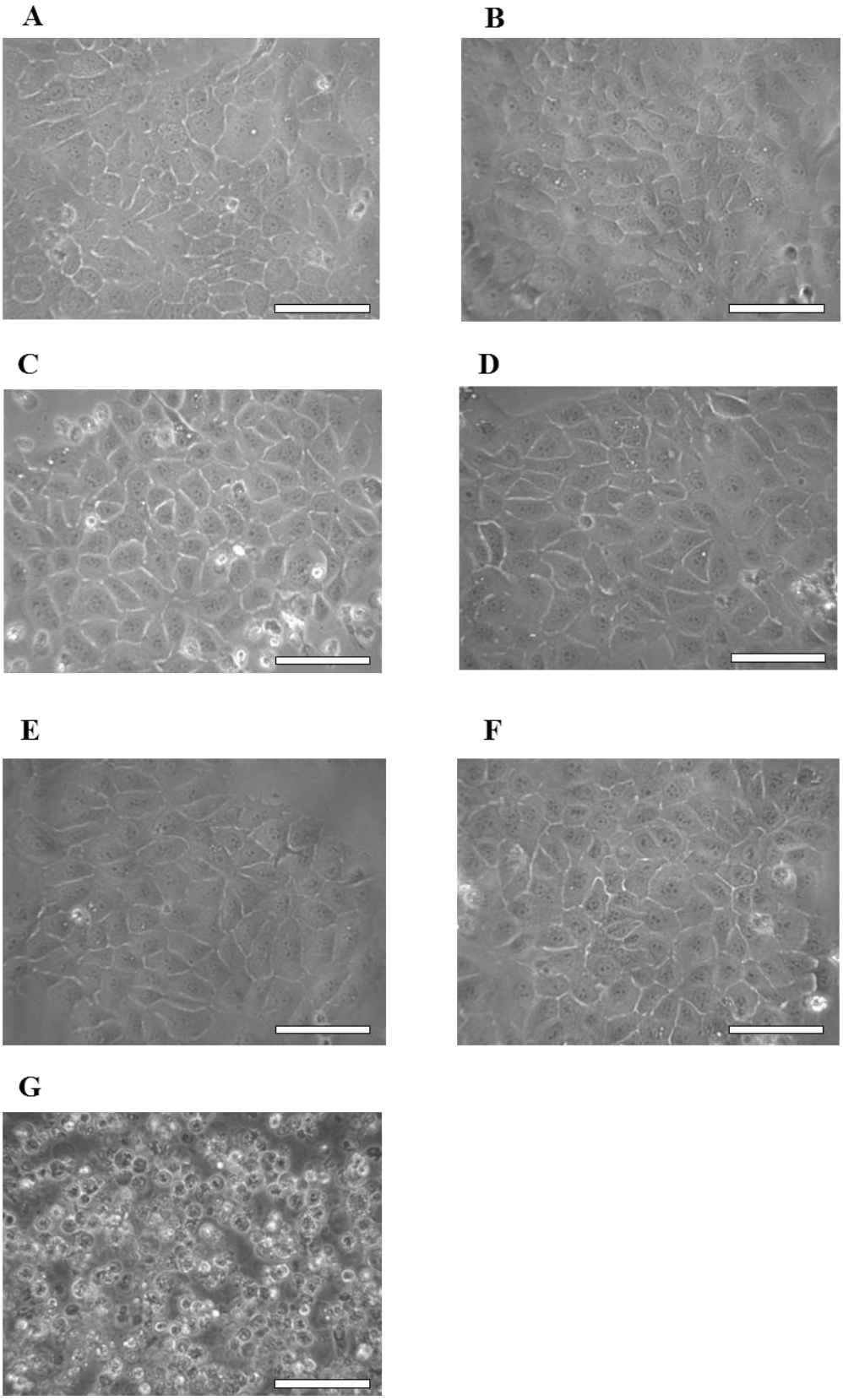

Figure 4.18: HaCaT morphology, cultured in the presence of (A) 0µg/ml, (B) 0.001µg/ml, (C) 0.01µg/ml, (D) 0.1µg/ml, (E) 1µg/ml, (F) 10µg/ml; and (G) 100µg/ml EBC-46 for 72h (*N=3*). Scale bar = 100µm.

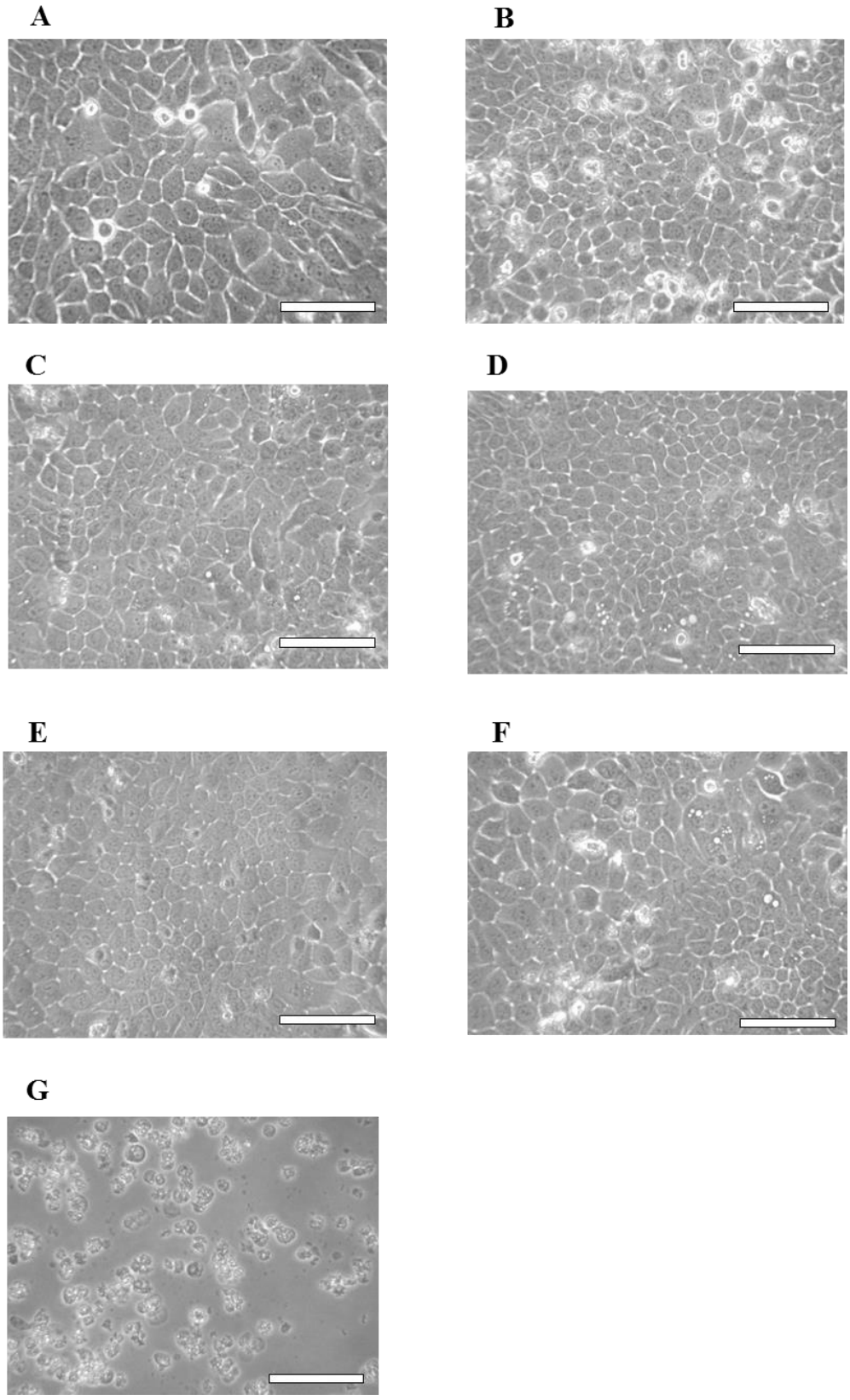

Figure 4.19: HaCaT morphology, cultured in the presence of (A) 0µg/ml, (B) 0.001µg/ml, (C) 0.01µg/ml, (D) 0.1µg/ml, (E) 1µg/ml, (F) 10µg/ml; and (G) 100µg/ml EBC-46 for 120h (*N=3*). Scale bar = 100µm.

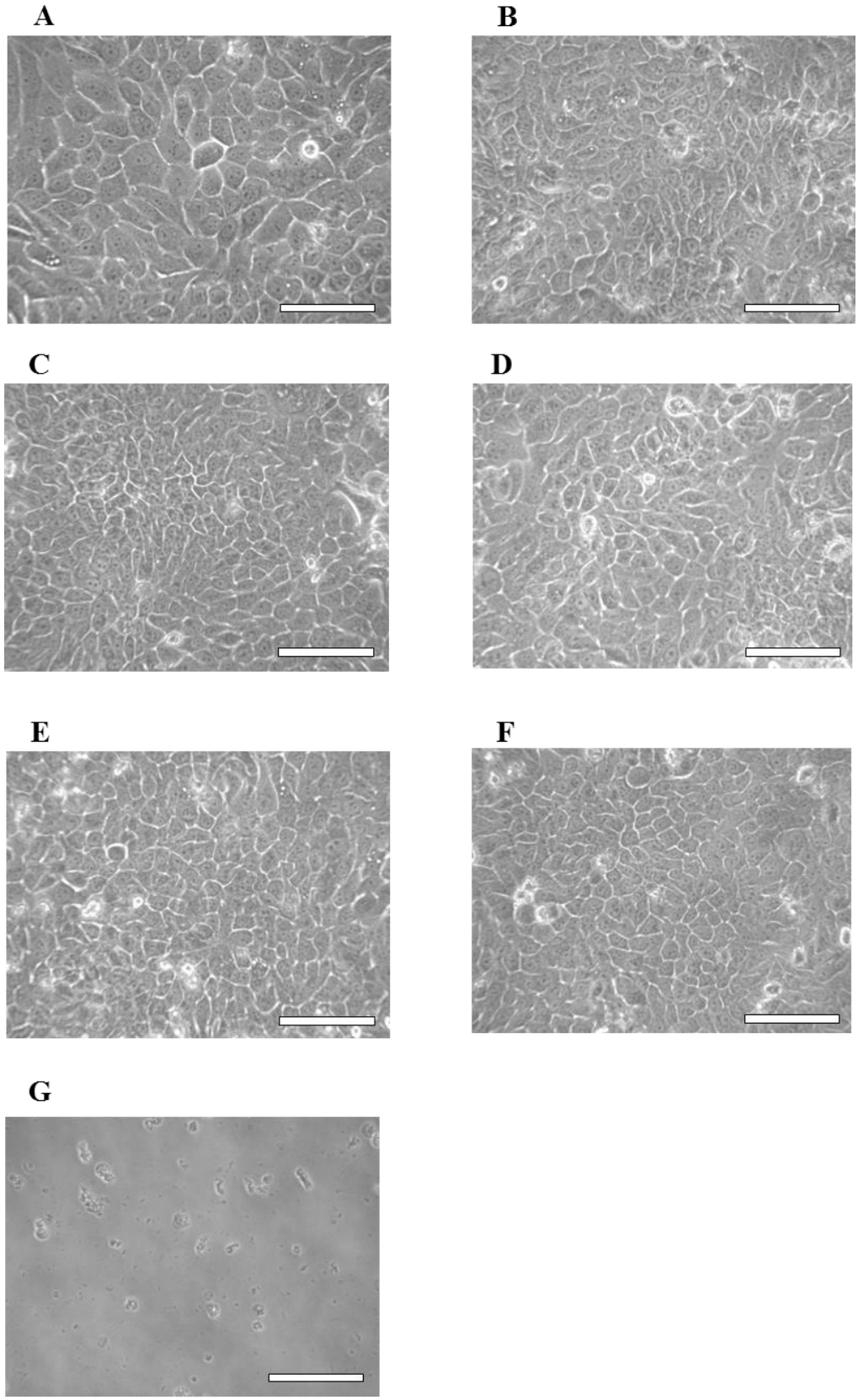

Figure 4.20: HaCaT morphology, cultured in the presence of (A) 0µg/ml, (B) 0.001µg/ml, (C) 0.01µg/ml, (D) 0.1µg/ml, (E) 1µg/ml, (F) 10µg/ml; and (G) 100µg/ml EBC-46 for 168h (*N=3*). Scale bar = 100µm.

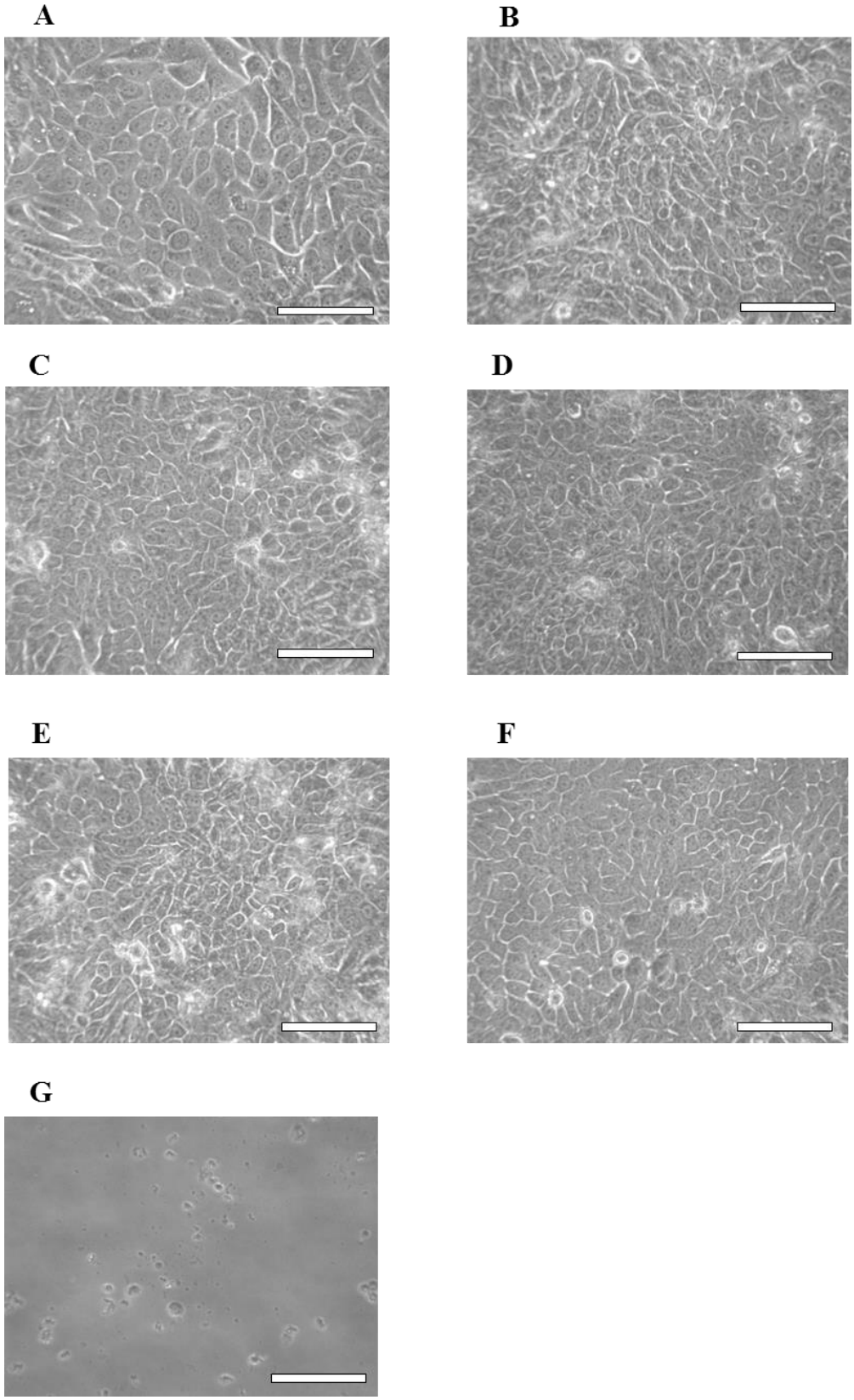

Figure 4.21: HaCaT morphology, cultured in the presence of (A) 0µg/ml, (B) 0.001µg/ml, (C) 0.01µg/ml, (D) 0.1µg/ml, (E) 1µg/ml, (F) 10µg/ml; and (G) 100µg/ml EBC-211 for 24h (*N=3*). Scale bar = 100µm.

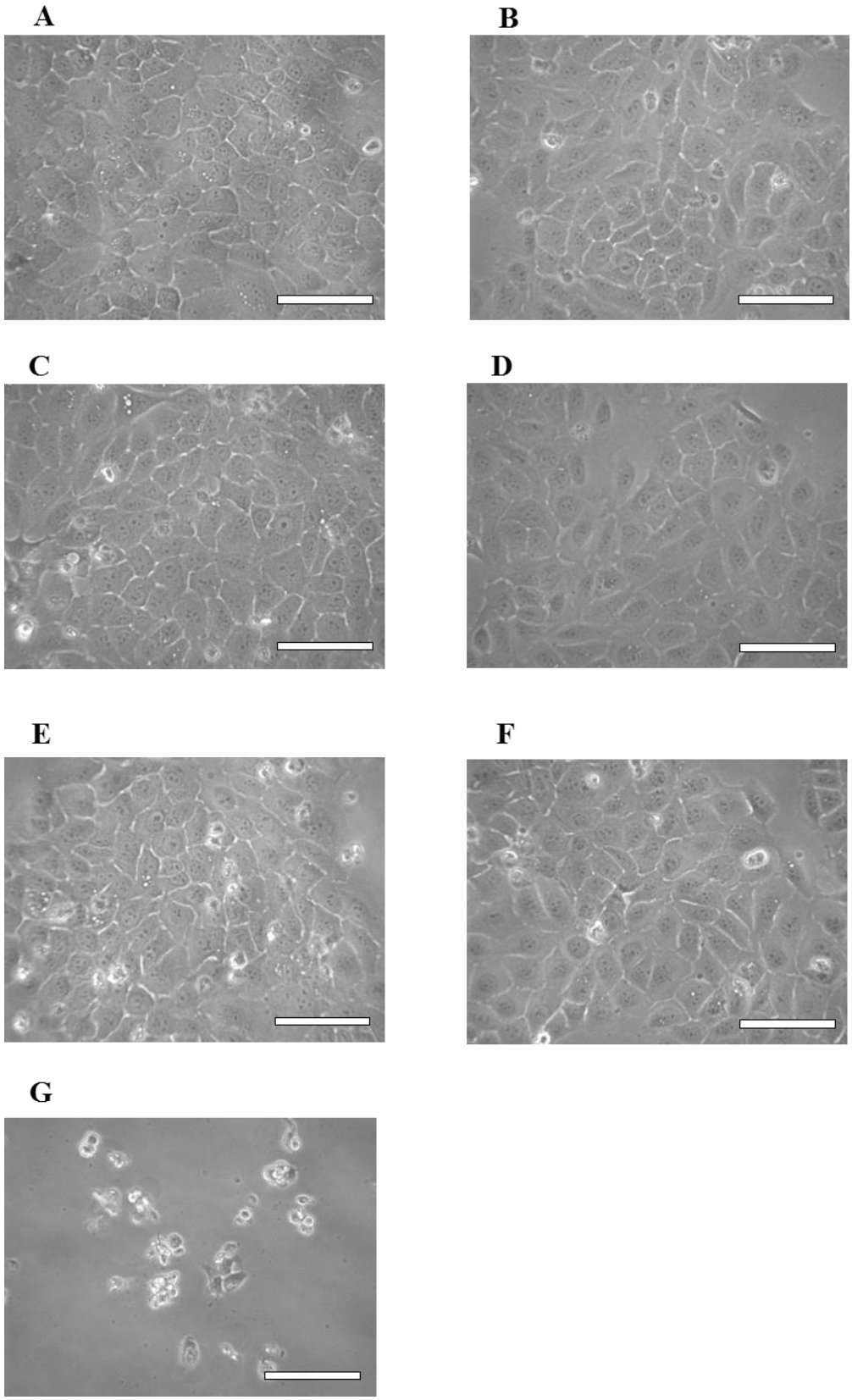

Figure 4.22: HaCaT morphology, cultured in the presence of (A) 0µg/ml, (B) 0.001µg/ml, (C) 0.01µg/ml, (D) 0.1µg/ml, (E) 1µg/ml, (F) 10µg/ml; and (G) 100µg/ml EBC-211 for 72h (*N=3*). Scale bar = 100µm.

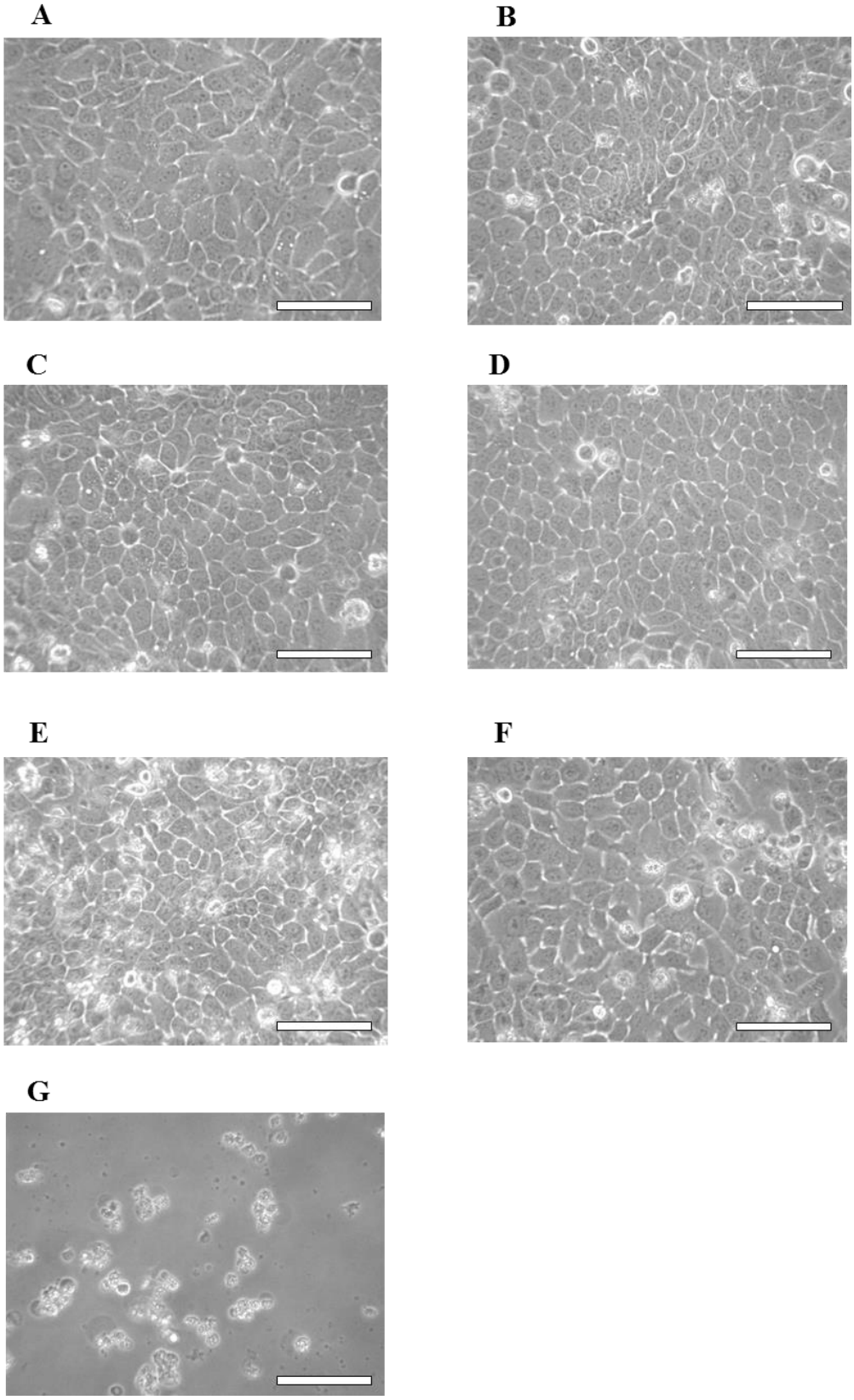

Figure 4.23: HaCaT morphology, cultured in the presence of (A) 0µg/ml, (B) 0.001µg/ml, (C) 0.01µg/ml, (D) 0.1µg/ml, (E) 1µg/ml, (F) 10µg/ml; and (G) 100µg/ml EBC-211 for 120h (*N=3*). Scale bar = 100µm.

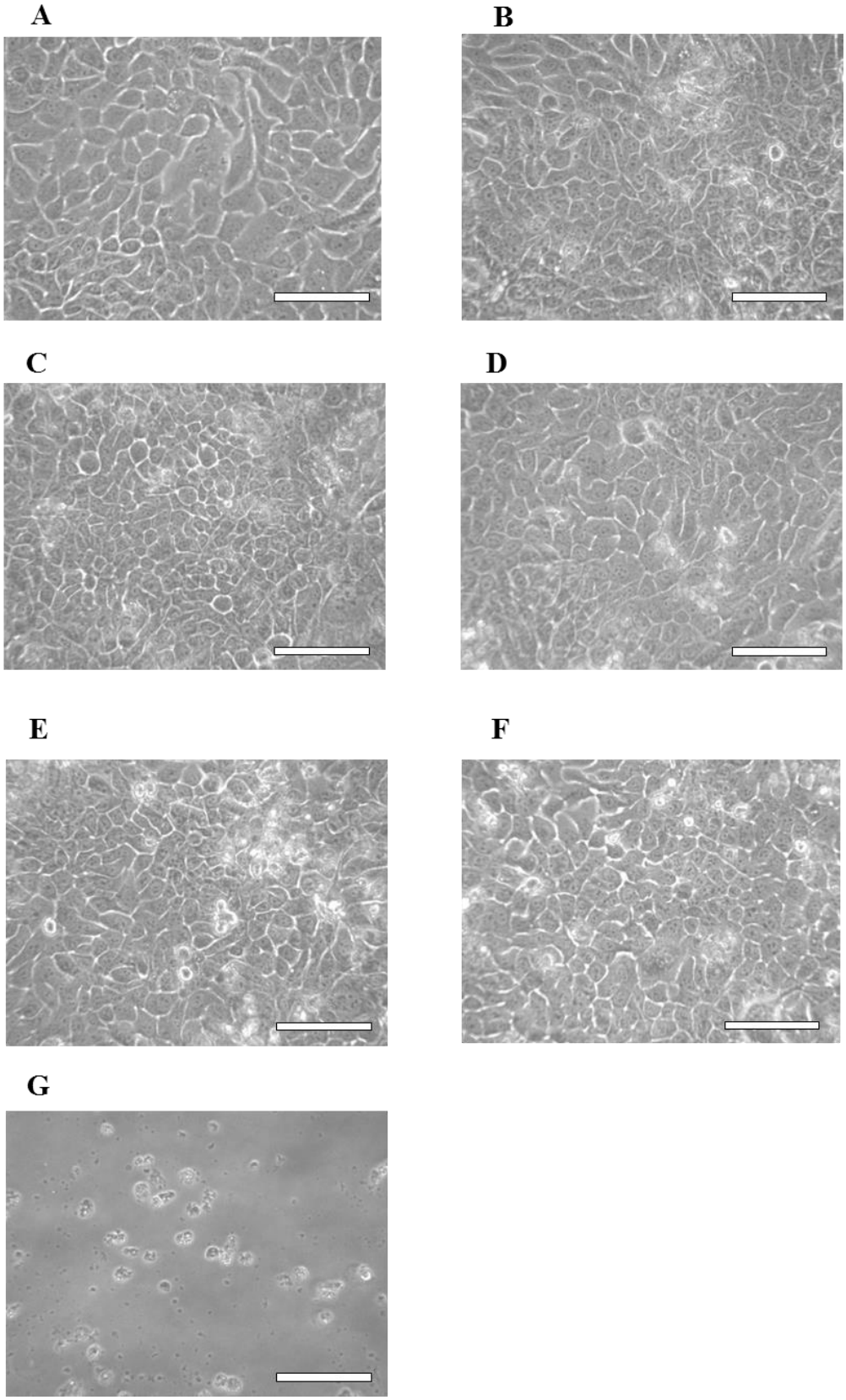

Figure 4.24: HaCaT morphology, cultured in the presence of (A) 0µg/ml, (B) 0.001µg/ml, (C) 0.01µg/ml, (D) 0.1µg/ml, (E) 1µg/ml, (F) 10µg/ml; and (G) 100µg/ml EBC-211 for 168h (*N=3*). Scale bar = 100µm.

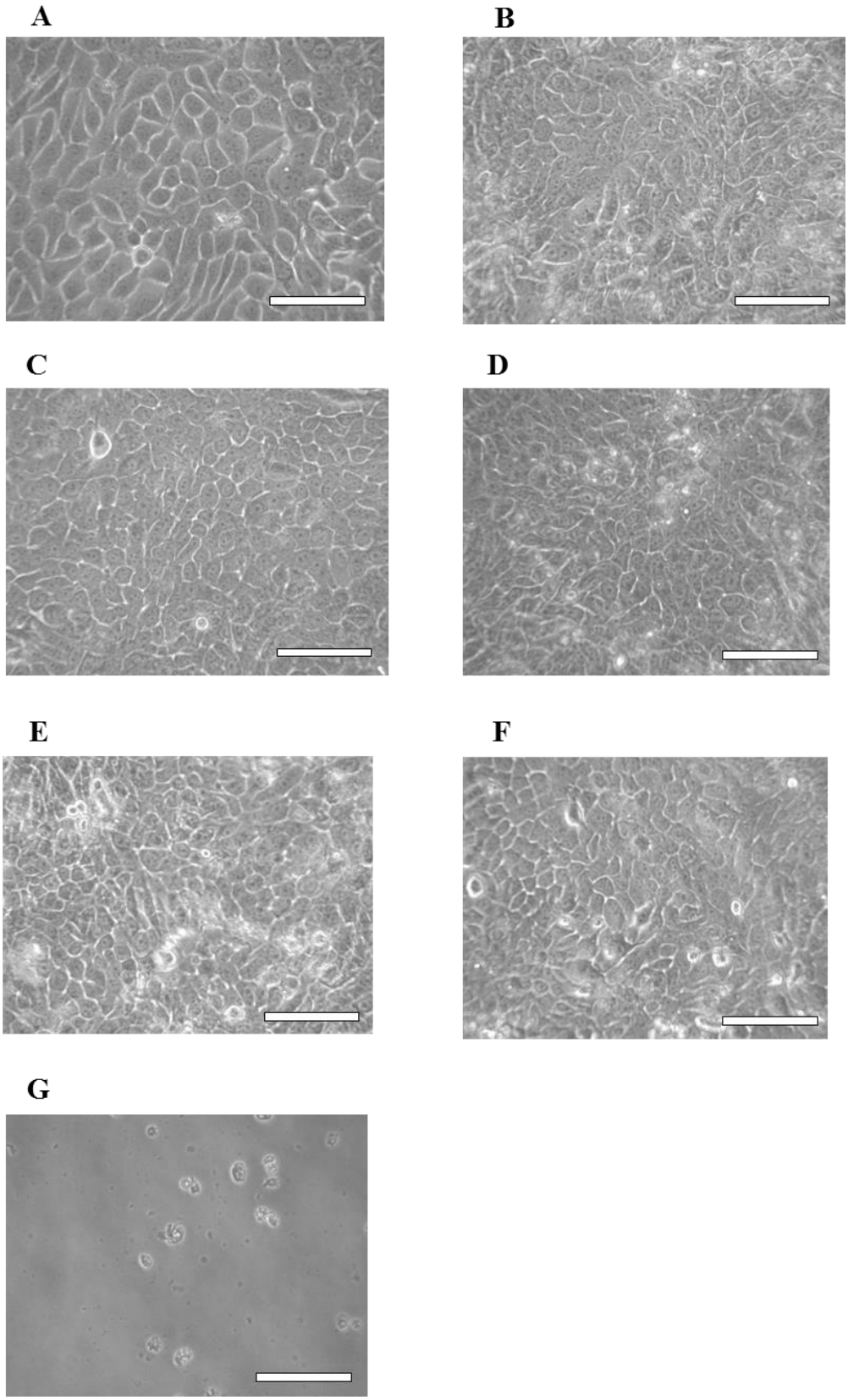

4.4.4 Effects of EBC-46 and EBC-211 on HaCaT Repopulation

Digital images obtained over 48h showed the repopulation of the denuded sites by HaCaTs. Cells were cultured in EBC-46 or EBC-211 (0.001µg/ml, 0.01µg/ml, 0.1µg/ml, 1µg/ml, 10µg/ml and 100µg/ml), with untreated controls (0µg/ml) included for comparison purposes (Figures 4.25 and 4.26, respectively). The digital images were converted into movies (Supplement 4.3), using LAS AF lite (Leica Software, Version 4.0.11706, Leica Microsystems (UK) Ltd), to show the repopulation of HaCaTs over the 48h time-period. HaCaTs in the untreated control migrated across the wound space, moving in a 'wave-like' action to repopulate the denuded area. The untreated control closed the wound over 48h, leaving approximately 50% of wound site remaining. The cytotoxic action of both EBC-46 and EBC-211 (at 100µg/ml) was again demonstrated through the apparent death of HaCaTs over the 48h time-period (Figure 4.25G and 4.26G, respectively).

Repopulation data for the other concentrations of EBC-46 (0.001-10µg/ml) was assessed, which demonstrated a greatly enhanced migratory response, when compared to untreated controls (Figure 4.25A-F). This was particularly evident at 0.001-0.01µg/ml EBC-46, with full wound closure observed in some cases at 48h (Figure 4.25B-C). A similar effect was observed upon culture with EBC-211 (Figure 4.26B-D). However, due to the lesser activity of EBC-211, this enhanced migratory response was observed across a larger range of EBC-211 concentrations, than previously seen with EBC-46 (Figure 4.25A-F). Enhanced repopulation was evident at 0.001-10µg/ml EBC-211 (Figure 4.26A-F), in comparison to untreated controls, with full wound closure observed at 0.001-0.1µg/ml EBC-211 after 48h (Figure 4.26B-D).

The HaCaT repopulation data was further analysed using ImageJ to identify any significant differences in wound repopulation and closure ability at both 24h and 48h, in the presence of EBC-46 and EBC-211 (0.001-100µg/ml); compared to the untreated controls (Figures 4.27A and 4.27B, respectively). At 24h, wound closure ability was not significantly different across the majority of EBC-46 concentrations (0.01-10µg/ml), compared with untreated controls ($p>0.05$; Figure 4.27A). However, at 0.001µg/ml EBC-46, the wound closure rate was significantly enhanced at 24h, compared to untreated controls ($p<0.01$; Figure 4.27A). At 48h, enhanced and

Figure 4.25: HaCaT scratch wound repopulation, in the presence of (A) 0µg/ml, (B) 0.001µg/ml, (C) 0.01µg/ml, (D) 0.1µg/ml, (E) 1µg/ml, (F) 10µg/ml; and (G) 100µg/ml EBC-46, over 48h (*N=3*). Red dashed lines show original scratch wound distance at 0h. Scale bar = 100µm.

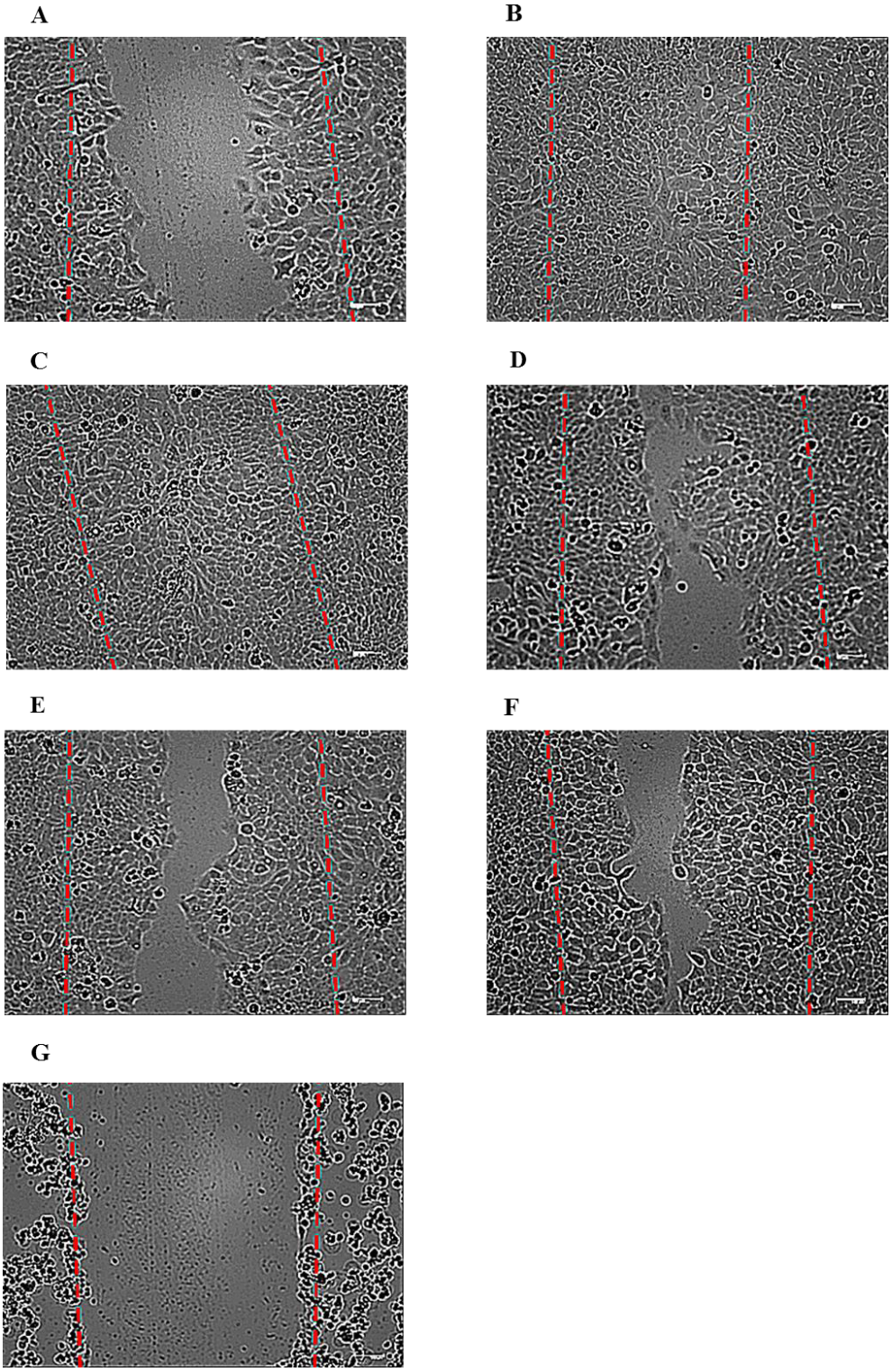

Figure 4.26: HaCaT scratch wound repopulation, in the presence of (A) 0µg/ml, (B) 0.001µg/ml, (C) 0.01µg/ml, (D) 0.1µg/ml, (E) 1µg/ml, (F) 10µg/ml; and (G) 100µg/ml EBC-211, over 48h (*N=3*). Red dashed lines show original scratch wound distance at 0h. Scale bar = 100µm.

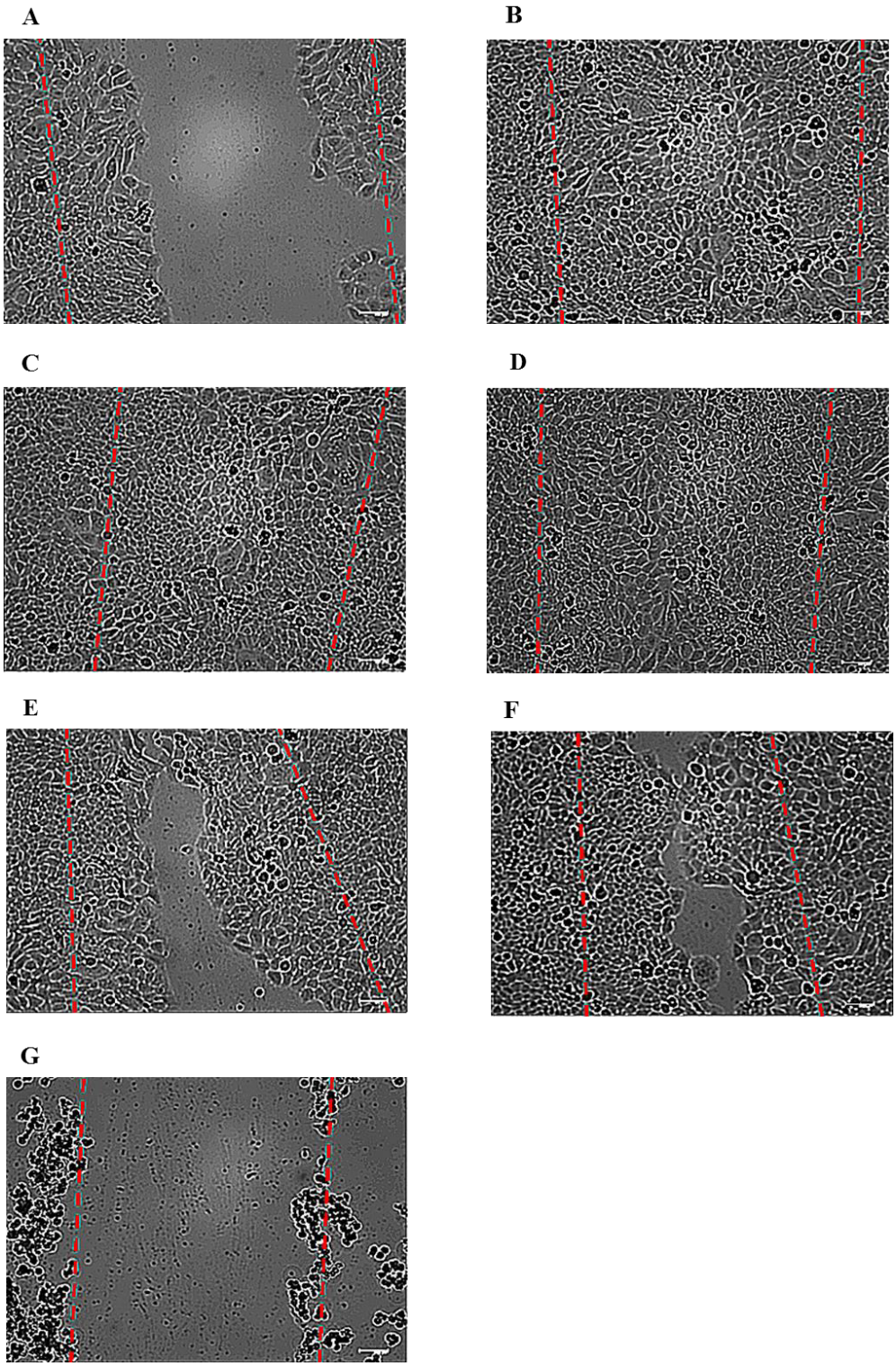

Figure 4.27: HaCaT scratch wound repopulation and closure analysis, in the presence of (A) EBC-46 or (B) EBC-211 (0.001-10µg/ml), versus untreated controls (0µg/ml) at 24h and 48h (*N=3, average±SE, with statistical analysis *p<0.05, **p<0.01, ***p<0.001*).

A

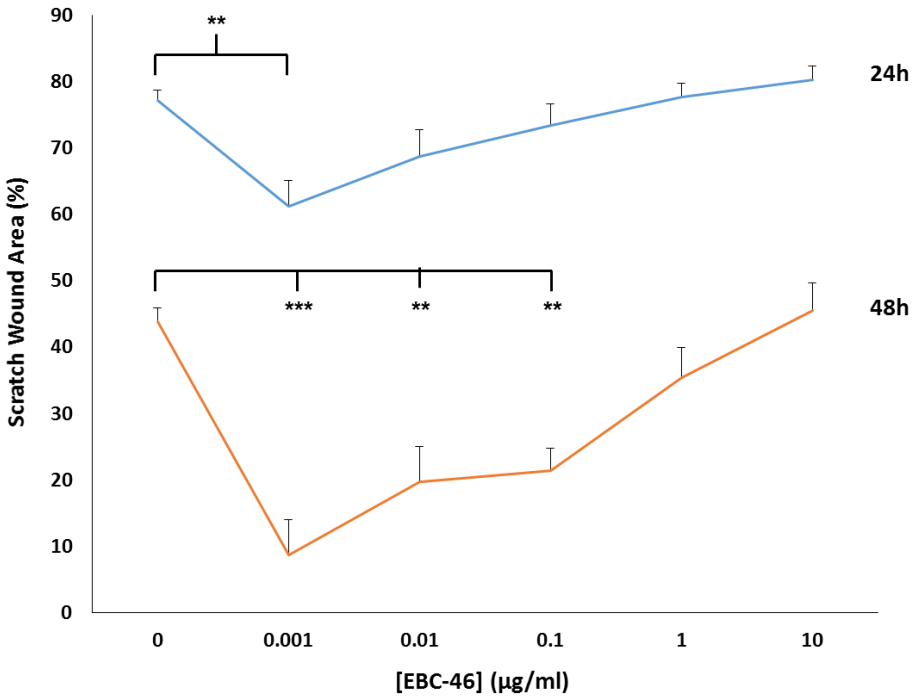

B

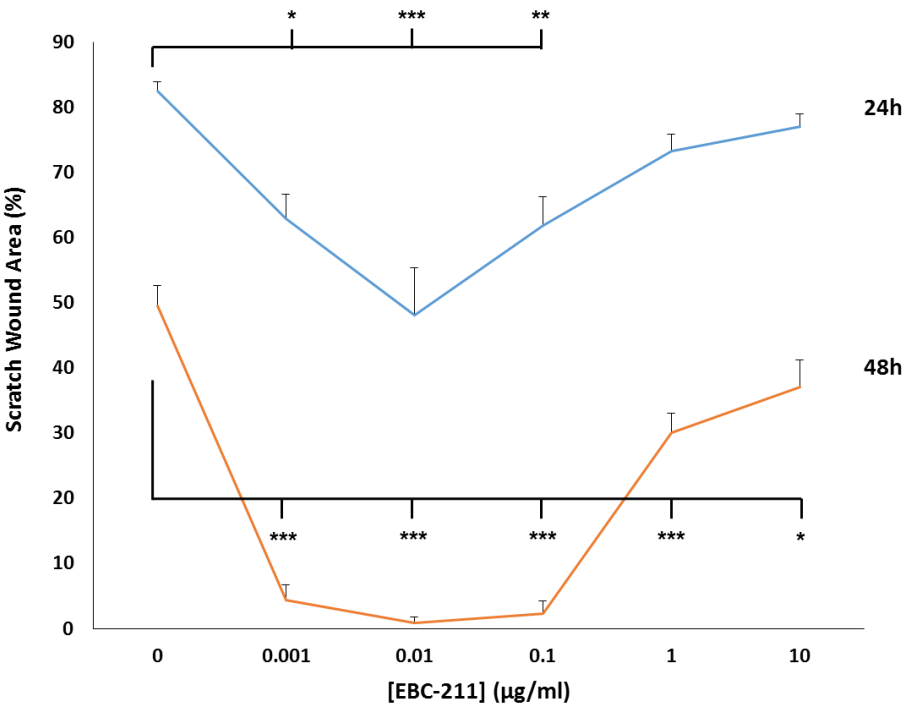

significant wound closure was evident at 0.001-0.1µg/ml EBC-46, compared to untreated controls ($p<0.001$-0.01; Figure 4.27A). However, in contrast, the higher concentrations of EBC-46 (1-10µg/ml) did not show enhanced or significant wound closure rates, compared to untreated controls, at either 24h or 48h ($p>0.05$; Figure 4.27A).

Wound closure rates were also significantly enhanced at 24h, following treatment with 0.001-0.1µg/ml EBC-211, compared to untreated controls ($p<0.001$-0.05; Figure 4.27B). At 24h, 0.01µg/ml EBC-211 exhibited the most significant wound closure rate, compared to these controls ($p<0.001$; Figure 4.27B). At 48h, the wound closure rates were significantly enhanced across the range of EBC-211 concentrations (0.001-10µg/ml), compared to untreated controls ($p<0.001$-0.05; Figure 4.27B). Treatment with 0.001-1µg/ml EBC-211 resulted in a highly significant enhancement of wound closure ability ($p<0.001$; Figure 4.27B); with 0.001-0.1µg/ml EBC-211 showing almost complete wound closure, corroborating the images previous observed (Figure 4.26B-D).

4.4.5 Effects of EBC-46 and EBC-211 on HaCaT Migration in Presence of Mitomycin C

Based on previous findings of the significantly enhanced HaCaT proliferative response following treatment with EBC-46 and EBC-211 (Figures 4.1A and 4.2A, respectively); the scratch wound repopulation was repeated in the presence of anti-proliferative agent, mitomycin C (Santhiago et al. 2012; Wang et al. 2012; Lü et al. 2013). This experiment aimed to determine the extent of which the significant proliferation responses in HaCaTs following treatment by EBC-46 and EBC-211, contribute to the enhanced *in vitro* scratch wound closure. As previously discussed, the optimal concentration of mitomycin C was initially determined, to produce a non-cytotoxic response to the HaCaTs, whilst also inducing an inhibition of proliferation (Section 2.3.4.1). This concentration was determined to be 1µg/ml mitomycin C (Supplement 4.4).

As before, digital images were obtained over 48h and converted into movies (Supplement 4.5), using LAS AF lite (Leica Software, Version 4.0.11706, Leica

Microsystems (UK) Ltd), to record the migration of HaCaTs cultured in either EBC-46 or EBC-211 across a range of concentrations (0.001-10µg/ml; Figures 4.28 and 4.29, respectively). These were compared to untreated controls, controls untreated with EBC-46 or EBC-211 or mitomycin C; and a control untreated with EBC-46 or EBC-211, but treated with 1µg/ml mitomycin C. This allowed the repopulation of denuded sites to be observed through the *in vitro* scratch wound assay and for wound closure rate to be determined, without the stimulatory proliferative effect on HaCaTs biasing the results. There was an enhanced migration rate for the lower concentrations of EBC-46-treated HaCaTs (0.001-1µg/ml), compared to controls with mitomycin C (Figure 4.28). However, this migration appeared to be enhanced even when compared to the control without mitomycin C, where the control HaCaTs without mitomycin C were capable of proliferation. However, there did not appear to be an enhanced migratory effect at 10µg/ml EBC-46, when compared to either untreated control at 48h.

As seen with EBC-46, there was a stimulated migratory response evident for the HaCaTs into denuded sites following treatment with 0.001-1µg/ml EBC-211, when compared to both untreated controls (Figures 4.29B-F). At certain concentrations of EBC-211 (0.01-0.1µg/ml), there appeared to be full wound closure at 48h, despite the lack of proliferation (Figures 4.29C-D). As before, the HaCaT migration data was further analysed using ImageJ to identify any significant differences in wound closure at both 24h and 48h. This was performed by analysing percentage wound closure, in the presence of EBC-46 and EBC-211 (0.001-100µg/ml) compared to the two untreated controls, in the absence and presence of mitomycin C (Figures 4.30A and 4.30B, respectively).

At 24h, wound closure ability was not significantly different across the majority of EBC-46 concentrations (0.01-10µg/ml), when compared with the untreated controls ($p>0.05$; Figure 4.30A). However, at 0.001µg/ml EBC-46, wound closure rates were significantly enhanced at 24h, compared to both untreated controls in the absence and presence of mitomycin C ($p<0.001$; Figure 4.30A). At 48h, significantly enhanced wound closure was evident at 0.001-1µg/ml EBC-46, compared to the untreated control treated with mitomycin C ($p<0.001$-0.05; Figure 4.30A). In addition,

Figure 4.28: HaCaT scratch wound repopulation, in the presence of mitomycin C (1µg/ml) and EBC-46 (A) 0µg/ml, (B) 0.001µg/ml, (C) 0.01µg/ml, (D) 0.1µg/ml, (E) 1µg/ml, (F) 10µg/ml; and (G) an untreated control in the absence of EBC-46 or mitomycin C, at 48h (*N=3*). Red dashed lines show original scratch wound distance at 0h. Scale bar = 100µm.

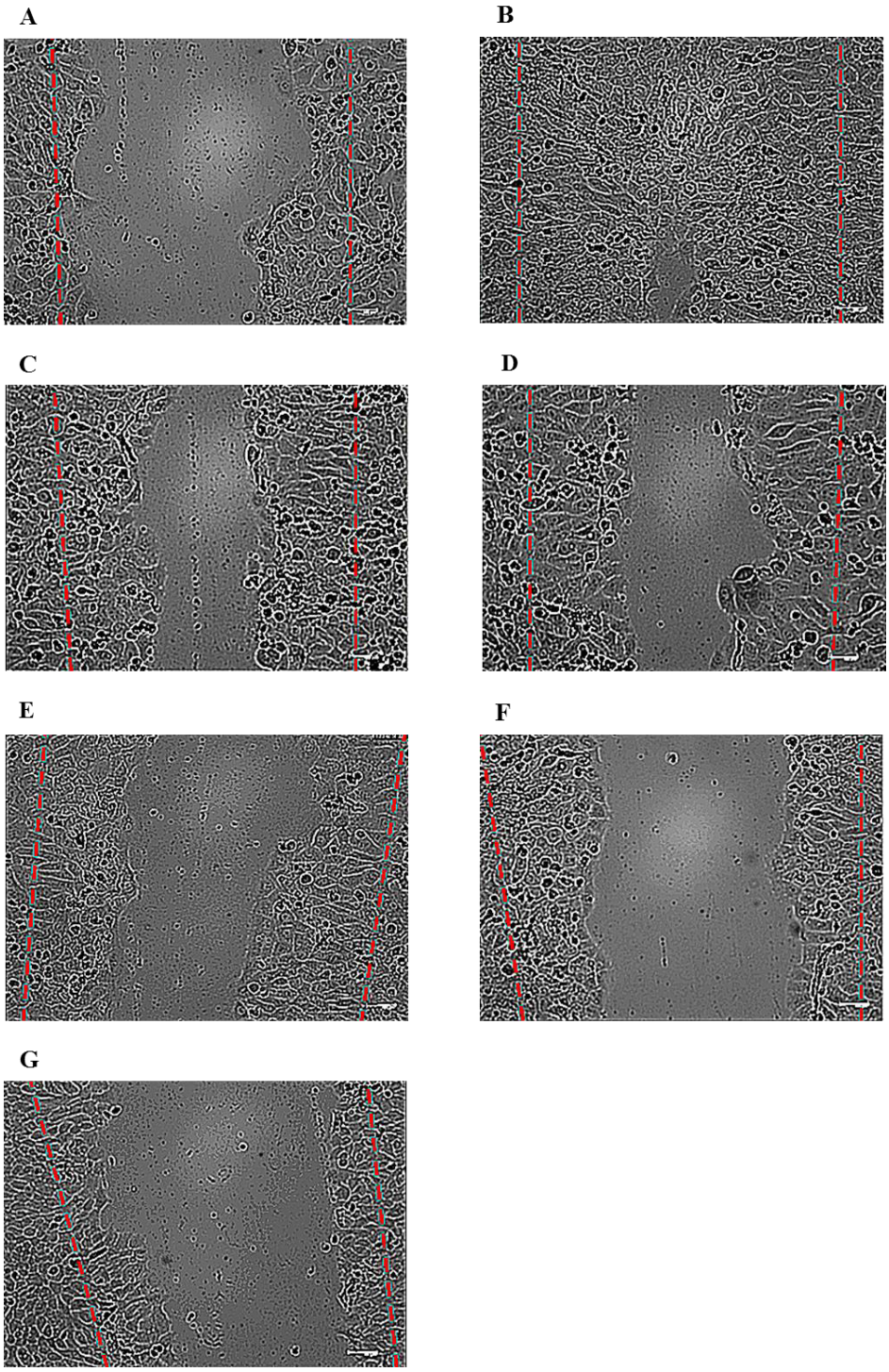

Figure 4.29: HaCaT scratch wound repopulation, in the presence of mitomycin C (1µg/ml) and EBC-211 (A) 0µg/ml, (B) 0.001µg/ml, (C) 0.01µg/ml, (D) 0.1µg/ml, (E) 1µg/ml, (F) 10µg/ml; and (G) an untreated control in the absence of EBC-211 or mitomycin C, at 48h (*N=3*). Red dashed lines show original scratch wound distance at 0h. Scale bar = 100µm.

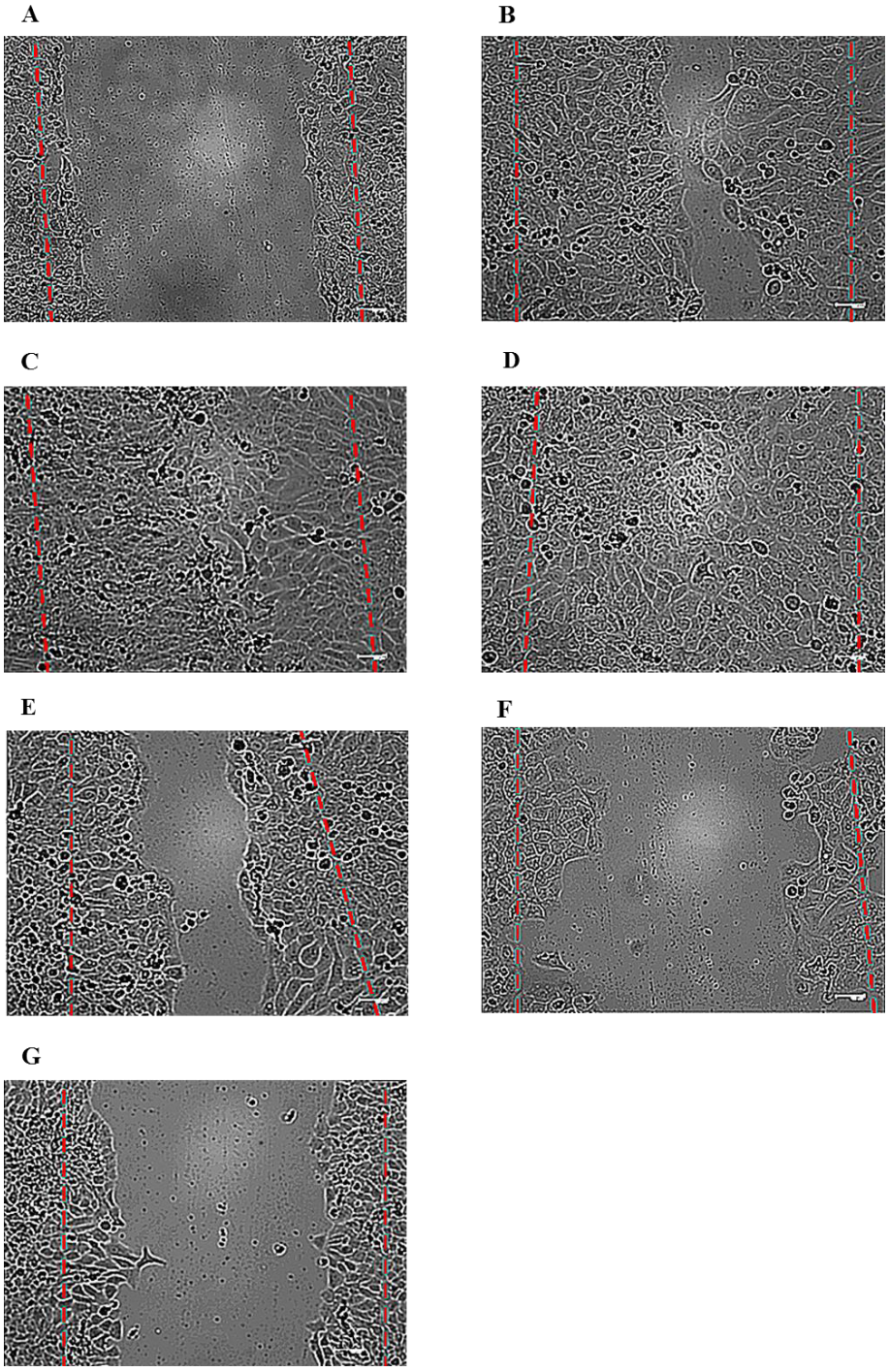

Figure 4.30: HaCaT scratch wound repopulation, in the presence mitomycin C (1µg/ml) and (A) EBC-46 or (B) EBC-211 (0.001-10µg/ml), with mitomycin-containing (1µg/ml) and mitomycin-free controls (0µg/ml) at 24h and 48h (*N=3, average±SE, with statistical analysis *p<0.05, **p<0.01, ***p<0.001*).

A

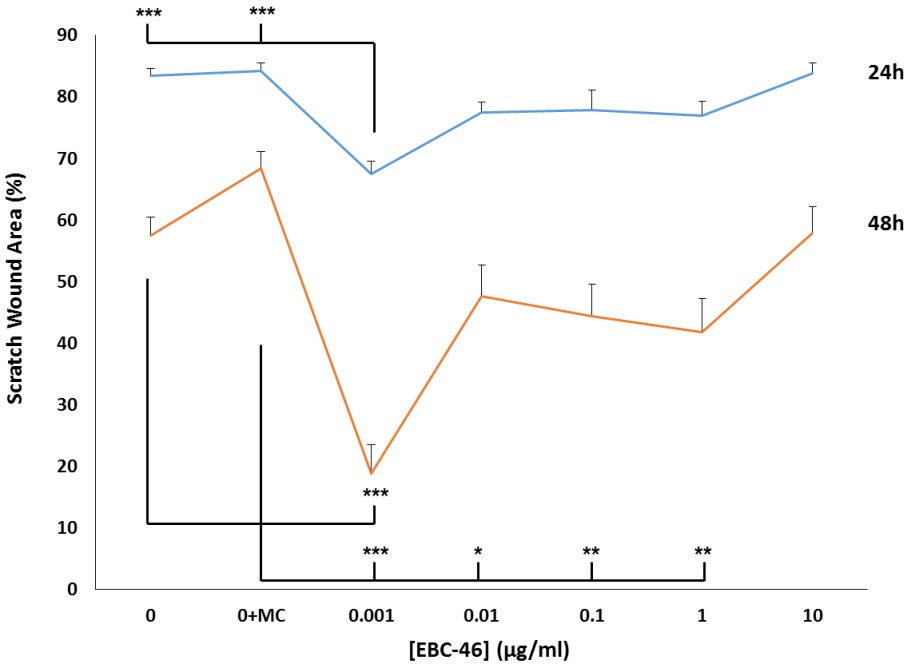

B

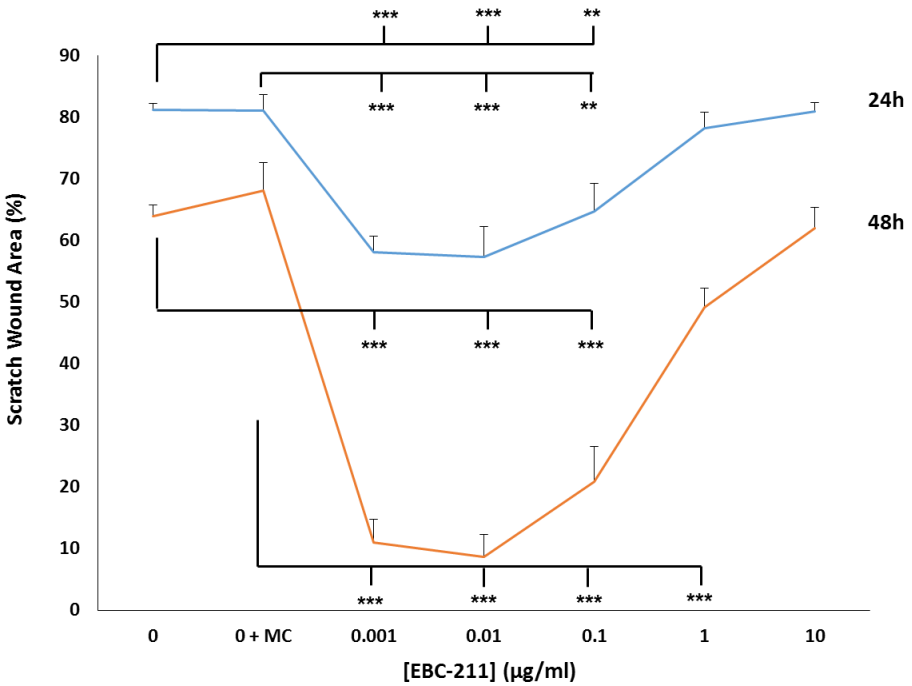

0.001µg/ml EBC-46 showed significantly enhanced wound closure ability, compared to the untreated control in the absence of mitomycin C ($p<0.001$; Figure 4.30A). The level of wound closure at 0.001µg/ml EBC-46 was dramatically enhanced compared to the other EBC-46 concentrations (0.01-10µg/ml), in addition to the two untreated controls. This was evident by the highly significant levels of wound closure at this concentration ($p<0.001$; Figure 4.30A). In contrast, the higher concentration of EBC-46 (10µg/ml) did not show enhanced or significant wound closure rates, compared to either untreated control at both 24h and 48h ($p>0.05$; Figure 4.30A).

Similar to previous findings, wound closure rates were significantly enhanced at 24h, following treatment with 0.001-0.1µg/ml EBC-211, compared to both untreated controls ($p<0.001$-0.01; Figure 4.30B). At 24h, treatment with 0.001-0.01µg/ml EBC-211 showed the most significant wound closure rates, compared to the untreated controls in the absence and presence of mitomycin C ($p<0.001$; Figure 4.30B). At 48h, wound closure rates were significantly enhanced across a range of EBC-211 concentrations (0.001-1µg/ml), compared to the untreated control treated with mitomycin C ($p<0.001$; Figure 4.30B). In addition, at 48h, wound closure rates were also significantly enhanced across the range of EBC-211 concentrations (0.001-0.1µg/ml), when compared to the control untreated with mitomycin C ($p<0.001$; Figure 4.30B).

4.5 Discussion

This Chapter examined the effects of the novel epoxy-tiglianes, EBC-46 and EBC-211, on HaCaTs, focusing on some of the vital functions carried out by keratinocytes during wound healing, such as proliferation and migration (Haase et al. 2003; Bader & Kao 2009; Portou et al. 2015). Veterinary case studies previously performed by QBiotics Ltd. have already demonstrated a remarkable wound closure ability *in vivo* with rapid re-epithelialisation, which would re-establish the protective barrier of the skin (Candi et al. 2005). As previously discussed, wound healing is a tightly regulated process and deviations from these normal mechanisms could result in a detrimental healing response, as seen with chronic wounds and complications from burn injuries (Schwacha et al. 2008; Dreifke et al. 2015). There are numerous genotypic and

phenotypic changes in preferential wound healing responses, such as early-gestational foetal and oral mucosal wounds; including reduced inflammatory response and rapid re-epithelialisation (Colwell et al. 2008; Turabelidze et al. 2014). A number of *in vitro* experiments were performed to determine the effect of treatment with the novel epoxy-tiglianes on HaCaT wound healing responses. HaCaTs were used instead of primary keratinocytes, as this immortalised cell line has been widely used to assess epidermal responses, due to their close similarity of functional response to normal adult epidermal keratinocytes (Boukamp et al. 1988; Pessina et al. 2001; Wilson 2014). HaCaTs have been shown to maintain key behavioural functions, similar to primary keratinocytes, such as retaining differentiation capacity. Little change to cell cycle related genes has also been observed, compared to primary keratinocytes (Sprenger et al. 2013). As a result of these beneficial properties, HaCaTs are considered suitable for use instead of primary keratinocytes and be representative of keratinocyte responses (Sprenger et al. 2013). In addition, use of primary keratinocytes can potentially result in a range of responses, due to variations in donor age, gender and localisation of biopsy (Sprenger et al. 2013).

The viability and proliferation assay was performed on HaCaTs for both EBC-46 and EBC-211. Likewise with the effects seen with fibroblasts, EBC-46 and EBC-211 were both cytotoxic to HaCaTs at 100µg/ml. This was extremely significant for both epoxy-tiglianes from 24h onwards, with no viable cells remaining ($p<0.001$). The effects were slightly reduced for EBC-211, again confirming the lesser activity of this epoxy-tigaline compared to EBC-46 (Reddell et al. 2014). As with the fibroblasts, it was possible that the HaCaTs were undergoing apoptosis at this concentration for both epoxy-tiglianes, followed by secondary necrosis, also referred to as apoptotic necrosis. This was visualised during the morphology and repopulation studies; as the cells were cultured *in vitro*, there was a lack of viable cells to phagocytose the apoptotic bodies, potentially resulting in this apoptotic necrosis process. This was visualised during the repopulation studies, where no viable cells remained by 24h and the cells were observed to shrink and condense (Saraste & Pulkki 2000; Ziegler & Groscurth 2004; Fink & Cookson 2005; Elmore 2007; Elliott & Ravichandran 2010).

Keratinocyte proliferation was studied due to its vital role in re-epithelialisation, through increasing the presence of keratinocytes at the wound site, in order to migrate across the wound and re-establish the protective barrier (Li et al. 2007; Bader & Kao 2009; Turabelidze et al. 2014; Portou et al. 2015). There was a significantly profound stimulation of proliferation observed at EBC-46 and EBC-211 concentrations of 0.001-10µg/ml, with a marked increase in proliferation evident throughout the 168h culture period. This was particularly apparent with respect to the untreated controls at 72h, 120h and 168h, with only 0.001µg/ml EBC-46 showing a significant proliferative effect at 24h. The largest proliferative response was observed at 72h, with all concentrations shown to be significant. Despite the continued increase in proliferation at each subsequent time-point, it was only at 72h that all concentrations of EBC-46 (0.001-10µg/ml) were considered to be significant, compared to untreated controls. In contrast, EBC-211 was considered to induce significant increases in proliferation across all concentrations (0.001-10µg/ml) at 72h and 168h. At the other time-points, increases in proliferation were still observed. However, this was not apparent across all epoxy-tigliane concentrations and not to the same significance in some cases, compared to the results seen at 72h. The results obtained at 120h and 168h for EBC-46 appear to show a biphasic response with significant proliferative responses observed at both the low and high concentrations, in particular at 0.001µg/ml and 1-10µg/ml, whereas 0.01µg/ml EBC-46 was not significantly increased at either of these time-points. In contrast, EBC-211 appeared to show a dose-dependent response. The lowest concentration of EBC-211 (0.001µg/ml) exhibited the greatest proliferative response, compared to untreated controls. Although the other concentrations were mostly significant compared to untreated controls, the proliferative ability was reduced with increasing concentration of EBC-211. At 120h, this reduced ability resulted in no significant difference being shown at 1-10µg/ml EBC-211, compared to untreated controls.

Due to the rapid increase in cell number, it was a consideration that the proliferative effect was partly dampened after 72h due to the wells becoming fully confluent and restricting the proliferative ability. Therefore, this study was repeated with a lower starting cell density to account for this potential issue. However, this study showed that the greatest proliferative response for both EBC-46 and EBC-211 was also at 72h,

despite the wells not being confluent at this point (Supplement 4.1). This potentially indicates that a proliferative burst on the HaCaTs occurs between 24h and 72h to produce this response. Visualisation of the cells during this study showed that no morphological changes were observed, indicating that the epoxy-tiglianes were not impacting the cytoskeletal structure of the HaCaTs.

Cell cycle progression after treatment with EBC-46 or EBC-211 was studied to further determine whether the significant proliferative response observed was related to the cell cycle. A number of time points were analysed to observe the progression through the phases, with epoxy-tigliane treated cells compared to untreated controls at each time-point. As expected, there was an increased progression through the cell cycle after treatment with EBC-46 and EBC-211. T0 was also analysed to confirm that all cells started in the same phase across the conditions. There was no significant difference or minimal significance compared to the untreated controls at the earlier time-points. However, at T26 and T40 in particular for both epoxy-tiglianes, there was a significant acceleration through the cell cycle phases. This was evident with the corresponding cell cycle histograms showing that the cells had progressed out of G1 phase into S phase, with some progressing into G2 phase; while a significant proportion of the control cells remain in G1 phase. As the cells cycled at a faster rate after 24h treatments, this was likely to contribute to the stimulated proliferative ability observed at 72h during proliferation studies.

Another key function of keratinocytes during wound healing is migration, where wound edge keratinocytes migrate across the ECM and re-epithelialise the denuded site. Repopulation studies were performed to analysis the effect of EBC-46 and EBC-211 on migratory ability, with time-lapse movies obtained over 48h and percentage wound closure rates analysed. The data clearly showed an enhanced wound repopulation into the denuded site after treatment with EBC-46 or EBC-211, compared to untreated controls. The enhanced repopulation following epoxy-tigliane treatment appeared to be dose-dependent, with the lower concentrations exhibiting greater wound closure ability. Due to the lesser activity of EBC-211, the beneficial response was present over a wider range of concentrations (0.001-10µg/ml), compared to EBC-

46 (0.001-0.1µg/ml), with all EBC-211 concentrations producing a significantly enhanced wound closure rate.

Although, the proliferative rates were significantly enhanced after epoxy-tigliane treatment, it is possible that this stimulated proliferation is biasing the repopulation results due to the increased cell number present in the EBC-46 and EBC-211 conditions, closing the wound site in a shorter time period. Therefore, these studies were repeated with the addition of anti-proliferative agent, mitomycin C, which prevents DNA synthesis through alkylating and cross-linking DNA and inhibiting subsequent mitosis (Santhiago et al. 2012; Jones et al. 2015). The mitomycin C concentration was optimised to inhibit proliferative ability, without having a cytotoxic effect on the cells (Santhiago et al. 2012). The migration studies performed with the addition of mitomycin C (1µg/ml) displayed a similar pattern to the previous repopulation studies. Low concentrations of both epoxy-tiglianes produced an accelerated wound closure by 24h, compared to untreated controls with mitomycin C. EBC-211 again showed a greater range of concentrations (0.001-0.1µg/ml) to produce the beneficial wound repopulation, whereas as before, only 0.001µg/ml EBC-46 showed a highly significant migratory response by 24h, compared to untreated controls with mitomycin C. By 48h, this significantly enhanced wound repopulation was observed across a greater range of both EBC-46 and EBC-211 (0.001-1µg/ml), compared to the untreated control with mitomycin C. An untreated control, without the addition of mitomycin C, was also included. These cells were able to proliferate as normal. Interestingly, the lower concentrations of both epoxy-tiglianes showed an enhanced wound closure ability, even against this control; with EBC-211 again showing this enhanced wound repopulation across a greater range of concentrations (0.001-0.1µg/ml), whereas this response is only observed at 0.001µg/ml EBC-46. This indicated that EBC-46 and EBC-211 are effecting the migratory ability of HaCaTs independent of proliferation at these low concentrations, producing a dual effect on the cells ability to repopulate wound sites.

This dual beneficial response on keratinocyte proliferation and migration observed during the *in vitro* studies may contribute to the exceptional wound healing response observed, during the *in vivo* animal wound healing studies, with rapid re-

epithelialisation evident (Reddell et al. 2014). Foetal keratinocytes have been observed to possess an increased proliferative potential, compared to adult keratinocytes, in addition to possessing longer telomeres and maintaining the ability to differentiate successfully into a stratified epidermal layer (Tan et al. 2014). As mentioned previously, oral keratinocytes also possess a dramatically increased proliferative capacity, compared to adult dermal keratinocytes. This enhanced proliferation, together with a stimulated migratory ability, may also contribute to the rapid re-epithelialisation process observed in scarless oral mucosal wound healing (Turabelidze et al. 2014).

As previously discussed, the migratory action of foetal keratinocytes is through a different mechanism, than in adult acute wound healing; via the use of the 'purse string closure' method, as opposed to lamellipodia formation and cell crawling (Martin 1997; Chen et al. 2010; Rolfe & Grobbelaar 2012). However, the rapid re-epithelialisation observed during oral mucosal wound healing undergoes migration in the same manner as adult acute wound healing (Turabelidze et al. 2014). *In vitro* studies performed by Turabelidze et al. (2014) have analysed wound closure rates in the oral mucosa. Migration studies were performed, independent of proliferative ability, which showed a higher rate of migration of oral keratinocytes, compared to adult skin keratinocytes. V-AKT murine thymoma viral oncogene homolog 3 (AKT3), is a serine/threonine-protein kinase involved in cell migration regulation, along with a number of other cellular functions. AKT3 was found to have a significantly higher expression in oral keratinocytes than epidermal skin keratinocytes (Turabelidze et al. 2014). This increased expression could be partly responsible for the enhanced proliferative and migratory ability, leading to the rapid re-epithelialisation observed in oral mucosal wounds (Turabelidze et al. 2014).

There are a number of stimulatory growth factors, EGF, TGF-α and KGF, involved in inducing re-epithelialisation, through stimulation of keratinocyte proliferation and migration. A number of integrins are also crucially involved, α5β1, αvβ6, αvβ5 and α2β1, which are responsible for lamellipodia movement, providing temporary adhesion for the keratinocytes migrating across the ECM (Martin 1997; Werner & Grose 2003; Ching et al. 2011; Seeger & Paller 2015). Therefore, such knowledge on

how to stimulate re-epithelialisation responses and the how the preferential responses are induced, will have major beneficial actions on chronic wounds and burn injuries; where these responses are impaired and will aid the re-establishment of the protective barrier (Candi et al. 2005; Seeger & Paller 2015).

In chronic wounds and burns, there is often a decreased migratory action, preventing this subsequent re-epithelialisation. For instance, the presence of β-catenin in chronic wounds has been associated with inhibition of keratinocyte migration, reducing the re-epithelialisation ability (Haase et al. 2003; Stojadinovic et al. 2005; Seeger & Paller 2015; Hameedaldeen et al. 2014; Pastar et al. 2014). Both chronic wounds and burn injuries have a stimulated presence of pro-inflammatory cytokines, causing sustained inflammation, which can result in impaired re-epithelialisation. This is potentially due to the increased and sustained presence of neutrophils, as it has been shown that an absence or reduction of neutrophils at a wound site can accelerate re-epithelialisation (Schwacha 2003; Dovi et al. 2004; Barrientos et al. 2008; Schwacha et al. 2008; Rowan et al. 2015; Rose & Chan 2016). Additionally, depending on the thickness of the burn, this may disrupt blood supply to the site and together with the presence of oedema at the site, may reduce access to immune cells and essential growth factors needed in normal acute wound healing (Edgar et al. 2011; Ching et al. 2011; Rose & Chan 2016). High presence of anaerobic bacteria in chronic wounds has been shown to impair keratinocyte proliferative and migratory responses, resulting in impaired re-epithelialisation (Stephens et al. 2003). This impaired response in chronic wounds is often a result of biofilm formation, composed primarily of *Staphylococcus*, *Pseudomonas*, *Corynobacterium* and a number of obligate anaerobic species. This has an inhibitory effect of keratinocyte ability to migrate across the wound site and undergo successful re-epithelialisation (Pastar et al. 2014).

These stimulatory effects on proliferation and migration could be especially beneficial in diabetic wounds, where both responses are impaired; inducing a rapid re-epithelialisation of the wound site would re-establish this barrier and reduce the clinical and economic burden of these long lasting chronic wounds (Hameedaldeen et al. 2014; Portou et al. 2015). Such reduced proliferative and migratory abilities have been observed in impaired healing, chronic wounds result from a loss of signalling

from growth factors, required to stimulate migration (Seeger & Paller 2015). There are contrasting opinions on keratinocyte proliferative ability in chronic wounds, with some studies indicating that keratinocytes become senescent; whereas other studies demonstrate an enhanced proliferative ability of keratinocytes at chronic wound edges and diabetic ulcer margins (Usui et al. 2008; Hameedaldeen et al. 2014; Pastar et al. 2014; Frykberg & Banks 2015).

However, despite this potentially hyperproliferative response, keratinocyte migration abilities at these wound edges are dramatically reduced (Usui et al. 2008; Hameedaldeen et al. 2014; Pastar et al. 2014; Portou et al. 2015). One pathway involved in this delayed migratory response is a result of excessive levels of the transcription factor, forkhead box O1 (FOXO1), seen in diabetic wounds. FOXO1 is essential for normal acute wound healing and keratinocyte migration, but elevated expression induces synthesis of pro-inflammatory molecules and subsequently reduces migration of keratinocytes (Hameedaldeen et al. 2014). Another potential contributor towards impaired keratinocyte migration in diabetic ulcers, is the reduced presence of a precursor form of laminin (LM-3A32). This precursor is involved in the activation of keratinocyte migration, through regulating the stable attachment of keratinocytes to the basement membrane (Usui et al. 2008). A greater understanding of the genotypic changes involved in epoxy-tigliane-mediated responses may elucidate which mechanisms are impacted to induce the beneficial wound healing responses and potentially stimulate successful repair of chronic wounds.

Studies performed by Boyle et al. (2014) show that EBC-46 predominantly acts through PKC-βI and -βII, and by PKC-α and -γ to a lesser degree, also marginally by PKC-δ and -θ. EBC-211 also acts through PKC-βI and -βII, although to a much reduced level and also very slightly through PKC-α and -γ isoforms (QBiotics Ltd.). There are a number of PKC isoforms present in keratinocytes, PKC-α, -β, -γ, -δ, -ε, -ζ, -η and -θ. PKC-β is present in HaCaTs, but not primary human keratinocytes (Mitev & Miteva 1999; Papp et al. 2003). Therefore, different PKC isoforms play important roles in regulating proliferation, differentiation and apoptosis (Mitev & Miteva 1999; Papp et al. 2003; Denning 2004; Breitkreutz et al. 2007). PKC-α and -β appear to have opposing roles, PKC-α is present in the actin cytoskeleton and involved in the

regulation of differentiation, with an inhibition of proliferation. In contrast, PKC-β is associated with an increase in proliferative ability and a reduction in differentiation (Papp et al. 2004; Breitkreutz et al. 2007; Zhang et al. 2015). Despite the opposing behaviours of PKC-α and -β and that they are both stimulated by EBC-46 and EBC-211, it is likely that the effect on proliferation is affected to a greater degree due to a higher activation of PKC-βI and -βII (QBiotics Ltd.). PKC-βII has also been shown to have an impact on epithelial migration, through enhanced formation of lamellipodia, aiding the wound closure process by cell crawling (Sumagin et al. 2013). Increased activation of PKC-β after treatment with novel epoxy-tiglianes may be the major pathway involved in the increased proliferative and migratory effect observed, both of which result in an enhanced re-epithelialisation (Papp et al. 2004; Sumagin et al. 2013). As an abnormal and sustained proliferation is often associated with tumour formation, studies have shown that overexpression of PKC-β producing an enhanced proliferative response does not result in tumour development through malignant cell transformation (Papp et al. 2004; Hanahan & Weinberg 2011).

The different isoforms of PKC exert different responses on HaCaTs, with PKC-α and PKC-δ associated with an inhibition of proliferation in favour of stimulating differentiation; whereas increased activation of PKC-δ has been shown to upregulate migration responses on collagen (Li et al. 2002; Papp et al. 2004). Despite the inhibited proliferative response associated with PKC-α, this isoform is also shown to play an important role in stimulating wound re-epithelialisation. Diminished PKC-α expression has been shown to delay this response, whereas an enhanced response occurs following excessive expression (Thomason et al. 2012). It is thought that this is related to the desmosomal adhesions, due to its presence at this site following wounding, rather than stimulated proliferation or migration. However, it is a necessary feature required for wound edge keratinocytes to migrate and has been noted that PKC-α is not present with the desmosomes in chronic wounds, which have been shown to have impaired re-epithelialisation responses (Thomason et al. 2012). However, increased expression of PKC-β and PKC-ε isoforms have been shown to increase HaCaT proliferation; whilst a reduction in PKC-βII expression has been observed in psoriatic skin, showing the vital importance of a careful balance in PKC expression in regulating cellular functions (Fisher et al. 1993; Papp et al. 2003, 2004). Downstream

signalling pathways from PKC activation also impact on wound healing responses, with a careful regulation required for successful healing to occur; phosphatidylinositide 3-kinase (PI3K) has been shown in some studies to increase proliferation of some cells (Fitsialos et al. 2007). However, other studies have shown an inhibitory effect of PI3K on proliferation and migration of keratinocytes, impairing re-epithelialisation (Fitsialos et al. 2007). In contrast, ERK1/2 and p38MAPK have a stimulatory effect on keratinocyte re-epithelialisation responses (Fitsialos et al. 2007). An inhibitor of ERK signalling pathway, U0126, has shown the importance of the ERK pathway on keratinocyte wound closure ability, with inhibited wound repopulation evident following treatment with U0126 (Fitsialos et al. 2007). It has also shown a connection to the EGF family of growth factors, with U0126 also inhibiting many of these growth factors. EGF family growth factors are strongly involved in the proliferative and migratory roles of keratinocytes (Fitsialos et al. 2007; Pastore et al. 2008; Mascia et al. 2012). Another beneficial response exerted through the ERK pathway is the reduced inflammatory response, through a decreased presence of pro-inflammatory cytokines. This is especially important as excessive inflammation has been observed in a number of non-healing wounds (Pastore et al. 2005). MAPK signalling pathway has also been shown to regulate keratinocyte migration, through an impact on motility (Haase et al. 2003). Wnt signalling pathway has been proposed to stimulate keratinocyte proliferation and reduce apoptosis, with an overexpression present in psoriasis, the hyperproliferative skin disorder. The inhibited keratinocyte apoptosis exacerbates the increased keratinocyte presence, following enhanced proliferation, as this alters the careful balance required for normal wound healing function (Zhang et al. 2015).

This Chapter has shown a significant stimulatory effect on keratinocyte proliferation, cell cycle progression and wound repopulation following treatment with EBC-46 or EBC-211. A greater range of EBC-211 concentrations appeared to induce these beneficial responses, especially regarding the wound repopulation studies. In addition, the lower concentrations of both EBC-46 and EBC-211, surprisingly, showed the greatest stimulatory responses. The proliferation studies showed an apparent dose-dependent response with the lower concentrations of EBC-211 inducing a greater proliferative response than the higher concentrations. A similar trend was observed in

the scratch wound repopulation studies, as EBC-211 possesses approximately 100-fold lesser activity than EBC-46, this stimulated wound repopulation response was observed over a wider therapeutic range. It appears that such stimulatory responses are likely a result of the activation of PKC-β isoforms (Papp et al. 2004; Boyle et al. 2014). The veterinary palliative trials have already demonstrated the *in vivo* response after treatment with EBC-46, displaying rapid wound closure with exceptional re-epithelialisation responses. However, before human clinical trials can commence, a greater understanding of the effect on the cells involved in the wound healing response is required.

Keratinocytes have a major involvement in acute skin wound healing process and there are cellular differences between the keratinocytes present in dermal wounds and the oral keratinocytes involved in the beneficial healing response. One of the main characteristics of preferential healing in regards to keratinocyte function is rapid re-epithelialisation, which is observed in both oral mucosal and early-gestational foetal wounds (Coolen et al. 2010; Rolfe & Grobbelaar 2012; Turabelidze et al. 2014). The veterinary studies performed by QBiotics Ltd. appear to be representative of these preferential responses. Although, further studies are required to determine whether there are important genotypic differences in keratinocytes following treatment with these novel epoxy-tiglianes, similar to those observed in early-gestational foetal skin and oral mucosal keratinocytes; and which pathways these genes and wound healing responses impact upon (Colwell et al. 2008; Turabelidze et al. 2014). For instance, gene analysis can be performed to determine the mechanisms involved in the increased proliferation and accelerated migratory responses, leading to the enhanced wound repopulation and closure responses observed. This could ultimately lead to the potential to treat impaired dermal healing conditions associated with altered or impaired keratinocyte wound healing responses (Colwell et al. 2008; Turabelidze et al. 2014).

Chapter 5 - Effects of EBC-46 and EBC-211 on Global Gene Expression in HaCaTs

Chapter 5 - Effects of EBC-46 and EBC-211 on Global Gene Expression in HaCaTs

5.1 Introduction

As discussed previously, acute skin wound healing is a tightly regulated process and changes in gene expression and resultant protein can have profound effects on this response. In some instances, this effect can result in a detrimental healing effect, as seen with keloid and hypertrophic scarring where excessive scarring occurs (Chen et al. 2003; Hahn et al. 2013; Jumper et al. 2015; Huang et al. 2015; Ma et al. 2015; Tan et al. 2015). Another detrimental response is observed in chronic wounds, where re-epithelialisation does not occur successfully and healing is impaired (Tomic-Canic & Brem 2004; Agren & Werthén 2007; Brem et al. 2007; Shih et al. 2012; Caley et al. 2015; Jumper et al. 2015). Alternatively, it has been documented that there are a number of differentially expressed genes associated with preferential healing responses, such as during early-gestational, foetal wound healing and oral mucosal healing (Colwell et al. 2008; Chen et al. 2010; Hu et al. 2014; Turabelidze et al. 2014). Some of the gene changes observed in these preferential processes are involved in cellular proliferation, cell cycle progression, DNA synthesis, repair and gene transcription; and in protein synthesis and degradation processes (Colwell et al. 2008; Helmo et al. 2013). Furthermore, it has been shown that the inflammatory phase is reduced in early-gestational foetal and oral mucosal wound healing, with a decreased presence of pro-inflammatory cytokines (Mak et al. 2009; Chen et al. 2010; Rolfe & Grobbelaar 2012; Yates et al. 2012; Helmo et al. 2013). There is also an increased expression of metalloproteinases in foetal and oral wounds, resulting in increased matrix degradation and subsequent extracellular matrix (ECM) turnover (Stephens et al. 2001; Rolfe & Grobbelaar 2012; Yates et al. 2012; Helmo et al. 2013). The objective of this study was to determine what genes were differentially expressed by the novel epoxy-tiglianes and whether any of these were associated with preferential healing responses, as observed with the healing processes, previously mentioned. This might elucidate whether the exceptional healing responses previously observed with epoxy-tiglianes during *in vivo* veterinary case

studies are a result of similar alterations in keratinocyte function, as seen in early-gestational foetal and oral mucosal wound healing (Colwell et al. 2008; Turabelidze et al. 2014).

From the previous studies, it had been shown that both EBC-46 and EBC-211 induce a beneficial wound healing response on epidermal keratinocytes, shown by the stimulation of both proliferation and migration in the keratinocyte cell line, HaCaTs. However, little is known about how these compounds exert these beneficial wound healing effects. In order to elucidate the mechanistic actions of both EBC-46 and EBC-211, global gene expression analysis was performed through the use of Microarray studies.

Due to the high-throughput of Microarray studies with thousands of genes analysed per sample and compared across conditions, a number of techniques were performed to narrow down the results produced with the aim of illuminating which genes were involved in producing the preferential wound healing response observed in the palliative veterinary studies. The process used in this global gene analysis was direct hybridisation, using the Eberwine protocol assay and Illumina's proprietary BeadArray technology, which has high sensitivity and reproducibility. Gene-specific probes are able to detect previously labelled cRNA in samples and detect transcriptional changes between samples through detecting mRNA transcripts and quantifying the expression (Schulze & Downward 2000; Miller & Tang 2009; Lovén et al. 2012).

5.2 Aims

The data obtained in Chapter 4 demonstrated the profound effects of EBC-46 and EBC-211 on HaCaT wound healing responses *in vitro*, altering genes and pathways to give rise to such preferential healing responses, such as with enhanced proliferation and migration, along with an accelerated cell cycle progression. Stimulation of proliferation and migration following epoxy-tigliane treatment would be immensely beneficial for the treatment of impaired healing situations, such as

chronic wounds and burn injuries, where rapid re-epithelialisation is necessary to re-establish the protective skin barrier (Candi et al. 2005).

5.3 Materials and Methods

5.3.1 Preparation of EBC-46 and EBC-211

EBC-46 and the lesser active analogue, EBC-211, were both supplied by QBiotics Ltd., Queensland, Australia. EBC-46 and EBC-211 were solubilised in DMSO (Section 2.1). For both compounds, concentrations of 0.001µg/ml, 0.01µg/ml, 0.1µg/ml, 1µg/ml and 10µg/ml were prepared in 1% K-SCM for the assessment of HaCaT wound healing responses (Section 2.2.2). The 100µg/ml was not included as it was previously shown to be cytotoxic to HaCaTs.

5.3.2 HaCaT Culture

The epidermal keratinocyte cell line (HaCaTs) were sourced, cultured, sub-cultured, counted, cryopreserved and mycoplasma screened, as previously described (Sections 2.2.2, 2.2.3, 2.2.4 and 2.2.5 respectively). HaCaTs were seeded and cultured for Microarray analysis *(n=4)*, with samples obtained at 24h and 48h after treatment. Samples were subsequently shipped to the QIMR Berghofer Medical Research Institute in Australia, in order to undertake the Microarray analysis (Section 2.4.1).

5.3.3 Assessment of HaCaT Gene Expression by Microarray Analysis

RNA was extracted from HaCaT samples, purified and quantified; RNA integrity and purity was analysed as previously described (Section 2.4.2 and 2.4.3). Biotinylated, amplified antisense RNA (cRNA) was generated and quantified; cRNA was hybridised to gene-specific sequence BeadChips, as previously described (2.4.4 and 2.4.5).

5.3.4 Microarray Data Acquisition and Data Analysis

BeadChips were scanned using the iScan System on Agilent GS2565 Microarray Scanner (Agilent Technologies Australia, Victoria, Australia); raw data files were filtered and normalised using BeadScan Software (Illumina®, Victoria, Australia). Data was subsequently imported into GeneSpring GX v12.5 expression analysis

software (Agilent Technologies), for normalisation, statistical analysis and heatmap visualization/clustering. Data from each treatment group *(n=4)* was grouped for combined analysis using Ingenuity Pathway Analysis (IPA®) for further analysis of Microarray data, as previously described (Section 2.4.6).

5.3.5 Statistical Analysis of Global Gene Expression Changes

Statistical analysis was carried out on the differences in gene expression by an unpaired T-Test unpaired, with Benjamini-Hochberg, multiple testing correction. Statistical significance was considered at $p<0.05$. Data from each experiment group *(n=4)* was combined for analysis, with hierarchical clustering analysis performed for the comparison between treated samples and untreated controls. Hierarchical clustering analysis allowed relationships between treatment groups to be observed, comparing EBC-46 (0.001µg/ml, 0.1 µg/ml and 10 µg/ml) and EBC-211 (0.001µg/ml, 0.1 µg/ml and 10 µg/ml) at 24h and 48h. Fold-changes in gene expression for each treatment group were identified; and compared to the untreated control for each respective time-point.

5.4 Results

5.4.1 Effects of EBC-46 and EBC-211 on Global Gene Expression

The Microarray analysis identified a number of genes differentially expressed after treatment with EBC-46 and EBC-211 (0.001µg/ml, 0.1 µg/ml and 10 µg/ml) at 24h and 48h, when compared to untreated controls at the same time-points. Due to the large number of genes analysed, only those differentially expressed ≥2 fold were focused upon.

Hierarchal clustering was performed in GeneSpring, producing heatmaps and organising the gene expression data, based on how similar their expression was and showed sections of genes which were differentially up- or down-regulated following treatment with EBC-46 or EBC-211 for 24h or 48h. This allowed comparison between each dataset condition and compared epoxy-tigliane treated cells to untreated controls, in addition to comparisons between the different concentrations of epoxy-tiglianes. In an attempt to see which genes were more significantly up-/down-

regulated, heatmaps were also produced showing the greater than 2-fold differentially expressed genes, compared to untreated controls, following 24h and 48h treatment (Figures 5.1A-B and 5.2A-B for EBC-46 and EBC-211, respectively). The heatmaps demonstrated that for the majority of genes analysed, the epoxy-tigliane treated cells produced similar changes in gene expression, compared to untreated controls, irrespective of the concentrations of epoxy-tigliane applied. This was observed through apparent similar levels of up- or down-regulation, compared to the respective untreated controls, for the majority of genes analysed. Any genes of interest were validated at a protein level (Chapter 6), to determine whether the genotypic differences observed after epoxy-tigliane treatment were replicated at a protein level and likely to result in a phenotypic response.

Tables 5.1 and 5.2 show the number of genes differentially expressed ≥2 fold, ≥3 fold, ≥5 fold and ≥10 fold, compared to untreated controls at the same time-points for EBC-46 and EBC-211, respectively. The fold differences in gene expression were determined through the use of GeneSpring GX11, a statistical tool for the analysis of Microarray data. Tables 5.1 and 5.2 show that the greatest number of genes differentially expressed occurred at the higher concentrations of both EBC-46 and EBC-211, especially at 48h post-treatment. This is also when the highest fold-changes in expression were evident. Due to large number of genes identified to be differentially expressed by the Microarray study, the raw data showing all genes differentially expressed is included in Supplement 5.1.

Key differentially expressed genes are displayed for keratins, cell cycle-related genes, cell proliferation-related genes, cell motility-related genes, proteinases, cytokines and chemokines, ECM component genes; and cell signalling-related genes (Supplement 5.2; Tables 5.1, 5.2, 5.3, 5.4, 5.5, 5.6, 5.7 and 5.8, respectively). All genes shown are differentially expressed by more than 2-fold, with some genes belonging to multiple categories due their exertion of a number of cellular functions. As shown in Supplement 5.2; Tables 5.1-5.8, some genes are present more than once on each BeadChip, with separate probe IDs/Entrez Gene ID. This provides additional validation of expression changes, compared to untreated controls. This resulted in more than one value produced for some differentially expressed genes compared to

Figure 5.1: Heatmap visualization through hierarchical clustering of genes differentially ≥2 fold expressed by HaCaTs (*n=4* biological samples), cultured in the presence of 0.001µg/ml, 0.1µg/ml or 10µg/ml EBC-46 at 24h (A) and 48h (B), and compared to an untreated control. (A) Lane 1 = Untreated HaCaT control; Lane 2 = 0.001µg/ml EBC-46; Lane 3 = 10µg/ml EBC-46. (B) Lane 1 = Untreated HaCaT control; Lane 2 = 0.001µg/ml EBC-46; Lane 3 = 0.1µg/ml EBC-46; Lane 4 = 10µg/ml EBC-46. Red = up-regulated genes, Green = down-regulated genes.

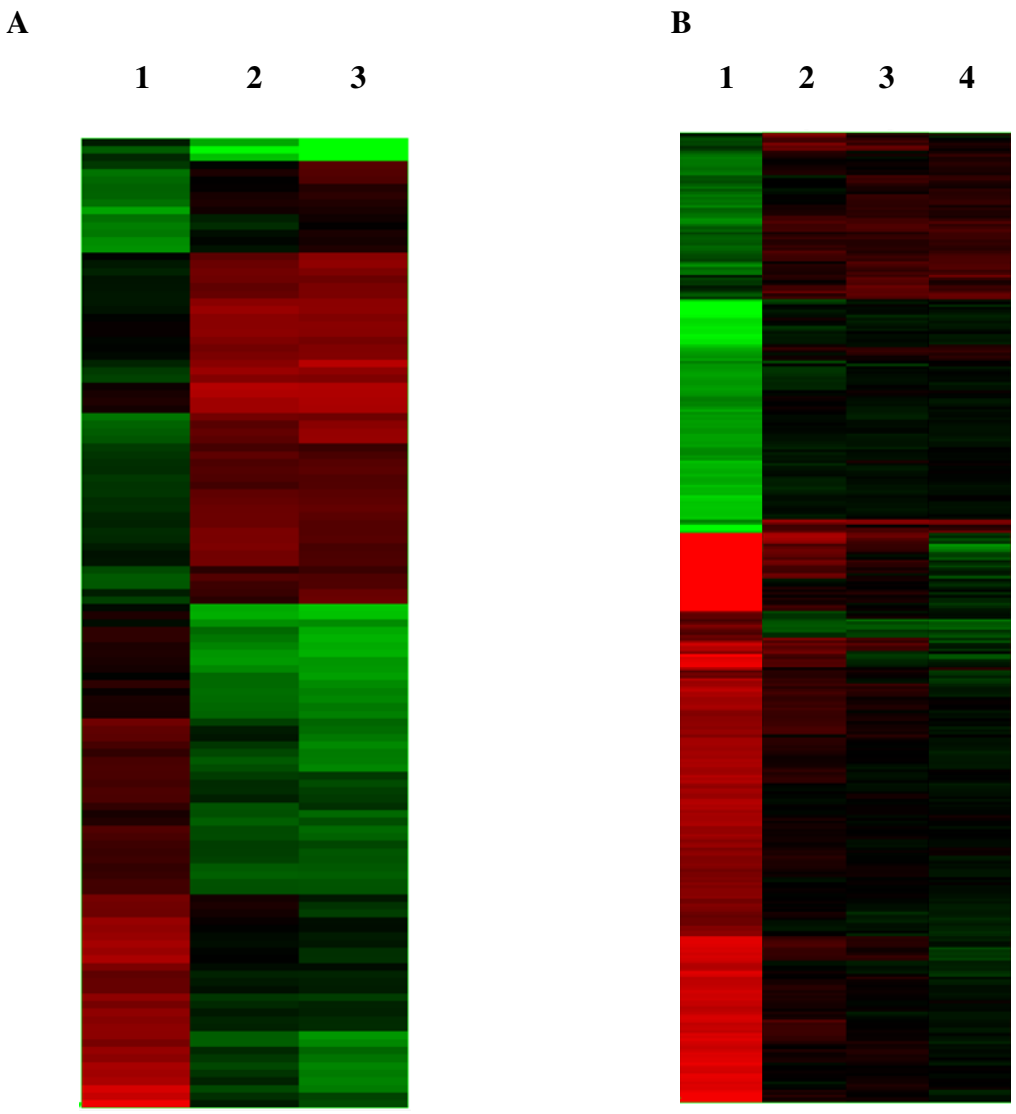

Figure 5.2: Heatmap visualization through hierarchical clustering of genes differentially ≥2 fold expressed by HaCaTs (*n=4* biological samples), cultured in the presence of 0.001µg/ml, 0.1µg/ml or 10µg/ml EBC-211 at 24h (A) and 48h (B), and compared to an untreated control. (A) Lane 1 = Untreated HaCaT control; Lane 2 = 0.001µg/ml EBC-211; Lane 3 = 10µg/ml EBC-211. (B) Lane 1 = Untreated HaCaT control; Lane 2 = 0.001µg/ml EBC-211; Lane 3 = 0.1µg/ml EBC-211; Lane 4 = 10µg/ml EBC-211. Red = up-regulated genes, Green = down-regulated genes.

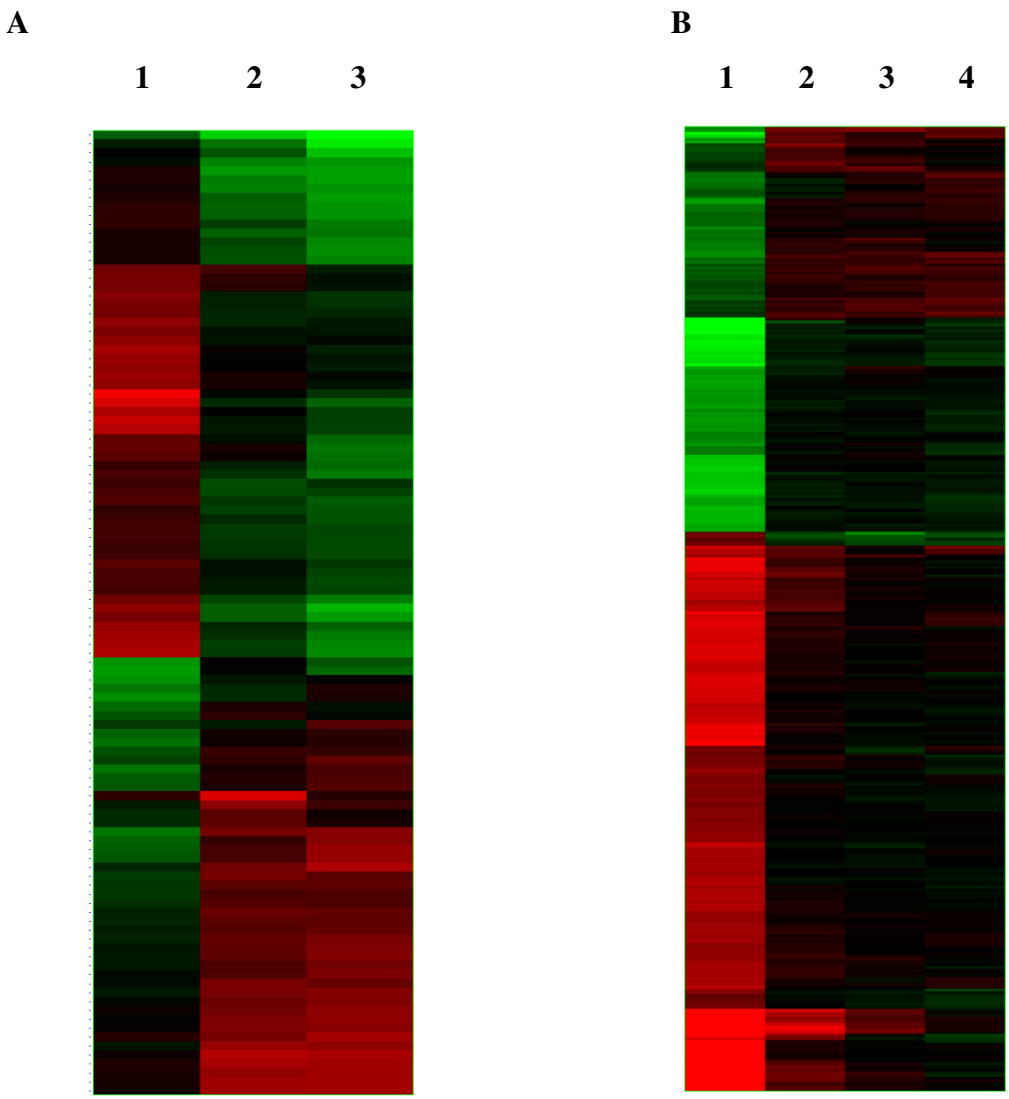

Table 5.1: Number of genes differentially expressed ≥ 2-fold, ≥ 3-fold, ≥ 5-fold and ≥ 10-fold in HaCaTs cultured with EBC-46 (0.001µg/ml, 0.1µg/ml or 10µg/ml) for 24h or 48h, in comparison to untreated controls.

	EBC-46									
	24h				48h					
	0.001µg/ml		10µg/ml		0.001µg/ml		0.1µg/ml		10µg/ml	
	Up-regulated	Down-regulated	Up-regulated	Down-regulated	Up-regulated	Down-regulated	Up-regulated	Down-regulated	Up-regulated	Down-regulated
≥ 2-fold	53	55	64	145	161	215	161	215	167	266
≥ 3-fold	2	9	5	40	34	64	34	64	35	111
≥ 5-fold	0	0	0	10	2	16	2	16	3	30
≥ 10-fold	0	0	0	1	0	0	0	0	0	6

Table 5.2: Number of genes differentially expressed ≥ 2-fold, ≥ 3-fold, ≥ 5-fold and ≥ 10-fold in HaCaTs cultured with EBC-211 (0.001µg/ml, 0.1µg/ml or 10µg/ml) for 24h or 48h, in comparison to untreated controls.

	EBC-211									
	24h				48h					
	0.001µg/ml		10µg/ml		0.001µg/ml		0.1µg/ml		10µg/ml	
	Up-regulated	Down-regulated	Up-regulated	Down-regulated	Up-regulated	Down-regulated	Up-regulated	Down-regulated	Up-regulated	Down-regulated
≥ 2-fold	37	33	62	126	146	138	159	215	130	220
≥ 3-fold	2	8	5	25	29	30	35	72	27	76
≥ 5-fold	0	0	0	6	3	5	1	13	2	22
≥ 10-fold	0	0	0	0	0	0	0	1	0	2

the untreated control, some genes are present on more than one BeadChip, resulting in two probe IDs for these genes. This can provide further confirmation of differentially expressed genes, if result observed for both BeadChips.

No genes were differentially expressed when the comparisons were made between the same concentration of EBC-46 and EBC-211, at each time-point ($p>0.05$). However, there were differentially expressed genes evident between 0.001µg/ml, 0.1µg/ml and 10µg/ml EBC-46 and EBC-211. This was particularly evident when comparing the lower concentrations of EBC-46 and EBC-211 (0.001 and 0.1µg/ml) to the higher concentration (10µg/ml); which may explain the superior wound repopulation responses evident at lower EBC-46 and EBC-211 concentrations (Supplement 5.2; Tables 5.9-16).

Ingenuity Pathway Analysis (IPA®) Software was used to analyse the Microarray data, using Ingenuity Knowledge Base to visualise gene pathways. Pathway analysis helped determine the resultant downstream effects of gene expression changes following novel epoxy-tigliane treatment. The regulator effect networks determined using IPA® software, shown in Figures 5.3-5.8, display predicted downstream phenotypic responses, according to the increase or decrease in expression of particular genes. Regulator effects were shown to predict stimulated proliferation of cells following 48h treatment with 0.001µg/ml or 0.1µg/ml EBC-46 (Figure 5.3). Significantly enhanced proliferative response was observed during the *in vitro* viability and proliferation studies (Figure 4.1A), although this study showed the enhanced proliferative ability for all concentrations of EBC-46. In addition, the growth and development of epithelial tissue was predicted to be stimulated following treatment with 0.001µg/ml and 0.1µg/ml EBC-46, but again not at 10µg/ml (Figure 5.4). This response was also observed following 48h treatment with 0.1µg/ml EBC-211, potentially contributing to the enhanced re-epithelialisation observed during the *in vivo* veterinary studies.

Figures 5.5-5.8 demonstrate that the result of epoxy-tigliane treatment and subsequent gene expression changes likely to produce a migratory response on the cells, which was previously seen in the observational experiments (Chapter 4). This

Figure 5.3: Regulator effects on HaCaTs after 48h treatment with 0.001µg/ml or 0.1µg/ml EBC-46; resulting in proliferation of cells.

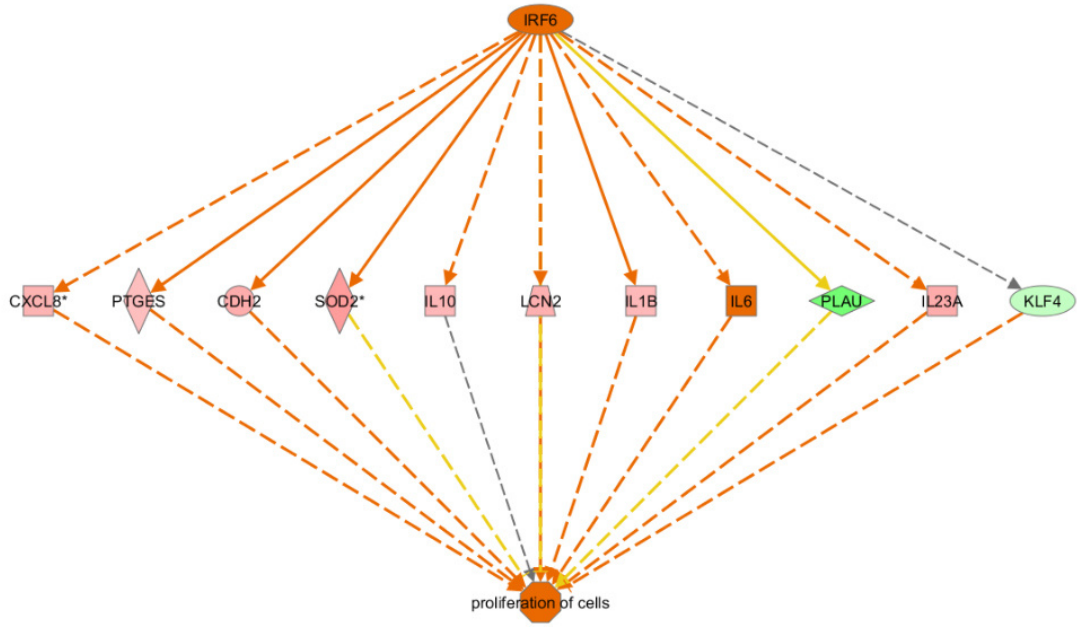

Figure 5.4: Regulator effects on HaCaTs after 48h treatment with 0.1µg/ml EBC-211; resulting in cell viability, leukocyte migration, growth of epithelial tissue, development of cardiovascular and epithelial tissue; and inhibited apoptosis of blood cells.

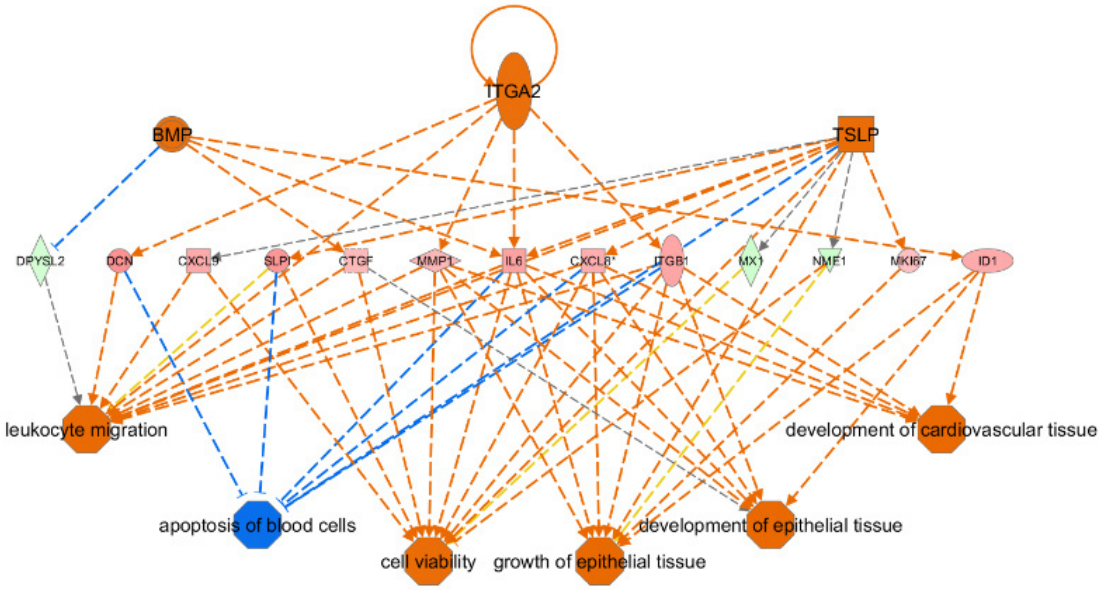

Figure 5.5: Regulator effects on HaCaTs after 48h treatment with 0.001µg/ml or 0.1µg/ml EBC-46; resulting in migration of cells, activation of cells, synthesis of nitric oxide and protein kinase cascade.

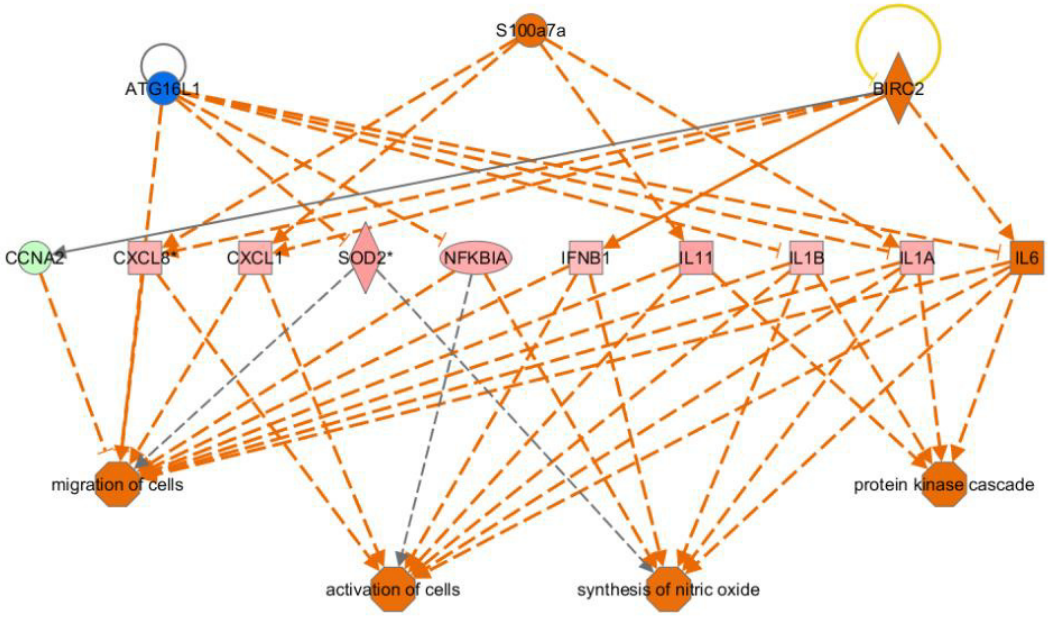

Figure 5.6: Regulator effects on HaCaTs after 48h treatment with 0.001µg/ml or 0.1µg/ml EBC-46, resulting in migration of cells, activation of cells, growth of epithelial tissue; and development of cardiovascular and epithelial tissue.

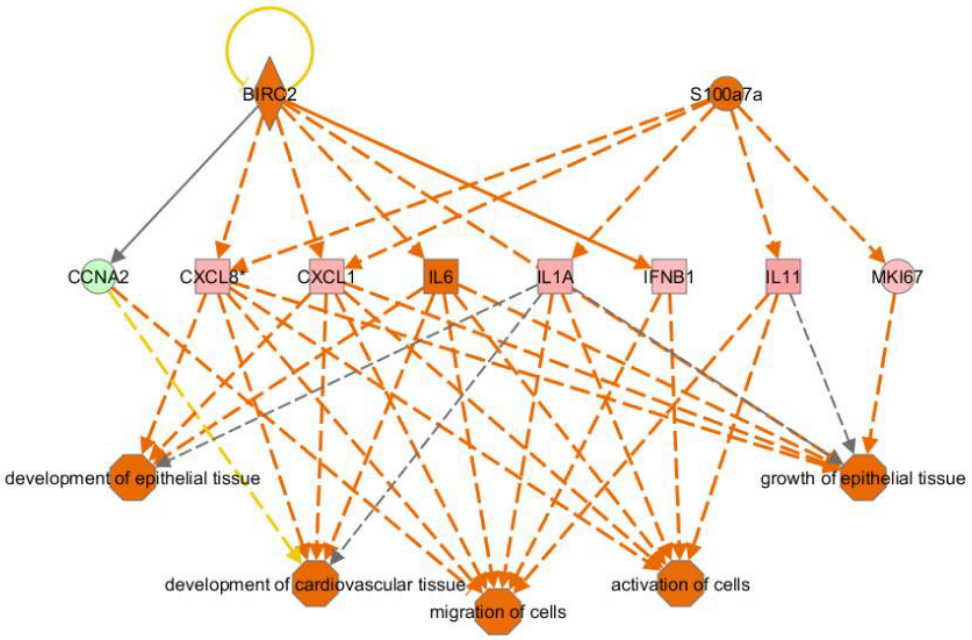

Figure 5.7: Regulator effects on HaCaTs after 48h treatment with 0.001µg/ml EBC-211; resulting in migration of cells.

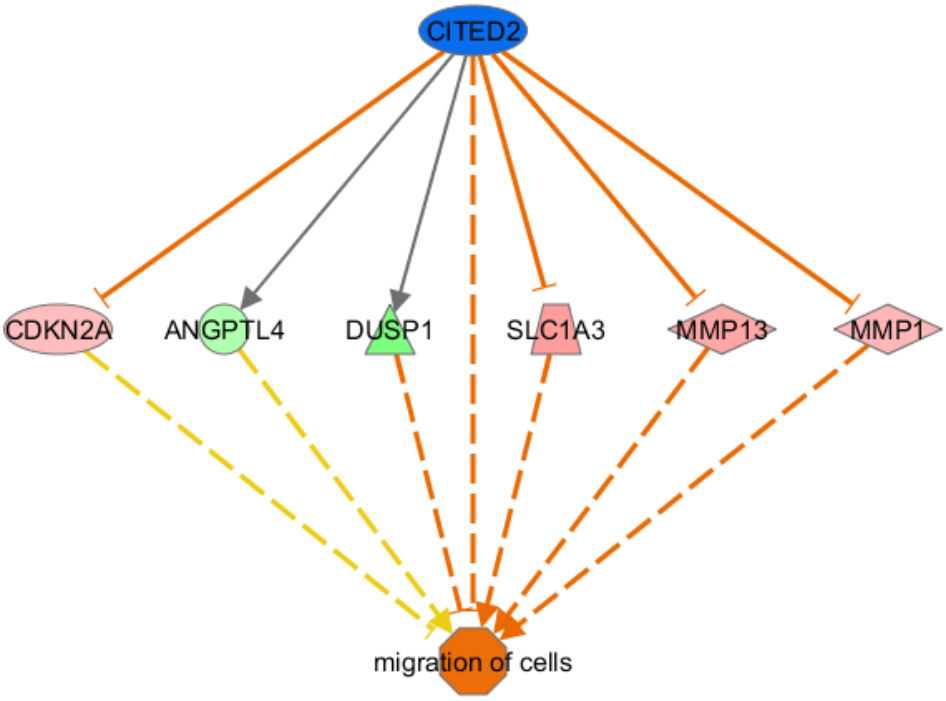

Figure 5.8: Regulator effects on HaCaTs after 48h treatment with 0.1µg/ml EBC-211; resulting in cell movement.

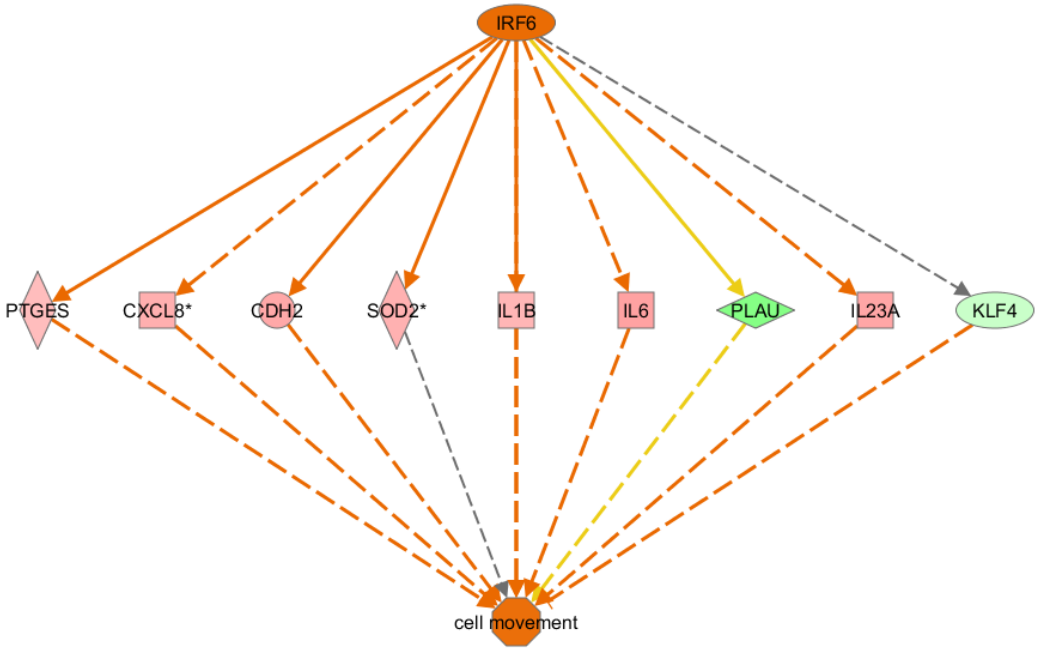

is particularly evident for Figures 5.5 and 5.6, where the migration of cells was predicted to be stimulated due to the differentially expressed genes shown. This was observed for 0.001µg/ml and 0.1µg/ml EBC-46, but not at 10µg/ml. This corroborates the *in vitro* wound repopulation studies, where significantly enhanced migration was evident for these two concentrations of EBC-46, but not 10µg/ml (Figure 4.27). Other regulator effects were shown to predict stimulated migration of cells or movement of cells, evident following 0.001µg/ml or 0.1µg/ml EBC-211 treatment, respectively (Figures 5.7 and 5.8, respectively). Migration of cells and movement of cells are listed as two separate functions, although there are a number of genes involved in both functions. Movement of cells may induce a motility response, whereas migration of cells may indicate a chemoattractant force stimulating a directional movement of cells. Significantly enhanced migration was also evident at the lower concentrations of EBC-211, shown through the *in vitro* wound repopulation studies (Figure 4.27).

Despite both EBC-46 and EBC-211 stimulating cell migration, there are different genes involved in these regulator effect responses. The regulator effect response for EBC-46 appears to involve chemokines, potentially inducing a chemoattractant gradient; whereas EBC-211 involved some metalloproteinases, so may induce the migratory response through degradation of the provisional matrix required for keratinocyte migration to occur (Michel et al. 1992; Pilcher et al. 1997; Engelhardt et al. 1998; Nagase et al. 2006; Kroeze et al. 2012; Nuutila et al. 2012). It is not fully understood yet why there are differences in these regulator responses, when the previous *in vitro* studies showed some similar responses between the two epoxy-tiglianes.

5.5 Discussion

The global gene analysis performed in this Chapter aimed to distinguish differentially expressed genes following EBC-46 and EBC-211 treatment at 24h and 48h, compared to untreated controls. The aim of this analysis was to identify which genes contribute to the beneficial HaCaT wound healing responses observed, both through the *in vitro* studies performed (Chapters 3 and 4) and the *in vivo* animal

palliative studies performed by QBiotics Ltd. As discussed previously, there are a number of genes involved in producing preferential or detrimental wound healing responses. Therefore, this study was undertaken to elucidate any potential expression changes in genes relevant to these HaCaT responses and the overall healing process. The aim was that some of these differentially expressed genes might explain the strong proliferative and migratory response in HaCaTs, along with the enhancement of cell cycle progression, following epoxy-tigliane treatment. As apparent in Tables 5.1 and 5.2, there are a large number of genes differentially expressed following EBC-46 and EBC-211 treatment, across all concentrations and time-points. IPA® software was instrumental in determining the impact these gene expression changes have on wound healing functions, narrowing down the genes of interest for further protein-based validation (Chapter 6).

There was a greater number of fold-changes in expression after 48h treatment for both epoxy-tiglianes, compared to 24h treatment. Similar patterns in differentially expressed genes were observed, when comparing the two epoxy-tiglianes at the same concentration and time-point; no genes were shown to be differentially expressed in this comparison. As previously mentioned, a number of genes were shown to be differentially expressed in comparisons between different concentrations of each epoxy-tigliane and compared to the other epoxy-tigliane, at the same time-point. These were predominantly the same genes, as observed when compared to the untreated controls. Due to the large number of genes analysed, the genes were further categorised by their function during the wound healing process and analysed accordingly. However, certain genes impart multiple cellular functions and therefore, fell into several categories. Therefore, these have been allocated into one category only for the purpose of displaying the results from this study. Despite the dramatic concentration differences evident during the *in vitro* studies, in particular during the wound repopulation and closure analysis, there was not a huge difference in expression fold-change across the concentrations for EBC-46 or EBC-211. In addition, the fold-changes observed were similar for EBC-46 and EBC-211 concentrations, compared to the untreated controls. However, there did appear to be a greater number of genes seen to be differentially expressed in each category of ≥ 2-

fold, ≥ 3-fold, ≥ 5-fold and ≥ 10-fold, with increasing concentration for both epoxy-tiglianes.

5.5.1 Keratins

Numerous keratins were found to be differentially expressed in this Microarray study following epoxy-tigliane treatment, when compared to untreated controls. This study showed that keratin (Krt)13, Krt15 and Krt9 were predominantly upregulated following 48h treatment with both epoxy-tiglianes, with Krt81 upregulated following 24h. In all cases, this upregulation was greater than 2-fold change in expression, compared to the respective untreated controls, with Krt13 and Krt15 upregulated approximately 4-7 fold.

The profound upregulation of Krt13 and Krt15 is of particular interest, as these are keratin types not typically found in adult skin epithelia. These keratins are present in non-keratinized, oral mucosal and foetal epithelia respectively, which are both recognised as preferential healing responses with rapid re-epithelialisation (Waseem et al. 1999; Turabelidze et al. 2014). A Microarray study by Turabelidze et al. (2014), showed an increased presence of Krt13 in oral mucosal epithelium, in contrast to the situation with skin epithelium (Bragulla & Homberger 2009). Additionally, Krt13 has also been documented to be present in the suprabasal layer of foetal epithelia and has a role in the regeneration of the epidermis (Kallioinen et al. 1995). Krt15 is present in basal keratinocytes and plays a major role in keratinocyte proliferation; this keratin is found to be upregulated and partner with Krt5 in the absence of Krt14 (Bragulla & Homberger 2009; Bose et al. 2013). Krt15 has been associated with tissue development and providing structural integrity to the developing basal layer, due to its' continuous presence in foetal epithelium compared to a discontinuous presence in the skin epithelium (Waseem et al. 1999; Bose et al. 2013). Krt15 has also been referred to as an epidermal stem cell marker and is present in the hair follicle bulge, an area that has been previously thought of as a stem cell niche (Liu et al. 2003; Bose et al. 2013). The upregulation of these two keratins following epoxy-tigliane treatment may be partly responsible for the

exceptional wound healing response observed, where the healing mechanism appears to be more representative of a regenerative healing model (Yates et al. 2012).

The Microarray analysis also showed a down-regulation of Krt6B, Krt16 and Krt17 at 2-4 fold, compared to untreated controls, at 24h and 48h. Krt16, Krt17 and Krt6B are typically absent from the epidermis in uninjured skin, but are induced following wounding and play a part in the wound healing response (Santos et al. 2002; Mazzalupo et al. 2003). These keratins form heterodimers and are associated with a hyperproliferative and migratory response, which is beneficial to wound healing situations in the repopulation of denuded sites if carefully controlled (Freedberg et al. 2001; Komine et al. 2001; Trost et al. 2010). Krt17 is typically found in complex epithelia, such as hair follicles, but not healthy epidermal skin (Shen et al. 2006; Jin & Wang 2014). Despite the roles of Krt6, Krt16 and Krt17 in the wound healing response, these keratins are also associated with a detrimental healing process. Downregulation of Krt6 has also been associated with increased keratinocyte migration and resultant re-epithelialisation (Wong & Coulombe 2003). The association between Krt17 expression and psoriasis is so well-established, that Krt17 expression levels are used diagnostically to determine the presence and severity of psoriatic disorders (Zhang et al. 2012). Additionally, an overexpression of Krt16, which occurs in aged skin, has been demonstrated to have an inhibitory effect on migratory potential of wound edge keratinocytes, although Krt16 has been associated with providing mechanical strength to these keratinocytes, instead of inducing migration (Trost et al. 2010). It has been hypothesised by Trost et al. (2010) that a careful balance between expressions of these keratins is necessary to provide strength at the wound edge, whilst also permitting the migration of keratinocytes across the wound site. The downregulation of these three keratins was not expected given their important role in wound healing. However, given that their expression is induced following wounding, this might explain the lack of upregulation observed following epoxy-tigliane treatment. Of particular interest was their inhibitory action on keratinocyte migration, the decreased expression of these keratins may contribute to the enhanced migratory responses observed during the *in vitro* wound repopulation studies and the animal *in vivo* studies.

5.5.2 Cell Cycle-Related Genes

A number of cell cycle-related genes were shown to be upregulated following epoxy-tigliane treatment, compared to untreated controls. This upregulation was in the range of 2-4 fold. Genes of particular interest that were upregulated included, cyclin B2 (CCNB2), cyclin B1 (CCNB1), cyclin A2 (CCNA2), cyclin-dependent kinase inhibitor 3 (CDKN3), ubiquitin-conjugating enzyme E2C (UBE2C), cell division cycle associated 7 (CDCA7), centrosomal protein 55kDa (CEP55) and E2F transcription factor 2 (E2F2). For the majority of these genes, the upregulation was only present at 48h. In contrast, cyclin-dependent kinase inhibitor 1A (CDKN1A) was downregulated following epoxy-tigliane treatment 2-3 fold across all conditions, compared to untreated controls.

Cyclin genes in particular were found to be upregulated, which are associated with the progression of cells into mitosis, along with cyclin-dependent protein kinases (CDKs), through the formation and dissociation of cyclin-CDK complexes (Hochegger et al. 2008; Huang et al. 2013). When cyclins bind to a CDK and subsequently activate, this signals to the cell to progress onto the next cell cycle phase (Alberts et al. 2002; Vermeulen et al. 2003; Huang et al. 2013). There is a specific association between cyclins and CDKs, an example is the complex formed between CCNB1 or CCNB2 and CDK1; this complex is involved in the progression of cells into M phase, initiating mitosis (Vermeulen et al. 2003; Hochegger et al. 2008; Huang et al. 2013). CCNB1, CCNB2 and CCNA2 promote G2-M transition, while CCNA2 also controls G1-S transition for DNA synthesis (Wu et al. 2010; Huang et al. 2013). The combined effect of these upregulated genes would result in the stimulated progression of cells into S phase and M phase, subsequently enhancing the proliferative effect on cells (Gong & Ferrell 2010). CCNB1 and CCNB2 are essential regulators of mitosis-promoting factor (MPF), through the formation of complexes with CDK1 or CDC2; although expression of these cyclins is also increased in cancers (Tschöp & Engeland 2007).

In addition to the cyclins required for mitosis to occur, cyclin-dependent inhibitors are also crucial. CDKN3 has been shown to regulate the G1 to S phase transition by arresting G1 phase, along with controlling the normal function of mitosis (Nalepa et

al. 2013). The loss or mutation of CDKN3 has been linked to the formation of several cancer types. As a result, this inhibitor is referred to as a tumour suppressor by preventing abnormal mitosis occurring (Nalepa et al. 2013). Another cyclin-dependent kinase inhibitor differentially expressed was CDKN1A, a potent inhibitor of cell cycle progression. CDKN1A acts through inhibiting the action of cyclin/CDK complexes, in particular complexes which contain CDK2, such as the complex formed with CCNA2. This subsequently prevents the transition of cells from G1 to S phase (Gartel & Tyner 2002; Koljonen et al. 2006). In this study, CDKN1A was downregulated after epoxy-tigliane treatment, reducing the inhibition of cell cycle progression and proliferative ability of the cells. Another essential factor for cell cycle progression differentially expressed after epoxy-tigliane treatment is UBE2C, which was upregulated greater than 3-fold at 48h with both EBC-46 and EBC-211. Cyclin-CDK complexes have to be disrupted to allow progression of cells into mitosis. UBE2C is involved in the breakdown of these cyclins, stimulating cell proliferation (Hao et al. 2012; Shen et al. 2013; Chou et al. 2014; Xie et al. 2014). However, overexpression of UBE2C can have a detrimental effect on the cell cycle profile, by the loss of certain crucial mitotic checkpoints. As a result, this gene has also been associated with a number of cancer types (Hao et al. 2012; Xie et al. 2014). Overall, these differentially expressed cell cycle-related genes result in an increased proliferative potential of keratinocytes, through enhanced cell cycle progression, maintenance of normal mitosis and a reduced inhibitory effect on cell cycle progression. This likely contributes to the enhanced cell cycle progression, following epoxy-tigliane treatment, observed during the flow cytometry studies; in addition, to the resultant increased proliferative ability observed during the *in vitro* viability and proliferation studies. The veterinary *in vivo* case studies showed enhanced wound re-epithelialisation, with increased keratinocyte proliferation potentially contributing to this response, this may be aided by the increased cell cycle progression due partly to these differentially expressed genes.

5.5.3 Cell Proliferation-Related Genes

There were a number of cell-proliferation genes differentially expressed following epoxy-tigliane treatment, including GINS complex subunit 2 (GINS2), polymerase (DNA directed), epsilon 2, accessory subunit (POLE2), KIAA0101 and parathyroid

hormone-like hormone (PTHLH). These genes were up-regulated in EBC-46- and EBC-211-treated cells between 2-4 fold, compared to untreated controls. GINS2 is a known gene involved in DNA replication, through its part in the replicative helicase allowing the progression of cells into S phase and subsequent cell division. GINS2 is also involved in the DNA damage response and DNA repair (Rantala et al. 2010; Gao et al. 2013; Zheng et al. 2014).

As previously discussed, keratinocyte wound healing responses have a paracrine feedback system with dermal fibroblasts, along with an autocrine feedback response (Bader & Kao 2009). One of the key genes involved in this feedback system is PTHLH, which is secreted by keratinocytes and acts on fibroblasts. PTHLH stimulates keratinocyte growth factor (KGF) expression in fibroblasts, a growth factor involved in keratinocyte wound healing responses (Blomme et al. 1999). PTHLH has been shown to have a proliferative effect on keratinocytes, with the expression increased throughout the cell cycle until mitosis is reached, where the greatest expression is observed (Feuerherm et al. 2013). Epoxy-tigliane induced upregulation of this gene may play a part in the increased keratinocyte proliferative response observed. These cell proliferation-related genes have been shown to directly or indirectly increase keratinocyte proliferative ability. This suggests their involvement in the enhanced proliferation observed during the *in vitro* studies. In addition, this upregulation may be involved in the potential increase in keratinocyte presence at the wound site during the animal *in vivo* case studies.

5.5.4 Cell Motility-Related Genes

The S100 proteins are a family of calcium binding proteins, with a wide array of functions through action on a range of cell types (Lee & Eckert 2007; Zibert et al. 2010). Some of the genes for this protein family were differentially expressed following epoxy-tigliane treatment, including S100A4, S100A7, S100A7A, S100A8, S100A9 and S100A12 (Mazzucchelli 2002; Lee & Eckert 2007; Zibert et al. 2010; Gross et al. 2014).

S100A4 was the only gene from this family that was upregulated at 48h with EBC-46 and EBC-211, with the up-regulation ranging between 2-3-fold, compared to

untreated controls. S100A4 has been shown to have a positive effect on cell proliferation, through affecting the cell cycle progression, with increased expression resulting in enhanced G1 to S phase transition. However, potentially due to this stimulatory effect on cell proliferation, along with a stimulatory effect on cell invasion, S100A4 has also been implicated in cancer progression, with a higher expression often correlating to a poor clinical outcome (Cajone & Sherbet 2000; Mazzucchelli 2002; Klingelhöfer et al. 2009). This enhanced proliferative effect can have detrimental outcomes, with an excessive expression of S100A4 also being linked to psoriasis (Zibert et al. 2010). This protein has also been shown to enhance a number of other cellular functions, such as cell motility, survival, differentiation and angiogenesis. The effect on cell motility may be a result of changes to the organisation of actin in the cell, increasing cell protrusions (Klingelhöfer et al. 2009; Sin et al. 2011).

S100A7, also known as psoriasin, and S100A7A (koebnerisin/S100A15) were down-regulated following epoxy-tigliane treatment, between 3-19-fold, compared to untreated controls. Increased expression of these two proteins has also been associated with psoriatic skin (Hattinger et al. 2013). They also have a chemoattractant activity, recruiting more immune cells to the site and subsequently enhancing the inflammatory reaction. However, due to the strongly similar structure of these two proteins, it is difficult to distinguish between them and determine which performs certain functions (Büchau et al. 2007; Wolf et al. 2011; Hattinger et al. 2013). S100A8 and S100A9, down-regulated between 2-11-fold and 4-8-fold respectively, are also expressed highly in psoriatic skin, along with S100A7; although despite psoriasis being a result of uncontrolled proliferation, a study has showed that over-expression of S100A8/A9 in HaCaTs reduces proliferation (Martinsson et al. 2005; Zibert et al. 2010; Voss et al. 2011). S100A8/A9 have been shown to be up-regulated after wounding, with the chemotaxis of immune cells to the site; and also where the epithelium is hyperproliferative (Thorey et al. 2001; Voss et al. 2011). S100A12 was down-regulated between 2-3-fold compared to untreated controls, along with a number of the other S100 family calcium binding proteins; S100A12 also has a chemoattractant effect on immune cells (Thorey et al. 2001; Gross et al. 2014). This protein is also found to be over-expressed in psoriatic

lesions, with expression correlating to severity of the skin disorder; expression is increased following stimulation by pro-inflammatory cytokines (Moroz et al. 2003; Wilsmann-Theis et al. 2015). The overall effect of these differentially expressed genes results in an enhanced proliferative response in keratinocytes, but would potentially inhibit the induction of a hyperproliferative response, as observed in psoriasis. In addition, increased cell mobility and decreased differentiation responses are potentially induced, as a result of these gene expression changes. This could lead to the enhanced proliferation and migration of keratinocytes observed *in vitro*, through proliferation and wound repopulation studies, respectively. As a rapid re-epithelialisation response was also observed during *in vivo* studies, these differentially expressed genes could contribute to this response, by enhancing keratinocyte proliferation and motility.

5.5.5 Proteinase and Proteinase Inhibitor Genes

In the proteinase and proteinase inhibitor gene category, some key wound healing proteases were differentially expressed between 2-6 fold, namely matrix metalloproteinase (MMP)-1, MMP-7 and MMP-10, which were upregulated following epoxy-tigliane treatment. Keratinocytes are the predominant producer of these three MMPs (Xue & Jackson 2015). However, no tissue inhibitors of metalloproteinases (TIMPs) were differentially expressed greater than 2-fold following epoxy-tigliane treatment.

Peptidase inhibitor 3, skin derived (PI3), also referred to as elafin, is a serine protease inhibitor and was shown to be profoundly downregulated following epoxy-tigliane treatment, between approximately 6-15-fold, when compared to untreated controls (Nakane et al. 2002; Pol et al. 2003). A number of serpin peptidase inhibitors (SERPINs) were differentially expressed following epoxy-tigliane treatment. SERPINA3, SERPINB3, SERPINB4 were all downregulated between approximately 2-8-fold, whereas SERPINB2 was upregulated approximately 2.3-fold at the lower concentrations of EBC-46 and EBC-211.

MMP-1 is a key proteinase in wound healing, which has a specific proteolysis action on type I collagen; this allows the migration of keratinocytes into the wound site and

for the subsequent re-epithelialisation process (Pilcher et al. 1997; Vu & Werb 2000; Agren et al. 2001; Dasu et al. 2003; Nagase et al. 2006; Muller et al. 2008; Nuutila et al. 2012; Rohani et al. 2014). Studies have shown that inhibiting MMP activity through use of broad spectrum inhibitors, GM 6001 or BB-94, resulted in a lack of keratinocyte migration, indicating the importance of MMP activity; however, re-epithelialisation did eventually occur despite constant presence of BB-94 (Agren et al. 2001; Mirastschijski et al. 2004; Mirastschijski et al. 2010). However, a careful balance of expression of MMPs is necessary as an increased expression for a longer time period can also be associated with non-healing wounds, such as chronic wounds; this excessive disruption of the ECM during chronic wounds has been shown to impede keratinocyte migratory ability, due to the fragmented nature of degraded ECM (Vaalamo et al. 1996; Pilcher et al. 1997; Trengrove et al. 1999; Cook et al. 2000; Saito et al. 2001; Mwaura et al. 2006; Beidler et al. 2008; Brandner et al. 2008; Eming et al. 2008; Muller et al. 2008; Alsaigh et al. 2011; Rohani & Parks 2015).

Conversely, keloid and hypertrophic scars have been shown to have decreased expression of MMP-1; with studies showing that increasing MMP-1 expression aids fibrosis through increased degradation of collagen, leading to therapies targeting increase of MMP-1 activity (Dasu et al. 2004; Cho et al. 2010; Eto et al. 2012; Aoki et al. 2014; Li et al. 2014; Rohani & Parks 2015). However, increased MMP-1 expression has been shown in some keloid studies, allowing the fibrotic response to extend past the wound margin, through a degradative action on collagen (Fujiwara et al. 2005; Shih et al. 2010).

MMP-7, also known as matrilysin, is typically found in mucosal epithelium and has been shown to be upregulated following bacterial infection and epithelial injury, where it plays a role in inflammation and repair (Kassim et al. 2007; Gill & Parks 2008; Chen et al. 2009; Rohani & Parks 2015). It has also been shown to degrade the basement membrane to allow keratinocyte migration and subsequent re-epithelialisation (Kassim et al. 2007; Chen et al. 2009; Philips et al. 2011). Increased levels of MMP-7 have been observed in chronic wounds or following exposure to *Staphylococcus aureus*; and associated with an increased degradative activity at the

wound site (Kanangat et al. 2006; Löffek et al. 2011; Puthenedam et al. 2011; Letra et al. 2013). MMP-10 (stromelysin-2) is expressed in wound edge keratinocytes and has been associated with keratinocyte migration following injury, through degradation of basement membrane collagens (Saarialho-Kere et al. 1994; Vaalamo et al. 1997; Rohani et al. 2015; Schlage et al. 2015). However, the function of MMP-10 on wound healing has yet to be fully elucidated. All three MMPs discussed appear to induce positive responses on keratinocyte migration, contributing to re-epithelialisation. Therefore, an increased expression of all in the Microarray studies following epoxy-tigliane treatment may account for the greatly enhanced migratory responses observed during the *in vitro* scratch wound repopulation studies; and the induction of a rapid re-epithelialisation during *in vivo* studies. Although, the *in vitro* migration assay was performed on tissue culture plastic and not an ECM, which would replicate *in vivo* settings more accurately (Kramer et al. 2013).

SERPINs are irreversible protease inhibitors involved in a number of wound healing functions, including coagulation, inflammation, angiogenesis and apoptosis (Janciauskiene 2001; Pike et al. 2002; Nuutila et al. 2012). A number of SERPINs are induced by tumour necrosis factor-α (TNF)-α, including SERPINB1, SERPINB2, SERPINB3 and SERPINB8; due to their protease inhibitory action, this may be a protective mechanism for the keratinocytes against increased inflammatory environments (Banno et al. 2004). SERPINA3, also known as α-1-antichymotrypsin (ACT), has been shown to be upregulated following injury and topical application enhanced wound repair in impaired healing situations, such as in diabetic wounds, through induction of granulation tissue formation and re-epithelialisation responses (Hoffmann et al. 2011).

SERPINB2, also known as plasminogen activator inhibitor (PAI)-2 is an inhibitor of urokinase-type plasminogen activator (uPA) and is upregulated following infection; this inhibits the role of uPA on keratinocyte cell cycle progression and subsequent proliferation (Reinartz et al. 1996; Hibino et al. 1999; Risse et al. 2000; Jang et al. 2010). PAI-2 has also been shown to have an increased presence in diabetic wound keratinocytes, contributing to impaired keratinocyte migration; although increased expression has been shown following wounding, stimulating keratinocyte

proliferation (Jensen & Lavker 1996; Zhang et al. 2015). SERPINB3, also known as squamous cell carcinoma antigen-1 (SCCA-1) and SERPINB4, also known as SCCA-2, are almost identical gene products within the SERPIN family (Katagiri et al. 2006; Katagiri et al. 2010). Both SCCA-1 and SCCA-2 have been shown to be present in abnormal skin disorders, such as psoriasis, associated with dysfunctional differentiation and a hyperproliferative profile (Titapiwatanakun et al. 2005; Katagiri et al. 2006; Mee et al. 2007; Yao et al. 2008; Katagiri et al. 2010). They both have also been implicated in inflammation, through increasing the expression of S100A8. Expression of SCCAs may lead to excessive inflammation and chronic wound situations (Sivaprasad et al. 2015). Of interest, protein levels of SCCA-1 were shown to be increased in rapidly healing diabetic wounds, as opposed to non-healing wounds (Fadini et al. 2014).

Some of the differentially expressed SERPIN functions are at contrast with the *in vitro* and *in vivo* results, previously observed. SERPINA3 was shown to be downregulated; whereas it is typically upregulated following injury and capable of stimulating enhanced wound repair in non-healing wounds. However, the samples used for this global gene analysis were not wounded. In addition, the upregulation of SERPINB2 resulting in inhibited keratinocyte proliferation conflicts with the enhanced proliferation observed during the *in vitro* studies. However, expression has been shown to be increased during re-epithelialisation, which may contribute to the rapid re-epithelialisation response observed during these *in vitro* and *in vivo* studies. The downregulation of SERPINB3 and SERPINB4, but enhanced wound repair during the *in vivo* animal studies, is in contrast to the enhanced healing observed in a study in diabetic wounds. The *in vitro* and *in vivo* studies have shown an increased proliferative ability of keratinocytes following epoxy-tigliane treatment, but this increased proliferation may be controlled, due to downregulation of a number of hyperproliferative-related genes.

5.5.6 Cytokine and Chemokine Genes

There was a down-regulation of a number of cytokines and chemokines following epoxy-tigliane treatment. These included tumour necrosis factor-α (TNF-α), interferon β1, fibroblast (IFNB1), chemokine (C-C motif) ligand 2 (CCL2), CCL3,

CCL5 (also known as RANTES), CCL8, CCL20, chemokine (C-X-C motif) ligand 1 (CXCL1), CXCL6; and CXCL10 (also known as IP-10; interferon γ-induced protein 10).

Expression of TNF-α is decreased approximately 2-4-fold at 48h with both EBC-46 and EBC-211, along with 10µg/ml EBC-46 and EBC-211, compared to untreated controls. A higher expression of TNF-α has been shown in non-healing chronic wounds, compared to normal acute skin wounds (Wallace & Stacey 1998; Barrientos et al. 2008; Brandner et al. 2008; Ashcroft et al. 2012; Gragnani et al. 2013). TNF-α stimulates KGF expression, which indirectly promotes re-epithelialisation through stimulating keratinocyte proliferation (Barrientos et al. 2008; Gragnani et al. 2013). However, if TNF-α expression is too high, it has been shown to inhibit the re-epithelialisation process, through increased keratinocyte adhesion and inhibition of keratinocyte proliferation, by keeping the cells in G1 phase (Wallace & Stacey 1998; Banno et al. 2004; Barrientos et al. 2008; Morhenn et al. 2013). It has also been shown to induce a positive response on keratinocyte migration, increasing re-epithelialisation response; although, this motility appeared to be more erratic, with cells migrating in and out of the denuded spaces (Banno et al. 2004; Scott et al. 2004). IFNB1, an inflammatory cytokine, was down-regulated between 3-5-fold following epoxy-tigliane treatment at both 24h and 48h, compared to untreated controls. IFNB1 has been shown to have antiviral properties, along with an anti-proliferative and enhanced differentiation effect on keratinocytes, acting through the Janus kinase/signal transducers and activators of transcription (JAK-STAT) pathway (Yaar et al. 1985; Dai et al. 2008; Ismail & Yusuf 2014; Takiguchi et al. 2014).

CCL5 and CCL2 (also known as MCP-1), are potent chemokines produced by keratinocytes involved in the wound healing process, by attracting immune cells to the wound site, including macrophages and neutrophils (Wetzler et al. 2000; Pastore et al. 2005; Suga et al. 2014; Balaji et al. 2015; Portou et al. 2015). Expression was downregulated following epoxy-tigliane treatment by approximately 2-5-fold, compared to untreated controls; this may result in a reduced inflammatory phase, similar to that seen in foetal wound healing (Larson et al. 2010; Balaji et al. 2015). CCL5 has a role in the majority of phases of the wound healing process: haemostasis,

inflammation and proliferation; in addition it exerts a mitogenic effect on keratinocytes, attracting more to the wound site (Spiekstra et al. 2007; Suga et al. 2014; Balaji et al. 2015). High expression of CCL2 is present in keratinocytes at the wound edge, with a hyperproliferative response. A significantly reduced expression of CCL2, following induction by TNF-α or IFN-γ, is observed in oral keratinocytes, compared to skin keratinocytes (Li et al. 2000). CXCL10, also known as IP-10, is another inflammatory chemokine which was down-regulated between 3-13-fold following epoxy-tigliane treatment, compared to untreated controls during all conditions. CXCL10 is an angiostatic chemokine and expression is induced following wounding; although, increased expression has been associated with detrimental wound healing, due to an elevated inflammatory response (Boorsma et al. 1998; Luster et al. 1998; Bodnar et al. 2006; Barrientos et al. 2008; Zaja-Milatovic & Richmond 2008; Yates-Binder et al. 2012; Lee et al. 2013). This chemokine has been shown to have a stimulatory response on the migratory response of undifferentiated keratinocytes, with delayed re-epithelialisation observed when the receptor for this chemokine, CXCR3, is dysfunctional (Satish et al. 2003; Satish et al. 2005; Behm et al. 2012; Kroeze et al. 2012; Yates-Binder et al. 2012; Zibert et al. 2013; Rees et al. 2015).

Due to the inflammatory response of these cytokines and chemokines on the wound healing process, the downregulation observed following epoxy-tigliane treatment, will potentially attenuate inflammation during wound healing. A dampened inflammatory phase is a characteristic feature of preferential healing responses, such as early-gestational foetal and oral mucosal healing (Liechty et al. 1998; Liechty et al. 2000; Turabelidze & DiPietro 2012; Turabelidze et al. 2014). These genes collectively exert opposing responses on keratinocytes, with expression of some inducing an anti-proliferative or senescent effect on keratinocytes. Reduction of this response may account for the greatly enhanced proliferative responses observed both during the *in vitro* proliferation studies. However, some of these genes are shown to induce migratory responses on keratinocytes, which is in contrast to the profoundly enhanced migration observed during the *in vitro* wound repopulation studies and the rapid re-epithelialisation seen during the *in vivo* studies.

There was a down-regulation of a number of other immune and inflammatory cytokines, including IL-1α, IL-6, IL-8, IL-28, IL-29 and IL-32. IL-1α is a key cytokine involved in skin homeostasis and is released by keratinocytes. This cytokine was down-regulated between 2-3-fold, for most epoxy-tigliane conditions at 48h (Mizutani et al. 1991; Corradi et al. 1995; Chen et al. 1995; Mee et al. 2005; Magcwebeba et al. 2012). It also plays a role in the paracrine feedback relationship between keratinocytes and fibroblasts, acting through c-Jun and JunB in fibroblasts to stimulate the release of KGF and granulocyte macrophage colony-stimulating factor (GM-CSF). These growth factors are strongly involved in stimulating keratinocyte proliferation and subsequent re-epithelialisation (Maas-Szabowski et al. 1999; Maas-Szabowski et al. 2000; Szabowski et al. 2000; Werner et al. 2007; Bader & Kao 2009; Wojtowicz et al. 2014).

There was a profound down-regulation of IL-6 and IL-8, ranging between 2-8-fold following epoxy-tigliane treatment. IL-6 has been shown to be involved in a number of functions, including inflammation, neovascularisation and re-epithelialisation; this was observed through IL-6 knockout mice studies, showing inhibited wound healing responses (Gallucci et al. 2004). Studies have indicated that the migratory response was not through a mitogenic response, as this was shown to be weak. However, it was potentially due to an indirect stimulation through the induction of motogenic factors from fibroblasts; this factor is currently unidentified, but potentially through the STAT3 pathway or through stromal cell-derived factor-1 (SDF-1), acting through extracellular signal-regulated kinases (ERK)/mitogen-activated protein kinases (MAPK) pathway (Gallucci et al. 2004; Hernández-Quintero et al. 2006; Quan et al. 2015). IL-6 and IL-8 appear to stimulate proliferative and migratory responses in keratinocytes, beneficial in wound healing if regulated; however, these can also contribute to the hyperproliferative aspect of such disorders, in addition to an involvement in excessive inflammation (Liechty et al. 1998; Liechty et al. 2000; Rennekampff et al. 2000; Sugawara et al. 2001; Gallucci et al. 2004; Hernández-Quintero et al. 2006; Jiang et al. 2012). There have also been studies showing IL-8 has a stimulatory effect on keratinocyte migration, by producing a chemokinetic gradient response for keratinocytes. This was thought to be mediated through the

phosphoinositide phospholipase C (PLC)-γ pathway, shown by the use of inhibitors (Rennekampff et al. 2000; Jiang et al. 2012).

IL-28 (α isoform) and IL-29 are part of the type III interferon family and are highly similar at an amino acid level (Uzé & Monneron 2007; Witte et al. 2010; Zahn et al. 2011; Fujie & Numasaki 2012). Both cytokines exert an antiviral activity through antiviral proteins and were down-regulated between approximately 2-3-fold following epoxy-tigliane treatment (Sheppard et al. 2003; Uzé & Monneron 2007; Wolk et al. 2008, 2010; Witte et al. 2010; Fujie & Numasaki 2012). There is a high presence of the common receptor for both of these cytokines, IL-28R1, in keratinocytes and has been shown to induce activity through STAT1 and STAT2 activation, as a result of activation of the JAK/STAT pathway (Sheppard et al. 2003; Witte et al. 2010; Wolk et al. 2010; Fujie & Numasaki 2012). Another action of these cytokines on keratinocytes is thought to be growth inhibition, shown by an anti-proliferative response on HaCaTs; although it has been shown that stimulation with the type III IFNs leads to the apoptosis of HaCaTs (Maher et al. 2008; Wolk et al. 2010). The cytokines discussed are immune or inflammatory-related genes and were all shown to be down-regulated following epoxy-tigliane treatment, which would contribute to a reduced inflammatory phase. An attenuated inflammatory response is a characteristic response of preferential healing, present in both early-gestational foetal and oral mucosal healing (Liechty et al. 1998, 2000; Turabelidze & DiPietro 2012; Turabelidze et al. 2014). In addition, these cytokines exert essential functions on keratinocytes, including neovascularisation, keratinocyte migration, re-epithelialisation; and an involvement in the paracrine feedback system between keratinocytes and fibroblasts (Maas-Szabowski et al. 2000; Gallucci et al. 2004; Bader & Kao 2009; Jiang et al. 2012). Some of these differentially expressed genes oppose the previously observed *in vitro* and *in vivo* results. In particular, the enhanced keratinocyte migration observed, which would be reduced with the down-regulated cytokines. However, there are a number of factors involved in controlling these functions, and the previous studies indicate that such responses are not inhibited despite the differentially expressed genes observed.

5.5.7 Extracellular Matrix Component Genes

There were a number of ECM component genes differentially expressed, following epoxy-tigliane treatment. Hyaluronan synthase 3 (HAS3), fibulin 1 and hyaluronan mediated motility receptor (HMMR) were up-regulated between 2-3-fold, following epoxy-tigliane treatment. Collagen type IV α5 (4A5), laminin-α3, laminin-ɣ2 and laminin-β3; and syndecan-4 were down-regulated between 2-3-fold, following epoxy-tigliane treatment.

HAS3 was shown to be upregulated 2-fold at 24h following epoxy-tigliane treatment. It has been shown to be present in the epidermal layer and upregulated following wounding, potentially contributing to re-epithelialisation (Sayo et al. 2002; Tammi et al. 2005). Although HAS3 synthesises extracellular hyaluronan in the epidermis, knockout studies have shown no effect on keratinocyte proliferation abilities, whereas levels of HAS3 are shown to decrease as the differentiation capacity of keratinocytes increases (Sayo et al. 2002; Malaisse et al. 2014, 2016). HMMR, also known as RHAMM, was up-regulated between 2-3-fold, following epoxy-tigliane treatment at 48h. RHAMM is a hyaluronan receptor, was named according to its role in mediating cell motility, and along with CD44, it is involved in hyaluronan signalling. (Hall et al. 1995; Lovvorn et al. 1998; Cheung et al. 1999; Turley et al. 2002; Niedworok et al. 2013; Tolg et al. 2014). Increased presence of HMMR has been associated with the transition from early-gestational foetal scarless wound healing to adult scarring healing, indicating a role in fibrosis (Lovvorn et al. 1998; Tolg et al. 2012). However, expression is also upregulated following wounding, this along with knockout studies have indicated an important role in wound repair and migration (Tolg et al. 2006, 2014). The induction of cell motility is believed to be due to serine/threonine kinase activation, through proto-oncogene tyrosine protein kinase (c-Src); this induces focal adhesion turnover and subsequent cell motility or invasion (Turley et al. 2002; Tolg et al. 2006). It is believed that cancer cells exploit this motility effect, which results in the tumour invasion response (Tolg et al. 2014).

Fibulin-1, transcript variant D, was also up-regulated, between approximately 2-3-fold, following epoxy-tigliane treatment at 48h. Fibulin-1 has been shown to be present in basement membranes, connective tissues and the epidermis, especially the

basal layer, dermal-epidermal junctional region, hair follicles and sebaceous glands (Roark et al. 1995). Fibulin-1 is present alongside elastin in elastic fibres and has been shown to bind to tropoelastin, in addition to fibronectin and fibrinogen (Tran et al. 1997; Argraves et al. 2003; Timpl et al. 2003). Collagen type IV α5 was down-regulated 2-fold following treatment with 10µg/ml EBC-46 and EBC-211, at 24h. Type IV collagens are typically found in the basement membrane, with α5 chain present in the skin basement membrane, at the dermal-epidermal junction. This α-chain is also present in early-gestational foetal skin, but to a lower level than adult skin (Hudson et al. 1993; Peissel et al. 1995; Tanaka et al. 1998; Khoshnoodi et al. 2008; Abreu-Velez & Howard 2012). Autoantibodies against α5 and α6 chain results in subepidermal blisters, indicating its important role in basement membrane integrity (Sado et al. 1998; Ghohestani et al. 2000, 2003).

Syndecan-4 is down-regulated 2-3-fold following epoxy-tigliane treatment at all conditions, apart from 0.001µg/ml EBC-211 at 24h. It has been shown to be up-regulated following injury, with excess expression at the wound edge; and knockout studies have demonstrated impaired wound healing (Echtermeyer et al. 2001; Araki et al. 2009; Bitoux et al. 2009). It has also been shown to play a role in keratinocyte migration, by stimulating focal adhesions formation, by binding to β4 integrin, inducing EGF-stimulated motility of the keratinocytes (Araki et al. 2009; Wang et al. 2015). Syndecan-4 acts through direct connection to PKC-α at focal adhesions, which is believed to activate the integrin and subsequently stimulating migration and wound repair (Morgan et al. 2007; Bass et al. 2011). However, syndecan-4 levels have been shown in some studies to be present at a reduced level during keratinocyte migration across the wound site, compared to the higher expression present in the hyperproliferating keratinocytes at the wound edge (Echtermeyer et al. 2001; Bitoux et al. 2009).

Laminin-5, also known as Laminin-332, is composed of α3, β3 and γ2 chains and present in the basal layer; these three chains were all down-regulated following epoxy-tigliane treatment (Korang et al. 1995; O'Toole et al. 1997; Akutsu et al. 2005; Baudoin et al. 2005; Schneider et al. 2007; Araki et al. 2009; Carulli et al. 2012). Laminin-332 was demonstrated to be synthesised at higher levels following

injury and play a role in wound repair, through migration and adhesion of keratinocytes (Amano et al. 2004). Some studies have indicated a positive role on keratinocyte migration, with increased expression from wound edge keratinocytes undergoing migration across the wound site (Amano et al. 2004; Schneider et al. 2007; Araki et al. 2009). It has been shown that the unprocessed form of laminin-332 is present at the wound edge and unprocessed laminin-α3 is deposited along a migratory path, resulting in increased keratinocyte migration (Schneider et al. 2007; Hamill et al. 2010). However, of interest is that oral mucosal keratinocytes do not deposit collagen type IV or laminin, during migration across the wound site, yet induce rapid re-epithelialisation responses (Larjava et al. 1993).

A number of extracellular matrix components were differentially expressed, following epoxy-tigliane treatment. HAS3, HMMR and fibulin-1 were all up-regulated, with fibulin-1 appearing to have an opposing action on keratinocyte migration, compared to HAS3 and HMMR. Increased expression of HMMR enhances migration, whereas increased fibulin-1 expression results in a reduced fibronectin-promoted migration. The expression for HAS3 and HMMR corroborate the previous *in vitro* studies, where greatly enhanced migration was occurred following EBC-46 or EBC-211 treatment; in addition to the enhanced re-epithelialisation responses during the *in vivo* studies. However, the fibulin-1 expression is in contrast to this response, although it appears to mainly impact on fibronectin-promoted migration and the *in vitro* wound repopulation studies occurred on tissue culture plastic dishes, as opposed to ECM. Collagen type IV α5, syndecan-4 and the subunits comprising laminin-332 (α3, β3 and γ2 chains) were all down-regulated following epoxy-tigliane treatment. Collagen type IV α5 was only down-regulated at 10μg/ml EBC-46 and EBC-211; and is associated with reduced integrity of the basement membrane. However, this concentration of both epoxy-tiglianes exhibited the least preferential responses, including lack of or reduced significantly enhanced migration and wound repopulation, compared to the lower concentrations. Syndecan-4 was shown to be down-regulated, following epoxy-tigliane treatment, but has been associated with enhanced keratinocyte migration. Laminin-332 components, α3, β3 and γ2 chains, were all individually down-regulated following epoxy-tigliane treatment. As with syndecan-4, laminin-332 expression is up-

regulated at wound sites, so may be induced following injury, whereas the cells during the Microarray study were not wounded, potentially preventing this increased expression. In addition, laminin deposition is not present in oral mucosal keratinocytes migrating across the wound site, yet they are still capable of inducing rapid re-epithelialisation.

5.5.8 Cell Signalling Genes

A number of cell signalling genes were shown to be differentially expressed between 2-4-fold following epoxy-tigliane treatment, compared to untreated controls; those downregulated included bone morphogenetic protein and activin membrane-bound inhibitor (BAMBI), Jun proto-oncogene (JUN, also referred as c-Jun), STAT1 and STAT2. In contrast, follistatin (FST) was upregulated between 2-4-fold following 24h of EBC-46 or EBC-211 treatment. FST was primarily upregulated at 24h for both EBC-46 and EBC-211, along with 0.1µg/ml EBC-211 at 48h, between 2-4-fold. FST has been shown to indirectly stimulate keratinocyte proliferation through acting as an antagonist to activin, inhibiting its action (Antsiferova & Werner 2012). It has been suggested that FST regulates keratinocyte proliferation, preventing hyperproliferative responses (Beer et al. 2000; Antsiferova et al. 2009; Antsiferova & Werner 2012).

BAMBI was shown to be downregulated between 2-4-fold, following EBC-46 and EBC-211 treatment at all conditions, for 24h and 48h, when compared to the respective untreated controls. It has been suggested that the inhibitory effect of BAMBI may reduce BMP and activin signalling. As mentioned previously, overexpression of activins inhibits *in vitro* keratinocyte proliferative and contributes to pathological scarring (Harrison et al. 2005; Antsiferova & Werner 2012). BAMBI has been shown, through Wnt signalling, to stimulate cell cycle progression and proliferation. However, this has been demonstrated in tumours, with overexpression leading to a tumorigenic response (Lin et al. 2008; Xavier et al. 2010; Zhou et al. 2013). c-Jun was shown to be downregulated between approximately 2-4-fold, following EBC-46 and EBC-211 treatment at most conditions, for 24h and 48h, when compared to the respective untreated controls. c-Jun is a member of the activator protein (AP)-1 family; knockout studies have indicated a negative impact

on keratinocyte proliferation *in vitro* (Zenz et al. 2003; Florin et al. 2004; Kappelmann et al. 2014). However, c-Jun has also been implicated in psoriasis and malignancies, with increased invasion, proliferation and motility of cells; although a lack of c-Jun has also been reported to impair keratinocyte migration (Mehic et al. 2005; Zenz & Wagner 2006). There are opposing studies regarding the wound healing response of c-Jun, with one indicating no difference in keratinocyte proliferation or migration observed using c-Jun knockout mice; in contrast, an inhibitor to c-Jun has been tested resulting in more rapid re-epithelialisation, compared to controls, with increased proliferation of HaCaTs evident (Zenz et al. 2003; Giles et al. 2008).

STAT1 and STAT2 was downregulated between 2-3-fold across all conditions, following 24h and 48h epoxy-tigliane treatment; STAT3 was also downregulated, although this was only at approximately 1.5-fold. The STAT protein family mediate a number of functions, with STAT1 and STAT3 inducing opposite responses on apoptosis and cell proliferation (Adámková et al. 2007). STAT1 is activated through IFN-α and IFN-γ signalling and has been shown to be required for the anti-proliferative effect of IFN-α on keratinocytes, through inhibited progression of cells into S phase (Bromberg et al. 1996; Ramana et al. 2000; Clifford et al. 2002; Ismail & Yusuf 2014). STAT2 is thought to be primarily located in the granular layer of the epidermis and involved in the IFN-α-mediated inhibition of cell growth, demonstrated through use of a double negative STAT2 protein expression. This inhibition is due to apoptosis, as opposed to an anti-proliferative response (Nishio et al. 2001; Clifford et al. 2003; Ismail & Yusuf 2014). STAT3 has been associated keratinocyte differentiation, with upregulation evident during conditions required for differentiation to occur (Hauser et al. 1998; Nishio et al. 2001). STAT3 has been shown to be involved in a number of processes involved in wound healing response and tumour formation, including inducing an anti-apoptotic response, cell cycle progression, proliferation and keratinocyte migration (Bromberg et al. 1999; Akira 2000; Grandis et al. 2000; Yu & Jove 2004; Dauer et al. 2005; Gartsbein et al. 2006). This enhanced migratory ability is partly due to the upregulation by STAT3 of a number of genes involved in inducing cell migration, such as CCL2 and CXCL2;

this was demonstrated through impaired epidermal repair in mice with disrupted STAT3 (Sano et al. 1999; Kira et al. 2002; Dauer et al. 2005).

BAMBI and c-JUN were both down-regulated, following epoxy-tigliane treatment, which appeared to induce opposing responses on re-epithelialisation, with decreased BAMBI expression reducing the inhibitory action on activin signalling, resulting in inhibited keratinocyte proliferation. Whilst decreased expression of c-Jun has been indicated by some studies to enhance re-epithelialisation responses, other studies suggest this impairs keratinocyte migration. FST was up-regulated following epoxy-tigliane treatment, which is believed to result in stimulated keratinocyte proliferation, due to reduced activin signalling. As all three STATs discussed were downregulated following epoxy-tigliane treatment, there may have been conflicting effects on the keratinocytes due to their opposing roles. Downregulation of STAT1 and STAT2 may contribute to the increased keratinocyte presence through reduced anti-proliferative and apoptotic responses. This could lead to the enhanced proliferative response observed in the *in vitro* viability and proliferation studies and contribute to the rapid re-epithelialisation observed during *in vivo* studies. Downregulation of STAT3 appears to oppose the *in vitro* and *in vivo* responses previously seen. However, downregulation of STAT3 was lower than STAT1 and lower than the 2-fold differentially expressed criteria, following epoxy-tigliane treatment, which its action typically conflicts with.

The Microarray study elucidated a number of key differentially expressed genes, following epoxy-tigliane treatment. Many of these appear to corroborate the previous *in vitro* and *in vivo* studies, due to their role in stimulating keratinocyte proliferation and migration. However, others appeared to oppose the responses previously observed. Although, it was necessary to confirm that these alterations in gene expression were also evident at the protein level. Genotypic changes are not always evident at a phenotypic level, due to post-translational modifications, preventing the differential change translated to a protein expression change or activity level. A number of key genes determined from this Chapter were subsequently selected for further protein level validation in Chapter 6.

Chapter 6 – Validation of Differential HaCaT Gene Expression Responses Induced by EBC-46 and EBC-211

Chapter 6 – Validation of Differential HaCaT Gene Expression Responses Induced by EBC-46 and EBC-211

6.1 Introduction

Wound healing is a carefully controlled process, to ensure successful wound closure and reformation of the dermal matrix and appendages (Grinnell 1992; Patel et al. 2006; Braiman-Wiksman et al. 2007; Li et al. 2007; Pastar et al. 2014). Alterations in this process can lead to impaired healing situations or pathological scarring, as seen in situations such as chronic wounds and keloids, respectively (Falanga 2005; Agren & Werthén 2007; Menke et al. 2007; Dreifke et al. 2015; Jumper et al. 2015). However, some alterations from the normal acute wound healing response have been shown to induce beneficial healing outcomes, through differentially expressed genes evident during early-gestational, foetal and oral mucosal wound healing. Both of these response are characterised as preferential healing, as a result of the rapid wound closure ability and the minimal scarring responses observed (Liechty et al. 1998; Liechty et al. 2000; Colwell et al. 2008; Lee et al. 2012; Rolfe & Grobbelaar 2012; Turabelidze et al. 2014).

Following the elucidation of a number of key differentially expressed genes during global gene analysis (Microarray) studies (Chapter 5), validation studies were performed to determine whether these expression changes occurred at the protein level, following epoxy-tigliane treatment. The global gene analysis was performed on HaCaTs to identify differentially expressed genes induced by EBC-46 and EBC-211, involved in keratinocyte wound healing responses (Chapter 4). However, due to the paracrine feedback between fibroblasts and keratinocytes, this can also impact on fibroblast wound healing responses (Maas-Szabowski et al. 1999; Werner & Smola 2001; Barrientos et al. 2008; Bader & Kao 2009). The Microarray study was able to provide information on more than 25,000 genes. Key genes shown to be differentially expressed by more than 2-fold, following treatment with EBC-46 or EBC-211 for 24 or 48h, were further analysed to determine protein expression or

activity level. The differentially expressed genes validated at a protein level included keratin 13 (Krt13), Krt15, Krt16, Krt17, Krt6B, cyclin A2, cyclin B1, cyclin B2, cyclin-dependent inhibitor 3 (CDKN3), CDKN1A, ubiquitin-conjugating enzyme E2C (UBE2C), matrix metalloproteinase (MMP)-1, MMP-7, MMP-10, interleukin (IL)-6, IL-8, chemokine (C-C motif) ligand 5 (CCL5); and chemokine (C-X-C motif) ligand 10 (CXCL10). The gene expression fold-changes for these validated proteins are shown in Tables 6.1 and 6.2, for EBC-46 and EBC-211, respectively. These genes and proteins also play important roles in mediating normal and pathological wound healing responses, in particular re-epithelialisation. This is achieved through increased keratinocyte proliferation and migration and is discussed in more detail in Sections 5.5.1, 5.5.2, 5.5.5 and 5.5.6 (Nagase et al. 2006; Bragulla & Homberger 2009; Toriseva & Kähäri 2009; Gong & Ferrell 2010; Hao et al. 2012; Koppel et al. 2014; Turabelidze et al. 2014).

Genotypic changes between normal, acute skin wound healing and preferential healing responses have been reported. These include enhanced keratinocyte proliferation, increased cell cycle progression; and enhanced protein synthesis and degradation (Colwell et al. 2008; Kim et al. 2013; Reddell et al. 2014; Tan et al. 2014; Turabelidze et al. 2014). In addition, a reduced inflammatory phase has been observed during preferential healing, including decreased IL-6 and IL-8 levels (Liechty et al. 1998; Liechty et al. 2000; Chen et al. 2010; Rolfe & Grobbelaar 2012; Yates et al. 2012). This is in contrast to the more prolonged inflammatory phase associated with chronic wounds and keloid scars (Yager & Nwomeh 1999; Menke et al. 2007; Shih et al. 2010; Wiegand et al. 2010; Gauglitz et al. 2011; Jumper et al. 2015). Variations in MMP levels have also been observed between normal adult, acute wound healing and early-gestational, foetal wounds, with increased MMP-1 expression in foetal wounds (Dang et al. 2003; Rolfe & Grobbelaar 2012). Studies have shown an increase in MMP activity in chronic wounds, indicating that they have a vital role in extracellular matrix (ECM) remodelling, through matrix degradation (Vaalamo et al. 1997; Lobmann et al. 2002; Mwaura et al. 2006; Eming et al. 2008; Wiegand et al. 2010; Thamm et al. 2015).

Table 6.1: Fold changes in key differentially expressed genes, following treatment with EBC-46 for 24h or 48h. Red = up-regulated genes, Green = down-regulated genes.

Gene	Control vs EBC-46, 0.001 24h	Control vs EBC-46, 0.001 48h	Control vs EBC-46, 0.1 48h	Control vs EBC-46, 10 24h	Control vs EBC-46, 10 48h
KRT13		5.3	5.3		6.3
KRT15		4.6	4.6	2.8	5.7
KRT16		4.3	4.3	3.1	4.1
KRT17		4.1	4.1	3.1	4.0
KRT6B		3.2	3.2		3.5
Cyclin A2		3.0	3.0		3.0
Cyclin B1		2.7	2.7		2.7
Cyclin B2		4.1	4.1		4.2
CDKN3		3.3	3.3		3.2
CDKN1A		2.0	2.0	3.2	2.2
UBE2C		3.8	3.8		4.3
MMP-1		5.8	5.8	2.5	5.1
MMP-7	2.4				
MMP-10					
IL-6		5.3	5.3	2.0	7.2
IL-8		5.6	5.6	4.4	8.1
CCL5	4.8	5.5	5.5	6.3	7.6
CXCL10	4.3	8.7	8.7	5.6	13.2

Table 6.2: Fold changes in key differentially expressed genes, following treatment with EBC-211 for 24h or 48h. Red = up-regulated genes, Green = down-regulated genes.

Gene	Control vs EBC-211, 0.001 24h	Control vs EBC-211, 0.001 48h	Control vs EBC-211, 0.1 48h	Control vs EBC-211, 10 24h	Control vs EBC-211, 10 48h
KRT13		6.9	5.6		4.7
KRT15		5.4	3.8		5.6
KRT16			3.2	3.0	4.0
KRT17		2.3	3.1	3.0	3.6
KRT6B			2.9		3.7
Cyclin A2		2.9	3.0		2.7
Cyclin B1		2.7	2.7		2.7
Cyclin B2		3.8	4.2		3.8
CDKN3		3.2	3.4		3.1
CDKN1A				2.8	2.1
UBE2C		3.6	3.6		3.7
MMP-1	4.1	6.0	4.7		6.2
MMP-7	2.7				
MMP-10	2.6	3.2	2.0		
IL-6		4.3	5.4		6.2
IL-8		2.8	3.8	3.2	6.3
CCL5	4.1	5.4	6.5	5.5	5.9
CXCL10	3.8	9.4	10.3	4.9	10.9

As preferential wound healing responses were observed during the *in vivo* animal wound healing studies performed by QBiotics Ltd., the aim of the global gene analysis and subsequent protein validation studies were to elucidate key genes and pathways involved in inducing these responses. Validation at the protein level is vital to determine whether the changes in genotypic response will result in a phenotypic effect, through increased translation of protein expression or activity. Differentially expressed genes may not result in any changes at a protein level, due to a number of post-transcriptional mechanisms (Hause et al. 2014). Therefore, important differentially expressed genes, may have no phenotypic impact following epoxy-tigliane treatment, compared to untreated controls.

6.2 Aims

The aim of this Chapter was to validate the key differentially expressed genes in HaCaTs at a protein level, following treatment with EBC-46 or EBC-211, for 24h or 48h. This was performed using a variety of techniques to confirm the protein expression or activity. Quantitative polymerase chain reaction (qPCR) analysis was initially used to validate Krt13, Krt15, Krt16, Krt17, Cyclin B2 and MMP-1 gene expression levels; while Western blot analysis was used to validate the protein levels of Krt13, Krt15, Krt16, Krt17, Krt6B, Cyclin A2, Cyclin B1, Cyclin B2, CDKN3, CDKN1A and UBE2C. MMP activity assays were used to validate MMP-1, MMP-7 and MMP-10 activities. Enzyme-linked immunosorbent assays (ELISAs) were performed to validate IL-6, IL-8, CCL5 and CXCL10 levels.

6.3 Materials and Methods

6.3.1 Preparation of EBC-46 and EBC-211

EBC-46 and the 'reduced activity' isomer, EBC-211, were both supplied by QBiotics Ltd., Queensland, Australia and solubilised in DMSO (Section 2.1). For both compounds, concentrations of 0.001µg/ml, 0.01µg/ml, 0.1µg/ml, 1µg/ml and 10µg/ml were prepared in F-SCM for dermal fibroblast (Section 2.2.1); 100µg/ml was not included as this concentration has previously been shown to be cytotoxic.

6.3.2 HaCaT Culture

Epidermal keratinocyte cell line (HaCaTs) were sourced, maintained, subcultured, counted, cryopreserved and screened for mycoplasma, as previously described (Sections 2.2.2, 2.2.3, 2.2.4 and 2.2.5 respectively).

6.3.3 Validation of Gene Expression Changes by Quantitative PCR (qPCR)

Keratinocyte cell line (HaCaT) gene expression changes were validation through qPCR for Krt13, Krt15, Krt16, Krt17, CCNB2 and MMP-1 at 24h and 48h, as previously described (Section 2.5.1).

6.3.4 Validation of Gene Expression Changes by Western Blotting

Keratinocyte cell line (HaCaT) gene expression changes were validation through analysing protein expression changes for Krt13, Krt15, Krt16, Krt17, Krt6B, Cyclin A2, Cyclin B1, Cyclin B2, CDKN3, CDKN1A and UBE2C by Western blotting, as described in Section 2.5.2.

6.3.5 Validation of Gene Expression Changes by Activity Assays

Keratinocyte cell line (HaCaT) gene expression changes were validation through analysing MMP-1, MMP-7 and MMP-10 activities at 24h and 48h, as previously described (Section 2.5.3).

6.3.6 Validation of Gene Expression Changes by ELISA

Keratinocyte cell line (HaCaT) gene expression changes were validation through analysing IL-6, IL-8, CCL5 and CXC10 protein expression at 24h and 48h, as previously described (Section 2.5.4).

6.4 Results

6.4.1 Validation of Gene Expression Changes by Quantitative PCR (qPCR)

qPCR was used to validate Krt13, Krt15, Krt16, Krt17, MMP-1 and Cyclin B2 at 24h and 48h, following EBC-46 and EBC-211 treatment. This was performed using the same epoxy-tigliane concentrations as in the Microarray studies (0.001µg/ml, 0.1µg/ml and 10µg/ml). Krt13 was previously shown in the Microarray studies to be upregulated following epoxy-tigliane treatment at 48h (Tables 6.1 and 6.2). In the qPCR studies, it was shown to be upregulated following EBC-46 and EBC-211 treatment, at both 24h and 48h (Figures 6.1A and 6.1B respectively). This upregulation was only considered to be significant for 0.001µg/ml and 10µg/ml EBC-46 at 24h ($p<0.05$); whereas at 48h, the upregulation was significant at all EBC-46 concentrations ($p<0.001$; Figure 6.1A), compared to untreated controls. A similar response was seen following EBC-211 treatment, with a significant upregulation of Krt13 expression at 0.001µg/ml EBC-211 at 24h ($p<0.001$; Figure 6.1B). Corroborating the Microarray studies, a significant upregulation of Krt13 at all EBC-211 concentrations ($p<0.001$) at 48h was seen, compared to untreated controls.

Krt15 gene expression was also shown to be upregulated following epoxy-tigliane treatment after 48h, during the Microarray studies. However, after 24h treatment with EBC-46 at 10µg/ml, there was a downregulation in expression of Krt15, compared to untreated controls (Tables 6.1 and 6.2). The qPCR data for EBC-46 showed this significant downregulation of Krt15 at both 0.001µg/ml and 10µg/ml, after 24h treatment ($p<0.001$); whereas EBC-211 only showed the significant downregulation at 24h for 10µg/ml, compared to untreated controls ($p<0.001$; Figures 6.2A and 6.2B, respectively). Following the same pattern as the Microarray studies (Tables 6.1 and 6.2), there was a significant upregulation of Krt15 expression after 48h treatment for EBC-46. This was significant at 0.1µg/ml and 10µg/ml EBC-46 ($p<0.001$) and to a lesser degree at 0.001µg/ml ($p<0.05$), compared to untreated controls. There was also a significant increase in Krt15 expression at 0.001µg/ml and 10µg/ml ($p<0.001$) at 48h, compared to untreated controls. It was also significantly

Figure 6.1: Krt13 expression in HaCaTs, cultured in the presence of 0.001µg/ml, 0.1µg/ml and 10µg/ml EBC-46 (A) or EBC-211 (B), compared to untreated controls (0µg/ml), at 24h and 48h. (*N=3, average±SE, statistical analysis displayed *p<0.05, ***p<0.001*).

A

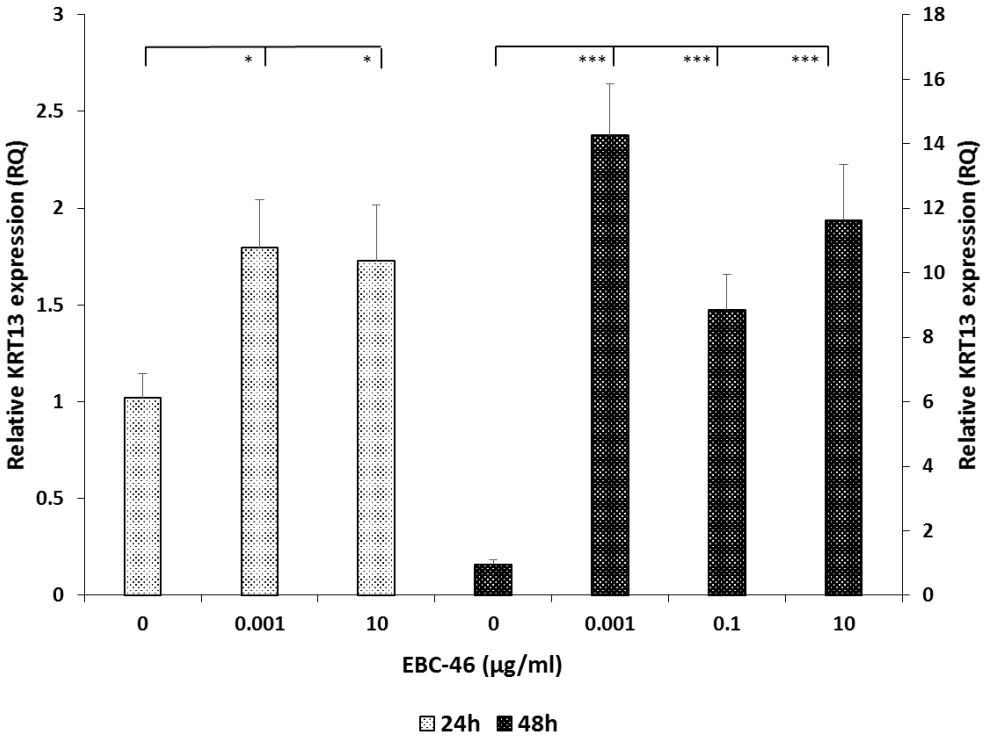

B

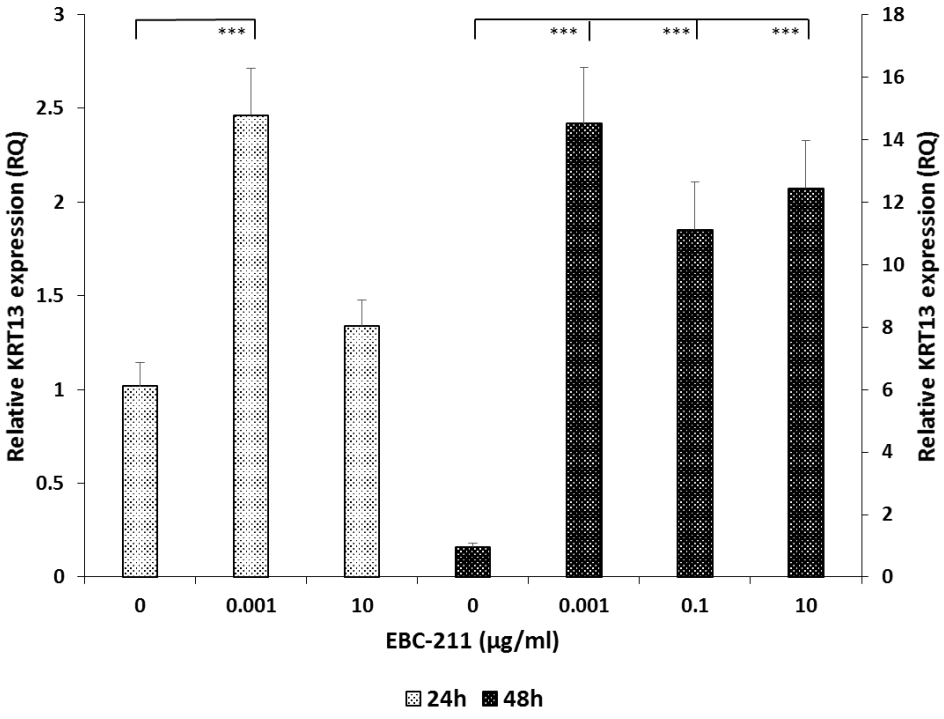

Figure 6.2: Krt15 expression in HaCaTs, cultured in the presence of 0.001µg/ml, 0.1µg/ml and 10µg/ml EBC-46 (A) or EBC-211 (B), compared to untreated controls (0µg/ml), at 24h and 48h. (*N=3, average±SE, statistical analysis displayed *p<0.05, **p<0.01, ***p<0.001*).

A

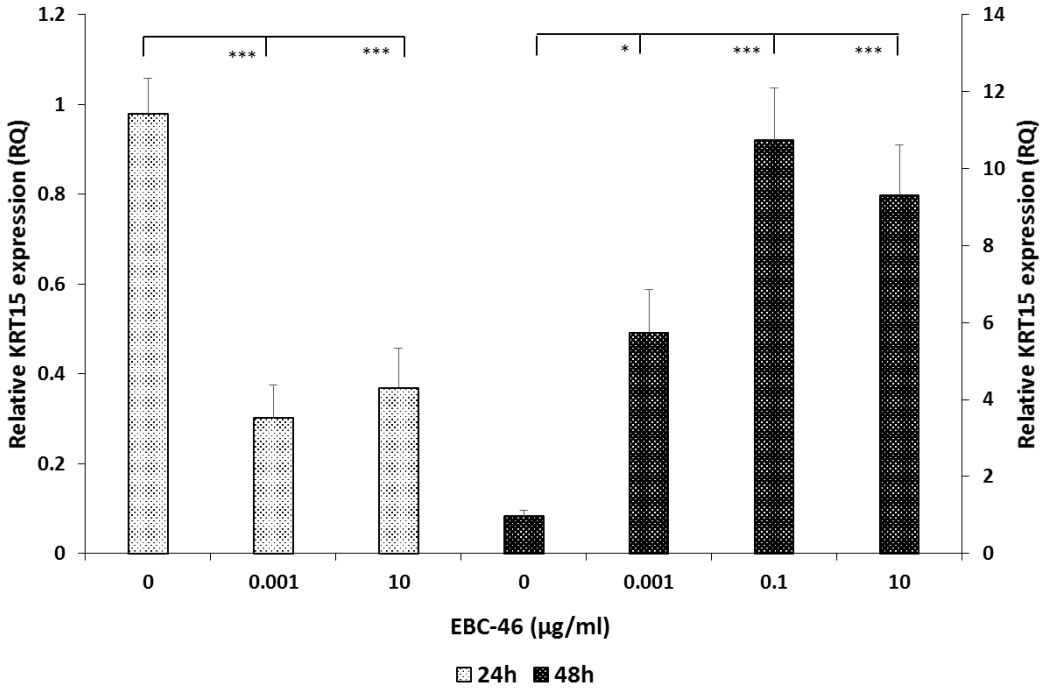

B

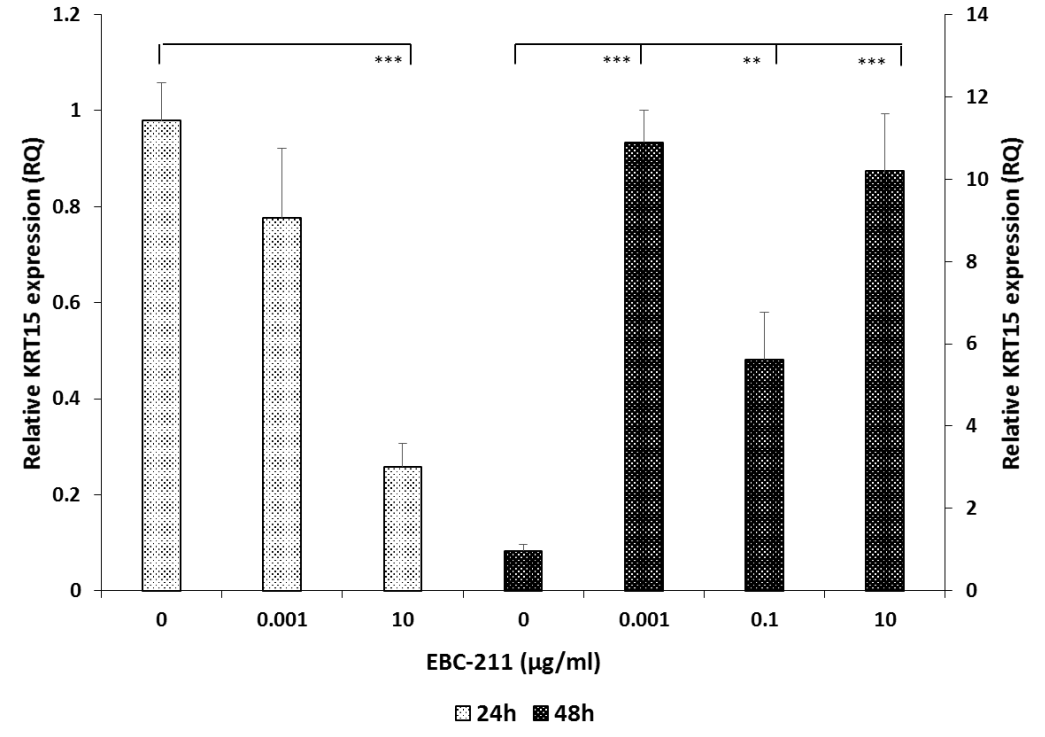

upregulated at 0.1µg/ml ($p<0.01$), although at a reduced level, in line with the Microarray data.

Krt16 was downregulated following epoxy-tigliane treatment at 24h, although this was not considered to be significant after EBC-46 treatment. However, there was a significant downregulation at 10µg/ml EBC-211 ($p<0.05$; Figures 6.3A and 6.3B, respectively). By 48h, there was a significant downregulation of Krt16 expression at 0.001µg/ml and 10µg/ml EBC-46 treatment ($p<0.001$-0.01), in addition to a significant downregulation at 0.1µg/ml ($p<0.05$). This pattern corroborated the fold changes in gene expression identified in the Microarray studies (Tables 6.1 and 6.2). Following 48h treatment with EBC-211, there was a significant downregulation of Krt16 expression at 0.1µg/ml and 10µg/ml, compared to untreated controls ($p<0.001$-0.01).

Krt17 was downregulated following EBC-46 and EBC-211 treatment at both 24h and 48h (Figures 6.4A and 6.4B, respectively), corroborating the Microarray studies (Tables 6.1 and 6.2). This downregulation was considered to be significant for EBC-46, at 24h and 48h, compared to the respective untreated controls ($p<0.001$). EBC-211 also showed a downregulation in Krt17 expression at 24h for 10µg/ml EBC-211 ($p<0.001$), and to a lesser degree at 0.001µg/ml ($p<0.05$). Corroborating the Microarray studies, there was a significant downregulation in Krt17 expression for all EBC-211 concentrations at 48h ($p<0.001$), compared to untreated controls.

MMP-1 expression was upregulated following epoxy-tigliane treatment, similar upregulation was observed during the Microarray studies, as shown in Tables 6.1 and 6.2. Although there appeared to be an upregulation at 24h following EBC-46 treatment, this was not considered to be significant ($p>0.05$; Figure 6.5A). In contrast, at 48h, there was a significant upregulation in MMP-1 expression at 0.1µg/ml ($p<0.001$), compared to untreated controls. As seen at 24h, although there was an appeared upregulation at 0.001µg/ml and 10µg/ml EBC-46, these were deemed to be non-significant ($p>0.05$). There was a significant upregulation of MMP-1 expression following 0.001µg/ml EBC-211 treatment at 24h ($p<0.05$; Figure 6.5B), compared to untreated controls; and a further significant upregulation with

Figure 6.3: Krt16 expression in HaCaTs, cultured in the presence of 0.001µg/ml, 0.1µg/ml and 10µg/ml EBC-46 (A) or EBC-211 (B), compared to untreated controls (0µg/ml), at 24h and 48h. (*N=3, average±SE, statistical analysis displayed *p<0.05, **p<0.01, ***p<0.001*).

A

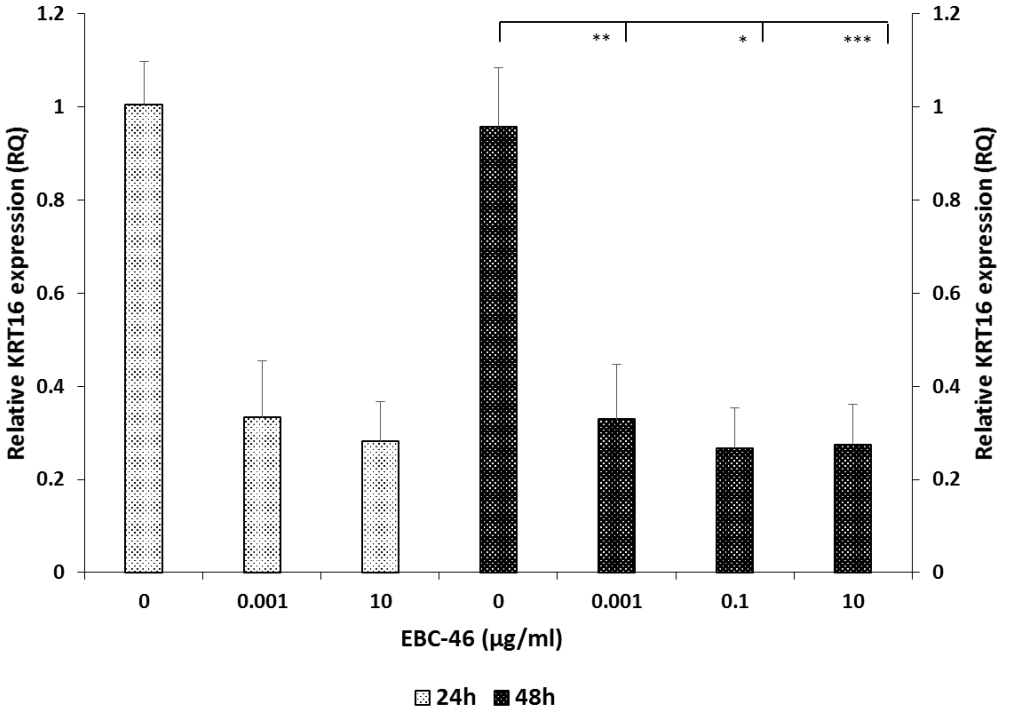

B

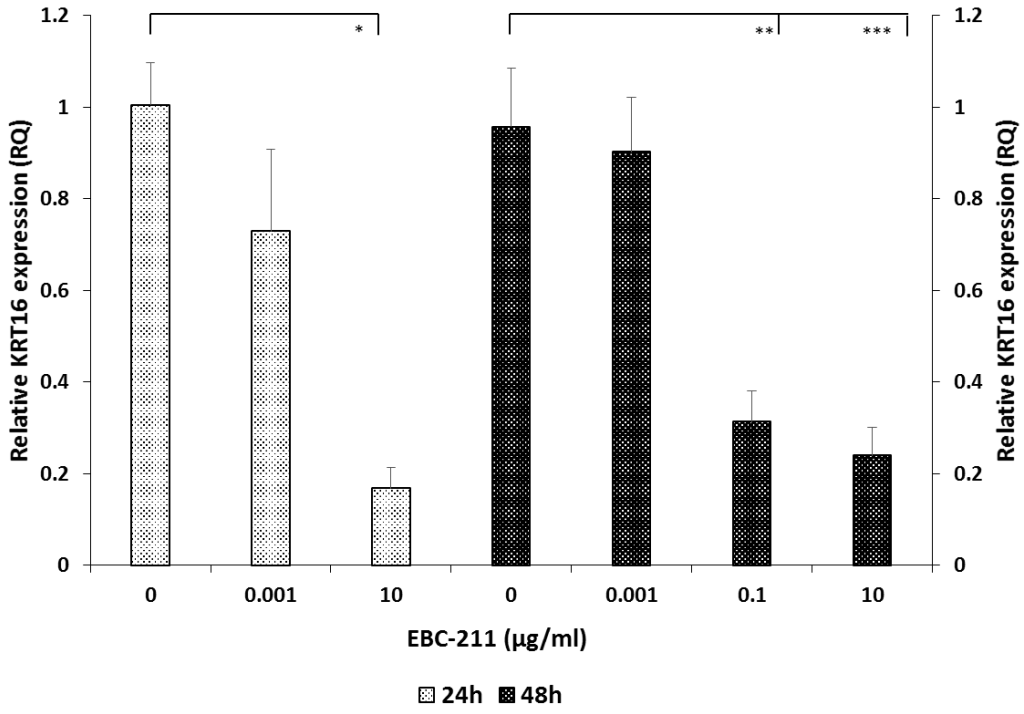

Figure 6.4: Krt17 expression in HaCaTs, cultured in the presence of 0.001µg/ml, 0.1µg/ml and 10µg/ml EBC-46 (A) or EBC-211 (B), compared to untreated controls (0µg/ml), at 24h and 48h. (*N=3, average±SE, statistical analysis displayed *p<0.05, ***p<0.001*).

A

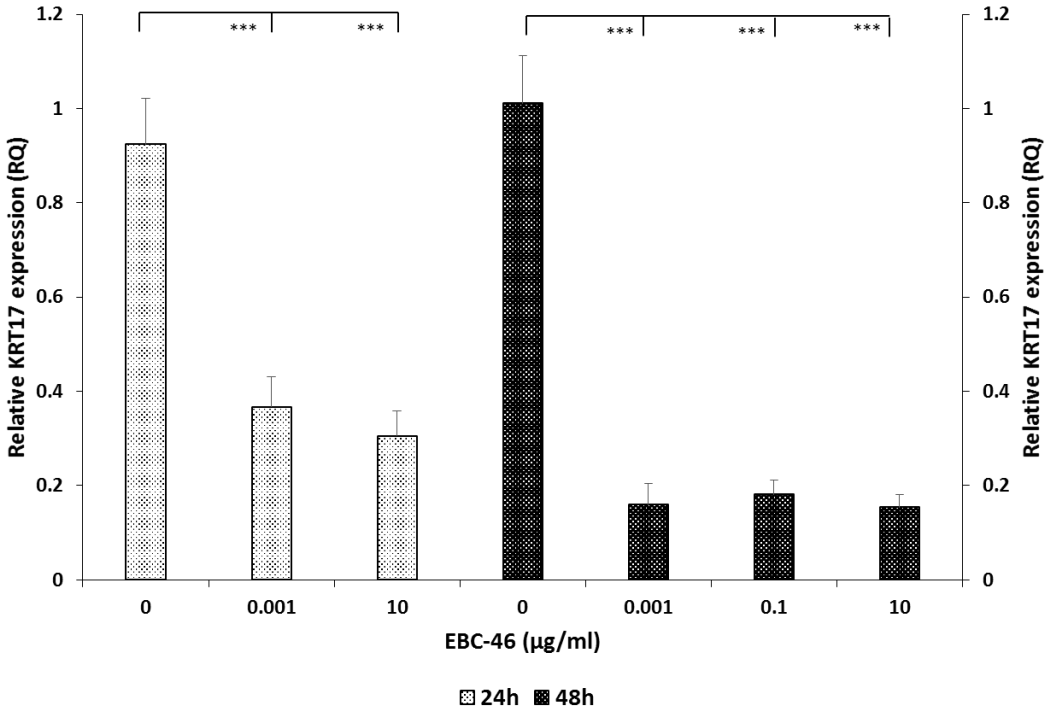

B

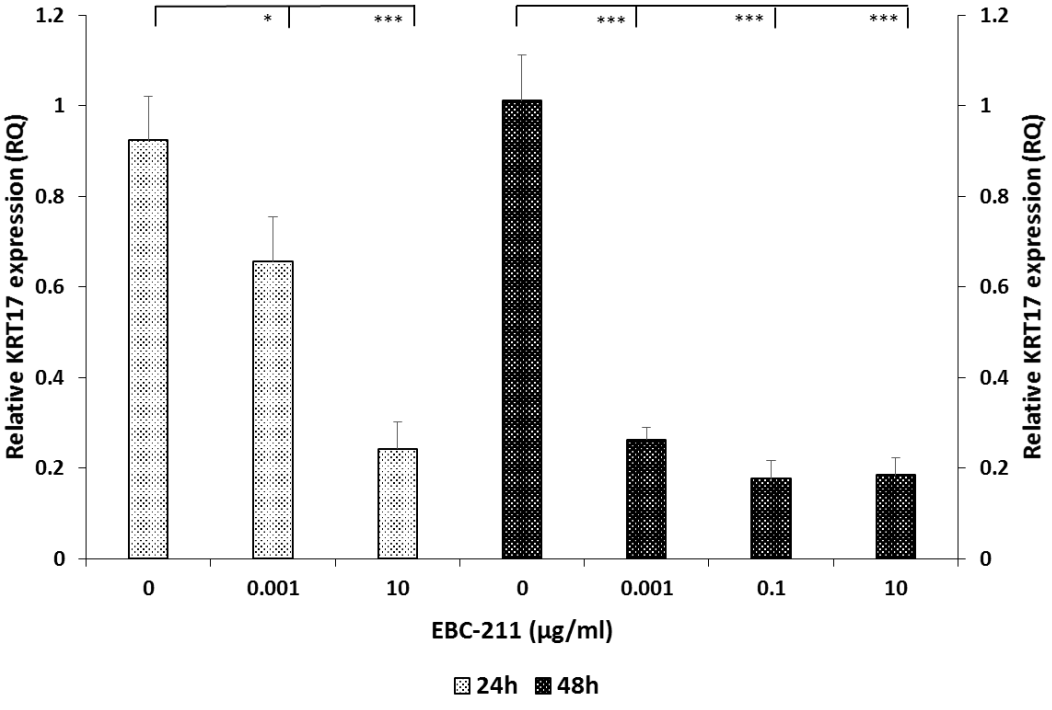

Figure 6.5: MMP-1 expression in HaCaTs, cultured in the presence of 0.001µg/ml, 0.1µg/ml and 10µg/ml EBC-46 (A) or EBC-211 (B), compared to untreated controls (0µg/ml), at 24h and 48h. (*N=3, average±SE, statistical analysis displayed *p<0.05, ***p<0.001*).

A

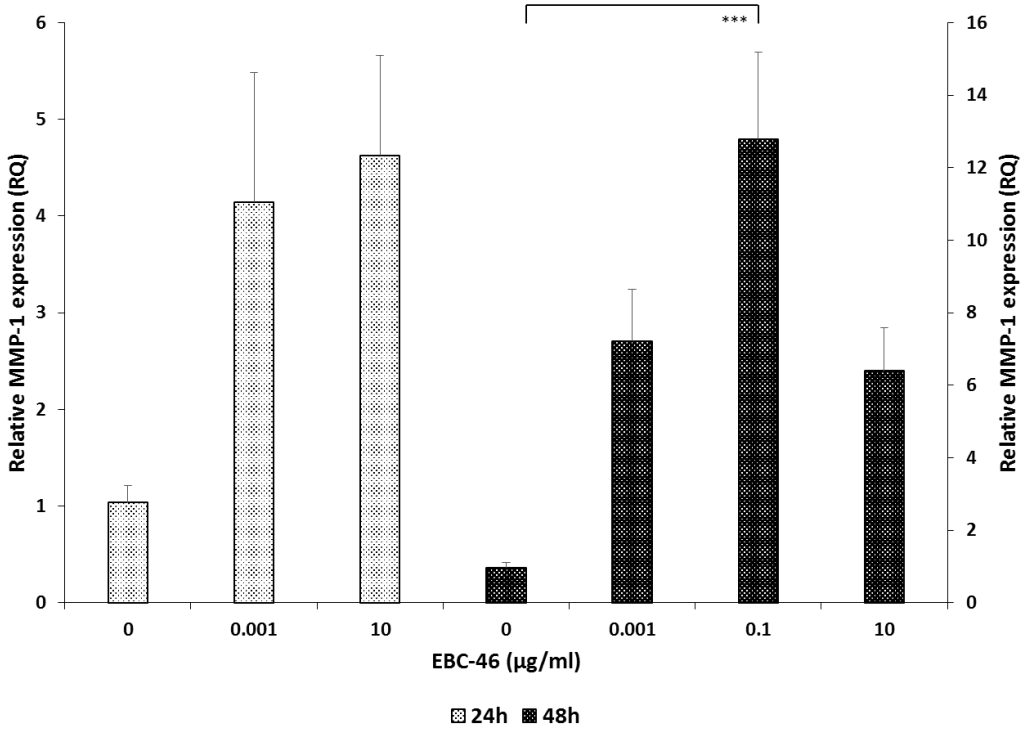

B

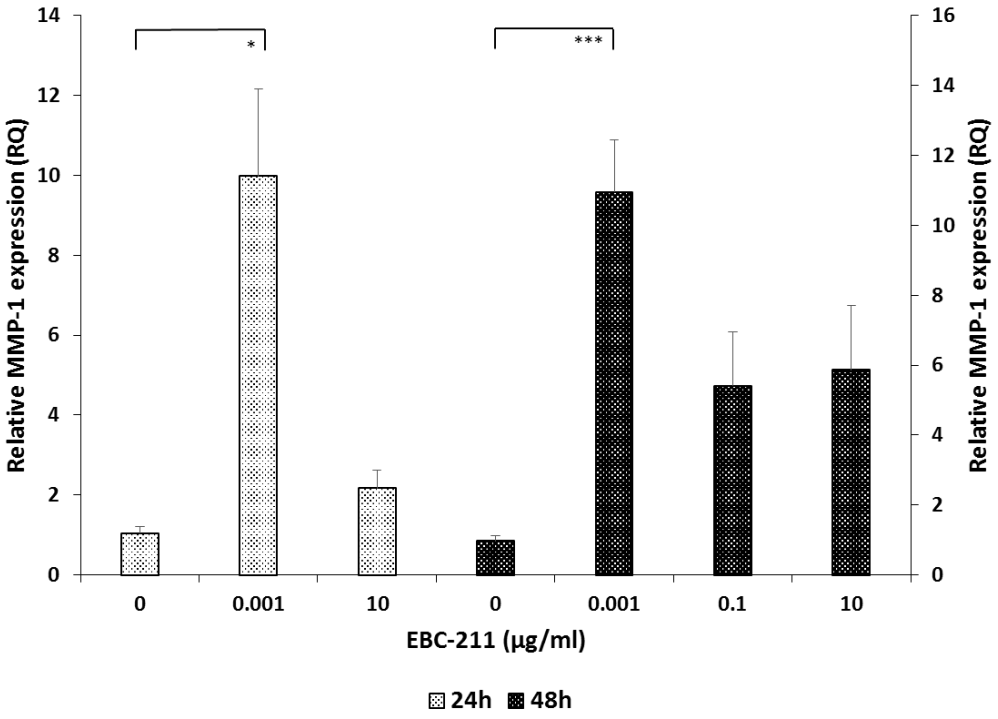

0.001µg/ml EBC-211 at 48h ($p<0.001$). However, the other concentrations were not considered to be significant, compared to untreated controls ($p>0.05$).

Cyclin B2 expression was shown to be upregulated at 48h for both EBC-46 and EBC-211 in the Microarray studies (Tables 6.1 and 6.2, respectively). The qPCR studies corroborated these results, showing no significant upregulation in Cyclin B2 expression following 24h treatment of EBC-46 or EBC-211 ($p>0.05$; Figures 6.6A and 6.6B, respectively). In contrast, at 48h, there was a significant increase in expression following 10µg/ml EBC-46 treatment, compared to untreated controls ($p<0.001$). The lower EBC-46 concentrations (0.001 and 0.1µg/ml) appeared to show an increase in expression, although these were not considered significant ($p>0.05$). Treatment with 0.1µg/ml EBC-211, at 48h, appeared to increase expression, although this again was not deemed significant ($p>0.05$). However, treatment with 0.001µg/ml and 10µg/ml EBC-211 significantly upregulated Cyclin B2 expression, compared to untreated controls ($p<0.01$-0.05).

Figure 6.6: Cyclin B2 expression in HaCaTs, cultured in the presence of 0.001µg/ml, 0.1µg/ml and 10µg/ml EBC-46 (A) or EBC-211 (B), compared to untreated controls (0µg/ml), at 24h and 48h. (*N=3, average±SE, statistical analysis displayed *p<0.05, **p<0.01, ***p<0.001*).

A

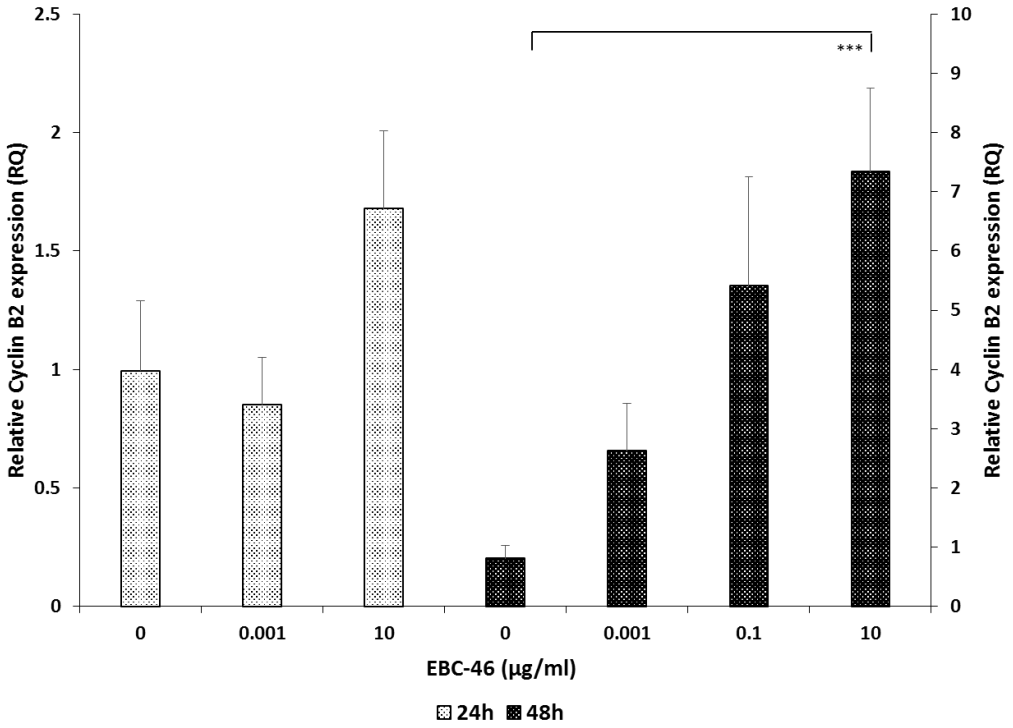

B

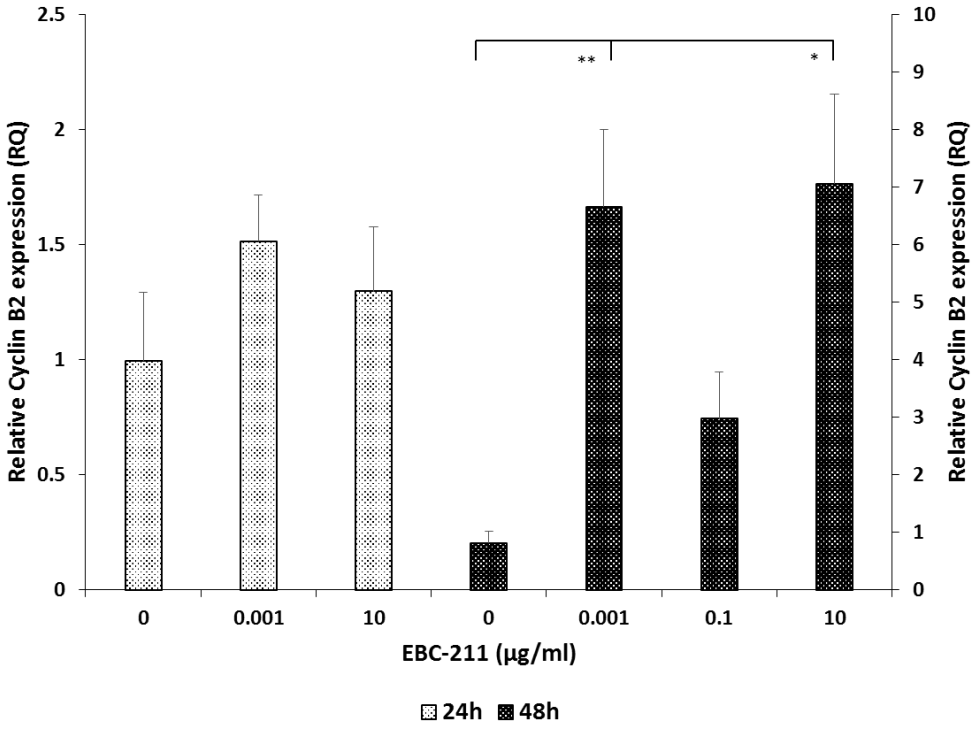

6.4.2 Validation of Gene Expression Changes by Western Blot

Western blot analysis was also performed to validate a number of differentially expressed genes identified during the Microarray studies, shown in Tables 6.1 and 6.2, for EBC-46 and EBC-211 respectively. These included Krt13, Krt15, Krt16, Krt17, Krt6B, Cyclin A2, Cyclin B1, Cyclin B2, CDKN3, CDKN1A and UBE2C. A number of keratins were shown to be upregulated or downregulated following epoxy-tigliane treatment. Krt13 and Krt15 were upregulated at 48h for all conditions analysed with both EBC-46 and EBC-211, although a downregulation was observed for Krt15 following 10μg/ml EBC-46 at 24h. Krt16, Krt17 and Krt6B were all shown to be downregulated following epoxy-tigliane treatment, predominantly at 48h.

Krt13 Western blots are shown in Figures 6.7A and 6.8A, for EBC-46 and EBC-211, respectively, with β-actin used as a loading control for each blot. The densitometry graphs are shown in Figures 6.7B-C and 6.8B-C, for EBC-46 and EBC-211, respectively. The Western blot for Krt13 following EBC-46 treatment appeared to indicate increased levels, compared to untreated controls, at both 24h and 48h (Figure 6.7A). The densitometry was performed on three separate blots, one per sample set. No significant change in Krt13 protein detection was observed at 24h ($p>0.05$; Figure 6.7B). However, at 48h, it appeared to show an increase across all EBC-46 concentrations, with this deemed significant at 0.1μg/ml and 10μg/ml EBC-46 ($p<0.01$-0.05; Figure 6.7C). Western blot analysis of EBC-211 effects appeared to show an increase in Krt13 levels at certain concentrations (0.001μg/ml, 0.1μg/ml and 10μg/ml), at 48h (Figure 6.8A). Densitometry analysis indicated that Krt13 detection following EBC-211 treatment may be increased at 24h for all concentrations (0.001-10μg/ml), although this was not considered to be significant ($p>0.05$; Figure 6.8B). At 48h, increased detection was also indicated; however, this was not considered to be significant ($p>0.05$; Figure 6.8C).

Krt15 Western blots are shown in Figures 6.9A and 6.10A, for EBC-46 and EBC-211, respectively, with β-actin used as a loading control for each blot. The densitometry graphs for each epoxy-tigliane are shown in Figures 6.9B-C and 6.10B-C. The Western blot for EBC-46 did not appear to show any change in Krt15 protein detection at 24h or 48h (Figure 6.9A). This was corroborated by no significant

Figure 6.7: Western blot analysis on (A) Krt13 in HaCaTs, at 24h and 48h; with densitometry analysis on Krt13 levels in HaCaTs, cultured in the presence of 0.001µg/ml, 0.01µg/ml, 0.1µg/ml, 1µg/ml and 10µg/ml EBC-46, compared to untreated controls (0µg/ml), at (B) 24h and (C) 48h. (*N=3, average±SE, statistical analysis displayed *p<0.05, **p<0.01*).

A

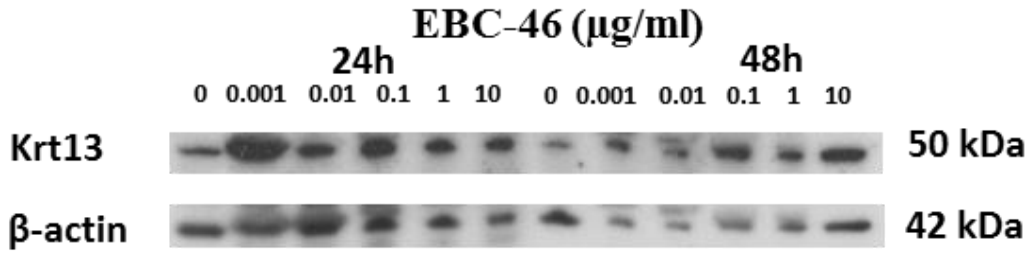

B

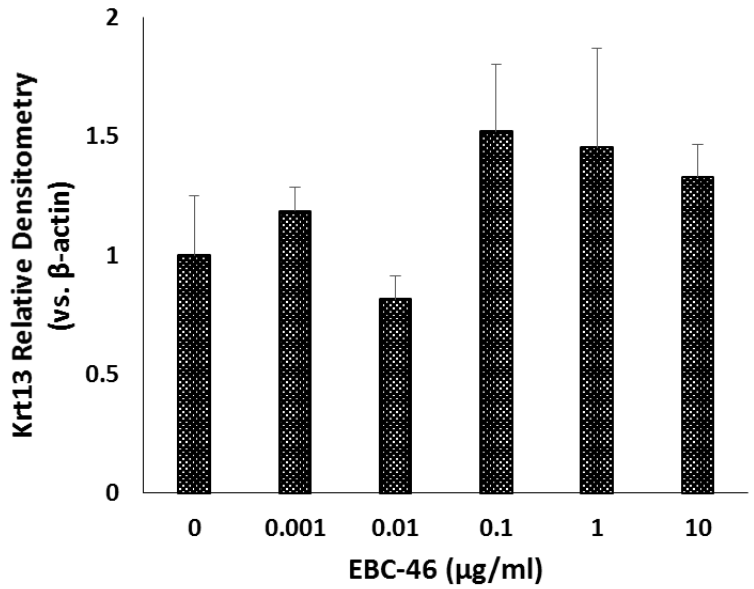

C

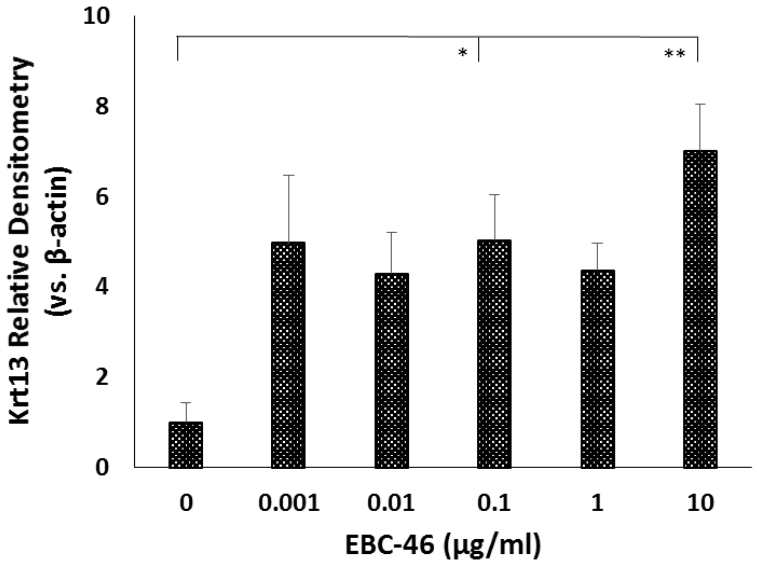

Figure 6.8: Western blot analysis on (A) Krt13 in HaCaTs, at 24h and 48h; with densitometry analysis on Krt13 levels in HaCaTs, cultured in the presence of 0.001µg/ml, 0.01µg/ml, 0.1µg/ml, 1µg/ml and 10µg/ml EBC-211, compared to untreated controls (0µg/ml), at (B) 24h and (C) 48h. (*N=3, average±SE).*

A

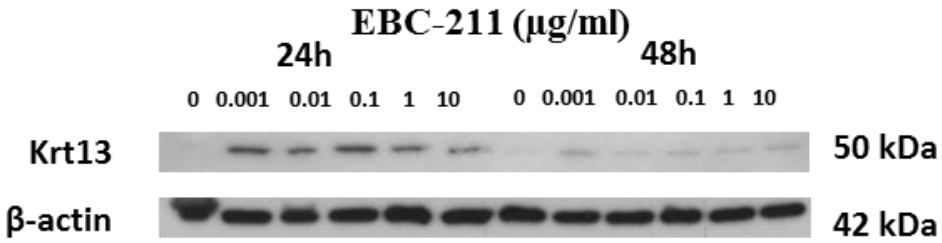

B

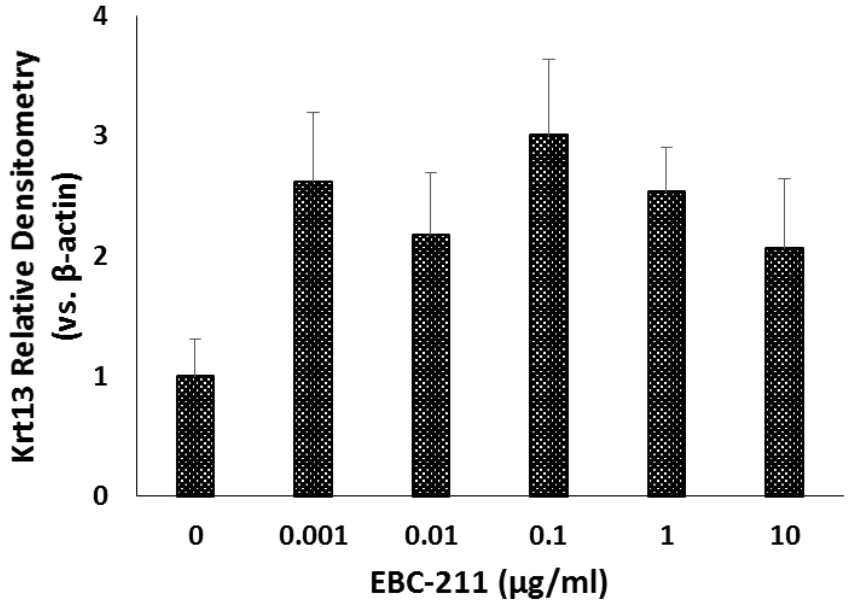

C

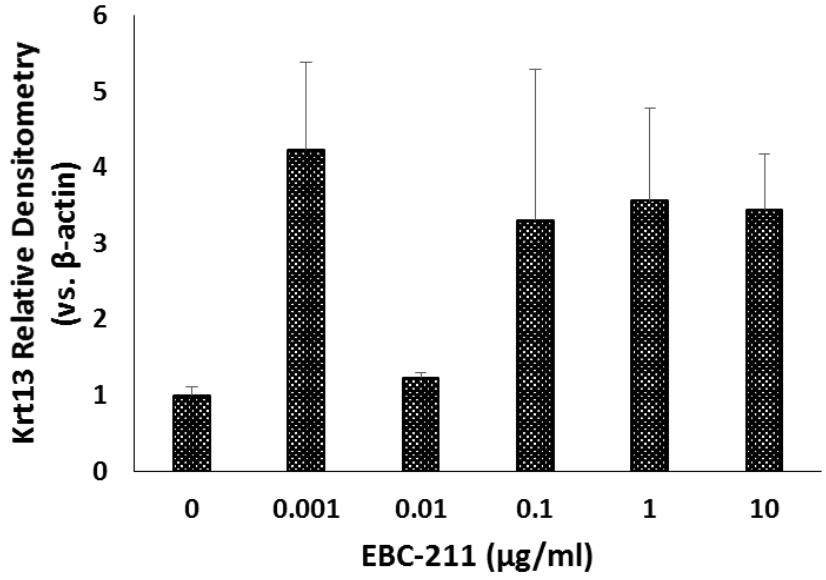

Figure 6.9: Western blot analysis on (A) Krt15 in HaCaTs, at 24h and 48h; with densitometry analysis on Krt15 levels in HaCaTs, cultured in the presence of 0.001µg/ml, 0.01µg/ml, 0.1µg/ml, 1µg/ml and 10µg/ml EBC-46, compared to untreated controls (0µg/ml), at (B) 24h and (C) 48h. (*N=3, average±SE).*

A

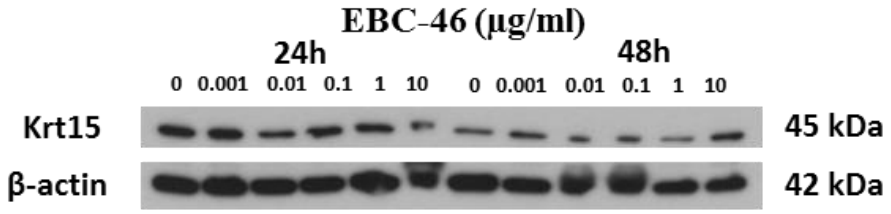

B

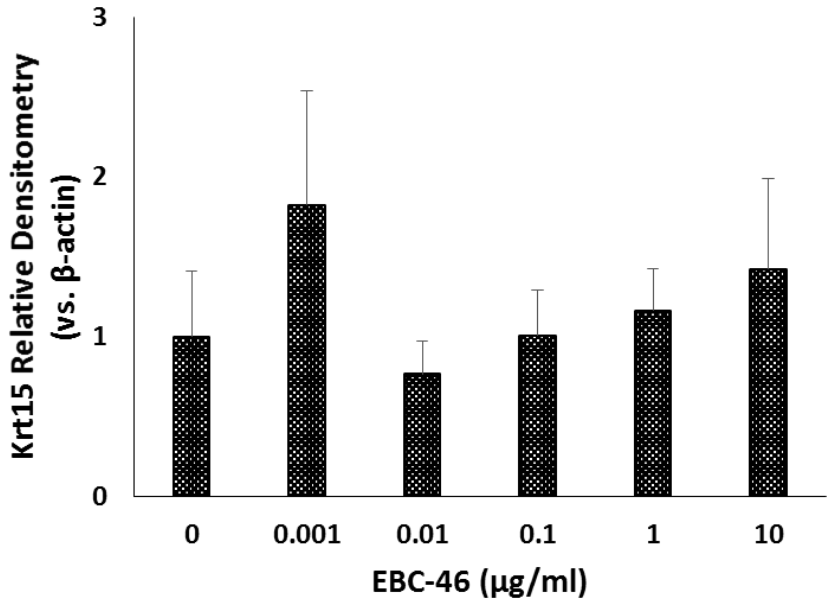

C

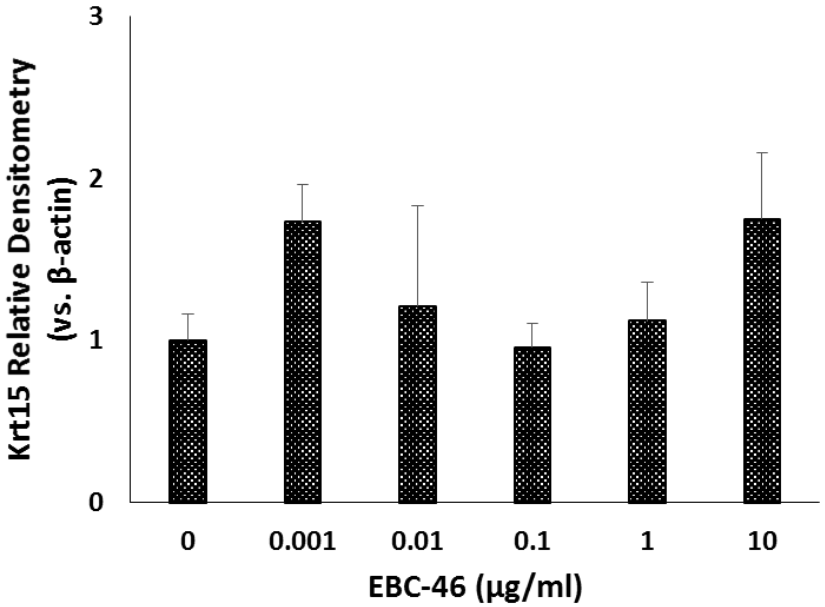

Figure 6.10: Western blot analysis on (A) Krt15 in HaCaTs, at 24h and 48h; with densitometry analysis on Krt15 levels in HaCaTs, cultured in the presence of 0.001µg/ml, 0.01µg/ml, 0.1µg/ml, 1µg/ml and 10µg/ml EBC-211, compared to untreated controls (0µg/ml), at (B) 24h and (C) 48h. (*N=3, average±SE).*

A

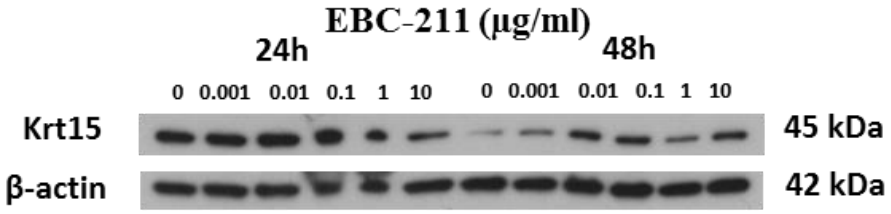

B

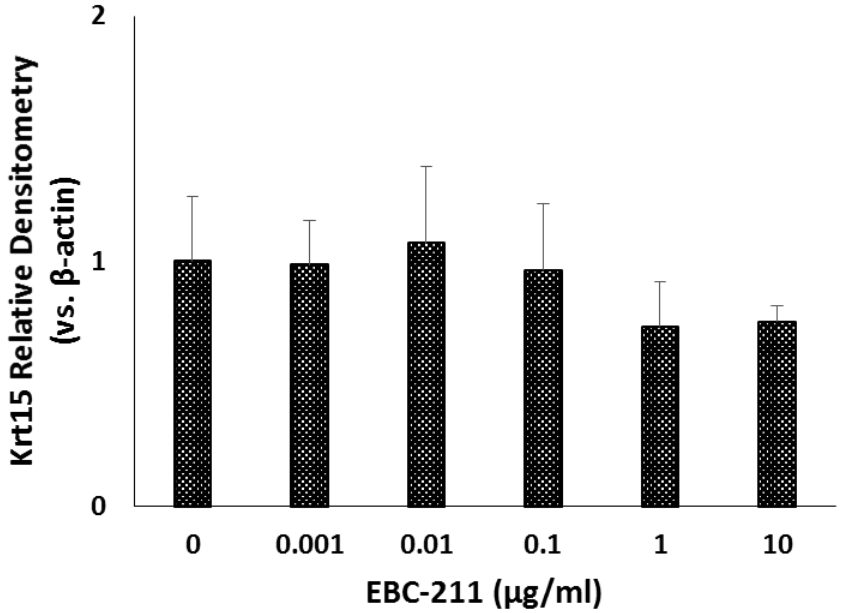

C

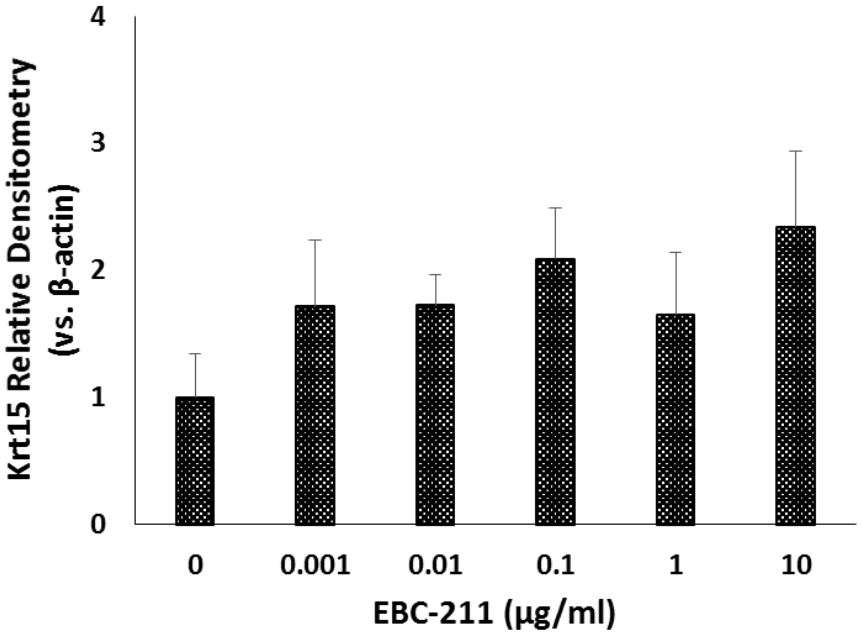

difference in detection, compared to untreated controls, observed in the densitometry analysis for 24h and 48h ($p>0.05$; Figures 6.9B and C). The Western blot for EBC-211 showed no noticeable difference in protein levels for Krt15 at 24h (Figure 6.10A). However, it appeared that levels were increased following EBC-211 treatment, at 48h. These effects were confirmed through the densitometry data, with no difference in Krt15 levels at 24h ($p>0.05$; Figure 6.10B); whereas, a perceived increase in Krt15 levels was seen at 48h, although this is deemed to not be significant ($p>0.05$; Figure 6.10C).

Krt16 Western blots are shown in Figures 6.11A and 6.12A, for EBC-46 and EBC-211, respectively, with β-actin used as a loading control for each blot. The densitometry graphs for each epoxy-tigliane are shown in Figures 6.11B-C and 6.12B-C. The Western blot for EBC-46 appeared to show a decrease in Krt16 protein detection, compared to untreated controls, at 48h, although a potential increase was observed at 24h (Figure 6.11A). The densitometry analysis showed a significant increase in Krt16 protein levels at 10μg/ml EBC-46 at 24h, in contrast to the Microarray findings ($p<0.05$; Figure 11B). In contrast, no significant difference in Krt16 levels were observed at 48h ($p>0.05$; Figures 6.11C). The Western blot for EBC-211 showed a potential decrease in Krt16 detection at 24h and 48h (Figure 6.12A). However, densitometry analysis showed no significant change in Krt16 levels at 24h or 48h ($p>0.05$; Figures 6.12B and C, respectively); although there was a perceived decrease in expression at 48h for 0.01μg/ml and 1μg/ml EBC-211, this was not considered to be significant ($p>0.05$).

Krt17 Western blots are shown in Figures 6.13A and 6.14A, for EBC-46 and EBC-211, respectively, with β-actin used as a loading control for each blot. The densitometry graphs for each epoxy-tigliane are shown in Figures 6.13B-C and 6.14B-C. The Western blot for EBC-46 did not appear to show any change in Krt17 protein detection at 24h or 48h (Figure 6.13A). The densitometry analysis corroborated this result, with no significant difference in Krt17 level observed following EBC-46 treatment, at 24h or 48h ($p>0.05$; Figures 6.13B and C, respectively). There was a perceived increase in Krt17 level at 24h, following 0.001μg/ml EBC-46 treatment; in addition to a decrease in Krt17 expression at

Figure 6.11: Western blot analysis on (A) Krt16 in HaCaTs, at 24h and 48h; with densitometry analysis on Krt16 levels in HaCaTs, cultured in the presence of 0.001µg/ml, 0.01µg/ml, 0.1µg/ml, 1µg/ml and 10µg/ml EBC-46, compared to untreated controls (0µg/ml), at (B) 24h and (C) 48h. (*N=3, average±SE; statistical analysis displayed *p<0.05).*

A

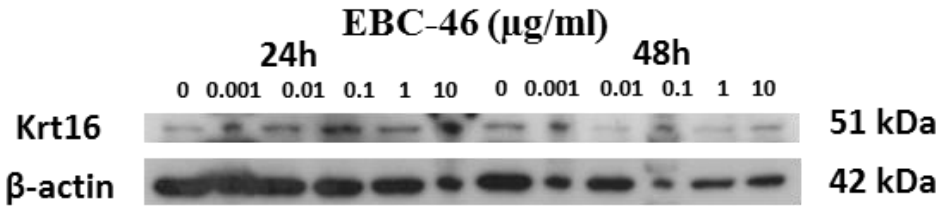

B

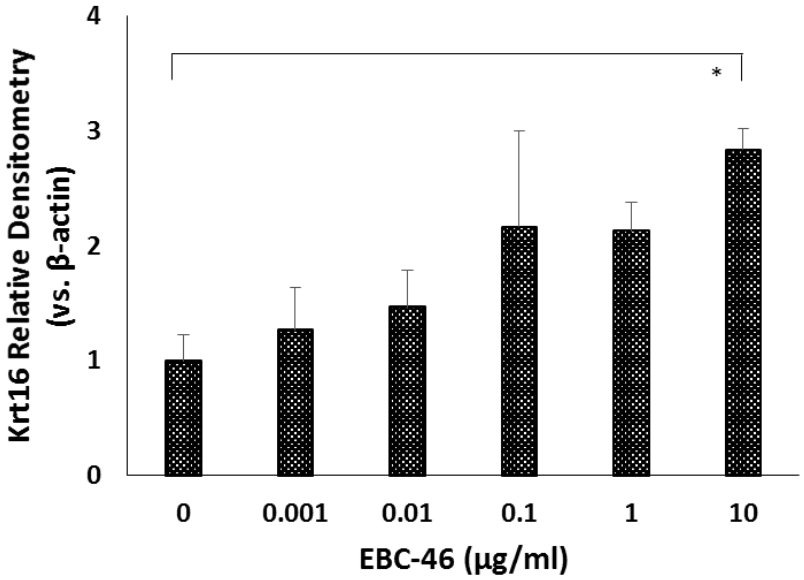

C

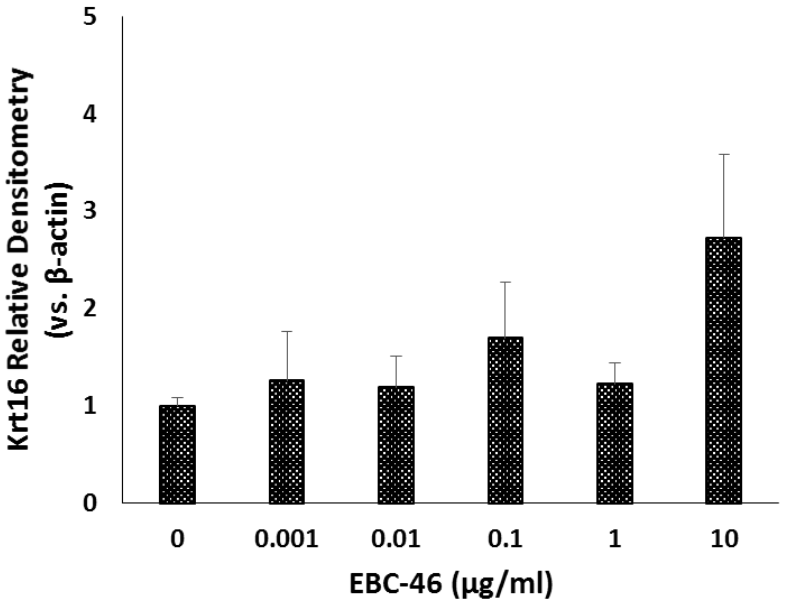

Figure 6.12: Western blot analysis on (A) Krt16 in HaCaTs, at 24h and 48h; with densitometry analysis on Krt16 levels in HaCaTs, cultured in the presence of 0.001µg/ml, 0.01µg/ml, 0.1µg/ml, 1µg/ml and 10µg/ml EBC-211, compared to untreated controls (0µg/ml), at (B) 24h and (C) 48h. (*N=3, average±SE).*

A

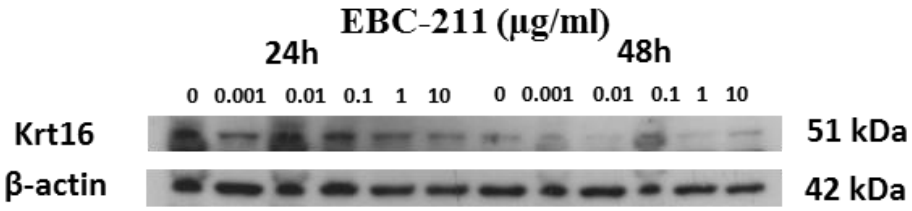

B

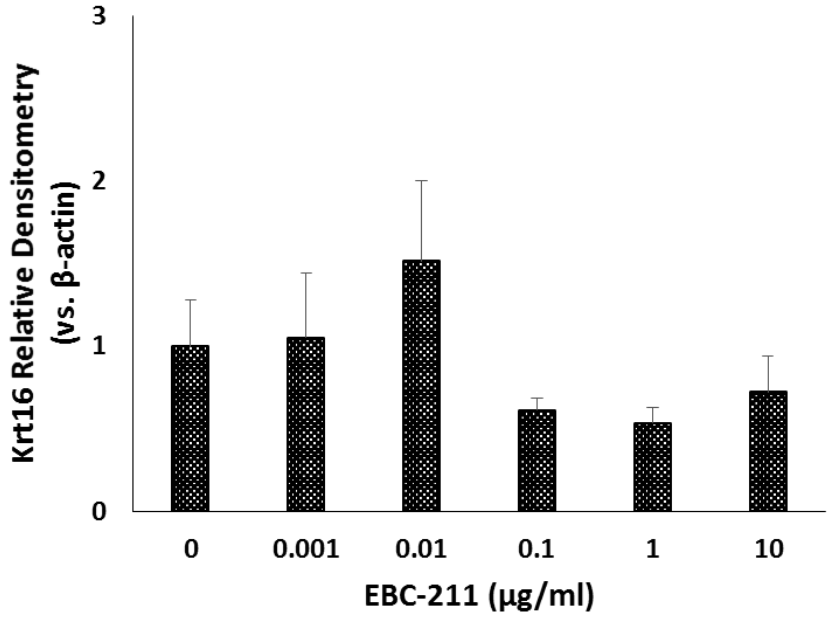

C

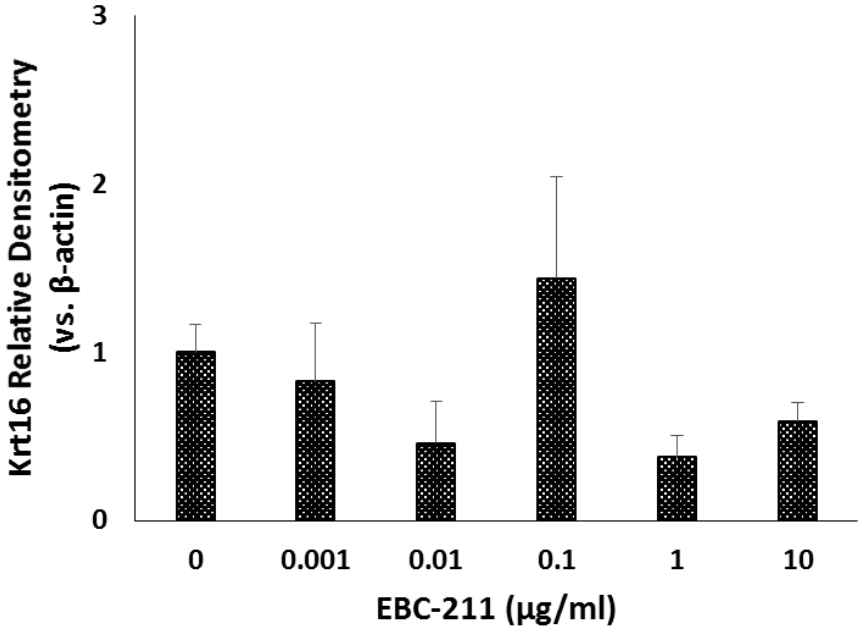

Figure 6.13: Western blot analysis on (A) Krt17 in HaCaTs, at 24h and 48h; with densitometry analysis on Krt17 levels in HaCaTs, cultured in the presence of 0.001µg/ml, 0.01µg/ml, 0.1µg/ml, 1µg/ml and 10µg/ml EBC-46, compared to untreated controls (0µg/ml), at (B) 24h and (C) 48h. (*N=3, average±SE).*

A

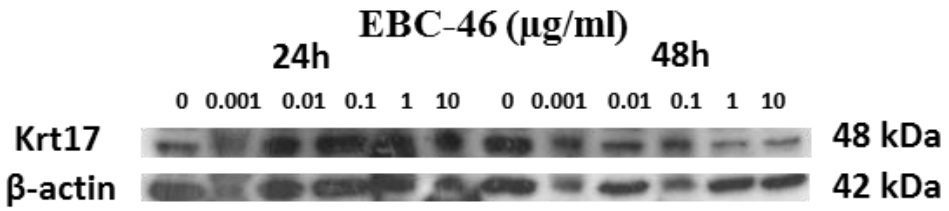

B

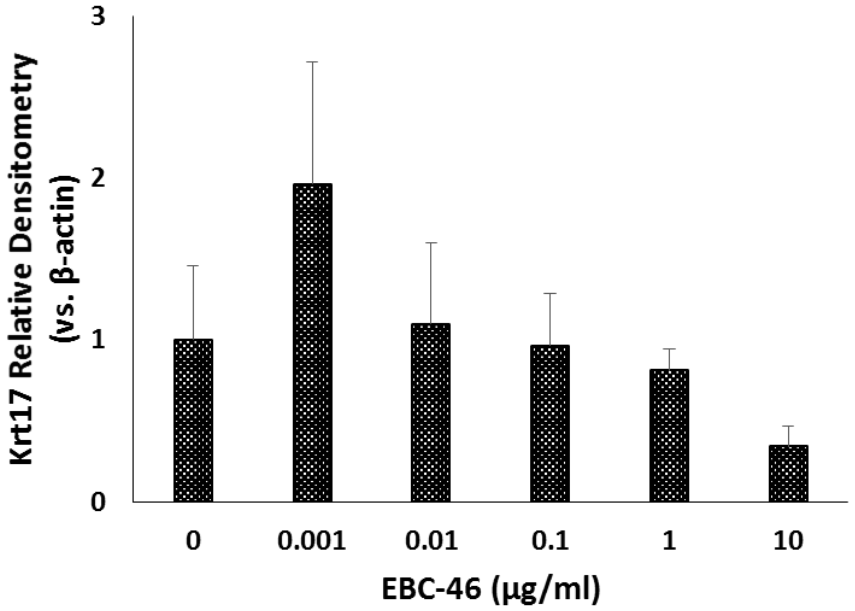

C

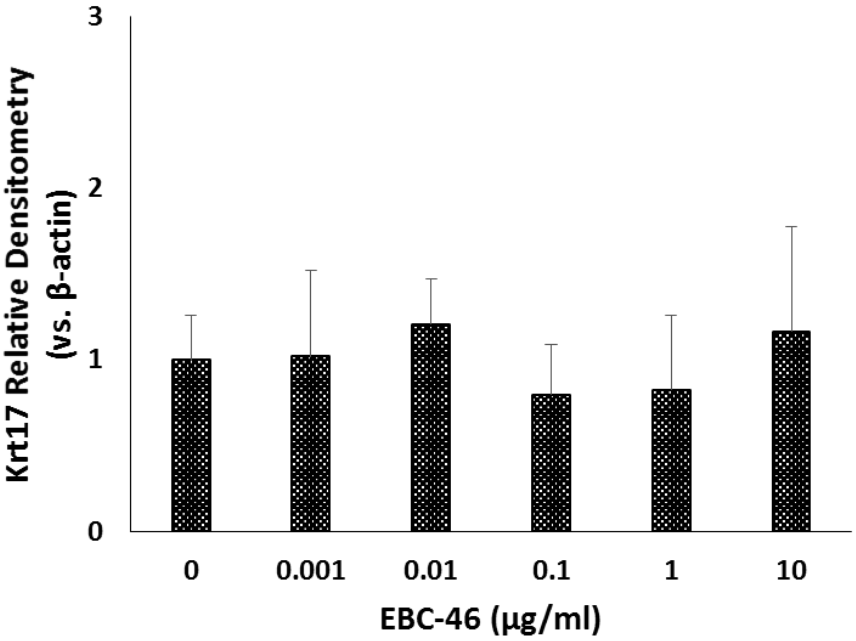

Figure 6.14: Western blot analysis on (A) Krt17 in HaCaTs, at 24h and 48h; with densitometry analysis on Krt17 levels in HaCaTs, cultured in the presence of 0.001µg/ml, 0.01µg/ml, 0.1µg/ml, 1µg/ml and 10µg/ml EBC-211, compared to untreated controls (0µg/ml), at (B) 24h and (C) 48h. (*N=3, average±SE).*

A

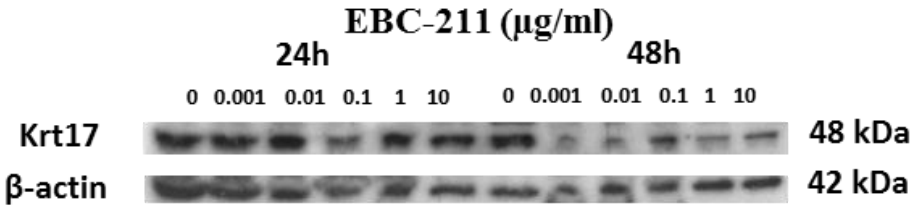

B

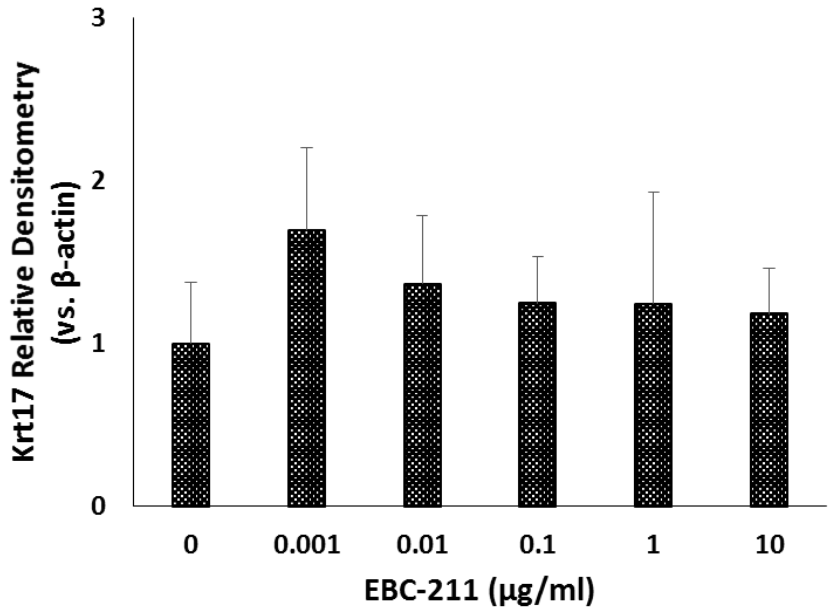

C

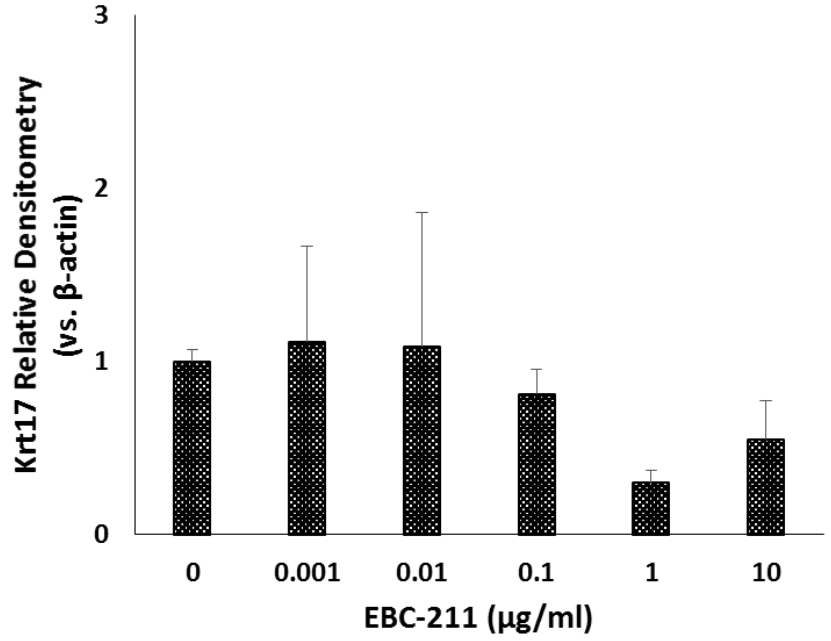

10μg/ml. However, both were shown not to be significant ($p>0.05$). The Western blot for EBC-211 showed no noticeable difference in Krt17 protein detection at 24h. Although, there was a decrease in Krt17 detection at 48h, compared to untreated controls (Figure 6.14A). However, the densitometry analysis showed no significant change in Krt17 levels following EBC-211 treatment, at 24h or 48h ($p>0.05$; Figures 6.14A and B, respectively). Although there was a perceived decrease in levels at 48h for 1μg/ml EBC-211, this was also not considered to be significant ($p>0.05$).

Krt6B Western blots are shown in Figures 6.15A and 6.16A, for EBC-46 and EBC-211, respectively, with β-actin used as a loading control for each blot. The densitometry graphs for each epoxy-tigliane are shown in Figures 6.15B-C and 6.16B-C. The Western blot for EBC-46 did not appear to show any change in Krt6B protein detection at 24h or 48h (Figure 6.15A). The densitometry analysis showed no significant difference in Krt6B levels at 24h or 48h ($p>0.05$; Figures 6.15B and C, respectively). There was a perceived increase in Krt6B levels at 24h and 48h, following EBC-46 treatment, although this was shown to not be significant ($p>0.05$). The Western blot for EBC-211 did not appear to show any change in Krt6B detection at 24h. However, it did show a potential decrease in Krt6B expression at 48h for 0.01μg/ml EBC-211 (Figure 6.16A). The densitometry analysis corroborated these results, showing no significant change in Krt6B levels at 24h ($p>0.05$; Figures 6.16B), although the perceived decrease in Krt6B levels for 0.01μg/ml and 1μg/ml EBC-211 was not considered to be significant ($p>0.05$; Figure 6.16C).

Figure 6.15: Western blot analysis on (A) Krt6B in HaCaTs, at 24h and 48h; with densitometry analysis on Krt6B levels in HaCaTs, cultured in the presence of 0.001µg/ml, 0.01µg/ml, 0.1µg/ml, 1µg/ml and 10µg/ml EBC-46, compared to untreated controls (0µg/ml), at (B) 24h and (C) 48h. (*N=3, average±SE).*

A

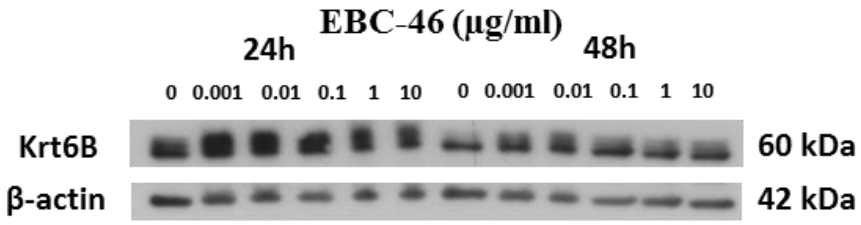

B

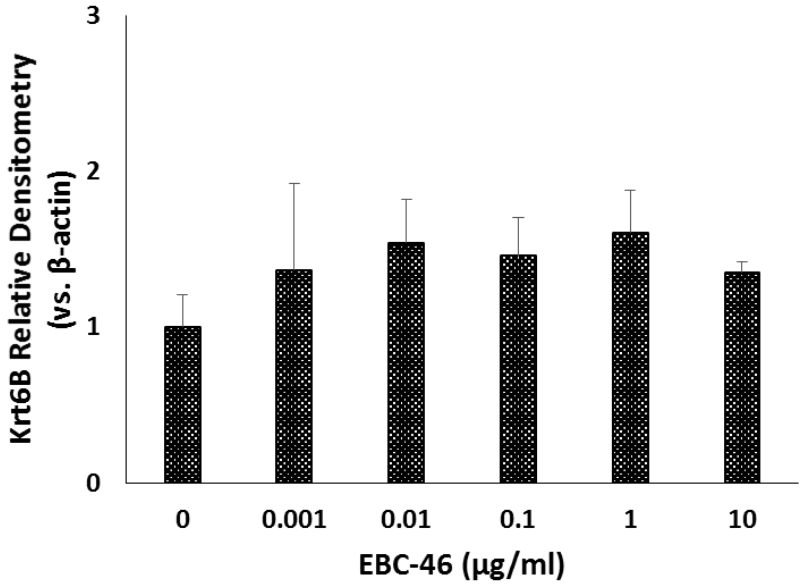

C

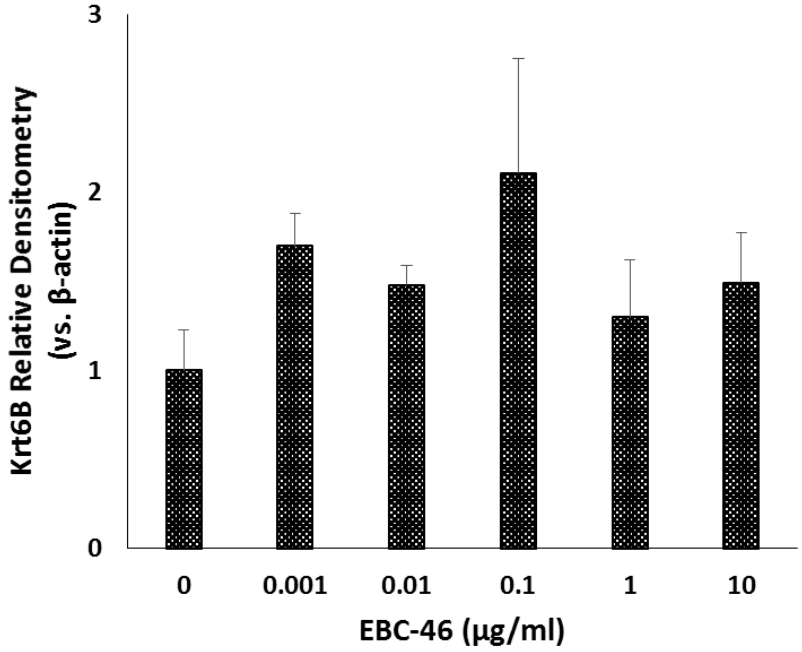

Figure 6.16: Western blot analysis on (A) Krt6B in HaCaTs, at 24h and 48h; with densitometry analysis on Krt6B levels in HaCaTs, cultured in the presence of 0.001µg/ml, 0.01µg/ml, 0.1µg/ml, 1µg/ml and 10µg/ml EBC-211, compared to untreated controls (0µg/ml), at (B) 24h and (C) 48h. (*N=3, average±SE).*

A

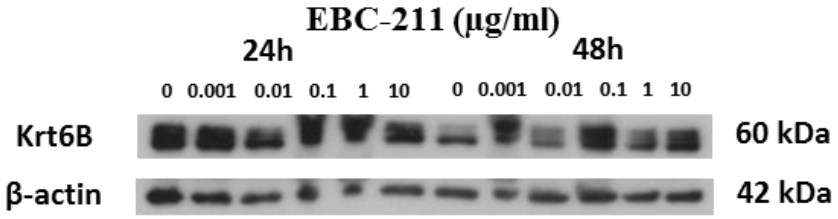

B

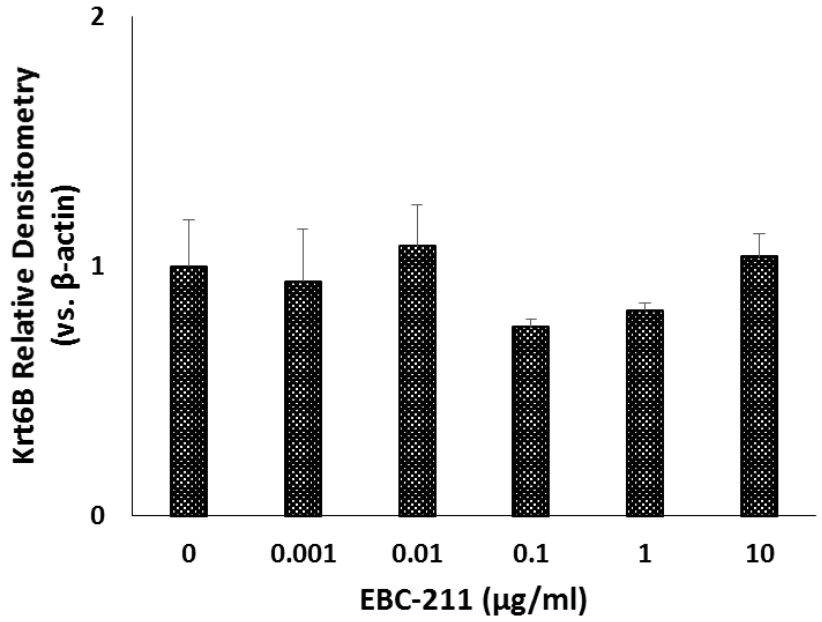

C

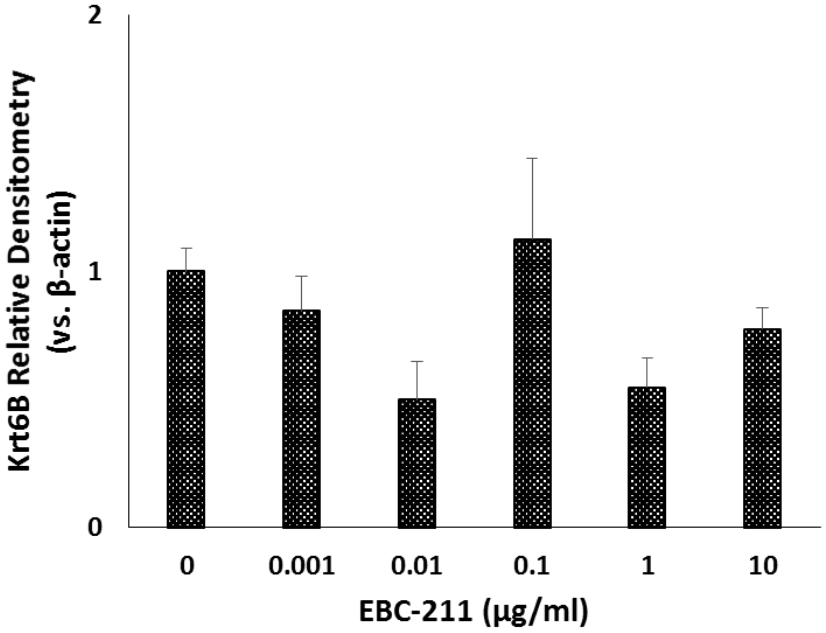

Western blot analysis was also performed on a number of cell cycle-related genes, as upregulation of Cyclin A2, Cyclin B1, Cyclin B2, CDKN3 and UBE2C, were observed during global gene analysis. The downregulation of CDKN1A was also seen (Tables 6.1 and 6.2, for EBC-46 and EBC-211 respectively).

Cyclin A2 Western blots are shown in Figures 6.17A and 6.18A, for EBC-46 and EBC-211, respectively, with β-actin used as a loading control for each blot. The densitometry graphs for each epoxy-tigliane are shown in Figures 6.17B-C and 6.18B-C. The Western blot for Cyclin A2 following EBC-46 treatment appeared to indicate reduced protein detection at 0.1-10μg/ml at 24h. However, there appeared to be a dose-dependent increase in Cyclin A2 levels with EBC-46 treatment at 48h, with increased detection particularly evident at higher concentrations (0.1-10μg/ml), compared to untreated controls (Figure 6.17A). The densitometry was performed on three separate blots, one per sample set. There were no significant changes in Cyclin A2 levels, following EBC-46 treatment at 24h ($p>0.05$; Figure 6.17B). At 48h, the dose-dependent increase in Cyclin A2 detection was confirmed, with a steady increase in levels evident with increasing concentration, from 0.001-10μg/ml EBC-46. However, despite this increase, only 10μg/ml was considered to be significant compared to untreated controls ($p<0.01$; Figure 6.17C). The Western blot for Cyclin A2 following EBC-211 treatment showed no change in protein level at 24h. However, a dose-dependent increase in Cyclin A2 levels was evident with EBC-211 treatment at 48h, with largest detection evident at higher concentrations (0.1-10μg/ml), compared to untreated controls (Figure 6.18A). Densitometry analysis confirmed these findings, with no noticeable or significant change in Cyclin A2 levels following EBC-211 treatment at 24h ($p>0.05$; Figure 6.18B). There was a perceived increase in Cyclin A2 levels following EBC-211 treatment (0.001-10μg/ml) at 48h. However, this was not considered to be significant ($p>0.05$; Figure 6.18C).

Cyclin B1 Western blots are shown in Figures 6.19A and 6.20A, for EBC-46 and EBC-211, respectively, with β-actin used as a loading control for each blot. The densitometry graphs for each epoxy-tigliane are shown in Figures 6.19B-C, and 6.20B-C. The Western blot for Cyclin B1 following EBC-46 treatment showed

Figure 6.17: Western blot analysis on (A) Cyclin A2 in HaCaTs, at 24h and 48h; with densitometry analysis on Cyclin A2 levels in HaCaTs, cultured in the presence of 0.001µg/ml, 0.01µg/ml, 0.1µg/ml, 1µg/ml and 10µg/ml EBC-46, compared to untreated controls (0µg/ml), at (B) 24h and (C) 48h. (*N=3, average±SE; statistical analysis displayed **p<0.01).*

A

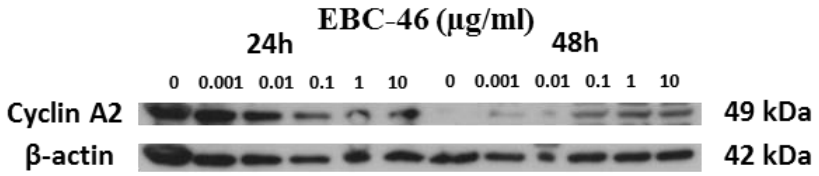

B

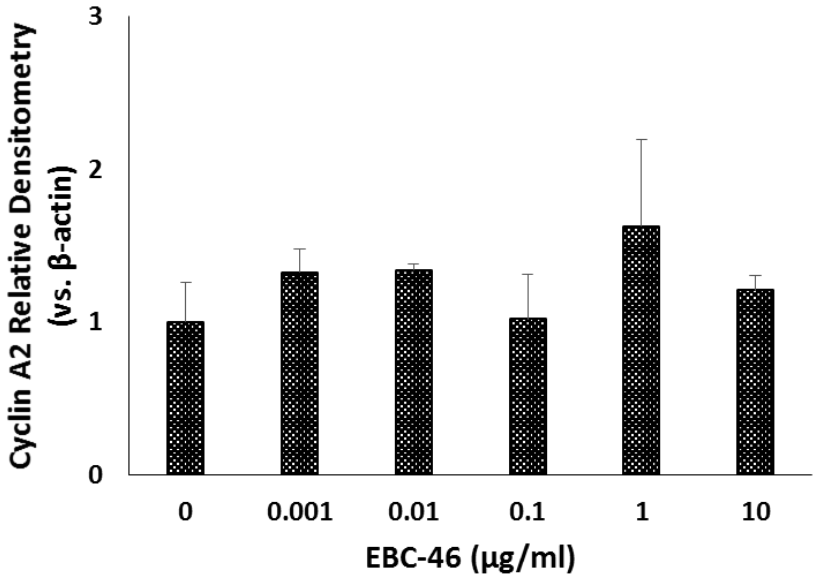

C

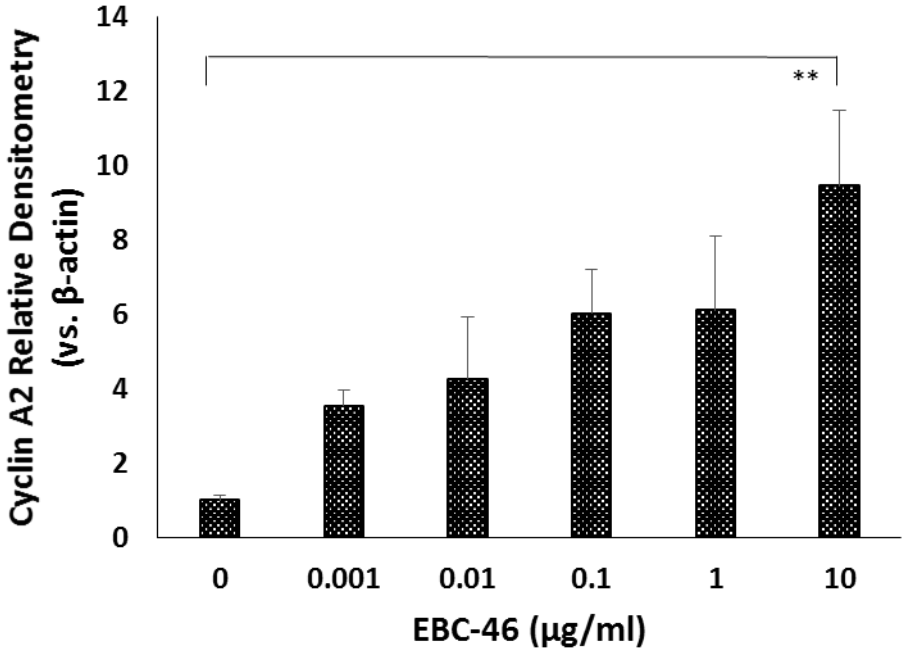

Figure 6.18: Western blot analysis on (A) Cyclin A2 in HaCaTs, at 24h and 48h; with densitometry analysis on Cyclin A2 levels in HaCaTs, cultured in the presence of 0.001µg/ml, 0.01µg/ml, 0.1µg/ml, 1µg/ml and 10µg/ml EBC-211, compared to untreated controls (0µg/ml), at (B) 24h and (C) 48h. (*N=3, average±SE).*

A

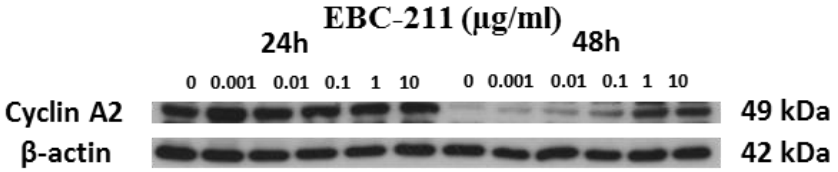

B

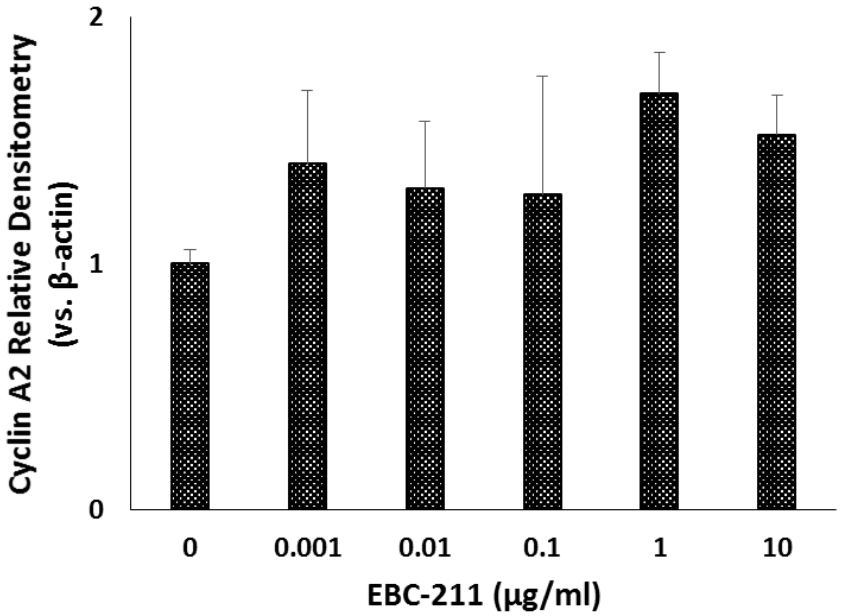

C

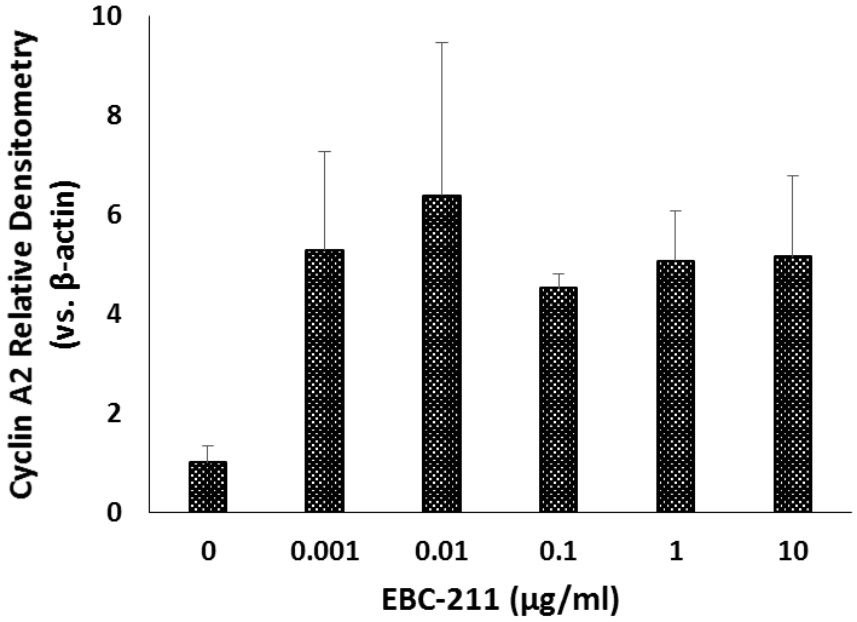

Figure 6.19: Western blot analysis on (A) Cyclin B1 in HaCaTs, at 24h and 48h; with densitometry analysis on Cyclin B1 levels in HaCaTs, cultured in the presence of 0.001µg/ml, 0.01µg/ml, 0.1µg/ml, 1µg/ml and 10µg/ml EBC-46, compared to untreated controls (0µg/ml), at (B) 24h and (C) 48h. (*N=3, average±SE; statistical analysis displayed *p<0.05, **p<0.01).*

A

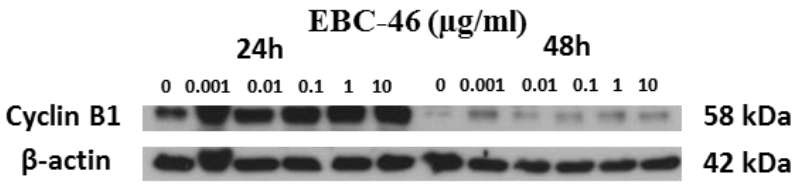

B

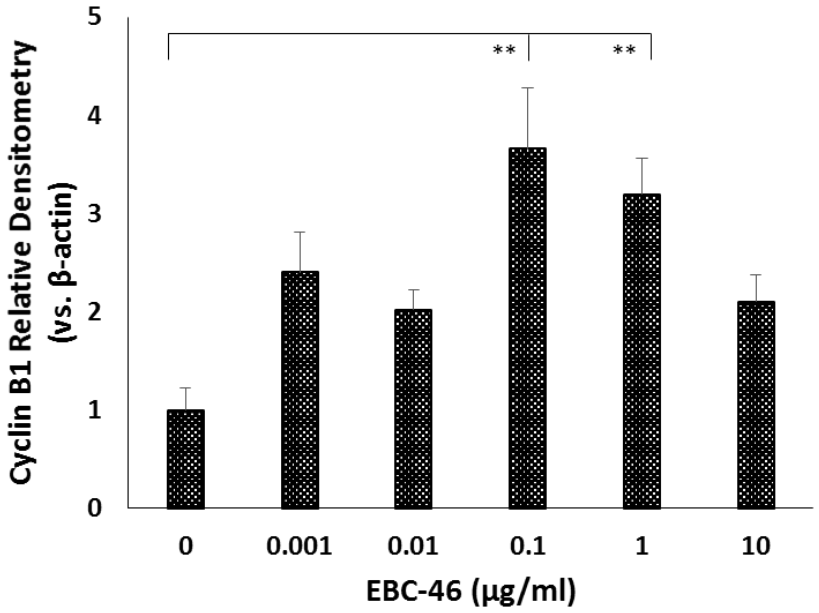

C

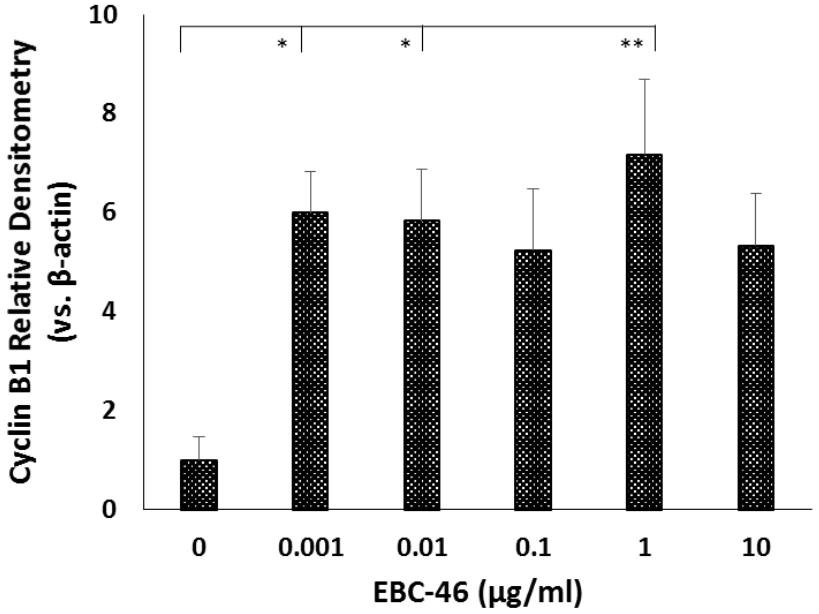

Figure 6.20: Western blot analysis on (A) Cyclin B1 in HaCaTs, at 24h and 48h; with densitometry analysis on Cyclin B1 levels in HaCaTs, cultured in the presence of 0.001μg/ml, 0.01μg/ml, 0.1μg/ml, 1μg/ml and 10μg/ml EBC-211, compared to untreated controls (0μg/ml), at (B) 24h and (C) 48h. (*N=3, average±SE; statistical analysis displayed **p<0.01).*

A

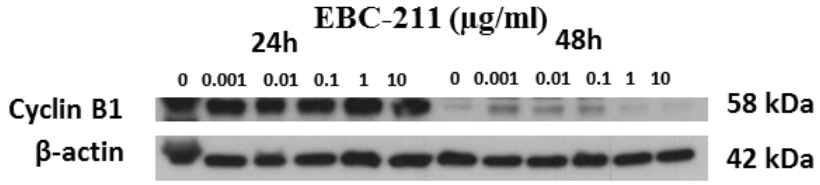

B

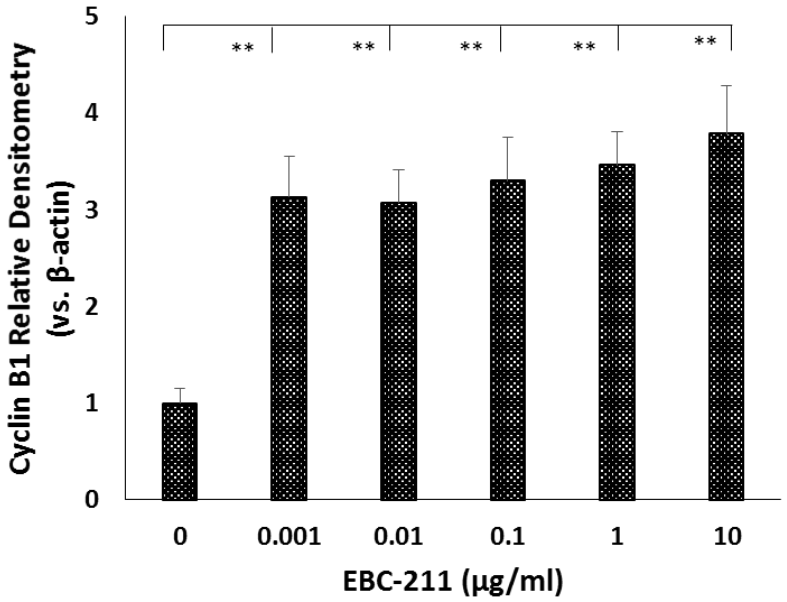

C

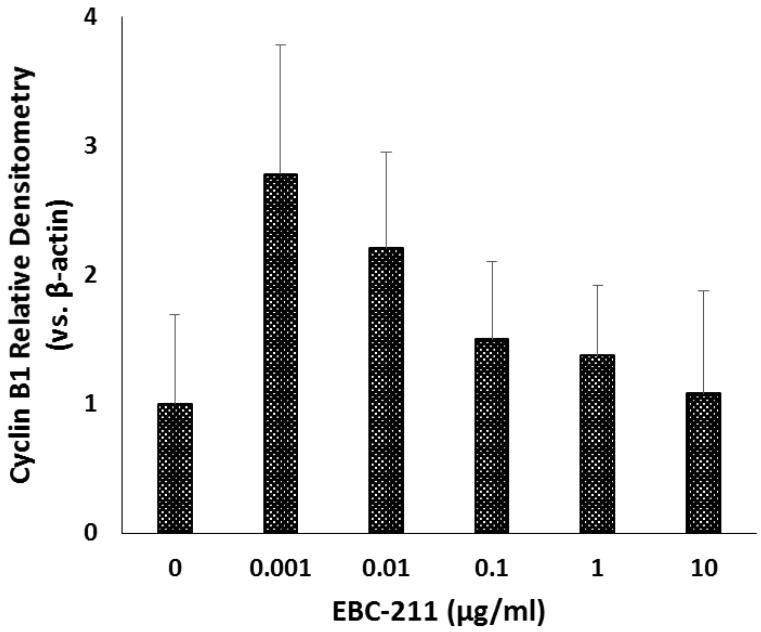

increased detection at 24h and 48h, compared to untreated controls (Figure 6.19A). The densitometry confirmed the increase at 24h, following EBC-46 treatment. However, despite this perceived increase across the range of concentrations (0.001-10μg/ml), it was only deemed to be significant at 0.1μg/ml and 1μg/ml EBC-46 ($p<0.01$; Figure 6.19B). At 48h, the increases in Cyclin B1 protein levels were also confirmed, with increased detection evident across the range of EBC-46 concentrations (0.001-10μg/ml). This was considered to be significant at 0.001μg/ml, 0.01μg/ml and 1μg/ml EBC-46 ($p<0.01$-0.05; Figure 6.19C). The Western blot for Cyclin B1 following EBC-211 treatment showed an increased detection at 24h and 48h, compared to untreated controls (Figure 6.20A). However at 48h, there appeared to be a greater increase in Cyclin B1 levels at the lower EBC-211 concentrations (0.001-0.1μg/ml); compared to the higher concentrations (1-10μg/ml), and the untreated controls. Densitometry analysis confirmed these findings, with a significant increase in Cyclin B1 detection at 24h for 0.001-10μg/ml EBC-211 (all $p<0.01$; Figure 6.20B). An increase in Cyclin B1 levels was also perceived at 48h following EBC-211 treatment, in an apparent dose-dependent manner, with the lower concentrations inducing the largest increases; however, this was deemed to not be significant ($p>0.05$; Figure 6.20C).

Cyclin B2 Western blots are shown in Figures 6.21A and 6.22A, for EBC-46 and EBC-211, respectively, with β-actin used as a loading control for each blot. The densitometry graphs for each epoxy-tigliane are shown in Figures 6.21B-C and 6.22B-C. The Western blot for Cyclin B2 following EBC-46 treatment showed increased detection at 24h and 48h, particularly at higher concentrations (0.1-10μg/ml) at 48h, compared to untreated controls (Figure 6.21A). The densitometry confirmed the increase at 24h, following EBC-46 treatment, although this increase was not considered to be significant ($p>0.05$; Figure 6.21B). At 48h, this increase in Cyclin B2 levels was also confirmed, with increased detection evident across the range of EBC-46 concentrations (0.001-10μg/ml); however, this was only considered to be significant at 10μg/ml EBC-46 ($p<0.05$; Figure 6.21C). The Western blot for Cyclin B2 following EBC-211 treatment showed increased detection at 24h and 48h, compared to untreated controls (Figure 6.22A). The densitometry analysis showed no

Figure 6.21: Western blot analysis on (A) Cyclin B2 in HaCaTs, at 24h and 48h; with densitometry analysis on Cyclin B2 levels in HaCaTs, cultured in the presence of 0.001µg/ml, 0.01µg/ml, 0.1µg/ml, 1µg/ml and 10µg/ml EBC-46, compared to untreated controls (0µg/ml), at (B) 24h and (C) 48h. (*N=3, average±SE; statistical analysis displayed *p<0.05).*

A

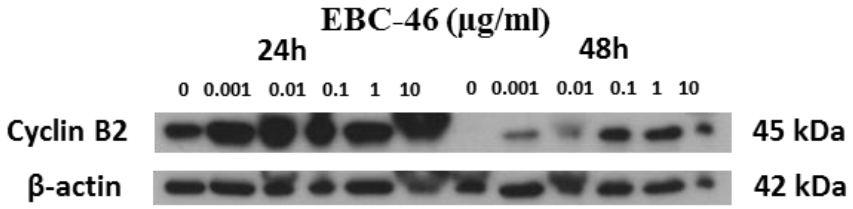

B

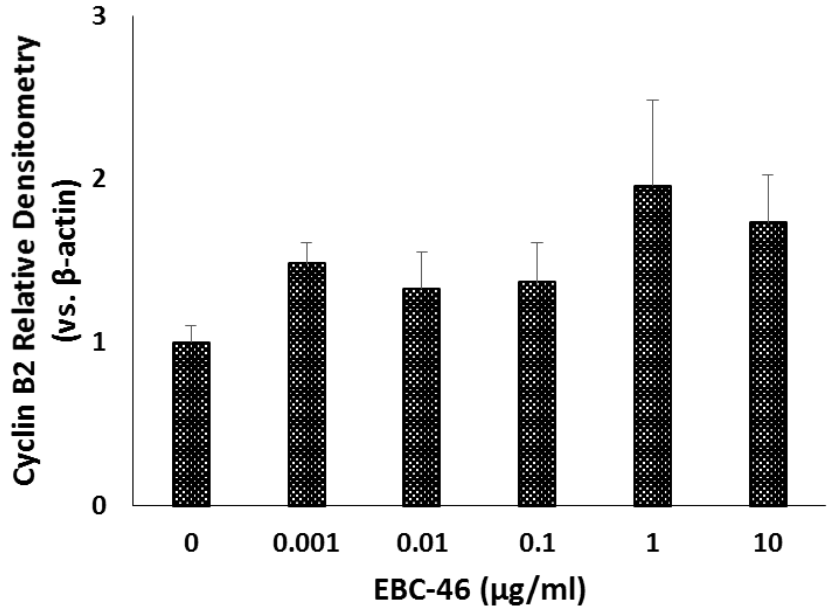

C

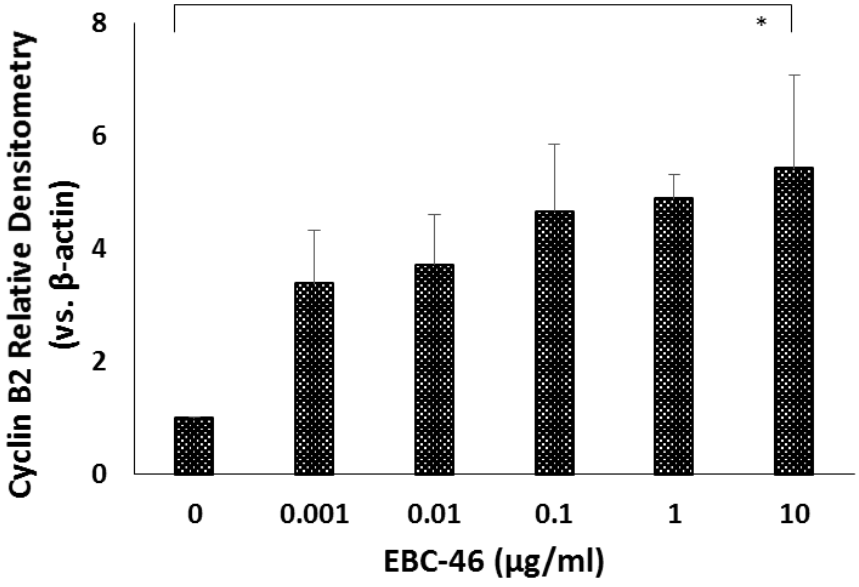

Figure 6.22: Western blot analysis on (A) Cyclin B2 in HaCaTs, at 24h and 48h; with densitometry analysis on Cyclin B2 levels in HaCaTs, cultured in the presence of 0.001µg/ml, 0.01µg/ml, 0.1µg/ml, 1µg/ml and 10µg/ml EBC-211, compared to untreated controls (0µg/ml), at (B) 24h and (C) 48h. (*N=3, average±SE).*

A

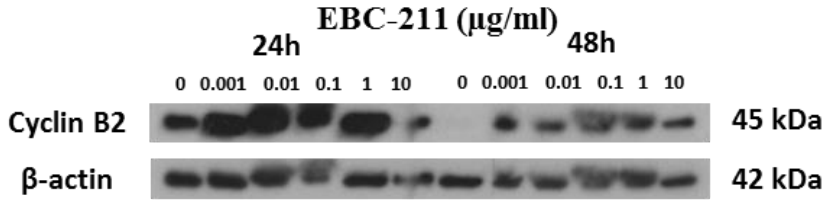

B

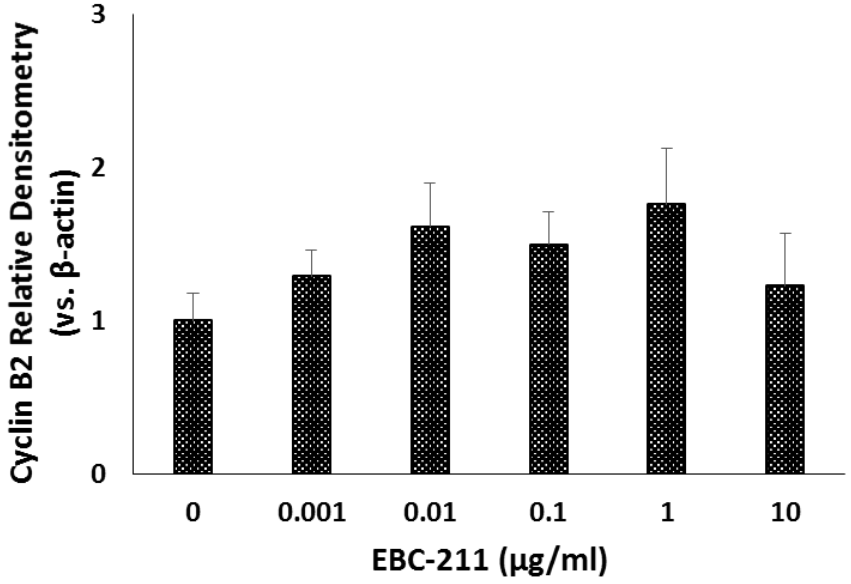

C

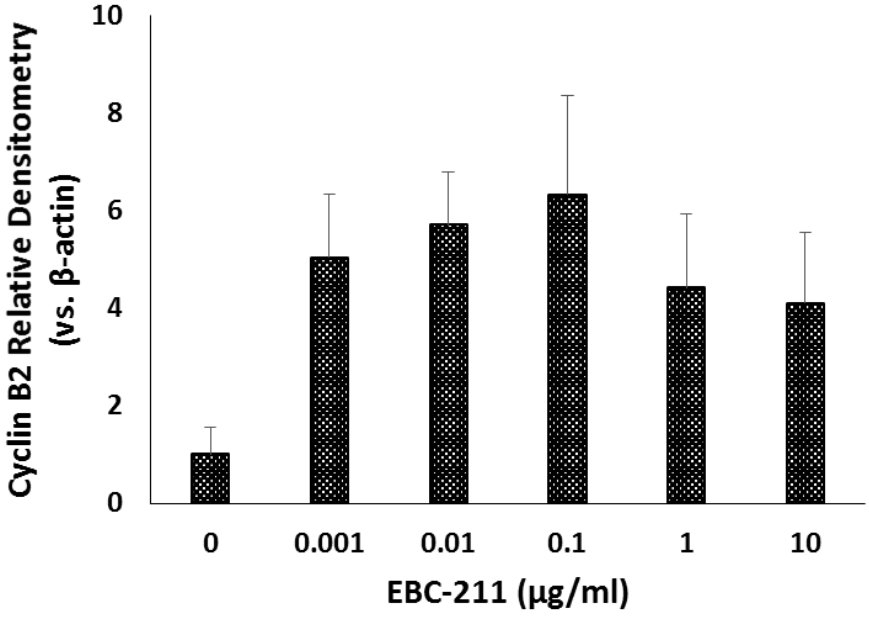

significant difference in Cyclin B2 protein levels at 24h, following EBC-211 treatment ($p>0.05$; Figure 6.22B). There was a perceived increase in Cyclin B2 levels at 48h, following EBC-211 treatment (0.001-10μg/ml). However, this was not considered to be significant, when compared to untreated controls ($p>0.05$; Figure 6.22C).

CDKN3 Western blots are shown in Figures 6.23A and 6.24A, for EBC-46 and EBC-211, respectively, with β-actin used as a loading control for each blot. The densitometry graphs for each epoxy-tigliane are shown in Figures 6.23B-C and 6.24B-C. The Western blot for CDKN3 following EBC-46 treatment showed no noticeable differences in detectable protein at 24h or 48h, compared to untreated controls (Figure 6.23A). The densitometry analysis showed that there was no significant difference in CDKN3 detection ($p>0.05$), following EBC-46 treatment at 24h, although a perceived downregulation was observed at 0.001μg/ml EBC-46. However, this was deemed to not be significant ($p>0.05$; Figure 6.23B). There was also no significant difference in CDKN3 levels following EBC-46 treatment at 48h, compared to untreated controls ($p>0.05$; Figure 6.23C). The Western blot for CDKN3 following EBC-211 treatment also showed no noticeable differences in detectable protein at 24h or 48h, compared to untreated controls (Figure 6.24A). The densitometry analysis showed a perceived upregulation of CDKN3 expression at 24h, following EBC-211 treatment, which was shown to be significant at 0.1μg/ml ($p<0.05$; Figure 6.24B). Confirming the Western blot data, the densitometry analysis showed no significant difference in CDKN3 detection at 48h, following EBC-211 treatment ($p>0.05$; Figure 6.24C).

CDKN1A Western blots are shown in Figures 6.25A and 6.26A, for EBC-46 and EBC-211, respectively, with β-actin used as a loading control for each blot. The densitometry graphs for each epoxy-tigliane are shown in Figures 6.25B-C and 6.26B-C. The Western blot for CDKN1A following EBC-46 treatment showed a profound reduction in detectable CDKN1A at 24h, after treatment with 0.001-10μg/ml EBC-46, compared to untreated controls (Figure 6.25A). Reduced levels were also observed at 10μg/ml EBC-46 at 48h, with no noticeable difference at the lower concentrations of EBC-46 (0.001-1μg/ml) at 48h, compared to untreated

Figure 6.23: Western blot analysis on (A) CDKN3 in HaCaTs, at 24h and 48h; with densitometry analysis on CDKN3 levels in HaCaTs, cultured in the presence of 0.001µg/ml, 0.01µg/ml, 0.1µg/ml, 1µg/ml and 10µg/ml EBC-46, compared to untreated controls (0µg/ml), at (B) 24h and (C) 48h. (*N=3, average±SE).*

A

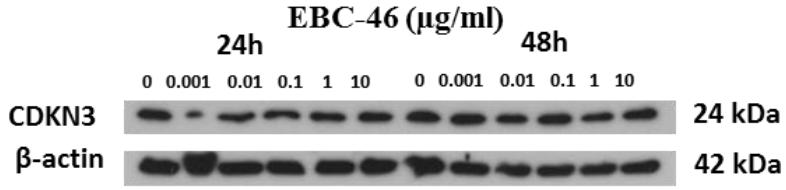

B

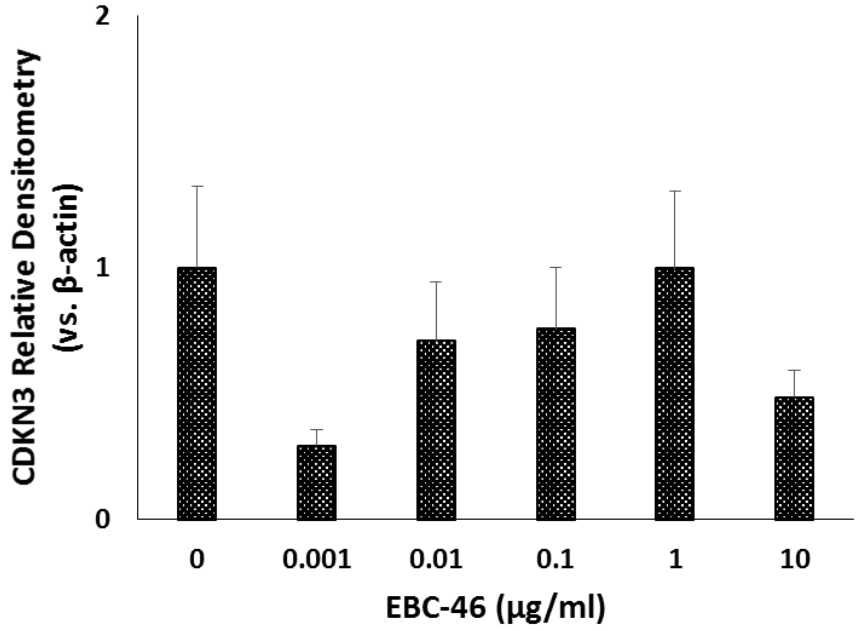

C

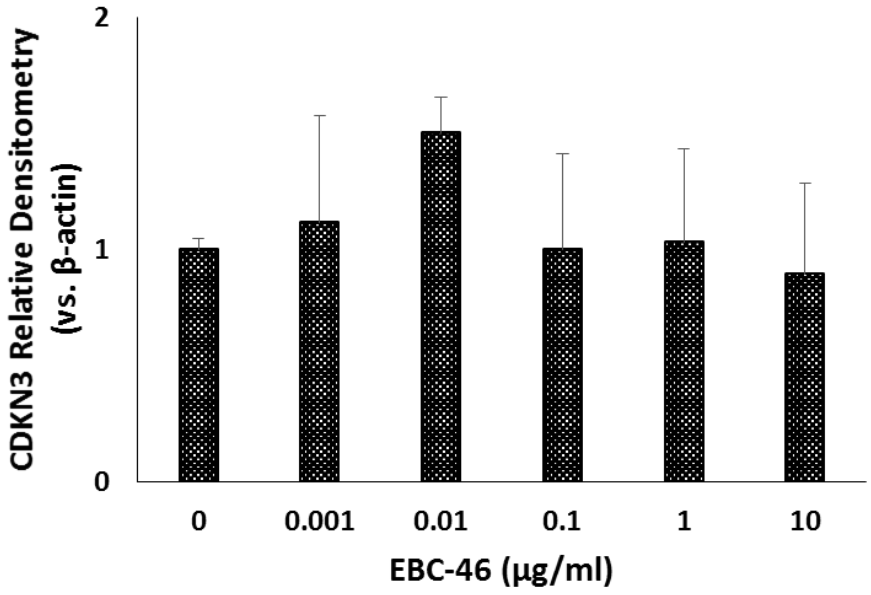

Figure 6.24: Western blot analysis on (A) CDKN3 in HaCaTs, at 24h and 48h; with densitometry analysis on CDKN3 levels in HaCaTs, cultured in the presence of 0.001µg/ml, 0.01µg/ml, 0.1µg/ml, 1µg/ml and 10µg/ml EBC-211, compared to untreated controls (0µg/ml), at (B) 24h and (C) 48h. (*N=3, average±SE; statistical analysis displayed *p<0.05).*

A

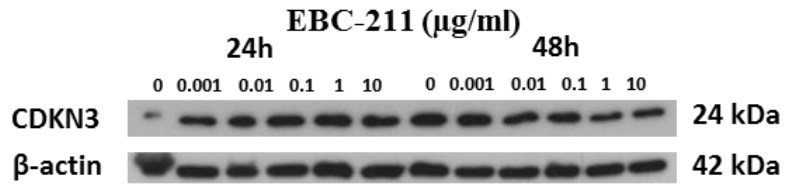

B

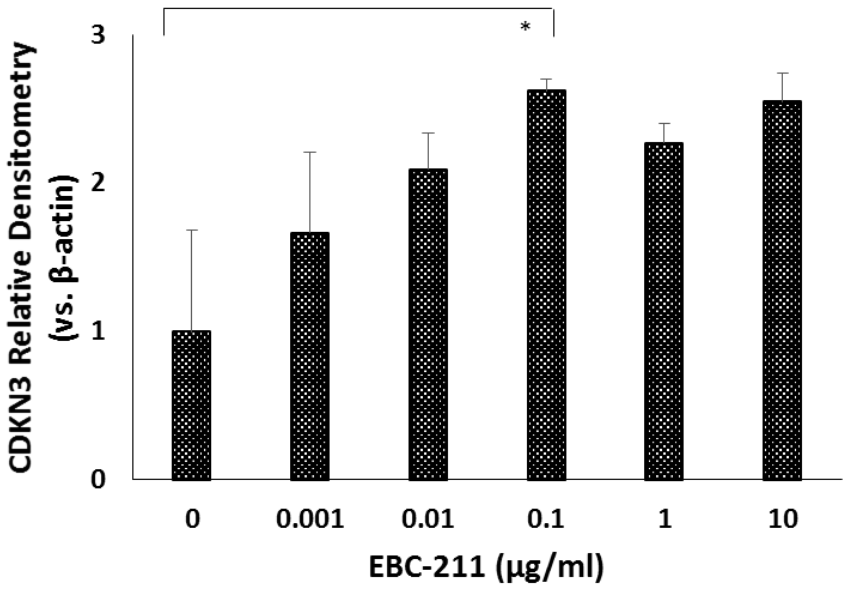

C

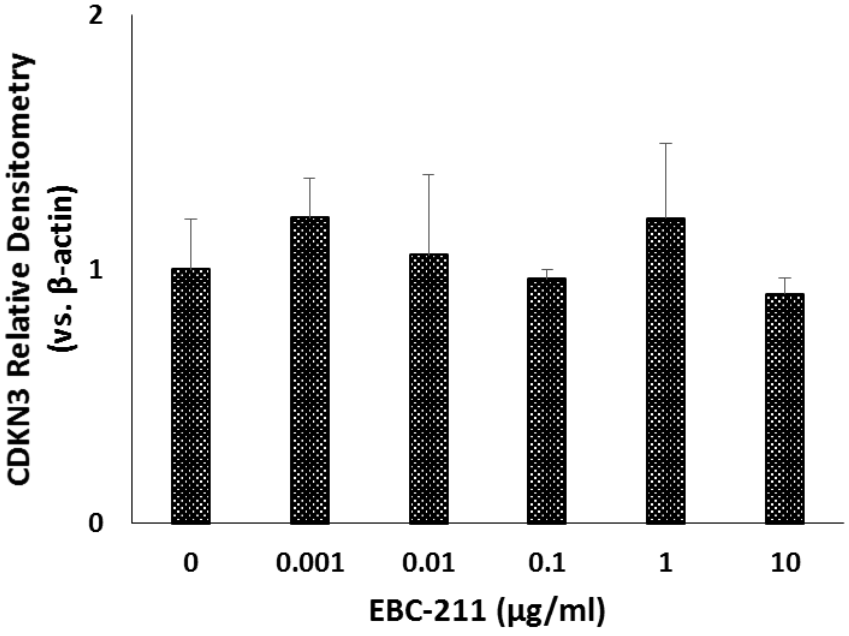

Figure 6.25: Western blot analysis on (A) CDKN1A in HaCaTs, at 24h and 48h; with densitometry analysis on CDKN1A levels in HaCaTs, cultured in the presence of 0.001µg/ml, 0.01µg/ml, 0.1µg/ml, 1µg/ml and 10µg/ml EBC-46, compared to untreated controls (0µg/ml), at (B) 24h and (C) 48h. (*N=3, average±SE; statistical analysis displayed **p<0.01).*

A

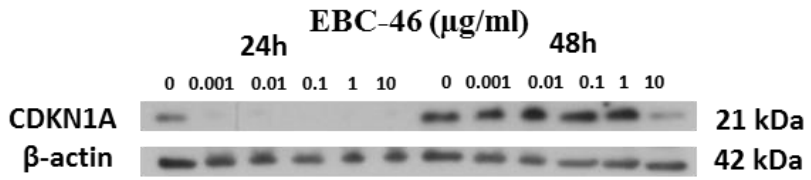

B

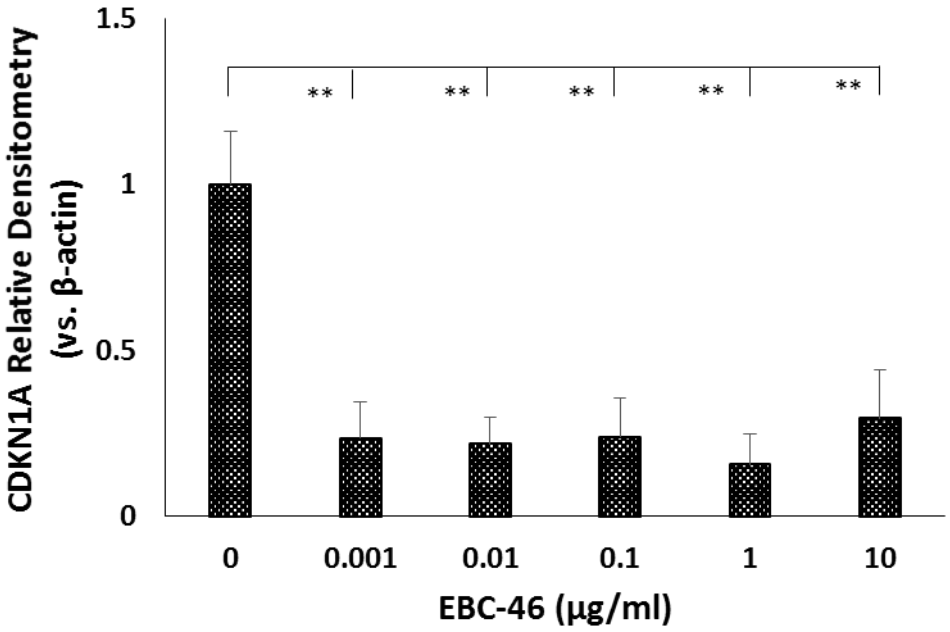

C

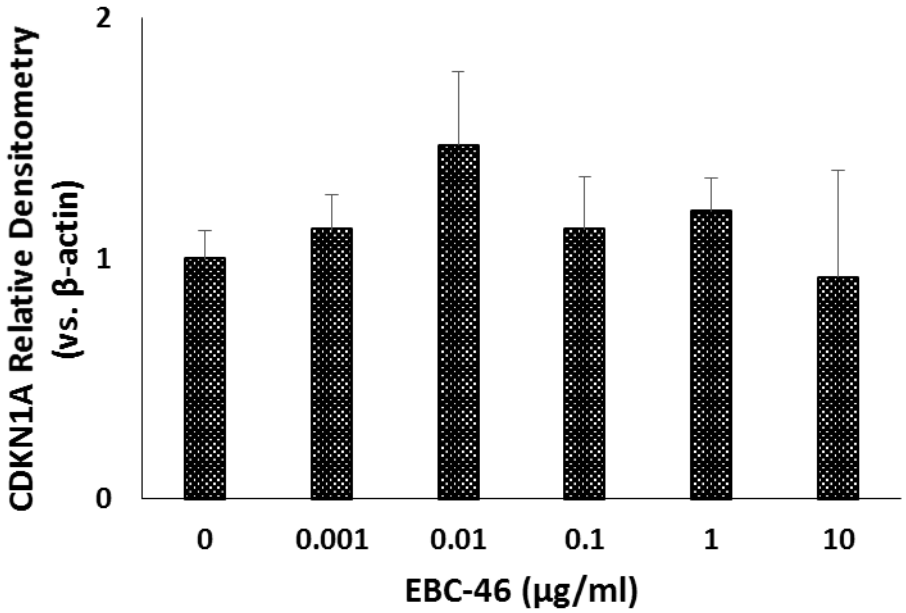

Figure 6.26: Western blot analysis on (A) CDKN1A in HaCaTs, at 24h and 48h; with densitometry analysis on CDKN1A levels in HaCaTs, cultured in the presence of 0.001µg/ml, 0.01µg/ml, 0.1µg/ml, 1µg/ml and 10µg/ml EBC-211, compared to untreated controls (0µg/ml), at (B) 24h and (C) 48h. (*N=3, average±SE; statistical analysis displayed **p<0.01).*

A

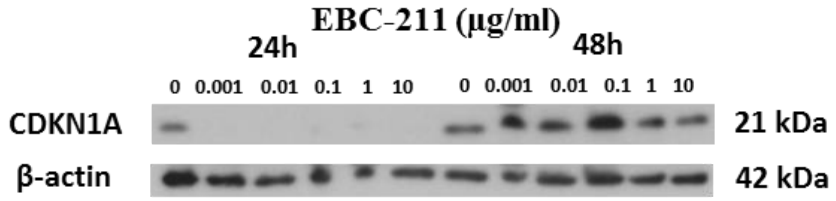

B

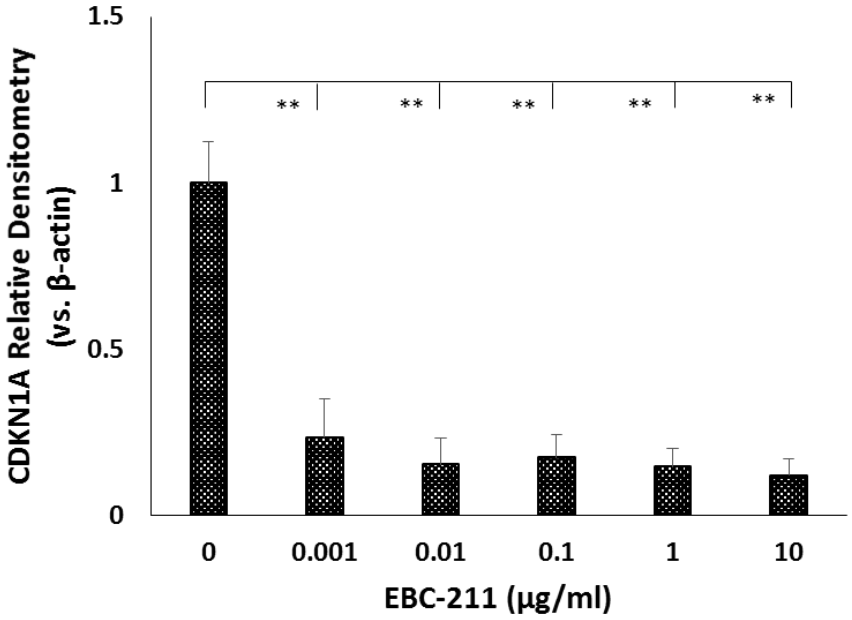

C

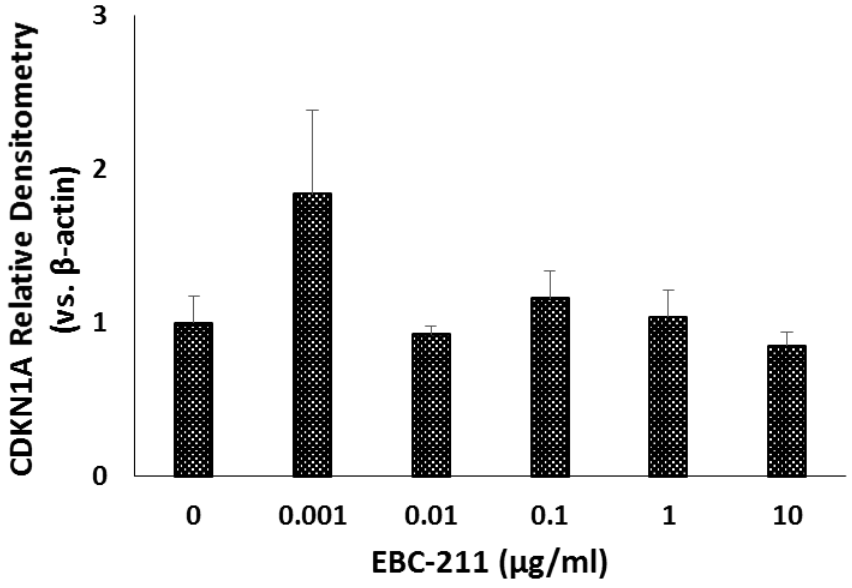

controls (Figure 6.25A). The densitometry analysis corroborated the profound decrease in CDKN1A, evident by the significant decreases in detectable protein levels across all EBC-46 concentrations (0.001-10μg/ml) at 24h ($p<0.01$; Figure 6.25B). However, at 48h, there was no significant difference in CDKN1A levels ($p>0.05$; Figure 6.25C). The Western blot for CDKN1A following EBC-211 treatment showed a similar response to EBC-46, with a profound reduction in CDKN1A levels at 24h. No obvious differences in CDKN1A levels were apparent at 48h, compared to untreated controls (Figure 6.26A). The densitometry analysis again confirmed this profound decrease in CDKN1A levels at 24h, with these decreases shown to be significant at 0.001-10μg/ml EBC-211 ($p<0.01$; Figure 6.26B). Confirming the Western blot data, the densitometry analysis showed no significant difference in CDKN1A levels at 48h, following EBC-211 treatment ($p>0.05$; Figure 6.26C).

UBE2C Western blots are shown in Figures 6.27A and 6.28A, for EBC-46 and EBC-211, respectively, with β-actin used as a loading control for each blot. The densitometry graphs for each epoxy-tigliane are shown in Figures 6.27B-C and 6.28B-C. The Western blot for UBE2C following EBC-46 treatment showed an increase in UBE2C detection following treatment with 0.001-0.1μg/ml EBC-46 at 24h. At 48h, an increase in UBE2C detection was also evident at 0.001μg/ml EBC-46, compared to untreated controls (Figure 6.27A). The densitometry analysis showed a perceived upregulation in UBE2C levels following EBC-46 treatment, at both 24h and 48h; however, this was not deemed to be significant ($p>0.05$; Figures 6.27B and C, respectively). The Western blot for UBE2C following EBC-211 treatment also showed an increased detection following EBC-211 treatment at both 24h and 48h. This appeared to be increased quite profoundly at 0.001-10μg/ml EBC-211 at 24h, compared to untreated controls (Figure 6.28A). However, the densitometry analysis showed no significant difference in UBE2C levels at 24h, following EBC-211 treatment ($p>0.05$; Figure 6.28B). UBE2C levels were shown to be increased at 48h, following EBC-211 treatment, compared to untreated controls; this was shown to be significantly increase at 0.1μg/ml EBC-211 ($p<0.05$; Figure 6.28C).

Figure 6.27: Western blot analysis on (A) UBE2C in HaCaTs, at 24h and 48h; with densitometry analysis on UBE2C levels in HaCaTs, cultured in the presence of 0.001µg/ml, 0.01µg/ml, 0.1µg/ml, 1µg/ml and 10µg/ml EBC-46, compared to untreated controls (0µg/ml), at (B) 24h and (C) 48h. (*N=3, average±SE).*

A

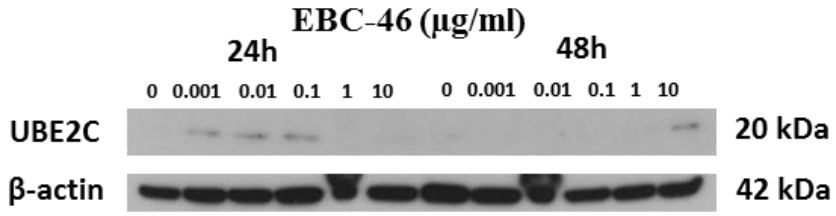

B

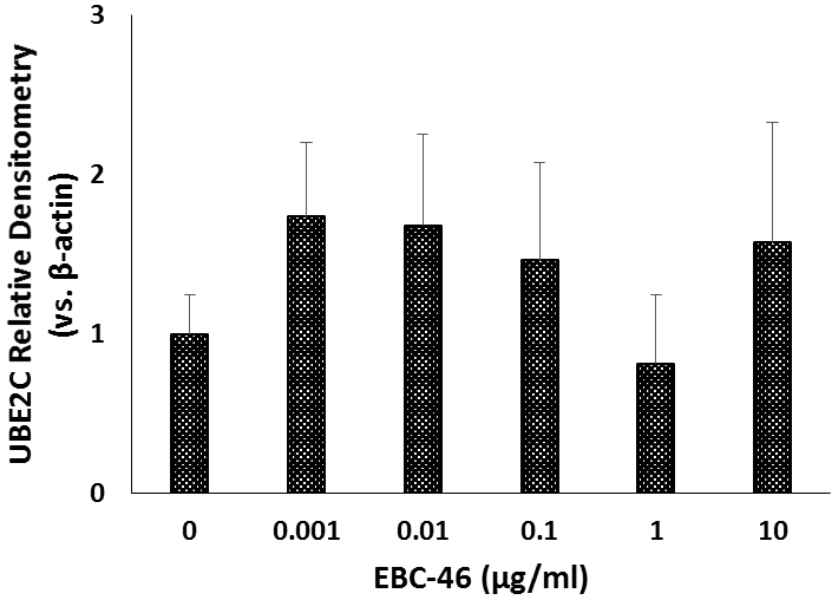

C

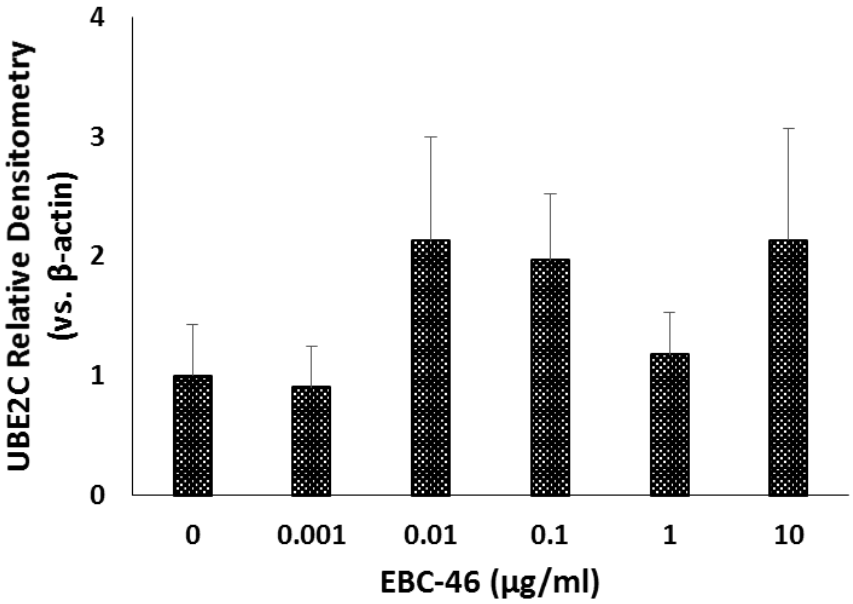

Figure 6.28: Western blot analysis on (A) UBE2C in HaCaTs, at 24h and 48h; with densitometry analysis on UBE2C levels in HaCaTs, cultured in the presence of 0.001µg/ml, 0.01µg/ml, 0.1µg/ml, 1µg/ml and 10µg/ml EBC-211, compared to untreated controls (0µg/ml), at (B) 24h and (C) 48h. (*N=3, average±SE; statistical analysis displayed *p<0.05).*

A

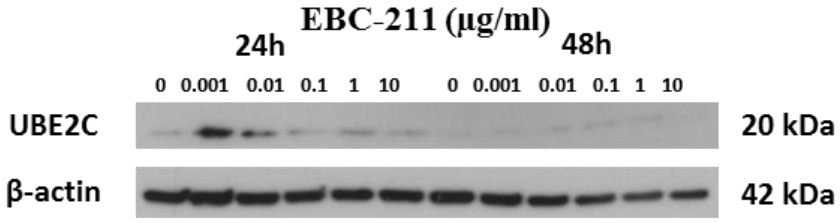

B

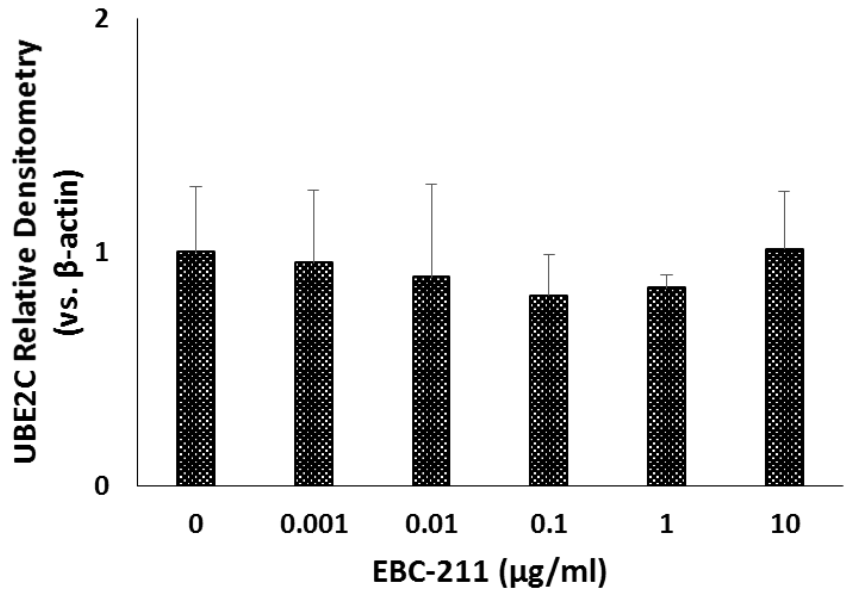

C

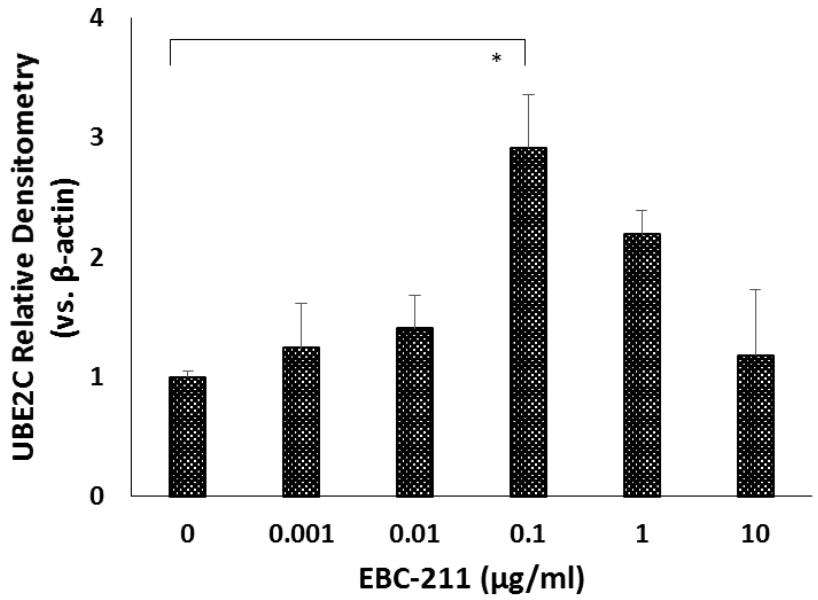

6.4.3 Validation of Gene Expression Changes by Activity Assays

MMP activity assays were performed on MMP-1, MMP-7 and MMP-10, as these MMPs were shown to be differentially expressed in HaCaTs, following treatment with the novel epoxy-tiglianes, compared to untreated controls (Tables 6.1 and 6.2). The results of these activity assays are shown in Figures 6.29, 6.30 and 6.31, respectively. There was a perceived increase in MMP-1 activity at 24h following EBC-46 treatment, although this was not considered to be significant ($p>0.05$; Figure 6.29A). However, at 48h, the elevated activity of MMP-1 was significant across all concentrations (0.001-10µg/ml; $p<0.001$-0.05), with the lower concentrations displaying a higher level of significance ($p<0.001$). In contrast, treatment with EBC-211 significantly increased MMP-1 activity at both 24h and 48h; particularly at 0.001-1µg/ml at 24h and 0.001-10µg/ml at 48h ($p<0.001$; Figure 6.29B).

MMP-7 activity was also increased following EBC-46 and EBC-211 treatment, at both 24h and 48h (Figures 6.30A and 6.30B, respectively). Following 24h treatment with EBC-46, there was a significant increase in MMP-7 activity at 0.001-0.1µg/ml EBC-46 ($p<0.01$-0.05; Figure 3.30A). This significant increase in activity was also evident at 0.001-0.01µg/ml, at 48h ($p<0.01$-0.05). The increased activity of MMP-7 was particularly observed at the lower concentrations of EBC-46 and potentially due to the lesser activity of EBC-211, this enhanced activity level was observed across a greater range of concentrations (0.001-1µg/ml; Figure 3.30B). This elevated activity following EBC-211 treatment was considered to be significant at 24h ($p<0.01$-0.05) and at 48h ($p<0.001$), for 0.001-1µg/ml EBC-211.

MMP-10 was only shown to be increased for EBC-211 in the Microarray studies (Tables 6.1 and 6.2). Corroborating this data, the perceived increases in MMP-10 activity following EBC-46 treatment were found to be not significant, compared to untreated controls (Figure 6.31A). However, treatment with EBC-211 was shown to increase MMP-10 activity at all concentrations (0.001-10µg/ml), at both 24h and 48h (Figure 6.31B). These increases were determined to be significant at 24h (all $p<0.001$) and at 48h ($p<0.001$-0.01).

Figure 6.29: MMP-1 activity in HaCaTs, cultured in the presence of 0.001µg/ml, 0.01µg/ml, 0.1µg/ml, 1µg/ml and 10µg/ml (A) EBC-46 or (B) EBC-211, compared to untreated controls (0µg/ml), at 24h and 48h. (*N=3, average±SE, statistical analysis displayed *p<0.05, **p<0.01, ***p<0.001*).

A

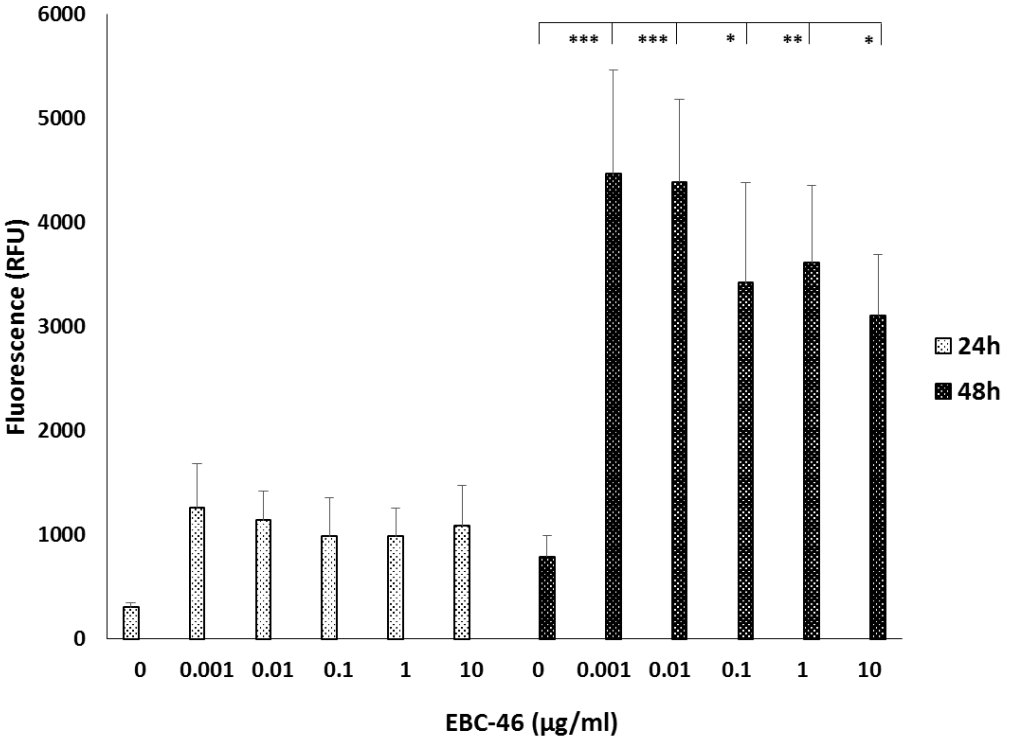

B

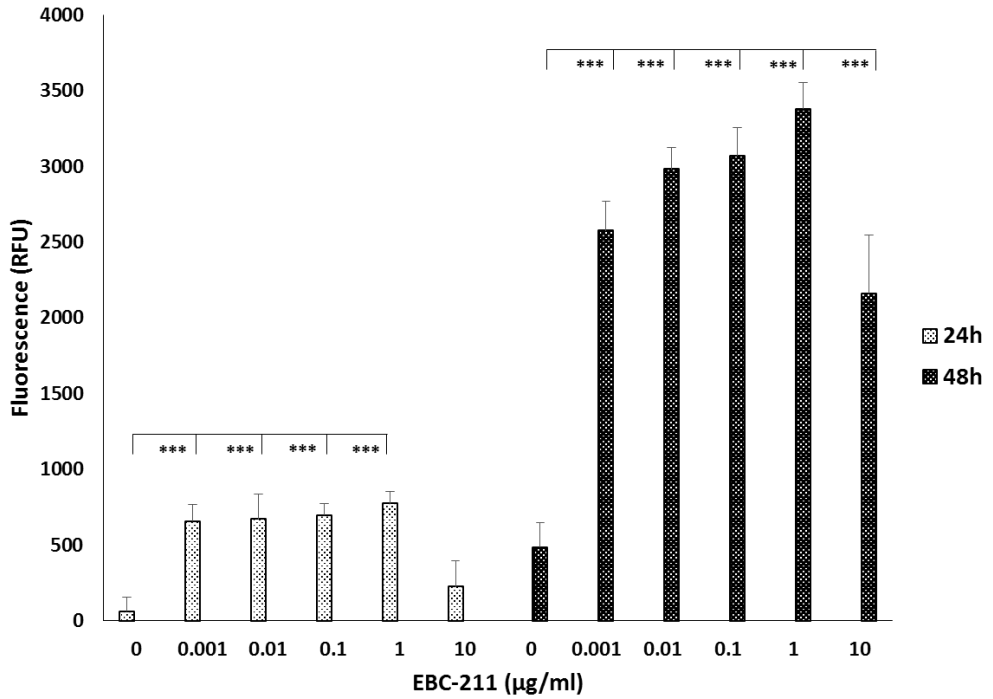

Figure 6.30: MMP-7 activity expression of HaCaTs, cultured in the presence of 0.001µg/ml, 0.01µg/ml, 0.1µg/ml, 1µg/ml and 10µg/ml EBC-46 (A) or EBC-211 (B), compared to untreated controls (0µg/ml), at 24h and 48h. (*N=3, average±SE, statistical analysis displayed *p<0.05, **p<0.01, ***p<0.001*).

A

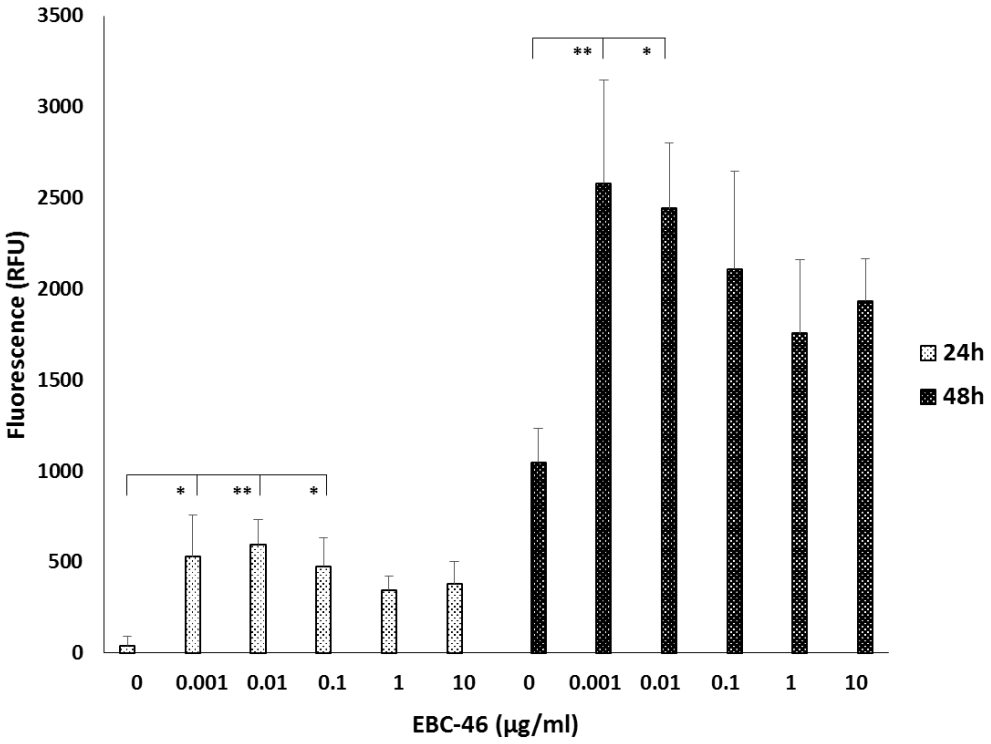

B

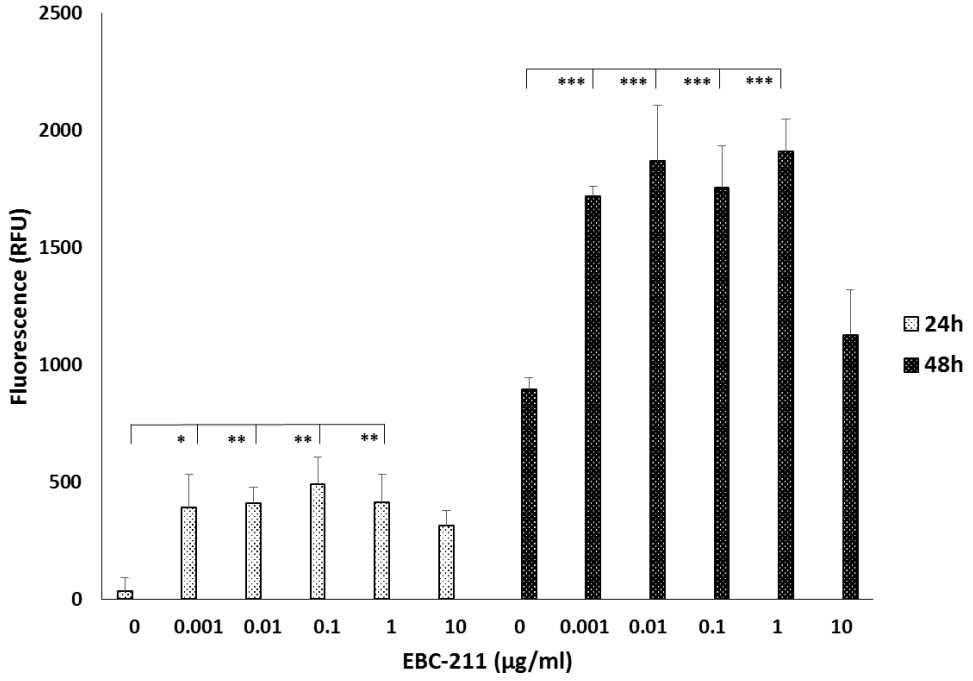

Figure 6.31: MMP-10 activity expression of HaCaTs, cultured in the presence of 0.001µg/ml, 0.01µg/ml, 0.1µg/ml, 1µg/ml and 10µg/ml EBC-46 (A) or EBC-211 (B), compared to untreated controls (0µg/ml), at 24h and 48h. (*N=3, average±SE, statistical analysis displayed **p<0.01, ***p<0.001*).

A

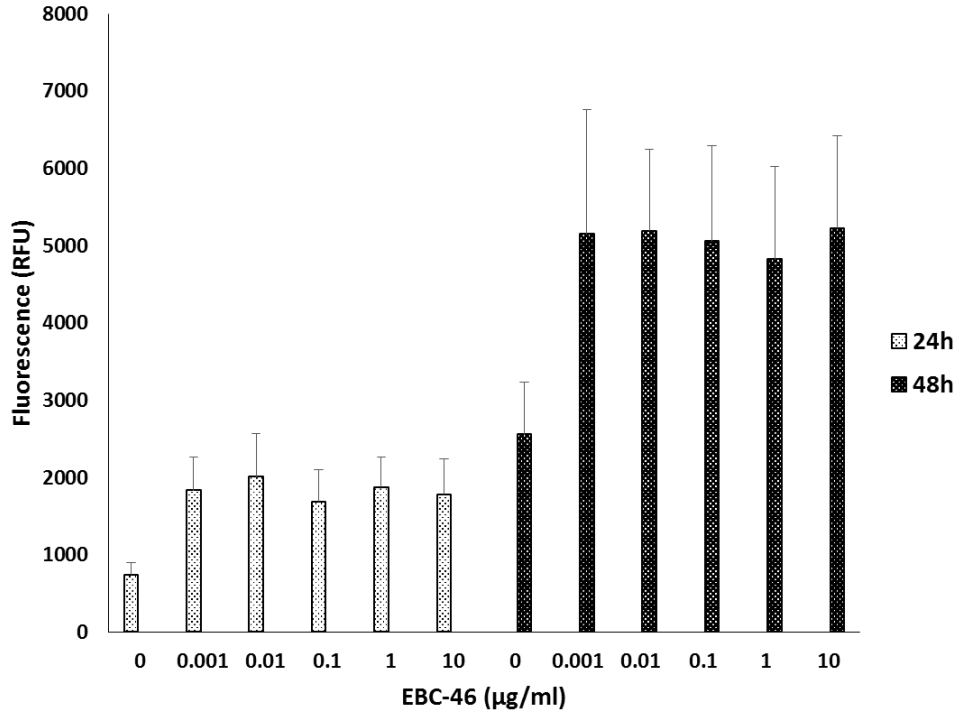

B

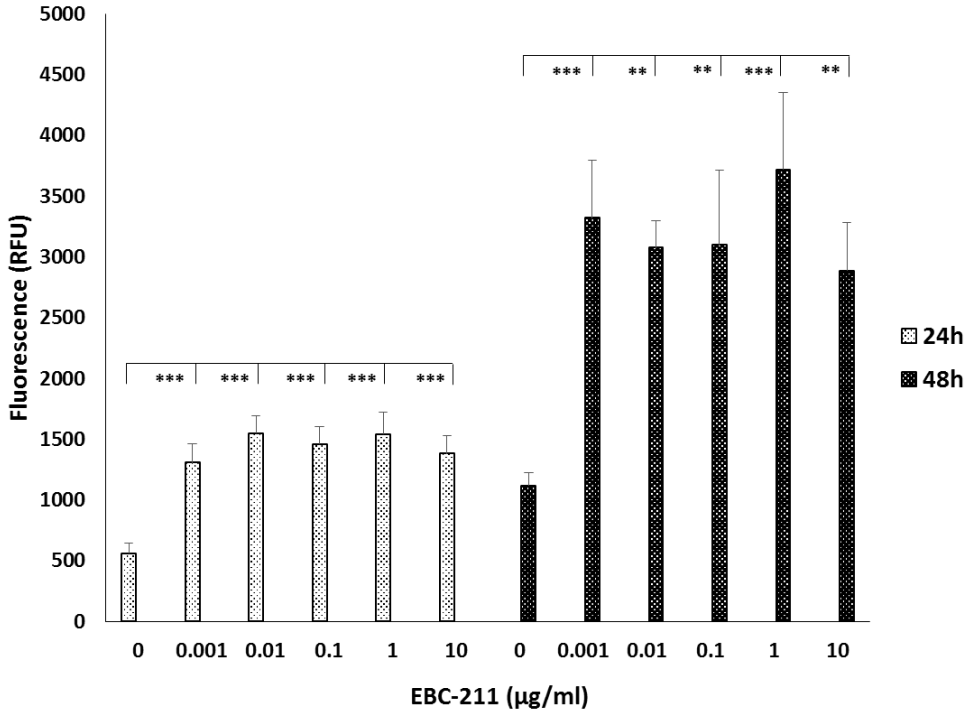

6.4.4 Validation of Gene Expression Changes by ELISA

ELISAs were performed on IL-6, IL-8, CCL5 and CXCL10 (Figures 3.32, 3.33, 3.34 and 3.35, respectively), as these genes were observed to be differentially expressed following epoxy-tigliane treatment, during the Microarray studies (Tables 6.1 and 6.2). IL-6 gene expression were predominantly shown to be downregulated following EBC-46 and EBC-211 treatment at 48h; this was corroborated by ELISA (Figures 6.32A and 6.32B, respectively). There were no significant changes following EBC-46 treatment at 24h ($p>0.05$). However, at 48h, there were significant decreases in IL-6 levels across all EBC-46 concentrations (0.001-10µg/ml; $p<0.001$-0.01), compared to untreated controls. Treatment with EBC-211 also showed an enhanced reduction in levels at 48h, with these decreases considered significant at all concentrations (0.001-10µg/ml; $p<0.001$). There was a slight increase in IL-6 levels at 24h for 10µg/ml EBC-211 ($p<0.05$), with no significant change for the remaining concentrations.

Microarray studies showed a profound downregulation in IL-8 gene expression, following EBC-46 and EBC-211 treatment. This was predominantly observed at 48h (Tables 6.1 and 6.2, respectively). ELISAs showed a dose-dependent increase in IL-8 levels for both EBC-46 and EBC-211 at 24h. This in contrast to the Microarray studies. This increase was significant for 0.01-10µg/ml EBC-46, with the peak increase at 0.01µg/ml ($p<0.001$-0.01). Some increases were shown to be significant between 0.1-10µg/ml for EBC-211 ($p<0.001$-0.05), with the greatest increase at 10µg/ml ($p<0.001$). In contract, the decrease in IL-8 levels observed in Microarray studies was corroborated at 48h with the ELISAs, for both EBC-46 and EBC-211 (Figures 6.33A and 6.33B, respectively); although this decrease was only considered significant for EBC-46 at 0.001µg/ml and 10µg/ml ($p<0.01$-0.05). In contrast, following EBC-211 treatment, the decrease was significant across all EBC-211 concentrations (0.001-10µg/ml; $p<0.001$-0.05), especially at 0.01-1µg/ml ($p<0.001$).

CCL5 was shown to be profoundly downregulated in the Microarray studies following epoxy-tigliane treatment. This was observed for all concentrations studied of EBC-46 and EBC-211, at 24h and 48h (Tables 6.1 and 6.2). This downregulation was corroborated at the protein level by ELISA, for both EBC-46 and EBC-211

Figure 6.32: IL-6 levels in HaCaTs, cultured in the presence of 0.001µg/ml, 0.01µg/ml, 0.1µg/ml, 1µg/ml and 10µg/ml EBC-46 (A) or EBC-211 (B), compared to untreated controls (0µg/ml), at 24h and 48h. (*N=3, average±SE, statistical analysis displayed *p<0.05, **p<0.01, ***p<0.001*).

A

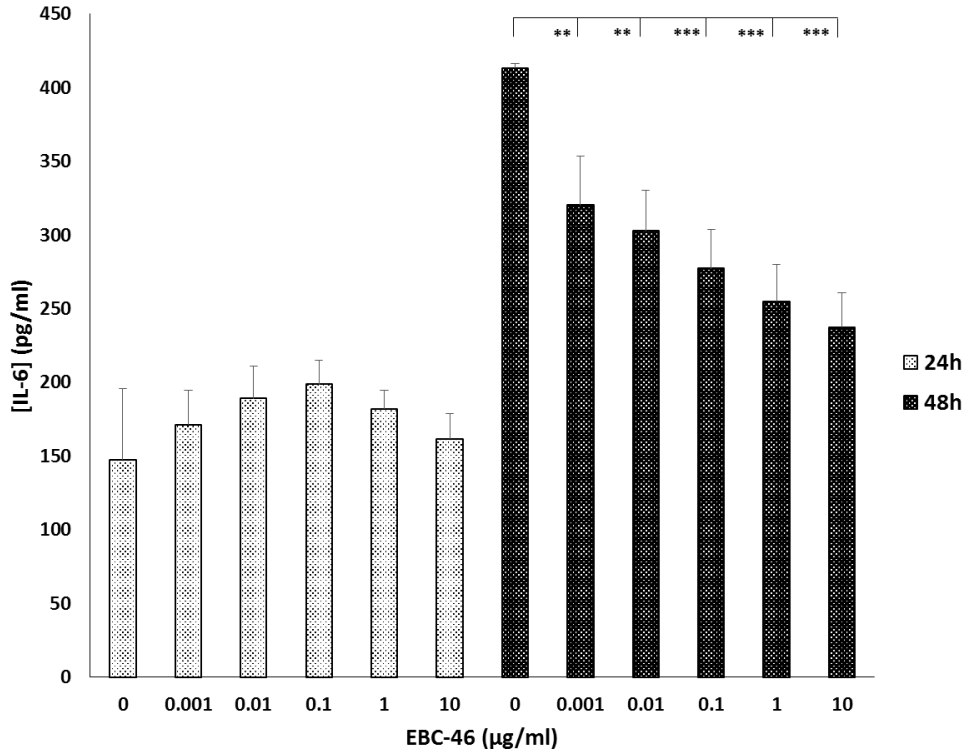

B

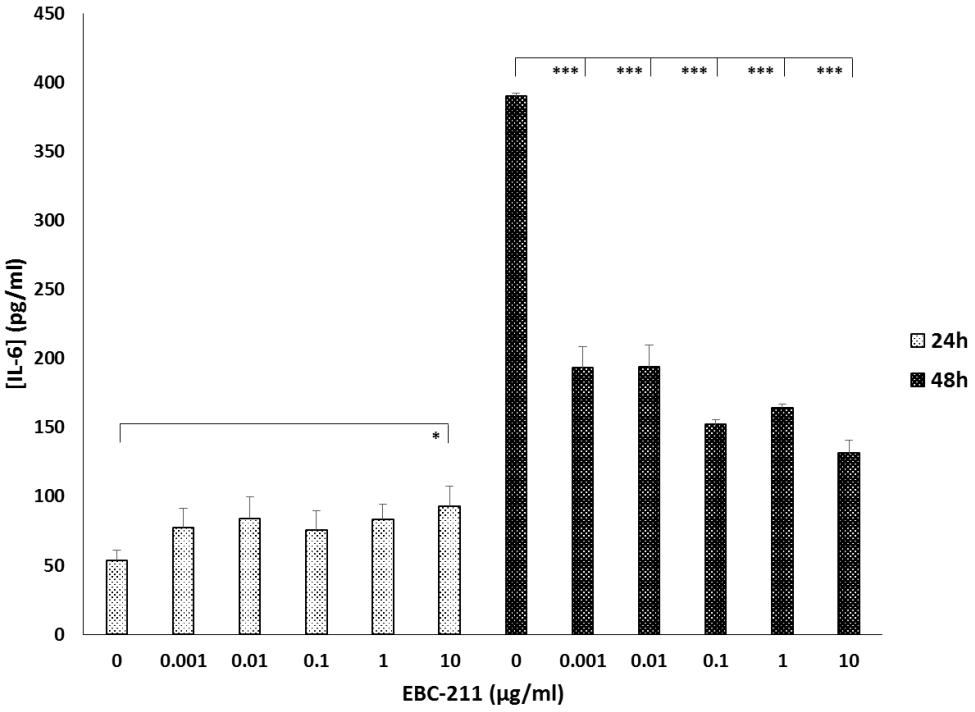

Figure 6.33: IL-8 levels in HaCaTs, cultured in the presence of 0.001µg/ml, 0.01µg/ml, 0.1µg/ml, 1µg/ml and 10µg/ml EBC-46 (A) or EBC-211 (B), compared to untreated controls (0µg/ml), at 24h and 48h. (*N=3, average±SE, statistical analysis displayed *p<0.05, **p<0.01, ***p<0.001*).

A

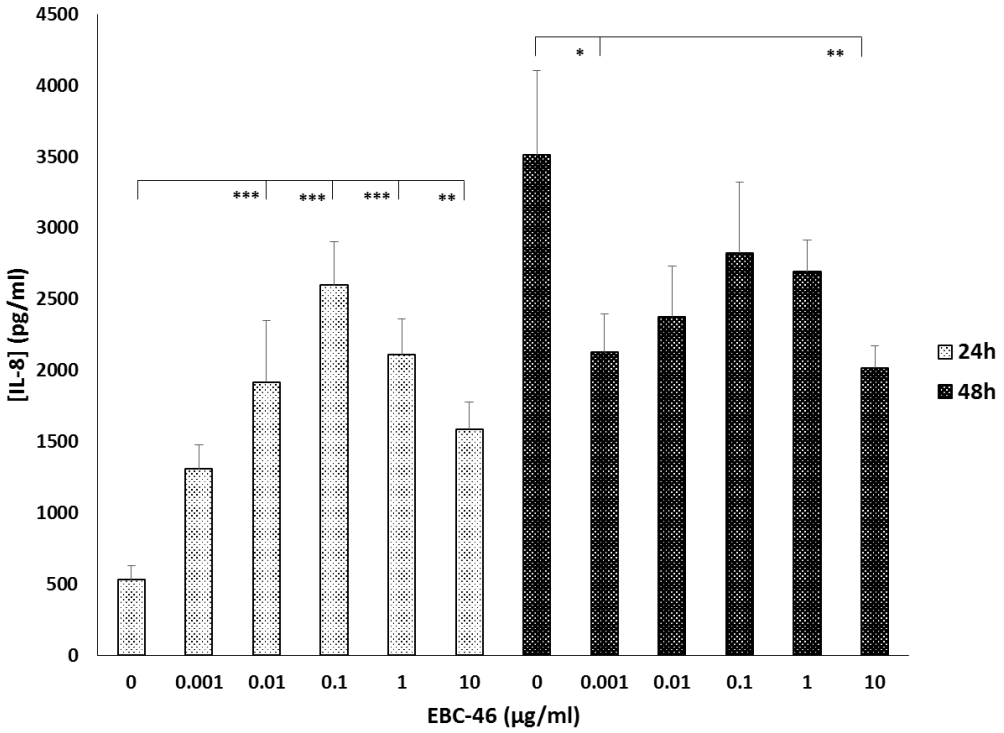

B

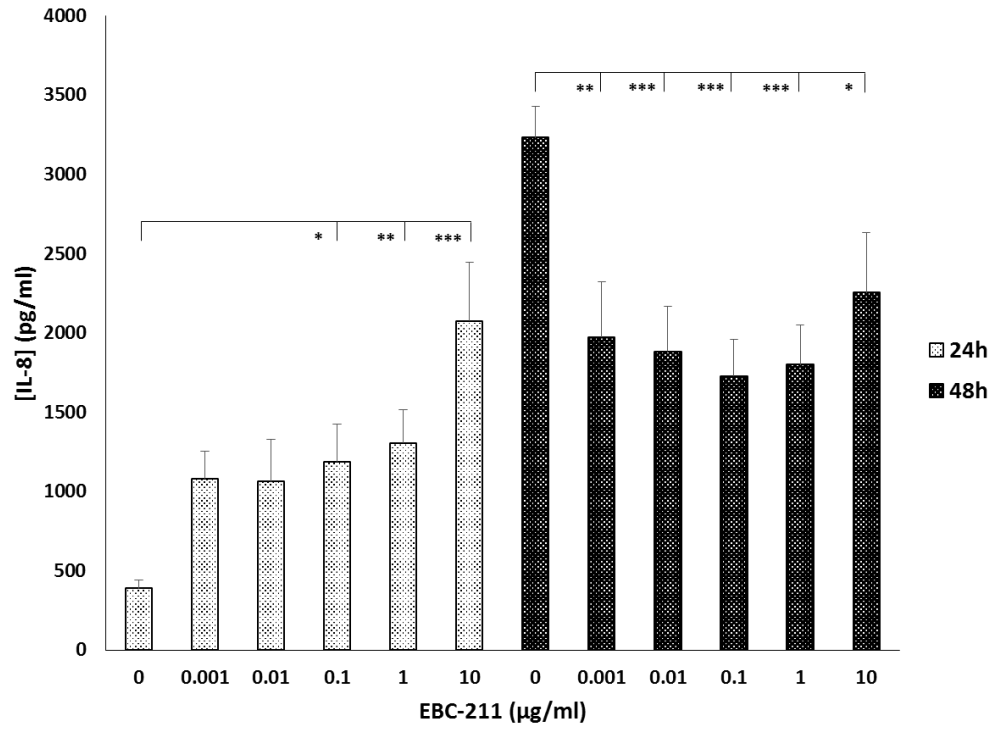

Figure 6.34: CCL5 levels in HaCaTs, cultured in the presence of 0.001µg/ml, 0.01µg/ml, 0.1µg/ml, 1µg/ml and 10µg/ml EBC-46 (A) or EBC-211 (B), compared to untreated controls (0µg/ml), at 24h and 48h. (*N=3, average±SE, statistical analysis displayed **p<0.01, ***p<0.001*).

A

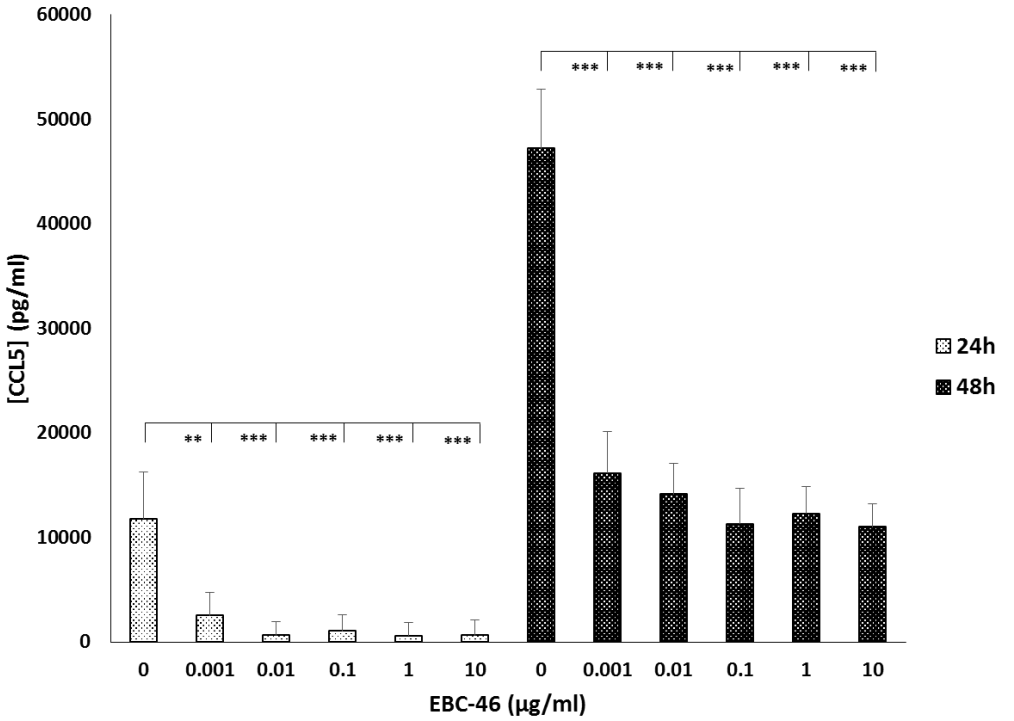

B

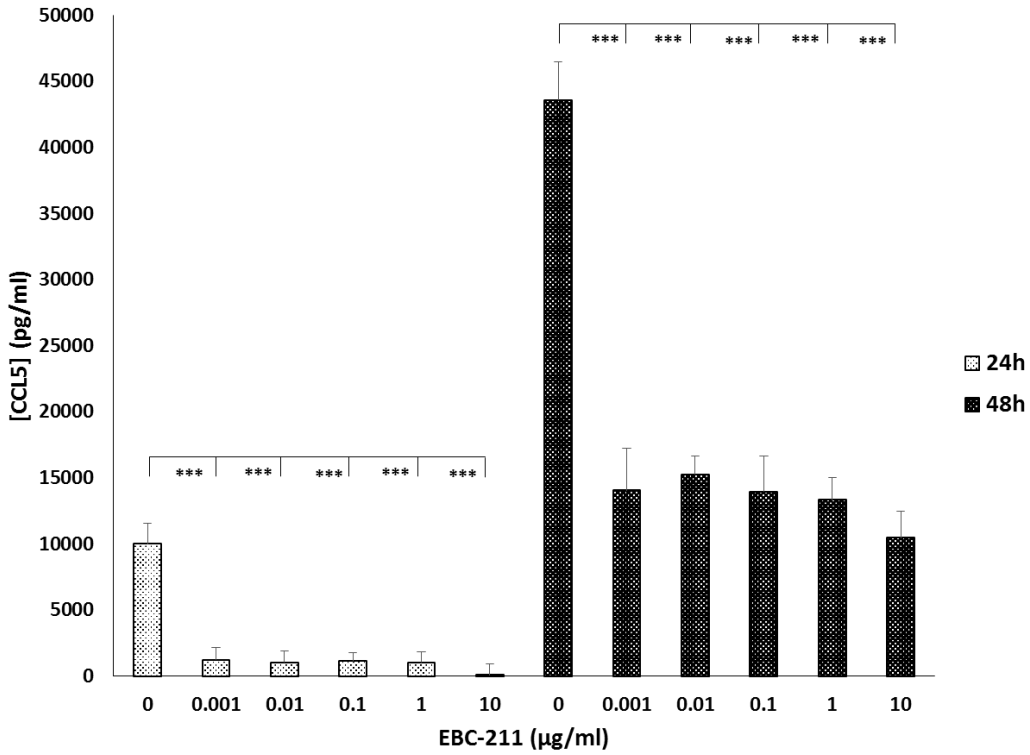

Figure 6.35: CXCL10 levels in HaCaTs, cultured in the presence of 0.001µg/ml, 0.01µg/ml, 0.1µg/ml, 1µg/ml and 10µg/ml EBC-46 (A) or EBC-211 (B), compared to untreated controls (0µg/ml), at 24h and 48h. (*N=3, average±SE, statistical analysis displayed **p<0.01, ***p<0.001*).

A

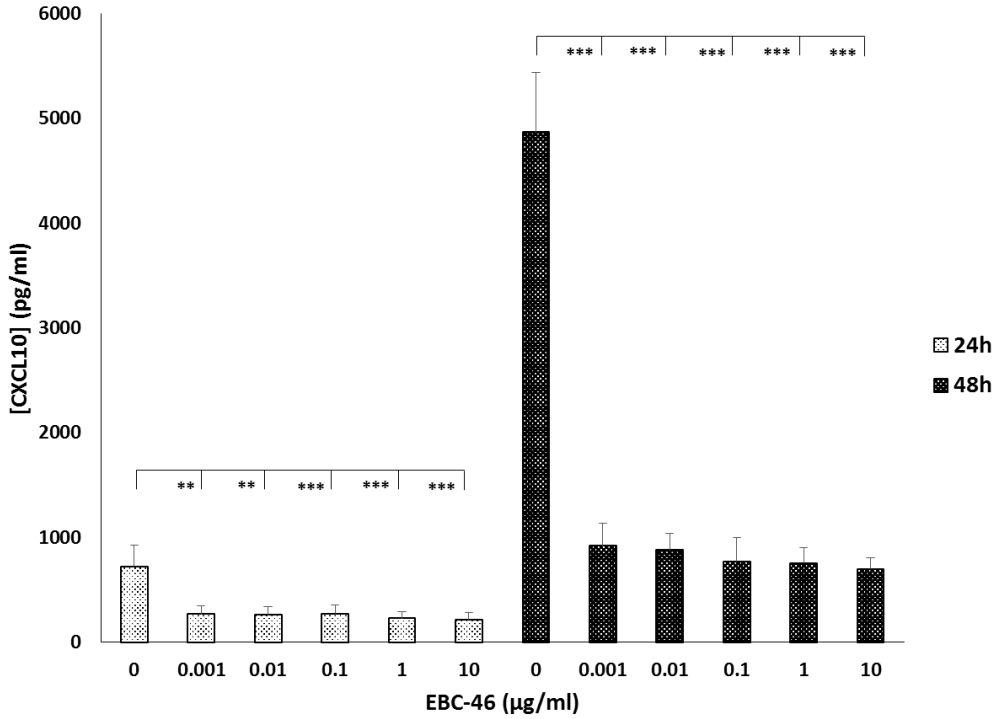

B

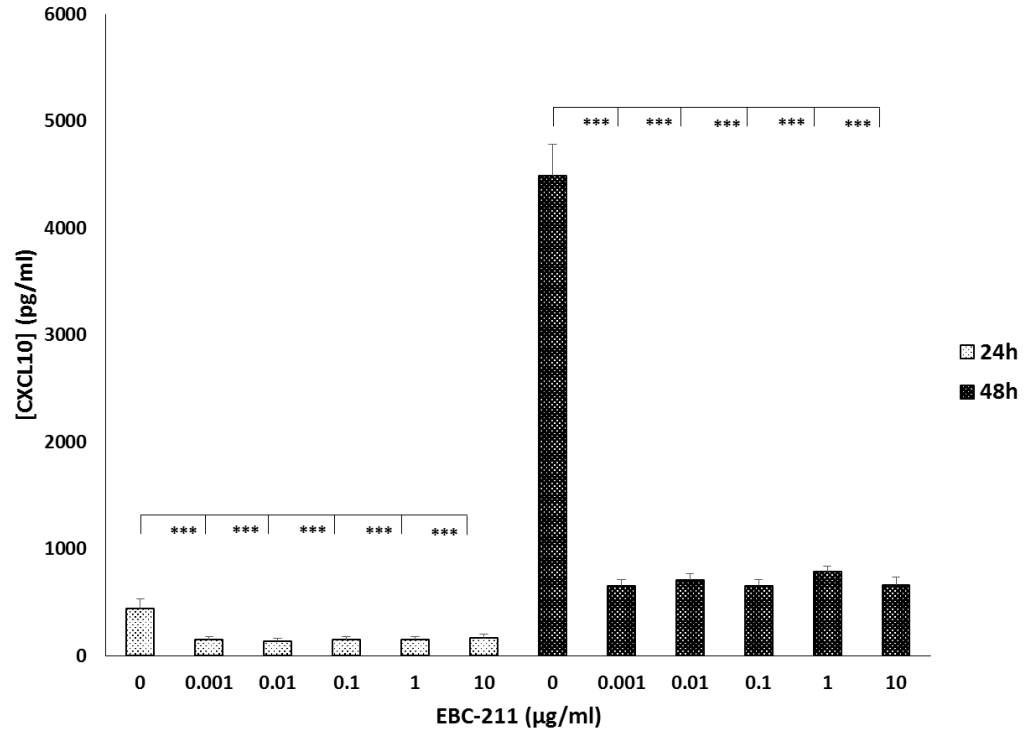

(Figures 6.34A and 6.34B, respectively). This reduced protein level was found to be significant for all EBC-46 concentrations (0.001-10µg/ml) at 24h ($p<0.001$-0.01); and to a greater significance at 48h (all $p<0.001$), compared to untreated controls. The reduced CCL5 protein levels following EBC-211 treatment was also significant at all concentration (0.001-10µg/ml), at both 24h and 48h (all $p<0.001$), compared to untreated controls.

Similarly, CXCL10 was shown to be greatly downregulated in the Microarray studies following EBC-46 or EBC-211 treatment, compared to untreated controls (Tables 6.1 and 6.2). This profound decrease was corroborated at the protein level by ELISA, for both EBC-46 and EBC-211 (Figures 6.35A and 6.35B, respectively). This reduction in protein level was found to be significant for all concentrations of EBC-46 (0.001-10µg/ml) at 24h ($p<0.001$-0.01); and again, to a greater significance at 48h (all $p<0.001$). The decrease in CXCL10 protein level following EBC-211 treatment was significant at all EBC-211 concentrations (0.001-10µg/ml) at both 24h and 48h (all $p<0.001$), compared to untreated controls.

6.5 Discussion

Following on from Chapter 5, which identified a number of key genes differentially expressed following treatment with EBC-46 or EBC-211, at 24h and 48h; this Chapter aimed to validate these changes in gene expression and at the protein level, thereby indicating whether such changes could result in phenotypic responses to epoxy-tigliane treatments. The genes chosen for validation were differentially expressed by more than 2-fold by epoxy-tigliane treatment, compared to untreated controls. These genes have also been shown to be involved in wound healing responses, as described in Section 5.5. Elucidation of the protein level changes following epoxy-tigliane treatment were required, as these may be responsible for the beneficial responses seen during the *in vitro* HaCaT studies, described in Chapter 4. In addition, these protein level changes may also determine how the beneficial veterinary *in vivo* responses following epoxy-tigliane treatment were potentially induced.

The qPCR studies were performed as further validation of genotypic response following epoxy-tigliane treatment (Section 6.4.1). This was analysed for a few key differentially expressed genes, identified during the Microarray studies (Chapter 5). Western blots were performed with subsequent densitometry analysis to validate the genotypic responses observed at the protein level for Krt13, Krt15, Krt16, Krt17, Krt6B, Cyclin A2, Cyclin B1, Cyclin B2, CDKN3, CDKN1A and UBE2C (Section 6.4.2). MMP activity assays were performed on MMP-1, MMP-7 and MMP-10, as these were all shown to be differentially expressed during Microarray analysis, following epoxy-tigliane treatment (Section 6.4.3). ELISAs were performed to validate the protein levels of IL-6, IL-8, CCL5 and CXCL10 (Section 6.4.4). These cytokines and chemokines were shown to be greatly downregulated in Microarray studies.

Krt13 was shown to be upregulated at 24h and 48h in these qPCR studies, corroborating the microarray analysis. The Western blots for Krt13 also showed a significant increase in protein detection at 48h following 0.1μg/ml and 10μg/ml EBC-46 treatments. However, for the other conditions for Krt13, no significant differences in protein levels were observed following epoxy-tigliane treatment, despite an upregulation in gene expression of Krt13. This keratin has been shown to be typically present in oral mucosal epithelia and early-gestational foetal epithelia, as opposed to adult skin epithelia (Kallioinen et al. 1995; Moll et al. 2008; Bragulla & Homberger 2009). The increased presence of this keratin may induce a beneficial healing outcome, due to the preferential rapid re-epithelialisation response associated with oral mucosal healing and the role that Krt13 plays in epidermal regeneration (Moll et al. 2008; Bragulla & Homberger 2009).

Krt15 was shown, through qPCR studies, to be downregulated at 24h following EBC-46 and EBC-211 treatment. However, it was significantly upregulated at 48h, following epoxy-tigliane treatment. Western blot analysis showed no significant differences in Krt15 protein levels for all conditions, following epoxy-tigliane treatment; this was despite an upregulation in gene expression for this keratin. Similarly to Krt13, Krt15 is typically found in early-gestational, foetal epithelia, another preferential wound healing tissue, and has also been considered as an

epidermal stem cell marker (Waseem et al. 1999; Liu et al. 2003; Bose et al. 2013). In addition, Krt15 has been shown to be strongly involved in keratinocyte proliferation, an important feature for re-epithelialisation. Rapid re-epithelialisation is a characteristic feature of early-gestational, foetal wound healing (Rolfe & Grobbelaar 2012; Bose et al. 2013).

Krt16 was shown in the qPCR studies to be downregulated at 48h for both EBC-46 and EBC-211; and at 24h for EBC-211. The Western blots for Krt16 showed a significant increase in Krt16 protein levels at 24h, following 10μg/ml EBC-46 treatment. However, for the other conditions for Krt16, no significant differences in protein levels were observed following epoxy-tigliane treatment, despite an observed downregulation in gene expression of Krt16. There was a perceived decrease in protein detection, but this was not considered to be significant. This keratin is typically associated with wound healing, due to its upregulation following wounding (Santos et al. 2002; Mazzalupo et al. 2003). However, it has also been shown to inhibit keratinocyte migration. Decreased migratory ability of keratinocytes could reduce re-epithelialisation response, due to a lack of keratinocytes migrating to the wound site and across the injury (Trost et al. 2010).

Krt17 was shown to be significantly downregulated in qPCR studies at 24h and 48h, for both EBC-46 and EBC-211. Western blot analysis showed no significant differences in Krt17 protein levels for all conditions, following epoxy-tigliane treatment; this was despite a downregulation in gene expression for this keratin. However, there was a perceived decrease in protein expression for Krt17, following EBC-211 treatment at 48h, but this was not deemed to be significant. This keratin is upregulated alongside Krt16 following wounding (Mazzalupo et al. 2003; Morley et al. 2003; Zhang et al. 2012). However, an increase in Krt17 has also been shown to be strongly implicated in the severity of psoriasis, a hyperproliferative skin disorder (Leigh et al. 1995; Zhang et al. 2012).

Krt6B was also shown to downregulated in Microarray studies, following epoxy-tigliane treatment, although there were no significant difference in protein levels identified through Western blot analysis for either EBC-46 or EBC-211. This keratin

is also upregulated following wounding and often forms a keratin pair with Krt16 (Moll et al. 2008; Bragulla & Homberger 2009; Hobbs et al. 2012). Despite its upregulation after injury, decreased Krt6B expression has been shown to increase keratinocyte migration and subsequent re-epithelialisation (Wong & Coulombe 2003).

MMP-1 expression was shown, through qPCR studies, to be significantly upregulated following epoxy-tigliane at both 24h and 48h for EBC-211; and at 48h for EBC-46. This result was corroborated with a significantly increased MMP-1 activity observed at 48h, following EBC-46 treatment. Significantly increased MMP-1 activity was also observed following EBC-211 treatment, at both 24h and 48h. This metalloproteinase degrades collagen, in particular type I and III collagens, the major collagen types present in the dermal matrix. This degradation aids keratinocyte migration into the wound site and subsequent re-epithelialisation (Dasu et al. 2003; Nagase et al. 2006; Muller et al. 2008). MMP-1 has also been shown to be downregulated in pathological scarring, such as keloids and hypertrophic scarring (Lee et al. 2015).

MMP-7 activity was also shown to be increased following EBC-46 and EBC-211 treatments at 24h and 48h. This increase was only significant at the lower concentrations of EBC-46 and over a greater range of concentrations of EBC-211, presumably due to the 'lesser activity' of this epoxy-tigliane. MMP-7 is also involved in aiding keratinocyte migration, through degradation of the basement membrane matrix components. This MMP has been shown to be upregulated following epithelial injury (Philips et al. 2011; Rohani & Parks 2015). MMP-10 activity was only shown to be significantly increased by EBC-211. This was evident at 24h and 48h; and corroborated Microarray studies. MMP-10 is highly expressed by wound edge keratinocytes and degrades the basement membrane to allow keratinocyte migration to promote re-epithelialisation (Gill & Parks 2008; Philips et al. 2011; Rohani & Parks 2015). Increased expression and activity of these three MMPs may subsequently lead to enhanced keratinocyte migration and re-epithelialisation.

Gene expression of Cyclin B2 was upregulated following epoxy-tigliane treatment, in the Microarray studies. It was also shown, through qPCR studies, to be upregulated at 48h, following EBC-46 and EBC-211 treatment. Protein levels were also elevated, seen through Western blot analysis; although this was only significant for 10µg/ml EBC-46 at 48h. This cyclin has been associated with increasing the transition from the G2 phase to mitosis, increasing cell proliferation (Wu et al. 2010; Huang et al. 2013). The increased presence of keratinocytes at the wound site would be beneficial by increasing the availability of migratory keratinocytes, thereby enhancing re-epithelialisation (Shaw & Martin 2009). Cyclin A2 was shown to be upregulated during the Microarray studies; although the protein expression was only significantly upregulated at 10µg/ml EBC-46 at 48h. Cyclin B1 gene expression was also upregulated following epoxy-tigliane treatment and the protein levels were also significantly increased at 24h and 48h for EBC-46; and at 24h for EBC-211. These cyclins are all involved in the progression of cells from G2 phase to mitosis, with Cyclin A2 also involved in the progression from G1 to S phase. Therefore, the combination of increased cell progression to S phase and mitosis will lead to enhanced keratinocyte proliferation and enhanced re-epithelialisation (Gong & Ferrell 2010; Wu et al. 2010; Huang et al. 2013).

CDKN3 was shown to be upregulated during Microarray studies, although the protein levels were not found to be significantly increased following EBC-46 treatment, but a significant increase was observed at 0.1µg/ml EBC-211 at 24h. This cyclin inhibitor control mitosis function and prevents abnormal mitosis occurring; downregulation of this inhibitor is often observed in tumours (Nalepa et al. 2013). Another cyclin inhibitor, CDKN1A, was found to be downregulated during Microarray studies. This was corroborated by Western blot analysis, showing significantly decreased protein levels at 24h for EBC-46 and EBC-211. CDKN1A has an inhibitory ability on cell cycle progression, through inhibiting cyclin/cyclin dependent kinase inhibitor (CDK) complexes and preventing cells progressing into S phase (Gartel & Tyner 2002; Koljonen et al. 2006). This results in a reduced proliferative ability. Therefore, downregulation of this gene and subsequent protein expression may increase proliferative ability, through reduction of this inhibitory action (Gartel & Tyner 2002). UBE2C was shown to be upregulated during

Microarray studies. Although protein expression upregulation observed through Western blot analysis was only considered significant at 0.1µg/ml EBC-211 at 48h. This is another essential factor for cell cycle progression and acts through the breakdown of cyclin/CDK complexes, required to progress cell into mitosis. Therefore, increased presence of this protein will enhance cell proliferation (Hao et al. 2012).

IL-6 protein levels were shown to be decreased at 48h, following EBC-46 or EBC-211 treatment. This decrease was shown to be significant, compared to untreated controls. IL-6 is a pro-inflammatory cytokine, which increases the presence of neutrophils and monocytes at the wound site through a chemoattractive effect (Barrientos et al. 2008). It has been shown that IL-6 has beneficial effects towards keratinocyte migration in acute skin wounds, increasing re-epithelialisation. However, there is a lowered presence observed in early-gestational, foetal and oral mucosal wounds, where rapid re-epithelialisation occurs along with reduced inflammatory phase (Szpaderska et al. 2003; Gallucci et al. 2004; Barrientos et al. 2008; Leung et al. 2012; Rolfe & Grobbelaar 2012). IL-8 levels were found to be significantly increased at 24h for both EBC-46 and EBC-211; whereas by 48h, it was shown to be significantly decreased for both epoxy-tiglianes. This decrease was more significant and over a greater range of concentrations with EBC-211, compared to untreated controls. IL-8 is another pro-inflammatory cytokine and has a strong chemoattractive effect on neutrophils. Levels have been shown to be increased in non-healing wounds, potentially due to the excessive inflammation associated with increased IL-8 presence (Liechty et al. 1998; Barrientos et al. 2008). In addition, IL-8 levels are shown to be lowered in early-gestational foetal wounds. Alongside lower IL-6 levels, the presence of reduced pro-inflammatory cytokine levels contributes greatly to the minimal inflammation that occurs in this preferential healing response (Liechty et al. 1998; Liechty et al. 2000; Szpaderska et al. 2003; Barrientos et al. 2008; Leung et al. 2012; Rolfe & Grobbelaar 2012). Therefore, the reduction of these cytokines following epoxy-tigliane treatment may impact on the inflammation phase of normal acute skin wound healing, producing an attenuated inflammatory response.

CCL5 was shown by Microarrays to be profoundly downregulated following EBC-46 or EBC-211 treatment at both 24h and 48h, compared to untreated controls. CCL5 is a potent chemokine for immune cells, including monocytes, macrophages, mast cells and leukocytes. Therefore, its increased presence can increase the inflammatory phase and higher expression of CCL5 has been detected in chronic wounds (Gillitzer & Goebeler 2001; Balaji et al. 2015; Rees et al. 2015). This chemokine can also induce a mitogenic response on keratinocytes, in addition to having a role in angiogenesis; although its main role appears to be inflammatory with the strong chemokine response on immune cells and facilitation of immune responses (Rees et al. 2015). Another chemokine validated was CXCL10, which was also shown by Microarrays to be profoundly downregulated following both EBC-46 and EBC-211 treatment, at 24h and 48h. CXCL10 is another chemokine with a potent chemoattractant effect on lymphocytes and monocytes, resulting in a pro-inflammatory effect due to increased immune cells at the wound site; and levels are increased in chronic inflammation (Barrientos et al. 2008; Turabelidze & Dipietro 2012; Balaji et al. 2015; Ding & Tredget 2015; Rees et al. 2015). This chemokine has also been shown to delay re-epithelialisation, through inhibition of epidermal growth factor (EGF)-mediated cell mobility in fibroblasts, impairing granulation tissue formation. Platelet-derived growth factor (PDGF) mediated cell migration is also thought to be inhibited and both of these growth factors are associated with promoting re-epithelialisation (Shiraha et al. 1999; Barrientos et al. 2008; Turabelidze & Dipietro 2012; Rees et al. 2015). This inhibited cell motility is thought to be induced through the inhibited de-adhesion of cell to the membrane, through m-calpain inhibition, important for retraction of the rear of the cell. In addition, activation of CXCR3, the receptor for CXCL10, is thought to convert fibroblasts to a contractile phenotype instead of migratory (Shiraha et al. 1999; Behm et al. 2012). CXCL10 has been shown to inhibit angiogenesis, through inhibiting vessel growth and neovascularisation. It is also believed to increase keratinocytes motility through promoting keratinocyte chemotaxis (Romagnani et al. 2004; Bodnar et al. 2006; Turabelidze & Dipietro 2012; Yates-Binder et al. 2012; Rees et al. 2015).

Chapter 5 elucidated a number of key differentially expressed genes during the Microarray studies, some of these were validated at a protein level during this chapter. An overview of these results are displayed in Tables 6.3 and 6.4, for EBC-46 and EBC-211, respectively. Some of these results from the validation studies corroborates the global gene analysis, although there are a few results which are in contrast to the gene analysis. Some of these genotypic and resultant phenotypic changes may contribute to the enhanced keratinocyte proliferative and migratory responses seen during the *in vitro* studies, described in Chapter 4. In addition, they may give greater understanding to the exceptional wound healing responses observed during the *in vivo* animal wound healing studies (Reddell et al. 2014). A number of key gene and protein changes involved with enhanced keratinocyte proliferation and migration were confirmed, following epoxy-tigliane treatment. This provides support for the rapid re-epithelialisation responses observed in these *in vitro* and *in vivo* studies; and confirms key mechanisms through which these epoxy-tiglianes exert exceptional wound healing responses. A number of the gene and protein changes observed were similar to the expression seen in preferential tissues, such as early-gestational, foetal and oral mucosal epithelia. This leads to the theory that treatment with these novel epoxy-tiglianes may induce a regenerative response, as opposed to the normal repair mechanism seen in adult dermal wound healing.

Table 6.3: Corroboration of global gene analysis by validation studies, following treatment with EBC-46. Red = up-regulated, Green = down-regulated, White = no significant change.

Gene/ Protein	Microarray Result	Validation Experiment	Validation Result
Krt13	Up-regulated	qPCR	Up-regulated
		Western Blot	Up-regulated
Krt15	Up-regulated	qPCR	Up-regulated
		Western Blot	No significant change
Krt16	Down-regulated	qPCR	Down-regulated
		Western Blot	Up-regulated
Krt17	Down-regulated	qPCR	Down-regulated
		Western Blot	No significant change
Krt6B	Down-regulated	Western Blot	No significant change
Cyclin A2	Up-regulated	Western Blot	Up-regulated
Cyclin B1	Up-regulated	Western Blot	Up-regulated
Cyclin B2	Up-regulated	qPCR	Up-regulated
		Western Blot	Up-regulated
CDKN3	Up-regulated	Western Blot	No significant change
CDKN1A	Down-regulated	Western Blot	Down-regulated
UBE2C	Up-regulated	Western Blot	No significant change
MMP-1	Up-regulated	qPCR	Up-regulated
		MMP Activity Assay	Up-regulated
MMP-7	Up-regulated	MMP Activity Assay	Up-regulated
IL-6	Down-regulated	ELISA	Down-regulated
IL-8	Down-regulated	ELISA	Down-regulated
CCL5	Down-regulated	ELISA	Down-regulated
CXCL10	Down-regulated	ELISA	Down-regulated

Table 6.4: Corroboration of global gene analysis by validation studies, following treatment with EBC-211. Red = up-regulated, Green = down-regulated, White = no significant change.

Gene/ Protein	Microarray Result	Validation Experiment	Validation Result
Krt13	Up-regulated	qPCR	Up-regulated
		Western Blot	No significant change
Krt15	Up-regulated	qPCR	Up-regulated
		Western Blot	No significant change
Krt16	Down-regulated	qPCR	Down-regulated
		Western Blot	No significant change
Krt17	Down-regulated	qPCR	Down-regulated
		Western Blot	No significant change
Krt6B	Down-regulated	Western Blot	No significant change
Cyclin A2	Up-regulated	Western Blot	No significant change
Cyclin B1	Up-regulated	Western Blot	Up-regulated
Cyclin B2	Up-regulated	qPCR	Up-regulated
		Western Blot	No significant change
CDKN3	Up-regulated	Western Blot	Up-regulated
CDKN1A	Down-regulated	Western Blot	Down-regulated
UBE2C	Up-regulated	Western Blot	Up-regulated
MMP-1	Up-regulated	qPCR	Up-regulated
		MMP Activity Assay	Up-regulated
MMP-7	Up-regulated	MMP Activity Assay	Up-regulated
MMP-10	Up-regulated	MMP Activity Assay	Up-regulated
IL-6	Down-regulated	ELISA	Down-regulated
IL-8	Down-regulated	ELISA	Down-regulated
CCL5	Down-regulated	ELISA	Down-regulated
CXCL10	Down-regulated	ELISA	Down-regulated

Chapter 7 – Discussion

Chapter 7 – Discussion

7.1 Overview

This PhD study aimed to determine the effects of the naturally occurring epoxy-tiglianes, EBC-46 and EBC-211, on dermal wound healing responses. This was performed through culturing dermal fibroblasts and an epidermal keratinocyte cell line (HaCaTs) with these novel epoxy-tiglianes and observing the effects on a number of key *in vitro* wound healing responses, including viability, proliferation, cell cycle progression, morphology, repopulation; and for fibroblasts, their differentiation to contractile myofibroblasts. Previous *in vivo* animal studies performed by QBiotics Ltd. have demonstrated the exceptional wound healing responses induced following epoxy-tigliane treatment, with treated skin displaying rapid re-epithelialisation, wound closure and minimal scarring (Reddell et al. 2014). Such findings justified the necessity to determine how EBC-46 and EBC-211 influence fibroblast and keratinocyte responses; and how these *in vivo* responses are induced. EBC-46 has been shown to act through classical protein kinase C (PKC) activation, in particular the PKC-β isoforms (Boyle et al. 2014).

7.2 Fibroblasts and Myofibroblasts

Fibroblasts cultured with 0.001-10µg/ml EBC-46 or EBC-211 demonstrated significant anti-proliferative responses, potentially partly due to the delayed cell cycle progression observed. Despite little significance shown, there was also a perceived inhibitory response of fibroblast wound repopulation and closure, following epoxy-tigliane treatment. In addition, apparent inhibition of fibroblast-myofibroblast differentiation was evident at certain concentrations of EBC-46 (0.1µg/ml) and EBC-211 (10µg/ml), demonstrated through lack of stress fibre formation and significantly reduced α-smooth muscle actin (SMA) expression (Gabbiani 2003).

Alterations in normal dermal fibroblast function are evident in both detrimental and preferential healing processes, such as excessive scarring and chronic wounds or early-

gestational foetal and oral mucosal healing, respectively (Menke et al. 2007; Bran et al. 2009; Shih et al. 2010; Frykberg & Banks 2015). Some aspects of the fibroblast responses to epoxy-tigliane treatment can be likened to impaired healing, such as the apparent inhibitory fibroblast proliferative and migratory responses and subsequent reduced wound repopulation (Menke et al. 2007). This has implications on the successful synthesis of new extracellular matrix (ECM), with a reduced presence of fibroblasts at the wound site resulting in a decreased replacement of the provisional fibrin matrix, reducing the tensile strength of the tissue (Menke et al. 2007; Eming et al. 2014; Frykberg & Banks 2015). In addition, chronic wound fibroblasts have also been demonstrated to possess reduced proliferative abilities, potentially a result of the proteolytic environment of the chronic wound degrading a number of key growth factors (Telgenhoff & Shroot 2005; Wall et al. 2008; Eming et al. 2014). In contrast, excessive scarring is a result of increased presence of fibroblasts, through enhanced migratory responses to the wound site as a result of chemotactic signals released by immune cells; along with an upregulated proliferative ability and resultant differentiation into the contractile myofibroblast phenotype (Gauglitz et al. 2011; Jumper et al. 2015; Kelsh et al. 2015). This indicates the extremely delicate balance between normal wound healing and the two opposing impaired healing responses.

The *in vivo* veterinary studies have elucidated the apparent dermal response following epoxy-tigliane treatment, with an exceptional cosmesis and wound closure ability, demonstrating an overall lack of scarring at the wound site (Reddell et al. 2014). This preferential healing response is evident despite the opposing fibroblast responses following epoxy-tigliane treatment to preferential healing, such as early-gestational foetal and oral mucosal wound repair, where fibroblast proliferative and migratory abilities are seen to be increased (Enoch et al. 2010; Yates et al. 2012; Helmo et al. 2013). In addition to the apparent impaired wound closure response, following epoxy-tigliane treatment, fibroblasts demonstrated an altered cytoskeletal structure. This was evident by the formation of multiple lamellipodia, as opposed to only one during normal cell crawling locomotion. This could be a result of alterations to ENA/VASP proteins, known to impact the elongation and branching of actin filaments and protrusion of lamellipodia (Kwiatkowski et al. 2003; Krause & Gautreau 2014). Additionally, the retraction of these projections does not occur in all instances,

especially evident during the time-lapse movies (Supplement 3.2), where trailing projections were shown to extend across large distances. Further studies would be required to determine whether this is a result of alteration in the actin cytoskeleton or other cytoskeletal proteins.

There are phenotypic differences between adult dermal fibroblasts and those present in preferential tissues, such as early-gestational, foetal and oral mucosal wounds. Oral mucosal fibroblasts have been described as having a 'younger phenotype' than dermal fibroblasts, resulting in a longer proliferative lifespan (Enoch et al. 2010). This is due to the delayed senescence, which is independent of telomerase activity (Enoch et al. 2009). Foetal fibroblasts have also been shown to possess increased levels of hyaluronan and its receptor, which has been associated with inducing fibroblast migration and contributing to the scarless healing response (Alaish et al. 1994; Bullard et al. 2003; Leung et al. 2012; Yagi et al. 2016). In addition, there is a variation in collagen type produced by foetal fibroblasts, with greater synthesis of type I collagen, compared to dermal fibroblast production; type I collagen fibres are finer and are difficult to discern from the surrounding uninjured tissue (Bullard et al. 2003; Leung et al. 2012; Yagi et al. 2016). Oral fibroblasts, like foetal fibroblasts, also exert a quicker migratory ability, compared to dermal fibroblasts. This combined with the extended proliferative lifespan, may result in an increased cell number at the wound site and contributes to the rapid wound closure seen in this preferential tissue (Bullard et al. 2003; Enoch et al. 2010; Yagi et al. 2016). In early-gestational, foetal wounds, there is an absence of myofibroblasts at day 14 following injury and subsequent reduced collagen contraction; oral fibroblasts have also shown to exert a reduced contraction than dermal fibroblasts (Cass et al. 1997; Lee & Eun 1999; Moulin & Plamondon 2002; Shannon et al. 2006; Leung et al. 2012; Yagi et al. 2016). This reduced contraction through myofibroblasts results in reduced scarring, which may be similar to the potentially inhibited myofibroblast formation, following epoxy-tigliane treatment, resulting in the production of minimal scarring (Enoch et al. 2008; Leung et al. 2012; Yagi et al. 2016). A degree of contraction has been thought to be beneficial through closure of the wound space, re-establishing a protective barrier for the underlying connective tissue (Li & Wang 2011; Eming et al. 2014). Although this mechanism needs to be tightly regulated, as too much or too little contraction can have

implications on the healing mechanism (Gabbiani 2003; Eckes et al. 2010; Li & Wang 2011). As previously mentioned, a lack of contraction may prevent successful closure of the wound, whilst excessive contraction can result in a fibrotic response and loss of function at the site (Gabbiani 2003; Eckes et al. 2010; Li & Wang 2011; Eming et al. 2014).

The altered fibroblast morphology and perceived inhibition of fibroblast-myofibroblast differentiation was of most interest, due to the potential anti-fibrotic implications following epoxy-tigliane treatment. The morphological studies showed a profound cytoskeletal change at 24h following epoxy-tigliane treatment, where the cells appeared to resemble a myofibroblast phenotype, with an increased morphology, stellate-structure and potential presence of stress fibres. The reversion of this morphology back to a typical spindle-shaped structure by 72h was intriguing and of interest; it led to the theory of a potentially reversible fibrosis response (Chitturi et al. 2015). This theory was developed upon during the differentiation studies and the inhibitory responses evident at certain concentrations of both epoxy-tiglianes. In this instance, it appeared that there was an inhibition of myofibroblast formation, as opposed to a reversion back to the normal fibroblast morphology as seen previously. It is still unknown what is inducing these responses and especially with the potential myofibroblast inhibition, why this response is only evident at 0.1µg/ml EBC-46 and 10µg/ml EBC-211. It would be of interest to know the comparable concentration used during the animal *in vivo* studies, which produced these anti-scarring responses, to determine whether this response also occurs *in vivo*. The *in vivo* studies previously performed have indicated that the healing responses are more characteristic of preferential healing, as observed in early-gestation foetal and oral mucosal wound responses. Therefore, treatment with these novel epoxy-tiglianes may induce regeneration at the wound site, instead of the typical repair mechanism, which occurs in adult wounds and results in scar formation. Of particular interest was the reformation of appendages during *in vivo* studies, which is typically absent following adult dermal repair and noted to occur during early-gestational foetal wound repair (Lorenz et al. 1993; Bullard et al. 2003; Werner & Grose 2003; Kishi et al. 2012; Leung et al. 2012).

Presence or absence of myofibroblasts in wounds has been shown to induce dysfunctional or preferential responses, respectively. A greatly increased presence is observed in keloid and hypertrophic scarring, resulting in excessive contraction of the wound site and resultant scarring (Gauglitz et al. 2011; Jumper et al. 2015; Kelsh et al. 2015). In contrast, it has been thought that, along with a decreased expression of transforming growth factor-β_1 (TGF-β_1), there is a reduced presence of myofibroblasts in early-gestational foetal healing; although their function is not fully known, due to a different wound closure method occurring in this healing response, instead of myofibroblast contraction (Larson et al. 2010; Rolfe & Grobbelaar 2012; Yates et al. 2012). The other widely noted preferential healing response, oral mucosal healing also possesses a decreased TGF-β_1 presence, along with a resistance to differentiation into myofibroblasts (Meran et al. 2007). This resistance is thought to be connected to the inhibited synthesis of hyaluronan in oral mucosal wounds, due to downregulated transcription of the related synthase enzymes, HAS2 (Meran et al. 2007). A global gene analysis could elucidate whether these synthase genes are some of the genes differentially expressed at those certain concentrations of EBC-46 and EBC-211, where differentiation appears to be inhibited. This may indicate whether this is the mechanism of myofibroblast inhibition and resultant scarless healing. As previously mentioned, it would be interesting to know the comparative concentration used during the *in vivo* studies, to understand which concentration results in the beneficial healing response observed in the case studies. This is of particular interest regarding the potential inhibition of myofibroblast formation and resultant minimal scarring, due to the apparent narrow range of concentrations of EBC-46 and EBC-211 which produce this response *in vitro*.

7.3 Keratinocyte Cell Line (HaCaTs)

In contrast to the dermal fibroblast responses, profound increases in HaCaT proliferative and migratory responses were evident, following culture with 0.001-10µg/ml EBC-46 or EBC-211. The most significant increased proliferation, compared to the untreated control, was evident following 72h treatment. This was shown to be a result of a proliferative burst occurring between 24h and 72h and a result of accelerated cell cycle progression. The cell cycle progression appeared to have a dose-dependent

response, with the lower concentrations initially exhibiting a similar progression to the untreated controls. In contrast, the enhanced HaCaT migratory responses were shown to be most significant at the lower concentrations of both epoxy-tiglianes, with complete wound closure evident at these lower concentrations; this was observed at 0.001-0.01µg/ml EBC-46 and 0.001-0.1µg/ml EBC-211. This enhanced response was evident across a wider therapeutic range for EBC-211, due to the lesser activity, compared to EBC-46. This increased range of enhanced wound repopulation may be of greater benefit from a clinical perspective, increasing the therapeutic range where exceptional wound healing responses can occur. The morphology and migration studies demonstrated no morphological change in the HaCaTs, indicating that the epoxy-tiglianes did not induce any differentiation responses in these cells.

Of interest was the dual response on wound repopulation ability, through independent upregulation of proliferative and migratory responses. This was demonstrated through analysing wound repopulation of an *in vitro* scratch wound, in the presence of mitomycin C, an inhibitor of proliferation (Santhiago et al. 2012; Wang et al. 2012; Lü et al. 2013). This was necessary to rule out whether the enhanced proliferation, observed previously, was biasing the wound repopulation outcome, through an overall increase in keratinocyte presence at the site. Keratinocyte presence at a wound site has extreme importance in the successful wound closure ability, through the re-epithelialisation process and re-establishment of the protective barrier, as described previously (Menon 2002; Candi et al. 2005; Portou et al. 2015).

Impaired wound closure has been shown in a number of chronic wound types and burn injuries, both of which result in impaired function and increased morbidity to the patient (Gorecki et al. 2009; Dreifke et al. 2015). Both proliferative and migratory response are shown to be impaired in chronic wounds, due to lack of response to signals, the reduced presence of growth factors stimulating motility, such as basic fibroblast growth factor (bFGF); and the proteolytic environment within chronic wounds capable of degrading a number of vital growth factors (Menke et al. 2007; Barrientos et al. 2008; Shirakata 2010). The inflammatory environment has also been thought to have implications on keratinocyte proliferation, with increased IL-8 shown to reduce proliferative responses (Barrientos et al. 2008). In addition, chronic wounds

possess a dysfunctional ECM. This may prevent the migration of keratinocytes across this wound bed, due to the necessity of a stable matrix for keratinocytes to migrate across and form focal adhesion complexes (Agren & Werthén 2007; Li et al. 2007).

The *in vivo* studies performed by QBiotics Ltd. have demonstrated exceptional healing of chronic wounds that were previously unresponsive to current wound care strategies. This indicates that the novel epoxy-tiglianes are able to induce a preferential wound healing response on these previously chronic wounds. This could have profound clinical implications, as chronic wounds and burn injuries cost the NHS approximately £5 billion to manage and treat (Posnett & Franks 2008; Guest et al. 2015; Harding 2015). A characteristic feature of preferential wound healing, both early-gestational foetal and oral mucosal, is induction of rapid re-epithelialisation, which appeared to occur during the *in vivo* studies (Coolen et al. 2010; Turabelidze et al. 2014). The *in vitro* studies suggest that the combination of the enhanced proliferative and migratory abilities, previously observed, will result in enhanced wound repopulation and potentially rapid re-epithelialisation. Enhanced keratinocyte proliferation has been observed in both early-gestational foetal and oral mucosal healing. In addition, enhanced migratory abilities are present in oral mucosal healing, which repopulates the wound in a similar manner to adult wound healing (Tan et al. 2014; Turabelidze et al. 2014). There are also a number of differentially expressed genes evident in both preferential healing responses, compared to adult dermal wound repair. Therefore, examination of genotypic expression following epoxy-tigliane was essential to determine the mechanisms behind this exceptional wound healing response (Colwell et al. 2008; Rolfe & Grobbelaar 2012; Turabelidze et al. 2014).

7.4 Genotypic and Phenotypic Responses

Following the exceptional responses observed in Chapter 4 on key keratinocyte wound healing functions, it was crucial to determine the genotypic responses following epoxy-tigliane treatment. There were a number of key differentially expressed genes identified following EBC-46 or EBC-211 treatment, with similar fold-changes in gene expression observed for both epoxy-tiglianes. This was noted despite slight variations in the *in vitro* results, with EBC-211 exhibiting a greatly enhanced migratory response,

compared to EBC-46. However, some cell-proliferation related genes, such as GINS complex subunit 2 (GINS2) and polymerase (DNA directed), ε2, accessory subunit (POLE2), were shown to be upregulated for 0.001µg/ml and 0.1µg/ml EBC-211 at 48h, but not at 10µg/ml, which may contribute to the reduced proliferative response seen in HaCaTs at the higher concentrations, following epoxy-tigliane treatment. In addition, matrix metalloproteinase (MMP)-1, MMP-7 and MMP-10 were shown to be upregulated at the lower concentrations (0.001µg/ml and 0.1µg/ml) of both epoxy-tiglianes, but not at the high concentration (10µg/ml). This was particularly evident for EBC-211 at 24h and 48h. This upregulation may contribute to the enhanced migratory responses observed at the lower concentrations, with some exhibiting full wound closure during the *in vitro* study. This response was further confirmed through pathway analysis on the differentially expressed genes predicting a stimulated migration of cells for 0.001µg/ml and 0.1µg/ml EBC-46 and EBC-211, but not at 10µg/ml. This corroborates the *in vitro* wound repopulation studies, where significantly enhanced migration was evident for the lower concentrations of both epoxy-tiglianes. The main areas of interest with differentially expressed genes, include cell cycle-related genes, cell-related genes, keratins and immune-related genes. The presence of certain keratins, only typically present in early-gestational foetal and oral mucosal epithelia, such as Krt13 and Krt15, respectively; were of particular interest, due to their roles in keratinocyte proliferation and epithelial regeneration (Kallioinen et al. 1995; Bose et al. 2013; Turabelidze et al. 2014). Of note, some crucial keratins that are typically induced following injury were shown to be downregulated, such as Krt16, Krt17 and Krt6B. This may be due to the lack of wounding to the cells during the *in vitro* experiment and would be interesting to observe the differential expression of these following a scratch wound study (Santos et al. 2002; Mazzalupo et al. 2003; Trost et al. 2010).

The previous *in vitro* cell cycle progression responses were shown to result from genotypic changes following epoxy-tigliane treatment, with enhancement of a number of cyclins and cyclin-dependent kinase inhibitors required for progression through the cell cycle (Tschöp & Engeland 2007; Hochegger et al. 2008; Nalepa et al. 2013). These differentially expressed genes, Cyclin A2, Cyclin B1 and Cyclin B2, confirmed the previous theory in Chapter 4, that G1 to S phase and G2 to mitosis transitions were

promoted. This was corroborated with a number of the upregulated cyclins involved in promoting this transition, seen at both the gene and protein level, contributing to the increased proliferative potential. In addition, proliferation was seen to be promoted through upregulation of a number of cell proliferation-related genes. Of interest, was the upregulation of factors, such as parathyroid hormone-like hormone (PTHLH), that are involved in the paracrine feedback system with fibroblasts, resulting in enhanced keratinocyte responses (Blomme et al. 1999; Bader & Kao 2009; Feuerherm et al. 2013). This leads us to question which genes of interest are differentially expressed in fibroblasts following epoxy-tigliane treatment, in particular those shown to be strongly linked to keratinocyte proliferation and migration, such as keratinocyte growth factor (KGF; Barrientos et al. 2008; Shirakata 2010).

Key MMPs were shown to be upregulated following epoxy-tigliane treatment. This can lead to beneficial or detrimental responses, as MMPs are vital for allowing migration of both keratinocytes and fibroblasts into the wound site to re-establish an epidermal barrier and re-form the underlying ECM (Vu & Werb 2000; Muller et al. 2008). However, if this upregulation is too excessive or prolonged, this could lead to the detrimental responses observed in chronic wounds, where high presence is observed (Menke et al. 2007; Frykberg & Banks 2015; Rohani & Parks 2015). As we already have confirmation of epoxy-tigliane efficacy from *in vivo* studies performed by QBiotics Ltd., it appears that the MMP levels are optimal for cell migration, without creating a chronic wound site. MMP-10 was the only proteinase that was shown to be differentially expressed for EBC-211, but not EBC-46. This result was confirmed through the MMP activity assays. However, as this MMP has been associated with the migration of keratinocytes at the wound edge, this result may contribute to the enhanced migratory response of EBC-211, compared to EBC-46 (Gill & Parks 2008; Philips et al. 2011; Rohani & Parks 2015). Although, the *in vitro* migration assay was performed on tissue culture plastic and not an ECM, which would replicate *in vivo* settings more accurately (Kramer et al. 2013).

A greatly important observation from the global gene analysis, corroborated at a protein level through ELISAs, was the profound downregulation of inflammatory cytokines and chemokines, such as IL-6, IL-8, CCL5 and CXCL10. This

downregulation and subsequent attenuated inflammatory phase are typically associated with preferential healing responses, again indicating that treatment with the novel epoxy-tiglianes, especially EBC-211, may induce a preferential response as opposed to the normal response associated with acute adult dermal wound healing (Barrientos et al. 2008; Leung et al. 2012; Rolfe & Grobbelaar 2012; Turabelidze & DiPietro 2012; Balaji et al. 2015). However, these inflammatory cytokines and chemokines have also been shown to induce keratinocyte migration to the wound site; with IL-8, this is through production of a chemokinetic gradient (Satish et al. 2003; Gallucci et al. 2004; Spiekstra et al. 2007; Jiang et al. 2012; Rees et al. 2015). However, as chronic wounds often possess an excessive inflammatory phase, treatment with these novel epoxy-tiglianes may attenuate this response and induce a rapid regenerative healing mechanism, as opposed to the typical repair response (Menke et al. 2007; Frykberg & Banks 2015).

7.5 Significance to Wound Healing Response

Of great interest, a number of the differentially expressed genes following epoxy-tigliane treatment have been associated with preferential healing responses, corroborating the enhanced wound repair responses observed through both the *in vitro* and animal *in vivo* studies (Rolfe & Grobbelaar 2012; Reddell et al. 2014; Turabelidze et al. 2014). The benefit of the prior performance of *in vivo* veterinary studies was the indication that treatment with the novel epoxy-tiglianes induced an exceptional wound healing response, with minimal scarring (Reddell et al. 2014). However, in order for these epoxy-tiglianes to progress as a novel pharmaceutical agent for enhanced wound repair, a greater understanding of the mechanism of action for these pharmaceuticals was required. EBC-46 has been shown to disrupt blood supply to the site during tumour ablation, increasing cell permeability at the wound site (Boyle et al. 2014). This is an interesting effect, as increased permeability has also been shown to occur in early-gestational foetal wound healing. This is potentially due to increased vascular endothelial growth factor (VEGF) expression, although there are conflicting studies on VEGF expression levels in foetal wounds (Bullard et al. 2003; Colwell et al. 2005; Henderson et al. 2011; Rolfe & Grobbelaar 2012; Johnson & Wilgus 2014; Yagi et al. 2016). However, the association between increased angiogenesis and scar formation

has been documented, with preferential healing responses exhibiting reduced angiogenesis (Szpaderska et al. 2005; Van Der Veer et al. 2011; DiPietro 2013). As mentioned previously, it is theorised that the epoxy-tiglianes are inducing a more regenerative wound healing response, reminiscent of early-gestational foetal wound healing (Leung et al. 2012; Rolfe & Grobbelaar 2012; Yates et al. 2012).

This theory that a regenerative healing response is induced is an area of immense interest and importance, through the potential as a treatment in impaired healing responses, such as chronic wounds and burn injuries, where large tissue sites are often impacted, requiring this stimulated wound closure ability (Menke et al. 2007; Dreifke et al. 2015; Frykberg & Banks 2015). In addition, the potentially anti-fibrotic response resulting from reduced fibroblast presence and perceived inhibition of myofibroblast differentiation, would be of great benefit in excessive scarring situations, such as keloid and hypertrophic scarring (Bran et al. 2009; Gauglitz et al. 2011; Viera et al. 2012). Despite the wide array of treatment options for fibrosis, it still presents a huge clinical burden and there is no gold standard treatment available yet. It was only in recent years that the formation of a larger keloid may occur at the wound site following surgical removal of keloids was discovered, which results in a higher disability to the patient (Gauglitz et al. 2011; Gold et al. 2014; Rabello et al. 2014). The perceived regenerative capability of epoxy-tigliane treatment may induce an anti-fibrotic response, through decreasing the proliferative and migratory action of the fibroblasts within the keloid and inhibition of myofibroblast formation, resulting in reduced wound contraction.

Furthermore, as discussed in detail in Chapter 1, current wound care strategies are not sufficient in the treatment of chronic wounds, resulting in persistent, non-healing wounds for many months; or for excessive dermal scarring situations, which can reduce patient functionality (Gauglitz et al. 2011; Viera et al. 2012; Rabello et al. 2014; Dreifke et al. 2015; Frykberg & Banks 2015). There is an urgent need for new treatment modalities and the novel epoxy-tiglianes show great promise in resolving these wounds and easing the huge impact on healthcare providers (Posnett & Franks 2008; Guest et al. 2015; Harding 2015). These epoxy-tiglianes have shown to induce these responses following topical application to the wound site and even show success

on long lasting chronic wounds, as in the veterinary case study with a deep necrosing chronic wound (Reddell et al. 2014). The *in vivo* veterinary trials have only involved EBC-46; although from the *in vitro* studies, it appears that both analogues exert their responses by the same mechanism, leading to the theory that EBC-211 would also be successful in the veterinary *in vivo* studies. However, an increased beneficial concentration range was observed following EBC-211 treatment, especially for wound repopulation, compared to EBC-46 responses; additionally, EBC-211 is considered to be of 'lesser activity' and has been demonstrated to possess a reduced cytotoxicity compared to EBC-46. Therefore, there is the possibility that EBC-211 may be considered as more promising therapeutically than EBC-46 for *in vivo* responses. However, despite these exceptional responses observed through the *in vitro* studies, there are numerous other cell types present within the epidermal and dermal layers, including a variety of stem cell and immune cell populations, impacting on the overall wound healing process; their responses to epoxy-tigliane treatment have not yet been investigated (Haake et al. 2001; Walters & Roberts 2002).

7.6 Future Research

EBC-46 and EBC-211 have been shown to induce the anti-cancer response, primarily through PKC-β isoforms, but also through PKC-α and -γ, to a lesser degree (Boyle et al. 2014; Reddell et al. 2014). It is theorised that the wound healing responses are acting through PKC pathways also, in particular the classical pathways (Boyle et al. 2014; Reddell et al. 2014). However, further studies are required to confirm this theory through a number of PKC studies, initially involving performing the proliferation and migratory studies in the presence of pan- and specific PKC inhibitors; such as BIM-1 and Gö6976 (Koivunen et al. 2004; Rotmann et al. 2006; Aaltonen & Peltonen 2010; Dang et al. 2011). Such studies will confirm a role for PKCs and specifically, classical PKCs in keratinocyte responses *in vitro*. In addition, PKC inhibition will be used to observe the impact of PKC activity, following epoxy-tigliane treatment, on the key differentially expressed genes identified during the global gene analysis. Gene and protein expression levels will be determined, following PKC inhibition, of key keratins, cell cycle-related genes, matrix metalloproteinase; and inflammatory cytokines and chemokines.

However, it has been indicated that PKC-β is present in HaCaTs only, not primary human keratinocytes. This may have implications for the wound healing studies and requires future experiments to be performed on primary keratinocytes to determine whether the same beneficial responses are observed (Mitev & Miteva 1999; Denning 2004). Although there are conflicting reports on this, with some stating that PKC-β is present in keratinocytes and that there is a reduction in expression of this isoform in the epidermal layer of psoriasis, compared to normal adult skin (Fisher et al. 1993; Papp et al. 2003). Other isoforms were also shown to be involved, albeit to a lesser level than PKC-β. However, these isoforms may predominate in the epoxy-tigliane mediated wound healing responses. As the *in vitro* studies performed in this thesis have indicated that the lower concentrations exert the greatest beneficial wound healing responses, resulting in the greater therapeutic range with EBC-211 treatment, low levels of PKC activation may be sufficient to induce these exceptional wound healing responses.

HaCaTs were used initially instead of primary keratinocytes, as this immortalised cell line has been widely used to assess epidermal responses, due to their close similarity of functional response to normal adult epidermal keratinocytes (Boukamp et al. 1988; Pessina et al. 2001; Wilson 2014). HaCaTs have been shown to maintain key behavioural functions, similar to primary keratinocytes, such as retaining differentiation capacity. Little change to cell cycle related genes have also been observed, compared to primary keratinocytes (Sprenger et al. 2013). As a result of these beneficial properties, HaCaTs are deemed suitable for use instead of primary keratinocytes, whilst being representative of epidermal keratinocyte responses (Sprenger et al. 2013). Primary keratinocytes have been reported to potentially induce a range of responses, due to variations in donor age, gender and localisation of biopsy (Sprenger et al. 2013). However, due to the potentially altered PKC isoform presence in HaCaTs, it would be necessary to perform studies on primary keratinocyte as well and compare to the previous results obtained from HaCaTs.

Correlating with the lesser activity of EBC-211, compared to EBC-46, the level of PKC activation by EBC-211 is thought to be much reduced (QBiotics Ltd.). Therefore,

the PKC inhibitors studies will elucidate whether both epoxy-tiglianes mediate their responses through the same mechanism of action, or if another pathway is involved in the responses observed by EBC-211. Once PKC activity has been determined, a number of mechanistic studies could identify the impact of specific PKC isoforms on the responses, previously observed. This analysis could focus on downstream signalling pathways of PKCs, including MAPK/ERK Kinase (MEK)1/2, extracellular signal-regulated kinase (ERK)1/2, mitogen-activated protein kinase (MAPK)1/2, phosphatidylinositide 3-kinase (PI3K), Akt, signal transducer and activator of transcription (STAT)1-3, janus kinase/signal transducers and activators of transcription (JAK-STAT) and SMAD. The impact on these downstream signalling pathway genes/proteins will be determined by quantitative polymerase chain reaction (qPCR) and Western blot analysis, respectively, through use of specific pathway inhibitors. These should also be performed in the absence of inhibition for comparison and those of interest will undergo further study through performing the proliferation and migratory studies in the HaCaTs in the presence of these certain inhibitors. As before, gene and protein expression levels should be determined, following inhibition of these downstream signalling pathways, of key keratins, cell cycle-related genes, matrix metalloproteinase; and inflammatory cytokines and chemokines.

As discussed, the profound response on fibroblast-myofibroblast differentiation, following epoxy-tigliane, requires further investigation, due to its potential as an anti-fibrotic agent. Following from the success of the keratinocyte Microarray studies, where a number of key genes were observed to be differentially expressed and helped elucidate the mechanism of action, global gene analysis could be performed during TGF-β_1-driven, dermal fibroblast-myofibroblast differentiation, following treatment with epoxy-tiglianes. This will be of great benefit to determine the pathways involved in inducing this unexpected and exceptional response. It may also elucidate key genes which result in inhibition of myofibroblast formation, especially at 0.1µg/ml EBC-46 and 10µg/ml EBC-211, which has been an area of great interest in the fibrosis field. In addition, a number of *in vitro* could be performed on keloid and hypertrophic fibroblasts, to determine whether treatment with the novel epoxy-tiglianes can induce an anti-fibrotic response on this highly proliferative and contractive cell type. This would be undertaken once the anti-fibrotic response has been confirmed for normal

dermal fibroblasts to determine whether this response is induced on this excessive scarring situation (Bran et al. 2009; Gauglitz et al. 2011).

Greater knowledge in the mechanism of action of these novel epoxy-tiglianes and how these apparent preferential wound healing responses are induced is vital for the continued development of a novel pharmaceutical. Additional *in vitro* studies could be performed, incorporating the strong paracrine feedback system between dermal fibroblasts and epidermal keratinocyte, through use of a 3D organotypic culture system. This could give an insight into how the epoxy-tiglianes induce their responses on each cell type, along with the basement membrane formation; however, this model does not incorporate all cell types involved in wound healing, such as immune cells (Maas-Szabowski et al. 1999; Lee & Cho 2005; Bader & Kao 2009; Lee et al. 2009; Safferling et al. 2013; Sriram et al. 2015). Another *in vitro* study which could be undertaken is a collagen lattice contraction assay, which measures the contractile ability of cells within the collagen matrix (Ngo et al. 2006; Ehrlich & Moyer 2013; Jin et al. 2015). This assay could potentially elucidate whether the contractile ability is reduced in fibroblasts cultured in the presence of TGF-β1, and 0.1µg/ml EBC-46 and 10µg/ml EBC-211, compared to untreated controls and other concentrations. This is due to the observation that treatment with both of these concentrations appeared to induce a resistance in fibroblast to myofibroblast differentiation.

Further *in vivo* studies could also be performed, through use of animal wound healing models, to determine the histology of the tissue following repair and observe the tensile strength of the regenerated tissue (Davidson 1998; Birch et al. 2005; Ansell et al. 2012). Due to the obvious benefit towards chronic non-healing wounds, use of a diabetic mouse model would be of great interest, such as the db/db mouse model, due to the impaired wound healing response associated with diabetic ulcers (Sullivan et al. 2004; Michaels et al. 2007; Trousdale et al. 2009). There are a number of other chronic wound animal models, including skin flap models inducing ischemic wounds and pressure wounds through use of magnets as a model for reperfusion of ischemic wounds; these are suitable models for ischemic ulcers and pressure ulcers, respectively (Davidson 1998; Ansell et al. 2012; Nunan et al. 2014). There have been limited animal models for pathological scarring, delaying the elucidation of full understanding

of the mechanism of action which results in keloid and hypertrophic scars (Morris et al. 1997; van den Broek et al. 2014; Alrobaiea et al. 2016). Part of the restriction for development of a hypertrophic scarring animal model is that these scars do not form in animal skin. An athymic nude mouse model has been developed, where full thickness human skin is grafted onto the mouse, which will overcome this problem. This model will provide greater understanding of excessive dermal fibrosis, as keloid skin or skin known to develop hypertrophic scars, can also be grafted onto the nude mouse; expected pathologies were evident for the excessive dermal fibrosis models (van den Broek et al. 2014; Alrobaiea et al. 2016). Wound closure ability and rate can be calculated following experimental treatment modalities, using these animal models. In addition, histological assessment can be performed to determine the composition and organisation of the underlying dermis (Sullivan et al. 2004; Trousdale et al. 2009; Alrobaiea et al. 2016). Immunohistochemical analysis on the athymic nude mouse model for hypertrophic scarring can determine the expression of α-SMA, as these scars contain myofibroblast-containing nodules (Rabello et al. 2014; Alrobaiea et al. 2016). The aim of undertaking these further studies would be to elucidate the mechanism of action of these novel epoxy-tiglianes and determine the resultant underlying dermal composition. This knowledge would enable progression into clinical trials for these epoxy-tiglianes for treatment of impaired healing situations, such as chronic wounds and burn injuries; in addition to treatment for excessive dermal fibrosis, including keloid and hypertrophic scarring.

Bibliography

Aaltonen, V. & Peltonen, J., 2010. PKCα/βI inhibitor Go6976 induces dephosphorylation of constitutively hyperphosphorylated Rb and G1 arrest in T24 cells. *Anticancer Research*, 30(10), pp.3995–3999.

Abreu-Velez, A.M. & Howard, M.S., 2012. Collagen IV in normal and in disease process. *North American Journal of Medical Sciences*, 4(1), pp.1–8.

Adámková, L., Součkova, K. & Kovařík, J., 2007. Transcription protein STAT1: Biology and relation to cancer. *Folia Biologica*, 53(1), pp.1–6.

Adzick, N.S. & Lorenz, H.P., 1994. Cells, matrix, growth factors, and the surgeon. The biology of scarless fetal wound repair. *Annals of surgery*, 220(1), pp.10–18.

Agale, S.V., 2013. Chronic Leg Ulcers : Epidemiology, Aetiopathogenesis, and Management. *Ulcers*, 413604, pp.1–9.

Ager, A., 1994. Lymphocyte recirculation and homing: roles of adhesion molecules and chemoattractants. *Trends in Cell Biology*, 4, pp.326–332.

Agren, M.S. et al., 2001. Topical synthetic inhibitor of matrix metalloproteinases delays epidermal regeneration of human wounds. *Experimental dermatology*, 10(5), pp.337–48.

Agren, M.S. & Werthén, M., 2007. The extracellular matrix in wound healing: a closer look at therapeutics for chronic wounds. *The international journal of lower extremity wounds*, 6(2), pp.82–97.

Ahn, J.Y. et al., 2011. The Inhibitory Effect of Ginsan on TGF-β Mediated Fibrotic Process. *Journal of Cellular Physiology*, 226(5), pp.1241–1247.

Akira, S., 2000. Roles of STAT3 defined by tissue-specific gene targeting. *Oncogene*, 19(21), pp.2607–2611.

Akita, S., Akino, K. & Hirano, A., 2012. Basic Fibroblast Growth Factor in Scarless Wound Healing. *Advances in Wound Care*, 2(2), pp.44–49.

Akutsu, N., Amano, S. & Nishiyama, T., 2005. Quantitative analysis of laminin 5 gene expression in human keratinocytes. *Experimental Dermatology*, 14(5), pp.329–335.

Alaish, S.M. et al., 1994. Biology of fetal wound healing: Hyaluronate receptor expression in fetal fibroblasts. *Journal of Pediatric Surgery*, 29(8), pp.1040–1043.

Al-Attar, A. et al., 2006. Keloid pathogenesis and treatment. *Plastic and reconstructive surgery*, 117(1), pp.286–300.

Alberts, B. et al., 2002. Intracellular Control of Cell-Cycle Events. In *Molecular Biology of the Cell*. New York: Garland Science.

Ali, A.S. et al., 2009. Exploitation of protein kinase C: A useful target for cancer therapy. *Cancer Treatment Reviews*, 35(1), pp.1–8.

al-Khateeb, T. et al., 1997. An investigation of preferential fibroblast wound repopulation using a novel in vitro wound model. *Journal Of Periodontology*, 68(11), pp.1063–1069.

Alrobaiea, S.M. et al., 2016. A Novel Nude Mouse Model of Hypertrophic Scarring Using Scratched Full Thickness Human Skin Grafts. *Advances in Wound Care*, 5(7), pp.299–313.

Alsaigh, T. et al., 2011. Acute venous occlusion enhances matrix metalloprotease activity: Implications on endothelial dysfunction. *Microvascular Research*, 81(1), pp.108–116.

Alster, T.S. & Nanni, C.A., 1998. Pulsed Dye Laser Treatment of Hypertrophic Burn Scars. *Plastic and Reconstructive Surgery*, 102, pp.2190–2195.

Alster, T.S. & Williams, C.M., 1995. Treatment of keloid sternotomy scars with 585 nm flashlamp-pumped pulsed-dye laser. *The Lancet*, 345(8959), pp.1198–1200.

Amadeu, T. et al., 2003. Vascularization pattern in hypertrophic scars and keloids: a stereological analysis. *Pathology, research and practice*, 199(7), pp.469–473.

Amano, M., Nakayama, M. & Kaibuchi, K., 2010. Rho-kinase/ROCK: A key regulator of the cytoskeleton and cell polarity. *Cytoskeleton*, 67(9), pp.545–554.

Amano, S. et al., 2004. Increase of laminin 5 synthesis in human keratinocytes by acute wound fluid, inflammatory cytokines and growth factors, and lysophospholipids. *British Journal of Dermatology*, 151(5), pp.961–970.

Ananthakrishnan, R. & Ehrlicher, A., 2007. The Forces Behind Cell Movement. *International*

Journal of Biological Sciences, 3(5), pp.303–317.
Andrae, J., Gallini, R. & Betsholtz, C., 2008. Role of platelet-derived growth factors in physiology and medicine. *Genes and Development*, 22, pp.1276–1312.
Andrews, J.P. et al., 2016. Keloids: The paradigm of skin fibrosis - Pathomechanisms and treatment. *Matrix Biology*, 51, pp.37–46.
Angel, P., Szabowski, a & Schorpp-Kistner, M., 2001. Function and regulation of AP-1 subunits in skin physiology and pathology. *Oncogene*, 20(19), pp.2413–2423.
Ansell, D.M., Holden, K.A. & Hardman, M.J., 2012. Animal models of wound repair: Are they cutting it? *Experimental Dermatology*, 21(8), pp.581–585.
Antsiferova, M. et al., 2009. Keratinocyte-derived follistatin regulates epidermal homeostasis and wound repair. *Laboratory investigation; a journal of technical methods and pathology*, 89(2), pp.131–41.
Antsiferova, M. & Werner, S., 2012. The bright and the dark sides of activin in wound healing and cancer. *Journal of cell science*, 125(Pt 17), pp.3929–37.
Aoki, M. et al., 2014. siRNA knockdown of tissue inhibitor of metalloproteinase-1 in keloid fibroblasts leads to degradation of collagen type I. *The Journal of investigative dermatology*, 134(3), pp.818–26.
Apikian, M. & Goodman, G., 2004. Intralesional 5-fluorouracil in the treatment of keloid scars. *Australasian Journal of Dermatology*, 45(2), pp.140–143.
Araki, E. et al., 2009. Clustering of Syndecan-4 and Integrin β1 by Laminin α3 Chain–derived Peptide Promotes Keratinocyte Migration. *Molecular Biology of the Cell*, 20, pp.3012–3024.
Argraves, W.S. et al., 1990. Fibulin is an extracellular matrix and plasma glycoprotein with repeated domain structure. *Journal of Cell Biology*, 111(6 II), pp.3155–3164.
Argraves, W.S. et al., 2003. Fibulins: physiological and disease perspectives. *EMBO Rep*, 4(12), pp.1127–1131.
Arin, M.J., 2009. The molecular basis of human keratin disorders. *Human Genetics*, 125(4), pp.355–373.
Armstrong, D.G., Lavery, L. a & Consortium, D.F.S., 2005. Negative pressure wound therapy after partial diabetic foot amputation: a multicentre, randomised controlled trial. *Lancet*, 366(9498), pp.1704–1710.
Arnold, I. & Watt, F.M., 2001. c-Myc activation in transgenic mouse epidermis results in mobilization of stem cells and differentiation of their progeny. *Current Biology*, 11(8), pp.558–568.
Arnott, C.H. et al., 2004. Expression of both TNF-alpha receptor subtypes is essential for optimal skin tumour development. *Oncogene*, 23, pp.1902–1910.
Arpino, V., Brock, M. & Gill, S.E., 2015. The role of TIMPs in regulation of extracellular matrix proteolysis. *Matrix biology : journal of the International Society for Matrix Biology*, 44-46, pp.247–54.
Ashcroft, G.S. et al., 2012. Tumor necrosis factor-alpha (TNF-α) is a therapeutic target for impaired cutaneous wound healing. *Wound Repair and Regeneration*, 20(1), pp.38–49.
Asilian, A., Darougheh, A. & Shariati, F., 2006. New combination of triamcinolone, 5-fluorouracil, and pulsed-dye laser for treatment of keloid and hypertrophic scars. *Dermatologic Surgery*, 32(7), pp.907–915.
Atiyeh, B.S., 2007. Nonsurgical management of hypertrophic scars: Evidence-based therapies, standard practices, and emerging methods. *Aesthetic Plastic Surgery*, 31(5), pp.468–492.
Atiyeh, B.S. & Costagliola, M., 2007. Cultured epithelial autograft (CEA) in burn treatment: Three decades later. *Burns*, 33(4), pp.405–413.
Attisano, L. & Wrana, J.L., 1998. Mads and Smads in TGFI3 signalling. *Current Opinion in Cell Biology*, 10, pp.188–194.
auf demKeller, U. et al., 2004. Keratinocyte growth factor: effects on keratinocytes and mechanisms of action. *European journal of cell biology*, 83(11-12), pp.607–12.
Aumailley, M. & Rousselle, P., 1999. Laminins of the dermo-epidermal junction. *Matrix biology : journal of the International Society for Matrix Biology*, 18(1), pp.19–28.
Bader, R.A. & Kao, W.J., 2009. Modulation of the Keratinocyte – Fibroblast Paracrine Relationship with Gelatin-Based Semi-interpenetrating Networks Containing Bioactive Factors for Wound Repair. *Journal of Biomaterials Science*, 20, pp.1005–1030.

Bainbridge, P., 2013. Wound healing and the role of fibroblasts. *Journal of wound care*, 22(8), pp.407–412.
Balaji, S. et al., 2015. Chemokine Involvement in Fetal and Adult Wound Healing. *Advances in Wound Care*, 4(11), pp.660–672.
Balato, A. et al., 2012. Pathogenesis of Psoriasis: The Role of Pro-Inflammatory Cytokines Produced by Keratinocytes. In D. J. Soung, ed. *Psoriasis*. InTech, pp. 9–28.
Bandyopadhyay, B. et al., 2006. A "traffic control" role for TGFβ3: Orchestrating dermal and epidermal cell motility during wound healing. *Journal of Cell Biology*, 172(7), pp.1093–1105.
Banno, T., Gazel, A. & Blumenberg, M., 2004. Effects of tumor necrosis factor-α (TNFα) in epidermal keratinocytes revealed using global transcriptional profiling. *Journal of Biological Chemistry*, 279(31), pp.32633–32642.
Bao, P. et al., 2009. The role of vascular endothelial groth factor in wound healing. *Journal surgery research*, 153(2), pp.347–358.
Barrientos, S., Stojadinovic, O., Golinko, M.S., Brem, H. & Tomic-Canic, M., 2008. Growth factors and cytokines in wound healing. *Wound repair and regeneration : official publication of the Wound Healing Society [and] the European Tissue Repair Society*, 16(5), pp.585–601.
Bartek, J., Lukas, C. & Lukas, J., 2004. Checking on DNA damage in S phase. *Nature reviews. Molecular cell biology*, 5(10), pp.792–804.
Bass, M.D. et al., 2011. A Syndecan-4 Hair Trigger Initiates Wound Healing through Caveolin- and RhoG-Regulated Integrin Endocytosis. *Developmental Cell*, 21(4), pp.681–693.
Battegay, E.J. et al., 1994. PDGF-BB modulates endothelial proliferation and angiogenesis in vitro via PDGF β-receptors. *Journal of Cell Biology*, 125(4), pp.917–928.
Baudoin, C., Fantin, L. & Meneguzzi, G., 2005. Proteolytic processing of the laminin α3 G domain mediates assembly of hemidesmosomes but has no role on keratinocyte migration. *Journal of Investigative Dermatology*, 125(5), pp.883–888.
Baum, C.L. & Arpey, C.J., 2005. Normal cutaneous wound healing: clinical correlation with cellular and molecular events. *Dermatologic surgery : official publication for American Society for Dermatologic Surgery [et al.]*, 31(6), pp.674–86; discussion 686.
Baumann, L., 2007. Skin ageing and its treatment. *Journal of Pathology*, 211, pp.241–251.
Bazin, S., Lous, M. Le & Delaunay, A., 1976. Collagen in Granulation Tissues. *Agents and Actions*, 6, pp.272–276.
Beanes, S.R. et al., 2003. Skin repair and scar formation: the central role of TGF-β. *Expert Reviews in Molecular Medicine*, 5(08), pp.1–22.
Bechtel, M.J. et al., 1998. Plasminogen activator inhibitor type 2 is expressed in keratinocytes during re-epithelialization of epidermal defects. *British Journal of Dermatology*, 138(1), pp.22–28.
Beer, H.D. et al., 2000. Expression and function of keratinocyte growth factor and activin in skin morphogenesis and cutaneous wound repair. *Journal of Investigative Dermatology Symposium Proceedings*, 5(1), pp.34–39.
Beer, H.D., Longaker, M.T. & Werner, S., 1997. Reduced expression of PDGF and PDGF receptors during impaired wound healing. *J.Invest Dermatol.*, 109(2), pp.132–138.
Behm, B. et al., 2012. Cytokines, chemokines and growth factors in wound healing. *Journal of the European Academy of Dermatology and Venereology*, 26(7), pp.812–820.
Beidler, S.K. et al., 2008. Inflammatory cytokine levels in chronic venous insufficiency ulcer tissue before and after compression therapy. *Journal of Vascular Surgery*, 16, pp.642–648.
Beldon, P., 2010. Basic science of wound healing. *Surgery*, 28(9), pp.409–412.
Belford, D.A., 1997. The mechanism of excisional fetal wound repair in vitro is responsive to growth factors. *Endocrinology*, 138(9), pp.3987–3996.
Bellini, A. & Mattoli, S., 2007. The role of the fibrocyte, a bone marrow-derived mesenchymal progenitor, in reactive and reparative fibroses. *Laboratory investigation; a journal of technical methods and pathology*, 87(9), pp.858–70.
Bennett, N.T. & Schultz, G.S., 1993. Growth factors and wound healing: biochemical properties of growth factors and their receptors. *American journal of surgery*, 165(6), pp.728–37.
Berg, D.T. et al., 2005. Smad6s Regulates Plasminogen Activator Inhibitor-1 through a Protein Kinase C-β-dependent Up-regulation of Transforming Growth Factor-β. *Journal of*

Biological Chemistry, 280(15), pp.14943–14947.
Berman, B., 2010. Biological agents for controlling excessive scarring. *American Journal of Clinical Dermatology*, 11(Suppl. 1), pp.31–34.
Berman, B. & Bieley, H.C., 1996. Adjunct Therapies to Surgical Management of Keloids. *Dermatologic surgery : official publication for American Society for Dermatologic Surgery*, 22(2), pp.126–30.
Berman, B. & Flores, F., 1997. Recurrence rates of excised keloids treated with postoperative triamcinolone acetonide injections or interferon alfa-2b injections. *Journal of the American Academy of Dermatology*, 37(5), pp.755–757.
Bettinger, D.A. et al., 1996. The Effect of TGF-β on Keloid Fibroblast Proliferation and Collagen Synthesis. *Plastic and reconstructive surgery*, 98(5), pp.827–833.
Bianchetti, L. et al., 2012. Extracellular matrix remodelling properties of human fibrocytes. *Journal of Cellular and Molecular Medicine*, 16(3), pp.483–495.
Bielefeld, K.A., Amini-Nik, S. & Alman, B.A., 2013. Cutaneous wound healing: Recruiting developmental pathways for regeneration. *Cellular and Molecular Life Sciences*, 70(12), pp.2059–2081.
Bigg, H.F. et al., 2007. Activity of matrix metalloproteinase-9 against native collagen types I and III. *FEBS Journal*, 274(5), pp.1246–1255.
Birch, M., Tomlinson, A. & Ferguson, M.W.J., 2005. Animal Models for Adult Dermal Wound Healing. In J. Varga, D. A. Brenner, & S. H. Phan, eds. *Methods in Molecular Medicine, Vol. 117: Fibrosis Research: Methods and Protocols*. Totowa, NJ: Humana Press Inc., pp. 223–236.
Bishop, J.R., Schuksz, M. & Esko, J.D., 2007. Heparan sulphate proteoglycans fine-tune mammalian physiology. *Nature*, 446(7139), pp.1030–1037.
Bitoux, M. Le et al., 2009. Syndecans and CD44 in Normal Human Keratinocyte Cultures: Modulation with Medium Composition and All-trans Retinoic Acid. *The Open Dermatology Journal*, 3, pp.32–41.
Blakaj, A. & Bucala, R., 2012. Fibrocytes in health and disease. *Fibrogenesis & Tissue Repair*, 5(Suppl 1), p.S6.
Blanpain, C. et al., 2004. Existence of Two Cell Populations within an Epithelial Stem Cell Niche. *Cell*, 118, pp.635–648.
Blasi, F., 1988. Surface receptors for urokinase plasminogen activator. *Fibrinolysin*, 2, pp.73–84.
Blomme, E.A.G. et al., 1999. Parathyroid hormone-related protein is a positive regulator of keratinocyte growth factor expression by normal dermal fibroblasts. , 152, pp.189–197.
Boateng, J. & Catanzano, O., 2015. Advanced Therapeutic Dressings for Effective Wound Healing - A Review. *Journal of Pharmaceutical Sciences*, 104(11), pp.3653–3680.
Bodnar, R.J., Yates, C.C. & Wells, A., 2006. IP-10 blocks vascular endothelial growth factor-induced endothelial cell motility and tube formation via inhibition of calpain. *Circulation Research*, 98(5), pp.617–625.
Boissy, R.E., 2003. Melanosome transfer to and translocation in the keratinocyte. *Experimental dermatology*, 12 Suppl 2, pp.5–12.
Bonnekoh, B. et al., 1995. Up-regulation of keratin 17 expression in human HaCaT keratinocytes by interferon-gamma. *The Journal of investigative dermatology*, 104(1), pp.58–61.
Boorsma, D.M. et al., 1998. Chemokine IP-10 expression in cultured human keratinocytes. *Archives of Dermatological Research*, 290(6), pp.335–341.
Borradori, L. & Sonnenberg, A., 1996. Hemidesmosomes : roles in adhesion , signaling and human diseases. *Current Opinion in Cell Biology*, 8, pp.647–656.
Bose, A. et al., 2013. Keratin K15 as a biomarker of epidermal stem cells. *International Journal of Molecular Sciences*, 14(10), pp.19385–19398.
Bosman, F.T. & Stamenkovic, I., 2003. Functional structure and composition of the extracellular matrix. *Journal of Pathology*, 200(4), pp.423–428.
Bottcher-Haberzeth, S., Biedermann, T. & Reichmann, E., 2010. Tissue engineering of skin substitutes. *Burns*, 36, pp.450–460.
Boukamp, P. et al., 1988. Normal keratinization in a spontaneously immortalized aneuploid human keratinocyte cell line. *The Journal of cell biology*, 106(3), pp.761–71.
Boulais, N. & Misery, L., 2007. Merkel cells. *J.Am.Acad.Dermatol.*, 57(1097-6787), pp.147–165.

Boulais, N. & Misery, L., 2008. The epidermis: a sensory tissue. *European journal of dermatology : EJD*, 18(2), pp.119–27.
Bouzari, N., Davis, S.C. & Nouri, K., 2007. Laser treatment of keloids and hypertrophic scars. *International Journal of Dermatology*, 46(1), pp.80–88.
Boyce, D.E. et al., 2001. Inflammatory-cell subpopulations in keloid scars. *British journal of plastic surgery*, 54(6), pp.511–6.
Boyle, G.M. et al., 2014. Intra-lesional injection of the novel PKC activator EBC-46 rapidly ablates tumors in mouse models. *PloS one*, 9(10), pp.1–12.
Bradley, M., 1999. The debridement of chronic wounds: A systematic review. *Health Technology Assessment*, 3(17 Pt1), pp.26–29.
Bragulla, H.H. & Homberger, D.G., 2009. Structure and functions of keratin proteins in simple, stratified, keratinized and cornified epithelia. *Journal of Anatomy*, 214(4), pp.516–559.
Braiman-Wiksman, L. et al., 2007. Novel insights into wound healing sequence of events. *Toxicologic pathology*, 35(6), pp.767–79.
Bran, G.M. et al., 2009. Keloids: Current concepts of pathogenesis (Review). *International Journal of Molecular Medicine*, 24(3), pp.283–293.
Brancato, S.K. & Albina, J.E., 2011. Wound macrophages as key regulators of repair: Origin, phenotype, and function. *American Journal of Pathology*, 178(1), pp.19–25.
Brandner, J.M. et al., 2008. Expression of Matrix Metalloproteinases, Cytokines, and Connexins in Diabetic and Nondiabetic Human Keratinocytes Before and After Transplantation Into an Ex Vivo Wound-Healing Model. *Diabetes Care*, 31(1), pp.114–120.
Breitkreutz, D. et al., 2007. Protein kinase C family: On the crossroads of cell signaling in skin and tumor epithelium. *Journal of Cancer Research and Clinical Oncology*, 133(11), pp.793–808.
Brem, H. et al., 2007. Molecular Markers in Patients with Chronic Wounds to Guide Surgical Debridement. *Molecular Medicine*, 13, pp.30–39.
van den Broek, L.J. et al., 2014. Human hypertrophic and keloid scar models: Principles, limitations and future challenges from a tissue engineering perspective. *Experimental Dermatology*, 23(6), pp.382–386.
Broker, B. et al., 1999. Comparison of growth factor expression in fetal and adult fibroblasts: a preliminary report. *Arch Otolaryngol Head Neck Surg*, 125, pp.676–680.
Bromberg, J.F. et al., 1999. Stat3 as an oncogene. *Cell*, 98(3), pp.295–303.
Bromberg, J.F. et al., 1996. Transcriptionally active Stat1 is required for the antiproliferative effects of both interferon alpha and interferon gamma. *Proceedings of the National Academy of Sciences of the United States of America*, 93(15), pp.7673–7678.
Broughton, G., Janis, J.E. & Attinger, C.E., 2006a. The basic science of wound healing. *Plastic and Reconstructive Surgery*, 117(Suppl), p.12S–34S.
Broughton, G., Janis, J.E. & Attinger, C.E., 2006b. Wound healing: an overview. *Plastic and Reconstructive Surgery*, 117(Suppl), p.1e–S–32e–S.
Broussard, K.C. & Powers, J.G., 2013. Wound dressings: Selecting the most appropriate type. *American Journal of Clinical Dermatology*, 14(6), pp.449–459.
Büchau, A.S. et al., 2007. S100A15, an antimicrobial protein of the skin: regulation by E. coli through Toll-like receptor 4. *The Journal of investigative dermatology*, 127(11), pp.2596–604.
Bugge, T.H. et al., 1996. Urokinase-type plasminogen activator is effective in fibrin clearance in the absence of its receptor or tissue-type plasminogen activator. *Proceedings of the National Academy of Sciences of the United States of America*, 93(12), pp.5899–904.
Bullard, K.M., Longaker, M.T. & Lorenz, H.P., 2003. Fetal wound healing: Current biology. *World Journal of Surgery*, 27(1), pp.54–61.
Bullen, E.C. et al., 1995. Tissue inhibitor of metalloproteinases-1 is decreased and activated gelatinases are increased in chronic wounds. *The Journal of investigative dermatology*, 104(2), pp.236–240.
Burdett, I.D.J., 1998. Aspects of the structure and assembly of desmosomes. *Micron*, 29(4), pp.309–328.
Burry, R.W., 2011. Controls for Immunocytochemistry: An Update. *Journal of Histochemistry & Cytochemistry*, 59(1), pp.6–12.
Butcher, E.C. et al., 1991. Leukocyte-endothelial cell recognition: Three (or more) steps to

specificity and diversity. *Cell*, 67(6), pp.1033–1036.
Cajone, F. & Sherbet, G. V, 2000. Stathmin is involved in S100A4-mediated regulation of cell cycle progression. *Clinical & Experimental Metastasis*, 17, pp.865–871.
Calderhead, R.G. & Goo, B.L., 2014. Handbook of Lasers in Dermatology. In K. Nouri, ed. *Handbook of Lasers in Dermatology*. London: Springer-Verlag.
Calderon, M., Lawrence, W.T. & Banes, A.J., 1996. Increased proliferation in keloid fibroblasts wounded in vitro. *The Journal of surgical research*, 61, pp.343–347.
Caley, M.P., Martins, V.L.C. & O'Toole, E.A., 2015. Metalloproteinases and Wound Healing. *Advances in wound care*, 4(4), pp.225–234.
Calkins, C.C. & Setzer, S. V., 2007. Spotting Desmosomes: The First 100 Years. *Journal of Investigative Dermatology*, 127(January), pp.E2–E3.
Callcut, R.A. et al., 2006. Clinical experience with Alloderm: A one-staged composite dermal/epidermal replacement utilizing processed cadaver dermis and thin autografts. *Burns*, 32(5), pp.583–588.
Campisi, J. & d'Adda di Fagagna, F., 2007. Cellular senescence: when bad things happen to good cells. *Nature reviews. Molecular cell biology*, 8(9), pp.729–40.
Candi, E., Schmidt, R. & Melino, G., 2005. The cornified envelope: a model of cell death in the skin. *Nature reviews. Molecular cell biology*, 6(4), pp.328–40.
Carulli, S. et al., 2012. Cell surface proteoglycans syndecan-1 and -4 bind overlapping but distinct sites in laminin α3 LG45 protein domain. *Journal of Biological Chemistry*, 287(15), pp.12204–12216.
Cass, D.L. et al., 1997. Wound size and gestational age modulate scar formation in fetal wound repair. *Journal of Pediatric Surgery*, 32(3), pp.411–415.
Cass, D.L., Meuli, M. & Adzick, N.S., 1997. Scar wars: Implications of fetal wound healing for the pediatric burn patient. *Pediatric Surgery International*, 12(7), pp.484–489.
Catalgol, B. et al., 2009. The proteasome is an integral part of solar ultraviolet a radiation-induced gene expression. *Journal of Biological Chemistry*, 284(44), pp.30076–30086.
Cesarman-maus, G. & Hajjar, K.A., 2005. Molecular mechanisms of fibrinolysis. *British Journal of Haematology*, 129, pp.307–321.
Chan, K.T., Cortesio, C.L. & Huttenlocher, A., 2011. Integrins in Cell Migration. *Cold Spring Harb Perspect Biol*, 3, pp.1–16.
Chen, J.D. et al., 1995. Interleukin-1α Stimulates Keratinocyte Migration Through an Epidermal Growth Factor/Transforming Growth Factor-α-Independent Pathway. *Journal of Investigative Dermatology*, 104(5), pp.729–733.
Chen, L. et al., 2010. Positional differences in the wound transcriptome of skin and oral mucosa. *BMC genomics*, 11(471), pp.1–15.
Chen, P. et al., 2009. MMP7 shedding of syndecan-1 facilitates re-epithelialization by affecting α2β1 integrin activation. *PLoS ONE*, 4(8), pp.25–29.
Chen, W. et al., 2003. Analysis of differentially expressed genes in keloids and normal skin with cDNA microarray. *Journal of Surgical Research*, 113(2), pp.208–216.
Chen, W. et al., 2007. Profiling of genes differentially expressed in a rat of early and later gestational ages with high-density oligonucleotide DNA array. *Wound Repair and Regeneration*, 15(1), pp.147–155.
Chen, W.Y.J. & Abatangelo, G., 1999. Functions of hyaluronan in wound repair. *Wound Repair and Regeneration*, 7(2), pp.79–89.
Cheng, W. et al., 2011. The content and ratio of type I and III collagen in skin differ with age and injury. *African Journal of Biotechnology*, 10(13), pp.2524–2529.
Cheung, W.-F., Cruz, T.F. & Turley, E.A., 1999. Receptor for hyaluronan-mediated motility (RHAMM), a hyaladherin that regulates cell responses to growth factors. *Biochemical Society Transactions link*, 27(2), pp.135–42.
Chin, D. et al., 2004. What is transforming growth factor-beta (TGF-β)? *British Journal of Plastic Surgery*, 57(3), pp.215–221.
Ching, Y.-H. et al., 2011. The use of growth factors and other humoral agents to accelerate and enhance burn wound healing. *Eplasty*, 11, pp.429–449.
Chiricozzi, A. et al., 2011. Integrative responses to IL-17 and TNF-α in human keratinocytes account for key inflammatory pathogenic circuits in psoriasis. *The Journal of investigative*

dermatology, 131(3), pp.677–87.
Chitturi, R.T. et al., 2015. The Role of Myofibroblasts in Wound Healing, Contraction and its Clinical Implications in Cleft Palate Repair. *Journal of International Oral Health*, 7(3), pp.75–80.
Cho, J.-W. et al., 2010. Onion extract and quercetin induce matrix metalloproteinase-1 in vitro and in vivo. *International journal of molecular medicine*, 25, pp.347–352.
Chou, C.P. et al., 2014. Ubiquitin-conjugating enzyme UBE2C is highly expressed in breast microcalcification lesions. *PLoS ONE*, 9(4), pp.1–11.
Chowdri, N.A., Mattoo, M.M.A. & Darzi, M.A., 1999. Keloids and hypertrophic scars: Results with intra-operative and serial postoperative corticosteroid injection therapy. *Australian and New Zealand Journal of Surgery*, 69(9), pp.655–659.
Chua, A.W.C. et al., 2011. The role of R-spondin2 in keratinocyte proliferation and epidermal thickening in keloid scarring. *The Journal of investigative dermatology*, 131(3), pp.644–54.
Chung, J.H. et al., 1996. Ultraviolet B irradiation-enhanced interleukin (IL)-6 production and mRNA expression are mediated by IL-1 alpha in cultured human keratinocytes. *The Journal of investigative dermatology*, 106(4), pp.715–20.
Cichorek, M. et al., 2013. Skin melanocytes: Biology and development. *Postepy Dermatologii i Alergologii*, 30(1), pp.30–41.
Circolo, A. et al., 1991. Differential regulation of the expression of proteinases/antiproteinases in fibroblasts. Effects of interleukin-1 and platelet-derived growth factor. *The Journal of biological chemistry*, 266(19), pp.12283–8.
Clainche, C.L.E. & Carlier, M., 2008. Regulation of Actin Assembly Associated With Protrusion and Adhesion in Cell Migration. *Physiol Rev*, 88, pp.489–513.
Clark, J.A. & Leung, K.S., 1996. The hypertrophic scar and microcirculation. *Burns*, 22(6), pp.447–450.
Clark, R.A., 2001. Fibrin and wound healing. *Annals of the New York Academy of Sciences*, 936, pp.355–367.
Clark, R.A.., 1996. Wound repair: Overview and general considerations. In R. A. . Clark, ed. *The Molecular and Cellular Biology of Wound Repair*. Plenum Press, pp. 3–50.
Clark, R.A.F. et al., 1982. Fibronectin and fibrin provide a provisional matrix for epidermal cell migration during wound reepithelialization. *Journal of Investigative Dermatology*, 79(5), pp.264–269.
Clifford, J.L. et al., 2003. Dominant negative signal transducer and activator of transcription 2 (STAT2) protein: stable expression blocks interferon alpha action in skin squamous cell carcinoma cells. *Mol Cancer Ther*, 2(5), pp.453–459.
Clifford, J.L. et al., 2002. Suppression of Type I Interferon Signaling Proteins Is an Early Event in Squamous Skin Carcinogenesis. *Clinical Cancer Research*, 8, pp.2067–2072.
Collen, D. & Lijnen, H.R., 2009. The tissue-type plasminogen activator story. *Arteriosclerosis, Thrombosis, and Vascular Biology*, 29(8), pp.1151–1155.
Collen, D. & Lijnen, H.R., 2005. Thrombolytic agents. *Thrombosis and Haemostasis*, 93, pp.627–630.
Colwell, A.S. et al., 2005. Increased angiogenesis and expression of vascular endothelial growth factor during scarless repair. *Plastic and reconstructive surgery*, 115(1), pp.204–12.
Colwell, A.S., Longaker, M.T. & Lorenz, H.P., 2008. Identification of differentially regulated genes in fetal wounds during regenerative repair. *Wound Repair and Regeneration*, 16(3), pp.450–459.
Conrad, P.A. et al., 1993. Relative distribution of actin, myosin I, and myosin II during the wound healing response of fibroblasts. *Journal of Cell Biology*, 120(6), pp.1381–1391.
Cook, H. et al., 2000. Defective extracellular matrix reorganization by chronic wound fibroblasts is associated with alterations in TIMP-1, TIMP-2, and MMP-2 activity. *The Journal of investigative dermatology*, 115(2), pp.225–33.
Coolen, N.A. et al., 2010. Comparison between human fetal and adult skin. *Archives of Dermatological Research*, 302(1), pp.47–55.
Cooper, D.M. et al., 1994. Determination of Endogenous Cytokines in Chronic Wounds. *Annals of Surgery*, 219(6), pp.688–691.
Cooper, G., 2000. Structure and organization of actin filaments. In G. Cooper, ed. *The Cell: A*

Molecular Approach. Sinauer Associates.
Corbett, S.A. et al., 1997. Covalent cross-linking of fibronectin to fibrin is required for maximal cell adhesion to a fibronectin-fibrin matrix. *Journal of Biological Chemistry*, 272(40), pp.24999–25005.
Cordeiro, M.F. et al., 2000. TGF-β1, -β2, and -β3 in vitro: Biphasic effects on Tenon's fibroblast contraction, proliferation, and migration. *Investigative Ophthalmology and Visual Science*, 41(3), pp.756–763.
Corradi, A., Franzi, A.T. & Rubartelli, A., 1995. Synthesis and Secretion of Interleukin-1α and Intedeukin-1 Receptor Antagonist during Differentiation of Cultured Keratinocytes. *Experimental Cell Research*, 217, pp.355–362.
Cowin, A.J. et al., 1998. Endogenous inflammatory response to dermal wound healing in the fetal and adult mouse. *Developmental Dynamics*, 212(3), pp.385–393.
Cox, T.R. & Erler, J.T., 2011. Remodeling and homeostasis of the extracellular matrix: implications for fibrotic diseases and cancer. *Disease models & mechanisms*, 4(2), pp.165–78.
Culav, E.M., Clark, C.H. & Mervyn, J., 1999. Connective Tissues : Matrix. *Physical Therapy*, 79(3), pp.308–319.
Cuttle, L. et al., 2005. Collagen in the scarless fetal skin wound: Detection with Picrosirius-polarization. *Wound Repair and Regeneration*, 13(2), pp.198–204.
D'Orazio, J. et al., 2013. UV radiation and the skin. *International Journal of Molecular Sciences*, 14(6), pp.12222–12248.
Dahlen, J.R. et al., 1998. Inhibition of soluble recombinant furin by human proteinase inhibitor 8. *Journal of Biological Chemistry*, 273(4), pp.1851–1854.
Dai, X. et al., 2008. The NF-κB, p38 MAPK and STAT1 pathways differentially regulate the dsRNA-mediated innate immune responses of epidermal keratinocytes. *International Immunology*, 20(7), pp.901–909.
Dang, C. et al., 2003. Scarless fetal wounds are associated with an increased matrix metalloproteinase-to-tissue-derived inhibitor of metalloproteinase ratio. *Plast Reconstr Surg*, 111(7), pp.2273–2285.
Dang, M. et al., 2011. Epidermal Growth Factor (EGF) ligand release by substrate-specific A disintegrin and metalloproteases (ADAMs) involves different protein kinase C (PKC) isoenzymes depending on the stimulus. *Journal of Biological Chemistry*, 286(20), pp.17704–17713.
Daniels, J.T. et al., 2003. Mediation of transforming growth factor-β1-stimulated matrix contraction by fibroblasts: a role for connective tissue growth factor in contractile scarring. *The American journal of pathology*, 163(5), pp.2043–2052.
Darby, I.A. et al., 2014. Fibroblasts and myofibroblasts in wound healing. *Clinical, Cosmetic and Investigational Dermatology*, 7, pp.301–311.
Darby, I.A. et al., 2016. The myofibroblast, a key cell in normal and pathological tissue repair. *Cellular and Molecular Life Sciences*, 73(6), pp.1145–1157.
Darlenski, R., Kazandjieva, J. & Tsankov, N., 2011. Skin barrier function: morphological basis and regulatory mechanisms. *Journal of Clinical Medicine*, 4(1), pp.36–45.
Dasu, M.R.K. et al., 2004. Gene expression profiles from hypertrophic scar fibroblasts before and after IL-6 stimulation. *Journal of Pathology*, 202(4), pp.476–485.
Dasu, M.R.K. et al., 2003. Matrix metalloproteinase expression in cytokine stimulated human dermal fibroblasts. *Burns*, 29, pp.527–531.
Dauer, D.J. et al., 2005. Stat3 regulates genes common to both wound healing and cancer. *Oncogene*, 24(21), pp.3397–408.
David-Raoudi, M. et al., 2008. Differential effects of hyaluronan and its fragments on fibroblasts: Relation to wound healing. *Wound Repair and Regeneration*, 16(2), pp.274–287.
Davidson, J.M., 1998. Animal models for wound repair. *Archives of Dermatological Research*, 290(14), pp.S1–S11.
Davison, S.P. et al., 2009. Efficacy of Intralesional 5-Fluorouracil and Triamcinolone in the Treatment of Keloids. *Aesthetic Surgery Journal*, 29(1), pp.40–46.
Davison, S.P. et al., 2006. Ineffective treatment of keloids with interferon alpha-2b. *Plastic and reconstructive surgery*, 117(1), pp.247–252.

Debelle, L. & Tamburro, A.M., 1999. Elastin: Molecular description and function. *International Journal of Biochemistry and Cell Biology*, 31(2), pp.261–272.

Demidova-Rice, T.N., Hamblin, M.R. & Herman, I.M., 2012a. Acute and Impaired Wound Healing: Pathophysiology and Current Methods for Drug Delivery, Part 1: Normal and Chronic Wounds: Biology, Causes, and Approaches to Care. *Adv Skin Wound Care*, 25(7), pp.304–314.

Demidova-Rice, T.N., Hamblin, M.R. & Herman, I.M., 2012b. Acute and Impaired Wound Healing: Pathophysiology and Current Methods for Drug Delivery, Part 2: Role of Growth Factors in Normal and Pathological Wound Healing: Therapeutic Potential and Methods of Delivery. *Adv Skin Wound Care.*, 25(8), pp.349–370.

Denning, M.F., 2004. Epidermal keratinocytes: regulation of multiple cell phenotypes by multiple protein kinase C isoforms. *The international journal of biochemistry & cell biology*, 36(7), pp.1141–1146.

Depianto, D. & Coulombe, P.A., 2004. Intermediate filaments and tissue repair. *Experimental Cell Research*, 301(1), pp.68–76.

Desmoulière, A. et al., 1997. Apoptosis during wound healing, fibrocontractive diseases and vascular wall injury. *International Journal of Biochemistry and Cell Biology*, 29(1), pp.19–30.

Desmoulière, A. et al., 1995. Apoptosis mediates the decrease in cellularity during the transition between granulation tissue and scar. *The American journal of pathology*, 146(1), pp.56–66.

Desmoulière, A. et al., 1993. Transforming growth factor-β1 induces α-smooth muscle actin expression in granulation tissue myofibroblasts and in quiescent and growing cultured fibroblasts. *The Journal of cell biology*, 122(1), pp.103–111.

Desmouliere, A., Chaponnier, C. & Gabbiani, G., 2005. Tissue repair, contraction, and the myofibroblast. *Wound Repair and Regeneration*, 13, pp.7–12.

Deuel, T.F. et al., 1982. Chemotaxis of monocytes and neutrophils to platelet-derived growth factor. *Journal of Clinical Investigation*, 69(4), pp.1046–1049.

Diegelmann, R.. & Evans, M.., 2004. Wound Healing: An Overview of Acute, Fibrotic and Delayed Healing. *Frontiers in Bioscience*, 9, pp.283–289.

ten Dijke, P. & Hill, C.S., 2004. New insights into TGF-β-Smad signalling. *Trends in Biochemical Sciences*, 29(5), pp.265–273.

Dillon, P.W. et al., 1994. The extracellular matrix of the fetal wound: hyaluronic acid controls lymphocyte adhesion. *The Journal of surgical research*, 57(1), pp.170–3.

Ding, J. & Tredget, E.E., 2015. The Role of Chemokines in Fibrotic Wound Healing. *Advances in wound care*, 4(11), pp.673–686.

DiPietro, L. a., 2013. Angiogenesis and scar formation in healing wounds. *Current Opinion in Rheumatology*, 25, pp.87–91.

DiStasi, M.R. & Ley, K., 2009. Opening the flood-gates: how neutrophil-endothelial interactions regulate permeability. *Trends in Immunology*, 30(11), pp.547–556.

Dong, X., Mao, S. & Wen, H., 2013. Upregulation of proinflammatory genes in skin lesions may be the cause of keloid formation. *Biomedical reports*, 1(6), pp.833–836.

Van Doren, S.R., 2015. Matrix metalloproteinase interactions with collagen and elastin. *Matrix biology : journal of the International Society for Matrix Biology*, 44-46(i), pp.224–31.

Dovi, J. V., Szpaderska, A.M. & DiPietro, L.A., 2004. Neutrophil function in the healing wound: Adding insult to injury? *Thrombosis and Haemostasis*, 92(2), pp.275–280.

Dreifke, M.B., Jayasuriya, A.A. & Jayasuriya, A.C., 2015. Current wound healing procedures and potential care. *Materials science & engineering. C, Materials for biological applications*, 48, pp.651–62.

Dumville, J. et al., 2015. Negative pressure wound therapy for treating leg ulcers. *Cochrane Database of Systematic Reviews*, (7), pp.1–36.

Dunn, C. et al., 2002. Molecular mechanism and biological functions of c-Jun N-terminal kinase signalling via the c-Jun transcription factor. *Cellular Signalling*, 14(7), pp.585–593.

Echtermeyer, F. et al., 2001. Delayed wound repair and impaired angiogenesis in mice lacking syndecan-4. *Journal of Clinical Investigation*, 107(2), pp.9–14.

Eckert, R.L. & Rorke, E.A., 1989. Molecular biology of keratinocyte differentiation. *Environmental Health Perspectives*, 80, pp.109–116.

Eckes, B., Nischt, R. & Krieg, T., 2010. Cell-matrix interactions in dermal repair and scarring. *Fibrogenesis & tissue repair*, 3, p.4.
Eckhart, L. et al., 2013. Cell death by cornification. *Biochimica et Biophysica Acta - Molecular Cell Research*, 1833(12), pp.3471–3480.
Edgar, D. et al., 2011. Local and systemic treatments for acute edema after burn injury: a systematic review of the literature. *J Burn Care Res*, 32(2), pp.334–347.
Edmonds, M. et al., 2000. New treatments in ulcer healing and wound infection. *Diabetes/metabolism research and reviews*, 16(Suppl 1), pp.S51–4.
Eferl, R. et al., 2003. Liver tumor development: c-Jun antagonizes the proapoptotic activity of p53. *Cell*, 112(2), pp.181–192.
Ehrlich, H.P. & Moyer, K.E., 2013. Cell-Populated Collagen Lattice Contraction Model for the Investigation of Fibroblast Collagen Interactions. In R. G. Gourdie & T. A. Myers, eds. *Wound Regeneration and Repair: Methods in Molecular Biology*. Humana Press, pp. 45–58.
Elliott, M.R. & Ravichandran, K.S., 2010. Clearance of apoptotic cells: Implications in health and disease. *Journal of Cell Biology*, 189(7), pp.1059–1070.
Elmore, S., 2007. Apoptosis: A Review of Programmed Cell Death. *Toxicol Pathol.*, 35(4), pp.495–516.
Eming, S. et al., 2008. The inhibition of matrix metalloproteinase activity in chronic wounds by a polyacrylate superabsorber. *Biomaterials*, 29(19), pp.2932–2940.
Eming, S. a, Krieg, T. & Davidson, J.M., 2007. Inflammation in wound repair: Molecular and cellular mechanisms. *Journal of Investigative Dermatology*, 127(3), pp.514–525.
Eming, S.A., Martin, P. & Tomic-canic, M., 2014. Wound repair and regeneration: Mechanisms, signaling, and translation. *Science Translational Medicine*, 6(265).
Engelhardt, E. et al., 1998. Chemokines IL-8, GROα, MCP-1, IP-10, and Mig Are Sequentially and Differentially Expressed During Phase-Specific Infiltration of Leukocyte Subsets in Human Wound Healing. *The American Journal of Pathology*, 153(6), pp.1849–1860.
English, R.S. & Shenefelt, P.D., 1999. Keloids and hypertrophic scars. *Dermatologic Surgery*, 25, pp.631–638.
Enoch, S., Peake, M.., et al., 2010. " Young " Oral Fibroblasts Are Geno / Phenotypically Distinct. *Journal of Dental Research*, 89(12), pp.1047–1413.
Enoch, S. et al., 2009. Increased oral fibroblast lifespan is telomerase-independent. *Journal of Dental Research*, 88(10), pp.916–21.
Enoch, S. et al., 2008. The oral mucosa: A model of wound healing with reduced scarring. *Oral Surgery*, 1(1), pp.11–21.
Eto, H. et al., 2012. Therapeutic potential of fibroblast growth factor-2 for hypertrophic scars: upregulation of MMP-1 and HGF expression. *Laboratory Investigation*, 92(2), pp.214–223.
Evans, R.A. et al., 2003. TGF-β1-mediated fibroblast-myofibroblast terminal differentiation - The role of Smad proteins. *Experimental Cell Research*, 282(2), pp.90–100.
Eyden, B., 2008. The myofibroblast in health and disease. *Revista Española de Patología*, 41(1), pp.3–10.
Fadini, G.P. et al., 2014. The molecular signature of impaired diabetic wound healing identifies serpinB3 as a healing biomarker. *Diabetologia*, 57(9), pp.1947–1956.
Falanga, V., 2005. Wound healing and its impairment in the diabetic foot. *Lancet*, 366(9498), pp.1736–1743.
Fan, J. et al., 2006. PKCδ clustering at the leading edge and mediating growth factor-enhanced, but not ecm-initiated, dermal fibroblast migration. *The Journal of investigative dermatology*, 126(6), pp.1233–1243.
Fang, R.C. & Galiano, R.D., 2008. A review of becaplermin gel in the treatment of diabetic neuropathic foot ulcers. *Biologics : targets & therapy*, 2(1), pp.1–12.
De Felice, B. et al., 2009. Differential apoptosis markers in human keloids and hypertrophic scars fibroblasts. *Molecular and Cellular Biochemistry*, 327(1-2), pp.191–201.
Ferguson, M.W.J. & Kane, S.O., 2004. Scar-free healing : from embryonic mechanisms to adult therapeutic intervention. *Phil. Trans. R. Soc. Lond. B*, 359, pp.839–850.
Fernandes, K.J.L. et al., 2004. A dermal niche for multipotent adult skin-derived precursor cells. *Nature Cell Biology*, 6(11), pp.1082–1093.
Feuerherm, A.J. et al., 2013. Platelet-activating factor induces proliferation in differentiated

keratinocytes. *Molecular and cellular biochemistry*, 384(1-2), pp.83–94.
Finch, P.W. et al., 1989. Human KGF is FGF-related with properties of a paracrine effector of epithelial cell growth. *Science (New York, N.Y.)*, 245(4919), pp.752–5.
Fink, S.L. & Cookson, B.T., 2005. Apoptosis, Pyroptosis, and Necrosis: Mechanistic Description of Dead and Dying Eukaryotic Cells. *Infection and Immunity*, 73(4), pp.1907–1916.
Fisher, G.J. et al., 1993. Differential Expression of Protein Kinase C Isoenzymes in Normal and Psoriatic Adult Human Skin: Reduced Expression of Protein Kinase C-βII in Psoriasis. *Journal of Investigative Dermatology*, 101(4), pp.553–559.
Fitsialos, G. et al., 2007. Transcriptional signature of epidermal keratinocytes subjected to in vitro scratch wounding reveals selective roles for ERK1/2, p38, and phosphatidylinositol 3-kinase signaling pathways. *Journal of Biological Chemistry*, 282(20), pp.15090–15102.
Fivenson, D.P. et al., 1997. Chemokine and inflammatory cytokine changes during chronic wound healing. *Wound repair and regeneration : official publication of the Wound Healing Society [and] the European Tissue Repair Society*, 5(4), pp.310–322.
Florin, L. et al., 2004. Identification of novel AP-1 target genes in fibroblasts regulated during cutaneous wound healing. *Oncogene*, 23, pp.7005–7017.
Frank, S. et al., 1995. Regulation of vascular endothelial growth factor expression in cultured keratinocytes: Implications for normal and impaired wound healing. *Journal of Biological Chemistry*, 270(21), pp.12607–12613.
Frank, S., Madlener, M. & Werner, S., 1996. Transforming Growth Factors β1, β2, and β3 and Their Receptors Are Differentially Regulated during Normal and Impaired Wound Healing. *The Journal of Biological Chemistry*, 271(17), pp.10188–10193.
Frantz, C., Stewart, K.M. & Weaver, V.M., 2010. The extracellular matrix at a glance. *Journal of cell science*, 123, pp.4195–4200.
Fraser, J.R., Laurent, T.C. & Laurent, U.B., 1997. Hyaluronan: its nature, distribution, functions and turnover. *Journal of internal medicine*, 242, pp.27–33.
Frazier, K. et al., 1996. Stimulation of fibroblast cell growth, matrix production, and granulation tissue formation by connective tissue growth factor. *The Journal of investigative dermatology*, 107, pp.404–411.
Freedberg, I. et al., 2001. Keratins and the Keratinocyte Activation Cycle. *Journal of Investigative Dermatology*, 116(5), pp.633–640.
Frykberg, R.G. & Banks, J., 2015. Challenges in the Treatment of Chronic Wounds. *Advances in wound care*, 4(9), pp.560–582.
Fu, D.J. et al., 2014. Keratin 9 is required for the structural integrity and terminal differentiation of the palmoplantar epidermis. *The Journal of investigative dermatology*, 134(3), pp.754–63.
Fu, X. et al., 2001. Dedifferentiation of epidermal cells to stem cells in vivo. *The Lancet*, 358, pp.1067–1068.
Fuchs, E., 1995. Keratins and the Skin. *Annu Rev Cell Dev Biol*, 11, pp.123–153.
Fuchs, E., 2007. Scratching the surface of skin development. *Nature*, 445(7130), pp.834–42.
Fuchs, E., 1990. The Bare Essentials Epidermal Differentiation : *The Journal of Cell Biology*, 111(6), pp.2807–2814.
Fujie, H. & Numasaki, M., 2012. Type III Interferons IL-28 and IL-29 : Novel Interferon Family Members with Therapeutic Potential in Cancer Therapy. In H. Arnouk, ed. *Advancements in Tumor Immunotherapy and Cancer Vaccines*. InTech.
Fujiwara, M., Muragaki, Y. & Ooshima, A., 2005. Keloid-derived fibroblasts show increased secretion of factors involved in collagen turnover and depend on matrix metalloproteinase for migration. *British Journal of Dermatology*, 153(2), pp.295–300.
Funayama, E. et al., 2003. Keratinocytes Promote Proliferation and Inhibit Apoptosis of the Underlying Fibroblasts: An Important Role in the Pathogenesis of Keloid. *Journal of Investigative Dermatology*, 121(6), pp.1326–1331.
Gabbiani, G., 1992. The biology of the myofibroblast. *Kidney International*, 41(3), pp.530–532.
Gabbiani, G., 2003. The myofibroblast in wound healing and fibrocontractive diseases. *The Journal of Pathology*, 200(4), pp.500–503.
Gailit, J. & Clark, R.A., 1994. Wound repair in the context of extracellular matrix. *Current Opinion in Cell Biology*, 6, pp.717–725.
Gailit, J., Clark, R.A.F. & Welch, M.P., 1994. TGF-β1 Stimulates Expression of Keratinocyte

Integrins During Re-Epithelialization of Cutaneous Wounds. *Journal of Investigative Dermatology*, 103(2), pp.221–227.
Galdino Jr, H. et al., 2014. Interleukin 32γ (IL-32γ) is highly expressed in cutaneous and mucosal lesions of American Tegumentary Leishmaniasis patients: association with tumor necrosis factor (TNF) and IL-10. *BMC infectious diseases*, 14, p.249.
Gallagher, J.T., Lyon, M. & Steward, W.P., 1986. Structure and function of heparan sulphate proteoglycans. *The Biochemical journal*, 236(2), pp.313–325.
Gallucci, R.M. et al., 2004. Interleukin 6 indirectly induces keratinocyte migration. *Journal of Investigative Dermatology*, 122(3), pp.764–772.
Gao, Y. et al., 2013. Roles of GINS2 in K562 human chronic myelogenous leukemia and NB4 acute promyelocytic leukemia cells. *Int J Mol Med*, 31(6), pp.1402–1410.
Garrod, D.R., 1993. Desmosomes and hemidesmosomes. *Current Opinion in Cell Biology*, 5(1), pp.30–40.
Gartel, A.L. & Tyner, A.L., 2002. The role of the cyclin-dependent kinase inhibitor p21 in apoptosis. *Mol Cancer Ther*, 1(8), pp.639–649.
Gartsbein, M. et al., 2006. The role of protein kinase C δ activation and STAT3 Ser727 phosphorylation in insulin-induced keratinocyte proliferation. *J Cell Sci*, 119(3), pp.470–481.
Gauglitz, G.G. et al., 2011. Hypertrophic scarring and keloids: pathomechanisms and current and emerging treatment strategies. *Molecular medicine (Cambridge, Mass.)*, 17(1-2), pp.113–25.
Gelse, K., Pöschl, E. & Aigner, T., 2003. Collagens—structure, function, and biosynthesis. *Advanced Drug Delivery Reviews*, 55(12), pp.1531–1546.
Geraldes, P. & King, G.L., 2010. Activation of protein kinase C isoforms and its impact on diabetic complications. *Circulation Research*, 106(8), pp.1319–1331.
Ghatak, S. et al., 2015. Roles of Proteoglycans and Glycosaminoglycans in Wound Healing and Fibrosis. *International Journal of Cell Biology*, 2015.
Ghohestani, R.F. et al., 2003. Crescentic glomerulonephritis and subepidermal blisters with autoantibodies to α5 and α6 chains of type IV collagen. *Lab Invest*, 83(5), pp.605–611.
Ghohestani, R.F. et al., 2000. The α5 chain of type IV collagen is the target of IgG autoantibodies in a novel autoimmune disease with subepidermal blisters and renal insufficiency. *Journal of Biological Chemistry*, 275(21), pp.16002–16006.
Gilcrease, M.Z., 2007. Integrin signaling in epithelial cells. *Cancer Letters*, 247, pp.1–25.
Giles, N. et al., 2008. A peptide inhibitor of c-Jun promotes wound healing in a mouse full-thickness burn model. *Wound Repair and Regeneration*, 16(1), pp.58–64.
Gill, S.E. & Parks, W.C., 2008. Metalloproteinases and their inhibitors: regulators of wound healing. *The international journal of biochemistry & cell biology*, 40(6-7), pp.1334–47.
Gillitzer, R. & Goebeler, M., 2001. Chemokines in cutaneous wound healing. *Journal of Leukocyte Biology*, 69(4), pp.513–521.
Glenisson, W., Castronovo, V. & Waltregny, D., 2007. Histone deacetylase 4 is required for TGFβ1-induced myofibroblastic differentiation. *Biochimica et Biophysica Acta - Molecular Cell Research*, 1773(10), pp.1572–1582.
Glim, J.E. et al., 2013. Detrimental dermal wound healing: What can we learn from the oral mucosa? *Wound Repair and Regeneration*, 21(5), pp.648–660.
Glim, J.E. et al., 2014. Extracellular matrix components of oral mucosa differ from skin and resemble that of foetal skin. *Archives of Oral Biology*, 59(10), pp.1048–1055.
Glim, J.E. et al., 2015. The number of immune cells is lower in healthy oral mucosa compared to skin and does not increase after scarring. *Archives of Oral Biology*, 60(2), pp.272–281.
Gold, M.H. et al., 2014. Updated international clinical recommendations on scar management: part 2--algorithms for scar prevention and treatment. *Dermatologic Surgery*, 40(8), pp.825–31.
Goldman, R., 2004. Growth factors and chronic wound healing: past, present, and future. *Advances in skin & wound care*, 17, pp.24–35.
Gong, D. & Ferrell, J.E., 2010. The Roles of Cyclin A2, B1, and B2 in Early and Late Mitotic Events. *Molecular Biology of the Cell*, 21, pp.3149–3161.
Gordon, M.K. & Hahn, R.A., 2011. Collagens. *Cell and Tissue Research*, 339(1), pp.247–257.
Gorecki, C. et al., 2009. Impact of pressure ulcers on quality of life in older patients: A systematic review: Clinical investigations. *Journal of the American Geriatrics Society*, 57(7), pp.1175–

1183.
Gorres, K.L. & Raines, R.T., 2010. *Prolyl 4-Hydroxylase*,
Gosain, A. & DiPietro, L.A., 2004. Aging and Wound Healing. *World Journal of Surgery*, 28(3), pp.321–326.
Graff, J.R. et al., 2005. The protein kinase Cβ-selective inhibitor, Enzastaurin (LY317615.HCl), suppresses signaling through the AKT pathway, induces apoptosis, and suppresses growth of human colon cancer and glioblastoma xenografts. *Cancer Research*, 65(16), pp.7462–7469.
Gragnani, A. et al., 2013. Keratinocyte growth factor, tumor necrosis factor-alpha and interleukin-1 beta gene expression in cultured fibroblasts and keratinocytes from burned patients. *Acta Cirúrgica Brasileira*, 28(8), pp.551–558. Available at: http://www.scielo.br/scielo.php?pid=S0102-86502013000800001&script=sci_arttext.
Grandis, J.R. et al., 2000. Constitutive activation of Stat3 signaling abrogates apoptosis in squamous cell carcinogenesis in vivo. *Proceedings of the National Academy of Sciences of the United States of America*, 97(8), pp.4227–4232.
Gras, M.P. et al., 2001. Downregulation of human type VII collagen (COL7A1) promoter activity by dexamethasone. Identification of a glucocorticoid receptor binding region. *Experimental dermatology*, 10(1), pp.28–34.
Graves, D.T., Wu, Y. & Badadani, M., 2014. Pyk2 contributes to reepithelialization by promoting MMP expression. Focus on "Delayed skin wound repair in proline-rich protein tyrosine kinase 2 knockout mice". *American journal of physiology. Cell physiology*, 306(10), pp.C887–8.
Greenhalgh, D.G. et al., 1990. PDGF and FGF stimulate wound healing in the genetically diabetic mouse. *The American journal of pathology*, 136(6), pp.1235–1246.
Greenhalgh, D.G., 1998. The role of apoptosis in wound healing. *The International Journal of Biochemistry & Cell Biology*, 30(9), pp.1019–1030.
Greiling, D. & Clark, R. a, 1997. Fibronectin provides a conduit for fibroblast transmigration from collagenous stroma into fibrin clot provisional matrix. *Journal of cell science*, 110(Pt 7), pp.861–870.
Grinnell, F., 1994. Fibroblasts, Myofibroblasts, and Wound Contraction. *The Journal of Cell Biology*, 124(4), pp.401–404.
Grinnell, F., 1992. Wound repair, keratinocyte activation and integrin modulation. *Journal of cell science*, 101(Pt 1), pp.1–5.
Grøndahl-Hansen, J. et al., 1988. Urokinase- and Tissue-Type Plasminogen Activators in Keratinocytes During Wound Reepithelialization In Vivo. *Journal of Investigative Dermatology*, 90, pp.790–795.
Grose, R. et al., 2002. A crucial role of beta 1 integrins for keratinocyte migration in vitro and during cutaneous wound repair. *Development*, 129(9), pp.2303–2315.
Gross, S.R. et al., 2014. Joining S100 proteins and migration: For better or for worse, in sickness and in health. *Cellular and Molecular Life Sciences*, 71(9), pp.1551–1579.
Gu, L.H. & Coulombe, P.A., 2007. Keratin function in skin epithelia: a broadening palette with surprising shades. *Current Opinion in Cell Biology*, 19(1), pp.13–23.
Gudmundsdottir, A.S. et al., 1999. Is an epitope on keratin 17 a major target for autoreactive T lymphocytes in psoriasis? *Clinical and Experimental Immunology*, 117(3), pp.580–586.
Guest, J.F. et al., 2016. Health economic burden that different wound types impose on the UK's National Health Service. *International Wound Journal*, Epub ahead.
Guest, J.F. et al., 2015. Health economic burden that wounds impose on the National Health Service in the UK. *BMJ open*, 5(12), p.e009283.
Guilloteau, K. et al., 2010. Skin Inflammation Induced by the Synergistic Action of IL-17A, IL-22, Oncostatin M, IL-1{alpha}, and TNF-{alpha} Recapitulates Some Features of Psoriasis. *Journal of immunology*, 184, pp.5263–5270.
Guimond, S.E. & Turnbull, J.E., 1999. Fibroblast growth factor receptor signalling is dictated by specific heparan sulphate saccharides. *Current Biology*, 9, pp.1343–1346.
Guo, L., Yu, Q.C. & Fuchs, E., 1993. Targeting expression of keratinocyte growth factor to keratinocytes elicits striking changes in epithelial differentiation in transgenic mice. *The EMBO journal*, 12(3), pp.973–86.
Guo, S. & DiPietro, L.A., 2010. Factors affecting wound healing. *Journal of Dental Research*,

89(3), pp.219–29.
Guo, W. et al., 2009. Abrogation of TGF-β1-induced fibroblast-myofibroblast differentiation by histone deacetylase inhibition. *Am J Physiol Lung Cell Mol Physiol.*, 297(5), pp.L864–L870.
Gurtner, G.C. et al., 2008. Wound repair and regeneration. *Nature*, 453, pp.314–321.
Haake, A., Scott, G. & Holbrook, K., 2001. Structure and function of the skin: overview of the epidermis and dermis. In R. Freinkel & W. DT, eds. *The Biology of the Skin*. The Parthenon Publishing Group Limited, pp. 19–45.
Haase, I. et al., 2003. Regulation of keratinocyte shape, migration and wound epithelialization by IGF-1- and EGF-dependent signalling pathways. *Journal of cell science*, 116(15), pp.3227–3238.
Van Haastert, P.J.M. & Devreotes, P.N., 2004. Chemotaxis: signalling the way forward. *Nature reviews. Molecular cell biology*, 5(8), pp.626–634.
Hahn, J.M. et al., 2013. Keloid-derived keratinocytes exhibit an abnormal gene expression profile consistent with a distinct causal role in keloid pathology. *Wound Repair and Regeneration*, 21(4), pp.530–544.
Häkkinen, L., Larjava, H. & Koivisto, L., 2011. Granulation tissue formation and remodeling. *Endodontic Topics*, 24(1), pp.94–129.
Hall, C.L. et al., 1995. Overexpression of the hyaluronan receptor RHAMM is transforming and is also required for H-ras transformation. *Cell*, 82(1), pp.19–28.
Hallock, G.G., 1999. The Cosmetic Split-Thickness Skin Graft Donor Site. *Plastic and reconstructive surgery*, 104(7), pp.2286–2288.
Hameedaldeen, A. et al., 2014. FOXO1, TGF-β regulation and wound healing. *International journal of molecular sciences*, 15(9), pp.16257–69.
Hamill, K.J., Paller, A.S. & Jones, J.C.R., 2010. Adhesion and Migration, the Diverse Functions of the Laminin α3 Subunit. *Dermatol Clin*, 28(1), pp.1–12.
Hampson, P. et al., 2010. Kinetics of ERK1/2 activation determine sensitivity of acute myeloid leukaemia cells to the induction of apoptosis by the novel small molecule ingenol 3-angelate (PEP005). *Apoptosis*, 15(8), pp.946–955.
Han, Y.-P., Yan, C. & Garner, W.L., 2012. Proteolytic Activation of Matrix Metalloproteinase-9 in Skin Wound Healing Is Inhibited by α-1-Antichymotrypsin. *Journal of investigative dermatology*, 29(6), pp.997–1003.
Hanahan, D. & Weinberg, R.A., 2011. Hallmarks of cancer: The next generation. *Cell*, 144(5), pp.646–674.
Hao, Z., Zhang, H. & Cowell, J., 2012. Ubiquitin-conjugating enzyme UBE2C: molecular biology, role in tumorigenesis, and potential as a biomarker. *Tumour biology : the journal of the International Society for Oncodevelopmental Biology and Medicine*, 33(3), pp.723–30.
Harding, K., 2015. Innovation and wound healing. *Journal of wound care*, 24(4), pp.7–13.
Hardwicke, J. et al., 2010. Bioresponsive Dextrin - rhEGF Conjugates: In Vitro Evaluation in Models Relevant to Its Proposed Use as a Treatment for Chronic Wounds. *Molecular Pharmaceuticals*, 7(3), pp.699–707.
Hardwicke, J. et al., 2008. Dextrin – rhEGF conjugates as bioresponsive nanomedicines for wound repair. *Journal of Controlled Release*, 130, pp.275–283.
Harris, P.A., 1998. Pre-confluent keratinocyte grafting: The future for cultured skin replacements? *Burns*, 24, pp.591–593.
Harrison, C. a et al., 2005. Antagonists of activin signaling: mechanisms and potential biological applications. *Trends in endocrinology and metabolism: TEM*, 16(2), pp.73–78.
Har-Shai, Y., Amar, M. & Sabo, E., 2003. Intralesional cryotherapy for enhancing the involution of hypertrophic scars and keloids. *Plastic and reconstructive surgery*, 111, pp.1841–1852.
Hasegawa, H. et al., 2007. The distributions of type IV collagen α chains in basement membranes of human epidermis and skin appendages. *Arch Histol Cytol*, 70(4), pp.255–265.
Hashimoto, K., 2000. Regulation of keratinocyte function by growth factors. *Journal of Dermatological Science*, 24, pp.S46–S50.
Hattinger, E. et al., 2013. Opposing functions of psoriasin (S100A7) and koebnerisin (S100A15) in epithelial carcinogenesis. *Current Opinion in Pharmacology*, 13(4), pp.588–594.
Hattori, N. et al., 2009. MMP-13 Plays a Role in Keratinocyte Migration, Angiogenesis, and Contraction in Mouse Skin Wound Healing. *The American Journal of Pathology*, 175(2),

pp.533–546.
Haukipuro, K. et al., 1991. Synthesis of type I collagen in healing wounds in humans. *Annals of surgery*, 213, pp.75–80.
Hause, R.J. et al., 2014. Identification and validation of genetic variants that influence transcription factor and cell signaling protein levels. *American Journal of Human Genetics*, 95(2), pp.194–208.
Hauser, P.J. et al., 1998. STAT3 Activation Accompanies Keratinocyte Differentiation. *Cell Growth & Differentiation*, 9(October), pp.847–855.
Hayflick, L., 1965. The limited in vitro lifetime of human diploid cell strains. *Experimental Cell Research*, 37(3), pp.614–636.
He, X. et al., 2015. Upregulation of hyaluronan-mediated motility receptor in hepatocellular carcinoma predicts poor survival. *Oncology Letters*, 10(6), pp.3639–3646.
Hedqvist, P.E.R., Gautam, N. & Lindbom, L., 2000. Interactions between Leukotrienes and Other Inflammatory Mediators / Modulators in the Microvasculature. *Am J Respir Crit Care Med*, 161, pp.117–119.
Heeg, M.H.J. et al., 2005. The antifibrotic effects of relaxin in human renal fibroblasts are mediated in part by inhibition of the Smad2 pathway. *Kidney International*, 68(1), pp.96–109.
Heinhuis, B. et al., 2011. Inflammation-dependent secretion and splicing of IL-32γ in rheumatoid arthritis. *Proceedings of the National Academy of Sciences of the United States of America*, 108(12), pp.4962–7.
Heino, J., 2007. The collagen family members as cell adhesion proteins. *BioEssays: news and reviews in molecular, cellular and developmental biology*, 29(10), pp.1001–10.
Heldin, C.H., Miyazono, K. & ten Dijke, P., 1997. TGF-β signalling from cell membrane to nucleus through SMAD proteins. *Nature*, 390(6659), pp.465–71.
Heldin, C.H. & Westermark, B., 1999. Mechanism of action and in vivo role of platelet-derived growth factor. *Physiological reviews*, 79(4), pp.1283–1316.
Heldin, P. et al., 2013. Deregulation of hyaluronan synthesis, degradation and binding promotes breast cancer. *Journal of Biochemistry*, 154(5), pp.395–408.
Helmo, F.R. et al., 2013. Fetal wound healing biomarkers. *Disease Markers*, 35(6), pp.939–944.
Henderson, J., Terenghi, G. & Ferguson, M.W.J., 2011. The reinnervation and revascularisation pattern of scarless murine fetal wounds. *Journal of Anatomy*, 218(6), pp.660–667.
Hernández-Quintero, M. et al., 2006. Interleukin-6 promotes human epidermal keratinocyte proliferation and keratin cytoskeleton reorganization in culture. *Cell and Tissue Research*, 325(1), pp.77–90.
Hibino, T. et al., 1999. Suppression of keratinocyte proliferation by plasminogen activator inhibitor-2. *Journal of Investigative Dermatology*, 112(1), pp.85–90.
Hinz, B., 2007. Formation and function of the myofibroblast during tissue repair. *The Journal of investigative dermatology*, 127(3), pp.526–37.
Hinz, B. et al., 2001. Mechanical tension controls granulation tissue contractile activity and myofibroblast differentiation. *The American journal of pathology*, 159(3), pp.1009–20.
Hinz, B. et al., 2012. Recent developments in myofibroblast biology: Paradigms for connective tissue remodeling. *American Journal of Pathology*, 180(4), pp.1340–1355.
Hinz, B. et al., 2007. The Myofibroblast. *The American Journal of Pathology*, 170(6), pp.1807–1816.
Hobbs, R.P., Lessard, J.C. & Coulombe, P. a, 2012. Keratin intermediate filament proteins - novel regulators of inflammation and immunity in skin. *Journal of cell science*, 125(Pt 22), pp.5257–8.
Hochegger, H., Takeda, S. & Hunt, T., 2008. Cyclin-dependent kinases and cell-cycle transitions: does one fit all? *Nature reviews. Molecular cell biology*, 9(11), pp.910–916.
Hoffman, M. et al., 1995. Factors IXa and Xa play distinct roles in tissue factor-dependent initiation of coagulation. *Blood*, 86(5), pp.1794–1801.
Hoffmann, A. et al., 2012. Role of Hyaluronic Acid Treatment in the Prevention of Keloid Scarring. *The Journal of the American College of Clinical Wound Specialists*, 4(2), pp.23–31.
Hoffmann, D.C. et al., 2011. Pivotal role for α1-antichymotrypsin in skin repair. *Journal of Biological Chemistry*, 286(33), pp.28889–28901.
Holmes, C. et al., 2013. Collagen-based wound dressings for the treatment of diabetes-related foot

ulcers: A systematic review. *Diabetes, Metabolic Syndrome and Obesity: Targets and Therapy*, 6, pp.17–29.
Howard, J.D. et al., 2014. Rapid granulation tissue regeneration by intracellular ATP delivery - A comparison with Regranex. *PLoS ONE*, 9(3), pp.1–14.
Hu, M.S. et al., 2014. Gene expression in fetal murine keratinocytes and fibroblasts. *Journal of Surgical Research*, 190(1), pp.344–357.
Huang, C. et al., 2013. Keloids and Hypertrophic Scars. *Plastic and Reconstructive Surgery Global Open*, 1(4), p.e25.
Huang, C., Jacobson, K. & Schaller, M.D., 2004. MAP kinases and cell migration. *Journal of cell science*, 117(Pt 20), pp.4619–28.
Huang, F. et al., 2015. IL-32B is the predominant isoform expressed under inflammatory conditions in vitro and in COPD. *COPD Research and Practice*, pp.1–11.
Huang, L., Gu, H. & Burd, A., 2008. A reappraisal of the biological effects of hyaluronan on human dermal fibroblast. *Journal of Biomedical Materials Research - Part A*, 90(4), pp.1177–1185.
Huang, L.P. et al., 2015. Screening of differentially expressed genes in pathological scar tissues using expression microarray. *Genetics and Molecular Research*, 14(3), pp.10743–10751.
Huang, Y., Sramkoski, R.M. & Jacobberger, J.W., 2013. The kinetics of G2 and M transitions regulated by B cyclins. *PLoS ONE*, 8(12), pp.30–35.
Hubmacher, D. & Apte, S.S., 2013. The biology of the extracellular matrix: novel insights. *Current opinion in rheumatology*, 25(1), pp.65–70.
Hübner, G. et al., 1996. Differential regulation of pro-inflammatory cytokines during wound healing in normal and glucocorticoid-treated mice. *Cytokine*, 8(7), pp.548–56.
Hudson, B.G., Reeders, S. & Tryggvason, K., 1993. Type IV Collagen: Structure, Gene Organization, and Role in Human Diseases. *Journal of Biological Chemistry*, 238(35), pp.26003–036.
Humphries, J.D., Byron, A. & Humphries, M.J., 2006. Integrin ligands at a glance. *Cell Science at a Glance*, 119, pp.3901–3903.
Igarashi, A. et al., 1993. Regulation of connective tissue growth factor gene expression in human skin fibroblasts and during wound repair. *Molecular biology of the cell*, 4(6), pp.637–45.
Igyarto, B.Z. & Kaplan, D.H., 2013. Antigen presentation by Langerhans cells. *Current Opinion in Immunology*, 25(1), pp.115–119.
Imaizumi, R. et al., 2009. Promoted activation of matrix metalloproteinase (MMP)-2 in keloid fibroblasts and increased expression of MMP-2 in collagen bundle regions: Implications for mechanisms of keloid progression. *Histopathology*, 54(6), pp.722–730.
Inman, G.J., Nicolás, F.J. & Hill, C.S., 2002. Nucleocytoplasmic shuttling of Smads 2, 3, and 4 permits sensing of TGF-beta receptor activity. *Molecular cell*, 10, pp.283–294.
Iozzo, R. V & Proteoglycans, L., 1999. The Biology of the Small Leucine-rich Proteoglycans. *The Journal of Biological Chemistry*, 274(27), pp.18843–18846.
Iozzo, R. V., 1998. Matrix Proteoglycans: From Molecular Design to Cellular Function. *Annual Review of Biochemistry*, 67(1), pp.609–652.
Isaac, A.L., Rose, J. & Armstrong, D.G., 2014. Mechanically powered negative pressure wound therapy as a bolster for skin grafting. *Plastic and reconstructive surgery*, 2(2), p.e103.
Ismail, A. & Yusuf, N., 2014. Type i interferons: Key players in normal skin and select cutaneous malignancies. *Dermatology Research and Practice*, 2014.
Izaguirre, G. et al., 2013. Identification of serpin determinants of specificity and selectivity for furin inhibition through studies of α1PDX (α1-protease inhibitor portland)-serpin B8 and furin active-site loop chimeras. *Journal of Biological Chemistry*, 288(30), pp.21802–21814.
Janciauskiene, S., 2001. Conformational properties of serine proteinase inhibitors (serpins) confer multiple pathophysiological roles. *Biochimica et Biophysica Acta - Molecular Basis of Disease*, 1535(3), pp.221–235.
Jang, S. et al., 2010. Role of plasminogen activator inhibitor-2 (PAI-2) in keratinocyte differentiation. *Journal of Dermatological Science*, 59(1), pp.25–30.
Javelaud, D. & Mauviel, A., 2004. Mammalian transforming growth factor-βs: Smad signaling and physio-pathological roles. *International Journal of Biochemistry and Cell Biology*, 36(7), pp.1161–1165.
Jenkins, R.H. et al., 2004. Myofibroblastic differentiation leads to hyaluronan accumulation

through reduced hyaluronan turnover. *Journal of Biological Chemistry*, 279(40), pp.41453–41460.
Jensen, P.J. & Lavker, R.M., 1996. Modulation of the plasminogen activator cascade during enhanced epidermal proliferation in vivo. *Cell growth & differentiation : the molecular biology journal of the American Association for Cancer Research*, 7(12), pp.1793–804.
Jiang, C.K. et al., 1993. Epidermal growth factor and transforming growth factor alpha specifically induce the activation- and hyperproliferation-associated keratins 6 and 16. *Proceedings of the National Academy of Sciences*, 90(14), pp.6786–6790.
Jiang, W.G. et al., 2012. Influence of interleukin-8 (IL-8) and IL-8 receptors on the migration of human keratinocytes, the role of plc-γ and potential clinical implications. *Experimental and Therapeutic Medicine*, 3(2), pp.231–236.
Jin, L. & Wang, G., 2014. Keratin 17: a critical player in the pathogenesis of psoriasis. *Medicinal Research Reviews*, 34(2), pp.438–454.
Jin, R. et al., 2013. Laser therapy for prevention and treatment of pathologic excessive scars. *Plastic and reconstructive surgery*, 132(6), pp.1747–58.
Jin, T. et al., 2015. A novel collagen gel-based measurement technique for quantitation of cell contraction force. *Journal of The Royal Society Interface*, 12(106), p.20141365.
Jinnin, M. et al., 2005. Regulation of fibrogenic/fibrolytic genes by platelet-derived growth factor C, a novel growth factor, in human dermal fibroblasts. *Journal of Cellular Physiology*, 202(2), pp.510–517.
Johnson, K.E. & Wilgus, T.A., 2014. Vascular Endothelial Growth Factor and Angiogenesis in the Regulation of Cutaneous Wound Repair. *Advances in wound care*, 3(10), pp.647–661.
Jones, C.D. et al., 2015. The Use of Chemotherapeutics for the Treatment of Keloid Scars. *Dermatology reports*, 7(5880), pp.15–19.
Jones, S.G., Edwards, R. & David, W., 2004. Inflammation and Wound Healing : The Role of Bacteria in the Immuno-Regulation. *Lower Extremity Wounds*, 3(4), pp.201–208.
Joo, C.K. & Seomun, Y., 2008. Matrix metalloproteinase (MMP) and TGFβ1-stimulated cell migration in skin and cornea wound healing. *Cell adhesion & migration*, 2(4), pp.252–253.
Jumper, N., Paus, R. & Bayat, A., 2015. Functional histopathology of keloid disease. *Histology and Histopathology*, 30(9), pp.1033–1057.
Kaibuchi, K., Kuroda, S. & Amano, M., 1999. Regulation of the Cytoskeleton and Cell Adhesion by the Rho Family GTPases in Mammalian Cells. *Annu. Rev. Biochem.*, 68, pp.459–486.
Kajanne, R. et al., 2007. EGF-R Regulates MMP Function in Fibroblasts Through MAPK and AP-1 Pathways. *Journal of cellular physiology*, 212, pp.489–197.
Kalinin, A.E., Kajava, A. V. & Steinert, P.M., 2002. Epithelial barrier function: Assembly and structural features of the cornified cell envelope. *BioEssays*, 24(9), pp.789–800.
Kallioinen, M. et al., 1995. Expression of cytokeratins in regenerating human epidermis. *British Journal of Dermatology*, 9, pp.830–835.
Kanangat, S. et al., 2006. Induction of multiple matrix metalloproteinases in human dermal and synovial fibroblasts by Staphylococcus aureus: implications in the pathogenesis of septic arthritis and other soft tissue infections. *Arthritis research & therapy*, 8(6), p.R176.
Kandasamy, R., Karumbayaram, S. & Packianathan, N., 2011. Hypertrophic Scar Management with a Flavonoid Fraction of Cyphomandra betacea. *Functional Plant Science and Biotechnology*, pp.4–6.
Kao, H.-K. et al., 2011. Peripheral Blood Fibrocytes. *Annals of surgery*, 254(6), pp.1066–1074.
Kappelmann, M., Bosserhoff, A. & Kuphal, S., 2014. AP-1/c-Jun transcription factors: Regulation and function in malignant melanoma. *European Journal of Cell Biology*, 93(1-2), pp.76–81.
Kassim, S.Y. et al., 2007. Individual matrix metalloproteinases control distinct transcriptional responses in airway epithelial cells infected with Pseudomonas aeruginosa. *Infection and Immunity*, 75(12), pp.5640–5650.
Kasuya, A. & Tokura, Y., 2014. Attempts to accelerate wound healing. *Journal of Dermatological Science*, 76(3), pp.169–172.
Katagiri, C. et al., 2006. Serpin squamous cell carcinoma antigen inhibits UV-induced apoptosis via suppression of c-JUN NH2-terminal kinase. *Journal of Cell Biology*, 172(7), pp.983–990.
Katagiri, C. et al., 2010. Up-regulation of serpin SCCA1 is associated with epidermal barrier disruption. *Journal of Dermatological Science*, 57(2), pp.95–101.

Kelly, D.J. et al., 2003. Protein kinase C beta inhibition attenuates the progression of experimental diabetic nephropathy in the presence of continued hypertension. *Diabetes*, 52(2), pp.512–8.
Kelsh, R.M., McKeown-Longo, P.J. & Clark, R.A.F., 2015. EDA Fibronectin in Keloids Create a Vicious Cycle of Fibrotic Tumor Formation. *Journal of Investigative Dermatology*, 135(7), pp.1714–1718.
Khamaisi, M. et al., 2016. PKC inhibition normalizes the wound-healing capacity of diabetic human fibroblasts. *Journal of Clinical Investigation*, 126(3), pp.837–853.
Khoshnoodi, J., Pedchenko, V. & Hudson, B.G., 2008. Mammalian Collagen IV. *Microsc Res Tech*, 71(5), pp.357–370.
Kielty, C.M., Sherratt, M.J. & Shuttleworth, C.A., 2002. Elastic fibres. *Journal of cell science*, 115(Pt 14), pp.2817–2828.
Kim, D.H. & Wirtz, D., 2013. Focal adhesion size uniquely predicts cell migration. *FASEB Journal*, 27(4), pp.1351–1361.
Kim, H.S. et al., 2013. Inducing re-epithelialization in skin wound through cultured oral mucosal keratinocytes. *Journal of the Korean Association of Oral and Maxillofacial Surgeons*, 39(2), pp.63–70.
Kim, J. et al., 1992. Integrin receptors and RGD sequences in human keratinocyte migration: unique anti-migratory function of alpha 3 beta 1 epiligrin receptor. *Journal of Investigative Dermatology*, 98, pp.764–770.
Kim, S.H., Turnbull, J. & Guimond, S., 2011. Extracellular matrix and cell signalling: The dynamic cooperation of integrin, proteoglycan and growth factor receptor. *Journal of Endocrinology*, 209(2), pp.139–151.
Kira, M. et al., 2002. STAT3 deficiency in keratinocytes leads to compromised cell migration through hyperphosphorylation of p130cas. *Journal of Biological Chemistry*, 277(15), pp.12931–12936.
Kirby, M., 2007. Negative pressure wound therapy. *The British Journal of Diabetes and Vascular Disease*, 7, pp.230–234.
Kischer, C.W., Shetlar, M.R. & Shetlar, C.L., 1975. Alteration of hypertrophic scars induced by mechanical pressure. *Archives of dermatology*, 111(1), pp.60–4.
Kishi, K. et al., 2012. Fetal skin possesses the ability to regenerate completely: Complete regeneration of skin. *Keio Journal of Medicine*, 61(4), pp.101–108.
Kisseleva, T. & Brenner, D. a, 2008. Mechanisms of fibrogenesis. *Experimental biology and medicine (Maywood, N.J.)*, 233(2), pp.109–22.
Kjeuin, L. & Lindahl, U., 1991. Proteoglycans: Structures and Interactions. *Annual Review of Biochemistry*, 60, pp.443–475.
Klingelhöfer, J. et al., 2009. Epidermal growth factor receptor ligands as new extracellular targets for the metastasis-promoting S100A4 protein. *The FEBS journal*, 276(20), pp.5936–48.
Knottenbelt, D.C., 2005. A suggested clinical classification for the equine sarcoid. *Clinical Techniques in Equine Practice*, 4(4), pp.278–295.
Köck, A. et al., 1990. Human keratinocytes are a source for tumor necrosis factor alpha: evidence for synthesis and release upon stimulation with endotoxin or ultraviolet light. *The Journal of experimental medicine*, 172(6), pp.1609–14.
Koh, T.J. & DiPietro, L.A., 2011. Inflammation and wound healing: the role of the macrophage. *Expert reviews in molecular medicine*, 13(e23), pp.1–12.
Koivisto, L., Häkkinen, L. & Larjava, H., 2012. Re-epithelialization of wounds. *Endodontic Topics*, 24, pp.59–93.
Koivunen, J. et al., 2004. Protein kinase C alpha/beta inhibitor Go6976 promotes formation of cell junctions and inhibits invasion of urinary bladder carcinoma cells. *Cancer research*, 64(16), pp.5693–701.
Kolega, J., Janson, L.W. & Taylor, D.L., 1991. The role of solation-contraction coupling in regulating stress fiber dynamics in nonmuscle cells. *Journal of Cell Biology*, 114(5), pp.993–1003.
Koljonen, V. et al., 2006. Cell cycle control by p21, p27 and p53 in Merkel cell carcinoma. *Anticancer Research*, 26(3 B), pp.2209–2212.
Koller, R. et al., 2002. The use of allogeneic cultivated keratinocytes for the early coverage of deep dermal burns - Indications, results and problems. *Cell and Tissue Banking*, 3(1), pp.11–14.

Komine, M. et al., 2000. Inflammatory versus proliferative processes epidermis. Tumor necrosis factor α induces K6b keratin synthesis through a transcriptional complex containing NFκB and C/EBPβ. *Journal of Biological Chemistry*, 275(41), pp.32077–32088.
Komine, M. et al., 2001. Interleukin-1 induces transcription of keratin K6 in human epidermal keratinocytes. *Journal of Investigative Dermatology*, 116(2), pp.330–338.
Kondo, T. & Ishida, Y., 2010. Molecular pathology of wound healing. *Forensic Science International*, 203(1-3), pp.93–98.
Kontochristopoulos, G. et al., 2005. Intralesional 5-fluorouracil in the treatment of keloids: an open clinical and histopathologic study. *Journal of the American Academy of Dermatology*, 52(3 Pt 1), pp.474–9.
Koppel, A.C. et al., 2014. Delayed skin wound repair in proline-rich protein tyrosine kinase 2 knockout mice. *American journal of physiology. Cell physiology*, 306(10), pp.C899–909.
Korang, K. et al., 1995. Differential cytokine modulation of the genes LAMA3, LAMB3, and LAMC2, encoding the constitutive polypeptides, α3, β3, and γ2, of human laminin 5 in epidermal keratinocytes. *FEBS Letters*, 368(3), pp.556–558.
Kovacs, D. et al., 2009. Keratinocyte growth factor down-regulates intracellular ROS production induced by UVB. *Journal of Dermatological Science*, 54(2), pp.106–113.
Koyama, S. et al., 2002. Vascular endothelial growth factor mRNA and protein expression in airway epithelial cell lines in vitro. *European Respiratory Journal*, 20(6), pp.1449–1456.
Kramer, N. et al., 2013. In vitro cell migration and invasion assays. *Mutation Research*, 752, pp.10–24.
Krampert, M. et al., 2004. Activities of the Matrix Metalloproteinase Stromelysin-2 (MMP-10) in Matrix Degradation and Keratinocyte Organization in Wounded Skin. *Molecular biology of the cell*, 15, pp.5242–5254.
Krause, M. & Gautreau, A., 2014. Steering cell migration: lamellipodium dynamics and the regulation of directional persistence. *Nature Reviews Molecular Cell Biology*, 15(9), pp.577–590.
Kretzschmar, M. & Massague, J., 1998. SMADs : mediators and regulators of TGF-β signaling. *Current Opinion in Genetics & Development*, 8, pp.103–111.
Krieg, T. & Aumailley, M., 2011. The extracellular matrix of the dermis: Flexible structures with dynamic functions. *Experimental Dermatology*, 20(8), pp.689–695.
Krishnaswamy, V.R. & Korrapati, P.S., 2014. Role of dermatopontin in re-epithelialization: implications on keratinocyte migration and proliferation. *Scientific reports*, 4, p.7385.
Kroeze, K.L. et al., 2012. Autocrine Regulation of Re-Epithelialization After Wounding by Chemokine Receptors CCR1, CCR10, CXCR1, CXCR2, and CXCR3. *Journal of Investigative Dermatology*, 132(1), pp.216–225.
Kumar, A. et al., 1997. Defective TNF-alpha-induced apoptosis in STAT1-null cells due to low constitutive levels of caspases. *Science*, 278(5343), pp.1630–1632.
Kupper, T.S., 1990. Immune and Inflammatory Processes in Cutaneous Tissues. *J.Clin.Invest.*, 86, pp.1783–1789.
Kwiatkowski, A. V., Gertler, F.B. & Loureiro, J.J., 2003. Function and regulation of Ena/VASP proteins. *Trends in Cell Biology*, 13(7), pp.386–392.
Lacci, K.M. & Dardik, A., 2010. Platelet-rich plasma: support for its use in wound healing. *The Yale journal of biology and medicine*, 83(1), pp.1–9.
Ladin, D.A. et al., 1998. P53 and Apoptosis Alterations in Keloids and Keloid Fibroblasts. *Wound Repair Regen*, 6(1), pp.28–37.
Lafuma, C. et al., 1994. Expression of 72-kDa gelatinase (MMP-2), collagenase (MMP-1), and tissue metalloproteinase inhibitor (TIMP) in primary pig skin fibroblast cultures derived from radiation-induced skin fibrosis. *The Journal of investigative dermatology*, 102(6), pp.945–50.
Larjava, H. et al., 1993. Expression of integrins and basement membrane components by wound keratinocytes. *Journal of Clinical Investigation*, 92(3), pp.1425–1435.
Larson, B.J., Longaker, M.T. & Lorenz, H.P., 2010. Scarless fetal wound healing: a basic science review. *Plastic and reconstructive surgery*, 126(4), pp.1172–80.
Larsson, C., 2006. Protein kinase C and the regulation of the actin cytoskeleton. *Cellular Signalling*, 18(3), pp.276–284.

Lauffenburger, D.A. & Horwitz, A.F., 1996. Cell Migration: A Physically Integrated Molecular Process. *Cell*, 84(3), pp.359–369.
Laurent, T.C., Laurent, U.B. & Fraser, J.R., 1995. Functions of hyaluronan. *Annals of the rheumatic diseases*, 54(5), p.429.
Le, M. et al., 2012. Transforming Growth Factor Beta 3 Is Required for Excisional Wound Repair In Vivo. *PLoS ONE*, 7(10), pp.1–10.
Leask, A. et al., 2008. Loss of protein kinase Cε results in impaired cutaneous wound closure and myofibroblast function. *Journal of cell science*, 121, pp.3459–3467.
Lech, M. & Anders, H.J., 2013. Macrophages and fibrosis: How resident and infiltrating mononuclear phagocytes orchestrate all phases of tissue injury and repair. *Biochimica et Biophysica Acta - Molecular Basis of Disease*, 1832(7), pp.989–997.
Lee, D.E. et al., 2015. High-mobility Group Box Protein-1, Matrix Metalloproteinases, and Vitamin D in Keloids and Hypertrophic Scars. *Plastic and reconstructive surgery. Global open*, 3(6), p.e425.
Lee, D.-Y. & Cho, K.-H., 2005. The effects of epidermal keratinocytes and dermal fibroblasts on the formation of cutaneous basement membrane in three-dimensional culture systems. *Archives for dermatological research. Archiv fur dermatologische Forschung*, 296(7), pp.296–302.
Lee, E.Y., Lee, Z.H. & Song, Y.W., 2013. The interaction between CXCL10 and cytokines in chronic inflammatory arthritis. *Autoimmunity Reviews*, 12(5), pp.554–557.
Lee, H.G. & Eun, H.C., 1999. Differences between fibroblasts cultured from oral mucosa and normal skin: Implication to wound healing. *Journal of Dermatological Science*, 21(3), pp.176–182.
Lee, K.C. & Eckert, R.L., 2007. S100A7 (Psoriasin)--mechanism of antibacterial action in wounds. *The Journal of Investigative Dermatology*, 127(4), pp.945–957.
Lee, S.Y. & Park, J., 2015. Postoperative electron beam radiotherapy for keloids: Treatment outcome and factors associated with occurrence and recurrence. *Annals of Dermatology*, 27(1), pp.53–58.
Lee, W. et al., 2009. Multi-layered culture of human skin fibroblasts and keratinocytes through three-dimensional freeform fabrication. *Biomaterials*, 30(8), pp.1587–1595.
Lee, W. et al., 2016. The Effect of MCP-1/CCR2 on the Proliferation and Senescence of Epidermal Constituent Cells in Solar Lentigo. *International Journal of Molecular Sciences*, 17(6), p.948.
Lee, Y.-S. et al., 2012. Wound Healing in Development. *Birth Defects Res C Embryo Today*, 96(3), pp.213–222.
Lehmann, G.M. et al., 2011. The aryl hydrocarbon receptor ligand ITE inhibits TGFβ1-induced human myofibroblast differentiation. *American Journal of Pathology*, 178(4), pp.1556–1567.
Leigh, I.M. et al., 1995. Keratins (K16 and K17) as markers of keratinocyte hyperproliferation in psoriasis in vivo and in vitro. *British Journal of Dermatology*, 133(4), pp.501–511.
de Leon, J.M. et al., 2009. Cost-effectiveness of negative pressure wound therapy for postsurgical patients in long-term acute care. *Advances in skin & wound care*, 22(3), pp.122–7.
Letra, A. et al., 2013. MMP-7 and TIMP-1, new targets in predicting poor wound healing in apical periodontitis. *Journal of Endodontics*, 39(9), pp.1141–1146.
Leung, A., Crombleholme, T.M. & Keswani, S.G., 2012. Fetal wound healing: implications for minimal scar formation. *Current Opinion in Pediatrics*, 24(3), pp.371–378.
Lev-Tov, H. et al., 2013. Cellular versus acellular matrix devices in treatment of diabetic foot ulcers: study protocol for a comparative efficacy randomized controlled trial. *Trials*, 14, pp.1–8.
Levy, D.S., Salter, M.M. & Roth, R.E., 1976. Postoperative Irradiation in the Prevention of Keloids. *American Journal of Roentgenology*, 127, pp.509–510.
Li, B. & Wang, J.H., 2011. Fibroblasts and myofibroblasts in wound healing: Force generation and measurement. *Journal of Tissue Viability*, 20(4), pp.108–120.
Li, J., Chen, J. & Kirsner, R., 2007. Pathophysiology of acute wound healing. *Clinics in Dermatology*, 25(1), pp.9–18.
Li, J., Farthing, P.M. & Thornhill, M.H., 2000. Oral and skin keratinocytes are stimulated to secrete monocyte chemoattractant protein-1 by tumour necrosis factor-alpha and interferon-gamma.

Journal of oral pathology & medicine : official publication of the International Association of Oral Pathologists and the American Academy of Oral Pathology, 29(3), pp.438–444.
Li, W. et al., 2002. An important role for protein kinase C-delta in human keratinocyte migration on dermal collagen. *Experimental cell research*, 273(2), pp.219–28.
Li, W. et al., 2004. Mechanism of Human Dermal Fibroblast Migration Driven by Type I Collagen and Platelet-derived Growth Factor-BB. *Molecular biology of the cell*, 15, pp.294–309.
Li, Y. et al., 2014. Kynurenine increases matrix metalloproteinase-1 and -3 expression in cultured dermal fibroblasts and improves scarring in vivo. *The Journal of investigative dermatology*, 134(3), pp.643–50.
Lian, X. & Yang, T., 2004. Plasminogen activator inhibitor 2: Expression and role in differentiation of epidermal keratinocyte. *Biology of the Cell*, 96(2), pp.109–116.
Lichtman, M.K., Otero-Vinas, M. & Falanga, V., 2016. Transforming growth factor beta (TGF-β) isoforms in wound healing and fibrosis. *Wound Repair and Regeneration*, pp.215–222.
Liechty, K.W. et al., 1998. Diminished interleukin-8 (IL-8) production in the fetal wound healing response. *The Journal of surgical research*, 77(1), pp.80–84.
Liechty, K.W., Adzick, N.S. & Crombleholme, T.M., 2000. Diminished Interleukin 6 (Il-6) Production During Scarless Human Fetal Wound Repair. *Cytokine*, 12(6), pp.671–676.
Lim, I.J. et al., 2002. Fibroblasts cocultured with keloid keratinocytes: normal fibroblasts secrete collagen in a keloidlike manner. *American journal of physiology. Cell physiology*, 283(1), pp.C212–C222.
Lim, I.J. et al., 2001. Investigation of the Infuence of Keloid-Derived Keratinocytes on Fibroblast Growth and Proliferation in Vivo. *Plastic and reconstructive surgery*, 107(3), p.787.
Lin, Z. et al., 2008. The pseudoreceptor BMP and activin membrane-bound inhibitor positively modulates Wnt/β-catenin signaling. *Journal of Biological Chemistry*, 283(48), pp.33053–33058.
Lin, Z.-Q. et al., 2003. Essential involvement of IL-6 in the skin wound-healing process as evidenced by delayed wound healing in IL-6-deficient mice. *Journal of leukocyte biology*, 73(6), pp.713–721.
Van Linthout, S., Miteva, K. & Tschöpe, C., 2014. Crosstalk between fibroblasts and inflammatory cells. *Cardiovascular Research*, 102(2), pp.258–269.
Lippens, S. et al., 2005. Death penalty for keratinocytes: apoptosis versus cornification. *Cell death and differentiation*, 12 Suppl 2, pp.1497–508.
Liu, Y. et al., 2009. Cell and molecular mechanisms of keratinocyte function stimulated by insulin during wound healing. *BMC cell biology*, 10, p.1.
Liu, Y. et al., 2003. Keratin 15 Promoter Targets Putative Epithelial Stem Cells in the Hair Follicle Bulge. *Journal of Investigative Dermatology*, 121(5), pp.963–968.
Lloyd, C. et al., 1995. The basal keratin network of stratified squamous epithelia: Defining K15 function in the absence of K14. *Journal of Cell Biology*, 129(5), pp.1329–1344.
Lo, D.D. et al., 2012. Scarless Fetal Skin Wound Healing Update. *Birth Defects Research (Part C)*, 96, pp.237–247.
Lobmann, R. et al., 2003. Autologous human keratinocytes cultured on membranes composed of benzyl ester of hyaluronic acid for grafting in nonhealing diabetic foot lesions: A pilot study. *Journal of Diabetes and its Complications*, 17(4), pp.199–204.
Lobmann, R. et al., 2002. Expression of matrix-metalloproteinases and their inhibitors in the wounds of diabetic and non-diabetic patients. *Diabetologia*, 45(7), pp.1011–1016.
Löffek, S., Schilling, O. & Franzke, C.W., 2011. Biological role of matrix metalloproteinases: A critical balance. *European Respiratory Journal*, 38(1), pp.191–208.
Longaker, M.T. et al., 2001. Fetal wound healing : Progress report and future directions. *Surgery*, 130(5), pp.785–787.
Longaker, M.T. et al., 1991. Studies in fetal wound healing. V. A prolonged presence of hyaluronic acid characterizes fetal wound fluid. *Annals of surgery*, 213(4), pp.292–296.
Longinotti, C., 2014. The use of hyaluronic acid based dressings to treat burns: A review. *Burns & Trauma*, 2(4), p.162.
Longmate, W.M. & DiPersio, C.M., 2014. Integrin Regulation of Epidermal Functions in Wounds. *Advances in Wound Care*, 3(3), pp.229–246.
Lorenz, H.P. et al., 1992. Scarless wound repair: a human fetal skin model. *Development*

(Cambridge, England), 114, pp.253–259.
Lorenz, H.P. & Adzick, N.S., 1993. Scarless skin wound repair in the fetus. *The Western journal of medicine*, 159(3), pp.350–5.
Loss, M. et al., 2000. Artificial skin, split-thickness autograft and cultured autologous keratinocytes combined to treat a severe burn injury of 93% of TBSA. *Burns*, 26(7), pp.644–652.
Lovén, J. et al., 2012. Revisiting global gene expression analysis. *Cell*, 151(3), pp.476–482.
Lovvorn, H.N. et al., 1998. Hyaluronan receptor expression increases in fetal excisional skin wounds and correlates with fibroplasia. *Journal of Pediatric Surgery*, 33(7), pp.1062–1070.
Lü, D. et al., 2013. Asymmetric Migration of Human Keratinocytes under Mechanical Stretch and Cocultured Fibroblasts in a Wound Repair Model. *PLoS ONE*, 8(9), pp.1–13.
Lu, P. et al., 2011. Extracellular matrix degradation and remodeling in development and disease. *Cold Spring Harb Perspect Biol*, 3(12), pp.1–24.
Lucas, T. et al., 2010. Differential roles of macrophages in diverse phases of skin repair. *Journal of immunology*, 184(7), pp.3964–77.
Luster, A. et al., 1998. Delayed wound healing and disorganized neovascularization in transgenic mice expressing the IP-10 chemokine. *Proc Assoc Am Physicians*, 110(3), pp.183–196.
Lyle, G.W., 2001. Silicone Gel Sheeting. *Safety and Efficacy Report*, 107(1), pp.272–275.
Ma, X. et al., 2015. Keloid-derived keratinocytes acquire a fbroblast-like appearance and an enhanced invasive capacity in a hypoxic microenvironment in vitro. *International Journal of Molecular Medicine*, 35(5), pp.1246–1256.
Maas-Szabowski, N., Shimotoyodome, a & Fusenig, N.E., 1999. Keratinocyte growth regulation in fibroblast cocultures via a double paracrine mechanism. *Journal of cell science*, 112 (Pt 1, pp.1843–1853.
Maas-Szabowski, N., Stark, H.J. & Fusenig, N.E., 2000. Keratinocyte growth regulation in defined organotypic cultures through IL-1-induced keratinocyte growth factor expression in resting fibroblasts. *Journal of Investigative Dermatology*, 114(6), pp.1075–1084.
Mackman, N., 2004. Role of Tissue Factor in Hemostasis, Thrombosis, and Vascular Development. *Arteriosclerosis, Thrombosis, and Vascular Biology*, 24, pp.1015–1022.
Magcwebeba, T. et al., 2012. Interleukin-1α Induction in Human Keratinocytes (HaCaT): An In Vitro Model for Chemoprevention in Skin. *Journal of Skin Cancer*, 2012, pp.1–10.
Magin, T., Vijayaraj, P. & Leube, R., 2007. Structural and regulatory functions of keratins. *Experimental Cell Research*, 313(10), pp.2021–2032.
Maguire Jr., H.C., 1965. Treatment of Keloids With Triamcinolone Acetonide Injected Intralesionally. *The Journal of the American Medical Association*, 192(4), pp.325–326.
Maher, S.G. et al., 2008. IFNalpha and IFNlambda differ in their antiproliferative effects and duration of JAK/STAT signaling activity. *Cancer biology & therapy*, 7(7), pp.1109–15.
Maheshwari, G. et al., 2000. Cell adhesion and motility depend on nanoscale RGD clustering. *Journal of cell science*, 113 (Pt 1), pp.1677–1686.
Mak, K. et al., 2009. Scarless healing of oral mucosa is characterized by faster resolution of inflammation and control of myofibroblast action compared to skin wounds in the red Duroc pig model. *Journal of Dermatological Science*, 56(3), pp.168–180.
Malaisse, J. et al., 2016. Hyaluronan Does Not Regulate Human Epidermal Keratinocyte Proliferation and Differentiation. *Journal of Biological Chemistry*, 291(12), pp.6347–6358.
Malaisse, J. et al., 2014. Hyaluronan metabolism in human keratinocytes and atopic dermatitis skin is driven by a balance of hyaluronan synthases 1 and 3. *The Journal of investigative dermatology*, 134, pp.2174–82.
Malik, T.A. et al., 2015. An insight into foetal wound healing and a future of scarless wound repair. *Wounds International*, 2(1), pp.6–11.
Martin, P., 1997. Wound Healing--Aiming for Perfect Skin Regeneration. *Science*, 276, pp.75–81.
Martin, P. & Leibovich, S.J., 2005. Inflammatory cells during wound repair: The good, the bad and the ugly. *Trends in Cell Biology*, 15(11), pp.599–607.
Martinsson, H., Yhr, M. & Enerbäck, C., 2005. Expression patterns of S100A7 (psoriasin) and S100A9 (calgranulin-B) in keratinocyte differentiation. *Experimental Dermatology*, 14(3), pp.161–168.
Martiny-Baron, G. & Fabbro, D., 2007. Classical PKC isoforms in cancer. *Pharmacological Research*, 55(6), pp.477–486.

Marynka-Kalmani, K. et al., 2010. The lamina propria of adult human oral mucosa harbors a novel stem cell population. *Stem Cells*, 28(5), pp.984–995.
Masamune, A. et al., 2006. Curcumin blocks activation of pancreatic stellate cells. *Journal of Cellular Biochemistry*, 97(5), pp.1080–1093.
Mascia, F. et al., 2012. The Black Box Illuminated: Signals and Signaling. *Journal of Investigative Dermatology*, 132(3), pp.811–819.
Mason, S.A. et al., 2010. The induction of senescence-like growth arrest by protein kinase C-activating diterpene esters in solid tumor cells. *Investigational New Drugs*, 28(5), pp.575–586.
Mast, B.A. et al., 1992. Scarless wound healing in the mammalian fetus. *Surgery, gynecology & obstetrics*, 174(5), pp.441–51.
Mazzalupo, S. et al., 2003. Role for keratins 6 and 17 during wound closure in embryonic mouse skin. *Developmental Dynamics*, 226(2), pp.356–365.
Mazzucchelli, L., 2002. Protein S100A4 : Too Long Overlooked by Pathologists ? *American Journal of Pathology*, 160(1), pp.7–13.
McCarty, S.M. & Percival, S.L., 2013. Proteases and Delayed Wound Healing. *Advances in wound care*, 2(8), pp.438–447.
Mccauley, R.L. et al., 1992. Alterd cytokines production in black patients with keloids. *Journal of clinical immunology*, 12(4), pp.300–308.
Mccubrey, J.A. et al., 2007. Roles Of The RAS/MEK/ERK pathway in Cell Growth, Malignant Transformation and Drug Resistance. *Biochimica et Biophysica Acta - Molecular Cell Research*, 1773(8), pp.1263–1284.
McDougall, S. et al., 2006. Fibroblast migration and collagen deposition during dermal wound healing: mathematical modelling and clinical implications. *Philosophical transactions. Series A, Mathematical, physical, and engineering sciences*, 364(1843), pp.1385–1405.
McGrath, J. & Uitto, J., 2010. Anatomy and organisation of human skin. In *Rook's Textbook of Dermatology*. Blackwell Publishing Ltd.
McGrath, J.A., Eady, R.A.J. & Pope, F.M., 2004. Anatomy and physiology of the skin. In T. Burns et al., eds. *Rook's Textbook of Dermatology*. Blackwell Publishing, Inc.
Mcheik, J.N. et al., 2014. Epidermal Healing in Burns. *Plastic and Reconstructive Surgery Global Open*, 2(9), p.e218.
Mcilwain, D.R., Berger, T. & Mak, T.W., 2013. Caspase Functions in Cell Death and Disease. *Cold Spring Harbor Perspectives in Biology*, 7(4), pp.1–28.
McInnes, R.L. et al., 2014. Contrasting host immuno-inflammatory responses to bacterial challenge within venous and diabetic ulcers. *Wound Repair and Regeneration*, 22(1), pp.58–69.
McKeown, S.T.W. et al., 2007. Matrix metalloproteinase-3 differences in oral and skin fibroblasts. *Journal of dental research*, 86, pp.457–462.
McLean, W.H.I. & Moore, C.B.T., 2011. Keratin disorders: From gene to therapy. *Human Molecular Genetics*, 20(R2), pp.189–197.
Mee, J.B. et al., 2005. Counter-regulation of interleukin-1α (IL-1α) and IL-1 receptor antagonist in murine keratinocytes. *Journal of Investigative Dermatology*, 124(6), pp.1267–1274.
Mee, J.B. et al., 2007. The Psoriatic Transcriptome Closely Resembles That Induced by Interleukin-1 in Cultured Keratinocytes. *The American Journal of Pathology*, 171(1), pp.32–42.
Mehic, D. et al., 2005. Fos and Jun proteins are specifically expressed during differentiation of human keratinocytes. *Journal of Investigative Dermatology*, 124(1), pp.212–220.
Mehta, K.D., 2014. Emerging role of protein kinase C in energy homeostasis: A brief overview. *World journal of diabetes*, 5(3), pp.385–92.
Meier, M. et al., 2007. Deletion of protein kinase C-β isoform in vivo reduces renal hypertrophy but not albuminuria in the streptozotocin-induced diabetic mouse model. *Diabetes*, 56(2), pp.346–354.
Mendez, M. V et al., 1998. Fibroblasts cultured from venous ulcers display cellular characteristics of senescence. *Journal of vascular surgery*, 28(5), pp.876–83.
Menke, N.B. et al., 2007. Impaired wound healing. *Clinics in dermatology*, 25(1), pp.19–25.
Menon, G.K., 2002. New insights into skin structure: scratching the surface. *Advanced drug*

delivery reviews, 54(Suppl 1), pp.S3–17.
Menon, S.N. et al., 2012. Modelling the interaction of keratinocytes and fibroblasts during normal and abnormal wound healing processes. *Proceedings. Biological sciences / The Royal Society*, 279(1741), pp.3329–38.
Merad, M., Ginhoux, F. & Collin, M., 2008. Origin, homeostasis and function of Langerhans cells and other langerin-expressing dendritic cells. *Nature reviews. Immunology*, 8(12), pp.935–47.
Meran, S. et al., 2008. Hyaluronan facilitates transforming growth factor-β1-mediated fibroblast proliferation. *The Journal of Biological Chemistry*, 283(10), pp.6530–45.
Meran, S. et al., 2007. Involvement of hyaluronan in regulation of fibroblast phenotype. *Journal of Biological Chemistry*, 282(35), pp.25687–25697.
Metz, C.N., 2003. Fibrocytes: A unique cell population implicated in wound healing. *Cellular and Molecular Life Sciences*, 60(7), pp.1342–1350.
Meyer, L.J.M. et al., 2000. Reduced hyaluronan in keloid tissue and cultured keloid fibroblasts. *Journal of Investigative Dermatology*, 114(5), pp.953–959.
Meyer, N. et al., 2010. IL-32 is expressed by human primary keratinocytes and modulates keratinocyte apoptosis in atopic dermatitis. *Journal of Allergy and Clinical Immunology*, 125(4).
Micallef, L. et al., 2012. The myofibroblast, multiple origins for major roles in normal and pathological tissue repair. *Fibrogenesis & tissue repair*, 5 Suppl 1, pp.1–5.
Michaels, J. et al., 2007. Db/Db Mice Exhibit Severe Wound-Healing Impairments Compared With Other Murine Diabetic Strains in a Silicone-Splinted Excisional Wound Model. *Wound Repair and Regeneration*, 15(5), pp.665–670.
Michel, G. et al., 1992. Interleukin-8 receptor-mediated chemotaxis of normal human epidermal cells. *FEBS Letters*, 305(3), pp.241–243.
Midgley, A.C. et al., 2015. Hyaluronan regulates bone morphogenetic protein-7-dependent prevention and reversal of myofibroblast phenotype. *Journal of Biological Chemistry*, 290(18), pp.11218–11234.
Midgley, A.C. et al., 2013. Transforming growth factor-β1 (TGF-β1)-stimulated fibroblast to myofibroblast differentiation is mediated by hyaluronan (HA)-facilitated epidermal growth factor receptor (EGFR) and CD44 co-localization in lipid rafts. *Journal of Biological Chemistry*, 288(21), pp.14824–14838.
Midwood, K.S. & Schwarzbauer, J.E., 2002. Elastic Fibers : Building Bridges Between Cells and Their Matrix. *Current Biology*, 12(02), pp.279–281.
Miller, L.S. et al., 2005. TGF-α Regulates TLR Expression and Function on Epidermal Keratinocytes. *The Journal of Immunology*, 174(10), pp.6137–6143.
Miller, M.B. & Tang, Y.W., 2009. Basic concepts of microarrays and potential applications in clinical microbiology. *Clinical Microbiology Reviews*, 22(4), pp.611–633.
Mimura, Y. et al., 2004. Epidermal growth factor induces fibronectin expression in human dermal fibroblasts via protein kinase C δ signaling pathway. *The Journal of investigative dermatology*, 122(6), pp.1390–8.
Mirastschijski, U. et al., 2010. Matrix metalloproteinase inhibition delays wound healing and blocks the latent transforming growth factor-β1-promoted myofibroblast formation and function. *Wound Repair and Regeneration*, 18(2), pp.223–234.
Mirastschijski, U. et al., 2004. Matrix metalloproteinase inhibitor GM 6001 attenuates keratinocyte migration, contraction and myofibroblast formation in skin wounds. *Experimental Cell Research*, 299(2), pp.465–475.
Mitev, V. & Miteva, L., 1999. Signal transduction in keratinocytes. *Experimental dermatology*, 8(2), pp.96–108.
Miyazono, K., 2000. TGF-?? signaling by Smad proteins. *Cytokine and Growth Factor Reviews*, 11(1-2), pp.15–22.
Mizutani, H., Black, R. & Kupper, T.S., 1991. Human keratinocytes produce but do not process pro-interleukin-1 (IL-1) beta different strategies of IL-1 production and processing in monocytes and keratinocytes. *Journal of Clinical Investigation*, 87(3), pp.1066–1071.
Mochly-Rosen, D., Das, K. & Grimes, K.K. V, 2012. Protein kinase C, an elusive therapeutic target? *Nature Reviews Drug Discovery*, 11(12), pp.937–957.

Moll, I. et al., 1987. Distribution of a special subset of keratinocytes characterized by the expression of cytokeratin 9 in adult and fetal human epidermis of various body sites. *Differentiation*, 33(3), pp.254–265.
Moll, I. et al., 2005. Human Merkel cells--aspects of cell biology, distribution and functions. *European journal of cell biology*, 84(2-3), pp.259–71.
Moll, R., Divo, M. & Langbein, L., 2008. The human keratins: Biology and pathology. *Histochemistry and Cell Biology*, 129(6), pp.705–733.
Monaco, J.L. & Lawrence, W.T., 2003. Acute wound healing an overview. *Clinics in Plastic Surgery*, 30(1), pp.1–12.
Morgan, M.R., Humphries, M.J. & Bass, M.D., 2007. Synergistic control of cell adhesion by integrins and syndecans. *Nature reviews. Molecular cell biology*, 8(12), pp.957–69.
Morhenn, V.B., Nelson, T.E. & Gruol, D.L., 2013. The rate of wound healing is increased in psoriasis. *J Dermatol Sci*, 72(2), pp.87–92.
Morizane, S. et al., 2012. Cathelicidin antimicrobial peptide LL-37 in psoriasis enables keratinocyte reactivity against TLR9 ligands. *The Journal of investigative dermatology*, 132(1), pp.135–43.
Morley, S.M. et al., 2003. Generation and characterization of epidermolysis bullosa simplex cell lines: Scratch assays show faster migration with disruptive keratin mutations. *British Journal of Dermatology*, 149(1), pp.46–58.
Moroz, O. V et al., 2003. Multiple structural states of S100A12: A key to its functional diversity. *Microscopy research and technique*, 60(6), pp.581–592.
Morris, D.E. et al., 1997. Acute and chronic animal models for excessive dermal scarring: quantitative studies. *Plastic and reconstructive surgery*, 100(3), pp.674–681.
Moseley, R. et al., 2004. Comparison of oxidative stress biomarker profiles between acute and chronic wound environments. *Wound Repair and Regeneration*, 12(4), pp.419–429.
Mosser, D.M. & Edwards, J.P., 2008. Exploring the full spectrum of macrophage activation. *Nature reviews. Immunology*, 8(12), pp.958–69.
Moulin, V. et al., 2004. Normal Skin Wound and Hypertrophic Scar Myofibroblasts Have Differential Responses to Apoptotic Inductors. *Journal of Cellular Physiology*, 198(3), pp.350–358.
Moulin, V. & Plamondon, M., 2002. Differential expression of collagen integrin receptor on fetal vs . adult skin fibroblasts : implication in wound contraction during healing. *British Journal of Dermatology*, 147, pp.886–892.
Moustakas, A. & Heldin, C.H., 2008. Dynamic control of TGF-β signaling and its links to the cytoskeleton. *FEBS Letters*, 582(14), pp.2051–2065.
Mouw, J.K., Ou, G. & Weaver, V.M., 2014. Extracellular matrix assembly: a multiscale deconstruction. *Nature reviews. Molecular cell biology*, 15(12), pp.771–785.
Muiznieks, L.D. & Keeley, F.W., 2013. Molecular assembly and mechanical properties of the extracellular matrix: A fibrous protein perspective. *Biochimica et Biophysica Acta - Molecular Basis of Disease*, 1832(7), pp.866–875.
Muller, M. et al., 2008. Matrix metalloproteinases and diabetic foot ulcers: The ratio of MMP-1 to TIMP-1 is a predictor of wound healing. *Diabetic Medicine*, 25(4), pp.419–426.
Mustoe, T.A., 2008. Evolution of silicone therapy and mechanism of action in scar management. *Aesthetic Plastic Surgery*, 32(1), pp.82–92.
Mutsaers, S.E. et al., 1997. Mechanisms of tissue repair: From wound healing to fibrosis. *The International Journal of Biochemistry and Cell Biology*, 29(1), pp.5–17.
Mwaura, B. et al., 2006. The impact of differential expression of extracellular matrix metalloproteinase inducer, matrix metalloproteinase-2, tissue inhibitor of matrix metalloproteinase-2 and PDGF-AA on the chronicity of venous leg ulcers. *European Journal of Vascular and Endovascular Surgery*, 31(3), pp.306–310.
Myllyharju, J., 2003. Prolyl 4-hydroxylases, the key enzymes of collagen biosynthesis. *Matrix Biology*, 22(1), pp.15–24.
Naba, A. et al., 2016. The extracellular matrix: Tools and insights for the “omics” era. *Matrix Biology*, 49, pp.10–24.
Naganuma, K. et al., 2014. Epigenetic alterations of the keratin 13 gene in oral squamous cell carcinoma. *BMC cancer*, 14(1), p.988.

Nagase, H., Visse, R. & Murphy, G., 2006. Structure and function of matrix metalloproteinases and TIMPs. *Cardiovascular Research*, 69(3), pp.562–573.
Nakane, H. et al., 2002. Elafin, a secretory protein, is cross-linked into the cornified cell envelopes from the inside of psoriatic keratinocytes. *Journal of Investigative Dermatology*, 119(1), pp.50–55.
Nalepa, G. et al., 2013. The tumor suppressor CDKN3 controls mitosis. *Journal of Cell Biology*, 201(7), pp.997–1012.
Nanney, L.B. et al., 1984. Comparison of epidermal growth factor binding and receptor distribution in normal human epidermis and epidermal appendages. *The Journal of investigative dermatology*, 83(5), pp.385–93.
Nardini, J.T. et al., 2016. Modeling keratinocyte wound healing dynamics : Cell – cell adhesion promotes sustained collective migration. *Journal of Theoretical Biology*, 400, pp.103–117.
Natarajan, V.T. et al., 2014. Multifaceted pathways protect human skin from UV radiation. *Nature chemical biology*, 10(7), pp.542–51.
Nauta, A., Gurtner, G.C. & Longaker, M.T., 2011. Wound healing and regenerative strategies. *Oral Diseases*, 17(6), pp.541–549.
Nedelec, B. et al., 2001. Myofibroblasts and apoptosis in human hypertrophic scars: The effect of interferon-α2b. *Surgery*, 130(5), pp.798–808.
Ngo, P. et al., 2006. Collagen Gel Contraction Assay. In S. P. Colgan, ed. *Methods in Molecular Biology*. Humana Press Inc., pp. 103–109.
Nickoloff, B.J. et al., 1991. Cellular localization of interleukin-8 and its inducer, tumor necrosis factor-alpha in psoriasis. *The American journal of pathology*, 138(1), pp.129–140.
Niedworok, C. et al., 2013. The impact of the receptor of hyaluronan-mediated motility (RHAMM) on human urothelial transitional cell cancer of the bladder. *PloS one*, 8(9), p.e75681.
Niessen, F.B. et al., 1999. On the Nature of Hypertrophic Scars and Keloids: A Review. *Plastic and reconstructive surgery*, 104(5), pp.1435–1458.
Niessen, F.B. et al., 1998. The use of silicone occlusive sheeting (Sil-K) and silicone occlusive gel (Epiderm) in the prevention of hypertrophic scar formation. *Plastic and reconstructive surgery*, 102, pp.1962–1972.
Nievers, M.G., Schaapveld, R.Q.J. & Sonnenberg, A., 1999. Biology and function of hemidesmosomes. *Matrix Biology*, 18(1), pp.5–17.
Niezgoda, J. a et al., 2005. Randomized clinical trial comparing OASIS Wound Matrix to Regranex Gel for diabetic ulcers. *Advances in skin & wound care*, 18(5), pp.258–266.
Nishio, H. et al., 2001. Immunolocalisation of the janus kinases (JAK)--signal transducers and activators of transcription (STAT) pathway in human epidermis. *Journal of anatomy*, 198(Pt 5), pp.581–9.
Nishiyama, T. et al., 2000. The importance of laminin 5 in the dermal-epidermal basement membrane. *Journal of Dermatological Science*, 24(Suppl. 1), pp.51–59.
Novak, N. et al., 2008. The immune privilege of the oral mucosa. *Trends Mol Med*, 14(5), pp.191–198.
Novokhatny, V. et al., 1995. Tissue-type plasminogen activator (tPA) interacts with urokinase-type plasminogen activator (uPA) via tPA's lysine binding site: An explanation of the poor fibrin affinity of recombinant tPA/uPA chimeric molecules. *Journal of Biological Chemistry*, 270(15), pp.8680–8685.
Nunan, R., Harding, K.G. & Martin, P., 2014. Clinical challenges of chronic wounds: searching for an optimal animal model to recapitulate their complexity. *Disease models & mechanisms*, 7(11), pp.1205–13.
Nuutila, K. et al., 2012. Human skin transcriptome during superficial cutaneous wound healing. *Wound repair and regeneration : official publication of the Wound Healing Society [and] the European Tissue Repair Society*, 20(6), pp.830–9.
Nwomeh, B.C. et al., 1998. Dynamics of the matrix metalloproteinases MMP-1 and MMP-8 in acute open human dermal wounds. *Wound repair and regeneration : official publication of the Wound Healing Society [and] the European Tissue Repair Society*, 6(2), pp.127–34.
Nyström, A. et al., 2013. C7 plays a dual role in skin wound healing. *Journal of Investigative Dermatology*, 133(8), p.S256.
O'Donnell, T.F. & Lau, J., 2006. A systematic review of randomized controlled trials of wound

dressings for chronic venous ulcer. *Journal of Vascular Surgery*, 44(5), pp.1118–1125.
O'Kane, S. & Ferguson, M.W.J., 1997. Transforming growth factor βs and wound healing. *The International Journal of Biochemistry & Cell Biology*, 29(1), pp.63–78.
O'Toole, E.A., 2001. Extracellular matrix and keratinocyte migration. *Experimental dermatology*, 26, pp.525–530.
O'Toole, E.A. et al., 1997. Laminin inhibits human keratinocyte migration. *Experimental Cell Research*, 233, pp.330–339.
Ogawa, H., 1996. The Merkel cell as a possible mechanoreceptor cell. *Progress in Neurobiology*, 49(4), pp.317–3334.
Ogawa, R. et al., 2003. Postoperative electron-beam irradiation therapy for keloids and hypertrophic scars: retrospective study of 147 cases followed for more than 18 months. *Plastic and reconstructive surgery*, 111(2), pp.547–53; discussion 554–5.
Ogawa, R., 2010. The most current algorithms for the treatment and prevention of hypertrophic scars and keloids. *Plastic and reconstructive surgery*, 125(2), pp.557–568.
Ogbourne, S.M. et al., 2004. Antitumor Activity of 3-Ingenyl Angelate : Plasma Membrane and Mitochondrial Disruption and Necrotic Cell Death Antitumor Activity of 3-Ingenyl Angelate : Plasma Membrane and Mitochondrial Disruption and Necrotic Cell Death. *Cancer Res.*, 64, pp.2833–2839.
Ohyama, M., 2007. Hair follicle bulge: A fascinating reservoir of epithelial stem cells. *Journal of Dermatological Science*, 46(2), pp.81–89.
Ojeh, N. et al., 2015. Stem cells in skin regeneration, wound healing, and their clinical applications. *International Journal of Molecular Sciences*, 16(10), pp.25476–25501.
Okamoto, O. et al., 2003. Normal Human Keratinocytes Bind to the α3LG4/5 Domain of Unprocessed Laminin-5 through the Receptor Syndecan-1. *Journal of Biological Chemistry*, 278(45), pp.44168–44177.
Oksala, O. et al., 1995. Expression of proteoglycans and hyaluronan during wound healing. *The journal of histochemistry and cytochemistry : official journal of the Histochemistry Society*, 43(2), pp.125–135.
Olczyk, P., Mencner, L. & Komosinska-Vassev, K., 2014. The role of the extracellular matrix components in cutaneous wound healing. *Biomed Res Int*, 2014, p.747584.
Oliveira, G. V. et al., 2009. Hypertrophic versus non hypertrophic scars compared by immunohistochemistry and laser confocal microscopy: Type I and III collagens. *International Wound Journal*, 6(6), pp.445–452.
Olson, E.R. et al., 2005. Inhibition of cardiac fibroblast proliferation and myofibroblast differentiation by resveratrol. *American Journal of Physiology. Heart and Circulatory Physiology*, 288(3), pp.H1131–1138.
Ong, C.T. et al., 2010. Comparative proteomic analysis between normal skin and keloid scar. *The British journal of dermatology*, 162(6), pp.1302–1315.
Otranto, M. et al., 2012. The role of the myofibroblast in tumor stroma remodeling. *Cell adhesion & migration*, 6(3), pp.203–219.
Ovaere, P. et al., 2009. The emerging roles of serine protease cascades in the epidermis. *Trends in Biochemical Sciences*, 34(9), pp.453–463.
Overall, C.M., Wrana, J.L. & Sodek, J., 1989. Independent regulation of collagenase, 72-kDa progelatinase, and metalloendoproteinase inhibitor expression in human fibroblasts by transforming growth factor-?? *Journal of Biological Chemistry*, 264(3), pp.1860–1869.
Pakyari, M. et al., 2013. Critical Role of Transforming Growth Factor Beta in Different Phases of Wound Healing. *Advances in wound care*, 2(5), pp.215–224.
Paladini, R.D. & Coulombe, P.A., 1998. Directed expression of keratin 16 to the progenitor basal cells of transgenic mouse skin delays skin maturation. *Journal of Cell Biology*, 142(4), pp.1035–1051.
Palecek, S.P. et al., 1997. Integrin-ligand binding properties govern cell migration speed through cell-substratum adhesiveness. *Nature*, 385(6616), pp.537–40.
Palta, S., Saroa, R. & Palta, A., 2014. Overview of the coagulation system. *Indian Journal of Anaesthesia*, 58(5), pp.515–523.
Panich, U. et al., 2016. Ultraviolet Radiation-Induced Skin Aging: The Role of DNA Damage and Oxidative Stress in Epidermal Stem Cell Damage Mediated Skin Aging. *Stem Cells*

International, 2016, pp.1–14.
Papanas, N. & Maltezos, E., 2010. Benefit-risk assessment of becaplermin in the treatment of diabetic foot ulcers. *Drug Safety*, 33(6), pp.455–461.
Papp, H. et al., 2004. Opposite roles of protein kinase C isoforms in proliferation, differentiation, apoptosis, and tumorigenicity of human HaCaT keratinocytes. *Cellular and Molecular Life Sciences*, 61(9), pp.1095–1105.
Papp, H. et al., 2003. Protein kinase C isozymes regulate proliferation and high cell density-mediated differentiation in HaCaT keratinocytes. *Experimental Dermatology*, 12(6), pp.811–824.
Parihar, A., Eubank, T.D. & Doseff, A.I., 2010. Monocytes and macrophages regulate immunity through dynamic networks of survival and cell death. *Journal of Innate Immunity*, 2(3), pp.204–215.
Parks, W.C., 1999. Matrix metalloproteinases in repair. *Wound Repair and Regeneration*, 7(6), pp.423–432.
Parrett, B.M. & Donelan, M.B., 2010. Pulsed dye laser in burn scars: Current concepts and future directions. *Burns*, 36(4), pp.443–449.
Parri, M. & Chiarugi, P., 2010. Rac and Rho GTPases in cancer cell motility control. *Cell communication and signaling*, 8, p.23.
Parsons, J.T., Horwitz, A.R. & Schwartz, M.A., 2010. Cell adhesion: integrating cytoskeletal dynamics and cellular tension. *Nat Rev Mol Cell Biol.*, 11(9), pp.633–643.
Pastar, I. et al., 2014. Epithelialization in Wound Healing: A Comprehensive Review. *Advances in wound care*, 3(7), pp.445–464.
Pastore, S. et al., 2005. ERK1/2 Regulates Epidermal Chemokine Expression and Skin Inflammation. *J Immunol*, 174, pp.5047–5056.
Pastore, S. et al., 2008. The epidermal growth factor receptor system in skin repair and inflammation. *The Journal of investigative dermatology*, 128(6), pp.1365–74.
Patel, G.K. et al., 2006. Numerous keratinocyte subtypes involved in wound re-epithelialization. *The Journal of investigative dermatology*, 126(2), pp.497–502.
Peake, M.A. et al., 2014. Identification of a transcriptional signature for the wound healing continuum. *Wound Repair and Regeneration*, 22(3), pp.399–405.
Peissel, B. et al., 1995. Comparative distribution of the α1(IV), α5(IV), and α6(IV) collagen chains in normal human adult and fetal tissues and in kidneys from X-linked alport syndrome patients. *Journal of Clinical Investigation*, 96(4), pp.1948–1957.
Penn, J.W., Grobbelaar, A.O. & Rolfe, K.J., 2012. The role of the TGF-β family in wound healing, burns and scarring: a review. *International journal of burns and trauma*, 2(1), pp.18–28.
Peplow, P. V & Chatterjee, M.P., 2013. A review of the influence of growth factors and cytokines in in vitro human keratinocyte migration. *Cytokine*, 62(1), pp.1–21.
Percival, S.L. et al., 2012. A review of the scientific evidence for biofilms in wounds. *Wound Repair and Regeneration*, 20, pp.647–657.
Pessina, A. et al., 2001. High sensitivity of human epidermal keratinocytes (HaCaT) to topoisomerase inhibitors. *Cell Proliferation*, 34(4), pp.243–252.
Petri, B. & Bixel, M.G., 2006. Molecular events during leukocyte diapedesis. *FEBS Journal*, 273(19), pp.4399–4407.
Petrie, R.J. & Yamada, K.M., 2012. At the leading edge of three-dimensional cell migration. *Journal of Cell Science*, 125(24), pp.5917–5926.
Pfundt, R. et al., 1996. Constitutive and inducible expression of SKALP/elafin provides anti-elastase defense in human epithelia. *Journal of Clinical Investigation*, 98(6), pp.1389–1399.
Philips, N. et al., 2011. Beneficial regulation of matrix metalloproteinases for skin health. *Enzyme research*, 2011, p.427285.
Pierce, G.F. et al., 1989. Platelet-derived growth factor and transforming growth factor-beta enhance tissue repair activities by unique mechanisms. *The Journal of cell biology*, 109(1), pp.429–40.
Pike, R.N. et al., 2002. Serpins: finely balanced conformational traps. *IUBMB life*, 54(1), pp.1–7.
Pilcher, B.K. et al., 1997. The activity of collagenase-1 is required for keratinocyte migration on a type I collagen matrix. *Journal of Cell Biology*, 137(6), pp.1445–1457.
Ploug, M., 2003. Structure-function relationships in the interaction between the urokinase-type

plasminogen activator and its receptor. *Curr Pharm Des.*, 9(19), pp.1499–1528.
Pober, J.S. & Sessa, W.C., 2007. Evolving functions of endothelial cells in inflammation. *Nat Rev Immunol*, 7(10), pp.803–815.
Pol, A. et al., 2003. Transcriptional regulation of the elafin gene in human keratinocytes. *The Journal of investigative dermatology*, 120(2), pp.301–307.
Poole, A.W. et al., 2004. PKC-interacting proteins: From function to pharmacology. *Trends in Pharmacological Sciences*, 25(10), pp.528–535.
Poomsawat, S. et al., 2003. Scatter factor regulation of integrin expression and function on oral epithelial cells. *Archives of Dermatological Research*, 295(2), pp.63–70.
Portou, M.J. et al., 2015. The innate immune system, toll-like receptors and dermal wound healing: A review. *Vascular Pharmacology*, 71, pp.31–36.
Posnett, J. & Franks, P.J., 2008. The burden of chronic wounds in the UK. *Nursing times*, 104(3), pp.44–5.
Powell, D.W. et al., 1999. Myofibroblasts. I. Paracrine cells important in health and disease. *Am J Physiol Cell Physiol*, 277(1), pp.C1–19.
Preissner, K.T. & Seiffert, D., 1998. Role of vitronectin and its receptors in haemostasis and vascular remodeling. *Thrombosis Research*, 89(1), pp.1–21.
Presland, R.B. & Dale, B.A., 2000. Epithelial Structural Proteins of the Skin and Oral Cavity: Function in Health and Disease. *Critical Reviews in Oral Biology & Medicine*, 11(4), pp.383–408.
Puig, L., Julià, A. & Marsal, S., 2014. The Pathogenesis and Genetics of Psoriasis. *Actas Dermo-Sifiliograficas*, 105(6), pp.535–545.
Puthenedam, M. et al., 2011. Matrilysin-1 (MMP7) cleaves galectin-3 and inhibits wound healing in intestinal epithelial cells. *Inflammatory Bowel Diseases*, 17(1), pp.260–267.
Quan, C. et al., 2015. Dermal fibroblast expression of stromal cell-derived factor-1 (SDF-1) promotes epidermal keratinocyte proliferation in normal and diseased skin. *Protein and Cell*, 6(12), pp.890–903.
Quan, T.E. et al., 2004. Circulating fibrocytes: Collagen-secreting cells of the peripheral blood. *International Journal of Biochemistry and Cell Biology*, 36(4), pp.598–606.
Rabello, F.B., Souza, C.D. & Farina Júnior, J.A., 2014. Update on hypertrophic scar treatment. *Clinics (São Paulo, Brazil)*, 69(8), pp.565–73.
Rad, M.M., Rad, N.M. & Mirdamadi, Y., 2015. Expression of TGF- β3 in isolated fibroblasts from foreskin. *Reports of Biochemistry & Molecular Biology*, 3(2), pp.76–81.
Raffetto, J. et al., 2001. Changes in cellular motility and cytoskeletal actin in fibroblasts from patients with chronic venous insufficiency and in neonatal fibroblasts in the presence of chronic wound fluid. *J Vasc Surg*, 33(6), pp.1233–1241.
Raica, M. & Cimpean, A.M., 2010. Platelet-derived growth factor (PDGF)/PDGF receptors (PDGFR) axis as target for antitumor and antiangiogenic therapy. *Pharmaceuticals*, 3(3), pp.572–599.
Rajan, V. & Murray, R.Z., 2008. The duplicitous nature of inflammation in wound repair. *Wound Practice and Research*, 16(3), pp.122 –129.
Ramana, C. V et al., 2000. Complex roles of Stat1 in regulating gene expression. *Oncogene*, 19(21), pp.2619–2627.
Ramms, L. et al., 2013. Keratins as the main component for the mechanical integrity of keratinocytes. *Proceedings of the National Academy of Sciences of the United States of America*, 110(46), pp.18513–8.
Rantala, J.K. et al., 2010. Integrative functional genomics analysis of sustained polyploidy phenotypes in breast cancer cells identifies an oncogenic profile for GINS2. *Neoplasia (New York, N.Y.)*, 12(11), pp.877–888.
Ravanti, L. et al., 2001. Expression of human collagenase-3 (MMP-13) by fetal skin fibroblasts is induced by transforming growth factor-b via p38 mitogen-activated protein kinase. *The FASEB Journal*, 15(6), pp.1098–1100.
Ravanti, L. et al., 1999. Transforming growth factor-beta induces collagenase-3 expression by human gingival fibroblasts via p38 mitogen-activated protein kinase. *The Journal of biological chemistry*, 274(52), pp.37292–300.
Rayment, E.A., Upton, Z. & Shooter, G.K., 2008. Increased matrix metalloproteinase-9 (MMP-9)

activity observed in chronic wound fluid is related to the clinical severity of the ulcer. *British Journal of Dermatology*, 158(5), pp.951–961.
Redd, M.J. et al., 2004. Wound healing and inflammation: embryos reveal the way to perfect repair. *Philosophical transactions of the Royal Society of London. Series B, Biological sciences*, 359(1445), pp.777–84.
Reddell, P.W. et al., 2014. Methods and compositions for wound healing.
Reddell, P.W. & Gordon, V.A., 2007. Tiglien-3-one derivatives.
Reed, C.C. & Iozzo, R. V., 2002. The role of decorin in collagen fibrillogenesis and skin homeostasis. *Glycoconjugate Journal*, 19(4-5), pp.249–255.
Rees, P.A. et al., 2015. Chemokines in Wound Healing and as Potential Therapeutic Targets for Reducing Cutaneous Scarring. *Advances in wound care*, 4(11), pp.687–703.
Rees, R.S. et al., 1999. Becaplermin gel in the treatment of pressure ulcers : a phase II randomized , double-blind , placebo-controlled study. *Wound Repair and Regeneration*, 7, pp.141–147.
Reilkoff, R.A., Bucala, R. & Herzog, E.L., 2011. Fibrocytes: Emerging effector cells in chronic inflammation. *Nature reviews. Immunology*, 11, pp.427–435.
Reinartz, J. et al., 1996. Plasminogen activator inhibitor type-2 (PAI-2) in human keratinocytes regulates pericellular urokinase-type plasminogen activator. *Experimental cell research*, 223(1), pp.91–101.
Reinke, J.M. & Sorg, H., 2012. Wound repair and regeneration. *European Surgical Research*, 49(1), pp.35–43.
Rendell, M.S. et al., 2002. Skin blood flow response in the rat model of wound healing: expression of vasoactive factors. *The Journal of surgical research*, 107(1), pp.18–26.
Rendell, M.S. et al., 1997. The Skin Blood Flow Response in Wound Healing. *Microvascular Research*, 53(3), pp.222–234.
Rennefahrt, U.E.E. et al., 2002. Constitutive JNK activation in NIH 3T3 fibroblasts induces a partially transformed phenotype. *Journal of Biological Chemistry*, 277(33), pp.29510–29518.
Rennekampff, H.O. et al., 2000. Bioactive interleukin-8 is expressed in wounds and enhances wound healing. *The Journal of surgical research*, 93, pp.41–54.
Reno, F., Grazianetti, P. & Cannas, M., 2001. Effects of mechanical compression on hypertrophic scars : prostaglandin E 2 release. *Burns : journal of the International Society for Burn Injuries*, 27, pp.215–218.
Revenu, C. et al., 2004. The Co-Workers of Actin Filaments: From Cell Structures to Signals. *Nature Reviews Molecular Cell Biology*, 5(August), pp.1–12.
Reyland, M., 2007. Protein kinase Cδ and apoptosis. *Biochem Soc Trans*, 35, pp.1001–1004.
Reynolds, L.E. et al., 2008. α3β1 integrin–controlled Smad7 regulates reepithelialization during wound healing in mice. *The Journal of Clinical Investigation*, 118, pp.965–974.
Ricard-Blum, S. & Ruggiero, F., 2005. The collagen superfamily: from the extracellular matrix to the cell membrane. *Pathologie-biologie*, 53(7), pp.430–42.
Rider, P. et al., 2011. IL-1α and IL-1β recruit different myeloid cells and promote different stages of sterile inflammation. *The Journal of Immunology*, 187(9), pp.4835–4843.
Risinger, G.M. et al., 2006. Matrix metalloproteinase-2 expression by vascular smooth muscle cells is mediated by both stimulatory and inhibitory signals in response to growth factors. *Journal of Biological Chemistry*, 281(36), pp.25915–25925.
Risinger, G.M. et al., 2010. TGF-beta suppresses the upregulation of MMP-2 by vascular smooth muscle cells in response to PDGF-BB. *American journal of physiology. Cell physiology*, 298(1), pp.C191–C201.
Risse, B.C. et al., 2000. Evidence for intracellular cleavage of plasminogen activator inhibitor type 2 (PAI-2) in normal epidermal keratinocytes. *Journal of Cellular Physiology*, 182(2), pp.281–289.
Rittié, L., 2016. Cellular mechanisms of skin repair in humans and other mammals. *Journal of Cell Communication and Signaling*, pp.103–120.
Roark, E.F. et al., 1995. The association of human fibulin-1 with elastic fibers: an immunohistological, ultrastructural, and RNA study. *The journal of histochemistry and cytochemistry : official journal of the Histochemistry Society*, 43(4), pp.401–411.
Robson, M.C., 1997. The role of growth factors in the healing of chronic wounds. *Wound Repair*

and Regeneration, 5(1), pp.12–17.
Rodier, F. & Campisi, J., 2011. Four faces of cellular senescence. *Journal of Cell Biology*, 192(4), pp.547–556.
Roffey, J. et al., 2009. Protein kinase C intervention-the state of play. *Current Opinion in Cell Biology*, 21(2), pp.268–279.
Rohani, M.G. et al., 2014. Cdc42 inhibits ERK-mediated collagenase-1 (MMP-1) expression in collagen-activated human keratinocytes. *The Journal of investigative dermatology*, 134(5), pp.1230–7.
Rohani, M.G. et al., 2015. MMP-10 Regulates Collagenolytic Activity of Alternatively Activated Resident Macrophages. *Journal of Investigative Dermatology*, 135(10), pp.1–8.
Rohani, M.G. & Parks, W.C., 2015. Matrix remodeling by MMPs during wound repair. *Matrix Biology*, 44-46, pp.113–121.
Rolfe, K.J. & Grobbelaar, A.O., 2012. A Review of Fetal Scarless Healing. *International Scholarly Research Notices*, 698034, pp.1–9.
Romagnani, P. et al., 2004. CXC chemokines: The regulatory link between inflammation and angiogenesis. *Trends in Immunology*, 25(4), pp.201–209.
Romani, N. et al., 2003. Langerhans cells - dendritic cells of the epidermis. *APMIS : acta pathologica, microbiologica, et immunologica Scandinavica*, 111(7-8), pp.725–40.
Rømer, J. et al., 1991. Differential Expression of Urokinase-Type Plasminogen Activator and Its Type-1 Inhibitor During Healing of Mouse Skin Wounds. *Journal of Investigative Dermatology*, 97, pp.803–811.
Rømer, J. et al., 1994. The Receptor for Urokinase-type Plasminogen Activator is Expressed by Keratinocytes at the Leading Edge During Re-Epithelialization of Mouse Skin Wounds. *Journal of Investigative Dermatology*, 102(4), pp.519–522.
Roper, J. a et al., 2015. Ultrasonic Stimulation of Mouse Skin Reverses the Healing Delays in Diabetes and Aging by Activation of Rac1. *Journal of Investigative Dermatology*, 135(January), pp.1–10.
Roques, C. & Téot, L., 2008. The use of corticosteroids to treat keloids: a review. *The international journal of lower extremity wounds*, 7(3), pp.137–45.
Rose, L.F. & Chan, R.K., 2016. The Burn Wound Microenvironment. *Advances in wound care*, 5(3), pp.106–118.
Ross, S. & Hill, C.S., 2008. How the Smads regulate transcription. *International Journal of Biochemistry and Cell Biology*, 40(3), pp.383–408.
Rotmann, A. et al., 2006. Activation of classical protein kinase C reduces the expression of human cationic amino acid transporter 3 (hCAT-3) in the plasma membrane. *The Biochemical journal*, 395(1), pp.117–123.
Rowan, M.P. et al., 2015. Burn wound healing and treatment: review and advancements. *Critical care*, 19(243), pp.1–12.
Ruehl, M. et al., 2002. The epithelial mitogen keratinocyte growth factor binds to collagens via the consensus sequence glycine-proline-hydroxyproline. *The Journal of biological chemistry*, 277(30), pp.26872–8.
Ruoslahti, E., 1988a. Fibronectin and Its Receptors. *Annual Review of Biochemistry*, 57, pp.375–413.
Ruoslahti, E., 1984. Fibronectin in cell adhesion and invasion. *Cancer and Metastasis Review*, 3(1), pp.43–51.
Ruoslahti, E., 1996. RGD and Other Recognition Sequences for Integrins. *Annu Rev Cell Dev Biol*, 12, pp.697–715.
Ruoslahti, E., 1988b. Structure and Biology of Proteoglycans. *Annual Review of Cell Biology*, 4, pp.229–255.
Russell, S.B. et al., 2010. Epigenetically altered wound healing in keloid fibroblasts. *The Journal of investigative dermatology*, 130(10), pp.2489–96.
Ruszczak, Z., 2003. Effect of collagen matrices on dermal wound healing. *Advanced Drug Delivery Reviews*, 55(12), pp.1595–1611.
Sa, C. et al., 2009. Dedifferentiation of Human Epidermal Keratinocytes Induced by UV In Vitro. *Journal of Health Science*, 55(5), pp.709–719.
Saarialho-Kere, U.K. et al., 1994. Distinct populations of basal keratinocytes express stromelysin-

1 and stromelysin-2 in chronic wounds. *Journal of Clinical Investigation*, 94(1), pp.79–88.
Saba, N.S. & Levy, L.S., 2012. Protein kinase C-beta inhibition induces apoptosis and inhibits cell cycle progression in acquired immunodeficiency syndrome-related non-hodgkin lymphoma cells. *Journal of investigative medicine : the official publication of the American Federation for Clinical Research*, 60(1), pp.29–38.
Sado, Y. et al., 1998. Organization and expression of basement membrane collagen IV genes and their roles in human disorders. *Journal of biochemistry*, 123(5), pp.767–76.
Saed, G.M. et al., 1998. Analysis of p53 Gene Mutations in Keloids Using Polymerase Chain Reaction–Based Single-Strand Conformational Polymorphism and DNA Sequencing. *Archives of dermatological research*, 134, pp.963–967.
Safferling, K. et al., 2013. Wound healing revised: A novel reepithelialization mechanism revealed by in vitro and in silico models. *Journal of Cell Biology*, 203(4), pp.691–709.
Saito, S. et al., 2001. Role of matrix metalloproteinases 1, 2, and 9 and tissue inhibitor of matrix metalloproteinase-1 in chronic venous insufficiency. *Journal of Vascular Surgery*, 34(5), pp.930–938.
Sano, S. et al., 1999. Keratinocyte-specific ablation of Stat3 exhibits impaired skin remodeling, but does not affect skin morphogenesis. *EMBO Journal*, 18(17), pp.4657–4668.
Santhiago, M.R., Netto, M. V & Wilson, S.E., 2012. Mitomycin C: biological effects and use in refractive surgery. *Cornea*, 31(3), pp.311–21.
Santoro, M.M. & Gaudino, G., 2005. Cellular and molecular facets of keratinocyte reepithelization during wound healing. *Experimental Cell Research*, 304(1), pp.274–286.
Santos, M. et al., 2002. The expression of keratin K10 in the basal layer of the epidermis inhibits cell proliferation and prevents skin tumorigenesis. *Journal of Biological Chemistry*, 277(21), pp.19122–19130.
Saraste, A. & Pulkki, K., 2000. Morphologic and biochemical hallmarks of apoptosis. *Cardiovascular Research*, 45(3), pp.528–537.
Sarrazin, S., Lamanna, W.C. & Esko, J.D., 2011. Heparan Sulfate Proteoglycans. , pp.1–33.
Sarrazy, V. et al., 2011. Mechanisms of pathological scarring: Role of myofibroblasts and current developments. *Wound Repair and Regeneration*, 19(Suppl. 1), pp.10–15.
Satish, L. et al., 2005. Interferon-inducible protein 9 (CXCL11)-induced cell motility in keratinocytes requires calcium flux-dependent activation of mu-calpain. *Molecular and cellular biology*, 25(5), pp.1922–41.
Satish, L. et al., 2004. Keloid fibroblast responsiveness to epidermal growth factor and activation of downstream intracellular signaling pathways. *Wound Repair and Regeneration*, 12(2), pp.183–192.
Satish, L. & Kathju, S., 2010. Cellular and molecular characteristics of scarless versus fibrotic wound healing. *Dermatology Research and Practice*, 790234, pp.1–11.
Satish, L., Yager, D. & Wells, A., 2003. Glu-Leu-Arg-negative CXC chemokine interferon γ inducible protein-9 as a mediator of epidermal-dermal communication during wound repair. *Journal of Investigative Dermatology*, 120(6), pp.1110–1117.
Sato, N. et al., 1993. Platelet-derived growth factor indirectly stimulates angiogenesis in vitro. *The American journal of pathology*, 142(4), pp.1119–1130.
Sawicki, G. et al., 2005. Interaction of keratinocytes and fibroblasts modulates the expression of matrix metalloproteinases-2 and -9 and their inhibitors. *Molecular and cellular biochemistry*, 269(1-2), pp.209–16.
Saxena, V. et al., 2004. Vacuum-assisted closure: microdeformations of wounds and cell proliferation. *Plastic and reconstructive surgery*, 114(5), pp.1086–1096; discussion 1097–1098.
Sayo, T. et al., 2002. Hyaluronan synthase 3 regulates hyaluronan synthesis in cultured human keratinocytes. *Journal of Investigative Dermatology*, 118(1), pp.43–48.
Scapini, P. et al., 2000. The neutrophil as a cellular source of chemokines. *Immunological reviews*, 177(4), pp.195–203.
Scarponi, C. et al., 2014. Inhibition of inflammatory and proliferative responses of human keratinocytes exposed to the sesquiterpene lactones dehydrocostuslactone and costunolide. *PLoS ONE*, 9(9), pp.1–10.
Schaefer, L. & Iozzo, R. V., 2008. Biological functions of the small leucine-rich proteoglycans:

From genetics to signal transduction. *Journal of Biological Chemistry*, 283(31), pp.21305–21309.
Schaefer, L. & Schaefer, R.M., 2010. Proteoglycans: From structural compounds to signaling molecules. *Cell and Tissue Research*, 339(1), pp.237–246.
Schafer, I.A. et al., 1985. Comparative observation of fibroblasts derived from the papillary and reticular dermis of infants and adults: Growth kinetics, packing density at confluence and surface morphology. *Mechanisms of Ageing and Development*, 31(3), pp.275–293.
Schäfer, M. & Werner, S., 2008. Oxidative stress in normal and impaired wound repair. *Pharmacological research : the official journal of the Italian Pharmacological Society*, 58(2), pp.165–71.
Scherer, S.S. et al., 2008. The mechanism of action of the vacuum-assisted closure device. *Plastic and reconstructive surgery*, 122(3), pp.786–97.
Schiller, M., Javelaud, D. & Mauviel, A., 2004. TGF-β-induced SMAD signaling and gene regulation: Consequences for extracellular matrix remodeling and wound healing. *Journal of Dermatological Science*, 35(2), pp.83–92.
Schlage, P., Kockmann, T., Sabino, F., et al., 2015. Matrix metalloproteinase 10 degradomics in keratinocytes and epidermal tissue identifies bioactive substrates with pleiotropic functions. *Molecular & cellular proteomics : MCP*, pp.3234–3246.
Schlage, P., Kockmann, T., Kizhakkedathu, J.N., et al., 2015. Monitoring matrix metalloproteinase activity at the epidermal-dermal interface by SILAC-iTRAQ-TAILS. *Proteomics*, pp.2491–2502.
Schneider, H., Mühle, C. & Pacho, F., 2007. Biological function of laminin-5 and pathogenic impact of its deficiency. *European Journal of Cell Biology*, 86(11-12), pp.701–717.
Schneider, L. et al., 2010. Directional cell migration and chemotaxis in wound healing response to PDGF-AA are coordinated by the primary cilium in fibroblasts. *Cellular Physiology and Biochemistry*, 25(2-3), pp.279–292.
Schreml, S. et al., 2010. Wound healing in the 21st century. *Journal of the American Academy of Dermatology*, 63(5), pp.866–81.
Schultz, G.S. & Wysocki, A., 2009. Interactions between extracellular matrix and growth factors in wound healing. *Wound Repair and Regeneration*, 17(2), pp.153–162.
Schulz, A. et al., 2016. A prospective clinical trial comparing Biobrane® Dressilk® and PolyMem® dressings on partial-thickness skin graft donor sites. *Burns*, 42(2), pp.345–355.
Schulze, A. & Downward, J., 2000. Analysis of gene expression by microarrays: cell biologist's gold mine or minefield? *Journal of cell science*, 113, pp.4151–4156.
Schwacha, M., Nickel, E. & Daniel, T., 2008. Burn Injury–Induced Alterations in Wound Inflammation and Healing Are Associated with Suppressed Hypoxia Inducible Factor-1α Expression. *Molecular Medicine*, 14(9-10), pp.628–633.
Schwacha, M.G., 2003. Macrophages and post-burn immune dysfunction. *Burns*, 29(1), pp.1–14.
Schwartz, M., 2004. Rho signalling at a glance. *Journal of Cell Science*, 117(23), pp.5457–5458.
Scott, K.A. et al., 2004. TNF-α regulates epithelial expression of MMP-9 and integrin αvβ6 during tumour promotion. A role for TNF-α in keratinocyte migration? *Oncogene*, 23(41), pp.6954–6966.
Scott, P.G. et al., 1995. Immunohistochemical localization of the proteoglycans decorin, biglycan and versican and transforming growth factor-β in human post-burn hypertrophic and mature scars. *Histopathology*, 26(5), pp.423–31.
Seeger, M.A. & Paller, A.S., 2015. The Roles of Growth Factors in Keratinocyte Migration. *Advances in wound care*, 4(4), pp.213–224.
Sen, C.K. et al., 2010. Human Skin Wounds: A Major Snoballing Threat to Public Health and Economy. *Wound Repair Regen. 2009*, 17(6), pp.763–771.
Seppa, H. et al., 1982. Platelet-derived Growth Factor Is Chemotactic for Fibroblasts Sources of Growth Factors Synthesis in Fibroblast Cultures. *J Cell Biol.*, 92(February), pp.584–588.
Serini, G. & Gabbiani, G., 1999. Mechanisms of myofibroblast activity and phenotypic modulation. *Experimental cell research*, 250(2), pp.273–83.
Serova, M. et al., 2008. Effects of protein kinase C modulation by PEP005, a novel ingenol angelate, on mitogen-activated protein kinase and phosphatidylinositol 3-kinase signaling in cancer cells. *Molecular cancer therapeutics*, 7(4), pp.915–922.

Shah, M., Foreman, D.M. & Ferguson, M.W.J., 1995. Neutralisation of TGF-β1 and TGF-β2 or exogenous addition of TGF-β3 to cutaneous rat wounds reduces scarring. *Journal of Cell Science*, 108, pp.985–1002.

Shah, V. V et al., 2016. 5-Fluorouracil in the Treatment of Keloids and Hypertrophic Scars: A Comprehensive Review of the Literature. *Dermatology and Therapy*, 6(2), pp.169–183.

Shannon, D.B. et al., 2006. Phenotypic differences between oral and skin fibroblasts in wound contraction and growth factor expression. *Wound Repair and Regeneration*, 14(2), pp.172–178.

Shaw, T.J. & Martin, P., 2009. Wound repair at a glance. *Journal of cell science*, 122(Pt 18), pp.3209–13.

Shen, Z. et al., 2006. Altered keratin 17 peptide ligands inhibit in vitro proliferation of keratinocytes and T cells isolated from patients with psoriasis. *Journal of the American Academy of Dermatology*, 54(6), pp.992–1002.

Shen, Z. et al., 2013. High expression of ubiquitin-conjugating enzyme 2C (UBE2C) correlates with nasopharyngeal carcinoma progression. *BMC cancer*, 13, p.192.

Sheng, W. et al., 2005. The Roles of Versican V1 and V2 Isoforms in Cell Proliferation and Apoptosis. *Molecular biology of the cell*, 16, pp.1330–1340.

Sheppard, P. et al., 2003. IL-28, IL-29 and their class II cytokine receptor IL-28R. *Nature immunology*, 4(1), pp.63–68.

Sheridan, R.L. & Tompkins, R.G., 1999. Skin substitutes in burns. *Burns*, 25(2), pp.97–103.

Sherratt, M.J., 2009. Tissue elasticity and the ageing elastic fibre. *Age*, 31(4), pp.305–325.

Shibani, S. & Gokul, S., 2012. Keratinization and its Disorders. *Oman Medical Journal*, 27(5), pp.348–357.

Shigeishi, H., Higashikawa, K. & Takechi, M., 2014. Role of receptor for hyaluronan-mediated motility (RHAMM) in human head and neck cancers. *Journal of cancer research and clinical oncology*, 140(10), pp.1629–1640.

Shih, B. et al., 2012. Identification of biomarkers in sequential biopsies of patients with chronic wounds receiving simultaneous acute wounds: A genetic, histological, and noninvasive imaging study. *Wound Repair and Regeneration*, 20(5), pp.757–769.

Shih, B. et al., 2010. Molecular dissection of abnormal wound healing processes resulting in keloid disease. *Wound Repair and Regeneration*, 18(2), pp.139–153.

Shiraha, H. et al., 1999. IP-10 inhibits epidermal growth factor-induced motility by decreasing epidermal growth factor receptor-mediated calpain activity. *Journal of Cell Biology*, 146(1), pp.243–253.

Shirakata, Y., 2010. Regulation of epidermal keratinocytes by growth factors. *Journal of dermatological science*, 59(2), pp.73–80.

Sin, C.G.T. et al., 2011. S100A4 downregulates filopodia formation through increased dynamic instability. *Cell adhesion & migration*, 5(5), pp.439–47.

Singer, A. & Clark, R., 1999. Cutaneous Wound Healing. *The New England Journal of Medicine*, 341, pp.738–746.

Singh, K. et al., 2016. Increased expression of TLR9 associated with pro-inflammatory S100A8 and IL-8 in diabetic wounds could lead to unresolved inflammation in type 2 diabetes mellitus (T2DM) cases with impaired wound healing. *Journal of Diabetes and its Complications*, 30(1), pp.99–108.

Singh, P., Carraher, C. & Schwarzbauer, J.E., 2010. Assembly of fibronectin extracellular marix. *Annu Rev Cell Dev Biol*, 26, pp.397–419.

Situm, M. et al., 2014. Chronic wounds as a public health problem. *Acta Med Croatica*, 68(Supplement 1), pp.5–7.

Sivamani, R., Garcia, M. & Isseroff, R., 2007. Wound re-epithelialization: modulating kerationcyte migration in wound healing. *Frontiers in Bioscience*, 12, pp.2849–2868.

Sivaprasad, U. et al., 2015. SERPINB3/B4 contributes to early inflammation and barrier dysfunction in an experimental murine model of atopic dermatitis. *J Invest Dermatol*, 135(1), pp.160–169.

Slemp, A.E. & Kirschner, R.E., 2006. Keloids and scars: a review of keloids and scars, their pathogenesis, risk factors, and management. *Current opinion in pediatrics*, 18(4), pp.396–402.

Smiell, J.M. et al., 1999. Efficacy and safety of becaplermin (recombinant human platelet-derived growth factor-BB)in patients with nonhealing, lower extremity diabetic ulcers: A combined analysis of four randomized studies. *Wound Repair and Regeneration*, 7(5), pp.335–346.

Smith, M.M. & Melrose, J., 2015. Proteoglycans in Normal and Healing Skin. *Advances in Wound Care*, 4(3), pp.152–173.

Snyder, R.J. et al., 2016. Macrophages: A Review of Their Role in Wound Healing and Their Therapeutic Use. *Wound Repair and Regeneration*, 24, pp.613–629.

Sogabe, Y. et al., 2006. Basic fibroblast growth factor stimulates human keratinocyte motility by Rac activation. *Wound Repair and Regeneration*, 14(4), pp.457–462.

Sohr, S. & Engeland, K., 2008. RHAMM is differentially expressed in the cell cycle and downregulated by the tumor suppressor p53. *Cell Cycle*, 7(21), pp.3448–3460.

Song, H.K., Wehrli, F.W. & Ma, J., 1997. In vivo MR microscopy of the human skin. *Magnetic Resonance in Medicine*, 37(2), pp.185–191.

Soo, C. et al., 2003. Ontogenetic transition in fetal wound transforming growth factor-beta regulation correlates with collagen organization. *The American journal of pathology*, 163(6), pp.2459–76.

Sorrell, J.M., Baber, M. a & Caplan, A.I., 2008. Human dermal fibroblast subpopulations; differential interactions with vascular endothelial cells in coculture: nonsoluble factors in the extracellular matrix influence interactions. *Wound repair and regeneration : official publication of the Wound Healing Society [and] the European Tissue Repair Society*, 16(2), pp.300–9.

Sorrell, J.M., Baber, M.A. & Caplan, A.I., 2004. Site-matched papillary and reticular human dermal fibroblasts differ in their release of specific growth factors/cytokines and in their interaction with keratinocytes. *Journal of Cellular Physiology*, 200(1), pp.134–145.

Sorrell, J.M. & Caplan, A.I., 2004. Fibroblast heterogeneity: more than skin deep. *Journal of cell science*, 117(Pt 5), pp.667–75.

Sozen, E. et al., 2014. Potential role of proteasome on c-jun related signaling in hypercholesterolemia induced atherosclerosis. *Redox Biology*, 2(1), pp.732–738.

Spiekstra, S.W. et al., 2007. Wound-healing factors secreted by epidermal keratinocytes and dermal fibroblasts in skin substitutes. *Wound repair and regeneration : official publication of the Wound Healing Society [and] the European Tissue Repair Society*, 15(5), pp.708–17.

Sprenger, A. et al., 2013. Consistency of the proteome in primary human keratinocytes with respect to gender, age, and skin localization. *Molecular & Cellular Proteomics*, 12, pp.2509–21.

Springer, T.A., 1994. Traffic signals for lymphocyte recirculation and leukocyte emigration: The multistep paradigm. *Cell*, 76(2), pp.301–314.

Sriram, G., Bigliardi, P.L. & Bigliardi-Qi, M., 2015. Fibroblast heterogeneity and its implications for engineering organotypic skin models in vitro. *European Journal of Cell Biology*, 94(11), pp.483–512.

Stadelmann, W.K., Digenis, A.G. & Tobin, G.R., 1998. Physiology and healing dynamics of chronic cutaneous wounds. *American Journal of Surgery*, 176(2 A).

Steinert, P., 2001. Keratins: Dynamic, flexible structural proteins of epithelial cells. *Curr. Probl. Dermatol*, 13, pp.193–198.

Stephens, P. et al., 2003. Anaerobic cocci populating the deep tissues of chronic wounds impair cellular wound healing responses in vitro. *British Journal of Dermatology*, 148, pp.456–466.

Stephens, P. et al., 2001. Phenotypic variation in the production of bioactive hepatocyte growth factor / scatter factor by oral mucosal and skin fibroblasts. *Wound Repair and Regeneration*, pp.34–43.

Stephens, P. et al., 2001. Skin and oral fibroblasts exhibit phenotypic differences in extracellular matrix reorganization and matrix metalloproteinase activity. *British Journal of Dermatology*, 144(2), pp.229–237.

Stephens, P. & Genever, P., 2007. Non-epithelial oral mucosal progenitor cell populations. *Oral diseases*, 13(1), pp.1–10.

Stevens, L.J. & Page-McCaw, A., 2012. A secreted MMP is required for reepithelialization during wound healing. *Molecular biology of the cell*, 23(6), pp.1068–79.

Stojadinovic, O. et al., 2005. Molecular Pathogenesis of Chronic Wounds. *The American journal of pathology*, 167(1), pp.59–69.

Strieter, R.M. et al., 2009. The role of circulating mesenchymal progenitor cells, fibrocytes, in promoting pulmonary fibrosis. *Transactions of the American Clinical and Climatological Association*, 120, pp.49–59.
Strik, M.C. et al., 2002. Distribution of the human intracellular serpin protease inhibitor 8 in human tissues. *The journal of histochemistry and cytochemistry : official journal of the Histochemistry Society*, 50(11), pp.1443–1454.
Suga, H. et al., 2014. TLR4, rather than TLR2, regulates wound healing through TGF-?? and CCL5 expression. *Journal of Dermatological Science*, 73(2), pp.117–124.
Suga, H. et al., 2014. Tracking the elusive fibrocyte: Identification and characterization of collagen producing hematopoietic lineage cells during murine wound healing. *Stem Cells*, 32(5), pp.1347–1360.
Sugawara, T. et al., 2001. Regulation and Role of Interleukin 6 in Wounded Human Epithelial Keratinocytes. *Cytokine*, 15(6), pp.328–336.
Sullivan, S.R. et al., 2004. Validation of a model for the study of multiple wounds in the diabetic mouse (db/db). *Plastic and reconstructive surgery*, 113(3), pp.953–960.
Sumagin, R. et al., 2013. Activation of PKCβII by PMA Facilitates Enhanced Epithelial Wound Repair through Increased Cell Spreading and Migration. *PLoS ONE*, 8(2), pp.1–12.
Sun, L.-D. et al., 2010. Association analyses identify six new psoriasis susceptibility loci in the Chinese population. *Nature genetics*, 42(11), pp.1005–9.
Sun, X. et al., 2011. Dedifferentiation of human terminally differentiating keratinocytes into their precursor cells induced by basic fibroblast growth factor. *Biological & pharmaceutical bulletin*, 34(7), pp.1037–45.
Suter, M.M. et al., 2009. The keratinocyte in epidermal renewal and defence. *Veterinary dermatology*, 20(5-6), pp.515–32.
Swensson, O. et al., 1998. Specialized keratin expression pattern in human ridged skin as an adaptation to high physical stress. *British Journal of Dermatology*, 139(5), pp.767–775.
Szabowski, A. et al., 2000. c-Jun and JunB antagonistically control cytokine-regulated mesenchymal-epidermal interaction in skin. *Cell*, 103(5), pp.745–755.
Szpaderska, A.M. et al., 2005. Distinct Patterns of Angiogenesis in Oral and Skin Wounds. *Journal of Dental Research*, 84, pp.309–314.
Szpaderska, A.M., Zuckerman, J.D. & DiPietro, L.A., 2003. Differential injury responses in oral mucosal and cutaneous wounds. *Journal of dental research*, 82(8), pp.621–626.
Szulgit, G. et al., 2002. Alterations in fibroblast alpha1beta1 integrin collagen receptor expression in keloids and hypertrophic scars. *The Journal of investigative dermatology*, 118(3), pp.409–15.
Takiguchi, T. et al., 2014. Cathelicidin antimicrobial peptide LL-37 augments interferon-β expression and antiviral activity induced by double-stranded RNA in keratinocytes. *British Journal of Dermatology*, 171(3), pp.492–498.
Tamburro, A.M., Bochicchio, B. & Pepe, A., 2005. The dissection of human tropoelastin: From the molecular structure to the self-assembly to the elasticity mechanism. *Pathologie Biologie*, 53(7), pp.383–389.
Tammi, R. et al., 2005. Hyaluronan synthase induction and hyaluronan accumulation in mouse epidermis following skin injury. *Journal of Investigative Dermatology*, 124(5), pp.898–905.
Tan, H. et al., 2015. Effective use of Biobrane as a temporary wound dressing prior to definitive split-skin graft in the treatment of severe burn: A retrospective analysis. *Burns*, 41(5), pp.969–976.
Tan, J. et al., 2015. iTRAQ-based proteomic profiling reveals different protein expression between normal skin and hypertrophic scar tissue. *Burns & Trauma*, 3(1), p.13.
Tan, K.K.B. et al., 2014. Characterization of fetal keratinocytes, showing enhanced stem cell-like properties: A potential source of cells for skin reconstruction. *Stem Cell Reports*, 3(2), pp.324–338.
Tan, K.T. et al., 2011. Characterization of hyaluronan and TSG-6 in skin scarring: Differential distribution in keloid scars, normal scars and unscarred skin. *Journal of the European Academy of Dermatology and Venereology*, 25(3), pp.317–327.
Tanaka, N. et al., 1998. Expression of the α1-α6 collagen IV chains in the dermoepidermal junction during human foetal skin development: Temporal and spatial expression of the α4 collagen

IV chain in an early stage of development. *British Journal of Dermatology*, 139(3), pp.371–374.
Tang, A. & Gilchrest, B.A., 1996. Regulation of keratinocyte growth factor gene expression in human skin fibroblasts. *Journal of Dermatological Science*, 11(1), pp.41–50.
Tarafder, A.K. et al., 2014. Rab11b Mediates Melanin Transfer between Donor Melanocytes and Acceptor Keratinocytes via Coupled Exo/Endocytosis. *The Journal of investigative dermatology*, 134, pp.1056–1066.
Tecchio, C. & Cassatella, M.A., 2016. Neutrophil-derived chemokines on the road to immunity. *Seminars in Immunology*, 28(2), pp.119–128.
Tecchio, C., Micheletti, A. & Cassatella, M.A., 2014. Neutrophil-derived cytokines: Facts beyond expression. *Frontiers in Immunology*, 5(OCT), pp.1–7.
Telgenhoff, D. & Shroot, B., 2005. Cellular senescence mechanisms in chronic wound healing. *Cell death and differentiation*, 12(7), pp.695–698.
Thamm, O.C. et al., 2015. Acute and chronic wound fluids influence keratinocyte function differently. *International Wound Journal*, 12(2), pp.143–149.
Thannickal, V.J. et al., 2003. Myofibroblast differentiation by transforming growth factor-β1 is dependent on cell adhesion and integrin signaling via focal adhesion kinase. *Journal of Biological Chemistry*, 278(14), pp.12384–12389.
Thomason, H.A. et al., 2012. Direct evidence that PKCα positively regulates wound re-epithelialization: Correlation with changes in desmosomal adhesiveness. *Journal of Pathology*, 227, pp.346–356.
Thorey, I.S. et al., 2001. The Ca2+-binding Proteins S100A8 and S100A9 are Encoded by Novel Injury-regulated Genes. *Journal of Biological Chemistry*, 276(38), pp.35818–35825.
Timpl, R. et al., 2003. Fibulins: a versatile family of extracellular matrix proteins. *Nat Rev Mol Cell Biol*, 4(6), pp.479–489.
Titapiwatanakun, B. et al., 2005. SCCA2-transfected human keratinocytes show increased secretion of IL-1α and IL-6, but not of TNF-α. *Archives of Dermatological Research*, 297(6), pp.274–277.
Tobin, D.J., 2016. Introduction to skin aging. *Journal of tissue viability*, ePub ahead.
Tolg, C. et al., 2012. A RHAMM mimetic peptide blocks hyaluronan signaling and reduces inflammation and fibrogenesis in excisional skin wounds. *American Journal of Pathology*, 181(4), pp.1250–1270.
Tolg, C., McCarthy, J.B., et al., 2014. Hyaluronan and RHAMM in Wound Repair and the "Cancerization"of Stromal Tissues. *BioMed Research Internationa*, pp.1–18.
Tolg, C. et al., 2006. Rhamm-/- fibroblasts are defective in CD44-mediated ERK1,2 motogenic signaling, leading to defective skin wound repair. *Journal of Cell Biology*, 175(6), pp.1017–1028.
Tolg, C., Telmer, P. & Turley, E., 2014. Specific sizes of hyaluronan oligosaccharides stimulate fibroblast migration and excisional wound repair. *PLoS ONE*, 9(2), pp.1–10.
Toma, J.G. et al., 2001. Isolation of multipotent adult stem cells from the dermis of mammalian skin. *Nature cell biology*, 3(9), pp.778–84.
Tomasek, J.J. et al., 2002. Myofibroblasts and mechano-regulation of connective tissue remodelling. *Nature reviews. Molecular cell biology*, 3(5), pp.349–63.
Tomic-Canic, M., Ågren, M.S. & Alvarez, O.M., 2004. Epidermal Repair and the Chronic Wound. In D. T. Rovee & H. I. Maibach, eds. *The Epidermis in Wound Healing*. CRC Press LLC, pp. 25–57.
Tomic-Canic, M. & Brem, H., 2004. Gene array technology and pathogenesis of chronic wounds. *American Journal of Surgery*, 188(1 Suppl. 1), pp.67–72.
Tonnesen, M.G., Feng, X. & Clark, R.A.F., 2000. Angiogenesis in wound healing. *The Journal of Investigative Dermatology Symposium Proceedings*, 5(1), pp.40–46.
Toriseva, M. & Kähäri, V.M., 2009. Proteinases in cutaneous wound healing. *Cellular and Molecular Life Sciences*, 66(2), pp.203–224.
Trace, A.P. et al., 2016. Keloids and Hypertrophic Scars: A Spectrum of Clinical Challenges. *American journal of clinical dermatology*, 17(3), pp.201–223.
Tracy, L.E., Minasian, R. a. & Caterson, E.J., 2016. Extracellular Matrix and Dermal Fibroblast Function in the Healing Wound. *Advances in wound care*, 5(3), pp.119–136.

Tramullas, M. et al., 2010. BAMBI (bone morphogenetic protein and activin membrane-bound inhibitor) reveals the involvement of the transforming growth factor-beta family in pain modulation. *J Neurosci*, 30(4), pp.1502–1511.
Tran, H., VanDusen, W.J. & Argraves, W.S., 1997. The self-association and fibronectin-binding sites of fibulin-1 map to calcium-binding epidermal growth factor-like domains. *Journal of Biological Chemistry*, 272(36), pp.22600–22606.
Traversa, B. & Sussman, G., 2001. The role of growth factors , cytokines and proteases in wound management. *Primary Intention*, 9(4), pp.161–167.
Trengrove, N.J. et al., 1999. Analysis of the acute and chronic wound environments:the role of proteases and their inhibitors. *Wound Repair and regeneration*, 7(6), pp.442–452.
Trost, A. et al., 2010. Aberrant heterodimerization of keratin 16 with keratin 6A in HaCaT keratinocytes results in diminished cellular migration. *Mechanisms of Ageing and Development*, 131(5), pp.346–353.
Trøstrup, H. et al., 2013. What Is New in the Understanding of Non Healing Wounds Epidemiology, Pathophysiology, and Therapies. *Ulcers*, 2013, pp.1–8.
Trousdale, R.K. et al., 2009. Wound Closure and Metabolic Parameter Variability in a db/db Mouse Model for Diabetic Ulcers. *Journal of Surgical Research*, 151(1), pp.100–107.
Tsatmali, M., Ancans, J. & Thody, A.J., 2002. Melanocyte Function and Its Control by Melanocortin Peptides. *Journal of Histochemistry & Cytochemistry*, 50(2), pp.125–133.
Tschöp, K. & Engeland, K., 2007. Cell cycle-dependent transcription of cyclin B2 is influenced by DNA methylation but is independent of methylation in the CDE and CHR elements. *FEBS Journal*, 274(20), pp.5235–5249.
Tsuboi, R. et al., 1993. Keratinocyte growth factor (FGF-7) stimulates migration and plasminogen activator activity of normal human keratinocytes. *The Journal of investigative dermatology*, 101(1), pp.49–53.
Tuan, T.L. & Nichter, L.S., 1998. The molecular basis of keloid and hypertrophic scar formation. *Molecular medicine today*, 4, pp.19–24.
Turabelidze, A. et al., 2014. Intrinsic differences between oral and skin keratinocytes. *PloS one*, 9(9), pp.1–10.
Turabelidze, A. & DiPietro, L.A., 2012. Inflammation and wound healing. *Endodontic Topics*, 24, pp.26–38.
Turley, E.A., Noble, P.W. & Bourguignon, L.Y.W., 2002. Signaling properties of hyaluronan receptors. *Journal of Biological Chemistry*, 277(7), pp.4589–4592.
Twal, W.O. et al., 2001. Fibulin-1 suppression of fibronectin-regulated cell adhesion and motility. *Journal of cell science*, 114(Pt 24), pp.4587–4598.
Uchi, H. et al., 2000. Cytokines and chemokines in the epidermis. *Journal of Dermatological Science*, 24, pp.S29–S38.
Uitto, J. et al., 1985. Altered steady-state ratio of type I/III procollagen mRNAs correlates with selectively increased type I procollagen biosynthesis in cultured keloid fibroblasts. *Proceedings of the National Academy of Sciences of the United States of America*, 82(17), pp.5935–9.
Ulrich, D. et al., 2010. Matrix metalloproteinases and tissue inhibitors of metalloproteinases in patients with different types of scars and keloids. *Journal of plastic, reconstructive & aesthetic surgery : JPRAS*, 63(6), pp.1015–1021.
Uppal, R.S. et al., 2001. The effects of a single dose of 5-fluorouracil on keloid scars: a clinical trial of timed wound irrigation after extralesional excision. *Plastic and Reconstructive Surgery*, 108(5), pp.1218–1224.
Usui, M.L. et al., 2008. Keratinocyte Migration, Proliferation, and Differentiation in Chronic Ulcers From Patients With Diabetes and Normal Wounds. *Journal of Histochemistry and Cytochemistry*, 56(7), pp.687–696.
Uzé, G. & Monneron, D., 2007. IL-28 and IL-29: Newcomers to the interferon family. *Biochimie*, 89(6-7), pp.729–734.
Vaalamo, M. et al., 1997. Distinct populations of stromal cells express collagenase-3 (MMP-13) and collagenase-1 (MMP-1) in chronic ulcers but not in normally healing wounds. *The Journal of investigative dermatology*, 109(1), pp.96–101.
Vaalamo, M. et al., 1996. Patterns of matrix metalloproteinase and TIMP-1 expression in chronic

and normally healing human cutaneous wounds. *The British journal of dermatology*, 135(1), pp.52–9.
Vaidya, M. & Kanojia, D., 2007. Keratins : Markers of cell differentiation or regulators of cell differentiation? *Journal of Biosciences*, 32, pp.629–634.
Varani, J. et al., 2009. Impaired keratinocyte function on matrix metalloproteinase-1 (MMP-1) damaged collagen. *Archives of Dermatological Research*, 301(7), pp.497–506.
Varani, J., 1998. Preservation of human skin structure and function in organ culture. *Histology and Histopathology*, 13, pp.775–783.
Vazquez, J.R. et al., 2003. Outcomes of hyaluronan therapy in diabetic foot wounds. *Diabetes Research and Clinical Practice*, 59(2), pp.123–127.
Van Der Veer, W.M. et al., 2011. Time course of the angiogenic response during normotrophic and hypertrophic scar formation in humans. *Wound Repair and Regeneration*, 19(3), pp.292–301.
Velnar, T., Bailey, T. & Smrkolj, V., 2009. The Wound Healing Process: An Overview of the Cellular and Molecular Mechanisms. *The Journal of International Medical Research*, 37(5), pp.1528–1542.
Verhaegen, P.D.H.M. et al., 2009. Differences in collagen architecture between keloid, hypertrophic scar, normotrophic scar, and normal skin: An objective histopathological analysis. *Wound Repair and Regeneration*, 17(5), pp.649–656.
Vermeulen, K., Van Bockstaele, D.R. & Berneman, Z.N., 2003. The cell cycle: A review of regulation, deregulation and therapeutic targets in cancer. *Cell Proliferation*, 36(3), pp.131–149.
Verrecchia, F., Mauviel, A. & Farge, D., 2006. Transforming growth factor-β signaling through the Smad proteins: Role in systemic sclerosis. *Autoimmunity Reviews*, 5(8), pp.563–569.
Veves, A., Sheehan, P. & Pham, H.T., 2002. A randomized, controlled trial of Promogran (a collagen/oxidized regenerated cellulose dressing) vs standard treatment in the management of diabetic foot ulcers. *Archives of Surgery*, 137(7), pp.822–827.
Vicente-Manzanares, M. & Horwitz, A., 2011. Cell migration: An overview. In C. Wells & M. Parsons, eds. *Cell Migration: Developmental Methods and Protocols*. Humana Press, pp. 1–24.
Viera, M.H., Vivas, A.C. & Berman, B., 2012. Update on Keloid Management: Clinical and Basic Science Advances. *Advances in wound care*, 1(5), pp.200–206.
Vikatmaa, P. et al., 2008. Negative Pressure Wound Therapy: a Systematic Review on Effectiveness and Safety. *European Journal of Vascular and Endovascular Surgery*, 36(4), pp.438–448.
Voigt, J. & Driver, V.R., 2012. Hyaluronic acid derivatives and their healing effect on burns, epithelial surgical wounds, and chronic wounds: a systematic review and meta-analysis of randomized controlled trials. *Wound repair and regeneration*, 20(3), pp.317–331.
Voss, A. et al., 2011. Expression of S100A8/A9 in HaCaT keratinocytes alters the rate of cell proliferation and differentiation. *FEBS Letters*, 585(2), pp.440–446.
Vu, T.H. & Werb, Z., 2000. Matrix metalloproteinases: Effectors of development and normal physiology. *Genes and Development*, 14(17), pp.2123–2133.
Wagner, W. & Wehrmann, M., 2007. Differential cytokine activity and morphology during wound healing in the neonatal and adult rat skin. *Journal of Cellular and Molecular Medicine*, 11(6), pp.1342–1351.
Wainwright, D.J., 1995. Use of an acellular allograft dermal matrix (AlloDerm) in the management of full-thickness burns. *Burns*, 21(4), pp.243–248.
Wall, I.B. et al., 2008. Fibroblast dysfunction is a key factor in the non-healing of chronic venous leg ulcers. *The Journal of investigative dermatology*, 128(10), pp.2526–40.
Wallace, H.J. & Stacey, M.C., 1998. Levels of tumor necrosis factor-α (TNF-α) and soluble TNF receptors in chronic venous leg ulcers-correlations to healing status. *The Journal of investigative dermatology*, 110(3), pp.292–6.
Walsh, P.N., 2003. Roles of factor XI, platelets and tissue factor-initiated blood coagulation. *Journal of Thrombosis and Haemostasis*, 1(10), pp.2081–2086.
Walters, K. & Roberts, M., 2002. Chapter 1, The Structure and Function of Skin. In *Dermatological and transdermal formulations*. Marcel Dekker, Inc.

Wang, H., Jin, H. & Rapraeger, A.C., 2015. Syndecan-1 and syndecan-4 capture epidermal growth factor receptor family members and the α3β1 integrin via binding sites in their ectodomains: Novel synstatins prevent kinase capture and inhibit α6β4-integrindependent epithelial cell motility. *Journal of Biological Chemistry*, 290(43), pp.26103–26113.

Wang, J. et al., 2008. Deep dermal fibroblasts contribute to hypertrophic scarring. *Laboratory investigation; a journal of technical methods and pathology*, 88(12), pp.1278–90.

Wang, Y. et al., 2012. Effect of mitomycin on normal dermal fibroblast and HaCat cell: an in vitro study. *Journal of Zhejiang University. Science. B*, 13(12), pp.997–1005.

Wankell, M. et al., 2003. The roles of activin in cytoprotection and tissue repair. *Annals of the New York Academy of Sciences*, 995, pp.48–58.

Waseem, A. et al., 1998. Isolation, sequence and expression of the gene encoding human keratin 13. *Gene*, 215(2), pp.269–279.

Waseem, A. et al., 1999. Keratin 15 expression in stratified epithelia: Downregulation in activated keratinocytes. *Journal of Investigative Dermatology*, 112(3), pp.362–369.

Van De Water, L., Varney, S. & Tomasek, J.J., 2013. Mechanoregulation of the Myofibroblast in Wound Contraction, Scarring, and Fibrosis: Opportunities for New Therapeutic Intervention. *Advances in wound care*, 2(4), pp.122–141.

Watt, F.M., 1998. Epidermal stem cells: markers, patterning and the control of stem cell fate. *Phil. Trans. R. Soc. Lond. B*, 353, pp.831–837.

Watt, F.M., 1989. Terminal differentiation of epidermal keratinocytes. *Current opinion in cell biology*, 1, pp.1107–1115.

Watt, F.M. & Fujiwara, H., 2011. Cell-extracellular matrix interactions in normal and diseased skin. *Cold Spring Harbor perspectives in biology*, 3(4).

Wawersik, M. & Coulombe, P.A., 2000. Forced expression of keratin 16 alters the adhesion, differentiation, and migration of mouse skin keratinocytes. *Mol Biol Cell*, 11(10), pp.3315–3327.

Webber, J., Meran, S., et al., 2009. Hyaluronan orchestrates transforming growth factor-β1-dependent maintenance of myofibroblast phenotype. *Journal of Biological Chemistry*, 284(14), pp.9083–9092.

Webber, J., Jenkins, R.H., et al., 2009. Modulation of TGFβ1-dependent myofibroblast differentiation by hyaluronan. *The American journal of pathology*, 175(1), pp.148–160.

Weber, R.S. et al., 1995. Split-Thickness Skin Graft Donor Site Management. *Arch Otolaryngol Head Neck Surg*, 121, pp.1145–1149.

Wei, J. et al., 2014. A synthetic PPAR-γ agonist triterpenoid ameliorates experimental fibrosis: PPAR-γ-independent suppression of fibrotic responses. *Ann Rheum Dis*, 73(2), pp.446–454.

Welgus, H.G., Jeffrey, J.J. & Eisen, A.Z., 1981. The Collagen Substrate Specificity of Human Skin Fibroblast Collagenase. *The Journal of Biological Chemistry*, 256(18), pp.9511–9515.

Wells, A., Nuschke, A. & Yates, C.C., 2015. Skin Tissue Repair: Matrix Microenvironmental Influences. *Matrix Biology*, 49, pp.1–12.

Werdin, F. et al., 2009. Evidence-based management strategies for treatment of chronic wounds. *Journal of Plastic Surgery*, 9, pp.169–179.

Werner, S., 1998. Keratinocyte Growth Factor : A Unique Player in Epithelial Repair Processes. *Cytokine + Growth Factor Reviews*, 9(2), pp.153–165.

Werner, S. & Grose, R., 2003. Regulation of wound healing by growth factors and cytokines. *Physiological Reviews*, 83(3), pp.835–870.

Werner, S., Krieg, T. & Smola, H., 2007. Keratinocyte – Fibroblast Interactions in Wound Healing. *The Journal of investigative dermatology*, 127(5), pp.998–1008.

Werner, S. & Smola, H., 2001. Paracrine regulation of keratinocyte proliferation and differentiation. *Trends in Cell Biology*, 11(4), pp.143–146.

Wetzler, C. et al., 2000. Keratinocyte-Derived Chemotactic Cytokines : Expressional Modulation by Nitric Oxide in Vitro and during Cutaneous Wound Repair in Vivo. *Biochemical and Biophysical Research Communications*, 274, pp.689–696.

Whitbread, L. a & Powell, B.C., 1998. Expression of the intermediate filament keratin gene, K15, in the basal cell layers of epithelia and the hair follicle. *Experimental cell research*, 244(2), pp.448–459.

Whitby, D.J. & Ferguson, M.W., 1991. The extracellular matrix of lip wounds in fetal, neonatal

and adult mice. *Development (Cambridge, England)*, 112(2), pp.651–668.
Wiedow, O. et al., 1990. Elafin: an elastase-specific inhibitor of human skin. Purification, characterization, and complete amino acid sequence. *The Journal of biological chemistry*, 265(25), pp.14791–14795.
Wiegand, C. et al., 2010. Protease and pro-inflammatory cytokine concentrations are elevated in chronic compared to acute wounds and can be modulated by collagen type i in vitro. *Archives of Dermatological Research*, 302(6), pp.419–428.
Wight, T.N. et al., 2014. Versican and the Regulation of Cell Phenotype in Disease. *Biochimica et biophysica acta*, 1840(8), pp.2441–2451.
Wikramanayake, T.C., Stojadinovic, O. & Tomic-Canic, M., 2014. Epidermal Differentiation in Barrier Maintenance and Wound Healing. *Advances in wound care*, 3(3), pp.272–280.
Wilgus, T. a et al., 2008. Regulation of scar formation by vascular endothelial growth factor. *Lab Invest*, 88(6), pp.579–590.
Wilgus, T. a, Roy, S. & McDaniel, J.C., 2013. Neutrophils and Wound Repair: Positive Actions and Negative Reactions. *Advances in wound care*, 2(7), pp.379–388.
Wilkie, A.O.M. et al., 1995. Functions of fibroblast growth factors and their receptors. *Current Biology*, 5(5), pp.500–507.
Wilsmann-Theis, D. et al., 2015. Among the S100 proteins, S100A12 is the most significant marker for psoriasis disease activity. *Journal of the European Academy of Dermatology and Venereology*, pp.10–15.
Wilson, A.M., 2013. Eradication of keloids: Surgical excision followed by a single injection of intralesional 5-fluorouracil and botulinum toxin. *Canadian Journal of Plastic Surgery*, 21(2), pp.87–91.
Wilson, V.G., 2014. Growth and Differentiation of HaCAT keratinocytes. In K. Turksen, ed. *Methods in Molecular Biology*. Springer New York, pp. 33–41.
Windoffer, R. et al., 2011. Cytoskeleton in motion : the dynamics of keratin intermediate filaments in epithelia. *Journal of Cell Biology*, 194(5), pp.669–678.
Wisdom, R., Johnson, R.S. & Moore, C., 1999. c-Jun regulates cell cycle progression and apoptosis by distinct mechanisms. *The EMBO journal*, 18(1), pp.188–97.
Witte, K. et al., 2010. IL-28A, IL-28B, and IL-29: Promising cytokines with type I interferon-like properties. *Cytokine and Growth Factor Reviews*, 21(4), pp.237–251.
Witte, R.P. & Kao, W.J., 2005. Keratinocyte-fibroblast paracrine interaction: the effects of substrate and culture condition. *Biomaterials*, 26(17), pp.3673–82.
Wojtowicz, A.M. et al., 2014. The importance of both fibroblasts and keratinocytes in a bilayered living cellular construct used in wound healing. *Wound repair and regeneration*, 22(2), pp.246–255.
Wolf, R., Ruzicka, T. & Yuspa, S.H., 2011. Novel S100A7 (psoriasin)/S100A15 (koebnerisin) subfamily: Highly homologous but distinct in regulation and function. *Amino Acids*, 41(4), pp.789–796.
Wolk, K. et al., 2008. Maturing dendritic cells are an important source of IL-29 and IL-20 that may cooperatively increase the innate immunity of keratinocytes. *Journal of leukocyte biology*, 83(5), pp.1181–93.
Wolk, K., Witte, K. & Sabat, R., 2010. Interleukin-28 and interleukin-29: novel regulators of skin biology. *J Interferon Cytokine Res*, 30(8), pp.617–628.
Wong, J.W. et al., 2009. Wound healing in oral mucosa results in reduced scar formation as compared with skin: Evidence from the red duroc pig model and humans. *Wound Repair and Regeneration*, 17(5), pp.717–729.
Wong, P. & Coulombe, P.A., 2003. Loss of keratin 6 (K6) proteins reveals a function for intermediate filaments during wound repair. *Journal of Cell Biology*, 163(2), pp.327–337.
Wong, T., Chiu, H. & Yip, K., 1994. Intralesional interferon alpha-2b has no effect in the treatment of keloids. *British Journal of Dermatology*, 130(5), pp.683–686.
Woo, S.H., Lumpkin, E.A. & Patapoutian, A., 2015. Merkel cells and neurons keep in touch. *Trends in Cell Biology*, 25(2), pp.74–81.
Wozniak, M.A. et al., 2004. Focal adhesion regulation of cell behavior. *Biochimica et biophysica acta*, 1692, pp.103–119.
Wu, T. et al., 2010. Regulation of cyclin B2 expression and cell cycle G2/m transition by menin.

The Journal of biological chemistry, 285(24), pp.18291–300.
Wynn, T.A., 2008. Cellular and molecular mechanisms of fibrosis. *J Pathol*, 214(2), pp.199–210.
Xavier, S. et al., 2010. BAMBI is expressed in endothelial cells and is regulated by lysosomal/autolysosomal degradation. *PLoS ONE*, 5(9).
Xie, C. et al., 2014. Ubiquitin-conjugating enzyme E2C: a potential cancer biomarker. *Int.J.Biochem.Cell Biol.*, 47(1878-5875 (Electronic)), pp.113–117.
Xie, J. et al., 2008. Effects of basic fibroblast growth factor on the expression of extracellular matrix and matrix metalloproteinase-1 in wound healing. *Clinical and Experimental Dermatology*, 33(2), pp.176–182.
Xu, F. & Graves, D.T., 2013. Abnormal Cell Repsonses and Role of TNF-α in Impaired Diabetic Wound Healing Abnormal Cell Repsonses and Role of TNF-α in Impaired Diabetic. *Biomed Res Int*, (754802), pp.1–9.
Xu, P., Liu, J. & Derynck, R., 2012. Post-translational regulation of TGF-?? receptor and Smad signaling. *FEBS Letters*, 586(14), pp.1871–1884.
Xu, X. et al., 1998. IFN-y Induces Cell Growth Inhibition by Fas-mediated Apoptosis: Requirement of STATI Protein for Up-Regulation of Fas and FasL Expression. *Cell*, 58(July), pp.2832–2837.
Xue, H., McCauley, R.L. & Zhang, W., 2000. Elevated interleukin-6 expression in keloid fibroblasts. *The Journal of surgical research*, 89(1), pp.74–7.
Xue, M. & Jackson, C.J., 2015. Extracellular Matrix Reorganization During Wound Healing and Its Impact on Abnormal Scarring. *Advances in wound care*, 4(3), pp.119–136.
Yaar, M. et al., 1985. Effects of alpha and beta interferons on cultured human keratinocytes. *J Invest Dermatol*, 85(1), pp.70–74.
Yager, D.R. et al., 1997. Ability of chronic wound fluids to degrade peptide growth factors is associated with increased levels of elastase activity and diminished levels of proteinase inhibitors. *Wound repair and regeneration*, 5(1), pp.23–32.
Yager, D.R. et al., 1996. Wound Fluids from Human Pressure Ulcers Contain Elevated Matrix Metalloproteinase Levels and Activity Compared to Surgical Wound Fluids. *Journal of Investigative Dermatology*, 107(5), pp.743–748.
Yager, D.R. & Nwomeh, B.C., 1999. The proteolytic environment of chronic wounds. *Wound Repair and Regeneration*, 7(6), pp.433–441.
Yagi, L.H., Watanuki, L.M., Isaac, C., Gemperli, R., Nakamura, Y.M. & Ladeira, P.R.S., 2016. Human fetal wound healing: a review of molecular and cellular aspects. *European Journal of Plastic Surgery*, 39(4), pp.239–246.
Yamada, Y. et al., 2004. Differential regulation by IL-1beta; and EGF of expression of three different hyaluronan synthases in oral mucosal epithelial cells and fibroblasts and dermal fibroblasts: Quantitative analysis using real-time RT-PCR. *Journal of Investigative Dermatology*, 122(3), pp.631–639.
Yamamoto, M. et al., 2005. Fibrin Stimulates the Proliferation of Human Keratinocytes through the Autocrine Mechanism of Transforming Growth Factor- α and Epidermal Growth Factor Receptor. *The Tohoku Journal of Experimental Medicine*, 207(1), pp.33–40.
Yamano, Y. et al., 2008. Hyaluronan-mediated motility: A target in oral squamous cell carcinoma. *International Journal of Oncology*, 32(5), pp.1001–1009.
Yamashita, T. et al., 2005. Non-invasive visualization of melanin and melanocytes by reflectance-mode confocal microscopy. *The Journal of investigative dermatology*, 124(1), pp.235–40.
Yang, L. et al., 1999. Active transforming growth factor-beta in wound repair: determination using a new assay. *The American journal of pathology*, 154(1), pp.105–11.
Yao, Y. et al., 2008. Type I interferon: Potential therapeutic target for psoriasis? *PLoS ONE*, 3(7).
Yarosh, D. et al., 2000. Regulation of TNFalpha production and release in human and mouse keratinocytes and mouse skin after UV-B irradiation. *Photodermatology, Photoimmunology and Photomedicine*, 16(6), pp.263–270.
Yates, C.C. et al., 2007. Delayed and Deficient Dermal Maturation in Mice Lacking the CXCR3 ELR-Negative CXC Chemokine Receptor. *The American journal of pathology*, 171(2), pp.484–495.
Yates, C.C. et al., 2009. Delayed reepithelialization and basement membrane regeneration after wounding in mice lacking CXCR3. *Wound Repair and Regeneration*, 17(1), pp.34–41.

Yates, C.C., Hebda, P. & Wells, A., 2012. Skin Wound Healing and Scarring: Fetal Wounds and Regenerative Restitution. *Birth Defects Res C Embryo Today*, 96(4), pp.325–333.
Yates-Binder, C.C. et al., 2012. An IP-10 (CXCL10)-derived peptide inhibits angiogenesis. *PLoS ONE*, 7(7), pp.1–14.
Yel, M., Güven, T. & Türker, H., 2014. Effects of ultraviolet radiation on the stratum corneum of skin in mole rats. *Journal of Radiation Research and Applied Sciences*, 7(4), pp.506–511.
Yu, H. & Jove, R., 2004. The STATs of cancer--new molecular targets come of age. *Nature reviews. Cancer*, 4(2), pp.97–105.
Zahn, S. et al., 2011. Evidence for a pathophysiological role of keratinocyte-derived type III interferon (IFNλ) in cutaneous lupus erythematosus. *The Journal of investigative dermatology*, 131(1), pp.133–140.
Zaja-Milatovic, S. & Richmond, A., 2008. CXC chemokines and their receptors: A case for a significant biological role in cutaneous wound healing. *Histology and Histopathology*, 23(11), pp.1399–1407.
Zeng, G. et al., 1996. Endogenous TGF-beta activity is modified during cellular aging: effects on metalloproteinase and TIMP-1 expression. *Experimental cell research*, 228(2), pp.271–6.
Zenz, R. et al., 2003. c-Jun regulates eyelid closure and skin tumor development through EGFR signaling. *Developmental Cell*, 4(6), pp.879–889.
Zenz, R. & Wagner, E.F., 2006. Jun signalling in the epidermis: From developmental defects to psoriasis and skin tumors. *International Journal of Biochemistry and Cell Biology*, 38(7), pp.1043–1049.
Zhan, R. et al., 2015. Nitric oxide enhances keratinocyte cell migration by regulating Rho GTPase via cGMP-PKG signalling. *PLoS ONE*, 10(3), pp.1–15.
Zhang, C. et al., 2010. Dedifferentiation derived cells exhibit phenotypic and functional characteristics of epidermal stem cells. *Journal of Cellular and Molecular Medicine*, 14(5), pp.1135–1145.
Zhang, C. et al., 2015. FOXO1 differentially regulates both normal and diabetic wound healing. *Journal of Cell Biology*, 209(2), pp.289–303.
Zhang, W. et al., 2012. The pro-inflammatory cytokine il-22 up-regulates keratin 17 expression in keratinocytes via stat3 and erk1/2. *PLoS ONE*, 7(7), pp.3–10.
Zhang, W. & Liu, H.T., 2002. MAPK signal pathways in the regulation of cell proliferation in mammalian cells. *Cell Research*, 12(1), pp.9–18.
Zhang, Y. et al., 1998. The G3 domain of versican enhances cell proliferation via epidermal growth factor-like motifs. *Journal of Biological Chemistry*, 273(33), pp.21342–21351.
Zhang, Y. et al., 2015. Wnt/β-Catenin and Wnt5a/Ca2+ Pathways Regulate Proliferation and Apoptosis of Keratinocytes in Psoriasis Lesions. *Cellular Physiology and Biochemistry*, 36(5), pp.1890–1902.
Zheng, M. et al., 2014. High GINS2 transcript level predicts poor prognosis and correlates with high histological grade and endocrine therapy resistance through mammary cancer stem cells in breast cancer patients. *Breast Cancer Research and Treatment*, 148(2), pp.423–436.
Zheng, X. et al., 2006. Proteomic analysis for the assessment of different lots of fetal bovine serum as a raw material for cell culture. Part IV. Application of proteomics to the manufacture of biological drugs. *Biotechnology Progress*, 22(5), pp.1294–1300.
Zhou, L. et al., 2013. The overexpression of BAMBI and its involvement in the growth and invasion of human osteosarcoma cells. *Oncology Reports*, 30, pp.1315–1322.
Zhu, Z., Ding, J. & Tredget, E.E., 2016. The molecular basis of hypertrophic scars. *Burns & Trauma*, 4(1), p.2.
Zibert, J.R. et al., 2013. Immunopathogenesis of psoriasis. *Physiological genomics*, 6(1), pp.45–56.
Zibert, J.R. et al., 2010. Significance of the S100A4 protein in psoriasis. *The Journal of investigative dermatology*, 130(1), pp.150–60.
Ziegler, U. & Groscurth, P., 2004. Morphological features of cell death. *News in physiological sciences : an international journal of physiology produced jointly by the International Union of Physiological Sciences and the American Physiological Society*, 19(10), pp.124–8.
Zimmermann, D.R. et al., 1994. Versican is expressed in the proliferating zone in the epidermis and in association with the elastic network of the dermis. *Journal of Cell Biology*, 124(5),

pp.817–825.
Ziyadeh, N. et al., 2011. A matched cohort study of the risk of cancer in users of becaplermin. *Advances in skin & wound care*, 24(1), pp.31–9.
Zouboulis, C.C. et al., 2002. Current developments and uses of cryosurgery in the treatment of keloids and hypertrophic scars. *Wound Repair and Regeneration*, 10(2), pp.98–102.
Zouboulis, C.C. et al., 1993. Outcomes of Cryosurgery in Keloids and Hypertrophic Scars. *Archives of dermatology*, 129, pp.1146–1151.
Zurada, J.M., Kriegel, D. & Davis, I.C., 2006. Topical treatments for hypertrophic scars. *Journal of the American Academy of Dermatology*, 55(6), pp.1024–1031.